



EUROCORR 2014

EUROPEAN CORROSION CONGRESS



The annual event of the European Federation of Corrosion

8-12 September 2014 | Pisa | Italy

organised by



ASSOCIAZIONE
ITALIANA
DI METALLURGIA



DECHEMA

BOOK OF ABSTRACTS

EUROCORR 2014

EUROPEAN CORROSION CONGRESS



The annual event of the European Federation of Corrosion

8-12 September 2014 | Pisa | Italy

BOOK OF ABSTRACTS



Printed in Italy
ISBN 978-3-89746-159-8

©Copyright 2014
By: DECHEMA e. V.

All rights reserved. This publication, or any part thereof, may not be reproduced in any form without the written permission of DECHEMA e. V.. The texts contained in this "Book of abstracts" are published as received from the authors and without any correction.

The publishers are not responsible for statements or opinion expressed in this publication.

Co-published by:

DECHEMA e.V., Theodor-Heuss-Allee 25, 60486 Frankfurt, Germany,
Tel. +49-(0)69-7564-209, +49-(0)69-7564-418, info@dechema.de - www.dechema.de
and

AIM – Associazione Italiana di Metallurgia, Piazzale Rodolfo Morandi, 2 - 20121 Milano, Italy,
Tel. +39-0276397770 / +39-0276021132, e-mail: aim@aimnet.it - www.aimnet.it

INTERNATIONAL SCIENTIFIC COMMITTEE

Co-Chairpersons

Luciano Lazzari, Lorenzo Fedrizzi, Arjan Mol

Ralph Bäßler
Federica Bassani
Roman Bender
Jean-Pierre Celis
Pierangela Cristiani
Jerome Crouzillac
Wilhelm Erning
Lorenzo Fedrizzi
Damien Feron
Ralf Feser
Wolfram Fürbeth
Mathias Galetz
Theo Hack
Fouzia Hannour
Don Harrop
Jürgen Heinemann
Andreas Heyn
Ulf H. Kivisakk
Philippe Marcus
Willi Meier
J.M.C. Arjan Mol
Delphine Neff
Steve Paterson
Michael Raupach
Marcel Roche
François Ropital
Günter Schmitt
Michael Schütze
Alda Simoes
Tamas Istvan Török
Tunc Tüken
Krzysztof Wolski

LOCAL ORGANISING COMMITTEE

Emma Angelini
Francesco Bellucci
Massimiliano Bestetti
Fabio Bolzoni
Pier Luigi Bonora
Marina Cabrini
Pierangela Cristiani
Flavio Deflorian
Massimo De Sanctis
Lorenzo Fedrizzi
Romeo Fratesi
Giovanna Gabetta
Luciano Lazzari
Gianfranco Lovicu
Giampiero Montesperelli
Cecilia Monticelli
Tommaso Pastore
Edoardo Proverbio
Stefano Trasatti
Roberto Venturini
Sergio M. Volontè

Local Organising Secretariat

Federica Bassani
Sabrina De Donato
Antonella Donzelli
Carlo Mapelli
Marco Molinaro
Elena Nicodemi

EFC Congress office

Roman Bender
Heike Geiling
Ines Honndorf
Willi Meier

PLENARY LECTURES

From the object scale to the nanometer: issues linked with corrosion of archaeological ferrous artefacts	1
P. Dillmann (PL-7838)	
1 . CORROSION AND SCALE INHIBITION	
Comparison of the corrosion protection effectiveness of vapor corrosion inhibitor and nitrogen blanketing system	5
B. Bavarian, J. Zhang, K. Lu, L. Reiner (KN-7108)	
New corrosion inhibitor for evaporative cooling systems	6
J. Matheis, A. Stratmann, W. Hater, F. Wolf, R. Lunkenheimer, C. Foret (O-7114)	
Corrosion inhibition of carbon steel in cooling water systems by means of chemicals used to modify heat transfer	7
O. Conejero, M. Cabañas, J. Arancón, D. Carrascal (O-7394)	
The impact of copper chrome boron (CCB) wood preservative on the corrosion of St37 steel	8
H. Gerengi, C. Tasçioğlu, C. Akçay, M. Kurtay (O-7169)	
Adsorption of imidazole, triazole, and tetrazole on oxidized copper surface	9
D. Peca, A. Kokalj (O-7581)	
Corrosion inhibition of a large evaporative cooling system	10
I. Baghni (O-7299)	
Protection of Cu70Ni30 alloy by fatty acids	11
H. Otmacic Curkovic, Z. Hajdari, K. Marusic (O-7289)	
Inhibitor for galvanically coupled copper/steel system	12
G. Tansug, T. Tuken, G. Sigircik, E.S. Giray, M. Erbil (O-7498)	
4,5-Dinitrobenzimidazole and 5-nitrobenzimidazole adsorption on copper surface. Electrochemical and XPS study	13
I. Arkhipushkin, D. Zhilenko, L. Kazansky (O-7352)	
Probing corrosion inhibitor behaviour using micelle detection	14
S. Rankin, E. Perfect, M. Achour, D. Blumer (O-7173)	
Evaluation of environmental-friendly corrosion inhibitors vs traditional corrosion inhibitors in oil and gas industry	15
C. Di Iorio, T. Cheldi, S. Correra, E. Lo Piccolo, G. Mortali (O-7255)	
Effect of an amine based inhibitor on CO₂ corrosion of carbon steel	16
G. Mori, A. Prethaler, E. Rosenberg, M. Rückemann, W. Havlik, G. Zehethofer, S. Hönig (O-7610)	
Investigation of corrosion problems in cooling water pipeline	17
S. Al Subai, A. Bairamov (O-7737)	
Inhibition of CO₂ corrosion of pipeline steel by some imidazoline derivatives	18
A. Obike, P.C. Okafor, U.J. Ekpe, X. Jiang, D.R. Qu (O-7728)	

On the irreversibility of adsorption of volatile corrosion inhibitors and protection of metals against atmospheric corrosion	19
O.A. Goncharova, Yu.I. Kuznetsov, E.A. Nad'kina (O-7658)	
Questioning the use of volatile corrosion inhibitors in polymer foils - a comparative study on corrosion protection capabilities	20
L. Igetoft, C. Mille, S. Arnell (O-7815)	
Inhibition efficiencies to adsorption thermodynamics: discussing the value of such measurements	21
R. Lindsay, C. Ruiz-Camargo, M.S. Walczak (O-7587)	
Mitigation of flow induced localized corrosion with inhibitors	22
G. Schmitt (O-7736)	
Methodology of laboratory assessment of the efficiency of carbon dioxide corrosion inhibitors in oilfield pipelines	23
N. Andreev, I.S. Sivokon, S.S. Vesely (O-7307)	
Experimental and theoretical evaluation of strawberry fruit extract and its active component as corrosion inhibitor for mild steel in HCl	24
S. Umoren (O-7303)	
Evaluation of two imidazole derivatives as possible green corrosion inhibitors for mild steel: comparison of simulation with experiment	25
I. Obot (O-7438)	
Corrosion mechanism and electrochemical performance of TiO₂ nanostructures synthesized in organic electrolytes at high voltage	26
N. Rayon, M. Vera, C. Cuevas (O-7778)	
Electrochemical and XPS studies of the corrosion inhibition of carbon steel in phosphoric acid pickling solutions by purpald	27
M. Traisnel, C. Jama, F. Bentiss, B. Hammouti (O-7234)	
Inhibition of mild steel corrosion in acidic medium by vanillin cationic surfactants	28
I. Aiad, M. El-Sukkary, M. Samy, S. Sayied, Y. Moshira (O-7280)	
Assessment of the corrosion inhibitors effectiveness and their influence on the concrete physical properties	29
F.M.A. Moreira, C. Resende, A.F. Diniz, H.F. Gorgulho, A.H.S. Bueno, P.B. Martelli (O-7674)	
Electrochemical studies of the inhibition effect of 2-dimethylamine on the corrosion of austenitic stainless steel type 304 in dilute HCl	30
R.T. Loto, C.A. Loto (O-7774)	
Inhibition efficiency by an aqueous extract of flower petals of <i>Cassia auriculata</i> on corrosive carbon steel	31
S. Rajendran, M. Sangeetha, J. Sathiyabama (O-7056)	
Sodium potassium tartrate (SPT) as a corrosion inhibitor for aluminium	32
M. Hakeem, S. Rajendran, P.P. Regis (O-7069)	
Corrosion resistance of austenitic and duplex stainless steels in chloride containing alkaline environments	33
H. Peltola, M. Martikainen, M. Lindgren (P-7182)	

Adsorption and passivation of copper in neutral solutions by some heterocyclic corrosion inhibitors	34
M.O. Agafonkina, Y.I. Kuznetsov, N.P. Andreeva (P-7212)	
Conversion coatings of lanthanide salts on aluminium alloy as a potential replacement of chromate coatings	35
B. Volaric, I. Milosev (P-7748)	
Green corrosion inhibition from aqueous extract of <i>Zygophyllum album</i> L for carbon steel in hydrochloric acid medium	36
H. Derfouf Talbi, Y. Harek (P-7461)	
Novel cationic surfactant based on triazole as a corrosion inhibitor for carbon steel in phosphoric acid produced by dihydrated wet process	37
M.A. Hegazy (P-7163)	
Effect of Zr on intergranular corrosion of low Cr ferritic stainless steel	38
J.H. Park, K.Y. Kim (P-7294)	
Orange peel as green corrosion inhibitor - assessment of hesperidin, naringin and synephrine efficiency	39
M.V.C. Monteiro, J.C. Rocha, J.A.C. Ponciano Gomes (P-7325)	
Influence of the lithium molybdate inhibitor on the corrosion resistance of a duplex stainless steel in LiBr absorption machine	40
M.J. Muñoz-Portero, J. Rubio-Cervera, R. Leiva-García, J. García-Antón (P-7517)	
2HEABu corrosion-inhibitor action in aggressive medium on API X70 substrate	41
M.R. Ortega Vega, S.R. Kunst, S. Mattedi, M. Iglesias, C.F. Malfatti (P-7558)	
Inhibition efficiency of 3,4-diaminobenzonitrile against steel corrosion	42
G. Sigircik, T. Tüken, M. Erbil (P-7567)	
Electrochemical study of the inhibitive effect a new prepared quinoline derivative on the corrosion of steel in 3.5% NaCl solution	43
N. Hassan, N.A. Abdelghany, R.M. El-Shishtawy, S. Khalil (P-7596)	
<i>Rosmarinus officinalis</i> use as eco-friendly corrosion inhibitor carbon steel in acid solution	44
M.A. Velázquez-González, J.G. Gozález-Rodríguez, M.G. Valladares-Cisneros (P-7126)	
The effect of chloride concentration on copper protection	45
N. Kicir, T. Tüken, M. Erbil (P-7814)	
Three novel bolaamphiphiles as corrosion inhibitors for carbon steel in hydrochloric acid: experimental and computational study	46
M.A. Hegazy, M.K. Awad (P-7164)	
Environmentally friendly carboxylate inhibitors for heating and cooling (HVAC) systems ...	47
M. Ahmed (P-7689)	
Corrosion inhibition of ground anchors steel in HCl by H₂S-scavenger in HCl solution	48
J. Malina, F. Kapor, A. Begic Hadzipasic (P-7710)	
Causes and control of corrosion in drinking water distribution systems	49
F. Rohuma, I. Ahmad (P-7172)	

Combination of stearic acid and benzotriazole as corrosion inhibitors for Cu and Cu₄₀Zn in artificial urban rain	50
G. Zerjav, I. Milosev (P-7745)	

2. CORROSION BY HOT GASES AND COMBUSTION PRODUCTS

Thermodynamic modelling of North Dakota lignite ash in air- and oxy-fuel fired boiler and comparison to collected ash from a 15MW boiler	51
B. Bordenet, R. Ganta, A. Levasseur (O-7756)	

Corrosion of welded coal boiler steels in oxyfuel flue gas	52
A. Kranzmann, M. Mosquera, G. Oder, P. Zimmer, S. Rehfeldt, F. Kluger (O-7598)	

Hot corrosion in the next generation of industrial gas turbines	53
A. Potter, J. Sumner, N.J. Simms, J.E. Oakey (O-7544)	

Thermodynamic and kinetic modeling for predicting the microstructural evolution in MCrAlY coatings	54
R. Pillai, W.G. Sloof, A. Chyrkin, V. Shemet, L. Singheiser, W.J. Quadackers (O-7059)	

Corrosion of materials in nitrate melts for molten salt solar receivers	55
M. Spiegel, A. Kilic (O-7781)	

High-temperature corrosion under conditions simulating biomass firing: depth-resolved phase identification	56
S.C. Okoro, M. Montgomery, F.J. Frandsen, K. Pantleon (O-7604)	

The development of nickel alloys for high temperature applications in the process and energy sectors	57
S.A. McCoy, B.A. Baker, G.D. Smith, L.E. Shoemaker (O-7539)	

Laser Raman microscopy study of the transition from high temperature alloy passivation to breakaway oxidation	58
D. Young, T. Gheno, D. Monceau (O-7109)	

Oxidation mechanisms of alloy 602 CA in different gas atmospheres relevant to gas separation membranes	59
M. Schiek, L. Niewolak, R. Vaßen, W.J. Quadackers (O-7140)	

Grain boundary sulphidation of nickel-based alloys applied in high-efficient coal-power plants	60
M.M. Lange, S. Borodin, F.U. Renner, M. Spiegel (O-7529)	

Effect of sulfur content on adhesion of thermal oxide scales grown on austenitic stainless steels	61
C. Pascal, E. Fedorova, V. Parry, M. Braccini, M. Mantel, D. Oquab, Y. Wouters, D. Monceau (O-7531)	

The effect of SO₄²⁻ ions on the corrosion of 15CrMo steels during shutting down and their oxide scale formation	62
Y. Meng, L. Zhang, D.Q. Zhang, L.X. Gao (O-7147)	

Behaviour of 25wt.%Cr-containing Fe-based alloys strengthened by hafnium carbides in oxidation between 1000 and 1200°C	63
P. Berthod, E. Conrath (O-7561)	

Effect of minor strengthening additions in Ni-base superalloys on oxide scale formation in high pO_2 environments	65
W. Nowak, A. Jalowicka, D. Naumenko, L. Singheiser, W.J. Quadackers (O-7252)	
Influence of water vapour in air and of TaC carbides in alloy on the high temperature oxidation of cobalt-based refractory alloys	66
L. Aranda, Th. Schweitzer, P. Berthod, A. Navet, A. Leroy (O-7568)	
Close-to-reality modelling of high temperature corrosion phenomena in steel industry by a novel designed lab-scale test rig	68
H. Rojacz, M. Varga, K. Adam, M. Rodríguez-Ripoll (O-7360)	
Effect of the presence of water vapour on the high temperature oxidation of Co-10Ni-30Cr and Co-10Ni-30Cr-0.5C alloys	69
A. Leroy, A. Navet, Th. Schweitzer, L. Aranda, P. Berthod (P-7573)	
Carbide transformations occurring between 1000 and 1100°C in the sub-surface of a Ni-25Cr-0.50C alloy induced by hot oxidation	70
P. Berthod, E. Conrath (P-7575)	
Kinetic of oxidation of chromium-rich HfC-containing Co-based and Ni-based alloys between 1000 and 1100°C	71
E. Conrath, P. Berthod (P-7615)	
Effect of sulfur on the KCl-induced high temperature corrosion of selected Fe-based and Ni-based alloys	73
S. Kiamehr, K.V. Dahl, T. Jonsson, M. Montgomery, M.A.J. Somers (P-7535)	
Kinetic of oxidation at 1000, 1100 and 1200°C of 32.5wt.% Cr-containing Co-based alloys reinforced by hafnium carbides	74
E. Conrath, P. Berthod (P-7611)	
3. NUCLEAR CORROSION	
Flow accelerated corrosion management using brt-cicero™: performances and future updates	76
S. Trévin, M.-P. Moutrille, P. Caylar, D. Delacoux, E. Gipon (KN-7691)	
Evaluation of the effects of pH and oxygen on mitigation of wall thinning of carbon steel due to flow-accelerated corrosion	77
S. Uchida, M. Naitoh, H. Okada (O-7104)	
Intergranular oxidation of alloy 600 exposed to simulated PWR primary water	78
J. Caballero Hinojosa, J. Crépin, T. Couvant, C. Duhamel (O-7133)	
Effect of alloying elements and surface preparation on the oxidation behaviour of nickel base alloys in superheated steam	79
F. Hamdani, H. Abe, B. Ter-Ovanesian, B. Normand, Y. Watanabe (O-7149)	
Image-based cohesive element modelling of low temperature crack propagation in alloy 82 weld metal	80
G. Klimaytys, A.P. Jivkov, D.L. Engelberg (O-7436)	
Detection and characterization of stress-corrosion cracking of stainless steel in simulated BWR environment	81
B. Zajec, M. Bajt Leban, A. Legat (O-7636)	

Characterization of Ni/NiO layers formed on alloy 182 weld metal in PWR water	82
C. de Araujo Figueiredo, R. Mendonça, M. Vankeerberghen, R-W. Bosch (O-7661)	
Experimental and numerical study of the iodine-induced stress corrosion cracking of zircaloy-4 nuclear fuel cladding tubes	83
T. Jezequel, Q. Auzoux, D. Le Boulch, E. Andrieu, C. Blanc, C. Delafoy, N. Barnel, C. Dal Bianco (O-7542)	
The influence of lithium ions on corrosion of zirconium alloys	84
A. Krausová, J. Macák, P. Sajdl, V. Renciuková, V. Vrtílková (O-7130)	
Effect of superheated steam on the corrosion behavior of advanced steels proposed as accident tolerant fuel cladding	85
R. Rebak, E. Dolley (O-7283)	
Study on the effect of phosphorous concentration on intergranular corrosion of stainless steel in boiling nitric acid solution	86
F. Ueno, A. Komatsu, T. Igarashi, M. Yamamoto (O-7096)	
Evaluation of the corrosion behavior of candidate materials for overpack applications under buried conditions	87
G. Nakayama, Y. Sakakibara (O-7176)	
The corrosion of carbon steel embedded in bentonite under anoxic conditions	88
N.R. Smart, A.P. Rance, B. Reddy, N. Diomidis (O-7503)	
Challenges related with the development of the closure plan for DNDR Baita Bihor România - corrosion monitoring	89
R. Fako, F. Dragolici, Gh. Barariu, F. Sociu, E. Neacsu (O-7429)	
Corrosion of carbon steel in the Callovo-Oxfordian claystone in the context of the French nuclear waste repository (in project) 1. Experimental set up and corrosion behaviour	90
S. Necib, D. Crusset, N. Michau, F. Foct, M. Schlegel, S. Daumas, S. Dewonck (O-7631)	
Iron corrosion products (CP) impact on the long term alteration of fractured nuclear glass: effects of transport and CP stability	91
L. Gentaz, D. Rebiscoul, D. Neff, P. Dillmann, S. Gin (O-7501)	
Galvanic corrosion of carbon steel under argillite layers in carbonated media	92
A. Romaine, R. Sabot, M. Jeannin, Ph. Refait (O-7156)	
Surface analytical and electrochemical measurements on Cu-coated steel specimens	93
R. Partovi-Nia, D.W. Shoesmith, R. Jacklin, J. Chen, D. Zagidulin, S. Ramamurthy, P.G. Keech (O-7603)	
Corrosion behaviour of Mg alloys cladding from nuclear reactors fuel in alkaline solutions	94
J. Agullo, B. Muzeau, C. Bataillon, V. L'Hostis (O-7381)	
Advanced Al₂O₃ coatings under extreme conditions	95
F. García Ferré, M. Ormellese, M. Beghi, F. Di Fonzo (O-7505)	
Oxidation of 316L(N) stainless steel in liquid sodium at high temperature	96
M. Rivollier, J.L. Courouau, M.L. Giorgi (O-7659)	

Corrosion of carbon steel in the Callovo-Oxfordian claystone in the context of the French nuclear waste repository (in project). 2. structural organization of corrosion products	97
M.L. Schlegel, S. Necib, S. Daumas, C. Blanc, E. Foy, D. Crusset, N. Michau (O-7486)	
Corrosion behaviour of structural steels exposed in supercritical water	98
J. Macák, P. Sajdl, A. Krausová, V. Bystrianský, L. Tuma, E. Krečanová, M. Zychová (O-7665)	
Investigation of the effect of water chemistry and temperature on the oxide layer formed on Alloy 182 in simulated PWR environment	99
R. de Mendonca, R.-W. Bosch, W. van Renterghem (P-7837)	
On the mechanism and kinetics of radiation induced corrosion of copper	100
Å. Björkbacka, S. Hosseinpour, M. Johnsson, C. Leygraf, M. Jonsson (P-7218)	
Corrosion susceptibility of steel drums containing cemented simulated incineration ashes as low level nuclear waste	101
G. Duffó, S. Farina, F. Schulz, F. Marotta (P-7086)	
Corrosion of high purity copper as engineering barrier in deep geological repositories	102
M. Ochoa, M. Rodríguez, S. Farina (P-7091)	
Corrosion resistance in multipass welding of thick UNS S31304 lean duplex stainless steel plates welded using SMAW, GMAW and FCAW processes	103
C.S. Souza, V.F.C. Lins, D.M. Silveira, C.G.F. Costa, R.C. Junior, F.R. Campos, A.Q. Bracarense (P-7719)	
Effect of cathodic hydrogen charging of titanium alloys on hydrogen absorption and hydride formation	104
S. Dejardin, V. Dusquesnes, N. Creton, R. Oltra, T. Montesin (P-7759)	
Water chemistry and corrosion issues of control rod and protection system in Russian LWGRS	105
E. Yurmanov, V. Yurmanov (P-7800)	
Sensitisation and IGSCC in type 321 SS NPP manifold welds	106
K. Shutko (P-7801)	
Behaviour of steam generator tube at different temperatures and levels of chloride	107
M. Schvartzman, F. Mansur, P. Nogueira, W.R.C Campos, M.A.D. Quinan (P-7600)	
Oxidation behavior and spallation of oxide scales after T91 oxidation in water vapor environment	108
M. Demizieux, C. Desgranges, J. Favergeon, L. Martinelli (P-7836)	
Hydrogen production by iron corrosion under irradiation	109
D. Stammose, M. Osmond, E. Barker, C. Wittebroodt (P-7664)	
4. ENVIRONMENT SENSITIVE FRACTURE	
Evaluating the pit-crack transition in an offshore pipeline steel	110
C. Evans, R. Akid (O-7490)	
Critical analysis of the role of ferrite content in the environment- sensitive cracking of duplex stainless steels	111
R. Pettersson, S. Wessman (O-7512)	

Influence of nitrate ions concentration, pH and applied potential on the susceptibility to corrosion and stress corrosion cracking of α-β brass in NaNO_3 solutions.....	112
C. Berne, E. Andrieu, J. Reby, J.-M. Sobrino, C. Blanc (O-7210)	
Mechanistic investigation of stress corrosion cracking of pipeline steel in near-neutral pH environment.....	113
R. Bogdanov, A. Marshakov, V. Ignatenko (O-7074)	
The relationships between microstructure and sulfide stress cracking resistance of high strength, low alloy OCTG steels.....	114
W. Huang, F. Cao, A. Aylor, W. Sun (O-7271)	
Cathodic charging during hydrogen embrittlement testing.....	115
Q. Liu, A. Atrens (O-7806)	
The Kelvin probe: towards rapid, in-situ evaluation of HISC susceptibility and undercoating corrosion.....	116
E.F. Turcu, M. Rohwerder (O-7391)	
Hydrogen induced stress cracking tests for offshore wind farm monopile foundations.....	117
D. Bangsgaard, T. Mathiesen, C. Christensen (O-7446)	
Investigation on Nickel base superalloy stem turbine bolts, fractured at high temperatures, a case history.....	118
G. Lovicu, R. Ishak, L. Rolla, C. Dellabiancia (O-7586)	
Analyses on coupled electrochemical noise and acoustic emission data applied on chloride stress corrosion cracking.....	119
L. Calabrese, F. Cappuccini, D. Di Pietro, M. Galeano, E. Proverbio (O-7523)	
Liquid metal embrittlement of the T91 steel in lead bismuth eutectic: effect of the loading rate and the oxygen content.....	120
I. Proriot Serre, C. Ye, J.-B. Vogt (O-7688)	
The effects of sulfide and flow rate on corrosion behavior of duplex steel 1.4462 in the artificial molasse basin fluid.....	121
J. Sobetzki, R. Bäßler, A. Boduch (O-7235)	
Influence of testing parameters on type of damage under cyclic loading.....	122
A. Visser, G. Mori, H. Leitner, M. Kapp, R. Fluch, B. Holper, M. Panzenböck (O-7605)	
CS-AFM study on the localized corrosion of 2507 duplex stainless steel.....	123
L. Qiao, M. Lin, L. Guo (O-7829)	
The transition between sulfide stress cracking and stress corrosion cracking of the 2304 DSS as a function of T and pH in H_2S environment.....	124
F. Ruel, S. Saedlou, S. Le Manchet, C. Lojewski, K. Wolski (O-7151)	
5. CORROSION MECHANISMS, METHODS AND MODELLING	
Critical factors in corrosion and biocompatibility of biodegradable Mg alloys.....	125
S. Virtanen (KN-7153)	
Application of time-of-flight secondary ions mass spectrometry (ToF-SIMS) to corrosion research.....	126
P. Marcus, A. Seyeux (KN-7695)	



Multiscale corrosion modelling	127
J. Deconinck, O. Dolgikh, P. Maciel, A. Demeter, H. Simillion, N. Van den Steen (KN-7708)	
Localised corrosion mechanisms of magnesium in methanol	128
H.N. McMurray, J.E. Board, G. Williams (O-7070)	
Effect of Si on formation of Fe-rich particles in pure Mg and its influence on corrosion	129
L. Yang, X. Zhou, S. Liang, R. Schmid-Fetzer, T. Hashimoto, H. Liu, X. Zhong, J. Robson, Z. Fan, G. Scamans, G.E. Thompson (O-7246)	
Corrosion of AZ31 Mg alloy in the presence of ammonium ion	130
D. Buggio, M. Trueba, S.P. Trasatti (O-7290)	
The dissolution of magnesium investigated with a microelectrochemical flow system	131
L. Rossrucker, N. Birbilis, G.S. Frankel, K.J.J. Mayrhofer (O-7545)	
Corrosion behaviour of magnesium electrodes investigated by real-time hydrogen measurement	132
M. Curioni (O-7310)	
Influence of plastic deformation on the corrosion resistance of TiAl6V4 and TiMo10Zr4 alloys in aqueous solution containing chloride ions	133
H. Krawiec, J. Loch, A. Lukaszczyk, V. Vignal (O-7626)	
Non-uniformity of anodized titanium surface under UV-light irradiation observed by ellipso-microscopy	134
K. Fushimi, K. Kurauchi, T. Nakanishi, Y. Hasegawa, M. Ueda, T. Ohtsuka (O-7278)	
pH at zinc and magnesium surfaces during atmospheric corrosion	135
C. Taxen, D. Thierry (O-7578)	
The development of a mechanistic model towards the simulation of atmospheric corrosion	136
H. Simillion, O. Dolgikh, P. Maciel, H. Terryn, J. Deconinck (O-7237)	
Role of pH on the L-cysteine action on zinc in 3 w/w % NaCl	137
V. Shkirskiy, P. Volovitch, K. Ogle, F. Leroux, T. Stimpfling, P. Keil, H. Hintze-Bruening (O-7417)	
In-situ atmospheric corrosion monitoring using resistometry	138
K. Azumi (O-7478)	
Corrosion performances of plasma electrolytic oxidized implant metals and alloys	139
S. Sinebryukhov, S.V. Gnedenkov, O.A. Khisanfova, A.V. Puz, V.S. Egorkin, A.G. Zavidnaya (O-7338)	
Effect of microstructure on the morphology of atmospheric corrosion pits in 304L stainless steel	140
H.B. Mohammed Ali, A.J. Davenport, M.M. Attallah (O-7676)	
Nanostructure and local properties of oxide layers grown in simulated pressurized water reactor environment	141
V. Maurice, T. Massoud, L.H. Klein, A. Seyeux, P. Marcus (O-7211)	
About point defects formation in Cr₂O₃ passive films	142
B. Malki, A. Pasturel, B. Baroux (O-7158)	

Kelvin probe force microscopy and atmospheric corrosion of cold-rolled grade 2205 duplex stainless steel	143
C. Örnek, D. Engelberg (O-7213)	
Relative humidity for onsets of pitting corrosion and repassivation of stainless steels under wet-dry cyclic conditions containing chloride	144
A. Nishikata, H. Nakamura, T. Nam, E. Tada (O-7275)	
Electrochemical AFM study of corrosion behavior of a 2507 super duplex stainless steel: influence of precipitated chromium nitrides	145
E. Bettini, U. Kivisäkk, C. Leygraf, J. Pan (O-7572)	
Influence of heat treatment on corrosion resistance of martensitic stainless steels 1.4034 and 1.4021	146
P. Rosemann, M. Babutzka, A. Heyn, T. Halle (O-7455)	
Stress corrosion cracking at room temperature of austenitic stainless steels in marine areas: the case of fixed guards for climbing	147
F. Deflorian, M. Dalvit, S. Rossi, C. Zanella, M. Fedel (O-7506)	
Passivity and corrosion behavior of duplex stainless steels after various surface preparations	148
V. Vignal, H. Krawiec, S. Le Manchet (O-7480)	
Stable and metastable pitting corrosion susceptibilities from physical properties of passive films	149
B. Ter-Ovanesian, B. Normand (O-7499)	
Chemical composition and nanostructure of passive films formed on FeCrNiMo austenitic stainless steel	150
H. Peng, V. Maurice, L.H. Klein, A. Seyeux, S. Zanna, P. Marcus (O-7217)	
Polarization behaviour of new aluminium alloys (AA2139 and AA2198) in neutral media	151
A. Balbo, V. Grassi, A. Frignani, F. Zucchi (O-7138)	
Mechanisms of scale dissolution on non-alloyed and silicon-alloyed steels	152
A. Alaoui Mouayd, E. Sutter, B. Tribollet A. Koltsov (O-7245)	
Critical aspects of electrochemical noise-based corrosion monitoring	153
A.M. Homborg, T. Tinga, X. Zhang, E.P.M. van Westing, G.M. Ferrari, J.H.W. de Wit, J.M.C. Mol (O-7313)	
A review on electrochemical noise measurement as a tool for evaluation of organic coatings and recent developments	154
D. Mills, S.S. Jamali (O-7697)	
Study of the relation between microstructure and corrosion properties of polycrystalline copper	155
E. Martinez Lombardia, L. Lapeire, V. Maurice, I. De Graeve, L. Klein, P. Marcus, K. Verbeken, L. Kestens, H. Terryn (O-7373)	
3D printed (flow) cells - a new approach in hydrogen embrittlement studies	156
G. Schimo, A.W. Hassel (O-7484)	
Corrosion of iron and steel: occurrence of iron(II) hydroxysalts	157
C. Remazeilles, I. Azoulay, M. Jeannin, R. Sabot, Ph. Refait (O-7137)	

Electrochemical characterization of corrosion behaviour of different metals in hot molten salt for solar thermal power plants	158
D. Ruckle, S. Kaesche, H. Garrecht, S. Virtanen (O-7204)	
Effect of HNO₃ and Cl⁻ on corrosion behaviour of AISI 304 and Cr-Mn austenitic stainless steels	159
N. Khobragade, A. Patil (O-7570)	
Grain-dependency of passive oxide film formed on iron in sulphuric acid	160
Y. Takabatake, K. Fushimi, T. Nakanishi, Y. Hasegawa (O-7167)	
Predictive modelling of the corrosion rate of carbon steel focusing on the effect of the precipitation of corrosion products	161
A. Marion, B. Vuillemin, R. Oltra, D. Crusset (O-7264)	
Development of a liquid-phase sulfide ion gun for localized sulfidation of metal surfaces	162
J.-S. Lee, K. Fushimi, T. Nakanishi, Y. Hasegawa (O-7364)	
Development of a sensor for interfacial pH measurements during pitting corrosion in situ observed by temporal series of micrographs	163
A. Mendes Zimer, M. Medina Da Silva, L. Helena Mascaro, E. Chaves Pereira (O-7618)	
Markov chain model to predict localised corrosion of stainless steels	164
A. Brenna, M. Ormellesse, L. Lazzari (O-7513)	
Mechanistic study of degradation of coil coated steel	165
Y. Liu, X. Zhou, G.E. Thompson, S.B. Lyon, T. Hashimoto, G. Smith, S. Gibbon, D. Francis, A. Gholinia, X. Zhong (O-7783)	
Finely distributed anodic and cathodic centers underneath organic coatings - characterization and effects on the delamination mechanism	166
M. Pichler, M. Fleischanderl, M. Wolpers, G. Fafilek (O-7641)	
Mechanism of corrosion protection of zinc-magnesium coatings on steel studied by electrochemical depth profiling	167
J. Rodriguez, M. Mouanga, A. Lanzutti, F. Andreatta, L. Fedrizzi, M.-G. Olivier (O-7132)	
A novel method to study corrosion resistance of galvanised steel against corrosive dropping electrolytes	168
S. Ziebermayr, M. Fleischanderl, G. Haslehner, K.H. Stellnberger, A.W. Hassel (O-7477)	
Nanoscope view on the initial stages of corrosion of hot dip galvanized Zn-Mg-Al coatings	169
J. Duchoslav, M. Arndt, T. Keppert, G. Luckeneder, K.H. Stellnberger, J. Hagler, C.K. Riener, G. Angeli, D. Stifter (O-7243)	
The effects of oxygen concentration and pH on the galvanic protection of tin	170
S. Geary, H.N. McMurray, A.C.A. de Vooy, N. Wint (O-7549)	
Investigation of passive layers on SiC-based ceramics by electrochemical impedance spectroscopy	171
M. Schneider, K. Kremmer, K. Sempf, M. Herrmann (O-7602)	
Corrosion features of the PEO-coated magnesium alloys	172
A. Gnedenkov, S. Sinebryukhov, D. Mashtalyar, S. Gnedenkov (O-7202)	

Corrosion layer growth on magnesium galvanic coupled to aluminium simulated by FEM	173
D. Höche (O-7142)	
Hydrogen diffusion mechanism in nickel base alloy 718	174
O. Golenishcheva, G. Andersohn, M. Oechsner, J. Kloewer, A. Aghajani (O-7434)	
Application of ENM to investigate the effect of different materials and methods of preparation of coating on anticorrosion quality of ZRP	176
B. Eremias, L. Mindos, L. Turek, L. Hochmannova (P-7068)	
Corrosion resistance of cold worked CrNi and CrNiMnN metastable austenites in defined strain states	177
P. Seemann, P. Gümpel (P-7155)	
Nanoscale oxide growth on nickel studied by reactive molecular dynamics	178
O. Assowe, L. Van Brutzel, A. Chartier (P-7175)	
Corrosion studies by depth profiling techniques	179
C. Olivero, P. Chapon, A. Tempez, S. Legendre (P-7404)	
Influence of surface treatments on localized corrosion behaviour of welded AISI 316L stainless steel	180
M. Halamová, G. Fumagalli, T. Liptáková, F. Bolzoni (P-7406)	
Comparitive corrosion resistance of dimensionally stable titanium based anodes and conventional lead alloy anodes in copper electrowinning	181
H. Potgieter (P-7409)	
Scanning vibrating electrode technique as a tool for investigating corrosion activities on coated mild steel in NaCl solutions	182
W. Shi, S.B. Lyon (P-7642)	
Qualification of stress and test methods for use in combined fatigue algorithms for riveted joints	183
J. Gehrke (P-7427)	
Pitting potential of materials during potentiodynamic polarization in a NaCl Solution	185
Y. Yi, M. Al Ameri, S. Al Saadi, P. Cho, C. Jang (P-7435)	
Effect of microstructure of X-65 in bioethanol for pipelines	186
M. Lucio, J.G. González Rodríguez, S. Serna, A. Torres-Islas (P-7770)	
Corrosion performance of TiO₂ nanostructures synthesized at low voltage applying electrochemical techniques	187
H. Herrera-Gutiérrez, C. Cuevas Arteaga, E. del Ángel Meraz (P-7771)	
Corrosion resistance of Zr 2.5Nb as material for permanent implants	188
S. Farina, A. Gomez Sanchez, S. Ceré (P-7090)	
Comparative corrosion behaviour of different Sn-based solder alloys	189
S. Farina, C. Morando (P-7092)	
Miniaturized cell for localized electrochemical measurements. Concept and examples of application	190
M. Bestetti, A. Vincenzo, S. Franz, M.F. Brunella, G. Puricelli, C. Borioli (P-7099)	

Dew-point corrosion resistance of alloys in geothermal fluids containing acid chloride	191
M. Cabrini, S. Lorenzi, T. Pastore, M. Favilla, R. Perini, B. Tarquini (P-7451)	
Corrosion resistance of ternary Ni-Ti alloys in 0.9% NaCl solution	192
C.D.R. Barros, J.A.C. Ponciano Gomes (P-7475)	
Electrochemical induced dissolution of silver points in sodium fluoride solution	193
C. Amaral, F. Ormiga, J.A.C. Ponciano Gomes (P-7476)	
EIS Studies of As-cast monotectic Al-Pb and Al-Bi alloys in a 0.5 M NaCl solution	194
E. Freitas, W. Osório, A. Silva, J. Spinelli, A. Garcia (P-7799)	
Effect of thermal treatments on the localized corrosion behaviour of alloy 718	195
R. Rebak, M. Rincon Ortiz, M. Iannuzzi, M. Kappes, M. Rodriguez (P-7284)	
Repassivation mechanism of Al alloys	196
D. Cicolin, E. Melilli, M. Pogliana, D. Guastaferro, M. Trueba, S.P. Trasatti (P-7291)	
The modified phosphate conversion coating on Zn-Mg alloy coated steel for corrosion protection	197
Y.J. Kwak, T.Y. Kim, D.Y. Lee, K.H. Nam, Y.H. Jung, W.S. Jung, M.J. Eom, S.J. Hong, J.K. Min, H.K. Sohn (P-7297)	
Local activation of iron in weakly alkaline medias containing halide-ions	198
S. Kaluzhina, N. Nafikova (P-7298)	
Bromide-ions additives effect on aluminium anodic behavior in borate buffer solution	199
S. Kaluzhina, T. Minakova, T. Popova, A. Chikova (P-7308)	
Application of micro-indentation techniques for investigation of seasonal corrosivity of Black Sea maritime atmosphere	200
O.V. Startsev, I.M. Medvedev (P-7312)	
Design criteria of reliability and safety in the design of corrosion protection of structural steel	201
V. Korolov, Y.B. Vysotsky, Y.V. Filatov, A.N. Gibalenko (P-7317)	
Electrochemical induced dissolution of silver points in sodium fluoride solution	202
C. Amaral, F. Ormiga, J.A.C. Ponciano Gomes (P-7326)	
Corrosion resistance of ternary Ni-Ti alloys in 0.9% NaCl solution	203
C.D.R. Barros, J.A.C. Ponciano Gomes (P-7332)	
Thermogravimetric study of hydrogen uptake and desorption in titanium alloys	204
V. Duquesnes, N. Creton, T. Montesin, E. Deloye (P-7762)	
Corrosion behavior of 18Cr-18Mn hot forging steel	205
A. Torres, R. Reyes, S. Serna, A. Bedolla, M.A. Lucio, J. Colin (P-7768)	
Evaluation of the pitting corrosion on an AISI 304 using scanning electrochemical microscopy	206
R. Sánchez-Tovar, R. Fernández-Domene, J. García-Antón (P-7504)	

Influence of submarine emissions from El Hierro volcano (Spain) on the corrosion resistance of stainless steels	207
R. Fernández-Domene, R. Sánchez-Tovar, C. Escrivà-Cerdán, R. Leiva-García, J. García-Antón (P-7514)	
Data processing and data mining applied to electrochemical noise technique for stress corrosion cracking recognition	208
L. Bonaccorsi, L. Calabrese, D. Di Pietro, M. Galeano, E. Proverbio (P-7515)	
FEM analysis of H-trapping diffusion model in pipeline steels	209
E. Fallahmohammadi, F. Bolzoni, G. Fumagalli, G. Re, L. Lazzari (P-7520)	
Sustainable water and facility management in the steel industry: influence of saline streams on pipeline corrosion	210
D. de la Fuente, M. Morcillo, P. Ivashechkin, V. Colla, T.A. Branca, M. De Sanctis, B.P. Vivas, M. Cabañas, A. Rassow, C. Lucca (P-7566)	
Corrosion behavior of tungsten heavy alloys in different aqueous solutions	211
Z. Abdel Hamid (P-7112)	
Influence of intermetallic phase content and microstructure on pitting potential of a duplex stainless steel	212
D.C. Dos Santos, R. Magnabosco (P-7078)	
Evaluation of elemental sulfur role on brittle failure in sour brine environment	213
M. Anselmi, L. Bonaccorsi, L. Calabrese, F. Cappuccini, A. Capri, A. Donato, E. Proverbio (P-7534)	
Quantum chemical study of adsorption of organic inhibitors of corrosion of Al on Al₂O₃ and Al(OH)₃ surfaces	214
G. Beloglazov, S. Beloglazov (P-7050)	
A probabilistic model for localized corrosion on a metallic pipe under D.C. stray current influence	215
G. Lucca (P-7066)	
The kinetic during atmospheric corrosion of a nickel cathode	217
S. Wibihal (P-7371)	
Hlfabar as effective inhibitor for zinc metal in aqueous solutions	218
O. Abdullatef, B. Abd-El-Naby (P-7677)	
Study of the influence of the different percentages of sigma phase in the resistance to pitting corrosion of a duplex stainless steel	219
C. Berlanga, G. Argandoña, M.V. Biezma, P. Linhardt (P-7696)	
6. CORROSION EDUCATION	
Corrosion awareness education a key for a better environment	220
A. Eliezer, G. Hays, E.H. Han, E. Leining, W. Burns (KN-7830)	
Corrosion education: present and future	221
A. Groysman (O-7062)	
Corrosion education in the framework of knowledge management	222
G. Gabetta (O-7713)	

The way to teaching corrosion based on visual inspection: student's opinions	223
M.V. Biezma, S. Braunstein Faldini (O-7709)	
Corrosion test rig for the amelioration of the service life of industrial components	224
M. Franchi, R. Cigna, O. Fumei, P. Pranovi (O-7206)	
 7. MARINE CORROSION	
Potential ennoblement of stainless steel in tropical seawaters	225
D. Thierry, N. Larche, S.L. Wijesinghe, S. Teo (O-7370)	
Effect of residual chlorine on the spontaneous potential of stainless steels in seawater	226
H. Yakuwa, M. Miyasaka, N. Shinoda, Y. Kuriki, J. Sakai (O-7735)	
Electrochemical monitoring of thermally sprayed aluminium coatings on steel in a simulated marine immersion environment	227
S. Paul, C. Gomez Gomez, M.D.F. Harvey (O-7458)	
Corrosion and cathodic protection of carbon steel in the tidal zone: Products, mechanisms and kinetics	228
P. Refait, R. Sabot, M. Jeannin, H. Antony, S. Pineau (O-7129)	
SEM/EDX-investigation of rust scales formed on an aluminium-steel friction weld under marine atmosphere	229
M. Schneider, U. Langklotz, U. Gierth (O-7144)	
Use of nanostructured materials in marine corrosion protection: an integrated approach	230
J. Tedim, F. Maia, A. Kuznetsova, A.P. Silva, R. Martins, A. Cunha, A. Almeida, S. Loureiro, R. Freitas, A.M.V.M. Soares, M.L. Zheludkevich, M.G.S. Ferreira (O-7627)	
The use of composite patches to repair ship structures: an electrochemical approach	231
A. Collazo, X.R. Nóvoa, C. Pérez (O-7790)	
The hydrogen permeation characteristics of high strength steel during splash zone corrosion process	232
Y.L. Huang, W.J. Qu, X.M. Yu (O-7808)	
Marine corrosion of SS 316L in Persian Gulf and protective coating	233
M. Najmi, D. Masouri (O-7606)	
Study on copper release from an antifouling coating and its influence on corrosion of aluminum alloy substrate	234
J. Cao, J. Sun, Y. Tang, Y. Zuo (P-7098)	
Corrosion resistance in multipass welding of thick UNS S31304 lean duplex stainless steel plates welded using SMAW, GMAW and FCAW processes	235
D.M. Silveira, V.F.C. Lins, A.Q. Bracarense, C.S. Souza, R. Cardoso Junior (P-7653)	
Behaviour of anti-corrosion coatings: comparison of the ageing in real environment in 2 different exposition sites	236
M. Tejero, J.B. Jorcin, A. Prieto, T. Alhambra, J. Ferreira (P-7714)	

**8. MICROBIAL CORROSION**

Role of green rusts in corrosion and biocorrosion of carbon steel in marine environment	237
P. Refait, R. Sabot, M. Jeannin, S. Sable, I. Lanneluc (KN-7848)	
Microbial corrosion of steel in argillite: complementarity of surface characterization (μRamanS and FESEM) and of microbiological approach	238
F. Mercier-Bion, Y. Léon, D. Neff, C. Wittebroodt, L. Urios, A. Perez, F. Marsal, M. Flachet, M. Magot, J.P. Gallien, Ph. Dillmann (O-7623)	
Evaluation of pH under-deposit using the dual-cell technique in flow conditions - The case of CuNi 70:30 in high bacteria contaminated fresh	239
M. Carvalho, E. Guerrini, S. Trasatti, P. Cristiani, M. Urquidi-Macdonald (O-7794)	
Electrochemical corrosion behavior of carbon steel exposed to low concentration agar with and without nutrients	240
A. Spark, L. Ward, I. Cole, D. Marney, D. Law (O-7353)	
Influence of Fe-S clusters of hydrogenase on mild steel corrosion	241
I. Rouvre, C. Gauquelin, I. Meynial-Salles, R. Basseguy (O-7384)	
Outer membrane associated redox active components in lithotrophic SRB trigger direct electron transfer during anaerobic electrical MIC	242
P. Beese-Vasbender, J. Garrelfs, S. Nayak, A. Erbe, K.J.J. Mayrhofer, M. Stratmann, F. Widdel (O-7077)	
Biofilm impact on the stainless steel passive film	243
A. Allion, S. Zanna, A. Seyeux, M.-H. Berger, P. Marcus (O-7703)	
Experimental study of wear and corrosion interaction in steel chains under working conditions	244
A. Lotfollahi Yaghin, R.E. Melchers (O-7084)	
A microelectrodes study for anaerobiosis profiles in biofilms	245
E. Guerrini, M. Grattieri, P. Cristiani, S.P.M. Trasatti (O-7533)	
Long-term corrosion of steels and steel piling in seawaters with elevated nutrient concentration	246
R. Melchers, R. Jeffrey (O-7199)	
Introducing a corrosion management approach to MIC assessment, control and monitoring in the oil and gas industry	247
T.L. Skovhus, H.E. Berge, R. Eckert, G. Koch (O-7229)	
A numerical model for copper biocorrosion	248
D. Fischer, C. Galarce, M. Walczak, G. Pizarro, I. Vargas (O-7613)	
Corrosion behaviour of titanium in the presence of Streptococcus Sanguinis	249
F. Yu, A. Davenport, O. Addison (O-7846)	
Effect of marine <i>Pseudoalteromonas</i> sp. on the microstructure and corrosion behaviour of 2205 Duplex stainless steel	250
M. Moradi, Z. Song (O-7334)	

Influence of sterilization methods on corrosion behavior of stainless steel in simulated cooling water containing sulfate reducing bacteria	251
H. Ge, X. Wang, M. Zhang, X. Meng (O-7683)	
Concrete deterioration by bacteriogenically induced sulfuric acid attack	252
C. Grengg, A. Baldermann, M. Dietzel, F. Mittermayr, M. Böttcher, A. Leis (O-7791)	
Microbiologically induced corrosion on tin bronze samples simulating uncommon archaeological corrosion	253
G. Ghiara, P. Piccardo, M. Stauder, C. Pruzzo (O-7377)	
MIC on bridge-building carbon steel in a tropical/Amazonian environment	255
M. Vastra, P. Salvin, C. Roos (O-7802)	
Meromictic lakes as field laboratory for corrosion studies in aerobic and anaerobic conditions	256
E. Guerrini, P. Cristiani, S.P.M. Trasatti, M.L. Carvalho, G. Storni (O-7797)	
Corrosion in biogas plants	257
R. Feser, A. Krebs (O-7322)	
Failure investigation of heat exchanger tubes in closed loop cooling water system	258
S. Almaaesab, H. Al-Mahamedh (O-7357)	
Electrochemical behavior of low-carbon steel within MIC-induced corrosion and cathodic protection	259
E. Leon, D.A. Koleva, H.M. Jonkers, J.M.C. Mol, K. Van Breugel (O-7301)	
Accelerated souring test of crude oil under the anaerobic condition	260
Y. Tanji, R. Hasegawa, K. Tohyama, K. Miyanaga (O-7075)	
Sulfate-reducing bacteria induced the corrosion of copper	261
D. Zhang, S. Chen, P. Wang (P-7089)	
The effects of Ag-Cu ions on the microbial corrosion of 316L stainless steel in the presence of <i>Desulfovibrio</i> sp.	262
T. Unsal, S. Arkan, E. Ilhan-Sungur, N. Cansever (P-7270)	
Influence of biofilm with mixed culture in corrosion rate of carbon steel	263
S.H. Oliveira, M.R.S. Vieira, D.R. Lima Junior, M.A.G.A. Lima, S.L. Urtiga Filho (P-7763)	
Effect of electromagnetic field on the corrosion behaviour of 2205 duplex stainless steel in the presence of <i>Pseudoalteromonas</i> sp.	264
Z. Song, M. Moradi (P-7809)	

9. CORROSION OF STEEL IN CONCRETE

Long-term survival of reinforced concrete structures in marine environments	265
R. Melchers, I. Chaves (O-7200)	
Corrosion behaviour of steel in fly-ash geopolymer mortars exposed to chloride solutions	266
C. Monticelli, M. Abbottoni, S. Manzi, C. Chiavari, A. Balbo, F. Zanutto, M.E. Natali, M.C. Bignozzi (O-7261)	

Study of reinforcing bar corrosion in solution simulating bacteria metabolites	267
M. Stefanoni, E. Volpi, S.P. Trasatti (O-7437)	
Investigations of chloride diffusion for reinforced geopolymer mortar	268
C. Monticelli, M. Abbottoni, S. Manzi, C. Chiavari, A. Balbo, F. Zanotto, M.E. Natali, M.C. Bignozzi (O-7551)	
Chloride threshold level for steel in concrete - rebar polarisation effects	269
M. Kosalla, M. Raupach (O-7550)	
A critical analysis of proposed test methods for measuring the chloride threshold value in reinforced concrete	270
U. Angst, B. Elsener (O-7060)	
Chloride threshold for corrosion initiation in reinforced concrete: the applicability of Ag/AgCl sensors revisited	271
F. Pargar, D.A. Koleva, P. Taheri, J.M.C. Mol, E.A.B. Koenders, K. van Breugel (O-7260)	
Effect of concrete pore solution composition on the electrochemical behaviour of C15 steel reinforcement	272
S. Chakri, E. Sutter, B. Tribollet, V. Vivier, I. Frateur (O-7553)	
Potentiostatic evaluation of the critical chloride threshold of 1.4362 stainless steel in concrete with mixed-in chloride	273
M. Gastaldi, F. Lollini, L. Bertolini (O-7624)	
Investigation of chloride-induced pitting corrosion of steel in concrete by a combination of electrochemical methods with X-ray tomography	274
G. Ebell, J. Mietz, A. Burkert (O-7207)	
Geo-polymeric and cementitious mortars with the same strength class: corrosion behaviour of steel and galvanized steel reinforcements	276
T. Bellezze, A. Mobili, G. Roventi, F. Tittarelli (O-7546)	
Stress corrosion cracking behaviour of the prestressing steel: influence of steel microstructure	277
I. Pepenar (O-7314)	
Simple concrete life extension	278
A. Borderon (O-7051)	
Smart controlled release corrosion inhibitors for steel reinforced concrete	279
D. Bastidas, I. Aguirre, S. Fajardo, I. Llorente, E. Medina, V. La Iglesia, V. González, J. Rodríguez, N. Birbilis, C. Monticelli, A. Balbo, V.J. Gelling (O-7265)	
Investigation of sodium molybdate's effect on the passive film of steel rebars in different simulated concrete pore solution environments	280
Y.T. Tan, S.L. Wijesinghe, D.J. Blackwood (O-7354)	
Application of gamma-ray radiography and gravimetric measurements after accelerated corrosion tests of steel embedded in mortar	281
G. Duffó, N. Gaillard, M. Mariscotti, M. Ruffolo (O-7088)	
Long term performance of migrating corrosion inhibitors to protect reinforced concrete structures in aggressive environments	282
B. Bavarian, L. Reiner (O-7107)	

The use of corrosion resistant steel reinforcement in chlorides contaminated concrete	283
N. Gartner, T. Kosec, A. Legat (O-7656)	
The synergetic effect of molybdenum and nitrogen alloying elements on austenitic stainless steels pitting resistance	284
V. Roche, I.N. Viçosa, C. Loable, R.P. Nogueira, E. Chauveau, M. Mantel, T.J. Mesquita (O-7701)	
Influence of the type of reinforcement on load bearing capacity of corroded reinforced concrete structures	285
A. Bossio, G.P. Lignola, T. Monetta, A. Prota, F. Bellucci, E. Cosenza, G. Manfredi (O-7842)	
Design, installation and performance of cathodic protection systems on Langeland Bridge, Denmark	286
R. Sorensen, J. Kok, K. Riis, F. Villumsen (O-7393)	
Altered cement hydration and subsequently modified porosity, permeability and compressive strength of mortar specimens due to electrical	287
A. Susanto, D.A. Koleva, K. van Breugel (O-7116)	
Monitoring steel corrosion in reinforced concrete beams with variable crack widths under sustained load	288
A. Blagojevic, D.A. Koleva, J.C. Walraven (O-7241)	
Active corrosion time affecting visual corrosion damage in carbonated concrete facades	289
A. Köliö, J. Lahdensivu (O-7741)	
Cross-border research for corrosion control in civil structures: recent research lines and novel approaches, employing electrochemistry, concrete materials science and nano-technology	290
D.A. Koleva (O-7557)	
Performance of conductive coatings used for cathodic protection of reinforced concrete structures under consideration of durability issues	291
C. Helm, M. Raupach (O-7583)	
The use of cathodic protection for life enhancement of immersed reinforced concrete structures	292
P. Chess, O. Klinghoffer, F. Grønvold, P.V. Nygaard (O-7662)	
Study the effect of heat and LASER treatments on the corrosion behavior of microalloyed carbon steels	293
F.M. Sayed, M.H. Hegazy, G.M. El-Mahdy, M.M. Eissa, A.M. Fathy (P-7044)	
Corrosion resistance of several metallic materials in contact with mortar	294
G. Duffó, S. Farina, F. Schulz (P-7087)	
FTIR study on the amorphous corrosion products of galvanized steel in carbonated concrete	295
G. Roventi, T. Bellezze, C. Conti, R. Fratesi (P-7457)	
Adsorption and inhibition corrosion of the biopolymer on carbon steel in simulated pores concrete solution	296
M. Martins, J. Tonholo, S.B.B. Uchoa (P-7764)	

Characterization and processing digital series obtained from electrochemical monitoring of reinforcing steel	297
R. Camacho-Chab, T. Pérez, B. Escobar-Morales (P-7632)	
Adsorption and inhibition corrosion of the biopolymer on carbon steel in simulated pores concrete solution	298
M. Martins, J. Tonholo, S.B.B. Uchoa (P-7637)	
Improving durability of reinforced concrete structures using migrating corrosion inhibitors	299
B. Bavarian, L. Reiner, J.J. Meyer (P-7855)	
10. CORROSION IN OIL & GAS PRODUCTION	
Comparison of martensitic stainless steels threshold properties in stress corrosion cracking phenomena	300
A. Scatena, M. Anselmi, F. Cappuccini, D. Di Pietro (O-7266)	
Effect of acetic acid on corrosion behaviour of modified martensitic stainless steels in high temperature sour environments	301
T. Sunaba, S. Okazaki, D. Ito, Y. Tomoe, S. Hirano (O-7171)	
Martensite-based stainless steel OCTG of 15Cr-based and 17Cr-based material for sweet and mild sour condition	302
Y. Ishiguro, T. Suzuki, E. Eguchi, T. Nakahashi, H. Sato (O-7368)	
Hydrogen stress cracking susceptibility of super duplex stainless steel 2507 in natural sea water	303
F. Vucko, N. Larché, D. Thierry (O-7154)	
Influence of thermal treatments between 650 and 850°C on the pitting corrosion behaviour of 2304 duplex stainless steel	304
F. Zucchi, F. Zanutto, V. Grassi, M. Merlin, A. Balbo (O-7253)	
Optimisation of the corrosion resistance of pipe butt welds in superduplex stainless steels	305
G. Byrne, G. Warburton, R. Francis, Z. Schulz (O-7805)	
Stress corrosion cracking of solution annealed and cold worked UNS S31603 stainless steel in H₂S containing production environments	306
T. Cassagne, C. Duret, C. Plennevaux (O-7821)	
Assessment of the crevice corrosion oxygen and temperature limits of CRAs for waste water injection wells	307
M.E. Wilms, S. Fletcher, W.D. Grimes, J.P. Smit, M. Klein, S. Abolghasemi (O-7576)	
Failure investigation: produced water re-injection tubing and equipment	308
H. Rese, P.I. Nice, A. Nelemans (O-7141)	
Galvanic effects in drilling equipment - challenges and solutions of corrosion resistance	309
S. Kolesov, R. Badrak, V. Chizhikov, A. Kharkiov, A. Alkhimenko (O-7776)	
In-situ surface strain mapping of pitting corrosion in a high strength carbon steel	310
P. Barnes, S.B. Lyon, D.L. Engelberg (O-7226)	

Sour corrosion - investigation of iron sulfide layer growth in saturated H₂S solutions	311
G. Genchev, K. Cox, A. Sarfraz, C. Bosch, M. Spiegel, A. Erbe (O-7233)	
Electrochemical noise analysis on modified 13%Cr stainless steels in sour environments under stress	312
M. Sakairi, J. Tatehara, Y. Mizukami, S. Hashizume (O-7095)	
Localised corrosion attack of pipeline steel associated with weldments in CO₂ containing environments	313
A. Abdurrahim (O-7106)	
Pipeline pigging and CP specialised electrical surveys: A unique integral strategy for pipeline integrity	314
L. Di Biase, O. Fumei, G. Fumei (O-7100)	
Electrochemical properties of iron sulphide in weak acid systems	315
M. Tjelta, J. Kvarekvål (O-7472)	
Cl-SCC attack in SS 316L branch connection welding	316
M. Al-Hammad (O-7724)	
Pittings occurrence in coupons of weight loss for corrosion monitoring in pipelines	317
N. Almeida, L. Tiroel, V. Ferrari, R. Moraes (O-7563)	
Effects of high flow rate on corrosion of carbon steel in high pressure CO₂ environment by means of linear polarization resistance	318
F. Todesco, M.E. Gennaro, S. Sgorlon, L. Torri (O-7510)	
Translating oilfield material exposures into laboratory tests	319
W. Grimes, M. Wilms (O-7571)	
Corrosion fatigue of aluminium drilling pipes: case study	320
L. Alleva, R. Porta, G. Hoxha (O-7491)	
An innovative design for top-of line corrosion assessment in laboratory	321
H. Mahmoud, A. Neville, A. Barnett (O-7439)	
Effect of plastic deformation on hydrogen permeation of API 5L X65 steel pipeline	322
E. Fallahmohammadi, F. Bolzoni, G. Fumagalli, G. Re, L. Lazzari (O-7508)	
Effective assessment of crude oil sourness for the material selection of refinery feeder pipeline	323
J. Khosravi (O-7407)	
Assessment of ionic liquids corrosivity: preliminary results	324
M.V. Diamanti, U. Velardi, A. Mele, M.P. Pedferri, M. Ormellese (O-7448)	
An alternative to H₂S in NACE corrosion test for sulphide and hydrogen-induced cracking risk assessment	325
C. Colombo, S. Corsinovi, G. Lovicu, R. Valentini (O-7684)	
Examination of line pipe strength and toughness in arctic environments combined with severe sour service	326
A. Smith, G. Mortali, G. Melis, O. Albores, E. Garcia (O-7395)	

Reducing sour corrosion using new, thermally stable hydrogen sulfide scavengers	327
S. Lehrer, V. Jovancevic, S. Ramachandran (O-7238)	
About the correspondence of test conditions with field conditions in materials selection	328
G. Gabetta, S. Correr, S. Sgorlon, S. Trasatti (O-7541)	
Methanesulfonic acid (MSA) as an acid used in the well stimulation procedure and corrosion of ²²Cr	329
J. Jackson, M. Finsgar (O-7465)	
The effect of deposit types on under-deposit corrosion behavior of carbon steel in sour environments	330
N. Alanazi, A. Sherik, A. Rasheed, S. Amar, M. Alneemi (O-7093)	
Improving oil and gas production infrastructure and equipment durability with active thermal sprayed coatings	331
F. van Rodijnen (O-7058)	
Failure of corrosion barriers in integrity management of subsea production systems - a statistical overview	332
B. Graver, F. Saint-Victor, K. Lønvik, B. Leinum (O-7488)	
Protective effect of molybdenum added to nickel based alloy in H₂S-Cl⁻ environment	333
A. Tomio, M. Sagara, T. Doi, H. Amaya, N. Otsuka, T. Kudo (O-7205)	
Wireline failures in oil & gas wells - case studies	334
D. Masouri, M. Askari, S. Afroukhteh (O-7619)	
Corrosion mitigation and inspection strategy for protection of assets in oil production facilities: an experience of Nafoora oilfield	335
I. Ahmad (P-7174)	
The influence of temperature on corrosion behavior of chromium steels in CO₂-containing environments	336
I.Yu. Pyshmintsev, I.V. Kostitsyna, V.P. Parshukov, A.G. Tyurin (P-7214)	
Hydrogen induced cracking of austenitic-ferritic stainless steels SAF 2205 and SAF 2507	337
S. Silva, J.A.C.P. Gomes (P-7328)	
Corrosion process of API 5L X52 in production water from oil well	338
O. Olivares-Xometl, M. Corrales-Luna, N.V. Likhanova, J.M. Hallen, I.V. Lijanov (P-7336)	
Assessment of localized corrosion resistance of 13Cr, 15Cr and 17Cr stainless steels in high chloride and CO₂ environments	339
E. Senatore, J.A.C.P. Gomes (P-7494)	
Corrosion resistance of rolled and rerolled supermartensitic steel in media containing chlorides and hydrogen sulfide	340
R. Braga Soares, D.C. de Sousa Garcia, M. Mendonça Lima, M.M. Reis de Castro, V. de Freitas Cunha Lins (P-7569)	
Improvement of 9% nickel steel for CO₂ reinjection in FSPOS and its corrosion resistance in brazilian pré-salt conditions - SSC and HIC	341
R. Kalume, L.I.L. Lima, M.C. Ferreira, B.I. Palmieri, G.V. Silva, C.R. D'Ávila, J.A. Carreno Velasco, R.V. Landim, S.M. de Souza (P-7813)	

Influence of molybdenum on UNS S32304 and UNS S31803 duplex stainless steels corrosion resistance	342
A. Viana, T. Oliveira, O. Mattos, K. Assis (P-7079)	
Effect of AC frequency on stress corrosion cracking behavior of X80 pipeline steel in carbonate/bicarbonate solution	343
C. Du, M. Zhu, X. Li, Z. Liu (P-7654)	
The influence of heat treatment on the corrosion behaviour of Inconel 718	344
L.C.M. Valle, A.I.C. Santana, L.H. de Almeida, O.R. Mattos (P-7047)	
A study by in situ Raman spectroscopy of carbon steel corrosion in CO₂ and H₂S environment	345
O. Delpoux, J. Kittel, F. Grosjean, S. Joiret, N. Desamais, C. Taravel-Condât (P-7777)	
Inhibitory protection of the installations of the oil-refining enterprises from corrosion	346
V.M. Abbasov, L.I. Alieva, T.A. Ismailov, Yu.G. Mamedaliev (P-7859)	
Corrosion monitoring of NPP equipment and pipelines by high-temperature on-line sensors	347
M.V. Sof'ın, F.V. Nikolaev, V.G. Kritsky, P.S. Styazhkin (P-7856)	
11.1. METALLIC COATINGS	
Galvanizability and corrosion properties of Zn-Mg-Al hot-dip coating with shot blasting pre-treatment	348
T.C. Kim, S.H. Kim, S.Y. Kim, M.S. Oh, J.S. Kim (O-7125)	
Corrosion and microstructure study of new ZnAlMg galvanized steel by single dip technology	349
A. Alvarez Pampliega, E. Thomas, A. Tomandl, C. Masquelier, J. Balduyck, T. Pinger, C. Buelens (O-7369)	
Corrosion behaviour of ZnAlMg coatings in tropical and coastal environments	350
A. Tomandl, E. Labrenz, A. Erni (O-7411)	
The effect of Mg composition on corrosion protection of steel using PVD Zn-Mg coatings	351
J. Davies, G. Williams (O-7430)	
Influence of organic sealants on the corrosion protection of thermally sprayed ZnAl 15 coating	352
R. Feser, A. Mertke (O-7323)	
Zinc flake coatings vs. zinc-nickel electroplating: new trends and developments	353
H. Sahrhage, M. Krumm, K. Wojczykowski, A. Hill (O-7773)	
XPS investigations of ZnCr coated steel after corrosion load	354
R. Steinberger, J. Duchoslav, M. Arndt, T. Steck, F. Lengwin, J. Faderl, D. Stifter (O-7244)	
Electrocodeposition of Al-Zn alloy by using double counter electrodes system	355
Y. Sato, K. Azumi (O-7399)	

Development of aluminum magnesium alloy coating by new mist air and nitrogen cooled thermal spraying gun	356
Y. Omori, Y. Nishiura, T. Kumai, T. Morimoto (O-7055)	
Antibacterial and protective properties of Cr/Ag nanocomposite coatings obtained by electrochemical techniques	357
E. García-Lecina, B. García-Blanco, I. García-Urrutia, J.A. Díez (O-7418)	
Study of corrosion resistance of electroless duplex NiP/NiB coatings in different media by potentiodynamic polarisation and SEM observation	358
V. Vitry, F. Tosar, F. Delaunois (O-7081)	
Friction and corrosion properties of electroless nickel nanocomposite coatings codeposited with MoS₂ or WS nanoparticles	359
C. Zanella, M. Righetti, A. Gracco, F. Deflorian (O-7625)	
Corrosion resistance of laser clad 304L stainless steel surfaces enriched with ruthenium additions exposed to sulphuric acid media	360
J.W. Van der Merwe, D. Tharandt, P.C. Masiu (O-7757)	
Anticorrosion composite coatings obtained by of plasma electrolytic oxidation	361
S. Gnedenkov, S. Sinebryukhov (O-7166)	
Corrosion protection property of corrosion products of zinc galvanized steels	362
H. Katayama, R. Miyahara, Y. Hoshi, I. Shitanda, M. Itagaki (P-7442)	
Pd-In and Pd-Fe as new type of "Ni-free" top coatings for decorative applications	363
S. Caporali, P. Marcantelli, U. Bardi (P-7470)	
Thin film hot dip galvanizing - the innovative revival of a traditional process	364
T. Pinger, J. Tomaszewski (P-7191)	
Influence of deposition techniques on properties of solar selective coatings on Cu and Al substrates	365
M. Shoeib, N. El-Mahallawy, Y. Ali (P-7580)	
Electrochemical behaviour of protective coatings in chloride solutions	366
G. Sundararajan, R. Rebak (P-7590)	
Electrodeposition of Ni-Mo-P electrodes for direct alcohol fuel cell applications	367
Z. Abdel Hamid (P-7111)	
Characterizing the structure of ZnAlMg-coated steel sheet via FIB-tomography	368
M. Arndt, J. Duchoslav, C.K. Rienr, G. Angeli, D. Stifter (P-7143)	
An electrodeposition process for fabrication of super-hydrophobic nickel film and its corrosion resistance	369
S. Khorsand, K. Raeissi, F. Ashrafizadeh, M.A. Arenas (P-7844)	
The effect of texture and surface morphology on the corrosion resistance of zinc electrodeposits	370
S. Khorsand, K. Raeissi, M.A. Golozar (P-7845)	
Anodic oxidation of galvanic Zn-Ni alloy coatings in the NaOH solutions	371
A. Maciej, W. Simka, J. Michalska, T. Gorewoda, G. Dercz (P-7274)	

Deposition of zinc powder on iron with cold spray application	372
A. Bossio, T. Monetta, C. Bitondo, F. Bellucci (P-7825)	

11.2. INORGANIC COATINGS

Development of a bilayer superhydrophobic electrophoretic sol-gel coating on stainless steel	373
A.M. Simoes, M.M. Lourenço, J.C. Fernandes (O-7775)	

Sol-gel derived protective coatings to prevent microbial induced corrosion	374
S. Pfeifer, A. Gutierrez, E. Kroke (O-7362)	

Novel nanoparticle-based coatings for the oxidation protection of steel compounds during press-hardening	375
B. Tigges, S. Benfer, A. Tenié, C. Klesen, M. Yekehtaz, W. Bleck, W. Fürbeth (O-7232)	

Characterization of conversion layers hexavalent chromium free applied in electrogalvanized steel	376
K. Provazi de Souza, C.R. Tomachuk, L.E.M. Palomino, C.M. Reis, I. Costa (P-7552)	

Behavior of alloying elements during anodizing of magnesium alloys	377
A. Němcová, P. Skeldon, G.E. Thompson, C. Olivero, P. Chapon (O-7666)	

Chemistry of Zr/Cr based solutions: application to sealing of anodized aluminium alloys	378
N. Chahboun, E. Rocca, D. Veys-Renaux, M. Augros, M. Boutoba, N. Caldeira (O-7593)	

Corrosion properties of PEO coatings obtained on Mg alloys with an electrolyte containing different concentrations of molybdate	379
L. Pezzato, K. Brunelli, M. Magrini, M. Dabalà (O-7239)	

Electrochemical and surface analysis of corrosion properties of nanometre-thick alumina coatings prepared by ALD on copper	380
S. Mirhashemihaghighi, J. Swiatowska, V. Maurice, A. Seyeux, L.H. Klein, E. Härkönen, M. Ritala, P. Marcus (O-7242)	

Experimental evaluation of the corrosion protection ability of PVD-coatings	381
U. Depner-Miller, G. Andersohn, M. Oechsner, K. Bobzin, N. Bagcivan, T. Brögelmann, R. Weiss (O-7428)	

Environmentally friendly CeCC for AA6060 aluminum alloy	382
A. De Nicolo, L. Pausa, F. Andreatta, A. Gobessi, C. Cepek, L. Fedrizzi (O-7584)	

Aluminium alloys anodizing: effect of the composition and the microstructure	383
N. Chahboun, E. Rocca, D. Veys-Renaux, M. Augros, M. Boutoba, N. Caldeira (O-7597)	

Investigation on defect morphology and corrosion behaviour of TiMgN hard coatings on steel substrate	384
T. Mueller, A. Heyn, M. Fenker, M. Balzer (O-7473)	

Performance and failure mode of diamond-like carbon coatings in simulated oil and gas conditions	385
A. Broughton, S.B. Lyon (O-7638)	

Synthesis and behavior of nano hard anodized layers	386
Z. Abdel Hamid (O-7113)	
Effect of PTFE and Al₂O₃ particles variation on corrosion and wear behavior of NiP-PTFE-Al₂O₃ nanodispersion coatings	387
A. Singh, P. Ankita (P-7201)	
Advanced environmentally friendly chemical surface treatments for cast magnesium helicopter transmission alloys preservation	388
F. Brusciotti, U. Izagirre Etxeberria, A. Unzurrunzaga Iturbe (P-7730)	
Bioceramic coatings on Ti6Al4V, developed by electrochemical plasma, laser printer with localized stripping and deposition electrophoresis	389
D. Peña, L. Ramos, H. Estupiñan (P-7707)	
Elaboration of silica hybrid coatings for corrosion protection of carbon steel: electrochemical study	390
T. Phan, C. Jama (P-7231)	
Influence of aluminium alloy type on the corrosion behaviour of formed alumina films	391
C. Girginov, S. Kozhukharov (P-7300)	
Corrosion behavior of nanostructured bioactive apatite coating on TiVAI alloys	392
A. Alshamsi (P-7304)	
Microstructure and optical appearance of anodized friction stir processed Al-metal oxide surface composites	393
V. Gudla, F. Jensen, K. Bordo, S. Canulescu, R. Ambat, A. Simar, R. Shabadi (P-7337)	
Electrochemical characterization of a zinc rich epoxy nano-coating primer on an X52 steel pipeline grade in flow conditions	394
E. Maya, V. Valencia, T. Hawkins, H. Castaneda (P-7341)	
Hybrid films modified with polyethylene glycol for corrosion protection of tin plate	395
H. Ribeiro Piaggio Cardoso, S.R. Kunst, M.R. Ortega Vega, T. Lemos Menezes, C. Fraga Malfatti (P-7509)	
Electrochemical characterization of a H2F6Zr film form on AISI/SAE 1006 steel	396
J. dos Anjos Moraes, R. Sánchez-Tovar, J. García-Antón, J. Zoppas-Ferreira (P-7525)	
Corrosion resistance of economical environmentally friendly anodization for Mg-3Zn-0.8Ca alloy	397
M. Shoeib, H. Soliman, S. Mikhail, M.E. Mousa (P-7565)	
Corrosion protection properties of the yttria stabilized sol-gel ZrO₂ thin film on 316L stainless steel	398
I. Bacic, H. Otmacic Curkovic, L. Curkovic (P-7591)	
Optical appearance of AC anodized Al/TiO₂ composite coatings	399
K. Bordo, V. Gudla, R. Ambat, F. Jensen (P-7601)	
Superficial patina: analytical interpretation of the ancient process of realization of Japanese Shakudo alloy	400
D. Ferro, D. Servidio, B. De Filippo, D. Loepp (P-7617)	

Effect of primer-free helical inserts to prevent galvanic corrosion	401
A.E. Eken, C. Yilmaz, E. Tan (P-7134)	
Corrosion resistance of H2F6Zr coatings in NaCl	402
J. dos Anjos Moraes, R. Sánchez-Tovar, R. Leiva-García, J. García-Antón, J. Zoppas-Ferreira (P-7530)	
Investigation of possibility to use glass-based layer to prevent internal corrosion of pipelines	403
M. Ronceray, A. Barnett, K.A. Raheem (P-7215)	
11.3. ORGANIC COATINGS	
A new way for corrosion research in an artificially produced micro-climate between alloys and organic coatings	404
S. Walkner, A.W. Hassel (O-7485)	
Delamination kinetics of chemisorbed polymer coatings on nano-structured metal surfaces	405
A. Bashir, D. Iqbal, A. Erbe, M. Rohwerder (O-7493)	
Strain induced defect formation in ultra-thin protective films on TWIP steels	406
C. Liu, O. Ozcan, T. Niendorf, F. Brenne, G. Grundmeier (O-7635)	
Effect of structure and stress-state interactions on water diffusion processes in epoxy coatings	407
G. Bouvet, S. Cohendoz, X. Feaugas, S. Mallarino, S. Touzain (O-7560)	
Anticorrosion atmospheric plasma coatings for metal protection	408
I. De Graeve, A. Kakaroglou, G. Scheltjens, B. Nisol, G. Van Assche, B. Van Mele, F. Reniers, H. Terry (O-7608)	
Electrochemical properties of graphene/epoxy coating	409
T. Monetta, A. Acquesta, F. Bellucci (O-7223)	
Advanced functional ormosil coatings modified with conductive fillers for corrosion protection of Mg alloys	410
F. Montemor, D. Snihirova, B. Martins, A. Zomorodian, Y. Morozov, S. Piçarra (O-7669)	
A new composite coating for corrosion protection of AZ31 and RZ5 magnesium alloys	411
M.C. Ferreira, A. Zomorodian, M.F. Montemor, J.C.S. Fernandes (O-7810)	
Elaboration of bisphenol A polybenzoxazine coatings for barrier protection applications on aluminum substrate	412
J. Escobar, M. Poorteman, L. Dumas, L. Bonnaud, P. Dubois, M.G. Olivier (O-7452)	
Poly(3,4-ethylenedioxythiophene)-poly(styrene sulfonate) as a primer coating for the inhibition of corrosion driven cathodic delamination and filiform corrosion on iron	413
C. Glover, G. Williams (O-7547)	
Structure property relationships in highly structured composite layers as corrosion protection coatings on mild steel	414
C. Becker-Willinger, S. Schmitz-Stoewe, M. Opsoelder, M. Jochum, S. Albayrak, E. Perre (O-7751)	

Inorganic-organic hybrid(TiO_2-MAPTS) coating on carbon steels for corrosion inhibition	415
W. Maeng, G. Song, M. Kim, J. Noh, M. You (O-7366)	
Possibilities of ex situ IR and in situ Raman spectroscopies for investigation of sol-gel anticorrosion coatings during anodic polarisation	416
A. Surca Vuk, M. Rodosek, A. Rauter, L. Slemenik Perse, D. Kek Merl (O-7177)	
Delamination of organic coatings on a zinc substrate investigated with a current measurement method	417
S. Wibihal, M. Pichler, G. Faflek, M. Fleischanderl (P-7372)	
Raman spectroscopy as a tool for investigation of fluoropolymer coatings on electronic boards	418
M. Rodosek, L. Slemenik Perse, M. Mihelcic, M. Kozelj, B. Orel, B. Bengu, O. Sunetci, P. Pori, A. Surca Vuk (P-7178)	
It's all relative, when it comes to protective coatings	419
D. Ferguson, P. Dove (P-7431)	
The study on failure process of acrylic polyurethane coating under alternate wetting and drying condition	420
Z. Fang, L. Zhang, X. Zhao, Y. Zuo (P-7094)	
Improved corrosion protection of graphene oxide reinforced siloxane-PMMA hybrid coatings	421
S.V. Harb, F.C. dos Santos, S.H. Pulcinelli, C.V. Santilli, P. Hammer (P-7194)	
Anodic protection produced by Smart Ink	422
R.S. Silva, V. Maggi, J.Z. Ferreira, A. Meneguzzi (P-7268)	
Protective compositions on base of wastes of vegetable oils production against atmospheric corrosion of steel goods	423
V.I. Vigdorovich, A.A. Uryadnikov, N.V. Shel, L.E. Tsygankova (P-7296)	
Fine textured polymer based composite materials as multifunctional low friction coatings with corrosion protection	424
D. Bentz, S. Schmitz-Stöwe, M. Wild, C. Becker-Willinger (P-7761)	
The effects of the nano-TiO_2 on the interfacial corrosion behavior of immersed coatings	425
J. Gao, H. Jiang, H. Qian, L. Lu, X. Li (P-7652)	
Study of the corrosion behavior of electrogalvanised steel/Cr(III) and Zr conversion layer/paint system by electrochemical and visual methods	426
F.M. Queiroz, P.R. Seré, C.I. Elsner, A.R. Di Sarli, C.R. Tomachuk, I. Costa (P-7124)	
Research into the causal effects and development of solutions to pinholing of powder coated galvanized steel	427
A. Speakman, C. Chisholm, M. El-Sharif, R. Ansell (P-7181)	
Behaviour of coatings at the defect - scribing tools for investigations of coatings on steel	428
R. Bentfeld (P-7363)	
New flange corrosion protection system	429
K. Flanagan (P-7857)	

11.4. PRETREATMENTS

Anti-corrosive conversion coating on aluminium alloys using high temperature steam with incorporated chemistries	430
R. Din, M.S. Jellesen, R. Ambat (O-7302)	
Comparative study between conventional tests and ACET technique for powder coatings used on steel with different phosphate pretreatments	431
J. Molina, J. Suay, J. Gracenea (O-7725)	
The role of surface modification by phosphating in corrosion protection of sintered Nd-Fe-B magnets	433
E. Isotahdon, E. Huttunen-Saarivirta, V.-T. Kuokkala (O-7752)	
Investigation of under film corrosion using pH sensitive microcapsules	434
T. Matsuda, K. Kashi, M. Jensen, V. Gelling (O-7262)	
Influence of different pretreatments of Mg4Y2Nd prior to NaF-coating on the electrochemical corrosion behaviour	435
C. Schille, E. Schweizer, J. Geis-Gerstorfer (P-7216)	
Employing electro-deposition technique for coating nano-bioactive ceramic coating on dental Ti-alloy implant	436
M. Shoeib, H. Shalaby, M. Nassif, A. Abdelrahman (P-7516)	
Establishment of a novel CV-method to measure real work pieces and comparison with the standard method	437
A. Schindel, J. Schodl, G. Fafilek, Ch. Kleber (P-7663)	

11.5. SELF-HEALING COATINGS

Highly ordered mesoporous silica loaded with dodecylamine for active anticorrosion coatings	438
J.M. Falcón, T. Sawcen, I.V. Aoki (O-7287)	
Self healing organic coatings on aluminium alloy	439
A. Firouzi, A. Bianco, G. Montesperelli (O-7187)	
Assessment of corrosion performances of cerium based silane-zeolite coatings on AA6061 substrate	440
L. Bonaccorsi, L. Calabrese, A. Capri, G. Gulli, E. Proverbio (O-7522)	
Numerical modelling as a tool for the design of self-healing dispersion coatings	441
M. Walczak (O-7412)	
L-cysteine intercalated layered double hydroxide as anticorrosive agent for organic coatings	442
T. Stimpfling, H. Hintze-Bruening, P. Keil, H. Theil, F. Leroux (O-7379)	
Micro-electrochemical study of organic corrosion inhibitors for AA2024	443
F. Andreatta, I. Recloux, L. Paussa, M. Mouanga, M. Olivier, L. Fedrizzi (O-7185)	
Coating self-healing effect by loading microcapsules with two-component epoxy film former	444
F. Cotting, I.V. Aoki (O-7585)	

Non-destructive in-situ characterization of microcapsules and self-healing coatings using confocal Raman spectroscopy	445
A. Lutz, I. De Graeve, H. Terryn (O-7282)	
Recent developments on microencapsulation for autonomous corrosion protection	446
L.M. Calle, W. Li, J.W. Buhrow, L. Fitzpatrick, S.T. Jolley, J.M. Surma, B.P. Pearman, X. Zhang (O-7195)	
Development of self healing polymer coatings on metals	447
A. Lutz, I. De Graeve, H. Terryn (O-7145)	
Design and analysis of multi-layer self-healing coatings tailored for smart corrosion protection	448
T. Tran, A. Vimalanandan, J. Fickert, K. Landfester, D. Crespy, M. Rohwerder (O-7228)	
Fundamental investigation on the mechanism of capsule based redox-responsive self-healing coatings	449
A. Vimalanandan, L-P. Lv, T. H. Tran, K. Landfester, D. Crespy, M. Rohwerder (P-7219)	
Self-healing properties of smart coating for hot dip galvanized steel	450
W-J. Li, C.Y. Tsai, C.J. Lu (P-7184)	
„Green“ encapsulation of corrosion inhibitors for smart coatings	451
A. Altin, M. Rohwerder, A. Erbe (P-7443)	
Encapsulation of corrosion inhibitors in a self-healing polymeric coating	452
H. Verbruggen, A. Lutz, H. Terryn, I. De Graeve (P-7374)	
11.6. COATINGS FOR HIGH TEMPERATURES	
Metal dusting protection by a novel coating, providing a classical oxide barrier as well as catalytic inhibition	453
S. Madloch, M.C. Galetz, M. Schütze (O-7168)	
Combination of CVD coatings and halogen effect to prevent high-temperature embrittlement in titanium aluminides	454
J. Grüters, M.C. Galetz, M. Schütze (O-7414)	
Surface modification of thermal barrier coatings by diffused and laser and phosphate treatments	455
M. Shoeib, K. Ahmed (O-7115)	
Improvement of turbine blade by using protective ceramic coating	456
S. Sohrabi, A. Saatchi, R. Ebrahimi (O-7316)	
Wavelet transform electrochemical noise analysis for intermetallic coatings at 750 °C in molten salt environment	457
A. Garcia, E.F. Díaz, S. Serna, J. Colin, A. Torres-Islas, M.A. Lucio-Garcia (P-7732)	
Development of Fe doped Ni-Co spinel for use in SOFC interconnects	458
A. Bervian, G.A. Ludwig, M.A. Korb, C.F. Malfatti (P-7588)	
Influence of CaO and CeO₂ coatings on the oxidation of nickel polycrystals	459
Z. Halem, N. Halem, S. Chekroude, M. Abrudeanu, G. Petot-Ervas (P-7574)	
The effect of the a double coating layer-oxide phase (NiFe₂O₄) combined with perovskite phase (La_{0.6}Sr_{0.4}CoO₃) on a ferritic stainless steel	460
D.A.S. Lima, G.A. Ludwig, M.A. Korb, A. Bervian, C.F. Malfatti, I.L. Müller (P-7667)	

Oxidation resistance ferritic stainless steel AISI 430 coated with spinel based Fe doped Ni-Co.....	461
A. Bervian, G.A. Ludwig, M.A. Korb, C.F. Malfatti (P-7668)	
 12. CORROSION IN THE REFINERY INDUSTRY	
Risk based inspection. The most rapid way in order to reduce maintenance and inspection costs.....	462
A. Pette (O-7726)	
Integrity assurance of process facilities at Adriatic LNG terminal through risk based inspection.....	463
F. Belloni, V. Colombo, G. Benassi (O-7740)	
Towards a first global assessment of corrosion issues in advanced biorefineries as preliminary learnings from ECORBio.....	464
G. Marlair, H.-L. Ngo, W. Benaissa, M. Nonus, C. Len, E. Hondjuila-Miokono, N. Thiébault, J. Garcia, B. Narcy, C. Sarazin, I. Gosselin, C. Triquenaux, A. Darraspen (O-7579)	
Corrosion behaviour of AISI 1006 steel in aqueous extracts of biodiesel and petrodiesel.....	465
L.F.P. Dick, M.D. Oliveira (O-7699)	
Corrosion in systems for storage and transportation of petroleum products and biofuels.....	466
A. Groysman (O-7061)	
Laboratory test method for corrosion under thermal insulation.....	467
O. Knudsen, J. Aaneby (O-7408)	
Corrosion mitigation in sulfur trains auxiliary burner.....	468
K. Al-Hajri (O-7841)	
Chemical treatment of untreated close water cooling system.....	471
F. Omer (O-7127)	
Successful trial of using non-metallic cladding in Saudi Aramco facility.....	472
M. Al Ridy (O-7102)	
3D TRASAR cooling water technology combined to refined knowledge system will help to optimize total cost of operation, to improve reliability at any time even during process leaks and to minimize the impact of process leaks on asset management.....	473
V. Bour Beucier (O-7817)	
Precipitation and dissolution of critical phases in alloy 625.....	474
R. Lackner, G. Mori, R. Egger, F. Winter, W. Grogger, M. Albu (O-7500)	
Laboratory examination of two olefin cracking radiant tube materials.....	475
J. Zhang, L. Allcock, A. Al-Meshari, E.M. Murillo, M. Diab, S. Ahmad (O-7554)	
Effective parameters on bottom plates corrosion phenomenon of storage tanks during construction time interval: A case study, investigations and solutions.....	476
H. Aldaghi, S. Easapour, Y. Haghighat (O-7120)	
Corrosion resistance of austenitic steels used in biodiesel fuel plant.....	477
A.P. Pereira, V.F.C. Lins, M.M.R. Castro, C.E.A.S. Torres (P-7721)	

Corrosion of steels used in a biodiesel fuel plant	478
A.P. Pereira, V.F.C. Lins, C.G.F. Costa, M.M.R. Castro, C.E.A.S. Torres (P-7720)	
In situ AFM and FTIR spectroscopy coupled with electrochemical techniques studies on naphthenic corrosion of API 5L X70 steel	479
E.C. Rios, A.L. Oliveira, A.M. Zimer, R.G. Freitas, R. Matos, L.H. Mascaro, E.C. Pereira (P-7645)	
Detection and sizing of corrosion under fireproofing (CUF) with welded wire mesh using MR-MWM-array	480
S.A. Dossary, A. Minachi, N. Goldfine, S. Denenberg (P-7858)	
 13. CATHODIC PROTECTION	
Electrochemical investigation of carbon-based conductive coatings for application as anodes in ICCP system of reinforced concrete structures	481
G. Ebell, M. Poltavtseva, J. Mietz (O-7489)	
Examples of C.P. remote monitoring installations carried out by a European gas transmission company	482
C. Aknouche, C. Calvi (O-7853)	
Corrosion of cathodically polarized TSA in subsea mud at high temperature	483
O. Knudsen, G. Clapp, G. Duncan, J. van Bokhorst (O-7413)	
Cased-pipeline: presentation and experience of annular space wax filling	484
P. de Bonnafoes (O-7833)	
The a.c. corrosion rate: A discussion of the influencing factors and the consequences on the durability of cathodically protected pipelines	485
M. Büchler (O-7080)	
Electrochemical phenomenon of a.c. corrosion likelihood of cathodically protected steel pipelines	486
F. Kajiyama (O-7148)	
Detecting and quantifying damage evolution of coated, cathodic protected buried pipelines by combining AC monitoring and stochastic analysis	487
X. Li, A. Yajima, R. Liang, H. Castaneda (O-7361)	
CORTracer TM, an innovative monitoring instrumentation for the ac corrosion risk assessment of cathodically protected buried pipelines	488
E. Fleury, D. Caron, M. Meyer, S. Fontaine (O-7543)	
Effects of anodic interference on carbon steel under cathodic protection condition	489
M. Ormellese, A. Brenna, L. Lazzari, F. Brugnetti (O-7518)	
Proposed method to define the maximal accepted error made in the metrology line of measurements	490
S. Fontaine (O-7834)	
CP design of internal components	491
H. Osvoll, J.C. Werenskiöld (O-7747)	
Cathodic protection of extended sheet piling in soil. A practical case	492
U. Marinelli, E. Barbaresi (O-7694)	

Cathodic protection assessment of oil storage tank farm	493
M. Diminich, F. Mari, B. Bazzoni, G. Lecardi, T. Caglioni, F. Duranti (O-7754)	
New tool for CP inspection	494
H. Osvoll, J.C. Werenskiold (O-7746)	
Evaluation of ICCP system over API X52 steel tested in two types soils in the state of Campeche, Mexico	495
C. Lizárraga, L. Quej-Aké, A. Contreras, V. Moo-Yam, T. Pérez (O-7333)	
Soil side corrosion of storage tank bottom plate, failure causes and mitigation provisions	496
S. Afroukhteh, M. Askari, D. Masouri (O-7634)	
Sacrificial anode key design parameters for the internal surfaces of vessel, tank and structures	497
H. Sabri, S. Al-Sulaiman (O-7146)	
EPIC new 16" Jet A1 fuel pipeline (external coating case study)	498
N. Hamdy (P-7041)	
Impressed current cathodic protection (ICCP) Ti-MMO grid system for 61m diameter methanol tank	499
F. Al-Fawaz (P-7739)	
 14. AUTOMOTIVE CORROSION	
Light weight technologies for innovative mobility society	500
A. Dogan (KN-7850)	
Effect of welding heat on microstructure and corrosion of ferritic stainless steel 409M	501
S.P. Ambade, Y.M. Puri, A.P. Patil (O-7315)	
Pickling process for high-strength steels before coating	502
C. Schreiber, S. Friedrich (O-7209)	
Limits of rapid heating for the press-hardening of ultra-high-strength steel from aluminum-silicon-coated blanks	503
T. Todzy, D. Worterg, B. Engel, M. Weyrich (O-7269)	
Controlling and monitoring the risks of hydrogen induced stress corrosion cracking in automotive body parts	504
R. Scharf, A. Muhr, G. Luckeneder, K.H. Stellnberger, J. Faderl, G. Mori (O-7433)	
Crevice corrosion of hot stamping steels for the automotive industry	505
M. Jönsson, L. Levander (O-7540)	
A century with salt spray testing; time for a final phasing-out by a replacement based on newly developed more capable test regimes	506
M. Ström (O-7639)	
Analysis of perforation corrosion morphology of steel sheets for automobiles using laser displacement meters	507
H. Kajiya, M. Omoda, M. Kimura (O-7655)	

Methodology for the definition of failure assessment diagram of AHSS exposed to aggressive environments	508
M. Beghini, L. Bertini, C. Colombo, B. Monelli, R. Valentini (O-7670)	
Influence of climatic parameters in accelerated test on the corrosion and mechanical properties of automotive joined materials	509
N. Lebozec, O. Clauzeau, D. Thierry (O-7193)	
Concentration effect of salt solution on the corrosion of carbon steels investigated by salt spray test	510
Y.H. Yoo, H.S. Park, Y.K. Song (O-7349)	
Adequacy between lighter multimaterial vehicle and car body corrosion resistance	511
P. Buttin, P.-Y. Cam, G.-A. Balmont, J. Bovin (O-7221)	
The influence of Ca²⁺ in de-icing salt on the corrosion behavior of AM50 magnesium alloy	512
M.W. Grabowski, S. Virtanen, D.B. Blücher, M. Korte (O-7161)	
Study of polymer coating delamination kinetics on zinc modified with zinc oxide of different morphologies	513
D. Iqbal, R. Singh Moirangthem, A. Bashir, A. Erbe (O-7526)	
Investigation on the effect of impurities on the corrosion behaviour of various A356 alloy	514
A. Niklas, R. González-Martínez, A.I. Fernández-Calvo, S. Mendez, A. Conde, J.J. de Arenas, J.J. de Damborenea (O-7224)	
Effect of experimental parameters on AA6xxx intergranular corrosion during immersion in acidified NaCl solutions (ISO11846)	515
L. Peguet, E. Chassagnolle, R. Bergeron, A. Afseth (O-7385)	
The effect of surface conditioning on the deposition of Zr-based conversion coatings on aluminium alloys	516
J. Cerezo, P. Taheri, I. Vandendael, R. Posner, J.H.W. de Wit, J.M.C. Mol, H. Terry (O-7511)	
Effect of Sr and Ti addition on the corrosion behavior of Al-7Si-0.3Mg alloy	517
M. Uludag, M. Kocabas, D. Dispinar, R. Çetin, N. Cansever (O-7614)	
Electrochemical profiling of multi-clad aluminium sheets used in automotive heat exchangers	518
K. Bordo, R. Ambat, L. Peguet, A. Afseth (O-7482)	
Investigation by electrochemical impedance spectroscopy of filiform corrosion of electrocoated steel substrates	519
A.-P. Romano, M.-G. Olivier (O-7152)	
Influence of water, chloride, sulphate and acetic acid on corrosion behavior of aluminum materials in ethanol-containing fuels	520
R. Reitz, G. Andersohn, M. Oechsner, O. Golenishcheva (O-7460)	
Time-dependent corrosion and layer formation reactions of EN AC-AISi10Mg in coolants for combustion engines under various boiling conditions	521
T. Duchardt, G. Andersohn, M. Oechsner, U. Depner-Miller (O-7481)	

The impact of condensates containing sulphate and chloride on automotive exhaust systems	522
R. Hashimoto, G. Mori, D. Knoll, U. Tröger, H. Wieser (O-7327)	
High-temperature corrosion of materials for cast exhaust-components	523
M. Ekström, B. Zhu, P. Szakalos, S. Jonsson (O-7383)	
Role of corrosion products in corrosion mechanisms of Zn(Mg)(Al) coatings on steel	524
P. Volovitch M. Salguero Azevedo, J.D. Yoo, C. Allely, C. Ogle (O-7678)	
Influence of corrosion on fatigue behaviour for automotive exhaust systems	525
U. Tröger, D. Knoll, H. Wieser, K. Duru, F. Haider (O-7497)	
Investigation on galvanic effect in automotive body corrosion	526
E. Szala, A. Dogan, F. Hannour (O-7854)	
 16. CORROSION OF POLYMER MATERIALS	
Application relevant polymer testing - impact of media on the viscoelastic behaviour of engineering polymers	527
P. Guttman, D. Oelzant, G. Pilz (O-7660)	
Compatibility of sealing materials with biofuels, biodiesel-heating oil blends and premium grade fuel at different temperatures	528
M. Weltschev, J. Werner, F. Heming, F. Jochems (O-7072)	
Monitoring the process of polymer degradation by imaging techniques	529
T. Schuster, S. Damodaran, K. Rode, R. Brüll, B. Gerets, M. Wenzel, M. Bastian (O-7248)	
Lifetime analysis for plastic pipes by statistical evaluation of creep rupture data	530
J. Heinemann, H. Haupt, A. Bockenheimer, M. Oechsner (O-7820)	
Fluoropolymers in corrosion resistance - long term experience opens a broad spectrum of applications	531
B. Neubauer, G. Maggi (O-7250)	
Fluorothermoplastic-lined steel and FRP equipment for highly corrosive environments - an overview	532
M. Lotz (O-7188)	
Fluoropolymers in corrosion resistance - protective organic coatings based on ECTFE	533
B. Neubauer, G. Maggi (O-7251)	
Corrosion of copper alloy fittings in a combined plastic/metal installation for hot drinking water	534
W. Erning (O-7183)	
Innovative high corrosion resistant systems for chrome plating on plastics	535
L. Thiery, H. Sahrhage, D. Dal Zilio, G.L. Schiavon (O-7831)	
Imaging techniques: tool for the quantification of oriented additives	536
T. Schuster, K. Rode, S. Damodaran, R. Brüll (P-7247)	
Three dimensional orientations by FTIR- and polarized light microscopy	537
S. Damodaran, T. Schuster, K. Rode, R. Brüll (P-7249)	

17. CORROSION & CORROSION PROTECTION OF DRINKING WATER SYSTEMS

Modeling water quality by water treatment for corrosion control in water distribution networks	538
A. Becker (O-7388)	
Observations on the graphitic corrosion of cast iron trunk main: mechanisms and implications	539
R. Logan, M. Mulheron, D. Jesson, P. Smith, T. Evans, N. Clay-Michael, J. Whiter (O-7466)	
Corrosion failure analysis of galvanized steel pipes in a closed water cooling system	540
A. Colombo, L. Oldani, S.P. Trasatti (O-7753)	
Material durability and biofilm development in drinking water network - comparison of stainless steel grades with commonly used materials	541
A. Allion, S. Jacques, J. Peultier, P. Boillot, J.-M. Damasse, M.-C. Bonnet (O-7548)	
Long term corrosion test of stainless steel for water heater applications	542
E. Johansson, S. Hägg Mameng (O-7424)	
Fatigue behavior of high quality steels in water	543
M. Borchert, M. Panzenboeck (O-7380)	
Influence of disinfection chemicals on corrosion of various metals for drinking water supply systems	544
M. Bajt Leban, T. Kosec (O-7358)	
Limiting conditions of pitting corrosion for lean duplex stainless steel as a substitute for standard austenitic grades	545
S. Hägg Mameng, R. Pettersson (O-7410)	
Effectiveness of induction annealing process for the ferritic stainless steel AISI 444	546
A. Acquesta, C. Bitondo, A. Bossio, A. Carangelo, M. Curioni, F. Bellucci (O-7852)	
Failure analyses of localised corrosion damages on stainless steels - practical examples	547
I. Juraga, V. Alar, V. Simunovic, I. Stojanovic (P-7396)	
Investigations of the corrosion behaviour of stainless steel in contact with ECA-generated disinfectant fluids	548
M. Dimper, A. Ahrens, S. Reimann (P-7405)	
Failure analysis of firewater pipeline	549
S. Al Subai, K. Barai, M. Esteban, E.M. Murillo (P-7738)	
In-plant corrosion investigation on steels in distillery effluents	550
A. Singh, C. Sharma, C. Ram (P-7281)	
Biocorrosion evolution in a laboratory copper pipe ageing system	551
D. Fischer, L. Daille, C. Galarce, R. De la Iglesia, G. Pizarro, I. Vargas (P-7609)	

18. CORROSION OF ARCHAEOLOGICAL AND HISTORICAL ARTEFACTS

Corrosion of gold imitations in illuminated manuscripts	552
M. Kouril, E. Jindrova, T. Jamborova, J. Dernovskova (O-7139)	

The bronze panel (paliotto) of San Moise in Venice: materials and causes of deterioration	553
C. Chiavari, C. Martini, S. Montalbani, E. Franzoni, M.C. Bignozzi, C. Passeri (O-7190)	
Single- and multiple-layer coatings for bronze statuary: preliminary study and in situ evaluation after five-year outdoor exposure	554
B. Salvadori, E. Cantisani, C.G.R. Tognon, M. Nesi, A. Cagnini, M. Galeotti, S. Porcinai (O-7464)	
In-situ EIS characterization of outdoor corrosion behaviour of bronze and gilded bronze	555
A. Balbo, M. Abbottoni, C. Chiavari, C. Martini, E. Bernardi, C. Monticelli (O-7259)	
Staining of bronze sculptures, determining the causes	556
A.R. Moreira, K. Barbosa, N.L. Almeida, Z. Panossian (O-7197)	
The role of microstructure on initial corrosion and metal release of Cu-Zn alloys in a chloride-containing laboratory atmosphere	557
X. Zhang, I. Odnevall Wallinder, C. Leygraf (O-7382)	
Atmospheric corrosion of fire gilded bronze: accelerated ageing in runoff conditions	558
C. Chiavari, C. Martini, E. Bernardi, S. Raffo, A. Balbo, M. Abbottoni, M.C. Bignozzi, C. Monticelli (O-7192)	
Dating copper-based archaeological materials using the voltammetry of microparticles	559
A. Doménech, S. Capelo, T. Doménech (O-7311)	
Prediction of long-term corrosion rate of copper alloy objects	560
K. Kreislova, H. Geiplova (O-7425)	
A multi-technique approach for characterizing patina formed on the surface of brass used for musical instrument of the XIX century	561
F. Cocco, M. Fantauzzi, G. Peschke, B. Elsener, A. Rossi (O-7787)	
In situ study of long term atmospheric corrosion of iron by μRaman spectroscopy	562
M. Bouchar, D. Neff, J.P. Gallien, P. Dillmann (O-7186)	
An integrated EIS-Raman approach to study the corrosion mechanism of iron artefacts	563
S. Grassini, M. Bouchar, E. Angelini, M. Parvis, D. Neff, P. Dillmann (O-7474)	
Study of iron sulphides origin in archeological artefacts by determination of sulphur isotopic ratio	564
S. Grousset, F. Mercier, A. Dauzères, D. Crusset, L. Raimbault, A. Galtayries, J.P. Gallien, P. Dillmann, D. Neff (O-7594)	
Study of archaeological ferrous objects in sulfide-containing media	565
J.A. Bourdoiseau, M. Jeannin, R. Sabot, C. Remazeilles, Ph. Refait (O-7136)	
Study of the role of ammonium ions on the corrosion of copper in sulphate containing media	566
H. de Melo, D.F. Abrahao (O-7651)	
Mill scale on historic wrought iron: impact on corrosion and coating performance	567
N. Emmerson, E. Nordgren, D. Watkinson (O-7496)	
Protective coatings for historic wrought iron: epoxy resins versus oil-based systems	568
N.J. Emmerson, D.E. Watkinson (O-7555)	

Pre-corroded electrical resistance sensors to mimic, monitor and guide the conservation of heritage iron	569
J. Dracott, S. Lyon, D. Watkinson, M. Rimmer (O-7589)	
Corrosion products transformations during sub-critical stabilization of archaeological iron artefacts	570
M. Bayle, D. Neff, Ph. de Viviés, J-B. Memet, Ph. Dillmann (O-7390)	
Predicting corrosion: chloride form and the response of archaeological iron to humidity	571
D. Watkinson, M. Rimmer (O-7258)	
Testing the durability of modified corrosion protection systems for iron monuments conservation	573
M. Raedel, M. Buecker (O-7734)	
Evaluation of the conservation state of metallic artefacts from the villa dei quintili in Rome	574
E. Angelini, S. Grassini, G. Galli, M.F. La Russa, S.A. Ruffolo (O-7671)	
Atmospheric corrosion effects of air pollution on materials and cultural property in Kathmandu, Nepal	575
J. Tidblad, K. Hicks, J. Kuylenstierna, B.B. Pradhan, P. Dangol, I. Mylvakanam (O-7459)	
Innovative biological approaches for metal conservation	576
E. Joseph, P. Letardi, M. Albini, L. Comensoli, W. Kooli, L. Mathys, E. Domon Beuret, L. Brambilla, C. Cevey, R. Bertholon, P. Junier, D. Job (O-7562)	
Insoluble decanoate salts as anticorrosion additives in acrylate varnish	577
J. Stoulil, V. Nikendey (O-7272)	
Protection of patinas on various bronzes by different types of inhibitors	578
T. Kosec, K. Marusic, P. Ropret, H. Otmacic Curkovic (O-7628)	
Plasma deposited DLC coatings for the conservation of bronze artefacts	579
E. Angelini, D. Caschera, F. Faraldi, S. Grassini, G.M. Ingo (O-7519)	
Self-assembling monolayers of organic acids for protection of bronze from polluted urban atmospheres	580
K. Marusic, N. Devetak, S. Spoljaric, H. Otmacic Curkovic (O-7319)	
Soil-induced corrosion of ancient roman brass: a case study	581
O. Papadopoulou, P. Vassiliou, V. Gouda, F. Faraldi, S. Grassini, E. Angelini (O-7727)	
Corrosion of sheet piling in the soil: results of a literature review and practical research	582
P. Kraaijenbrink, G.A.M. van Meurs, S. Jansen, H. Senhorst (O-7843)	
Effects of <i>Juniperus communis</i> leaves extracts on tin bronze corrosion	583
R. Ben Channouf, N. Souissi, S. Zanna, H. Ardelean, N. Bellakhal, P. Marcus (O-7376)	
Pollutant permeability in acrylate varnishes	584
J. Svadlena, J. Stoulil (P-7273)	
Corrosion of cans in collections: the case study of Burghalde museum	585
L. Brambilla, S. Mischler, L. Nicolay, R. Schmitt, C. von Arx, I. Böhmler, R. Bertholon (P-7847)	

19. CORROSION IN AEROSPACE

Investigation into the impact of lithium additions on the corrosion response of Al-Cu alloys for aerospace applications	586
D. Carrick, S. Hogg, G. Wilcox (O-7421)	
Effect of microstructure on the corrosion resistance of AA2524-T3 and AA2198 T-851 aluminum alloys used in the aeronautic industry	587
A.F.S. Santos, S. Zaccarelli, S.R. Araujo, M. Terada, I. Costa (O-7622)	
Corrosion resistance of direct metal laser sintering (DMLS) AlSiMg alloys	588
M. Cabrini, S. Lorenzi, T. Pastore, D. Manfredi, S. Biamino, P. Fino, C. Badini (O-7536)	
Effect of deicing compounds on aircraft materials	589
A. Bjørgum, A.-K. Kvernbråten, A. Støre, T.A. Gustavsen, P.I. Lohne, G.W. Karlsen (O-7196)	
Surface treatments in space environment	590
A. Zapata (O-7785)	
Complex oxide morphologies by potentiodynamic anodizing of aluminium	591
M. van Put, O. Elisseeva, J. de Kok, S.T. Abrahami, J.M.C. Mol, H. Terryn (O-7180)	
Application of surface wetness sensors for the evaluation of corrosivity of the atmosphere to aerospace aluminium alloys	592
O.V. Startsev, I.M. Medvedev (O-7784)	
Choosing a corrosion prevention compound surface science helping to preserve aeronautical equipment	593
C. Bilke-Krause, Chr. Rulison (O-7577)	
The prevention of corrosion and stress-corrosion cracking on European space programme	595
T. Ghidini, A. Tesch, A. Graham (O-7803)	
The role of anodic oxide chemistry in the interfacial bonding of aluminium in the aerospace industry	596
S.T. Abrahami, J. de Kok, J.M.C. Mol, H. Terryn (O-7179)	
Plasma electrolytic oxidation processes for aeronautic applications and their technical application	597
N. Godja, M. Pölzer, A. Schindel, J. Wosik, A. Gavrilovic, Ch. Kleber (O-7208)	
Tartaric/sulphuric acid anodizing of aluminium-copper-lithium alloy AA2198	598
A. Schindel, N. Godja, T. Vanka, J. Wosik, Ch. Kleber (O-7367)	
Characterization and performance of passive layers generated from lithium based inhibitors for corrosion protection of AA 2024-T3	599
P. Visser, J.M.C. Mol, H. Terryn (O-7616)	
Experimental study of the effect of mass transfer on the efficiency of inhibitors released from an inhibited-primer	600
F. Peltier, R. Oltra, G. Zalamansky (O-7263)	
Advanced protective coatings for AA2024 alloys with combination of pH- sensitive active containers filed with corrosion inhibitors	601
D. Snihirova, S.V. Lamaka, M.F. Montemor, P. Taheri, J.M.C. Mol (O-7700)	

Self-healing anticorrosive hybrid sol-gel coatings based on loaded nanocontainers for 2XXX serie aluminium alloys	602
R. Noiville, M. Gressier, M-J. Menu, J-P. Bonino, S. Duluard, B. Fori, C. Gazeau, P. Bares (O-7749)	
Silica mesoporous thin films hosting benzotriazole for protection of 2024 aluminum alloy - Study of healing mechanism	603
I. Recloux, M. Mouanga, F. Khelifa, M-G. Olivier (O-7131)	
Eco-friendly primer treatments for corrosion protection of Al 2024	604
I. Bertoli, M. Trueba, S.P. Trasatti (O-7292)	
Characterization of corrosion resistance of chromium-free coatings for aeronautical application	605
L. Belsanti, E. Forchin, R. Stifanese, M. Toselli, P. Traverso (P-7715)	
Anticorrosion sol-gel coatings for anodised aluminium	606
M. Oubaha (P-7760)	
A study of the films formed on an AA2024 alloy clad layer by hydrothermal treatments involving cerium (III) and propylene glycol	607
W.I.A. Santos, V.R. Capelossi, S. Hinder, M.A. Baker, R. Grilli, I. Costa (P-7680)	
A. WS: CO₂-CORROSION IN INDUSTRIAL-APPLICATIONS	
Mitigating corrosion in sweet gas units: a comparison between laboratory data and field survey	608
J. Kittel, M. Bonis, G. Perdu (O-7811)	
Corrosive and protective behaviour of MEA in dense phase CO₂	609
A. Dugstad, M. Halseid, B. Morland (O-7743)	
Thermally sprayed corrosion resistant alloy coatings on carbon steel for use in CCS	610
S. Paul (O-7456)	
Effect of microstructure on scale protectiveness and corrosion rate of carbon steel in CCTS environments	611
M. Cabrini, S. Lorenzi, T. Pastore (O-7524)	
Safe transport of dense phase CO₂ - how much flue gas impurities can be accepted?	612
A. Dugstad, M. Halseid, B. Morland (O-7744)	
Corrosion susceptibility of steels under transport and injection exploitation conditions possible in CCS process chain	613
O. Yevtushenko, R. Bäßler, D. Bettge (O-7157)	
B. WS: CORROSION RELIABILITY OF ELECTRONICS DEVICES	
Perspectives on the climatic reliability issues of electronic devices	614
R. Ambat (O-7822)	
Brief introduction to the mechanism of electrochemical migration	615
H. Schweigart (O-7819)	

Influence of the printed circuit board design on electrochemical migration and surface insulation	616
M. Nowotnick, S. Mattern (O-7818)	
Electrochemical migration in electronics: effect of contamination and bias conditions	617
V. Verdingovas, M.S. Jellesen, R. Ambat (O-7447)	
Contamination profile of printed circuit board assemblies in relation to soldering types and conformal coating	618
H. Conseil, M.S. Jellesen, R. Ambat (O-7082)	
Corrosion reliability of electronics: the influence of solder temperature on the decomposition of flux activators	619
K. Piotrowska, H. Conseil, M.S. Jellesen, R. Ambat (O-7495)	
Cleaning in electronics: understanding Today's needs	620
J. Cetier, P.J. Duchi, A.M. Laugt (O-7227)	
Solder paste residue corrosivity assessment: Bono test	621
J. Cetier, C. Puechagut, A.M. Laugt, E. Guene, R. Anisko (O-7225)	
Corrosion in electronics: overview of failures and countermeasures	622
M.S. Jellesen, V. Verdingovas, H. Conseil, R. Ambat (O-7426)	
Salt spray corrosion test methods - an overview	623
A.B. Kentved, K.A. Schmidt (O-7521)	
An on-site atmospheric-corrosion sensor	624
R. Minamitani (O-7203)	
Environmental stress corrosion of polybutylenterephthalate: a common material for electronic housings	625
G. Klett, M. Fürtsch, A. Hachtel, L. Müller (O-7824)	
The effect of a post-electroplating electrochemical oxidation treatment on whisker formation from tin coatings	626
M.A. Ashworth, D. Haspel, L. Wu, G.D. Wilcox, R.J. Mortimer (O-7236)	
Tin electrodeposits produced using non-aqueous ionic liquid electrolytes: whisker formation	627
C.J. Stuttle, M.A. Ashworth, G.D. Wilcox, R.J. Mortimer (O-7403)	
Basic physics of moisture challenges in electronic packaging - a tutorial overview	628
J. Jacobsen, A. Holm, J.P. Krog, L. Rimestad, A. Riis (O-7823)	
Climatic durability of modern assembly technologies in electronics	629
P. Zák, K. Kreislová, D. Majtás (P-7453)	
Understanding moisture protection of coated electronic circuits in terms of water permeation and electrochemical corrosion	630
J. Krog, M. Ahmed, M.S. Jellesen, J.B. Jacobsen, R. Ambat (P-7826)	
Development and evaluation of atmospheric corrosion sensors using printed circuits	631
E. Roblero, F. Corvo, V. Moo-Yam, E. García-Ochoa, T. Pérez (P-7335)	

C. JS: HIGH TEMPERATURE CORROSION IN THE REFINERY, PETROCHEMICAL & CHEMICAL INDUSTRIES

Influence of single surface ash layer on dual corrosion	632
M. Mosquera Feijoo, A. Kranzmann, A. Baselga Zapater (O-7400)	
Acoustic emission analysis coupled with thermogravimetric experiments dedicated to high temperature corrosion studies on metallic alloys	633
V. Peres, O. Al Haj, E. Serris, M. Cournil, F. Grosjean, J. Kittel, F. Ropital (O-7240)	
Integrated risk management program to allow safe profitable processing of opportunity naphthenic acid crudes	634
P. Thornthwaite, K. Clarke, J. Davies (O-7135)	
Passivation behaviour of stainless steel (UNSN-08028) in industrial phosphoric acid contaminated with chlorides and sulfates at 80°C	635
M. Ben Salah, R. Sabot, E. Triki, L. Dhoubi, P. Refait, M. Jeannin (P-7386)	
Failure analysis of boiler furnace wall tube	636
M. Al Muaisub, A. Bayramov (P-7423)	

E. JS: CATHODIC PROTECTION IN MARINE ENVIRONMENTS

Heavy metal inputs from anodic dissolution of Al-Zn-In galvanic anodes to the marine environment: TALINE project	637
S. Pineau, J. Deborde, A.M. Grolleau, P. Refait, C. Caplat, O. Basuyaux, M.L. Mahaut, S. Le Glatin, P. Bustamante, J.L. Gonzalez, C. Brach-Papa, P. Honoré (O-7222)	
Design of cathodic protection retrofitting of subsea pipelines assisted by FEM modeling	638
P. Marcassoli, M. Ginocchio, B. Bazzoni, A. Msallem, A. Ibrahim (O-7729)	
Volume synthesis of a calcareous deposit on steel under cathodic protection by impressed current	639
A. Zanibellato, R. Sabot, P. Refait, M. Jeannin (O-7306)	

F. WS: MARINE CORROSION IN RENEWABLE ENERGY

Coating deterioration and corrosion on offshore wind power structures: a review of inspection results	640
A. Momber (O-7792)	
Cathodic protection for marine structures: 3 case studies	641
S. Ayyar, J. Jansson (O-7375)	
Corrosive environment inside offshore monopile structures and challenges in monitoring	642
B. Jensen, F. Grønvold (O-7365)	
Durability of coating repair systems for offshore service	643
A.R. Black, P.K. Nielsen (O-7230)	

I. JS: INTERPLAY OF MECHANICS AND CORROSION IN SURFACE AND BULK DEGRADATION

Kinetic of passivation of two stainless steel microstructures under tribocorrosion solicitations	644
V. Dalbert, N. Mary, B. Normand, C. Verdu, S. Saedlou (O-7528)	
Tribocorrosion behaviour of stainless steel under cathodic potential	645
N. Mary, V. Dalbert, N. Normand, B. Ter-Ovanessian, T. Borgna, L. Lefebvre, S. Saedlou (O-7532)	
The effect of surface condition on the friction coefficient of different dental archwires	646
T. Kosec, P. Mocnik, U. Mezeg, J. Primožic, A. Legat (O-7630)	
New advances and perspectives in the electrochemical study of tribocorrosion	647
M. Keddam, P. Ponthiaux, V. Vivier (O-7798)	
Sensitivity to liquid metal embrittlement of the T91 steel by the liquid sodium : influence of the pre-immersion in liquid sodium	648
I. Proriot Serre, O. Hamdane, J-B. Vogt, J.-L. Courouau (O-7687)	
Tribocorrosion effects on offshore mooring chain steel	649
A. Lopez, F. Pagano, R. Bayon, A. Igartua (O-7772)	
Tribocorrosion behavior of commercially pure titanium in biomedical application of dental and orthopaedic implants	650
Y. Yang, P. Ponthiaux (P-7330)	

J. WS: MULTIMATERIALS IN HYBRID STRUCTURES FOR AUTOMOTIVE AND AEROSPACE APPLICATIONS - CORROSION PREVENTION

Corrosion investigations of ultrasound supported friction stir welded Al/Mg-hybrid joints	651
S. Benfer, B. Straß, G. Wagner, W. Fürbeth (O-7170)	
Study of the corrosion behaviour of friction stir welded AA 2024-T3 using global and local electrochemical techniques	652
C. Molena de Assis, I.V. Aoki, V. Vivier (O-7643)	
Active self-healing coating for galvanically coupled multi-material assemblies	653
M. Serdechnova, S. Kallip, D. Vieira, L.F.S. Barbosa, M.G.S. Ferreira, M.L. Zheludkevich (O-7257)	
A controlled experimental approach of the effect of confinement on the damage inside an aluminium alloy lap joint	654
T.M.L. Le, R. Oltra, A. Zimmer (O-7789)	
Corrosion behaviour of titanium in lightweight construction	655
S. Wibihal, G. Fafilek, T. Hack, M. Beneke (O-7786)	
Inhibitor-enriched composite protective coating for WE43 magnesium alloy	656
S. Lamaka, M. Lourenço, D. Ivanov, M. Zheludkevich, M. Ferreira, T. Hack (O-7640)	
The influence of hot forming on the microstructure and corrosion behaviour of magnesium alloy	657
J. Alias, X. Zhou, G.E. Thompson (O-7415)	

In-situ Al/TiC nanocomposites: the effect of sintering temperature on the corrosion behavior	658
B. Dikici, M. Gavgali, F. Bedir, T. Kiyak (O-7198)	

K. WS: MEANS OF PREVENTION AND RECOVERY AGAINST DECAY/DETERIORATION OF VALUABLE BUILDING AND URBAN DECORATION

Research activity for the restoration and maintenance of the Pisan art objects at the University of Pisa	659
A. Andreotti, I. Bonoduce, V. Castelvetro, F. Ciardelli, M.P. Colombini (O-7835)	

World War One fortresses and artifacts in Trento area: from historical corrosion to a durable maintenance work	660
F. Meneghelli (O-7828)	

Cutting-edge technologies for the renewal of historical buildings the thirty-year experience gained in restoring the painted facades	661
G. Di Tanna, G. Bozzo (O-7807)	

Genoa's elevated highway (Soprelevata) : 1964 -1984 -2014 - a successful maintenance project	662
P. Bonora (O-7816)	

More than 20 years of proven durability of fluorinated architectural coatings onto concrete; 1992/2014 Genoa's Aquarium case	663
A. Locaspi (O-7812)	

The effect of soiling and oxidation on architectural titanium	664
M.V. Diamanti, M.P. Pedferri (O-7450)	

Study of protective coatings for outdoor bronzes by means of in situ electrochemical techniques	665
A. Colombo, S. Goidanich, E. Guerrini, S. Porcinai, A. Cagnini, M. Galeotti, B. Salvadori, A. Vincenzo, L. Brambilla, L. Rosetti, S. Trasatti (O-7849)	

Corrosion resistance of anticorrosive film formed on Mg alloy by steam coating	666
T. Ishizaki, N. Kamiyama (O-7782)	

CAVALLARO MEDAL LECTURE

Development of inhibitor-containing zeolites for protection coatings	667
M.G.S. Ferreira (O-7860)	

From the object scale to the nanometre: issues linked with corrosion of archaeological ferrous artefacts.

Philippe Dillmann

LAPA SIS2M/NIMBE CEA Saclay, France and IRAMAT UMR5060 CNRS, France.

Corrosion of archaeological ferrous artefacts is a main issue for conservation of cultural heritage. Actually objects realised with this metal constitute the main part of archaeological metals stored in Museums or used in ancient monuments. Depending on the environment, several corrosion patterns are observed on the metal, forming a thick layer constituted of various phases and heterogeneous at different scales. The physico-chemical properties of this layer will drive the corrosion kinetics and conduct to different main mechanisms and average corrosion rates after centuries of alteration. To develop reliable diagnosis but also to optimise the possible protection or inhibition treatments, it is necessary to understand these mechanisms in detail, and their synergies from the nanometre to the millimetre.

The purpose of this talk is to illustrate by several examples the various mechanisms and the main issues dealing with these mechanisms. Some specific methodologies, adapted to the particular case of very long term corrosion, including the “analogue approach”, will be showed.

**SCIENTIFIC
SESSIONS AND
JOINT SESSIONS**



Comparison of the Corrosion Protection Effectiveness of Vapor Corrosion Inhibitor and Nitrogen Blanketing System

Behzad Bavarian, Jia Zhang, Keyang Lu and Lisa Reiner

Dept. of Manufacturing Systems Engineering & Management
College of Engineering and Computer Science
California State University, Northridge, USA 91330

Abstract

Corrosion behavior of steel samples used for storage tanks and cross casing pipe applications were investigated using two different protection mechanisms: vapor corrosion inhibitor and nitrogen blanketing system. The objective of this project was to demonstrate which technique provides more protection in corrosive environments, especially where there are restricted geometries such as crevices, threads, notches, and under-deposits.

Corrosion behavior of steel samples were studied in two different conditions; the first contained 200 ppm chloride solution + 10% corrosion inhibitor addition, the second included 200 ppm chloride solution with a nitrogen blanketing system at 10 psi applied pressure. The corrosion rate of the exposed samples were monitored for more than five months (~3,600 hours) using linear polarization resistance (LPR) and electrical resistance (ER) probe techniques.

The corrosion data have demonstrated that vapor phase corrosion inhibitors have superior advantages over the nitrogen blanketing system in the presence of excessive salt and moisture. On average, the LPR corrosion rate measured less than 0.06 mpy for samples immersed in VCI solution, no sign of corrosion was observed. The immersed and nitrogen blanketing samples, in contrast, showed a corrosion rate of 1.68 mpy and the samples were covered with a thick red rust. ER probes showed a corrosion rate of 0.18 mpy for VCI treated while the nitrogen blanketing samples showed a 2.12 mpy corrosion rate and probes were heavily corroded. It is interesting to report that when VCI was injected into the nitrogen blanketing corrosion cell, the corrosion rate of the corroded steel probes dropped to less than 0.26 mpy in under 20 hours. This shows a significant reduction in the corrosion rate by more than eight times.

New Corrosion Inhibitor for Evaporative Cooling Systems

Matheis J.; Stratmann, A.; Hater, W.; BK Giulini GmbH, Duesseldorf, Germany
Wolf, F.; Lunkenheimer, R.; BK Giulini GmbH, Ludwigshafen, Germany
Foret, C. ; ICL France SAS, Vaas, France

Corrosion of heat exchangers and installations in evaporative cooling systems is a serious problem of industry, as it may lead to increased maintenance effort, damages, up to plant shut-down causing high cost. Furthermore, there may be a high environmental impact due to the discharge of blow-down water containing heavy metals or hazardous compounds, which may enter the water system via leakages.

State of the art corrosion inhibitor programs are based on phosphate, phosphonates, zinc and combinations thereof. Although generally satisfying control of corrosion can be achieved, all programs suffer more or less severe drawbacks, such as lack of biodegradability, content of heavy metals or necessity of pH control combined with acid dosage.

Consequently, there is a need of corrosion inhibitors having an improved environmental profile and/or an improved performance. This papers shows the results obtained with a newly developed corrosion inhibitor. The molecule is free of heavy metals.

Corrosion tests have been carried out with carbon steel specimen in dependence of inhibitor concentration, water composition and water temperature. Electrochemical methods, e.g. voltammetry and polarization resistance, were applied as well as beaker tests and long term tests in cooling circuit simulating devices. Thereby, the efficiency of the new inhibitor as such as well as of combinations with other organic inhibitors has been studied. Finally, the new inhibitor has been tested in a pilot cooling tower under practical conditions.

The results of the corrosion tests clearly show an excellent efficiency of the new corrosion inhibitor. Significant synergies could be identified between the new substance and other inhibitors. Pilot plant studies of a formulation based on the new corrosion inhibitor show a better or at least the same performance compared to commercially available corrosion inhibitors, but a marked reduction of the phosphorous entry into the waste water.

Corrosion inhibition of carbon steel in cooling water systems by means of chemicals used to modify heat transfer

O. Conejero, ITMA Materials Technology, Avilés / Spain

M. Cabañas, J. Arancón, D. Carrascal, ArcelorMittal Global R&D, Avilés / Spain;

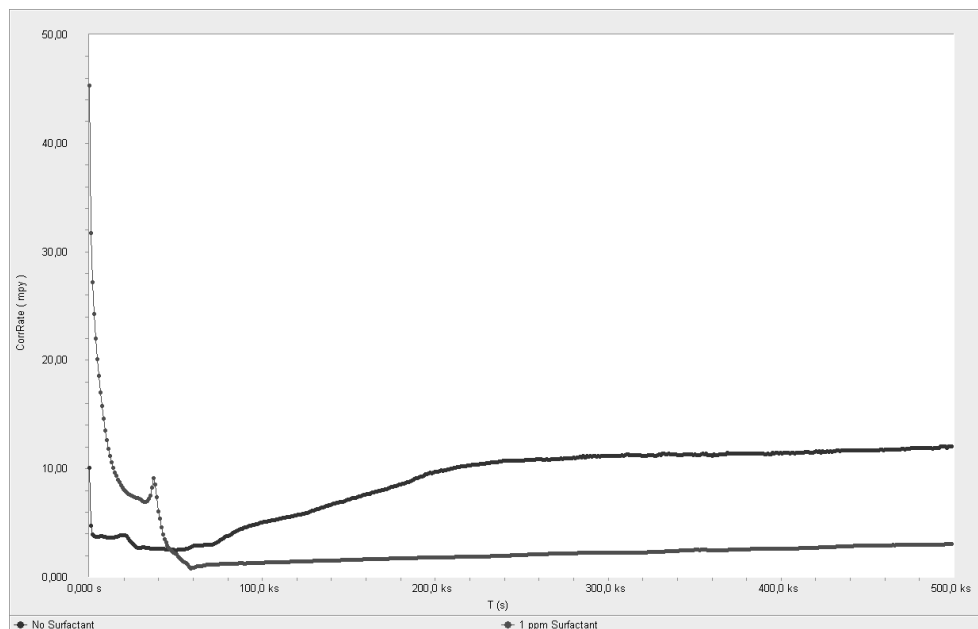
Abstract

Surfactants are being studied in the ArcelorMittal steelmaking plants as water additives.

The use of water additives is a method that can be employed to modify the heat transfer characteristics of water. Surfactants are chemicals that are being studied to be employed for this purpose in different steelmaking processes.

As a side effect, the corrosivity of any new additive has to be assessed. For this reason, a study of the corrosivity of a commercial product was carried out in the laboratory and also in a semi-industrial pilot plant.

The results obtained show that the addition of this type of products lowers the corrosion rate of carbon steel in the investigated system. The corrosion rate can be up to four times lower in water with 1ppm of the chemical product as compared to the same water without it.



The Impact of Copper Chrome Boron (CCB) Wood Preservative on the Corrosion of St37 Steel

Husnu Gerengi^{a,}, C. Taşçioğlu^b, C. Akçay^b, M. Kurtay^a*

^aCorrosion Research Laboratory, Kaynasli Vocational College, Duzce University,
81900 Kaynasli, Duzce, Turkey

^bDepartment of Forest Products Engineering, Faculty of Forestry, Duzce University,
81620 Duzce, Turkey

Abstract

Copper Chrome Boron (CCB) is a well-known new generation wood preservative. The corrosion inhibition performance of CCB on St37 steel in 3.5% (w/v) NaCl was examined using dynamic electrochemical impedance spectroscopy (DEIS), Tafel polarisation and scanning electron microscopy techniques. Corrosion test results of the system being investigated revealed that CCB displayed inhibitor properties and behaved predominantly as an anodic inhibitor. The adsorption of CCB was found to follow Langmuir's adsorption model. Scientifically, this work can contribute to the understanding of the mechanism of corrosion of st37 steel fasteners used with CCB-treated and untreated wood.

Keywords: Corrosion; Copper Chrome Boron (CCB); St37; Wood Preservative

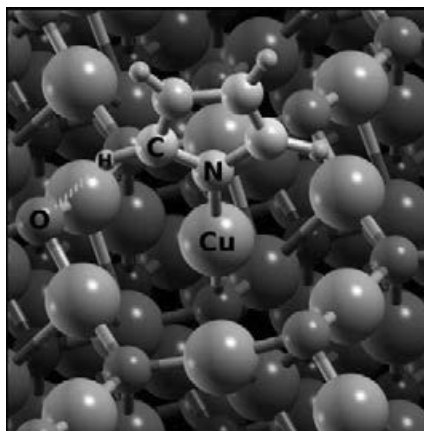
* Corresponding author Tel.: +90-5053987953; E-mail: husnugerengi@duzce.edu.tr

Adsorption of imidazole, triazole, and tetrazole on oxidized copper surface

Dunja Peca, Anton Kokalj

Jožef Stefan Institute, Jamova 39, Ljubljana, Slovenia

Azole molecules are known for their ability to significantly slow down the corrosion of metals. Because molecular adsorption represents an important step in achieving the inhibitory effect, several density functional theory (DFT) studies have been performed recently with the aim to ascertain molecular level understanding of the bonding of azole molecules to copper surfaces, e.g., see Refs. [1-4]. The focus of these studies was the interaction of azole inhibitors with only unoxidized copper surfaces. However, it is known that metal surfaces are often oxidized and consequently surface-oxides play an important role in the adsorption process of inhibitors. For this reason we have studied by means of DFT molecular modeling the interaction of imidazole, triazole, and tetrazole molecules with the $\text{Cu}_2\text{O}(111)$ surface. We find that there are significant differences with respect to unoxidized $\text{Cu}(111)$. Namely, it was shown previously that only deprotonated molecules bond strongly to the $\text{Cu}(111)$, while the molecules in neutral form bind weakly with the bonding energy of about 0.5 eV [3]. In contrast, neutral molecules can adsorb rather strongly to $\text{Cu}_2\text{O}(111)$ with the bonding energy of about 1.6 eV, provided that they bond to the coordinatively unsaturated copper sites, while the bonding to the saturated sites is similar as on $\text{Cu}(111)$. On the other hand, the bonding of deprotonated molecules to $\text{Cu}_2\text{O}(111)$ is either similar or even reduced with respect to $\text{Cu}(111)$. These results, therefore, imply that on oxidized copper surfaces the molecules in neutral form may play more important role for inhibiting the corrosion than on unoxidized Cu surfaces.



- [1] A. Kokalj, S. Peljhan, M. Finšgar, I. Milošev, *J. Am. Chem. Soc.*, **2010**, 132, 16657-16668.
- [2] N. Kovačević, A. Kokalj, *J. Phys. Chem. C*, **2011**, 115, 24189-24197.
- [3] N. Kovačević, A. Kokalj, *Corros. Sci.*, **2013**, 73, 7-17.
- [4] A. Kokalj, S. Peljhan, J. Koller, *J. Phys. Chem. C*, **2014**, doi:10.1021/jp409719c

Corrosion Inhibition of a large evaporative cooling system

Issa M. Baghni, Engineering Academy, Tajoura - Libya

Abstract: Cooling tower plays an important role in total energy balance of chemical process and gas plant industries, particularly with respect to total water conservation. The increasing use of desalinated water for cooling systems has raised various problems that were not faced in cooling systems when using ground water, one of those problems is selection of proper corrosion inhibitor that is compatible with biological water treatment scheme.

In this case study, efforts were made to share the experience of a large evaporative cooling system water treatment, with discussion of remedial actions taken to reduce corrosion rate.

Keywords: Corrosion inhibitors, Corrosion, Cooling system, Water treatment. bio-fouling.

Protection of Cu70Ni30 Alloy by Fatty Acids

Helena Otmačić Ćurković, Zana Hajdari and Katarina Marušić

*Faculty of Chemical Engineering and Technology, University of Zagreb, Savska 16,
10000 Zagreb, Croatia*

Cupronickel alloys are often used for applications in marine environment due to their relatively high corrosion resistance based on the formation of protective oxide layer. Their service life in such aggressive environment can be prolonged by protection with corrosion inhibitors. However, marine environment is sensitive to toxic compounds that are often used as corrosion inhibitors. For this reason it is very important to develop new corrosion inhibitors that are not harmful to marine ecosystems.

Fatty acids are known to adsorb on some of the metal oxides and form self-assembled monolayer that might act as a barrier to diffusion of aggressive species towards metal surface. They are also environment friendly compounds.

The objective of this study is to examine several fatty acids as possible corrosion inhibitors for Cu70Ni30 alloy in seawater. Protective layer is formed by immersion in ethanol solution of fatty acid. Influence of the application conditions, such as immersion time, fatty acid concentration, temperature and surface pretreatment, on inhibiting efficiency and stability of fatty acids monolayer is examined.

Studies are performed by electrochemical methods: polarization measurements and electrochemical impedance spectroscopy. Surface layer is characterized by FTIR spectroscopy and SEM/EDX. Contact angle measurements are conducted to examine increase of the surface hydrophobicity in the presence of fatty acids.

Results of this investigation show that fatty acids increase the corrosion resistance of cupronickel alloys and prolong their service life in seawater.

Acknowledgments: The research leading to these results has received funding from Croatian Science Foundation under grant agreement 9.01/253.

Inhibitor for Galvanically Coupled Copper/Steel System

*Gozde Tansug, Tunc Tuken, Gokmen Sigircik, Elife Sultan Giray, Mehmet Erbil
Cukurova University, Adana, Turkey*

In much industrial application, diverse metals are employed together mandatorily; heat exchangers, cooling water systems etc. Inevitably, such systems are subjected to galvanic corrosion, copper/steel couple is a typical example. Protection of these systems involves particular interest, especially in acidic chloride environment, at which both copper and steel is highly vulnerable against corrosion. Azole group organic inhibitors are pronounced with their ability to form polymer like protective film on copper, via interacting with copper ions. The mercapto group containing inhibitors are strongly adsorbed on oxide free metal surfaces. They could also form stable complex with copper ions via the thiolate bond. Generally, this kind of inhibitor molecules is modified with an aromatic ring, in order to increase hydrophobicity on top of protective layer.

Methyl 3-((2-mercaptophenyl)imino) butanoate (MMPB) was studied as corrosion inhibitor for protection of galvanically coupled copper and steel systems. The efficiency was examined in acidic chloride media by means of various electrochemical and spectroscopy techniques. The measurements were realized for single copper, steel electrodes and once for galvanically coupled samples. Scanning electron microscopy and energy dispersive X-ray analysis proved that MMPB offers significant protection against corrosion of copper and steel, for extending periods. The inhibition efficiency against coupled systems was investigated with electrochemical measurements between galvanically coupled copper and steel samples, which were immersed in test solution and coupled to each other with an external connection wire. Galvanic current and potential difference between these electrodes was measured. Solution assay analysis was realized for quantification of corrosion rates of each metal. It was proved that the inhibitor offers high efficiency for such systems, at which steel becomes highly vulnerable against corrosion when it is coupled with copper. The azole and thiol groups of molecule generate strong adsorptive interaction with the surface of both metals. The azole group could also form highly stable complex with Cu(I) ions, which are freshly released due to oxidation of copper at the interface. The carboxylate end group of molecule leads to significant intermolecular attraction between the adsorbed inhibitor molecules, because of notably dipole character.

References

1. M. M. Antonijevic, B. M. B. Petrovic, Int. J. Electrochem. Sci. 3 (2008) 1-28.
2. M. M. Antonijevic, S. M. Milic, M. B. Petrovic, Corros. Sci. 51(2009) 1228-1237.
3. Sudheer, M.A. Quraishi, Corros. Sci. 70 (2013) 161-169.

4,5-Dinitrobenzimidazole and 5-nitrobenzimidazole adsorption on copper surface. Electrochemical and XPS study*

Arkhipushkin I.A.^{1,2}, Zhilenko D.Yu.¹ Kazansky L.P.²

¹ *Mendeleyev University of Chemical Technology of Russia, Miusskaya square, 9, Moscow, Russia*

² *Institute of physical chemistry and electrochemistry, Russian Academy of sciences, Leninski pr.31 Moscow, Russia*

Corresponding author: arhi90@mail.ru

As many constructional metals copper suffers from corrosion in aqueous solutions and therefore it needs protection. One of the most effective protection methods is usage of corrosion inhibitors, often organic compounds. For copper - azoles and their derivatives are especially interesting.

Rather effective ones are believed to be 4,5-dinitrobenzimidazole and 5-nitrobenzimidazole, whose structures are shown below.



5-nitrobenzimidazole



4,5-dinitrobenzimidazole

In the present study using XPS and electrochemistry we have investigated the mentioned substances when they adsorbed on copper samples in neutral borate buffer (pH 7.4) with and without 0.5M NaCl. XPS analysis of copper samples shows that both inhibitors adsorb on the surface and remain there even after thorough ultrasonic washing. It is evidenced by the presence of two N1s peaks, one for -NO₂ group (406.1 eV) and another for -N- in azole group (399.8 eV) with expected different peak intensities. When adsorbed, the N1s azole peak shifts from the peak position observed for azole powder (400.5 eV). At the same time, the peak width (2.39 eV) decreases in comparison with azole powder (2.62 eV). It may result from deprotonation of azole nitrogen atom, equalization of the charges on them and their coordination with Cu⁺ ions. The Cu2p3 spectrum reveals the only peak at 932.8 eV witnessing the absence of Cu⁺⁺. The Auger spectra CuL₃M₄₅M₄₅ electrons may be deconvoluted into three individual curves assigned to Cu⁰ (568 eV), Cu₂O (570 eV) and complex CuL₂, where L - inhibitor molecule. The maximum at 572.5 eV of the third component belongs to this copper - inhibitor complex due to formation Cu-N bonding. According to interpretation of XPS data 5-nitrobenzimidazole and 4,5-dinitrobenzimidazole form polymolecular complex film which thickness increases in time of exposure and can reach 9 nm in several hours.

Potentiodynamic curves of the copper electrode have shown gradual decreasing the anodic current upon addition the substances under study in pure borate buffer containing 0.01M NaCl and in 0.5M NaCl solution. Corrosion protection effect of 5-nitrobenzimidazole and 4,5-dinitrobenzimidazole is compared and discussed.

*This work is partly financed by RFBR grant №13-03-00354

Probing Corrosion Inhibitor Behaviour Using Micelle Detection

Cameron Mackenzie, LUX Assure, Edinburgh UK;

Mohsen Achour and David Blumer, ConocoPhillips, Bartlesville OK, USA

The preparation of commercial corrosion inhibitors draws on a wealth of research, experience and expertise to provide an effective solution which is both environmentally and economically acceptable. In oil and gas production the package usually contains one or more chemical surfactant families along with other additives. However the competitive environment means that many details of the formulations are trade secrets resulting in a general opacity and a lack of specific data or research on the behaviour of these chemicals at the molecular level in oilfield environments.

Micelles are molecular aggregates formed when a surfactant is present above a specific concentration and temperature and their measurement can provide a useful tool for probing the behaviour of inhibitors at the functional molecular level whilst maintaining the secrecy required by manufacturers. Two main themes will be presented. Firstly, the use of micelle detection in the laboratory environment provides rapid insights in to the behaviour of different chemicals in different physical and chemical environments. For example, the effect of varying water-cuts, oil and water chemistry and pH was explored and the results demonstrated the significant and often unpredictable changes which can occur. Secondly, the differences between measuring simulated samples, samples measured in the field and samples shipped from the field are explored.

The results discussed in this work reinforce the observation that corrosion inhibitors are complex and sensitive to their environment. Apparently insignificant changes in conditions can have dramatic effects on the behaviour of the active chemicals. It is therefore imperative that corrosion inhibitor is analysed as close to field conditions as possible and that where simulations are used, the results are treated with appropriate caution.

Evaluation of environmental friendly corrosion inhibitors vs traditional corrosion inhibitors in oil and gas industry

*C. Di Iorio, T. Cheldi, S. Correra
eni e&p, S. Donato Milanese*

*E. Lo Piccolo, G. Mortali
Centro Sviluppo Materiali, Roma*

Carbon and low alloy steels are widely used construction materials for oil and gas process and transportation facilities. In order to guarantee the integrity of the plant a very effective corrosion management strategy is mandatory with these materials. The most extensively used method in controlling internal corrosion threats is represented by chemical inhibition.

A large number of commercial corrosion inhibitors is available to handle a lot of different corrosive conditions.

Unfortunately, most of the chemical molecules more effective as corrosion inhibitor are non-biodegradable and toxic for marine and terrestrial living species. That is why international regulations are changing, forcing chemical manufacturers and operators to dismiss harmful and hazardous chemicals in favour of eco-friendly compounds.

Concerning eco-friendly corrosion inhibitors the main questions arising between operators are:

- Are environmental friendly corrosion inhibitors effective as traditional ones?
- Are they really environmental friendly?

In the attempt to answer to these questions a laboratory testing activity was carried out by eni e&p with the support of specialized laboratories.

This paper describes the applied testing protocol and the results of the comparative evaluation of eight different corrosion inhibitors, both traditional (red) and environmental-friendly (green).

Four service companies were asked to provide two different corrosion inhibitors, a red and a green one.

The efficiency, in corrosion control, of the eight chemicals was evaluated, at the same conditions, by means of electrochemical techniques, both under static and dynamic conditions.

The toxicity of the chemicals was evaluated by means of the assessment of their specific EC₅₀ value.

The comparison of the different laboratory test results was carried out between products of the same supplier.

Effect of an amine based inhibitor on CO₂ corrosion of carbon steel

*Gregor Mori, Andreas Prethaler, Montanuniversität Leoben, Leoben
Erwin Rosenberg, Melanie Rückemann, Technical University of Vienna, Vienna
Wolfgang Havlik, Gerald Zehethofer, Stefan Hönig, OMV E&P GmbH, Gänserndorf*

Abstract

Inhibition is, besides coating technology, the most applied technique of corrosion protection in oil and gas production. Understanding of inhibitors is in many cases insufficient and follows more general rules of thumb than scientific theories. This lack of understanding hinders researchers to formulate more efficient corrosion inhibitors.

In the present work an amine based gas condensate inhibitor applicable below 100 °C has been investigated both, in a laboratory flow loop and a jet impingement cell. Inhibitor concentration was varied in these flow experiments. As test material an L80 chromium quenched and tempered steel with 1 % has been used. Tubes with different diameters have been fabricated from a rod for the flow loop experiments to enable different flow regimes and flow velocities. After leaving the flow loop, the residual inhibitor concentration in the artificial brine has been analysed. From the same material small coupons have been machined and tested in a jet impingement cell. These tests under flow conditions have all been done at flow velocities (flow loop) and impact velocities (jet impingement cell), respectively between 10 and 30 m/s.

In addition partitioning of inhibitor in oil-water-gas mixtures has been determined as well as critical micelle concentration (cmc). Analysis of inhibitor has been done by gas chromatography coupled with a mass spectrometer. Electrochemically potential and polarization resistance have been determined for different concentrations under stagnant conditions.

Data generated show that the functional substances of the inhibitor are quaternary amines with a chain length between C₁₀ and C₁₈. Inhibitor is mainly water soluble and only little fugitive. Inhibitor shows a good performance as long as concentration is higher than cmc. This is verified in flow loop and jet impingement experiments, both resulting in reasonable data compared to the field.

Keywords: CO₂ corrosion, corrosion inhibitor, critical micelle concentration

Investigation of Corrosion Problems in Cooling Water Pipeline

Saud G. Al subai and A. K. Bairamov

Saudi Basic Industries Corporation, P.O Box 11669, Jubail 31961, Saudi Arabia, T +966 (3) 359 9134, F +966 (3) 359 9112, subaisg@sabic.com

This paper describes the investigation of the corrosion problems observed in cooling water pipe lines. The pipes have been in service for six years at the time of this investigation. The first leakage was observed within one year after commissioning. Corrosion investigations revealed that the leakage problems encountered in the lines are due to under deposit corrosion. The supplied cooling water was contaminated with organic material and solid particles. The internal pipe surface was heavily covered with deposit and consequently the water chemical treatment was unable to prevent localized corrosion from taking place.

Carbon Steel material is the most cost effective and technically acceptable material to be used if the deposits accumulation problem is avoided and effective water treatment is utilized. Thus, water quality limits should be clearly defined and adhered to. Additionally, due to the hot surrounding environment, the exterior surfaces of Carbon Steel pipes should be coated.

Inhibition of CO₂ Corrosion of Pipeline Steel by some Imidazoline Derivatives

A. I. Obike^{1,2,3}, P. C. Okafor^{1*}, U.J. Ekpe¹, X. Jiang³ and D. R. Qu³

¹Department of Pure & Applied Chemistry, University of Calabar, P. M. B. 1115, Calabar, Nigeria

²Department of Pure & Industrial Chemistry, Abia State University, Uturu, P. M. B. 2000, Abia State, Nigeria

³SINOPEC Research Institute of Safety Engineering, 218, Yan'an 3rd RD, Qingdao, P. R. China, 266071

[2-(2-Henicos-10-enyl-4,5-dihydro-imidazol-1-yl)-ethyl]-methylamine (HDEM), 2-(2-Henicos-10-enyl-4,5-dihydro-imidazol-1-yl)-ethanol (HDE) and 2-Henicos-10-enyl-4,5-dihydro-1H-imidazole (HDI) were synthesized by assisted organic synthesis (MAOS) method and characterized by FT-IR. The corrosion inhibition properties of these compounds on mild steel L360 in 3.5% NaCl was investigated by weight loss, potentiodynamic polarization, electrochemical impedance and scanning electron microscopic techniques. Results from the study showed that the inhibition efficiency increased with increase in the concentration of the inhibitor to a maximum and decreased with rise in temperature. An adherent layer of inhibitor molecules on the surface is proposed to account for their inhibitive action in which the organic molecules adsorb on the active anodic and cathodic sites following Langmuir isotherm. The effectiveness of these inhibitors has been correlated to their chemical structures and were in the order of HDEM > HDE > HDI. The values of activation energy, free energy of adsorption, heat of adsorption, enthalpy of activation and entropy of activation were also calculated to elaborate the mechanism of corrosion inhibition. The potentiodynamic polarization data show that the compounds studied are mixed type inhibitors. Electrochemical impedance was used to investigate the mechanism of corrosion inhibition. The surface characteristics of inhibited and uninhibited metal samples were investigated by scanning electron microscopy (SEM).

* Correspondence: pcokafor@unical.edu.ng; pcokafor@gmail.com. Tel.: +234-803-429-5604

On the irreversibility of adsorption of volatile corrosion inhibitors and protection of metals against atmospheric corrosion

Goncharova O.A., Nad'kina E.A., Kuznetsov Yu.I.

Russian academy of sciences A.N. Frumkin Institute of Physical chemistry and Electrochemistry RAS (IPCE RAS), Moscow, RF

Increase of the irreversibility of the adsorption of volatile corrosion inhibitors (VCI) necessary to strengthen the protective action of nanosized layers formed by them.

Adsorption and its irreversibility are studied with the help of ellipsometric and electrochemical methods. It has been shown that VCI adsorption together with volatile silanes intensify their protective activity not only in relation to ferrous metals, but also to aluminum alloys and copper.

It has been revealed that in some cases it is more efficient to adsorb VCI and volatile silanes in sequentially, since they form a barrier siloxane layer in the process of their hydrolization in a humid atmosphere.

It prevents not only the VCI desorption, but also penetration of aggressive components from the environment to the metal. This conclusion is confirmed by direct corrosion tests in a humid atmosphere.

Questioning the use of volatile corrosion inhibitors in polymer foils – a comparative study on corrosion protection capabilities

Lars Igetoft, Christian Mille, Sylva Arnell

ABB Corporate Research, Västerås, Sweden.

A common method of protecting products and components from corrosion damage is to use polymer foils. Within ABB, foils are often used to wrap products for protection during transportation to the site and storage until installation. These foils often include volatile corrosion inhibitors (VCI) or added metal grains, both for improved barrier action and corrosion protection. Some foils, designed for very demanding environments, have both VCI and metal grains incorporated. The price of these foils varies greatly, from 0,6 USD/m² for pure polymer up to 7,3 USD/m² for the more expensive products.

In this study, seven commercially available foils have been exposure tested in order to evaluate their corrosion protection capacity. Metal coupons were encapsulated in melt sealed bags from the seven foils. These bags were then exposed to three different test atmospheres.

Bags containing copper coupons and unprotected reference were exposed to a flowing mixed gas test for two months. The reference turned black in a few days while the protected coupons remained unaffected and were unaffected during the exposure. This was the case for all seven foils.

Bags containing zinc coupons and one unprotected reference were exposed in a wooden box outdoors for one year. The reference turned gray-white while all seven protected foils remained unaffected throughout the exposure.

Bags containing steel coupons and one unprotected reference were exposed to a salt accelerated outdoor test for one year. The reference was completely consumed by corrosion after the test period. One coupon had small rust dots across the whole sample, indicating insufficient barrier properties of the foil. Two foils had a hole that came from mechanical damage in the corner which occurred during folding the material. This lead to rust spots close to the holes. The other foils, including the one containing only polymer, were intact.

In conclusion, the most important factor when sealing a material is to make sure no mechanical damage occurs. The foils should not be too thin or sensitive to wrinkles. When it comes to selecting the barrier material, no significant difference in barrier properties or corrosion protection among the seven tested foils could be seen. It is obvious that significant savings can be made by avoiding expensive packing foil. Also, based on the results in this study, the value of adding corrosion inhibitors in packing foils can be questioned.

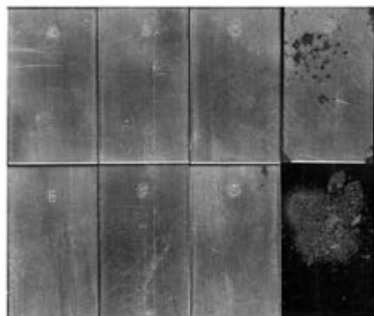


Figure 1. The seven sealed bags (A-G) and the unprotected coupon (bottom right).

Inhibition efficiencies to adsorption thermodynamics: Discussing the value of such measurements

*Robert Lindsay, Cariño Ruiz-Camargo, Monika S. Walczak
University of Manchester, Manchester, UK*

Many studies assessing the corrosion inhibition performance of organic compounds in acidic solutions evaluate inhibition efficiency (IE) as a function of the concentration of the organic species in bulk solution. Typically, it is found from such measurements that IE increases asymptotically up to a limiting value. Often these data are fitted with a function describing an adsorption isotherm (e.g. Langmuir), and a value for the free energy of adsorption is determined. Such work is relatively straightforward, and can apparently provide significant insight into adsorption thermodynamics. However, great care must be taken to ensure the validity of this approach, as there are a number of potential issues, which may lead to erroneous output.

Here, concerns associated with the determination of adsorption thermodynamics from plots of IE versus inhibitor concentration are addressed. Typical assumptions are outlined, and their likely validities are critically discussed. To this end, IE data acquired for mercaptobenzimidazole (MBI) and benzotriazole (BTA) inhibiting the corrosion of carbon-steel in 1 M HCl are presented, and compared to surface coverages extracted from X-ray photoelectron spectra. This comparison indicates that IE is not always directly proportional to surface coverage, which is a necessary prerequisite for reliable elucidation of adsorption thermodynamics. For MBI, for example, IE more rapidly approaches a maximum as a function of inhibitor concentration than surface coverage. This result suggests that active surface sites for corrosion are preferential locations for MBI binding, i.e. the substrate is essentially *fully* inhibited at well below monolayer MBI coverage.

Mitigation of Flow Induced Localized Corrosion with Inhibitors

Günter Schmitt

IFINKOR - Institute for Maintenance and Corrosion Protection Technologies n.f.p.Ltd.
Kalkofen 4, D-58638 Iserlohn, Germany
gue.schmitt@t-online.de

In flowing media corrosion inhibitors mitigate flow induced localized corrosion (FILC) not only by adsorption on solid surfaces but also by decreasing the friction (wall shear stress) between solid surface and the fluid. Due to the drag reducing properties of some corrosion inhibitors the critical wall shear stress for the initiation of FILC can be increased. The mechanism of this effect was not understood for a long time. The problem was that the initiation of FILC generally occurs by a crack/spall mechanism of protective scales or film. However, the wall shear stresses encountered in technical flow systems are several orders of magnitude too small to provide the fracture stresses needed to crack protective scales hydrodynamically.

The “Freak Energy” approach developed in our laboratory offers a solution for this problem. It assumes that high-energy near-wall turbulence elements create freak events which impinge the surface vertically with forces higher than the fracture stress. It was proved that corrosion inhibitors can reduce the impact energy of such freak events below the fracture stress of scales thus preventing initiation of FILC. Mechanistically this phenomenon is explained by flow-induced concentration and aggregation of inhibitor molecules in or near the viscous sublayer of the turbulent boundary layer causing a cushion effect for impinging near-wall turbulence elements. Demands for the molecular structure of drag reducing organic molecules are discussed.

Methodology of laboratory assessment of the efficiency of carbon dioxide corrosion inhibitors in oilfield pipelines

N.N. Andreev, I.S. Sivokon, and S.S. Vesely

*A. N. Frumkin Institute of Physical Chemistry and Electrochemistry, Russian Academy of Sciences, Leninskii pr. 31, Moscow, 119071 Russian Federation
n.andreev@mail.ru*

Oil production and processing are impossible without the application of corrosion inhibitors. The selection of corrosion inhibitors is very broad. The choice of the most efficient products for practical use generally relies on pilot testing that is laborious, time consuming, and expensive. It is no wonder that it is preceded by laboratory testing aimed at rejecting the least efficient products and selecting the most promising ones. Choosing the methods and conditions of laboratory testing acquires primary importance for this purpose.

The typical conditions of corrosion and inhibitor protection in various oilfield pipelines and the capabilities of a broad range of laboratory methods for corrosion testing are compared. The effects of the phase composition of model environments, hydrodynamic conditions, temperature, oxygen concentration, testing duration, corrosion inhibitor concentration, and specimen preparation methods on the kinetics of carbon dioxide corrosion of steel under various model conditions have been studied. The methods and conditions of laboratory estimation of the efficiency of corrosion inhibitors for oilfield pipelines ensuring a rational selection of products for testing under natural conditions have been determined.

Experimental and Theoretical Evaluation of Strawberry Fruit Extract and its Active Component as Corrosion Inhibitor for Mild Steel in HCl

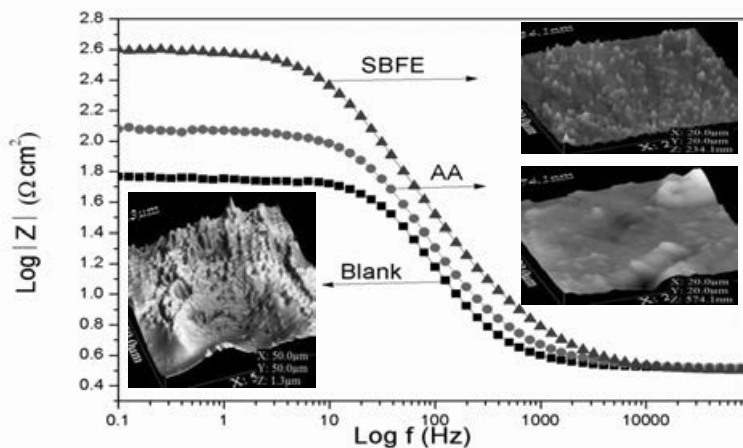
Saviour A. Umoren

Centre of Research Excellence in Corrosion, Research Institute, King Fahd University of Petroleum and Minerals, Dhahran 31261, Kingdom of Saudi Arabia

For correspondence: Email: umoren@kfupm.edu.sa (S.A.Umoren); Phone: +966 3 860 7902; Fax: +966 3 860 3996.

Abstract

The corrosion inhibition effect of strawberry fruit extract (SBFE) for mild steel in 1 M HCl was investigated using gravimetric and electrochemical methods at 25 and 60 °C. Ascorbic acid (AA) the principal constituent of strawberry in its pure form was also studied under the same experimental conditions with the intent of ascertaining its contribution to the overall inhibition effect of SBFE. Results obtained showed that both SBFE and AA inhibited the acid-induced corrosion of mild steel. Inhibition efficiency increased with increase in the concentration of the additives but decreased with increase in temperature. The maximum inhibition efficiency of SBFE and AA were 95 and 79% respectively at the inhibitors' concentration of 2.0 g L⁻¹ at 25 °C from gravimetric measurements indicating that AA contributed about 8% to the overall inhibition effect of SBFE. The enhanced inhibition effect of SBFE could be attributed to synergistic interactions between AA and other components present in SBFE. The potentiodynamic polarization studies revealed that SBFE and AA functions as mixed-type inhibitors. The inhibition was assumed to occur via adsorption of the inhibitor molecules on the mild steel surface which can be approximated by Langmuir adsorption isotherm model. Quantum chemical calculations and molecular dynamics simulations have been used to provide insights into the mechanism of interaction of AA with mild steel. The morphology of the corroding steel surface in the absence and presence of the inhibitors was visualized using scanning electron microscopy (SEM) as well as the atomic force microscopy (AFM) analysis.



Evaluation of two imidazole derivatives as possible green corrosion inhibitors for mild steel: Comparison of simulation with experiment

I. B. Obot

Centre of Research Excellence in Corrosion, Research Institute, King Fahd University of Petroleum and Minerals, Dhahran 31261, Kingdom of Saudi Arabia

Abstract

Corrosion inhibition performances of two imidazole derivatives namely, vinylimidazole (VI) and allylimidazole (AI) for mild steel corrosion in 1 M HCl was predicted theoretically using quantum chemical calculations and molecular dynamics simulations. Global reactivity indicators such as E_{HOMO} , E_{LUMO} , the energy gap ($E_{\text{LUMO}} - E_{\text{HOMO}}$), dipole moment etc., and the local site selectivity such as Fukui indices were computed and correlated with the reactivity of VI and AI. DFT calculations indicated that VI is more reactive towards steel surface than AI. Equilibrium adsorption behaviour of VI and AI molecules on Fe_2O_3 (010) surface was further investigated using molecular dynamics (MD) simulations. The adsorption energy followed the order: VI > AI. Theoretical conclusions were subsequently validated experimentally using potentiodynamic polarization, linear polarization resistance, electrochemical impedance and surface analytical techniques (SEM and AFM). The experimental results indicated that inhibition efficiency depends on the concentration and molecular structure of the investigated compounds. The two compounds acted as mixed-type inhibitors. The studied inhibitors follow Langmuir adsorption isotherm. Surface analysis support the formation of a protective inhibitor film on the steel surface. VI inhibited the corrosion of mild steel effectively than AI. The theoretical prediction agrees well with experimental results.

Keywords: Mild steel, DFT, vinylimidazole, allylimidazole, Molecular Dynamics Simulations.

Email: obot@kfupm.edu.sa (I.B.OBOT); Phone: +966 3 860 8283;

Fax: +966 3 860 3996.

Corrosion mechanism and electrochemical performance of TiO₂ nanostructures synthesized in organic electrolytes at high voltage.

N. Rayón López, M. Vera Jiménez, Cecilia Cuevas Arteaga, FCQI-CIICAp- Universidad Autónoma del Estado de Morelos, Av. Universidad 1001, Col. Chamilpa, 62209, Cuernavaca, Mor., México.

In this work the synthesis and corrosion characterization of TiO₂ nanostructures are reported. The synthesis was made by electrochemical anodization at high voltage using titanium foils exposed in organic electrolytes (glycerol/water/NH₄F) [3-5]. TiO₂ nanostructures have had great interest in recent years due to their exceptional variety in their functional properties and their applications based on the semiconductivity and bio-compatible nature [1,2]. With respect to the synthesis the optimal experimental conditions were obtained (especially anodization time and pre-treatments of titanium foils) [6]. The electrolyte used in this process was glycerol/water (50:50 % Vol) + 0.27M NH₄F. 2x2x0.025 cm, 99.7% purity Ti foils were used, which were mirror polished, degreased through ultrasonically in acetone, iso-propanol, DI water and then dried in a warm stream nitrogen. The anodization process was carried out at 20V using a two electrodes cell, the working electrode (Ti foils) and an auxiliary Pt electrode. The experiments were made at room temperature using a power source equipment. In order to determine the morphology, the TiO₂ nanostructures films were analyzed by scanning electron microscopy. The optimum time was 2:30 h, obtaining nanoporous of 66 nm diameter with a wall thickness of 40 nm (See Fig. 1). In order to determine the electrochemical stability of TiO₂ nanoporous films, the corrosion mechanism was studied exposing the films in an aqueous solution 1M Na₂SO₄. Some electrochemical techniques were applied: polarization curves and electrochemical impedance spectroscopy. As comparison, four samples were studied: pure titanium, passivated titanium through a galvanostatic test, amorphous TiO₂ nanostructures, and crystallized TiO₂. Electrochemical techniques showed that both TiO₂ nanostructures presented a better corrosion resistance than that of pure and passivated Ti, showing a smaller density corrosion current and a major charge transfer resistance, especially that crystallized. Nyquist diagram presented a semi-circle behavior, which means that the controlled process was by activation. It can be concluded that dissolution of TiO₂ in a nanostructured form is rarely observed. Fig. 1.a shows the TiO₂ nanostructured film obtained at an optimal time of 2:30 h, whereas Fig. 1.b shows the dissolution of TiO₂ nanostructure after 2:40 h of anodization, which means that these films are susceptible to dissolution in the electrolyte contained ammonium fluoride.

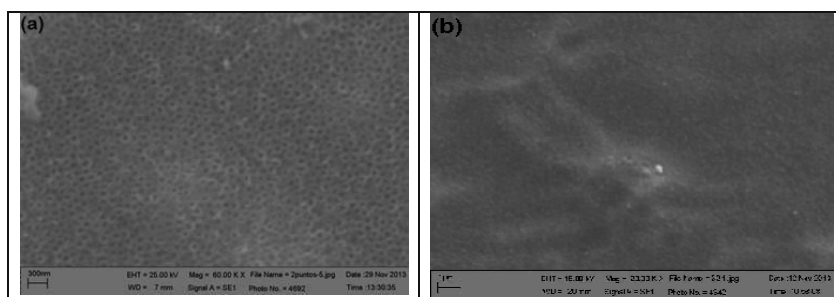


Fig. 1. TiO₂ nanostructured (a), and TiO₂ dissolved (b) when exposed in an electrolyte of glycerol/water/NH₄F.

Electrochemical and XPS studies of the corrosion inhibition of carbon steel in phosphoric acid pickling solutions by purpald

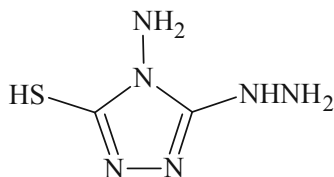
Michel Traisnel^a, Charafeddine Jama^a, Fouad Bentiss^{a,b}, Belkheir Hammouti^c

^a UMET-ISP, CNRS UMR 8207, ENSCL, Université Lille Nord de France, BP 90108, F-59652 Villeneuve d'Ascq Cedex, France

^b Laboratoire de Catalyse et de Corrosion des Matériaux (LCCM), Faculté des Sciences, Université Chouaib Doukkali, B.P. 20, M-24000 El Jadida, Morocco

^c LCAE-URAC18, Faculté des Sciences, Université Mohammed I^{er} B.P. 717, M-60000 Oujda, Morocco

In continuation of our work on development of triazole derivatives as corrosion inhibitors in acidic media, we have studied the corrosion inhibiting behaviour of purpad, namely 4-amino-3-hydrazino-5-mercapto-1,2,4-triazole (AHMT), on carbon steel in phosphoric acid (2 M H₃PO₄) medium. In the present work, the corrosion inhibition properties of purpald (AHMT)) on carbon steel in 2 M H₃PO₄ solution has been examined and characterized by weight loss, Tafel polarization, electrochemical impedance spectroscopy (EIS) and X-ray photoelectron spectroscopy (XPS) methods.



AHMT

The experimental results reveal that the compound has a good inhibiting effect on the carbon steel in 2 M H₃PO₄ solution. The protection efficiency increases with increasing inhibitor concentration, but the temperature has hardly effect on the inhibition efficiency of AHMT. The adsorption of AHMT is found to obey the Langmuir adsorption isotherm. Thermodynamic data and XPS analysis clearly show that the adsorption mechanism of AHMT on carbon steel surface in 2 M H₃PO₄ solution is mainly electrostatic-adsorption. Potentiodynamic polarization studies have shown that AHMT acts as a mixed-type of inhibitor. Data obtained from EIS studies were analyzed to model inhibition process through appropriate equivalent circuit model.

Inhibition of mild steel corrosion in acidic medium by Vanillin cationic surfactants

Ismail Aiad, Mohamed M. El-Sukkary, Samy, M. Shaban

Sayied Soliman, Moshira Y. El-Awady,*

Petrochemical Department, Egyptian Petroleum Research Institute,

**Faculty of Science, Ain Shams University, Cairo, Egypt*

Abstract

Three cationic surfactants based on Schiff base were laboratory prepared. These compounds are N-(3-((4-hydroxy-3-methoxybenzylidene)amino)propyl)-N,N-dimethyldecan-1- ammonium bromide (I), N-(3-((4-hydroxy-3-methoxybenzylidene)amino)propyl)-N,N-dimethyldodecan-1- ammonium bromide (II) and N-(3-((4-hydroxy-3-methoxybenzylidene)amino)propyl)-N,N-dimethylhexadecan-1- ammonium bromide (III). The chemical structure was confirmed by different techniques, FTIR, ¹HNMR and mass spectroscopy. Three techniques were used for the corrosion inhibition evaluation, namely; weight loss, polarization and electrochemical impedance. The serial dilution method was used to evaluate the inhibiting effect of these compounds on Bacterial growth. The results showed that the prepared compounds have good antimicrobial activities against gram positive and gram negative bacteria and fungi as well as they have higher efficiency as corrosion inhibitors for carbon steel in 1.0 M HCl.

Key Words:

Corrosion inhibition, biological activity, cationic surfactants

Assessment of the corrosion inhibitors effectiveness and their influence on the concrete physical properties

F. M. A. Moreira ^a, C. Resende ^{a*}, A. F. Diniz ^a, H. F. Gorgulho ^a, A. H. S. Bueno ^a, P. B. Martelli ^a

^a Universidade Federal de São João Del Rei, Departamento de Engenharia Mecânica, Praça Frei Orlando 170, CEP 36.307-352 - São João Del Rei, Minas Gerais, Brasil.

Abstract

This study investigated the influence of two corrosion inhibitors on the mechanical properties of reinforcing concrete. In that case, the variation of the mechanical properties after the addition of inhibitors in concrete were evaluated by the compressive strength and modulus of elasticity tests. In addition, potentiodynamic polarization curves, measurements of potential versus time and electrochemical impedance tests were performed to assess the effectiveness of inhibitors against corrosion caused by chloride ions. It was observed that the inhibitor sodium nitrite induced reduction of concrete compressive strength. Higher passivation domain in polarization tests and higher impedance values were obtained for solutions with inhibitors when compared to the solution without inhibitor. Testing of scanning electron microscopy and optical microscopy confirmed the results obtained in the electrochemical tests for all inhibitors. In other words, the surface metals tested without corrosion inhibitors presented more quantities of pitting corrosion than the conditions with inhibitors.

Electrochemical studies of the inhibition effect of 2-dimethylamine on the corrosion of austenitic stainless steel type 304 in dilute hydrochloric acid

R.T. Loto^{a,b*} and C. A. Loto^{a,b}

^aDepartment of Mechanical Engineering, Covenant University, Ota, Ogun State, Nigeria;

^bDepartment of Chemical, Metallurgical & Materials Engineering, Tshwane University of Technology, Pretoria, South Africa

*tolu.loto@gmail.com

+2348084283392

The inhibiting action of 2-dimethylamine on the electrochemical behaviour of austenitic stainless steel (type 304) in dilute hydrochloric was evaluated through weight-loss method, open circuit potential measurement and potentiodynamic polarization tests at specific concentrations of the organic compound. Results obtained reveal that the compound performed effectively giving a maximum inhibition efficiency of 79% at 12.5% concentration from weight loss analysis and 80.9% at 12.5% concentration from polarization tests. The average corrosion potential of -321 mV was obtained the same concentration from other tests which is well within passivation potentials on the steel thus, providing good protection against corrosion in the acid solutions. 2-dimethylamine acted through physiochemical interaction at the steel/solution interface from thermodynamic calculations and obeyed the Langmuir adsorption isotherm. The values of the inhibition efficiency determined from the three methods are in reasonably good agreement. Polarization studies showed that the compounds behaved as cathodic type inhibitor.

Keywords: corrosion; 2-dimethylamine; inhibition; adsorption; hydrochloric acid.

Inhibition efficiency by an aqueous extract of flower petals of cassia auriculata on corrosive carbon steel

S. Rajendran^{1,2*}, M. Sangeetha¹, J. Sathiyabama¹

1. PG and Research Department of Chemistry, GTN Arts College, Dindigul – 624005, Tamil Nadu, India, E-mail:sangeethamanirevathi@gmail.com
2. Corrosion Research Centre, Department of Chemistry, RVS School of engineering and Technology, Dindigul – 624005, E-mail:srmjoany@sify.com

Abstract

The inhibition efficiency (IE) of flower petals of cassia auriculata extract (CAE)-Zn²⁺ system in controlling corrosion of carbon steel in an aqueous solution has been evaluated by weight loss method. Weight loss study reveals that the formulation consisting of 8 ml of CAE and 25 ppm of Zn²⁺ has 95% inhibition efficiency in controlling corrosion of carbon steel immersed in an aqueous solution. Synergistic parameters suggest that a synergistic effect exists between CAE and Zn²⁺. Polarization study reveals that this formulation controls the anodic reaction predominantly. AC impedance spectra reveal that a protective film is formed on the metal surface. The FTIR spectra reveal that the protective film consists of Fe²⁺-Di-(2-ethyl) hexyl phthalate complex.

Key words: Corrosion inhibition, carbon steel, green inhibitor, environmentally friendly inhibitor, cassia auriculata

Sodium potassium tartrate (SPT) as a corrosion inhibitor for aluminium

M. Hakeem, Department of Chemistry, Hajee Karutha Rowther Howdia College, Uthamapalayam, Theni District, Tamil Nadu, sheikhchandra@rediffmail.com

S. Rajendran, Department of Chemistry, RVS School of Engineering and Technology, Dindigul-624005, Tamil Nadu, India, srmjoany@sify.com

Peter Pascal Regis, Associate Professor, Department of Chemistry, St. Joseph's College, Tiruchirappalli – 620002, srisrielango@rediffmail.com

Abstract

The present study is to use sodium potassium tartrate (SPT) as corrosion inhibitor for aluminium in an aqueous solution containing 60 ppm Cl^- ion was chosen as the inhibitor. Zn^{2+} is selected as the synergist, as Zn^{2+} ions in association with SPT inhibitor is considered environmental friendly inhibitor for aluminium corrosion in alkaline (pH=11) media. The environment chosen is aqueous solution containing 60 ppm Cl^- ions. To investigate the nature of the protective film, surface analytical techniques such as, Scanning Electron Microscopy (SEM), Atomic Force Microscopy (AFM) have been studied. The formation of protective film has been confirmed using the electrochemical techniques such as polarization study and AC impedance spectral study. The above studies support the weight loss study.

Corrosion resistance of austenitic and duplex stainless steels in chloride containing alkaline environments

*Heljä Peltola, Mika Martikainen, Mari Lindgren
Outotec Research Center, Pori/Finland*

In the industrial water treatment applications, stainless steels are normally used as a material of construction in the most aggressive environments containing high levels of chlorides. The combined effect of chlorides with the other constituents of industrial waters is still somewhat unknown, as the dissolved ions and the prevailing temperature may affect on the corrosion rates. Five stainless steels were laboratory tested in water solutions corresponding to several kinds of industrial waters. The grades included the austenitic stainless steels 304 and 316L, and the duplex stainless steels LDX2101, 2304, and 2205. Gypsum water with different pH values and with different chloride, sulfate, calcium and sodium contents was prepared and used as the corrosive media at various temperatures. Reference tests in cation free aqueous solutions with high levels of chlorides and varying pH were conducted for 316L and LDX2101 as well. The samples equipped with crevice formers were immersed in the test solutions for four weeks. After the tests, the uniform corrosion rates were calculated from the weight losses, and the existence of pitting and crevice corrosion on the surfaces was investigated by microscopy. The effects of cations, chloride concentration, pH, and temperature are described. The differences in the pitting behavior of 316L and LDX2101 are discussed.

Adsorption and passivation of copper in neutral solutions by some heterocyclic corrosion inhibitors

*Kuznetsov Yu.I., Agafonkina M.O., Andreeva N.P.,
Institute of Physical Chemistry and Electrochemistry RAS
yukuzn@gmail.com*

Triazoles are well known class of corrosion inhibitors for copper, in particular 1,2,3-benzotriazole (BTA), its chloro derivative - 5-chloro-BTA and 3-amino-1,2,4-triazole (3-AT). The passivation of copper by triazoles in neutral solutions and its stabilization in the presence of corrosive anions begins with their adsorption. The ellipsometric method is used to evaluate its adsorption in borate buffer pH 7.4 at the applied potential $E = 0.0$ V (NHE).

The adsorption of 5-chloroBTA is shown to begin at concentrations $\lg C_{in}$ (mol/l) = -10.0, and is not limited to the formation of a monolayer. With increasing inhibitor concentration a multilayer coverage of a surface takes place. For 5-chloroBTA and 3-AT, the free adsorption energy for a monolayer ($-\Delta G_a^0$) is obtained equal to 58.7 and 55.5 kJ/mol, respectively. This is somewhat higher than calculated ($-\Delta G_a^0$) = 50.5 kJ/mol for BTA. That suggests chemisorption of the inhibitor on the copper surface.

Another noteworthy class of heterocyclic inhibitors of copper corrosion are porphyrins. Recently, we have shown that for the passivation of copper in chloride solutions ($C_{Cl^-} = 10^{-2}$ mol/l) only 10^{-5} mol/l (6.8 mg/l) of protoporphyrin IX - dimegin, (disodium salt of dicarboxylic acid) are needed that is 3 orders of magnitude lower than a concentration of the aggressive Cl^- [1]. The protective properties of dimegin are also superior to BTA, and its adsorption on copper has a high value ($-\Delta G_a^0$) = 55.5 kJ/mol. Due to its chemisorption on copper the dimegin may be used as a surface modifier for subsequent adsorption of triazoles on it. Thus, if the pre-adsorbed on the copper with 0.4 monolayer of dimegin ($\lg C = -7.70$), it improves the adsorption of BTA: its (ΔG_a^0) increases from 50 kJ/mol to 63 kJ/mol.

Corrosion tests of copper in a chamber with periodic water condensation have shown that without passivation treatment with aqueous solution of inhibitor, the first corrosion spots on the surface appear as early as 2 days. When treated by 1 mmol/l BTA solution the corrosion does not begin until 11 days, and when preliminary treated by dimegin with $C = 0.04$ mol/l ($\lg C = -7.40$, coverage $\Theta = 0.17$ obtained from the adsorption isotherm) and then treated by BTA ($C = 1$ mmol/l), copper remains fully protected during 19 days.

1. Yu. I. Kuznetsov, M. O. Agafonkina, N. P. Andreeva, and A. B. Solov'eva
Modification of Iron Surface by Dimegin and Adsorption of 1,2,3-Benzotriazole //
Protection of Metals and Physical Chemistry of Surfaces, 2010.- Vol. 46.- N 7.-P.
807-811

CONVERSION COATINGS OF LANTHANIDE SALTS ON ALUMINIUM ALLOY AS A POTENTIAL REPLACEMENT OF CHROMATE COATINGS

Barbara Volarič, Ingrid Milošev, Department of Physical and Organic Chemistry, Jožef Stefan Institute, Jamova cesta 39, 1000 Ljubljana, Slovenia

Aluminium alloy 7075-T6 is due to the good physical and chemical properties commonly used material in different applications in industry. To protect aluminium alloys against corrosion chromate conversion coatings have been applied for many decades.¹ Today their use is strongly restricted due to toxicity. As alternative, rare earth salts, especially cerium, have been identified.² Lanthanide compounds are environmental friendly, their price is reasonable and are available in natural sources. The aim of this study was to investigate various lanthanide salts as potential corrosion inhibitors for AA7075-T6. Conversion coatings were prepared using 0.01 M chloride and nitrate lanthanide salts, i.e., cerium chloride, cerium nitrate, lanthanum chloride and lanthanum nitrate, at room temperature and at 60 °C with the addition of hydrogen peroxide. The corrosion properties of bare substrate and substrates modified by conversion coatings were studied by electrochemical measurements in 0.1 M NaCl solution. Surface morphology and composition of the coatings were also analyzed, and corrosion protection was confirmed by testing in salt spray chamber.

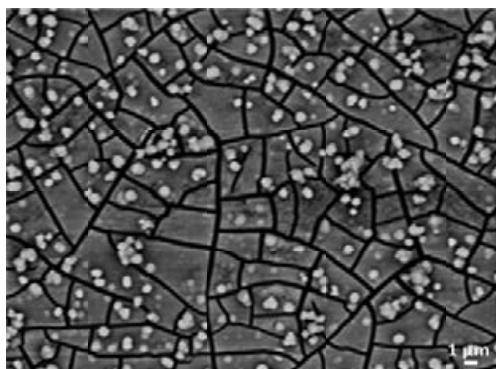


Figure 1: SEM image of CeCl₃ conversion coating deposited at room T.

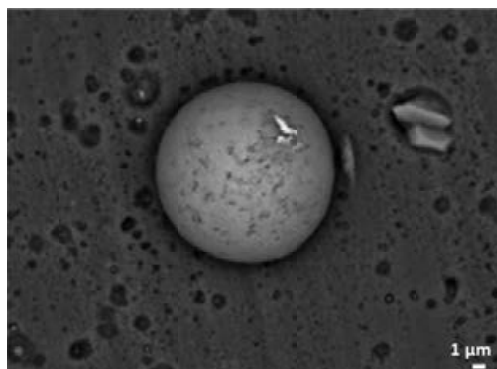


Figure 2: SEM image of LaCl₃ conversion coating deposited at room T.

Reference:

1. M. W. Kending, R.G. Buchheit, Corrosion Inhibition of Aluminum and Aluminum Alloys by Soluble Chromates, Chromate Coatings, and Chromate-Free Coatings, *Corrosion*, **2003**, Vol. 59, No. 5, 379-400.
2. M. Bethencourt; F. J. Botana, J. J. Calvino, M. Marcos, M. A. Rodríguez-Chacón, Lanthanide Compounds as Environmentally-friendly Corrosion Inhibitors of Aluminium Alloys: a Review. *Corrosion Science*, **1998**, 40, 1803–1819.

Green corrosion inhibition from aqueous extract of *Zygophyllum Album L* for carbon steel in hydrochloric acid medium

H. Derfouf-Talbi, Bechar University, Bechar/ Algeria, Y. Harek, Aboubakr Belkaid University, Tlemcen/ Algeria.

Abstract:

The use of inhibitors for the control of corrosion of metals and alloys which are in contact with aggressive environment is an accepted practice. Large numbers of organic compounds were studied and are being studied to investigate their corrosion inhibition potential. But, unfortunately most of these compounds are not only expensive but also toxic to living beings. In recent days many alternative eco-friendly corrosion inhibitors have been developed. Plant extract have become important because are biodegradable and environment friendly. They are the rich sources of ingredients which have very high inhibition efficiency.

The efficiency of *zygophyllum album L* aqueous extract as a corrosion green inhibition for carbon steel in acid medium (1M HCl) was investigated by gravimetric and electrochemical measurements. According to the experimental results, *Zygophyllum Album L* extract acts as a good corrosion inhibitor, value of inhibition efficiency attains approximately 89 %. Inhibition on metal surface was verified by plotting Langmuir's adsorption isotherm. Scanning electron microscopy observation of the steel surface confirmed the protective roles of the inhibitor.

Key words: Corrosion. Green inhibitor. *Zygophyllum Album L*. Polarization. Hydrochloric acid.

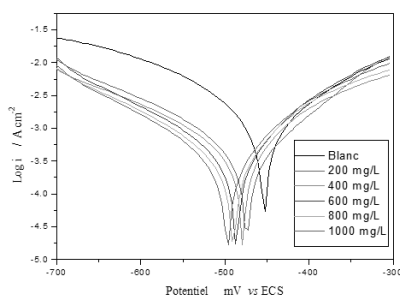
Results and Discussion

Inhibition efficiency increased with increasing inhibition concentration (Table.1.). Polarization curves with and without inhibitor indicated that the inhibitor works in cathodic mode of inhibition (Figure.1.).

Table 1: corrosion rate and inhibition efficiency

Concentration (mg/l)	W_{cor} ($10^{-3} \cdot g \cdot h^{-1} \cdot cm^{-2}$)	P(%)
0	0,77730	-
200	0,17806	77,31
600	0,09184	88,11
800	0,10045	88,29
1000	0,08827	88,71

Figure.1. Polarization curves for carbone steel in 1M HCl containing different concentration of *Zygophyllum Album L*



Novel cationic surfactant based on triazole as a corrosion inhibitor for carbon steel in phosphoric acid produced by dihydrated wet process

M.A. Hegazy*

Egyptian Petroleum Research Institute (EPRI), Nasr City 11727, Cairo, Egypt

Abstract

The corrosion inhibition effect of Novel cationic surfactant based on triazole derivatives on carbon steel in 7 M H_3PO_4 solution has been evaluated by weight loss, potentiodynamic polarization, electrochemical impedance spectroscopy (EIS) and scanning electron spectroscopy (SEM) methods. The inhibition efficiency increases with increasing inhibitor concentration, but it decreases with increasing temperature. The adsorption of inhibitor is physical adsorption and found to obey the Langmuir adsorption isotherm. Potentiodynamic polarization studies have shown that inhibitor acts as a mixed type of inhibitor. Data obtained from EIS studies were analyzed to model inhibition process through appropriate equivalent circuit model. SEM images indicate that the synthesized cationic surfactant has good performance on corrosion inhibition of carbon steel in 7 M H_3PO_4 .

Keywords: Carbon steel; Weight loss; Polarization; EIS; SEM; Adsorption.

Effect of Zr on intergranular corrosion of low Cr ferritic stainless steel

Jin Ho Park, Kyoo Young Kim

Graduate Institute of Ferrous Technology, Pohang University of Science and Technology (POSTECH), Pohang 790-784, KOREA

The intergranular corrosion (IGC) of stainless steel is commonly known to occur due to Cr-depletion in grain boundary area by formation of Cr-carbide. The general commercial practice to prevent IGC is to add stabilizers, such as Ti and/or Nb. However, IGC still occurs in stabilized ferritic stainless steel (FSS). Our previous study suggested IGC mechanism of Ti-Nb stabilized low-Cr FSS by intergranular Cr segregation without formation of Cr-carbide[1]. According to this new mechanism, new alloy design will be suggested.

Zr has higher C affinity than conventional stabilizers, such as Ti and Nb, and it is good intermetallic compound former such as Fe-Zr intermetallic compounds. Therefore, Zr can be one of the candidates for preventing IGC of low-Cr FSS. In this study, effect of Zr on IGC of low-Cr FSS will be investigated.

By comparing Nb, Ti-Nb and Zr stabilized FSS, only Zr stabilized specimen prevent intergranular sensitization and consequent IGC. TEM and 3DAP analysis indicate that Zr forms ZrC and $\text{Fe}_{23}\text{Zr}_6$ along grain boundary during heat treatment, and they prevent IGC by two-fold effect; one as a strong carbide former to inhibit formation of Cr-carbide and the other as diffusion barrier against the solute Cr diffusion toward grain boundary.

Orange peel as green corrosion inhibitor – Assessment of hesperidin, naringin and synephrine efficiency

M. V. C. Monteiro¹, J. C. da Rocha¹, J. A. C. Ponciano Gomes¹

¹Federal University of Rio de Janeiro-LabCorr, Rio de Janeiro/Brazil

The use of inhibitors is one of the most practical methods for protecting against the corrosion in acidic media. Inhibitors protect the metals by getting effectively adsorbed on its surface, blocking the active sites of metal dissolution and/or hydrogen evolution, thereby retarding overall metal corrosion in aggressive environments. Currently, a lot of research has focused on plants to extract natural inhibitors that can replace synthetic compounds. But, there are few researches about the use of by-product as green corrosion inhibitor. This study investigated the possibility of using natural extracts obtained from domestic / industrial by-products as corrosion inhibitors of carbon steel in acidic media. In Brazil, fruit processing for the extraction of juices creates a large amount of by-product from the industrial processing, such as seeds and peels. These by-products have attracted considerable scientific interest for their potential use as natural antioxidants. Therefore, the possibility of using industrial waste as a corrosion inhibitor is quite interesting due to economics and environmental aspects. The use of aqueous extracts of fruit peels as inhibitors adds value to the residues of the juice industry, in addition to being environmentally friendly, orange peels are rich sources of antioxidant compounds such as polyphenols, carotenoids and vitamins C and E. The major constituents in orange peel are flavonoids, specially hesperidin, naringin and alkaloids, mainly synephrine. On the previous work, the orange peel extract was characterized by Fourier transform infrared (FTIR) spectroscopy, using the KBr disk technique in order to identify the major containing molecules. The inhibitive action of the aqueous extracts of orange peel against corrosion of carbon steel in a 1 M HCl solution was previously investigated using electrochemical techniques, such as anodic and cathodic polarization curves and electrochemical impedance. It was concluded that this extract significantly reduced the corrosion rate of a carbon steel. Thus, the inhibitory effect observed in polarization curves and electrochemical impedance diagrams results likely occurs via the adsorption of the phenolic compounds present in the orange peel extracts onto the steel surface. However the obtained results obtained with separate molecules - hesperidin, naringin and synephrine - do not seem to explain the corrosion inhibition observed with the orange peel extract. Probably other components present in the orange peel extracts might have promoted the observed inhibition effect and that a complex synergistic relationship between the major constituents and other components of orange peel may have been responsible for the inhibition efficiency.

Influence of the lithium molybdate inhibitor on the corrosion resistance of a duplex stainless steel in LiBr absorption machines

*M.J. Muñoz-Portero, J. Rubio-Cervera, R. Leiva-García, J. García-Antón
Universidad Politécnica de Valencia, Camino de Vera s/n 46022 Valencia/Spain*

Introduction

Lithium Bromide (LiBr) is one of the most widely used absorbents in refrigeration technology. However, the operating conditions can generate corrosion problems in the structural materials. The addition of inhibitors in the medium can decrease these corrosion problems. Duplex stainless steel could be employed in LiBr absorption machines due to their good mechanical properties and corrosion resistance. The aim of this work is the study of the influence of the lithium molybdate inhibitor in the corrosion resistance of a duplex stainless steel on concentrated lithium bromide solutions.

Experimental procedure

Cyclic potentiodynamic curves and electrochemical impedance measurements at open circuit potential (OCP) of samples of Alloy 900 (EN 1.4462) were carried out in LiBr solutions at two concentrations (400 g/L and 992 g/L) in the absence and in the presence of different concentrations of lithium molybdate inhibitor (5, 10, 15, and 20 ppm) at 25 °C. After the tests, images of the electrode surface were obtained using the laser scanning confocal microscope.

Results

According to the cyclic potentiodynamic curves, the corrosion current density of Alloy 900 decreases with the concentration of lithium molybdate inhibitor. Corrosion potential and pitting potential of Alloy 900 move to a more positive value with the increase in the concentration of lithium molybdate inhibitor.

On the other hand, electrochemical impedance measurements were carried out in the different test conditions. All the measurements were fitted to an equivalent circuit in order to obtain the different electrochemical parameters of the passive films. According to the results obtained the polarisation resistance of Alloy 900 increases with the concentration of lithium molybdate inhibitor; these results are in agreement with those observed in the cyclic potentiodynamic curves.

Furthermore, the corrosion resistance of Alloy 900 increases with the concentration of lithium molybdate inhibitor.

Acknowledgements: We wish to thank to UPV (CEI-01-11), to FEDER, to Programas de Apoyo a la Investigación y Desarrollo (PAID-06-10) de la UPV, to MICINN (CTQ2009-07518), and to Dr. Asunción Jaime for her translation assistance.

2HEABu corrosion-inhibitor action in aggressive medium on API X70 substrate.

Maria Rita Ortega Vega, Universidade Federal do Rio Grande do Sul, Porto Alegre/Brazil; Sandra Raquel Kunst, Universidade Federal do Rio Grande do Sul, Porto Alegre/Brazil; Silvana Mattedi, Universidade Federal da Bahia, Salvador/Brazil; Miguel Iglesias, Universidade Federal da Bahia; Célia de Fraga Malfatti, Universidade Federal do Rio Grande do Sul, Porto Alegre/Brazil.

Protic Ionic Liquids (PILs) are organic compounds, liquid at room temperature and formed by an anion and a cation, given by the reaction of a carboxylic acid and an amine. PILs show interesting properties when in contact with a metallic substrate, since they are adsorbed on its surface which insulates the metal from aggressive media; i. e. PILs are suitable as adsorption-type corrosion inhibitors.

The aim of this paper is to study the electrochemical behaviour of the addition of different concentrations of the PIL 2-hydroxiethylammonium butanoate (2HEABu) in a 0.01 NaCl solution, to evaluate the corrosion inhibition performance for this PIL in an aggressive medium. The chosen substrate is API X70 steel, which is a widely used material in the oil and gas industry. 2HEABu was chosen as corrosion inhibitor because, in former works, it shows a good electrochemical performance in aqueous medium; so, it is necessary to find the most adequate concentrations to obtain optimal corrosion protection.

2 cm x 2 cm API X70 steel plates need to be cleaned, sanded, washed and dried. Wettability tests will be carried out to evaluate the surface interaction between the substrate, the PIL and the NaCl solution. Electrolytic solution were constituted by 0.01 M NaCl solution with addition of 2HEABu in concentrations of 100, 1000, 10000 ppm; in order to compare, tests with 0.01 M NaCl and 50 wt% 2HEABu were conducted. To evaluate the electrochemical performance, open circuit potential monitoring and electrochemical impedance spectroscopy were carried out for different immersion times (1, 3, 5, 24 and 48 hours, 1 and 2 weeks). Samples morphology after the electrochemical tests was evaluated by scanning electronic microscopy (SEM).

Preliminar results shown that the OCP for API X70 substrate in NaCl 0.01 M solution with addition of 50 wt% 2HEABu presented a less active OCP compared to the NaCl 0.01 M solution without ionic liquid addition. However the impedance results showed a progressive variation of the electrochemical behaviour with the immersion time, which represents that the different barrier effect modifications that take place. The higher the concentration of 2HEABu in the electrolytic solution the more inhibited corrosion of the substrate.

Inhibition Efficiency of 3,4-diaminobenzonitrile Against Steel Corrosion

Gökmen Sığircık, Tunç Tüken, Mehmet Erbil

Çukurova University, Science & Arts Faculty, Chem. Dept., 01330, Adana, Turkey

Inhibitor application is one of the most convenient ways for slowing down and/or get under control corrosion in various industrial applications. The efficiency of an inhibitor is strictly related to its molecular structure. Organic molecules functionalized with electronegative functional group and aromatic ring are mostly used as corrosion inhibitor; nitrile, azole and thiol compounds etc. These molecules are strongly adhered to metal surface and block the active centers, generally forming a protective film. Therefore, most of the inhibitor compounds are designed in order to have these kinds of functional groups and additional substituents for tailoring the surface properties of protective film. Amine substituted benzonitrile compounds are also generally pronounced as good inhibitor for steel and its alloys. Since, amine compounds are also known as film generating inhibitor compounds on various metals, especially on copper.

In this study, the inhibition efficiency of 3,4-diaminobenzonitrile has been investigated for mild steel corrosion in 0.5M HCl solution. The effect of amine groups, regarding to their position with respect to nitrile group has been discussed. Electrochemical impedance spectroscopy and potentiodynamic measurements were realized for different concentration and temperature conditions, for understanding the inhibition mechanism against steel corrosion. Besides, surface analysis was also carried out by scanning electron microscopy technique, for illumination of the surface exposed to corrosive environment. All the results showed that this inhibitor has a good inhibition effect on mild steel in 0.5 M HCl solution.

References

1. K.S. Jacob, G. Parameswaran, Corrosion Science 52 (2010) 224-228.
2. M. Gopiraman, N. Selvakumaran, D. Kesavan, R. Karvembu, Progress in Organic Coatings 73 (2012) 104-111.

Inhibitive Effect a new prepared Quinoline Derivative on the Corrosion of mild Steel in NaCl solution

Nazly Hassan¹, Reda M. El-Shishtawy^{2,3} and Said Khalil⁴

¹Composites and Nano Structured Dept., New materials and advanced Technology Institute, City of Scientific Research and Technology Applications, New Borg Elarab, Alexandria, Egypt. E.mail: na_hassan12@yahoo.com

²Chemistry Department, Faculty of Science, King Abdulaziz University, P.O. Box 80203, Jeddah 21589, Saudi Arabia.

³Dyeing, Printing and Textile Auxiliaries Department, Textile Research Division, National Research Center, Dokki, Cairo 12622, Egypt e.mail: elshishtawy@hotmail.com

⁴Faculty of Science, Department of chemistry, Alexandria University, Alexandria, Egypt.
e.mail: chemistsaidmohamed@yahoo.com

Abstract:

Since N and O-containing compounds have been described as good inhibitors to reduce the corrosion rate of metals, we designed a Quinoline-8-carboxamide derivative to investigate its inhibition effect on the corrosion behavior of mild steel in 3.5% sodium chloride solution. The influence of the prepared compound as corrosion inhibitor was examined by means of weight loss, potentiodynamic polarization and electrochemical impedance spectroscopy. The inhibition efficiency was found to vary with the inhibitor concentration and bath temperature. The achieved data proved that the compound has a good anticorrosive activity. Thermodynamic parameters for the inhibition process were also calculated and discussed

Keywords: Corrosion inhibition, Steel, new Inhibitor, weight loss, polarization, EIS

***Rosmarinus officinalis* use as eco-friendly corrosion inhibitor carbon steel in acid solution**

Ma. Abigail Velázquez González¹, José Gonzalo González Rodríguez¹, Ma. Guadalupe Valladares Cisneros¹.

¹Universidad Autónoma del Estado de Morelos

Av. Universidad 1001, col. Chamilpa, C.P.62209, Cuernavaca, Morelos

aby_purple0411@hotmail.com; ggonzalez@uaem.mx; mgpevalladares@gmail.com

The hexanic extract of *Rosmarinus officinalis* was evaluated as a corrosion inhibitor of carbon steel, exposed to a 0.5 M H₂SO₄ aqueous solution. Used techniques weight loss, polarization curves and electrochemical impedance spectroscopy (EIS), which were applied to different concentrations (100, 200, 400, 600, 800 and 1000 ppm) and different temperatures (25°C, 40°C and 60°C). The results revealed that the hexanic extract of *Rosmarinus officinalis* acted as a mixed type of inhibitor with cathodic effects. The *R. officinalis* showed a maximum efficiency of 99.57%, as corrosion inhibitor, at a temperature of 25°C with a concentration of 1000 ppm. It was also observed that the efficiency of *R. officinalis* as corrosion inhibitor for carbon steel increased with increasing its concentration, also the temperature dropped the inhibitory action of *R. officinalis*, since a drop in the efficiency was observed with increasing temperature.

The effect of chloride concentration on copper protection

Nur Kıcı, Tunç Tüken, Mehmet Erbil

nurkicir@hotmail.com, ttuken@cu.edu.tr, merbil@cu.edu.tr

Çukurova University, Science & Arts Faculty, Chem. Dept., 01330, Adana, Turkey

The success of inhibitor application for copper protection is highly sensitive against temperature and composition of corrosive environment. Different corrosion mechanisms work for copper, depending on pH and presence of species like chloride, mercapto functionalized organics etc. During the copper corrosion, primarily generated Cu (I) ions are able to make many insoluble complex structures on the surface and directly influence the mechanism. Cu (I) chloride is one of the most stable compound being formed on the surface, whenever copper is subjected to corrosion in chloride solution. Therefore the chloride concentration is crucial for the efficiency of organic inhibitor on the metal surface. Ionic liquids (ILs) are involved with organic and inorganic groups. ILs offer very extreme physico-chemical properties, good thermal stability, low vapour pressure, high electrical conductivity. Moreover, various non-toxic imidazolium derivatives have been reported recently, for their effective inhibitory performance against steel corrosion. In this study, the effect of chloride concentration was investigated on inhibitory effect of 1-ethyl-3-methylimidazolium dicyanamide (EMID) on copper, statistically. The chloride and inhibitor concentrations were selected as independent variables which determine the corrosion rate.

The inhibition efficiency of EMID was investigated against copper corrosion in 0.1 M HCl and 0.1 M H₂SO₄ solutions. The behaviour of copper with EMID, its protection mechanism and effect of chloride ions was discussed in several NaCl concentrations (10-100 ppm) containing in the presence and absence of 50 mM EMID solutions 0.1 M H₂SO₄ at various temperatures (25-50°C). The electrochemical impedance spectroscopy (EIS) and atomic absorption spectroscopy (AAS) were utilized for evaluating the chloride concentration effect. In order to investigate the morphology and structural composition of the surface energy-dispersive X-ray spectroscopy (EDX) and scanning electron microscopy (SEM) analysis were realized. In the presence of chloride ions, the surface is covered with CuCl protective layer which is stable and insoluble compound and so blocking copper surface. The SEM and EDX analysis showed that the surface was covered with Cu-EMID complex film. In fact, CuCl may be formed in defective areas of the Cu-EMID complex film so Cu-EMID complex film together with CuCl was protected the surface successfully. Since the Cu (I) chloride complex made contribution to corrosion protection too, the critical chloride quantities were discussed, for effective protection and corrosive risk.

Keywords: Copper, Chloride ions, 1-ethyl-3-methylimidazolium dicyanamide.

References:

1. T. Tüken, N. Kıcı, N. T. Elalan, G. Sığircık, M. Erbil, Appl. Surf. Sci. 258 (2012) 6793-6799.
2. T. Tüken, F. Demir, N. Kıcı, G. Sığircık, M. Erbil, Corros. Sci. 59 (2012) 110-118.
3. M. M. Antonijevic, S. M. Milic, M. B. Petrovic, Corros. Sci. 51 (2009) 1228-1237.

Three novel bolaamphiphiles as corrosion inhibitors for carbon steel in hydrochloric acid: experimental and computational study

M.A. Hegazy^a and M.K. Awad^b

^a *Egyptian Petroleum Research Institute (EPRI), Nasr City 11727, Cairo, Egypt*

^b *Chemistry Department, Theoretical Applied Chemistry Unit (TACU), Faculty of Science, Tanta University, Tanta, Egypt.*

Abstract

Three novel bolaamphiphiles were synthesized and investigated as corrosion inhibitors for carbon steel in 1M HCl using weight loss, potentiodynamic polarization and electrochemical impedance spectroscopy (EIS) measurements. The results reveal that the synthesized surfactants have a good inhibiting effect on the carbon steel in 1 M HCl solution. The results suggest that these inhibitors act as mixed-type inhibitors for acid corrosion of mild steel. The adsorption of bolaamphiphiles on the carbon steel surface in 1M HCl was found to obey Langmuir isotherm. Polarization results have shown that, these inhibitors act as a mixed type inhibitors. Quantum chemical calculations were also carried out to verify the inhibition efficiency obtained from all experiments.

Keywords: Carbon steel; Weight loss; Polarization; EIS; Adsorption; Computational.

Environmentally friendly carboxylate inhibitors for heating and cooling (HVAC) systems

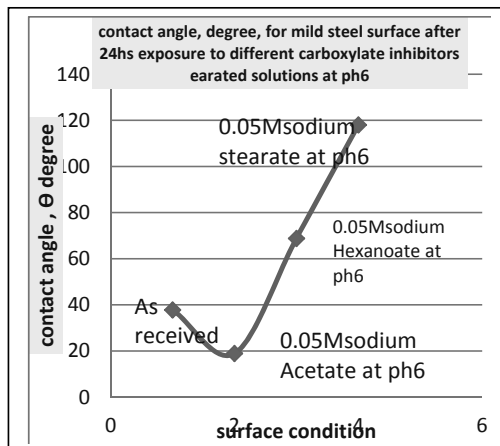
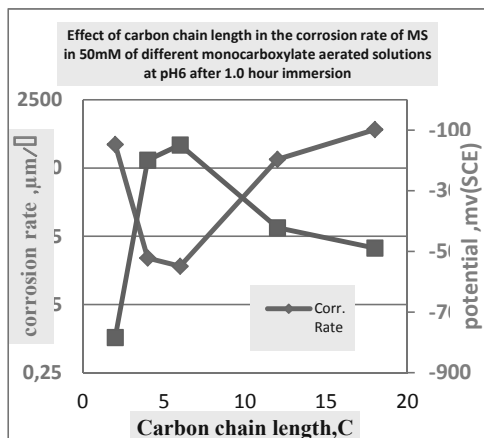
Mohamad Ali-Ahmed and Stuart Lyon

Corrosion and Protection Centre, School of Materials, University of Manchester, M13 9PL, UK

Abstract

The environmental toxicity of inorganic corrosion inhibitors has promoted the search for green organic inhibitors as they are biodegradable and do not contain heavy metals and any other toxic compounds. Aliphatic mono- and di- sodium carboxylates were used in this study with straight chain lengths from C = 2 to 18. The objective was to investigate the effect of de-aeration, carbon chain length and aggressive ion (chloride) concentration on the inhibition of mild steel in a stagnant cooling water system by use of electrochemical and surface analytical tools.

Results obtained in this study showed that the mono carboxylates can be excellent inhibitors for mild steel in cooling waters but that their effectiveness is critically dependent upon the chain length and dissolved oxygen content. The inhibition efficiency for mono-carboxylates reached a maximum value of 95% in stagnant aerated solutions at a chain length of C=6 and the critical inhibition concentration was 6mM in the presence of 10mM NaCl. However the inhibition efficiency was gradually reduced as the number of carbon atoms in the chain length increased to more than 8, or less than 4, and this was in agreement with surface hydrophobicity and contact angle results. For di-carboxylates the inhibition efficiency was improved for mild steel in 10mM NaCl at a given chain length compared with mono-carboxylates, and also increases up to C=10, the maximum so far tested. The oxygen content of the cooling water plays an important role in protection as long-term linear polarisation resistance experiments showed a drop in inhibition efficiency under de-aerated conditions. Results of potentiodynamic polarization experiments showed a large shift of OCP towards noble values due to the presence of these organic molecules and this was attributed to an anodic inhibition mechanism. Further research aims to identify molecular coverage and orientation on the steel substrate as a function of external parameters; including dissolved oxygen, temperature and chloride content.



Corrosion inhibition of ground anchors steel in HCl by H₂S-scavenger

J. Malina¹, F. Kapor², A. Begić Hadžipašić¹

*¹University of Zagreb/ Faculty of Metallurgy, ²University of Zagreb/ Faculty of Mining,
Geology and Petroleum Engineering, Zagreb/ Croatia*

The objective of the submitted work is to study the H₂S-scavenger effect as a corrosion inhibitor for ground anchors steel in 1M HCl solution. Laboratory measurements were performed using electrochemical techniques. With the aim to obtain the apparent activation energies of the corrosion process, the temperature dependence of the corrosion rates in the absence and presence of different concentrations of scavenger were obtained. It was found that the activation energy in the presence of scavenger is higher than that in uninhibited HCl solution.

The experimental data were modeled with several adsorption isotherms at different temperatures in order to determine the standard free energies of the adsorption process. It allowed to gain more information on the mode of scavenger interaction with steel surface. The inhibition process was attributed to the formation of an adsorbed film on the metal surface that protects the metal against corrosive agents. The inhibition efficiency increased with increase in scavenger concentration.

Causes and Control of Corrosion in Drinking Water Distribution Systems

Fadi Rahuma
Great Man Made River Project
Benghazi (Libya)
Email: fadi_n_r@hotmail.com

Iftikhar Ahmad
Arabian Gulf Oil Company (AGOCO)
Benghazi (Libya)

Corrosion is a common issue in drinking water supplies. In drinking water distribution systems, materials that could be affected by corrosion and leach increased amounts of contaminants include metal pipes and fittings, cement in pipe linings and polyvinyl chloride (PVC) pipes. Corrosion in drinking water distribution systems can be caused by several factors, including the type of materials used, the age of the piping and fittings, the stagnation time of the water and the water quality in the system, including its pH. The most influential properties of drinking water when it comes to the corrosion and leaching of distribution system materials are pH and alkalinity. Other drinking water quality parameters of interest are temperature, calcium, free chlorine residual, chloramines, chloride, sulphate and natural organic matter (NOM). Any change to the drinking water treatment process may impact corrosion in the distribution system and in household plumbing.

The intent of this paper is to provide responsible authorities, such as municipalities with guidance on assessing corrosion and implementing corrosion control for distribution systems in residential settings. It also provides sampling protocols and corrective measures for non-residential buildings, including schools, day care facilities and office buildings, for those authorities that are responsible for the health and safety of the occupants of such buildings. Although there are no direct health effects linked to corrosion in drinking water distribution systems but corrosion may cause the leaching of contaminants that would be a concern for the health of population. This paper outlines the steps that should be taken to reduce population exposure to contaminants. Concerns related to contaminants whose concentrations may be affected by corrosion, such as lead, copper and iron, are also briefly discussed.

Combination of stearic acid and benzotriazole as corrosion inhibitors for Cu and Cu40Zn in artificial urban rain

Gregor Žerjav, Ingrid Milošev, Department of Physical and Organic Chemistry, Jožef Stefan Institute, Ljubljana, Slovenia

Copper is a very useful material because of its excellent electrical and thermal conductivity properties. To improve its mechanical properties, copper is alloyed with Zn to produce brasses (Cu40Zn, wt(Zn)=40%). Copper and brasses provide superior functions in many applications and environments. However, during the exposure to environment, they may be subjected to corrosion. There are many ways to protect them against corrosion [1].

Cu and Cu40Zn can be protected against corrosion with the use of organic corrosion inhibitors [2]. Benzotriazole (BTAH) is one of the most effective inhibitors for copper and its alloys. BTAH provides a cheap and effective corrosion inhibition in most aqueous environments even at low concentration [3]. Another protection method is to modify the metal surface with stearic acid (SA) to make it hydrophobic and thus not wetted by aqueous liquids. Stearic acid forms self-assembled layer by adsorption to the positively charged metal surfaces via carboxyl groups, producing a hydrophobic layer [4].

In this study we investigate the use of a mixture of SA and BTAH to modify the surface of Cu and Cu40Zn in order to increase their hydrophobicity and corrosion resistance. The surface of was modified by immersing the sample in the ethanol solution of (i) SA, (ii) BTAH, (iii) mixture of (BTAH + SA) and (iv) layer-by-layer BTAH_SA. Modified samples were then tested in artificial urban rain (0.2 g/l Na₂SO₄, 0.2 g/l NaHCO₃, 0.2 g/l NaNO₃, pH=5).

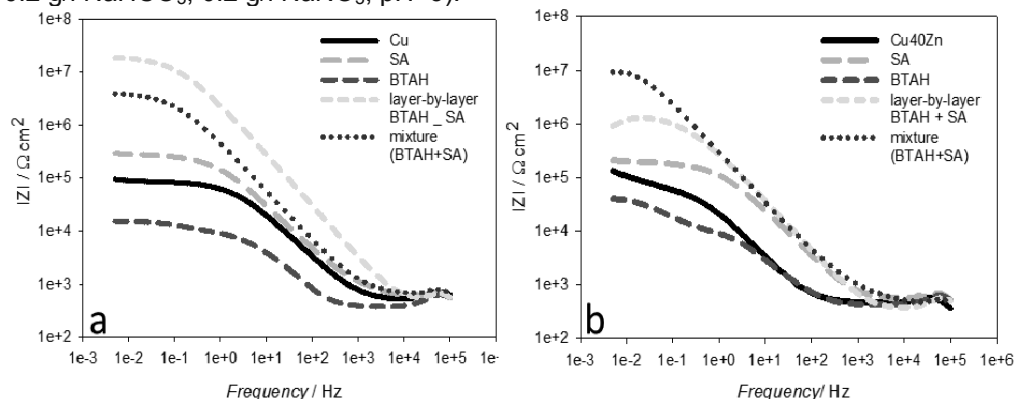


Figure show impedance data recorded for Cu (a) and Cu40Zn (b) after 24 h immersion in artificial urban rain. Cu and Cu40Zn are better corrosion protected when modified by the combination of BTAH and SA than when using these inhibitors individually. For Cu40Zn, this combination was more effective as a mixture (BTAH+SA), while for Cu layer-by-layer combination (BTAH_SA) provided better results.

1. M. M. Antonijević, M.B. Petrović, *Int. J. Electrochem. Sc.*, **2008**, 3, 1-28.
2. H. Otmačić, E. Stupnišek-Lisac, *Electrochim. Acta*, **2003**, 48, 985-991.
3. M. Finšgar, I. Milošev, *Corros. Sci.*, **2010**, 52, 2737-2749.
4. I. Milošev, T. Kosec, M. Bele, *J. Appl. Electrochem.*, **2010**, 40, 1317-1323.

Thermodynamic modelling of North Dakota lignite ash in air- and oxy-fuel fired boiler and comparison to collected ash from a 15MW_{th} boiler

*Bettina Bordenet, Alstom (Switzerland) Ltd, Baden / Switzerland,
R. Ganta, A. Levasseur, Alstom Power Inc., Windsor, CT / USA*

In oxy-combustion, combustion air is replaced by oxygen and flue gas is recycled back to the boiler to limit the flame temperature and avoid excessive slagging and fouling. Since nitrogen is removed, the combustion products may contain greater concentrations of CO₂, CO, SO₂, HCl, etc., which may increase the potential for corrosion of boiler components.

The ash and gas composition was modeled for air- and an oxy-fuel fired PC boiler with North Dakota Lignite. The results of the thermodynamic model were compared to measurements of the gas and ash composition from Alstom's 15MW_{th} boiler simulation facility (BSF) firing ND Lignite. The comparison of modeled and measured data has shown that the thermodynamic modeling approach is a suitable tool for the determination of the ash / gas composition.

From the measured SO₃-content of ≤3vol% of the total SO_x-content, the gas composition can be modeled for a temperature of around 1'000°C. Even if the flue gas is cooling down downstream, the residence time is not long enough to reach equilibrium values.

For the prediction of ashes deposited on heat exchanger surfaces, the model predicts too high SO₃-content in the ash, when the real material surface temperatures (superheater / re-heater area) are applied. Therefore the modeling temperature has to be adjusted depending on the ash type.

The chemical composition of the ash is similar for air-firing and oxy-fuel firing, only the SO₃-content is varying depending on the recycling scheme. For an oxy-fuel firing with flue gas desulfurization in the recirculation loop, the SO_x-content in the flue gas is nearly as low as in the air-firing. The changes of CO₂-, H₂O- and N₂-content between air- and oxy-fuel firing seem not to influence the modeled formation temperature of sulphate-compounds.

From the thermodynamic modeling and the results from the 15MW_{th} Boiler Simulation Facility (BSF), the following conclusions for the corrosion behavior can be drawn. As the general ash composition is comparable for air and oxy-fuel, similar corrosion mechanisms are expected.

Corrosion of Welded Coal Boiler Steels in Oxyfuel Flue Gas

*A. Kranzmann¹, M. Mosquera¹, G. Oder¹, Bundesanstalt für Materialforschung und –
prüfung, Berlin, Germany*

P. Zimmer, Vattenfall Europe Generation AG, Cottbus, Germany

S. Rehfeldt, Hitachi Power Europe GmbH, Duisburg, Germany

F. Kluger, ALSTOM Boiler Deutschland GmbH, Stuttgart, Germany

The experimental simulation of oxyfuel working conditions is the objective of our experiments. Like in real steam power plants internal pressure is applied using flowing steam at 270 bar pressure. The corrosive part of external flue gas is a gas mixture containing CO_2 , O_2 , SO_2 and H_2O . It could be demonstrated that the corrosion rate will be not the limiting factor of welded tubes within their typical temperature working regime. The corrosion scales were inspected by different methods. In this paper we will present corrosion scale thickness measurements and analytical results obtained from optical microscopy and microprobe measurements. The microstructure and the chemical analysis of the scales show the expected phases formed under oxidizing conditions such as Magnetite and Haematite. Indications of high carbon activity and subsequent carburization of the material which was demonstrated in earlier experiments applying a H_2O - CO_2 gas were not observed here.

Hot corrosion in the next generation of industrial gas turbines

A Potter, J Sumner, N J Simms, J E Oakey

Cranfield University, Cranfield, Bedfordshire, MK43 0AL, United Kingdom

To meet the target of a 20% reduction in CO₂ emissions by 2020, the European Council concluded that the implementation of CCS (carbon capture and storage) is essential. The next generation of combined cycle power plants could use the gasification of various fuels to produce a H₂ rich syngas which is then combusted in the gas turbine. The European funded H₂IGCC (H₂-integrated gasification combined cycle) project aims to solve some of the technical difficulties associated with the implementation of using H₂ rich syngases in such gas turbines and the problems of plant flexibility.

Combusted gas composition changes will affect the turbine components' working environments. This research investigates the type I and type II hot corrosion performance of selected superalloys, under consideration for use in gas turbine components, in various environmental conditions. To achieve this research, a series of 'deposit recoat' corrosion tests have been carried out in controlled atmosphere furnaces. The gas phase compositions were designed to replicate the following possible operating conditions: combustion of H₂ rich syngas, combustion of natural gas and combustion of syngas with a high level of H₂S contamination. The materials tested are used for the combustor can (Hastalloy X), turbine blades (GTD 111, Rene 80 and PW1483) and turbine vanes (MarM 509). Tests were carried out at both 700 and 900 °C for an exposure time of up to 500 hours with recoats every 100 hours.

The degree of corrosion was quantified by comparing pre-exposure contact metrology and post-exposure image analysis to give a dimensional metal loss. Additionally, the changes in morphology have been investigated using an environmental scanning electron microscope equipped with energy dispersive X-ray analysis. The data produced will contribute to turbine materials selection for the next generation of IGCC power plants as well as being integral to component life models.

Thermodynamic and kinetic modeling for predicting the microstructural evolution in MCrAlY coatings

R. Pillai¹, W.G. Sloof², A. Chyrkin¹, V. Shemet, L. Singheiser¹, W.J. Quadackers¹

¹Forschungszentrum Jülich, Institute of Energy and Climate Research (IEK-2),
52425 Jülich, Germany

²Delft University of Technology, Department of Materials Science and Engineering, 2628 CD Delft, NL

Coated Ni-base superalloys combine the excellent creep rupture strength of superalloys with the prolonged oxidation and corrosion resistance of overlay coatings or bondcoats. One of the widely used types of coatings are MCrAlY (M = Ni, Co) bondcoats, which ensure the growth of a slowly growing adherent alumina scale and thus protect the underlying substrate from rapid oxidation attack. Aluminium from the bondcoat is lost to the thermally grown oxide (TGO) on the coating surface and to the substrate by interdiffusion resulting in dissolution of the β -NiAl phase. Coating life generally corresponds to the operating life of the components and is usually measured in terms of the depletion of the β -NiAl phase as it serves as an Al-reservoir for the growth of the protective alumina scale.

A new computational approach to model the microstructural evolution in coating systems and thereby evaluate the lifetime of bondcoats was undertaken in the present study for typical bondcoats on Ni-based superalloys. Scanning electron microscopy (SEM) and electron microprobe analysis (EPMA) provide local element concentrations in a multiphase microstructure. This results in significant spatial concentration variations, which complicates the comparison with computed results. Glow discharge optical emission spectroscopy (GDOES) enabled depth profiling of the coating and substrate composition, thereby providing average element concentrations. Phases were identified by electron backscatter diffraction (EBSD) and correlated with SEM analyses.

Microstructural development in the alloy was modelled by considering simultaneously occurring oxidation and interdiffusion processes. Using available thermodynamic and kinetic data for all occurring phases from Thermo-Calc the current work distinguishes itself from contemporary modelling methodologies. Element concentrations and phase distribution were obtained by scanning electron microscopy (SEM).

Good agreement was found between the measured and computed element concentrations and phase distributions after specific time intervals. The computational approach assists in estimating the lifetime of the bondcoat and provides a tool to predict composition dependent microstructural changes in coating systems.

Keywords: MCrAlY, oxidation, interdiffusion, lifetime assessment, thermodynamic-kinetic modeling,

Presenting author's email: r.pillai@fz-juelich.de

Corrosion of materials in nitrate melts for molten salt solar receivers

M. Spiegel and A. Kilic

Salzgitter Mannesmann Forschung GmbH, Ehinger Strasse 200, 47259 Duisburg, Germany

Solarthermic Power Plants (SPP) are an alternative energy source which uses concentrated sun-light for the production of steam which is converted to electrical power by a steam turbine. Especially tower receivers are most efficient in collecting sun radiation. However, a liquid medium is necessary to transport the heat to a heat exchanger and to store it overnight. According to the high heat capacity, molten nitrates are in use for the transport which occurs through thin walled metallic tubes. The requirements for the tube materials are reasonable resistance against thermo-cyclic fatigue at temperatures of 550 – 650 °C as well as an excellent stability in the presence of the molten salt.

A selection of materials representing the classes of ferritic martensitic, austenitic and nickelalloys were exposed to a $\text{KNO}_3\text{-NaNO}_3$ eutectic mixture in air and nitrogen for 500 h at 600 °C in order to estimate the corrosion loss of the different classes of alloys and to evaluate the corrosion mechanisms. In some alloy severe nitridation occurs, especially with alloying elements with a high affinity to nitrogen like Ti and Al.

High-temperature corrosion under conditions simulating biomass firing: depth-resolved phase identification

Sunday Chukwudi Okoro, Technical University of Denmark (DTU), Department of Mechanical Engineering, 2800 Kongens Lyngby, Denmark.

Melanie Montgomery, COWI A/S/ DTU-Mechanical Engineering, Parallelsvej 2, 2800 Kongens Lyngby, Denmark.

Flemming Jappe Frandsen, DTU, Department of Chemical and Biochemical Engineering, 2800 Kongens Lyngby, Denmark.

Karen Pantleon, DTU, Department of Mechanical Engineering, 2800 Kongens Lyngby, Denmark.

To solve the corrosion issues that have bedevilled thermal power plants firing biomass, there is strong need to understand the principal corrosion mechanisms. However, owing to the complexity of both deposit and flue gas compositions during biomass firing, proper understanding of the corrosion mechanisms under realistic, although laboratory, conditions is still lacking. In most laboratory studies, only HCl and H₂O are employed in order to simplify the process. Consequently, the influence of other flue gas components such as SO₂ and CO₂ is neglected.

Laboratory exposure of an austenitic stainless steel (TP 347H) under conditions simulating firing of straw was carried out. Samples cut from unexposed superheater tubes were coated with a synthetic deposit consisting of KCl. The KCl coated samples were exposed isothermally at 560 °C in a furnace in a gaseous atmosphere for one week. The gaseous mixture of HCl, SO₂, CO₂, O₂ and H₂O was employed to simulate the flue gas composition during firing of straw.

The exposed samples were cross-sectioned and analysed by Light Optical Microscopy (LOM) and Scanning Electron Microscopy (SEM) as well as Energy Dispersive Spectroscopy (EDS). In addition, qualitative phase analysis was carried out by X-ray diffraction (XRD) in combination with successive removal of the corrosion products. These XRD measurements were further combined with microscopy (applying SEM) and chemical element analysis (EDS) on the corresponding surfaces after each removal step. These complementary methods (including both cross-section and plane view analysis) revealed site-specific information on the morphology and chemical nature of the various layers within the grown oxide scale. This finally allowed the identification of corrosion products as a function of distance from surface and, thus, supports clarification of the corrosion mechanism which is responsible for high-temperature corrosion due to straw firing.

The development of Nickel alloys for high temperature applications in the Process and Energy Industrial Sectors

S.A.McCoy, B.A.Baker, G.D.Smith. L. E. Shoemaker, Special Metals Corporation, Huntington, U.S.A.

Nickel-base alloys designed for elevated temperature service can offer a high degree of mechanical integrity and corrosion resistance for extended service. Proper selection of a material for a particular application involves consideration of several important factors. Corrosion resistance is a major deciding factor and many relevant corrosion modes must be considered, such as oxidation, carburization, metal dusting, nitridation, sulfidation, and attack by halide salts and gaseous halogen-containing species.

Mechanical properties are an important consideration as well and would include elevated temperature tensile, rupture and creep strength as well as fatigue strength and toughness. Fabrication issues associated with the application of these materials in a range of intermediate and high temperature service environments are also considered. This paper provides a summary of high temperature corrosion properties for a range of high temperature nickel base alloys, including recent alloy developments in the Fe-Ni-Cr, Ni-Cr-Al and Ni-Co-Cr families, for high temperature applications in the Process and Energy industrial sectors.

Laser Raman microscopy study of the transition from high temperature alloy passivation to breakaway oxidation

D. Young, T. Gheno, University of New South Wales, Sydney/AUS; D. Monceau, ENSIACET, Toulouse/F

Model chromia-forming alloys were exposed to flowing gas mixtures of Ar-20CO₂, Ar-20CO₂-5H₂O and Ar-20CO₂-20H₂O (volume %) at 650°C for periods of up to 336 h. The alloys were ferritic Fe-20Cr and Fe-25Cr (weight %), austeno-ferritic Fe-20,25Cr-10Ni and austenitic Fe-20,25Cr-20Ni. Initially, slow oxidation was observed for all alloys, but subsequent acceleration in the reaction rates led to unacceptably high rates of alloy consumption. In contrast, reaction in air led to stable, protective oxidation of these alloys.

Laser Raman microscopy was used to observe the evolution in oxide phase constitution accompanying the transition from protective to breakaway oxidation. In the protective stage of reaction, a passivating scale of Cr₂O₃ was formed by all alloys. Microanalysis by energy dispersive X-ray spectrometry of alloy subsurface regions allowed quantification of chromium depletion, and confirmation via a mass balance that the chromia scale contained negligible iron. Local fluctuations in chromia scale thickness (and the accompanying extent of alloy depletion) were observed to develop during the protective stage.

Acceleration in alloy reaction rates was due to nucleation and growth of additional iron-rich oxide nodules. Raman analysis showed that early in their lives, these nodules consisted of iron-rich M₂O₃ overlying a seemingly intact layer of chromium-rich M₂O₃ which was continuous with the protective scale surrounding the nodule. Beneath the chromia layer, internal precipitation of spinel, Fe_{3-x}Cr_xO₄, developed within the alloy. In the case of alloy Fe-20Cr, these nodules spread and coalesced to form a thick, continuous scale. This scale was found by Raman analysis to consist of a thin, outermost layer of Fe₂O₃ surmounting a thick Fe₃O₄ layer, a thin intermediate band of spinel ($x = 1.6$) and an inner two-phase layer of spinels with $x = 0.3$ and 1.2 .

An Fe-25Cr alloy was more resistant to breakaway oxidation, forming some areas of thick, iron-rich oxide growths, but also some areas of “rehealed” oxide. The latter consisted of rather thin iron-rich M₂O₃ and M₃O₄ layers over a layer of chromium-rich oxide, either spinel or M₂O₃. Nickel-bearing alloys developed qualitatively similar scales. Nodule development on the 20Cr alloys was slower than on the ferritics, as a result of slow diffusing NiFe₂O₄ formation in the inner layer. At the 25 Cr level, both nickel bearing alloys formed nodules which were extremely slow growing, and too small for analysis.

The morphological evolution of fast growing, layered oxide scales from initially protective chromia is discussed in terms of alloy depletion leading to formation of spinel at sites of local damage to the chromia. This spinel permits outward iron diffusion and inward oxygen transport. Lateral diffusion then leads to nodule spreading both above and below the prior chromia layer, its consequent destabilisation and absorption into the scale.

Oxidation Mechanisms of Alloy 602 CA in Different Gas Atmospheres Relevant to Gas Separation Membranes

M. Schiek, L. Niewolak, R. Vaßen, W. J. Quadakkers

*Forschungszentrum Jülich GmbH, Institute of Energy and Climate Research (IEK)
Jülich/Germany*

Carbon capture and storage (CCS) technologies are being considered for reducing CO₂ emissions from fossil fuel fired power plants. The main task thereby is to separate the CO₂ from the exhaust gases, using several new power plant design concepts such as e.g. oxyfuel combustion. In a number of applications this requires the use of ceramic gas separation membranes at elevated temperatures. Because ceramic membrane materials are prone to mechanically induced failure, porous metallic carriers are needed to support them. The main requirements for the metallic carrier are: good oxidation resistance in the process relevant environments, limited evaporation of Cr-species, thermal expansion coefficient close to that of the ceramic membrane material and a slow reaction rate with the membrane material. Depending on the actual membrane material being used, these requirements can be fulfilled by alumina forming nickel base alloys.

The actual service environment to which the membrane material is subjected depending on the actual CCS technology used and may contain variable amounts of oxygen, water vapour and/or carbon dioxide. In the present study the effect of atmosphere composition on the formation and stability of an external alumina scale is being investigated. With this aim, isothermal oxidation studies were carried out in different model gases using the marginal alumina forming alloy 602 CA in the temperature range 800°C – 1100°C. The mass change data up to 72 h exposures in Ar-20%O₂, Ar-2%CO₂ and Ar-7%H₂O gas was continuously recorded using a Setaram TGA facility. Compositions and morphologies of the oxide scales formed at the high test temperatures were analysed by optical metallography (OM), scanning electron microscopy equipped with energy dispersive X-ray spectroscopy (SEM/EDX), Raman spectroscopy and X-ray diffraction (XRD). Additionally, elemental concentration profiles in the oxide scales and underlying alloy were determined using plasma secondary neutral mass spectrometry (Plasma-SNMS) and glow discharge optical emission spectroscopy (GDOES).

It was found that the investigated alloy 602 CA oxidised at 800°C forms an external alumina scale with various amounts of transient, Cr-rich oxides in all used test atmospheres. Increasing the oxidation temperature to 900°C and above results in formation of an external chromia scale and an internal oxidation zone (IOZ) containing alumina precipitates. Furthermore, the formation of Cr-rich carbides in the alloy matrix was affected by the oxidation process. Thereby the subscale dissolution of carbides was not only affected by oxidation induced chromium depletion but also by Al-depletion as a result of external or internal aluminium oxide formation.

Differences in oxidation mechanisms in the various environments will be discussed.

Grain Boundary Sulphidation of Nickel-Based Alloys applied in High-Efficient Coal-Power Plants

M. M. Lange¹, S. Borodin¹, F. U. Renner¹ and M. Spiegel²

1. Max-Planck-Institut für Eisenforschung GmbH, Department for Interface Chemistry and Surface Engineering, D-40237 Düsseldorf, Germany

2. Salzgitter Mannesmann Forschung GmbH, D-47259 Duisburg, Germany

New materials with low creep rates and a good high temperature resistance are required for the development of high-efficient 700°C coal-power technologies. Nickel-based alloys are promising for such applications. However, high temperature corrosion can affect the creep behavior e.g. by embrittlement. Therefore, a fundamental understanding of the alloy's corrosion behaviour, especially of grain boundary sulphidation, is needed in order to promote the corrosion stability of the material by grain boundary strengthening. Here we focus on the nickel-based Alloy 617 B which was exposed in a 700° C coal-power plant and showed grain boundary sulphidation.

In the present study we used a method which enabled us to determine the sulphur attack along the grain boundary even for low concentration by means of electron spectroscopy. First, samples from A 617 B after sulphidation were investigated in conventional cross section to get an overview of the different corrosion morphology. In selective areas samples were fractured in-situ and subsequently investigated by means of Auger Electron Spectroscopy (AES). In case of an intercrystalline fracture possible segregated elements at the grain boundary are present over the whole surface and they can be detected due to the higher concentration per surface area. Ion sputtering on these surfaces results in depth profiles from the grain boundary to the matrix.

The investigated alloy 617B after sulphidation under high-temperature working conditions fractures fully intercrystalline. Sulphur penetration in the material along grain boundaries was found up to a certain depth from the fireside. Beyond this depth sulphur was not detected. Obviously, the grain boundary is an easy pathway for sulphur diffusion into the alloy from the fireside, however, the bulk metal properties are not affected so far. By monitoring depth profiles, a reaction sequence can be formulated with respect to the chemistry of the unaffected grain boundary. Moreover, the role of adsorbed chlorine and oxygen from the flue gas atmosphere was studied and will be discussed in correlation to sulphur.

Effect of sulfur content on adhesion of thermal oxide scales grown on austenitic stainless steels

C. Pascal ⁽¹⁾, E. Fedorova ⁽²⁾, V. Parry ⁽¹⁾, M. Braccini ⁽¹⁾, M. Mantel ^(1,3), D. Oquab ⁽⁴⁾,
Y. Wouters ⁽¹⁾, D. Monceau ⁽⁴⁾

⁽¹⁾ SiMaP, University of Grenoble, France

⁽²⁾ Polytechnic Institute of Siberian Federal University, Krasnoyarsk, Russia

⁽³⁾ UGITECH SA, Ugine, France

⁽⁴⁾ CIRIMAT, University of Toulouse, France

Two austenitic stainless steels, AISI 304L (EN 1.4307) and AISI 303 (EN 1.4305) with close compositions, containing 0.025 and 0.249 wt.% S respectively were oxidized at 1000°C for 50 hours in synthetic air. The chemical compositions of the oxide scales, investigated by Raman spectroscopy and X-Ray diffraction, indicate that the oxide scales are duplex. For 303, the oxide scale is composed of hematite (Fe_2O_3), a rhombohedral solid solution of $(\text{Fe,Cr})_2\text{O}_3$ and of spinel type oxide $((\text{Fe,Cr})_3\text{O}_4)$. For 304L, only $(\text{Fe,Cr})_2\text{O}_3$ and $(\text{Fe,Cr})_3\text{O}_4$ solid solutions are present in the scale.

Isothermal oxydation kinetics of the two austenitic stainless steels was studied through ThermoGravimetric Analysis. The parabolic rate constant of AISI 303 is about one order of magnitude higher than AISI 304L one ($2.9 \cdot 10^{-5} \text{ mg}^2\text{cm}^{-4}\text{h}^{-1}$ and $3.5 \cdot 10^{-6} \text{ mg}^2\text{cm}^{-4}\text{h}^{-1}$ respectively).

During SEM *in situ* tensile test (Figure 1), the behaviours of the oxide layers are quite different: (i) the crack patterns are different, (ii) the critical strain at which first cracks appear is about 1.6% and 3.4% for the 303 and 304L respectively, (iii) spallation occurs only in the oxide scale of the 303 steel.

A correlation between the specific mass change, the oxide chemistry, the scale microstructure and the adhesion properties is performed and results are discussed in relation with sulfur content and oxide growth mechanism.

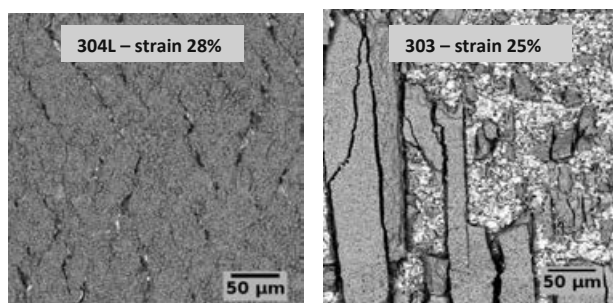


Fig. 1 Surface SEM view (BSE) of the oxide scale during SEM *in situ* tensile test

The effect of SO_4^{2-} ions on the corrosion of 15CrMo steels during shutting down and their oxide scale formation

Yu Meng, Li Zhang, Da Quan Zhang, Li Xin Gao

Department of Environmental Engineering, Shanghai University of Electric Power,
Shanghai 200090, PR China

Abstract: The corrosion of 15CrMo steels caused by sulfate ions are evaluated in the stimulated condensed water system. The increase of the concentration of sulfate ions renders a negative shift of the corrosion potentials and improves the corrosion current densities evidently. The high temperature oxidation test was performed for 15CrMo steels with and without the pre-corroded film on its surface. Microstructure and composition of the oxide scale of 15CrMo steels were characterized using scanning electron microscopy/energy dispersive X-ray spectroscopy (SEM/EDS), and X-ray diffraction (XRD). It shows that the corrosion damage by sulfate ions attacking during shut-down significantly affects the structure of the oxide scale formed by the high temperature of 15CrMo.

Behaviour of 25wt.%Cr-containing Fe-based alloys strengthened by hafnium carbides in oxidation between 1000 and 1200°C

Patrice Berthod, Elodie Conrath

*Institut Jean Lamour (UMR CNRS 7198), department CP2S,
team "Surface and Interface, Chemical Reactivity of Materials",
University of Lorraine
B.P. 70239, 54506 Vandoeuvre-lès-Nancy, France*

Applications at high temperature in which pieces are subjected to static or varying mechanical stresses need very refractory alloys with matrixes refractory enough and if possible intrinsically resistant [1]. Unfortunately, the base elements able to bring these two properties are either expensive or difficult to shape. However, thanks to the very high melting points of chromium but also of iron, many Cr-rich Fe-based alloys are very refractory alloys and remain not so costly. Unfortunately, since most of them keep a ferritic (back centred cubic) structure from room temperature up to their solidus temperature, they are not mechanically resistant enough to be used at high temperature under stresses. Their cast versions can be successfully reinforced by eutectic TaC carbides mixed with the matrix in the interdendritic spaces [2]. Although they are much better than chromium carbides in this field, the TaC carbides are not sufficiently stable to allow high temperature strength over long times: they tend to get fragmented and to decrease in volume fraction. Fortunately, other MC-type carbides, the HfC ones, are less sensitive to these phenomena, in cobalt-based alloys [3] but also in chromium-rich iron-based alloys [4,5], and it appears possible to benefit simultaneously of the high refractoriness of the Fe(Cr) base and of the ideally shaped and positioned HfC carbides, to obtain alloys very resistant against creep deformation.

However, hafnium is an element which is generally added to alloys in very low quantities either to improve ductility or some aspects of oxidation behaviour (e.g. resistance to oxide spallation in thermal cycling). The presence of a so reactive element in quantities as high as 4 to 6 wt.%Hf, contents necessary to develop significant volume fractions in HfC carbides, risk to be not neutral for the general behaviour of HfC-reinforced Fe(Cr)-based alloys.

In this work, several 25wt.%Cr-containing Fe-based alloys in which significant fractions in HfC carbides are present thanks to rather high amounts in carbon (0.25 to 0.50wt.%) and in hafnium (3.7 to 5.6wt.%), were subjected to 46 hours-long oxidation tests in dry air at temperatures ranging between 1000 and 1200°C, in thermo-balance. The mass gains were treated using the $\{m \times dm/dt = K_p - K_v \times m\}$ method [6] when applicable and the oxidized samples were subjected to post-mortem characterization. The contained oxidation kinetic was not always regular enough to correctly extract the two constants K_p and K_v (chromia volatilization for T equal to 1100 or 1200°C), but this was possible in some cases. The external oxide was mainly composed of $(Cr,Fe)_2O_3$ oxide and they also contained some HfO_2 islands. Accelerated oxidation seemed starting in some locations of the surface of the 1200°C-oxidized samples, which let think that catastrophic oxidation ought to generalize beyond the 46 hours of these tests. Obviously these alloys need to be enriched in chromium to delay such scenario, or to benefit of a protective coating.

References:

- [1] Donachie, M. J., Donachie, S. J., Superalloys: A Technical Guide (2nd Edition), ASM International (Materials Park, 2002).
- [2] Berthod, P., Hamini, Y., Aranda, L., Héricher, L., « Experimental and thermodynamic study of tantalum-containing iron-based alloys reinforced by carbides: Part I – case of (Fe,Cr)-based ferritic steels”, Computer Coupling of Phase Diagrams and Thermochemistry, Vol. 31 (2007), pp. 351-360.
- [3] Berthod, P., “High temperature properties of several chromium-containing Co-based alloys reinforced by different types of MC carbides (M=Ta, Nb, Hf and/or Zr)”, Journal of Alloys and Compounds, Vol. 481 (2009), pp. 746-754.
- [4] Berthod, P., “Hafnium carbides in cast chromium-rich refractory alloys. Part 3: Case of iron-based alloys”, Materials Science: An Indian Journal, Vol. 9 (2013), pp. 453-458.
- [5] Conrath, E., Berthod, P., “Microstructure evolution at high temperature of chromium-rich iron-based alloys containing hafnium carbides”, International Journal of Materials Research (formerly: Zeitschrift für Metallkunde), submitted.

Effect of minor strengthening additions in Ni-base superalloys on oxide scale formation in high pO_2 environments

W. Nowak, A. Jalowicka, D. Naumenko, L. Singheiser and W.J. Quadackers

*Institute for Energy and Climate Research, IEK-2
Forschungszentrum Jülich GmbH, 52425, Jülich, Germany*

Abstract

Ni-base superalloys are commonly used in the hottest sections of power generating gas turbines due to a combination of excellent mechanical properties at elevated and room temperature and exceptional high-temperature corrosion and oxidation resistance. Apart from the major alloying elements, Cr, Co, Al, W, Ti, modern Ni-based superalloys contain minor (between 0.01 and 1 at.%) additions of elements such as Hf, Zr or B for obtaining improved mechanical properties, in particular grain boundary strengthening. However, these minor elements also form thermodynamically very stable oxides and can therefore participate in the oxidation process.

To elucidate the effect of the above mentioned minor alloying additions on the oxidation resistance of Ni-base superalloys, in the present work commercially available (Rene80, CM247) as well as several cast model alloys were exposed in the temperature range between 950°C and 1050°C up to 500 hours in atmospheres simulating typical gas turbines environments. After exposure the oxidized samples were investigated with a number of surface analytical methods, including glow discharge optical emission spectroscopy (GD-OES), optical and scanning electron microscopy and X-Ray diffraction.

The strengthening additions were found to become incorporated into the oxide scale. Their exact effect on the oxidation process was, however, dependent on the exposure conditions being stronger at higher exposure temperatures and more pronounced in aggressive atmospheres with high H_2O and/or SO_2 partial pressures.

Influence of water vapour in air and of TaC carbides in alloy on the high temperature oxidation of cobalt-based refractory alloys

Lionel Aranda, Thierry Schweitzer, *Patrice Berthod*, Alexandre Navet, Albert Leroy

*Institut Jean Lamour (UMR CNRS 7198), department CP2S,
team "Surface and Interface, Chemical Reactivity of Materials",
University of Lorraine*

B.P. 70239, 54506 Vandoeuvre-lès-Nancy, France

Besides nitrogen and oxygen, other gaseous species (CO , CO_2 , SO_2 , H_2O ...) are generally present in the hot atmosphere in which refractory alloys are in service [1], and their presence influences the behaviour of alloys in high temperature oxidation [2], often in the wrong direction, i.e. with rather detrimental effect. Notably, it is widely recognized that water vapour plays an important role, but not necessarily unfavourable for the sustainability of the metallic component. If it is true that the presence of water vapour in air tends to provoke the volatilization of SiO_2 and Al_2O_3 protecting the silica or alumina-forming alloys, and to accelerate of Cr_2O_3 covering the chromia-forming ones, some advantages were also noticed: sometimes a slow-down in speed for the oxidation rate and frequently an improvement of the scale adherence when temperature varies [2,3].

In the case of the Cr_2O_3 -former alloys and superalloys many studies dealing with the effect of water vapour, the high temperature oxidation concern nickel-based alloys while, in contrast, the cobalt-based alloys, although they constitute also an important family of cast and wrought chromia-forming high temperature alloys, were curiously a little less studied in this field. Since such alloys are also used in the hottest parts of aero-engines [4] and in the hottest pieces involved of various industrial processes (such glass working [5]), with in both cases the possible presence of water vapour even in little concentration, it appears interesting to better know the effect of water vapour on the behaviour in oxidation at high temperature for this family of alloys.

In this work, a model Co-10Ni-30Cr-0.5C-7.5Ta was considered (all contents in wt.%). This rather simple alloy, which is however close to commercial Co-based superalloys as MarM-509 and others, was elaborated by casting of pure elements with a high frequency induction furnace under inert atmosphere. Thermogravimetry runs were performed at 1000, 1100 and 1200°C in dry synthetic air as well as in the same but humidified with a special apparatus. The mass gain files were analysed according to the $\{m \times dm/dt = K_p - K_v \times m\}$ method [6] to determine the oxidation rate and the chromia-volatilization one, simultaneously. The heating part and the cooling parts of the mass gain files were also exploited to study the eventual effect of water vapour on the oxidation start temperature and on the parameters characterizing the resistance of the scale to spallation.

The effect of the existence of many interdendritic eutectic TaC carbides in the present alloy on the water-vapour dependence of the high temperature oxidation behaviour was investigated by comparison with results obtained in parallel for analogous test conditions for more simple alloys with the same Co, Ni Cr, and C alloys [7].

References:

- [1] Donachie, M. J., Donachie, S. J., Superalloys: A Technical Guide (2nd Edition), ASM International (Materials Park, 2002).
- [2] Young, D., High Temperature Oxidation and Corrosion of Metals, Elsevier Corrosion Series (Amsterdam, 2008).
- [3] Berthod, P., Aranda, L., Mathieu, S., Vilasi, M., "Influence of water vapour on the rate of oxidation of a Ni-25wt.%Cr alloy at high temperature", Oxidation of Metals, Vol. 79, No. 3-4 (2013), pp. 517-527.
- [4] Sims, C.T., Hagel, W.C., The superalloys, John Wiley & Sons (New York, 1972).
- [5] Berthod, P., Bernard, J.L., Liébaut, C., Patent WO99/16919.
- [6] Berthod, P., "Kinetics of high temperature oxidation and chromia volatilization for a binary Ni-Cr alloy", Oxidation of Metals, Vol. 64, No. 3-4 (2005), pp. 235-252.
- [7] Leroy, A., Navet, A., Schweitzer, Th., Aranda, L., Berthod, P., "Effect of the presence of water vapour on the high temperature oxidation of Co-10Ni-30Cr and Co-10Ni-30Cr-0.5C alloys", poster presented at Eurocorr 2014, Pisa (Italy), 8-12 September 2014.

Close-to-reality modelling of high temperature corrosion phenomena in steel industry by a novel designed lab-scale test rig

H. Rojacz¹, M. Varga¹, K. Adam², M. Rodríguez-Ripoll¹

¹ AC²T research GmbH, 2700 Wiener Neustadt, Austria

² voestalpine Stahl Linz GmbH, 4020 Linz, Austria

The harsh environment in sintering plants for the preparation of iron ore, coke and limestone for the pig iron production causes high temperature (HT) corrosion, which is one of the most crucial effects causing downtime and maintenance costs of the sintering plant. Materials working in such applications not only require wear resistance, but also excellent HT corrosion and oxidation resistance at temperatures up to 1100°C.

In the present study, the corrosives present in the sintering atmosphere were examined in detail. Comprehensive studies revealing various corrosives were performed, using detailed characterisation of the application and corrosives. The analysis revealed combined chlorine and carbonate corrosion, carburization (metal dusting) and sulphidation in the solid, liquid and gaseous phase. Analyses of the different corrosives are given in Fig. 1.

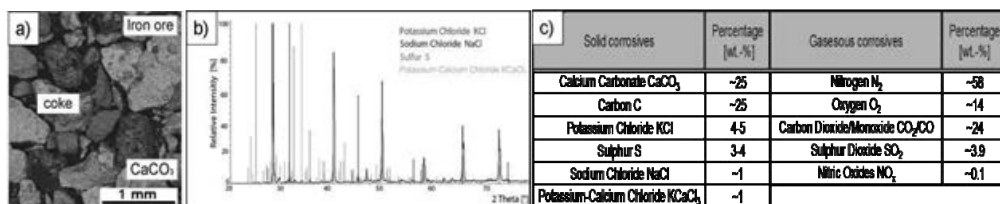


Fig. 1: a) SEM-Investigations of the sintering ash, b) XRD-Patterns of the soluble corrosive salts, c) Corrosives and their average concentration – solid corrodents are given in percentage of the sintering ash.

To replicate this harsh environment in close to reality conditions, a HT-Corrosion Test (HT-CT) was developed, enabling corrosion in solid/molten environment combined with different atmospheric gases up to 1500°C. As solid corrosive precipitated sintering ash was chosen; corrosive gases were adjusted according to the performed application measurements. Different Cr- and Ni-alloyed steels were chosen to investigate influences of different alloying elements in the specific environment of a sintering plant. Corrosion mechanisms and the formed protective layers are analysed in detail via EDX-mappings at metallographic cross sections. An exemplary EDX-mapping of an austenitic steel is given in Fig. 2.

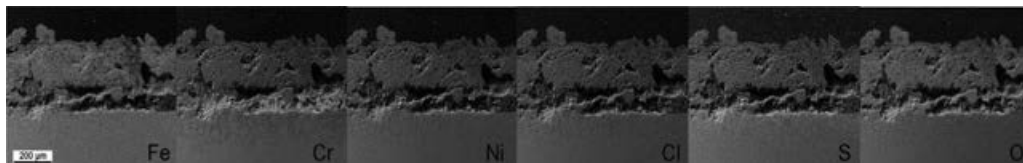


Fig. 2: EDX-mapping of the steel 1.4301 (18 % Cr, 10 % Ni, 0.07 % C, bal. Fe)

Different forms of corrosion could be detected for different steel classes. Corrosion models for different steel groups were evolved based on the gained data. The results indicate that the HT corrosion depends strongly on the alloyed elements, which stabilise the materials against corrosion.

Effect of the presence of water vapour on the high temperature oxidation of Co-10Ni-30Cr and Co-10Ni-30Cr-0.5C alloys

Albert Leroy, Alexandre Navet, Thierry Schweitzer, Lionel Aranda, Patrice Berthod

*Institut Jean Lamour (UMR CNRS 7198), department CP2S,
team "Surface and Interface, Chemical Reactivity of Materials",
University of Lorraine
B.P. 70239, 54506 Vandoeuvre-lès-Nancy, France*

Water vapour is known to influence the general behaviour of refractory alloys and superalloys in oxidation at high temperature [1], in terms of isothermal oxidation rate, volatilization of the protective scale formed (alumina, chromia or silica), and of oxide scale spallation in thermal cycling. After having studied the double kinetic of both mass gain of oxidation and mass loss by chromia volatilization in the case of chromia-forming nickel-based alloys [2], it was wished here to characterize the effect on oxidation of water vapour in the case of cobalt alloys, with thermogravimetry recording followed, here too by using the $\{m \times dm/dt = K_p - K_v \times m\}$ method [3] for the isothermal part, and by examining their heating and cooling parts.

Cobalt-based superalloys are generally rich in chromium (several tens weight percents) and are strengthened by carbides. Many of them additionally contain several weight percents in nickel to stabilize the FCC network of the matrix. These are the reasons why the two simple model alloys considered in this work are: first a carbide-free Co-10Ni-30Cr ternary alloy to study the specific behaviour of the matrix, and second a Co-10Ni-30Cr-0.5C to examine the case of the same alloy but containing significant fraction in chromium carbides.

These two alloys were elaborated by high frequency induction melting from pure elements, in inert gas. The parallelepiped samples were cut and ground with smoothing of edges and corners, then subjected to thermogravimetry runs performed in dry synthetic air and in humidified air (temperatures of test: 1000, 1100 and 1200°C, duration: 50 hours). The analysis of the three parts (heating, isothermal oxidation, cooling) of the mass gain files, as well as the post-mortem metallographic characterization of the oxidized samples, allowed evidencing the effect of water vapour on numerous characteristics of the high temperature oxidation of these cobalt-based alloys.

References:

- [1] Young, D., High Temperature Oxidation and Corrosion of Metals, Elsevier Corrosion Series (Amsterdam, 2008).
- [2] Berthod, P., Aranda, L., Mathieu, S., Vilasi, M., "Influence of water vapour on the rate of oxidation of a Ni-25wt.%Cr alloy at high temperature", Oxidation of Metals, Vol. 79, No. 3-4 (2013), pp. 517-527.
- [3] Berthod, P., "Kinetics of high temperature oxidation and chromia volatilization for a binary Ni-Cr alloy", Oxidation of Metals, Vol. 64, No. 3-4 (2005), pp. 235-252.
- [4] Sims, C.T., Hagel, W.C., The superalloys, John Wiley & Sons (New York, 1972).
- [5] Donachie, M. J., Donachie, S. J., Superalloys: A Technical Guide (2nd Edition), ASM International (Materials Park, 2002).

Carbide transformations occurring between 1000 and 1100°C in the sub-surface of a Ni-25Cr-0.50C alloy induced by hot oxidation

Patrice Berthod, Elodie Conrath

*Institut Jean Lamour (UMR CNRS 7198), department CP2S,
team "Surface and Interface, Chemical Reactivity of Materials",
University of Lorraine
B.P. 70239, 54506 Vandoeuvre-lès-Nancy, France*

Alloys and superalloys elaborated by foundry practice are often strengthened by carbides. They constitute an important family of refractory alloys for applications at high temperature [1]. Since the metallic carbide-forming elements present in the reinforcing carbides are easily oxidable [2], when they are used in hot conditions in aggressive environments, such alloys are subjected to changes of the carbides initially present in the sub-surface [3,4] induced by high temperature oxidation occurring on surface. These microstructure modification may possibly modify the local refractoriness [5] as well as the local mechanical properties in sub-surface. They can be of different types: (eventually) development of a carbide-free zone, local coarsening of carbides, nature change of the carbides initially present, precipitation of new ones...

This study focuses on the oxidation-induced phenomena encountered in the sub-surfaces by ternary Ni-Cr-C alloys, with additionally the study of the effect of the temperature and duration of oxidation. The phenomena are interpreted using thermodynamic calculations [6,7].

References :

- [1] Donachie, M. J., Donachie, S. J., Superalloys: A Technical Guide (2nd Edition), ASM International (Materials Park, 2002).
- [2] Young, D., High Temperature Oxidation and Corrosion of Metals, Elsevier Corrosion Series (Amsterdam, 2008).
- [3] Berthod, P., Michon, S. et al, "Thermodynamic calculations for studying high temperature oxidation of superalloys", Calphad, Vol. 27 (2003), pp. 279-288.
- [4] Berthod, P., Vébert, C. et al, "Study of carbide transformations during high-temperature oxidation of nickel-base superalloys", Oxidation of Metals, Vol. 63, No. 1/2 (2005), pp. 57-72.
- [5] Berthod, P., "Experimental and thermodynamic study of nickel-based alloys containing chromium carbides. Part II: Study of the sub-surface characteristics of Ni-30 wt.%Cr-xC alloys oxidized at high temperature using thermodynamic calculations", Calphad, Vol. 32 (2008), pp. 492-499.
- [6] Thermo-Calc version N, "Foundation for Computational Thermodynamics", Stockholm (Sweden), Copyright (1993, 2000), www.thermocalc.com
- [7] SGTE: Scientific Group Thermodata Europe Database, Update 1992.

Kinetic of oxidation of chromium-rich HfC-containing Co-based and Ni-based alloys between 1000 and 1100°C

Elodie Conrath, Patrice Berthod

*Institut Jean Lamour (UMR CNRS 7198), department CP2S,
team "Surface and Interface, Chemical Reactivity of Materials",
University of Lorraine
B.P. 70239, 54506 Vandoeuvre-lès-Nancy, France*

Many cobalt-based superalloys and some nickel-based ones are reinforced by interdendritic carbides for allowing to use them in hot conditions [1]. Such carbides must be stable enough at high temperature in term of geometry/shape as well in term of volume fraction. The TaC carbides which reinforce some cobalt-based alloys do not rapidly evolve while TaC carbides are much less stable in chromium-rich nickel-based alloys (and even less stable than the chromium carbides in this second family of alloys [2]). HfC are among the carbides which are more stable at high temperature than the tantalum carbides, much more in the case of the nickel-based alloys [3] and already a little more in the case of the cobalt-based ones [4,5].

Hafnium carbides may potentially lead to nickel-based and cobalt-based alloys very resistant against creep deformation at high temperature but it was recently found that the HfC carbides network may be rather neutral for the behaviour of the nickel-based alloys in oxidation at high temperature [6], but detrimental for the alloys which are based on cobalt [7].

The good stability of the HfC carbides in the same families of alloys can be also exploited at lower temperatures such as 1100 and 1000°C. It appeared that it can be interesting to characterize the behaviour in oxidation at these temperatures of the same alloys already studied at 1200°C [6,7], in order to see if the behaviour of the cobalt-based alloys notably is improved 100°C or 200°C lower.

Thus several new alloys with the same carbon (0.25 and 0.50 wt.%) and hafnium (3.7 to 7.4 wt.%) contents as the alloys previously studied at 1200°C were elaborated by foundry and tested in oxidation at 1100°C and 1000°C. The final mass gains, natures of oxides present externally and the values of parabolic constant and chromia volatilization constant (both extracted from the mass gain versus time file according to the $\{m \times dm/dt = K_p - K_v \times m\}$ method [8], clearly show that the behaviour of these alloys are really better, especially in the case of the cobalt alloys.

References:

- [1] Donachie, M. J., Donachie, S. J., Superalloys: A Technical Guide (2nd Edition), ASM International (Materials Park, 2002).
- [2] Berthod, P., Aranda, L., Vébert, C., Michon, S. "Experimental and thermodynamic study of the high temperature microstructure of tantalum containing nickel-based alloys", *Calphad*, Vol. 28, No. 4 (2004), pp. 159-166.
- [3] Berthod, P., "Hafnium carbides in cast chromium-rich refractory alloys. Part 1: Case of nickel-based alloys", *Materials Science: An Indian Journal*, Vol. 9 (2013), pp. 359-365.

- [4] Berthod, P., "High temperature properties of several chromium-containing Co-based alloys reinforced by different types of MC carbides (M=Ta, Nb, Hf and/or Zr)", *Journal of Alloys and Compounds*, Vol. 481 (2009), pp. 746-754.
- [5] Berthod, P., "Hafnium carbides in cast chromium-rich refractory alloys. Part 2: Case of cobalt-based alloys", *Materials Science: An Indian Journal*, Vol. 9 (2013), pp. 420-427.
- [6] Conrath, E., Berthod, P., "Kinetic of high temperature oxidation and chromia volatilization for HfC-containing nickel-based alloys", *Oxidation of Metals*, in press (DOI 10.1007/s11085-013-9449-0)
- [7] Conrath, E., Berthod, P., "Kinetic of high temperature oxidation of chromium rich HfC reinforced cobalt based alloys", *Corrosion Engineering Science and Technology*, in press (DOI 10.1179/1743278213Y.0000000105)
- [8] Berthod, P., "Kinetics of high temperature oxidation and chromia volatilization for a binary Ni-Cr alloy", *Oxidation of Metals*, Vol. 64, No. 3-4 (2005), pp. 235-252.

Effect of Sulfur on the KCl-induced High Temperature Corrosion of Selected Fe-based and Ni-based Alloys

Saeed Kiamehr*, Kristian V. Dahl*, Torbjörn Jonsson**, Melanie Montgomery*, Marcel A.J. Somers*

* *Department of Mechanical Engineering, Technical University of Denmark (DTU), Produktionstorvet, Building 425, 2800 Kgs. Lyngby, Denmark; [Saeed Kiamehr](#)*

** *Environmental Inorganic Chemistry, Department of Chemical and Biological Engineering, Chalmers University of Technology, S-412 96, Göteborg, Sweden*

The influence of sulfur on the KCl-induced high temperature corrosion of two commercial alloys, austenitic stainless steel TP347HFG and Ni-based super alloy Nimonic 80A, has been studied. Samples of these alloys were covered by KCl(s) particles and were exposed to $\text{N}_2(\text{g}) + 5\text{vol.}\% \text{O}_2(\text{g}) + 300\text{ppmSO}_2(\text{g})$ at 600°C for 168h. A sulfur-free exposure was also performed as the reference experiment. The extent of the attack was measured by residual metal thickness measurements. Corrosion morphology and products were investigated by Light Optical Microscopy (LOM), Scanning Electron Microscopy (SEM) and Energy Dispersive X-Ray Spectroscopy (EDS). On the basis of the results role of sulfur in KCl-induced high temperature degradation of alloys is clarified.

Key words: high temperature corrosion, deposit, biomass combustion, potassium chloride, potassium sulfate, chromium depletion.

Kinetic of oxidation at 1000, 1100 and 1200°C of 32.5wt.%Cr-containing Co-based alloys reinforced by hafnium carbides

Elodie Conrath, Patrice Berthod

*Institut Jean Lamour (UMR CNRS 7198), department CP2S,
team "Surface and Interface, Chemical Reactivity of Materials",
University of Lorraine
B.P. 70239, 54506 Vandoeuvre-lès-Nancy, France*

Interdendritic carbides are often used to strengthen cast superalloys working in hot conditions [1]. These carbides have to be extremely stable at high temperature when the envisaged temperatures of service alloys are especially high. The volume fractions and geometrical shapes of chromium carbides, which are among the most often involved in refractory alloys to achieve mechanical properties improvements, evolve too rapidly in such conditions with consequently a loss in creep resistance. More stable carbides as the TaC ones are themselves not sufficient since they also undergo fraction reduction and fragmentation phenomena [2]. The HfC ones, which appeared much more resistant to such phenomena [3], and also which show a script-like shape recognized for its efficiency in creep resistance improving, are fortunately available for mechanical reinforcement on long times. Hafnium, which is an element essentially known for its efficiency in high temperature oxidation behaviour improvement [4,5] when added to alloys in rather low quantities in commercial superalloys, is also able to allow developing significant interdendritic HfC carbides in cast cobalt-based alloys if present in higher quantity in presence of carbon [6].

However it was recently seen that a significant interdendritic network of eutectic HfC carbides, able to bring high resistance to creep deformation, may also threaten the resistance of the concerned cobalt-based alloys in oxidation at high temperature, by leading to a not chromia-forming behaviour [7]. As evocated in the conclusions of [7] as future works, it was thus attempted here to increase the chromium content in these alloys, from the 25wt.% which was not high enough. Thus several new alloys with the same carbon (0.25 and 0.50 wt.%) and hafnium (3.7 and 7.4 wt.%) contents but with 7.5wt.%Cr more, were elaborated by foundry and tested in oxidation at 1200°C for 50 hours in dry synthetic air. The final mass gains, natures of oxides present externally and the values of parabolic constant and chromia volatilization constant (both extracted from the mass gain versus time file according to the $\{m \times dm/dt = K_p - K_v \times m\}$ method [8]) clearly show that the behaviour of these alloys became significantly improved, what let think that these new alloys may be candidate to uses at very high temperature on long times, in term of creep-resistance as well as in term of oxidation resistance.

References:

- [1] Donachie, M. J., Donachie, S. J., Superalloys: A Technical Guide (2nd Edition), ASM International (Materials Park, 2002).
- [2] Berthod, P., Michon, S., Aranda, L., Mathieu, S., Gachon, J.C., "Experimental and thermodynamic study of the microstructure evolution in cobalt-base superalloys at high temperature", Calphad, Vol. 27, No. 4 (2003), pp. 353-359.

- [3] Berthod, P., "High temperature properties of several chromium-containing Co-based alloys reinforced by different types of MC carbides (M=Ta, Nb, Hf and/or Zr)", *Journal of Alloys and Compounds*, Vol. 481 (2009), pp. 746-754.
- [4] Lee, S., Kim, G.M., "The effect of Hf, Y and Zr additions on the oxidation behaviour of Ni-based Inconel 601 at high temperature", *Han'guk Pusik Hakhoechi*, Vol. 24 (1995), pp. 124-133.
- [5] Maragoudakis, N., Tsipas, D., Eggonopoulos-Papadopoulos, V., "The role of reactive elements on scale adherence in high-temperature oxidation behaviour of metals and alloys", *Romanian Journal of Physics*, Vol. 49 (2004), pp. 245-250.
- [6] Berthod, P., Conrath, E., "As-cast microstructures and behaviour at high temperature of chromium-rich cobalt-based alloys containing hafnium carbides", *Materials Chemistry and Physics*, Vol. 143 (2014), pp. 1139-1148.
- [7] Conrath, E., Berthod, P., "Kinetic of high temperature oxidation of chromium rich HfC reinforced cobalt based alloys", *Corrosion Engineering Science and Technology*, in press (DOI 10.1179/1743278213Y.0000000105)
- [8] Berthod, P., "Kinetics of high temperature oxidation and chromia volatilization for a binary Ni-Cr alloy", *Oxidation of Metals*, Vol. 64, No. 3-4 (2005), pp. 235-252.

FLOW ACCELERATED CORROSION MANAGEMENT USING BRT-CICERO™: PERFORMANCES AND FUTURE UPDATES

S. Trévin, M-P. Moutrille, P. Caylar, D. Delacoux, E. Gipon - EDF/DPIH/DTG, Grenoble/France

Flow accelerated corrosion is very effective for nuclear power plant. This generalized corrosion can lead to the rupture of pipe and in some dramatic cases killed operators. EDF has developed during these 20 last years a software called BRT-CICERO™ for the surveillance of the secondary piping system of its Pressurized Water Reactors (PWRs). This software enables the operator to calculate the FAC wear rates taking into account all the influencing parameters such as: pipe isometrics, chromium content of the steel, chemical conditioning and operating parameters of the secondary circuit (temperature, pressure, etc.). This is a major tool for the operators to organize the maintenance and to plan the inspections.

In the framework of the French pressure vessel law issued on March 15th 2000, the software BRT-CICERO™ has been recognized by the French authority for the FAC surveillance on the secondary pressure piping lines of the EDF 58 NPPs. It takes advantage of the experience feedback of the French fleet, of the R&D improvements and is frequently updated. A guideline is associated to BRT-CICERO™ to define the rules and the pipelines include into the susceptibility analysis, take advantage of all functionalities and take into account the rapid experience feedback.

This paper deals with the maintenance optimization performed at EDF with industrial key factors such as:

- chemical conditioning specifications
- non-destructive testing shared on all units
- spare parts management with guaranteed chemical alloy contents
- development of specific technical features in BRT-CICERO™ integrating the effects of local chemistry, specific thermodynamic behavior, statistical analysis of wall thickness measurement and computational fluid dynamics.

Evaluation of the effects of pH and oxygen on mitigation of wall thinning of carbon steel due to flow-accelerated corrosion

Shunsuke Uchida, Masanori Naitoh and Hidetoshi Okada
Institute of Applied Energy, Tokyo, Japan

Six calculation steps were prepared for predicting flow-accelerated corrosion (FAC) occurrence and evaluating wall thinning rate (Figure 1). Flow pattern and temperature in each elemental volume along the flow path are obtained with a one dimensional (1D) computational fluid dynamics (CFD) code (Step 1) and then corrosive conditions, e.g., [O₂] and electrochemical corrosion

potential, along the flow path are calculated with the O₂-N₂H₄ reaction code (Step 2).¹ A 1D FAC code developed by applying 1D mass transfer coefficient (MTC) and geometrical factors can determine regional maximum wall

thinning rate, which could evaluate the high FAC risk zone (Step 3). As a result of verification and validation evaluation, it was confirmed that estimation accuracy of the wall thinning rate obtained with the 1D FAC code was within a factor of 2.¹ At the indicated high FAC risk zone, precise flow patterns around the structure surface are calculated with a 3D CFD code and then distributions of MTCs at the surface are obtained (Step 4). 3D wall thinning rates are calculated with the coupled models of static electrochemical model and dynamic oxide layer growth model (Step 5) (Table 1). As a final evaluation, residual lifetime of the pipes and applicability of countermeasures against FAC are evaluated in Step 6.

One of the promising countermeasures for FAC risk mitigation is to increase pH in the cooling water. Increasing pH from 9.2 through 10 might extend the time margin for pipe rupture. At present time not only ammonia but also morpholine, ethanoline and so on are injected to control pH in the PWR secondary coolant. High temperature magnetite solubility applied for the 1D and 3D FAC codes is expressed as a function of pH_{RT} determined by ammonia. Temperature dependent pH for many chemicals are determined (Figure 2) to evaluate the effects of pH on FAC wall thinning mitigation.

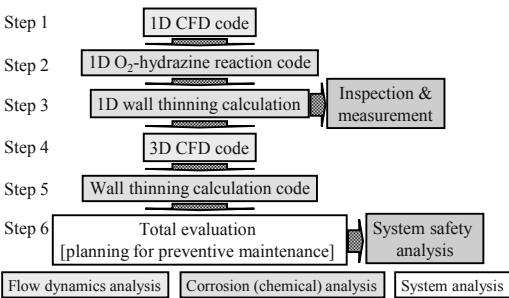


Figure 1 Evaluation inspection steps for wall thinning due to FAC

Table 1 Coupled electrochemistry/oxide layer growth model for wall thinning calculation

Sub-model	electrochemistry model (static model)	oxide layer growth model (dynamic model)
Input	temperature, [O ₂], pH, k _m , mass transfer coefficient (h _m) oxide film thickness, oxide properties	temperature anodic/cathodic current densities ECP
Output	anodic/cathodic current densities ECP	oxide film thickness properties (Fe ₂ O ₃ /Fe ₃ O ₄ ratio)
Final output	anodic/cathodic current densities wall thinning rate	

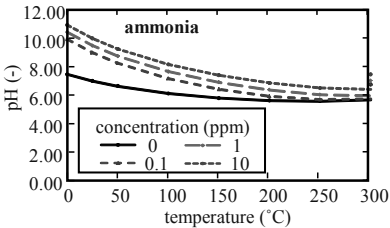


Figure 2 Temperature dependent pH

References

1) H. Suzuki, et.al., Nucl. Technol., 183, 194 (2013).

Intergranular oxidation of Alloy 600 exposed to simulated PWR primary water

Jacqueline Caballero, Centre des Matériaux - Mines ParisTech/ EDF R&D, Moret sur Loing Cedex/France

Jérôme Crépin, Centre des Matériaux – Mines ParisTech CNRS UMR 7633, Evry Cedex/France

Thierry Couvant, EDF R&D, Moret sur Loing Cedex/France

Cécilie Duhamel, Centre des Matériaux – Mines ParisTech CNRS UMR 7633, Evry Cedex/France

Several components present in the primary circuit of Pressurized Water Reactors (PWR) were manufactured with alloy 600. Field experience of the primary circuit of PWRs showed that alloy 600 may suffer intergranular stress corrosion cracking (IGSCC).

Many studies investigated IGSCC of alloy 600 and an empirical initiation model was developed to predict the time to initiation as a function of temperature, mean applied stress and a microstructural parameter mainly related to the precipitation. However, this model suffers a lack of predictability.

The current study proposes to focus on oxidation, especially along grain boundaries emerging at the surface exposed to the primary water. Intergranular oxidation is characterized as a function of time, metallurgical parameters (precipitation, chromium content) and environmental properties (dissolved hydrogen content).

The main objective is to propose an alternative initiation model based on local parameters, such as intergranular oxidation kinetics, instead of macroscopic parameters.

Effect of alloying elements and surface preparation on the oxidation behaviour of nickel base alloys in superheated steam

*F. Hamdani^{a,b}, H. Abe^a, T. Higashi^a, B. Ter-Ovanessian^b, C. Alemany-Dumont^b,
B. Normand^b, Y. Watanabe^a*

^a *Graduate School of Engineering, Tohoku University, 6-6-01-2 Aoba, Aramaki, Aoba-Ku, Sendai, 980-8579, Japan*

^b *INSA-Lyon, MATEIS CNRS UMR5510, F-69621 Villeurbanne, France*

Nickel base alloys have been selected to use in stream generator (SG) tubing in pressurized water reactor (PWR) due to their good corrosion resistance. These materials are eventual candidate to use in superheated steam generator for advanced ultra-supercritical power plants as well. So far, few oxidation studies of Ni-base alloys in superheated steam were conducted. However it was reported that some of Ni-base alloys composition can suffer from stress corrosion cracking (SCC) such as alloy 600 (Ni-16Cr-8Fe), thus presently higher chromium Alloy 690 (Ni-30Cr-8Fe) is used. Since this later shows a good resistance to SCC. It is commonly known that a sufficient Cr content in Ni-base alloys has a promoting effect on the oxidation resistance. On the other hand, the enhanced oxidation resistance of higher chromium alloys remains not clearly explained. This study is launched in order to determine the threshold of Cr content required to form a continuous Cr-enriched layer in superheated steam at 700°C in atmospheric pressure. This can be achieved by investigating the oxidation behaviour of Ni-Cr model alloys with Cr content in the range of 14-30 wt.%. Currently in the production lines, Ni-base alloys contain 8 wt.% of iron to reduce the manufacturing cost and improve their workability. Therefore, ternary Ni-xCr-8Fe (x=14,22 and 30) are also studied to point out the contribution of iron in the oxidation process. In the present study the oxidation rate was evaluated by weight gain (WG) measurements. A meticulous characterisation of the oxide scale is performed and the threshold of Cr content was suggested considering both oxide features and oxidation rates. Furthermore, the effect of surface preparation on the oxidation rate is examined. It was demonstrated that reducing the hardened layer which results from the surface preparation can be an accurate method to emphasize the effect of alloying elements on the oxidation rate and to avoid the synergetic effect with the cold-work. The hardened layer was reduced by mechanical polishing and completely removed by electro-polishing in order to reveal the effect of surface deformations on the oxidation behaviour. According to the present study, the threshold of Cr content was 26 wt. % for mirror polished surface. While, a discontinuous chromium oxide precipitates were observed beneath mirror polished surfaces of materials with Cr content in the range of 14-22 wt.%.

Image-based Cohesive Element Modelling of Low Temperature Crack Propagation in Alloy 82 Weld Metal

G. Klimaytys, A.P. Jivkov, D.L. Engelberg

*Materials Performance Centre, The University of Manchester,
Sackville Street, M13 9PL, United Kingdom*

Exposure of Alloy 82 welds to hydrogen containing, de-oxygenated aqueous environments at temperatures below 150°C can result in embrittlement, manifested by a significant reduction of its resistance to cracking. The embrittlement is brought about by nano-scale niobium and titanium rich carbonitrides at grain boundaries which act as hydrogen traps. The presence of stresses may then result in low temperature crack propagation (LTCP).

The work reported in this paper provides a better understanding of the effect of grain boundary micro- and meso-structure on LTCP susceptibility. The grain boundary morphology of an Alloy 82 weld microstructure was characterised using image analysis methods, and microstructure-faithful grain boundary profiles imported into Abaqus Finite Element (FE) software. A 2D model of the grain boundary meso-structure was generated using cohesive elements to simulate intergranular LTCP. Stress-assisted diffusion was used to calculate the rate of hydrogen ingress along grain boundaries. Changes in local hydrogen concentrations were then used to obtain the failure energy of each cohesive element. This controls the energy required to advance a crack locally. Grain boundary morphology, crystallography, and coverage of intergranular precipitates can also be included in the cohesive element model.

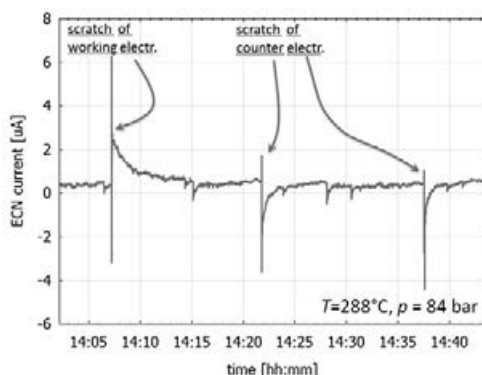
The model was compared to in-situ observations of crack propagation in fatigue pre-cracked Alloy 82 microstructures exposed to 54°C hydrogenated water. A windowed-autoclave test facility in conjunction with slow strain rate testing was used to observe a propagating crack along grain boundary segments. Digital image correlation (DIC) was then employed to estimate local crack growth rates and obtain fracture pathway information. Results obtained by in-situ observations were then used to calibrate cohesive model parameters. Post-mortem fractographic assessment was carried out to determine modes of failure.

Detection and characterization of stress-corrosion cracking of stainless steel in simulated BWR environment

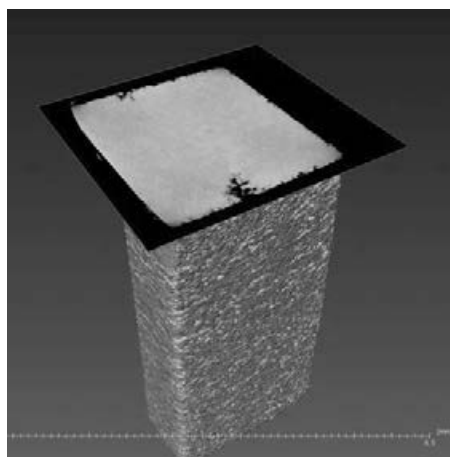
Bojan Zajec, Mirjam Bajt Leban, Andraž Legat, Slovenian National Building and Civil Engineering institute, Ljubljana, Slovenia

Stress corrosion cracking (SCC) is one of the most insidious corrosion processes, which can also be a critical degradation phenomena concerning safety of Nuclear Power Plants (NPPs), and integrity of high-radioactive waste (HRW) containers. This process can lead to catastrophic failures of structural components. SCC occurs in specific combination of three essential conditions: tensile stress or strain of a sufficient level, an aggressive local environment, and a susceptible material. Any technique for in-situ corrosion monitoring with the capability to detect SCC initiation in high temperature water environments is thus highly desirable.

In the present report we describe our work towards establishing an experimental setup for SCC detection and characterization in stainless steel samples in BWR environment using primarily electrochemical noise analysis while acoustic emission served as a complementary method. BWR environment ($T=288^{\circ}\text{C}$, pressure above 73 bar) was simulated in the autoclave equipped with the load cell and a unique scratching device, though without the circulation loop that resulted in water conductivity on the order of few $\mu\text{S}/\text{cm}$. Samples made of intentionally sensitized stainless steel were exposed to slow-strain rate test (SSRT) while the electrochemical noise (ECN) current and potential were recorded and acoustic emission signal were monitored. It was found that the SCC onset is highly sensitive to the sample surface preparation and can result in failure that is not primarily caused by SCC. Scratching and subsequent re-passivation kinetics is well manifested in the ECN current and potential signal. Post-mortem analysis of cracked samples by SEM, X-ray microtomography and metallography were performed to confirm the true nature of the fracture mechanism.



1. Electrode scratching as reflected on ECN current signal.



2. X-ray CT image with cross section plane of the cracked sample.

Characterization of Ni/NiO layers formed on Alloy 182 weld metal in PWR water

*Célia de Araújo Figueiredo^a, Renato Mendonça^b, Marc Vankeerberghen^c
and Rik-Wouter Bosch^c*

^aCDTN/CNEN, Av. Pres. Antônio Carlos, 6627, 31270-901 Belo Horizonte/Brazil
^bCAPES^b, Setor Bancário Norte, Q. 2, B. L. L. 6, 70040- 020 Brasília/Brazil
^cSCK•CEN, Boeretang 200, 2400 Mol/Belgium

It is known that Ni-based Alloys are susceptible to Stress Corrosion Cracking (SCC) when exposed to Pressurized Water Reactor (PWR) water for many years. The crack growth rate of Ni-based Alloys exhibits a maximum at a certain dissolved hydrogen concentration that also depends on the temperature. This maximum in crack growth rate is assumed to be related to the nickel/nickel oxide (Ni/NiO) phase transition. When the electrochemical corrosion potential of the system (reflected by temperature and dissolved hydrogen concentration) is equal to the Ni/NiO equilibrium potential, a maximum in SCC susceptibility is thus observed. The combination of temperature and dissolved hydrogen where the Ni/NiO transition occurred is still not well established as different values are found in the literature.

In this paper the effect of temperature on the Ni/NiO transition curve for a dissolved hydrogen concentration of 30 cc/kg was studied by means of electrochemical tests (Electrochemical Impedance Spectroscopy – EIS, and Mott-Schottky). The aim is to find the Ni/NiO transition temperature and relate the electrochemical results to the maximum in SCC susceptibility. Alloy 182 dissimilar metal weld was used in the tests. On-line electrochemical tests under PWR conditions (high temperature water with B and Li) were carried out in a temperature range of 300°C to 360°C together with the oxidation of samples for post test analysis. The impedance of Alloy 182 specimens was measured during the exposure time (2 weeks), once per day. The oxidized Alloy 182 specimens were used to measure the capacitance by means of Mott-Schottky tests in a buffer solution (0.05 mol/l H_3BO_3 + 0.075 mol/l $\text{Na}_2\text{B}_4\text{O}_7$) at room temperature after these two weeks of exposure. The oxide layer formed on other, specially-prepared, specimens (Alloy 182 weld metal and also pure Ni metal) was examined using Scanning Electron Microscopy (SEM) after the exposure time.

The first results showed that no oxide layer was formed on pure Ni metal in the temperature range of 300°C – 315°C. On Alloy 182, however, it was observed that a needle like oxide was formed on the surface, in the same temperature range. The capacitance measurements revealed the existence of a straight line with positive slope for potentials higher than – 0.5 V in the temperature range of 300°C – 315°C. However, a straight line with a negative slope was only seen at 315°C, for potentials lower than – 0.5 V. It indicates that the oxide layer behaves as n-type semiconductor in the temperature range 300°C – 315°C, but p-type behavior could be observed only at 315°C. Results from impedance and Mott-Schottky tests for 300°C – 360°C will be presented along with the material characterization.

Experimental and numerical study of the iodine-induced stress corrosion cracking of Zircaloy-4 nuclear fuel cladding tubes

T. Jezequel, Q. Auzoux, D. Le Boulch, CEA Saclay, Gif-sur-Yvette/France; E. Andrieu, C. Blanc, CIRIMAT/INPT, Toulouse/France; C. Delafoy AREVA NP, Lyon/France; N. Barnel, EDF R&D, Moret-sur-Loing/France, C. Dal Bianco, EDF SEPTEN, Lyon/France

After exposure to the pressurized water nuclear reactors, the initial gap between the pellet and the cladding of nuclear fuels is reduced to zero due to combine effects of irradiation and water pressure. This phenomenon is called Pellet-Cladding Interaction (PCI). During accidental power transient under PCI conditions, the synergistic effect of the hoop tensile stress and strain imposed on the cladding by the fuel thermal expansions and corrosion by iodine released as a fission product, may lead to cladding failure by Iodine-induced Stress Corrosion Cracking (I-SCC).

In this study, internal pressure tests were conducted on 90 mm long cladding tubes of unirradiated cold-worked stress-relieved Zircaloy-4 under an iodine vapor environment. The aim was to investigate the influence of loading mode (constant pressure tests, constant circumferential strain rate tests or constant circumferential strain tests) and test temperature (320°C, 350°C or 380°C) on the I-SCC process. Fractured samples were observed by scanning electron microscopy (SEM) in order to identify the initiation and propagation mechanisms. Moreover, tests were simulated by finite element analysis using a viscoplastic mechanical model combined with an I-SCC damage model.

The experimental results obtained with different loading modes highlighted a very good consistency. The apparent threshold hoop stress for I-SCC was found to be independent of the test temperature.

SEM micrographs of the fractured and the inner surfaces of the tested samples showed common features. Many pits were distributed over the inner surface; they tended to coalesce into large pits in which a microcrack initiated. Fractographic examination showed an elliptical and relatively brittle area characteristic of I-SCC, where intergranular and transgranular patterns – quasi-cleavage and fluting – were observed with also a lot of pits mainly located at the beginning of the crack propagation.

A model was developed, based on both test simulation by finite element analysis using a specific viscoplastic constitutive equation and time-to-failure predictions by a modified Kachanov's damage growth. This model succeeded in predicting the time-to-failure under various conditions, considering both the mechanical and the chemical contributions.

Another facet of this study was the use of complementary experimental means (secondary ion mass spectrometry, Raman and infrared spectroscopy) to analyze the chemical interactions between the iodine compounds and the zirconium. The aim was a better understanding of the chemical mechanisms notably about the iodine speciation.

The influence of lithium ions on corrosion of zirconium alloys

Aneta Krausová¹, Jan Macák¹, Petr Sajdl¹, Veronika Renčiuková², Věra Vrtílková²,

¹ Institute of Chemical Technology, Prague, Czech Republic

² UJP Prague, Czech Republic

The influence of lithium ions on corrosion of different types of zirconium alloys was investigated using electrochemical impedance spectroscopy (EIS). The long-term (up to 1000 hours) in-situ corrosion tests were carried out in the experimental high-pressure high-temperature loop (280 °C, 8 MPa). The experiments were performed in lithiated environment as well as under VVER simulating conditions. The concentration of 70 ppm Li is considered as a significant limit value at which the enhanced corrosion rate starts to occur. The influence of a higher concentration of lithium (200 ppm) on corrosion characteristic of zirconium alloys was also compared. Impedance spectra were processed using suitable equivalent circuit to determine the transfer and diffusion parameters of the oxide layers. Especially significant are the values of the polarization resistance which are related to the instant corrosion rate. The oxide thickness was determined using Jonscher's analysis and by application of a model based on Stern-Geary approach. Weight gain measurements were chosen as a reference method to electrochemical measurements. The Mott-Schottky approach was employed to finding the semiconducting character and dopant density of the corrosion film.

Effect of Superheated Steam on the Corrosion Behaviour of Advanced Steels Proposed as Accident Tolerant Fuel Cladding

Raul B. Rebak, and Evan J. Dolley
GE Global Research

1 Research Circle, Schenectady, NY 12309, USA 1

The US Department of Energy (DOE) started a research program focused on accident tolerant fuels (ATF), in part as a response to the events of 11 March 2011 in North East Japan. In comparison with the traditional UO₂–Zirconium based system, the ATF fuels need to tolerate loss of active cooling in the core for a considerably longer time period while maintaining or improving the fuel performance during normal operation conditions. The current research focuses on the replacement of zirconium alloy cladding for advanced steels such as iron-chromium-aluminum (FeCrAl) alloys since they offers a series of improved benefits under accident conditions. Commercial and experimental alloys were tested for several periods of time in 100% superheated steam from 600°C to 1475°C. The candidate new alloys (e.g. APMT, and Alloy 33) offer orders of magnitude improvement over the current zirconium based material both from the mechanical properties and corrosion performance under normal operation conditions and under accident conditions (Figure 1).

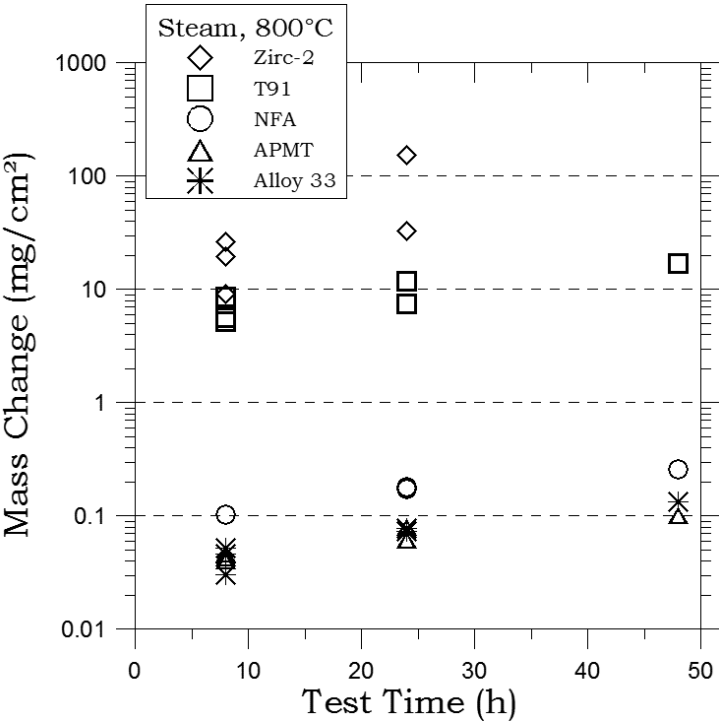


Figure 1. Mass change as a function of testing time in 100% steam at 800°C

Study on the effect of phosphorous concentration on intergranular corrosion of stainless steel in boiling nitric acid solution

Fumiyoshi UENO, Atsushi KOMATSU, Takahiro IGARASHI, Masahiro YAMAMOTO
Japan Atomic Energy Agency
2-4, Shirakata-Shirane, Tokai-mura, Ibaraki, 319-1195, Japan

In PUREX fuel reprocessing process, the plant materials are exposed in severe corrosion environment with boiling nitric acid solution. In the environment, austenitic stainless steels, which are used to concentrators and dissolvers, indicate intergranular corrosion (IC) surfaces. Many reports have concluded that concentration of minor elements (e.g., C, Si, P, S) in grain boundary (GB) were effective on IC progress. In this paper, the effect of phosphorous concentration in GB on IC progress was studied by experimental and numerical method.

Used material was an extra high purity (EHP) alloy¹⁾ which includes total concentration of minor elements within 100ppm. In this study, type 310 EHP stainless alloy²⁾ added with 270ppm P was used after thermal aged for 1.2×10^6 s at 873K to investigate an effect of P concentration in GB on IC. Specimen was corroded under the constant quantity of electric charge at controlled potential of 1.1V (vs. Ag/AgCl) in boiling $8 \text{ mol} \cdot \text{dm}^{-3}$ nitric acid³⁾. Figure 1 shows cross-section of corroded surface. Corroded GB shows triangular cross-section. The analysis result of three-dimensional atom probe (3DAP) in the corroded GB shows approximately 1.4at% of P as shown in Fig.2. From the experiments, IC rate was considered to be effective by P concentration change in GB.

Relation between P profile in GB and IC rate was studied by numerical simulation using cellular automaton method⁴⁾. Solution, grain and GB were simplified into two-dimensional model as shown in Fig.3. In this method, corrosion rate was represented as the changing rate from grain or GB cells to solution cells. For the numerical simulation, both IC rate and grain surface corrosion rate were assumed and introduced to the simulation. In the case of considering with local concentration of P in a GB, IC was accelerated and triangular shape was changed to sharp in cross-section as shown in Fig.4.

As the results, concentration of P in GB was detected and new simulation method of IC progress considering with P profile in GB was developed. It can be concluded that P concentration change around 1.4at% in GB of type 310 EHP stainless steel causes IC rate change in boiling nitric acid solution.

References : 1) J. Nakayama, et al., *Kobe Steel Engineering Reports*, 59-2, p.94 (2009). 2) I. Ioka, et al., *Proc. ICONE16*, ICONE16-48776, (2008). 3) A. Komatsu, et al., *Zairyo-to-Kankyo*, in press. 4) T. Igarashi, et al., *Zairyo-to-Kankyo*, in press.

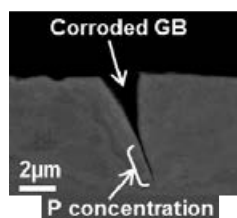


Fig.1 Cross-section of Corroded grain boundary

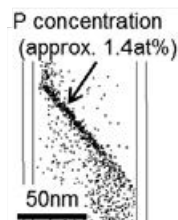


Fig.2 P profile in GB by 3DAP analysis

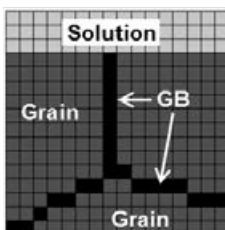


Fig.3 Two-dimensional cellular automata model

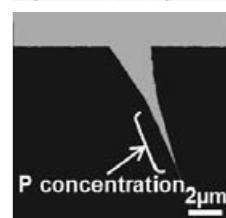


Fig.4 Simulation result of corrosion behavior in P concentrated GB

Evaluation of the corrosion behavior of candidate materials for overpack applications under buried conditions

Gen Nakayama, Yohei Sakakibara, IHI Corporation, Yokohama/Japan;

1. Estimation of the general corrosion rate of carbon steel

Tests were conducted to measure the corrosion rates of three carbon steel round bar electrodes, each of diameter 6 mm and immersion depth of 30 mm, according to procedures specified by ASTM G199-09 for mixing water and bentonite at a ratio of 1:2 in an ambient atmosphere and also heated at 40°C. The times for the immersing potential and the open-circuit current are shown in Fig.1 for a two-hour duration with 138.5 hours of elapsed time. The corrosion rate was computed at $1.05 \mu\text{Acm}^{-2}$ based on data obtained after the test had been initiated with data obtained as $\sigma_E=1.06\text{mV}$, and $\sigma_i=0.254\mu\text{A}$. Despite the presence of dissolved oxygen brought to the test system from the ion-exchanged water, the mass transfer of DO was restricted by the presence of bentonite. Changes in the general corrosion rate, *GCR*, of the carbon steel over time, as immersed in the mixture of water and bentonite at 40°C, are shown in Fig.2. *GCR* was found to have declined to a level of around $10\mu\text{myr}^{-1}$ after 100 hours had elapsed.

2. Estimation of the general corrosion rate of titanium

The *GCR* values of titanium computed based on the test-time dependence of the *GCR* obtained from the passivity-sustaining current density, i_{pass} during potentiostatic tests of +0.5V vs .SHE, and other values becomes steady during the test period after 100 to 1,000 hours have elapsed; reaching a value of between 1 and $0.01 \mu\text{myr}^{-1}$ as shown in Fig. 2.

The *GCR* values of stainless steel similarly obtained are smaller than those of titanium, which suggests that although titanium is considered less susceptible to local corrosion under certain environments, it is not the final solution to general corrosion loss. Furthermore, the *GCR* of carbon steel under conditions of restricted mass transfer is as low as $10\mu\text{myr}^{-1}$, suggesting that the proposed uses of titanium may be impractical.

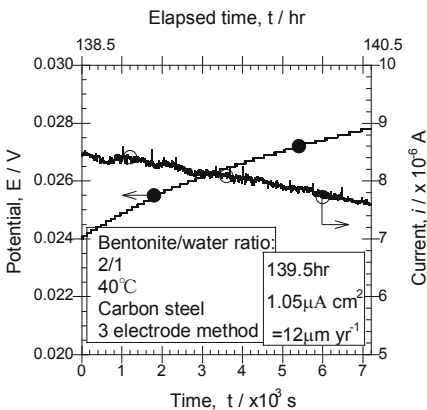


Fig. 1 Times to immersion potential and open circuit current of carbon steel.

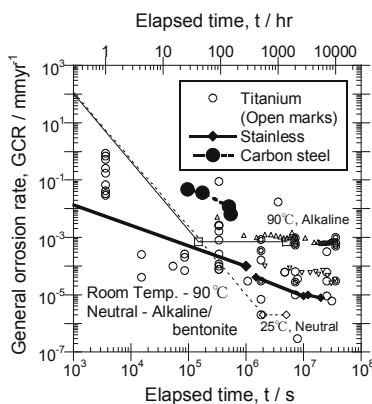


Fig.2 Changes in the general corrosion rates of titanium, stainless steel, and carbon steel over time.

The corrosion of carbon steel embedded in bentonite under anoxic conditions

Nicholas R. Smart¹, Andrew P. Rance¹, Bharti Reddy¹, Nikitas Diomidis²

¹ *Amec, Clean Energy – Europe, Building 150, Harwell Oxford, Didcot, Oxfordshire, OX11 0QB, United Kingdom.*

² *Nagra, National Cooperative for the Disposal of Radioactive Waste, Hardstrasse 73, Postfach 280, 5430 Wettingen, Switzerland.*

The concept for the Swiss national program for the disposal of spent fuel and high level radioactive waste consists of a deep geological repository at a depth of 650-900m in Opalinus Clay host rock. The repository will be based on a series of excavated tunnels within which disposal canisters containing spent fuel assemblies or vitrified waste will be set on pedestals made from compressed bentonite blocks. After emplacement of the canisters, the tunnel will be backfilled with granular bentonite and sealed. According to the current reference canister design concept, the canisters will be cylindrical with flat ends that incorporate a handling feature. They will be made from forged low carbon steel.

After closure of the repository the conditions in the disposal tunnels will gradually evolve. Ingress of porewater from the host rock will increase the relative humidity until the bentonite is fully saturated. In parallel, oxygen which existed in the bentonite pores and the excavation disturbed zone will gradually be consumed by corrosion, microbial activity or other processes until anoxic conditions prevail. Saturated and anoxic conditions are expected to remain indefinitely and will therefore be present for the vast majority of the lifetime of the disposal canisters.

The corrosion rate of carbon steel embedded in saturated bentonite under anoxic conditions was measured using barometric gas cells. The evolution of the corrosion rate was monitored for over three years until quasi steady-state conditions were reached. The measured corrosion rates are in agreement with weight loss measurements and with previous tests under similar conditions.

Dismantling one of the gas cells and characterisation of the surface of the corrosion coupons and the steel/bentonite interface provided an insight into the prevailing mechanisms under relevant repository conditions. The main corrosion product was identified as being magnetite, while there were also indications of other iron oxy-hydroxides. Surface microstructural analysis and profilometry indicated that some roughening of the surface and localised phenomena had occurred.

Challenges related with the development of the closure plan for DNDR Băița Bihor România –Corrosion Monitoring

R. Fako¹, F. Dragolici², Ghe. Barariu¹, F. Sociu¹, E. Neacșu²,

1) RATEN – Center of Technologies and Engineering for Nuclear Objectives (CITON), Măgurele/România;

2) Horia Hulubei National Institute of Physics and Nuclear Engineering (IFIN-HH), Măgurele, Romania

The aim of the paper is to emphasise the advancements of a corrosion monitoring schedule within a Joint Applied Research Project developed by three Romanian research and design organizations in order to demonstrate the safety of the proposed Closure Plan for the Radioactive Waste National Repository Băița Bihor (DNDR-BB). The DNDR – BB facility is developed in former uranium mine, accepts short-lived low institutional radioactive wastes and was commissioned in 1985. It is presently considered that the disposal activities will continue until 2040. During time there were proposed and implemented improvements of the operation schedule. All modifications were carefully demonstrated based on international experience and regulatory framework in order to guarantee repository safety for population and environment on the intended time frame. The improvements were internationally supported into the frame of several PHARE projects.

In order to realise an assessment of the performance of the Closure System proposed for DNDR Băița Bihor several experimental arrangements were developed both in laboratory and in-situ (in an experimental gallery at DNDR Băița Bihor). Even in incipient phase, the preliminary results of these programs could be considered as valuable inputs for modelling and anticipation of several damage mechanisms that could arise in the disposal system. All data registered for the exposed corrosion specimens will be analysed and interpreted considering relevant mechanical data obtained on tested specimens, permeability data for the conditioning matrices used for corrosion specimens, leaching data and any other information regarding the exposure environment and time dependent alterations of the exposure conditions.

The experiments are in progress and it is anticipated that they will increase the knowledge database on corrosion mechanisms and kinetics in the disposal system at DNDR Băița Bihor (both before and after the implementation of the Closure Plan). Also, the corrosion experimental program outputs will be important data for demonstration of the disposal system stability during the repository service design life (based on forecasted interactions between metallic surfaces and sealing/backfilling materials).

References

1. The Strategy Development for Closing the DNDR Baita Bihor, Based on the Optimization of Engineering Barriers (SARAWAD-BB), PN-II-PCCA-2011-3.2-0334, Project 156/2012-Stage II, SITON/IFIN-HH/UTCB (2013);

Acknowledgments

This work was supported by a grant of the Romanian National Authority for Scientific Research, project number 156/2012.

Corrosion of carbon steel in the Callovo-Oxfordian claystone in the context of the French nuclear waste repository¹ (in project) 1.

Experimental set up and corrosion behaviour

S.Necib¹ sophia.necib@andra.fr, D.Crusset², N.Michau², F.Foct³, M.Schlegel⁴, S.Daumas⁵, S.Dewonck¹

1.Andra, Meuse/Haute Marne Center, 52290 Bure, France 2. Andra, 92290 Châtenay-Malabry, France 3. EDF 4.CEA, DEN, DPC/SEARS/LISL, F91191 Gif-sur-Yvette; France 5.CFG Services, 13009 Marseille, France

Carbon steel (C-steel) is studied to be the material for the metallic components of the high level waste (HLW) in the French repository (in project).

There are two main metallic components involved. One is called "liner" and its main function is to ensure mechanical resistance. The second one called "overpack", is to prevent water from reaching the vitrified HLW during the thermal phase.

In situ experiment has been conducted at the Meuse/Haute-Marne underground laboratory to investigate the corrosion behaviour of different grades of C-steel coupons at a maximum temperature of 85°C. Two environments have been studied; porewater and gas coming from the Callovo - Oxfordian (Cox) host rock, in which the future vitrified nuclear waste will be disposed of. Three series of rods, containing C-steel coupons, have been introduced, at different times, to a test chamber composed of two media: porewater and gas. The series were composed of seven, three and four rods respectively. Each rod contained up to twenty coupons (ten in the porewater phase and ten in the gas phase). The rods have been retrieved at a particular given time to measure the corrosion rate of the C-steel coupons. In addition, corrosion products characterisation, chemical and microbial analyses have been carried out to well understand the corrosion processes.

After 36 months of experiment, the different grades of C-steel have revealed similar corrosion behaviours for a given rod. The first series of rods have shown two main corrosion behaviours. Some rods presented coupons showing corrosion rate inferior to 20 µm/yr, while, others revealed corrosion rate going up to 200 µm/yr. Chemical analyses revealed the presence of an acidic pH transient going down to 4.8, which lasted about 200 days. Corrosion products characterisation showed that for the coupons revealing higher corrosion rate, a layer of β -Fe₂(OH)₃Cl hydroxychloride was present at the inner interface, while for the coupons corroding at lower corrosion rate, only siderite or chukanovite was present in close contact with the metal.

The second and last series of rods, which were not exposed to the acidic transient, revealed low corrosion rate below 20 µm/yr.

Results from microbial analyses showed the presence of sulphate reducing bacteria (SRB) and thiosulphate reducing bacteria (TRB), both in the corrosion products and in porewater. Their metabolism was confirmed by a decrease of the sulphate concentration present in clay porewater. On the other hand, in the gas phase, the corrosion products did not reveal neither SRB nor TRB. The impact of micro-organisms on the corrosion processes is still being investigated as well as the characterisation of the corrosion products of the coupons from the second and third series of rods.

Acknowledgements : The authors wish to acknowledge Solexperts (particularly Thomas Fierz and Yanick Lettry) for supplying the equipment of this experiment.

¹ For the corrosion products characterisation studies, see „Corrosion at the carbon steel-clay porewater interface in a nuclear waste repository.

2. Structural organization of corrosion products, M.L. Schlegel et al."

Iron corrosion products (CP) impact on the long term alteration of fractured nuclear glass: effects of transport and CP stability

Gentaz L.^a, Neff D.^a, Rebiscoul D.^b, Dillmann P.^a et Gin S.^b,

^a - LAPA SIS2M UMR3299 CEA/CNRS, CEA Saclay, 91191 Gif sur Yvette, France

^b - LCLT SECM, CEA Marcoule, 30207 Bagnols-sur-Cèze, France

Keywords: Nuclear glass, iron, corrosion, archaeological artefacts, anoxic environment, SON68

Abstract

In the context of long term nuclear waste repository, the reference system is based on a multi-barriers concept: nuclear glass is placed in a low-alloy iron steel overpack stored in clay media saturated by water. The water will in time corrode the overpack and alter the fractured glass. In order to accurately simulate the storage analogues of long term alteration, archaeological artefacts buried under similar conditions, were used. Representative corrosion products (RCP) were extracted from 450 year old archaeological iron nail corroded in clay media saturated with anoxic carbonated water at Glinet reference site.

The interactions between glass and iron can have a catalytic effect the glass alteration mechanisms as iron-rich phases possess a strong affinity for silicon. Laboratory experiments under anoxic conditions have shown an increase in the glass alteration rate when in contact with iron and/or its corrosion products. The extent of the alteration and the underlying mechanisms depend on the phase nature and its specific surface area. Affinity to silicon will also differ between synthesized corrosion products and RCP, due to their porosity limiting or enhancing the transport through the iron corrosion layer and the stability of iron corrosion products which will impact on the availability of iron in solution.

For this study, the fractured glass system is simulated by a model-fissure of SON68 glass (the inactive surrogate of French nuclear R7T7 glass) in contact with iron, iron RCP or iron CP synthesized in storage conditions. Experiments were conducted in cell at 50°C in contact with synthetic groundwater solution. The analyses of the resulting samples were conducted through systematic multi-scale and multi-instrumental analyses: optic microscopy, scattering and transmission electronic microscopy, μ RAMAN spectrometry, μ XRD and STXM at the Fe and Si-edge.

The results will provide information on the transport of silicon in the system, migration through the porous material and retention due to affinity with iron. The distance between the glass-solution interface and the source of iron will impact on the rate of alteration as well as on the nature of the secondary products formed.

Galvanic corrosion of carbon steel under argillite layers in carbonated media

A. Romaine^{a,b}, R. Sabot^a, M. Jeannin^a, Ph. Refait^a

^a Laboratoire des Sciences de l'Ingénieur pour l'Environnement (LaSIE),
FRE 3474 CNRS-Univ. La Rochelle, Bât. Marie Curie, Av. Michel Crépeau,
F-17042 La Rochelle cedex 01, France.

^b ANDRA, Parc de la Croix Blanche, 1/7 rue Jean Monnet, F-92298 Châtenay-Malabry, France.

This study relates to the problem of long-term interim storage of nuclear wastes. In France, it is envisaged that high-level radioactive wastes will be confined in a glass matrix, stored in a stainless steel canister, itself placed in a carbon steel overpack. The wastes will then be stored at a depth of ~450 m in a deep geological disposal, drilled in a very stiff (indurated) clay (argillite) formation. Because of the intense radioactivity, a temperature as high as 90°C is expected at the steel surface. In these conditions, magnetite, siderite and chukanovite are the main expected corrosion products of steel [1].

One of the possible risks of localized corrosion of the carbon steel overpack is the galvanic coupling that might happen between two zones of the metal covered with different corrosion products or in contact with different electrolytes. This phenomenon is also known in the oil and gas industry and often described as mesa-corrosion.

To address this problem, the effects of the galvanic coupling between a magnetite electrode and a bare carbon steel electrode were investigated at 25°C and 80°C. Both electrodes were covered by a ~5 mm thick argillite layer that strongly hinders the transport of oxygen and more generally the transport of matter [1-2], and immersed in a NaHCO_3 (0.01 mol L^{-1}) + NaCl (0.01 mol L^{-1}) solution. The current density between the two electrodes was monitored thanks to a ZRA (zero resistance ammeter) method for different surfaces ratios ($S_{\text{anode}}/S_{\text{cathode}}$). To simulate a local source of sulfide species (sulfate reducing bacteria or pyrite FeS_2 , a mineral present in argillite), the galvanic coupling between a first carbon steel electrode immersed in a sulfide-containing solution and another immersed in a NaHCO_3 + NaCl solution was studied at 80°C, the electrodes being covered by a ~5 mm thick argillite layer. In both kinds of experiment, μ -Raman spectroscopy was used to identify the compounds formed on the electrodes at the end of the experiment.

In both cases, galvanic corrosion could be observed, associated with significant galvanic current densities ($10\text{-}60 \mu\text{A/cm}^2$). The galvanic current proved more important between magnetite (cathode) and steel (anode) at 80°C. In most cases, the galvanic current tended to decrease with time. Raman analysis revealed that the electrodes coupled with magnetite were covered by a corrosion products layer made of an inner stratum of magnetite and an outer stratum of siderite and chukanovite. The magnetite stratum was not homogeneous, implying that anodic areas were still remaining on the carbon steel surface.

[1] A. Romaine, R. Sabot, M. Jeannin, S. Necib, Ph. Refait. *Electrochimica Acta*. 114, (2013) 152-158.

[2] M. Jeannin, D. Calonnec, Ph. Refait. *Electrochimica Acta*. 56 (2011) 1466-1475.

Surface Analytical and Electrochemical Measurements on Cu-Coated Steel Specimens

Raheleh Partovi-Nia¹, Rebecca Jacklin², Jian Chen¹, Dimitrij Zagidulin¹, Sridhar Ramamurthy², Peter G. Keech³ and David W. Shoesmith^{1, 2}

¹*Department of Chemistry, Western University, 1151 Richmond St, London, Canada*

²*Surface Science Western, Western University, 999 Collip Circle, London, Canada*

³*Nuclear Waste Management, 22 St Clair Ave, Toronto, Canada*

A proposed concept for permanent storage of spent nuclear fuel involves the use of a deep geological repository, with multiple engineered barriers to contain and isolate the used fuel from environment. The corrosion behaviour of the container materials becomes critical to ensure reliable confinement of high-level nuclear waste for such a long repository period. Copper has been selected mainly because of its calculated thermodynamic immunity to spontaneous corrosion in near pH neutral anoxic oxygen-free water. One reference Canadian used fuel container consists of dual vessel comprised of outer shell of copper and an inner shell of low alloy steel ; this container is conceptually similar to the SKB KBS-3 container, in that the inner steel 100 mm component will provide structural support, even under glacial loading, while the outer 25-50 mm copper casing will provide a corrosion barrier.¹ Because of the challenges in manufacturing, including the requirement of a very narrow gap between the copper and steel components (<1.5 mm over 4 m length), and the need to produce a self-supporting copper sleeve of a minimum wall thickness in excess of 50 mm during extrusion, an alternative design is being explored within the Canadian program, which involves directly coating copper onto steel to produce a layered single container capable of withstanding suitable mechanical loading and corrosion phenomena. Two coating methods are currently considered for manufacturing the outer shell of these containers, namely cold-spray and electrodeposition. The purpose of this study is to provide a preliminary corrosion evaluation of the cold-spray and electrodeposited copper deposited on A516 Gr. 70 low alloy steel substrate and comparing this corrosion behavior to that of the standard SKB copper (low oxygen). Initial surface condition and the surface properties were determined using optical microscopy, scanning electron microscopy coupled with energy dispersive X-ray analysis (SEM/EDX), and confocal laser scanning microscopy (CLSM). A series of electrochemical tests were performed using constant applied current to accelerate the dissolution of the copper. A current density of 10 $\mu\text{A}/\text{cm}^2$ was applied for a series of 24 hour periods. The electrochemically-treated specimens were then analyzed by SEM/EDX, X-ray diffraction (XRD) to determine the structure, morphology, and composition of the corrosion products. In addition, CLSM and profilometry techniques were also used to determine the changes in the roughness and topography of the electrochemically-treated interface. To-date no significant differences in corrosion behaviour between the SKB and cold-spray and electrodeposited copper have been observed.

Reference:

1.Scully, J. R.; Edwards, M. "Review of the NWMO Copper Corrosion Allowance," Nuclear Waste Management Organization. NWMO TR-2013-04, **2013**.

Corrosion behaviour of Mg alloys cladding from nuclear reactors fuel in alkaline solutions

J. Agullo¹, B. Muzeau¹, C. Bataillon², V. L'Hostis¹, CEA Saclay, Gif-sur-Yvette/France

¹ CEA, DEN, DANS, DPC, SECR, Laboratoire d'Etude du Comportement des Bétons et des Argiles, F-91191 Gif-sur-Yvette (France)

² CEA, DEN, DANS, DPC, SCCME, Laboratoire d'Etude de la Corrosion Aqueuse, F-91191 Gif-sur-Yvette (France)

The reprocessing of spent fuel from the French UNGG (Graphite Gas Natural Uranium) nuclear power plants generates cladding wastes such as Mg-Mn alloys. A storage strategy is to encapsulate these wastes into cement matrix. The main issue is hydrogen evolution as the main consequence of the corrosion of Mg alloys, regardless of concrete radiolysis. In fact Mg acts as an anode in most of galvanic corrosion systems and the hydrogen can be produced either by water reduction or by Anodic Hydrogen Evolution (AHE). In the last case, an increase in the rate of hydrogen production with increasing applied potential is observed. This phenomenon called "Negative Different Effect" (NDE) is in contradiction with the conventional Tafel equation. The corrosion of magnesium may produce Mg^+ cations which react quickly with water to produce hydrogen and stable Mg^{2+} cations.

The interstitial solution in concrete pores is characterized by a very high pH. To reproduce the pH solution around 13, 0.1M NaOH solutions were prepared and used as electrolytes from electrochemical experiments. Stainless steel, platinum and graphite were used as cathode to investigate basic galvanic coupling as it can be encountered in the real wastes.

The purpose of this work was to investigate the galvanic corrosion of Mg alloys in the high pH solutions. The study of Mg corrosion behaviour was carried out using electrochemical measurement: ZRA mode. The analysis of the surface and the corrosion products were performed by Raman spectroscopy. The first results showed a galvanic corrosion rate more important with stainless steel rather than with graphite.

Advanced Al_2O_3 coatings under extreme conditions

F. García Ferré, Center for Nano Science and Technology, Istituto Italiano di Tecnologia, Via Pascoli 70/3, 20133 Milano, Italia

M. Ormellese, Dipartimento di Chimica, Materiali e Ingegneria Chimica, Politecnico di Milano, Via Mancinelli 7, 20131 Milano, Italia

M. Beghi, Dipartimento di Energia, Politecnico di Milano, Via Ponzio 34/3, 20133 Milano, Italia

F. Di Fonzo, Center for Nano Science and Technology, Istituto Italiano di Tecnologia, Via Pascoli 70/3, 20133 Milano, Italia

In future generation nuclear systems cooled by Heavy Liquid Metals (HLMs), such as lead or lead-bismuth eutectic (LBE), fuel cladding will be exposed to an extremely harsh environment, in which radiation dose will approach 150 displacements per atom (dpa) at a temperature of up to 800°C. In addition, corrosion of structural steels by HLMs stands as a major bottleneck.

In this work, we propose the use of a nanocrystalline Al_2O_3 /amorphous Al_2O_3 composite coating as a corrosion barrier for high temperature operation of steels in HLMs [1]. The barrier layer is grown by Pulsed Laser Deposition (PLD) at room temperature, 400°C and 600°C. The mechanical properties of the coating are assessed with high accuracy and precision through a novel opto-mechanical method [2], based on the combination of ellipsometry, Brillouin spectroscopy and nanoindentation. The adhesive strength is evaluated by nanoscratch tests. In the room temperature process, and up to 400°C, the coating attains an unusual combination of compactness, strong interfacial bonding, moderate stiffness ($E=195\pm9$ GPa and $\nu=0,29\pm0,02$) and significant hardness ($H=10\pm1$ GPa), resulting in superior plastic behavior and a relatively high ratio of hardness to elastic modulus ($H/E=0,049$). These features are correlated to the nanostructure of the coating, which comprises a regular dispersion of ultra-fine crystalline Al_2O_3 nano-domains (2-5 nm) in a dense and amorphous alumina matrix. For the coating grown at 600°C, strong adhesion is still observed, along with an increase of stiffness and a significant enhancement of hardness ($E=277\pm9$ GPa, $\nu=0,27\pm0,02$ and $H=25\pm1$ GPa), suggesting an outstanding resistance to wear ($H/E=0,091$). Corrosion aspects are examined by short- and mid-term exposure of samples to stagnant HLMs at 600°C. Post-test analysis reveal no signs of corrosion, confirming the strong chemical inertia of the coatings [1]. The performance of the alloy substrate-ceramic coating system under high dose radiation damage is studied by irradiation with heavy ions up to 150 dpa at 600°C. Finally, other coating materials and structures of interest, including cermets and graded barriers with an engineered composition, are proposed and discussed.

References

- [1] F. García Ferré, M. Ormellese, F. Di Fonzo, M.G. Beghi. *Corr Sci* 77 (2013) 375
- [2] F. García Ferré et al. *Acta Mater* 61 (2013) 2662

Oxidation of 316L(N) stainless steel in liquid sodium at high temperature

Matthieu Rivollier¹; Jean-Louis Courouau¹; Marie-Laurence Giorgi²

¹CEA, DEN, DANS, DPC, SCCME, Laboratoire d'Etude de la Corrosion Non Aqueuse, F-91191 Gif-sur-Yvette, France ;

²CNRS, RA4038, Laboratoire Génie des Procédés et Matériaux, F-92295 Chatenay-Malabry, France

The sodium cooled fast reactor is selected in France as the 4th generation of nuclear power plant. 4th generation's reactor vessel, primary loop structures and heat exchangers will be made of austenitic stainless steels. 316LN is the reference material. To assess reactor service life time, corrosion of austenitic stainless steel by liquid sodium is studied in normal operating conditions as well as transient conditions either expected or not.

Based on corrosion tests performed in the static sodium testing device ("CorroNa") at 550°C, sodium chromite scale (NaCrO_2) is observed in slightly oxidizing conditions. Below the oxide scale, a chromium depleted layer is observed (Figure 1). This paper presents the morphology of this oxide scale, and its properties (expected corrosion behavior).

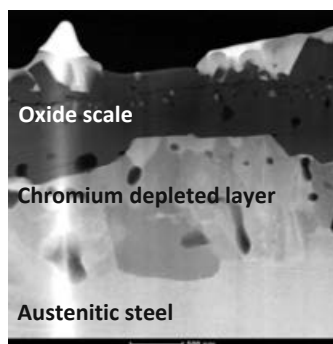


Figure 1 - TEM cross section observation

To predict long term corrosion effects on materials (40-60 years), the oxidation's mechanisms are investigated, in order to identify the corrosion limiting step, as well as to understand the basic phenomenon at play in this complex corrosion mechanisms. One of the first issues is to determine the direction of growth of the oxide scale. Inert corrosion marker tests, as well as isotopic markers corrosion test (^{16}O - ^{18}O) are presented. Characterizations are then performed by to Rutherford Backscattered Spectroscopy (RBS), Glow Discharge (GDMS + GDOES), and Secondary Ion Mass Spectroscopy (SIMS). The direction of growth is found to be inwards. In addition, these results are used to assess the oxygen diffusion coefficient in the sodium chromite scale.

Corrosion of carbon steel in the Callovo-Oxfordian claystone in the context of the French nuclear waste repository (in project). 2. Structural organization of corrosion products.

M. L. Schlegel^a, S. Necib^b, S. Daumas^c, C. Blanc^a, E. Foy^d, D. Crusset^e, N. Michau^e

^aCEA, DEN, DPC/SEARS/LISL, F-91191 Gif-sur-Yvette; France;

^aANDRA, Meuse-Haute Marne research Center, DRD/SCM, F-55290 Bure, France

^cCFG Services, 117 Avenue de Luminy, F-13009 Marseille, France

^dCEA, DSM, IRAMIS/SIS2M/LAPA, F-91191 Gif-sur-Yvette; France

^eANDRA, DRD/SCM, F-92298 Châtenay-Malabry, France

Claystone is considered as a prime host rock for the setup of deep geological repositories of high-level nuclear waste (HLW). In such repositories, the HLW is to be confined within carbon steel overpacks for a few centuries. Technical gaps should be present between the overpack and a steel liner which allows reversibility for ~100 years, and between the liner and the clay formation. These gaps will gradually be refilled by clay porewater. Meanwhile radioactive decay would result in a temperature transient with a maximum at 90°C. To investigate the impact of the gaps and of this transient, *in situ* experiments have been conducted at the Meuse-haute Marne Underground Research Laboratory, in which carbon steel coupons were in contact with clay porewater and submitted to heating up to 85°C (experimental details are given in a companion communication). Corrosion coupons reacted from 7 to 28 months were embedded and impregnated with resin, sectioned, and the sample sections polished, using only absolute ethanol as lubricant. Then, corrosion interfaces were characterized using micro-spectroscopic techniques [1-3].

Two series of samples with either extensive or limited damage were identified. For extensively corroded coupons, several layers of inner corrosion products were observed. The innermost layer was made of Cl-rich Fe (hydr)oxide, later evolving to $\beta\text{-Fe}_2(\text{OH})_3\text{Cl}$ sometimes crossed by magnetite columns, or laterally replaced by green rust for the 28-months samples. The second inner layer was made of Fe hydrated silicate with a sponge-like morphology, a local sub-molecular structure reminiscent of clay minerals, and interconnecting cementite particles. This porous layer locally contained massive nodules of siderite and chukanovite, which morphed to a more continuous layer close to the trace of the original surface. The layers external to this original surface were discontinuous and made of successively siderite, Fe sulphide (likely related to bacterial activity), S-rich Fe silicate, and finally pyrite nodules and siderite. The extensive corrosion damage and nature of interfacial corrosion products could be related to an initial transient in pH (monitored down to 4.8). For the samples with limited damage, no $\beta\text{-Fe}_2(\text{OH})_3\text{Cl}$ layer was observed, siderite or chukanovite were in close contact to metal, sometimes with interfacial magnetite, and the Fe hydrated silicate veinlets were less developed. External layers of Fe sulphide and siderite were observed. This suggests that these slightly corroding samples could have been altered in more confined conditions due to artefact in experimental conditions.

References

- [1] M.L. Schlegel, C. Bataillon, et al. *Appl. Geochem.* 23, 2619-2633 (2008).
- [2] M.L. Schlegel, C. Bataillon, et al. *Environ. Sci. Technol.* 44, 1503-1508 (2010).
- [3] G. de Combarieu, M.L. Schlegel, et al. *Appl. Geochem.* 26, 65-79 (2011).

Corrosion behaviour of structural steels exposed in supercritical water

Jan Macák¹, Petr Sajdl¹, Aneta Krausová¹, Václav Bystrianský¹, Lukáš Tůma¹, Eliška Křečanová^{1,2}, Markéta Zychová²;

¹ICT Prague, Czech Republic

²CVŘ, s. r. o., Czech Republic

Different types of creep-resisting steels were exposed in supercritical water (SCW) experimental loop (580-600°C, 25MPa) for up to 1000 hours under varied conditions (oxygen concentration, pH, subcritical-supercritical transition etc.). Materials under study included highly alloyed austenitic steels and ferritic-martensitic steels having chromium content between 8,5 and 12%. All the materials selected for the tests are designated for the construction either of supercritical boiler pressure parts or of turbine components.

Chemical composition, electronic and chemical structure, morphology and thickness of oxide layers formed during interaction with the SCW were ex-situ characterized by the electrochemical methods and by the methods of surface analysis (XPS, Raman spectroscopy). The electrochemical approach included electrochemical impedance spectroscopy (EIS), capacitance vs potential measurements (the Mott-Schottky plots) and double loop electrochemical potentiokinetic reactivation tests (DL-EPR). Characteristics of the oxide films formed in SCW were discussed on the basis of the chemical conditions of exposure and on the chemical composition of the base metal (in particular to the chromium content). In general, duplex and semi-conductive character of the oxides was confirmed. DL-EPR tests revealed intensive sensitization of some of the austenitic steels after the 1000 hours exposure in SCW.

Investigation of the effect of water chemistry and temperature on the oxide layer formed on Alloy 182 in simulated PWR environment

*Renato de Mendonça, Rik-Wouter Bosch, Wouter Van Renterghem,
SCK•CEN (Belgian Nuclear Research Centre), Mol, Belgium*

Summary

Stress Corrosion Cracking (SCC) is still a major issue in plant life management of ageing Light Water Reactors. One class of materials in a nuclear power plant that shows an increased susceptibility to stress corrosion cracking are the so-called Ni-based alloys used for dissimilar welds, e.g. between the stainless steel piping and the carbon steel reactor vessel. These Ni-based alloys show a peak in SCC susceptibility at a certain temperature and hydrogen concentration. This peak is related to the electrochemical condition where the Ni to NiO transition takes place. One assumption is that the oxide layer at this condition is not properly developed and so the material is not optimally protected to SCC. Therefore the oxide layer formed on alloy 182 is investigated as a function of the water chemistry and temperature. The main aim of this work is to correlate the susceptibility to crack initiation and SCC to the behaviour and composition of the different oxide layers formed in high temperature water. Exposure tests have been performed with alloy 182 and Ni coupons in a PWR environment (1000 ppm B, 2 ppm Li and 35 cc/kg H₂) as a function of temperature. The temperature ranges from 300 to 345 °C since in this temperature range the Ni/NiO transition is located based on thermodynamic calculations. Post-test analysis of the formed oxide layers have been carried out by Scanning Electron Microscopy, Energy Dispersive X-Ray Spectroscopy and X-Ray Photoelectron Spectroscopy. The first results showed that there is a large difference between the low (300°C) and high (345°C) exposure temperature w.r.t. the oxide layer morphology. At low temperature, a thin spinel type oxide is present whereas at high temperature a complex bilayer with deposited oxide layer is present. Exposure tests at intermediate temperatures are going on to reveal where the transition temperature for Ni/NiO is located for this given water chemistry.

On the mechanism and kinetics of radiation induced corrosion of copper

Åsa Björkbacka¹, Saman Hosseinpour², Magnus Johnsson², Christofer Leygraf², Mats Jonsson¹;

¹School of Chemical Science and Engineering, Applied Physical Chemistry, KTH Royal Institute of Technology, Stockholm, Sweden

²School of Chemical Science and Engineering, Surface and Corrosion Science, KTH Royal Institute of Technology, Stockholm, Sweden

Copper metal has been used extensively by humans since ancient times. The metal and its alloys are ductile, strong and corrosion resistant. In anoxic water, copper is thermodynamically stable and copper containing archaeological artefacts have been found quite intact under such conditions.^{1,2} This is the main motivation why copper is a material considered for encapsulation of spent nuclear fuel for future multi-barrier deep geological repositories for nuclear waste. The spent fuel will be sealed inside copper canisters with cast iron insert, placed 500 metres below ground and stored for approximately 100 000 years.³ Gamma radiation originating from the spent nuclear fuel will penetrate the canisters and induce radiolysis when absorbed by water. Two radiolysis products, hydrogen peroxide and hydroxyl radicals, have significantly higher standard reduction potentials than copper and are therefore able to initiate corrosion of the canister.^{1,4,5}

A series of experiments were performed where the gamma radiation induced corrosion of copper was studied. Copper samples submerged in anoxic water were irradiated by total doses within the range relevant for a deep repository for spent nuclear fuel. Unirradiated reference samples were used throughout. Qualitative surface characterizations were performed using x-ray photoelectron spectroscopy, XPS, and infrared reflection absorption spectroscopy, IRAS. Quantitative surface characterization was performed using cathodic reduction. Dissolution of copper was analysed using inductively coupled plasma atomic emission spectroscopy, ICP-AES. The experimental results show that the oxide layer thickness as well as the dissolution increase upon irradiation.^{6,7} The main corrosion product formed is cuprite, Cu₂O, but the presence of tenorite, CuO, cannot be completely ruled out.

¹ R.R. Conry, in *Encyclopedia of Inorganic Chemistry* 2nd ed. R.B. King, Editor p. 940-945, Wiley, New York, 2005.

² Nuclear waste containment materials, TR-01-25. Swedish Nuclear Fuel and Waste Management Co., Stockholm, 2001.

³ SKB, 2011. Long-term safety for the final repository for spent nuclear fuel at Forsmark. Main report of the SR-Site project. Swedish Nuclear Fuel and Waste Management Co., Stockholm, 2011.

⁴ W.H. Koppenol and J.F. Liebman, *Journal of Physical Chemistry*, 88, 99-101, 1984.

⁵ F.A. Cotton and G. Wilkinson, *Advanced inorganic chemistry*, 3 ed., 416, Wiley Interscience, New York (1972).

⁶ Björkbacka, Å., et al., *Electrochemical and Solid-State Letters* 15, C5-C7, 2012.

⁷ Björkbacka, Å., et al., *Radiation Physics and Chemistry* 92, 80-86, 2013.

Corrosion susceptibility of steel drums containing cemented simulated incineration ashes as low level nuclear waste

Gustavo S. Duffó, CNEA, CONICET, UNSAM, Buenos Aires, Argentina

Silvia B. Farina, CNEA, CONICET, UNSAM, Buenos Aires, Argentina

Fátima M. Schulz Rodriguez, CONICET, UNSAM, Buenos Aires, Argentina

Francesca Marotta, Politecnico de Milano, Milano, Italia

Cementation processes are used as immobilization techniques for low or intermediate level radioactive waste for economical and safety reasons and for being a simple operation. In particular, ion-exchange resins commonly used for purification of radioactive liquid waste from nuclear reactors are immobilized before being stored to improve the leach resistance of the waste matrix and to maintain mechanical stability. Combustible solid radioactive waste can be incinerated and the resulting ashes can also be immobilized before storage. The immobilized resins and ashes are then contained in steel drums that may undergo corrosion depending on the presence of certain contaminants. The results concerning the effect of the contaminated cemented ion-exchange resins on the corrosion behaviour of steel drums were already published. This work focuses on the corrosion susceptibility of steel drums in contact with cemented incineration ashes; that contain chloride ions in their composition. A special type of specimen was designed to simulate the cemented waste in the drum. The evolution of the corrosion potential and the corrosion rate -measured with the Linear Polarization Resistance technique- as well as the electrical resistivity of the matrix were monitored over a time period of 3.7 years. The work was complemented with an analysis of the corrosion products formed on the steel in each condition, as well as the morphology of the corrosion products. The results show that the corrosion potential and the corrosion rate depend on the incineration ash content of the matrix (Figure 1). When applying the results obtained in the present work to estimate the corrosion depth of the steel drums containing the cemented radioactive waste after a period of 300 years (foreseen durability of the Low Level Radioactive Waste facility in Argentina), it is found that the corrosion penetration will be considerably lower than the thickness of the wall of the steel drums. So, it is concluded that the cementation of incineration ashes seems not to pose special risks regarding the corrosion of the steel drums that contained them.

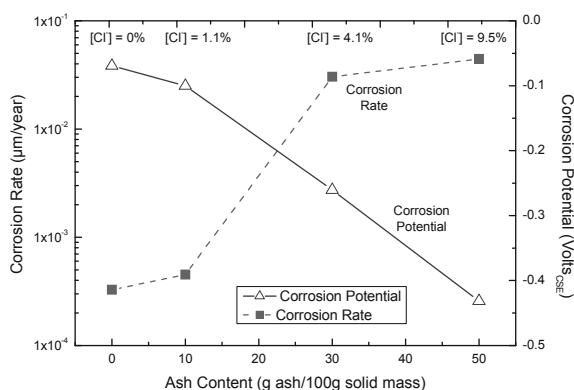


Figure 1.- Corrosion rate and corrosion potential of the steel as a function of the ash content. The chloride content of the matrix respect to the cement mass is included.

Corrosion of High Purity Copper as Engineering Barrier in Deep Geological Repositories

Maité Ochoa, Comisión Nacional de Energía Atómica (CNEA) - Instituto Sabato, Univ. de San Martín (UNSAM), Av. Gral Paz 1499 (1650) San Martín, Argentina
Martín A. Rodríguez, CNEA - Comisión Nacional de Investigaciones Científicas y Técnicas (CONICET) - Instituto Sabato (UNSAM), Av. Gral Paz 1499 (1650) San Martín, Argentina

Silvia B. Farina, CNEA - CONICET - UNSAM, Av. Gral Paz 1499 (1650) San Martín, Argentina

Pure copper with oxygen content below 5 ppm (to minimize segregation at grain boundaries) and doped with phosphorus (to increase creep resistance) is the chosen material for the corrosion-resistant barrier of the High Level Radioactive Waste (HLRW) containers in the Swedish and Finnish repository models. These models include the construction of the repository below the water table, which is a reducing environment in which copper has excellent resistance to general and localized corrosion in aqueous electrolytes.

Copper is a candidate material for the construction of the HLRW container in Argentina. The aim of this work is contribute to determine the durability of the material, given that deep geological repositories of HLRW are designed to ensure the protection of the environment for periods of hundreds of thousands years. As a first step in a more general analysis the effects of chloride, one of the main aggressive species to corrosion, are evaluated.

To this purpose corrosion potential was determined and anodic polarization curves were performed in NaCl deaerated solutions varying the chloride concentration between 0.01 and 1M and the temperature between 30 and 90°C. Several electrochemical techniques were used: the evolution of corrosion potential was measured, anodic polarization curves were obtained and electrochemical impedance tests were performed.

The analysis was complemented with microscopic observations of the type of corrosive attack, as well as determinations of the eventual corrosion products formed using Energy-Dispersive X-ray Analysis.

Results show the aggressiveness of chloride ions: the corrosion potential decreases with the increase of chloride concentration and with the increase of temperature. A correlation of the corrosion potential as a function of temperature and chloride concentration was obtained, with the purpose of making predictions in variable conditions. The current density increases both with temperature and with chloride concentration. A pitting potential is observed under certain conditions. Corrosion products formed showed a composition of 30wt% Cl and 70wt% Cu.

Corrosion resistance in multipass welding of thick UNS S31304 lean duplex stainless steel plates welded using SMAW, GMAW and FCAW processes

*Carla Soares Souza¹, Vanessa de Freitas Cunha Lins², Dalila Moreira da Silveira²,
Cintia Gonçalves Fonseca Costa², Ronaldo Cardoso Junior³, Frederico Rodrigues
Campos⁴, Alexandre Queiroz Bracarense⁴*

1 Fiat Automobile S.A., Materials Science Technology Center, Betim, Brazil

2 Federal University of Minas Gerais, Chemistry Engineering Department, Belo Horizonte, Brazil

3 ESAB Industry and Trade LTD, Contagem, Brasli;

4 Federal University of Minas Gerais, Mechanical Engineering Department, Belo Horizonte, Brasil

The UNS S32304 lean duplex stainless steel presents a lower cost compared to other duplex steels due to the partial substitution of nickel by nitrogen as an element that stabilizes austenite. During the welding of duplex stainless steels, the desired material properties can be radically altered by a process which locally melts and recasts the steel. In this work, samples of the lean duplex stainless steel welded using GMAW, SMAW and FCAW processes and two types of consumable, 2209 (22% wt Cr, 9% wt Ni and 3% wt Mo) and 2307 (23% wt Cr and 7% wt Ni) were analyzed by electrochemical impedance spectroscopy and potentiodynamic anodic polarization to evaluate the corrosion resistance of the material in NaCl 3.5% m/v aqueous solution. The electrochemical impedance spectroscopy results showed that the top of the weld had a higher corrosion resistance in saline solution than the root of the weld, except for the welded joint using the GMAW process and the consumable 2209. The welded joint using the GMAW process and the 2209 consumable showed the highest corrosion resistance in NaCl aqueous solution. Electrochemical processes with two time constants were obtained for the samples welded using the GMAW and FCAW process with the two consumables, and for the samples welded using the SMAW process with the 2209 consumable. One capacitive arc in the Nyquist diagram, and one time constant in the Bode diagram, was observed for the samples welded using the SMAW process with the 2307 consumable. The anodic potentiodynamic polarization indicated that the welded joints using the GMAW process showed a higher breakdown potential and a lower passivation current density than the samples welded using the SMAW and FCAW processes, for the two types of consumable. After the polarization tests, all samples exhibited the highest degree of corrosion in the heat affected zone.

Effect of cathodic hydrogen charging of titanium alloys on hydrogen absorption and hydride formation

S. Dejardin, V. Dusquesnes, N. Creton, R. Oltra, T. Montésin, Laboratoire ICB - UMR 6303 CNRS - Université de Bourgogne - 9 av. Alain Savary - 21000 Dijon, France.

At exposition of titanium alloys to electrolytes, the formation of hydride layer and hydride precipitates or hydrogen dissolution into the metal appear to be depending on solution chemistry and pH, applied potential, temperature and time of charging [1,2,3].

In a global study of titanium alloys behavior in specific aqueous solution (embrittlement, corrosion and corrosion under stresses), the present study focuses on the effect of electrochemical parameters of cathodic hydrogen charging in order to obtain a significant rate of hydrogen in the solid solution of α -Ti and $\alpha+\beta$ -Ti lattice and the hydride phase to be formed.

Alkaline and acid solutions have been tested taking into account solution concentration, level of cathodic polarization and time of charging. The influence of oxide film has also been taken into account. In each case, hydrogen absorption and formation of hydride phase have been studied by microstrural observations (optical microscopy and scanning electron microscopy), X-ray diffraction method and ATG measurement. Analyses showed that hydrogen absorption is lower in alkaline than in acid solutions and that increased cathodic polarization causes the increase of hydride phase rate and also the increase of hydrogen concentration into hydride phase. These results allowed to determine significant electrochemical parameters in cathodic hydrogen charging in order to perform accelerate aging test of titanium U-Bend samples into autoclave.

Key words : cathodic charging, titanium alloys, hydrogen

[1] E. Lunarska, O. Chernyayeva, D. Lisovytski, "Hydride formation at cathodic charging of α -Ti", *Advances in materials science*, Vol. 8, No 1(15), 2008, pp. 105-114

[2] Toshio Ogawa, Ken'ichi Yokoyama, Kenzo Asaoka, Jun'ichi Sakai, "Distribution and thermal desorption behavior of hydrogen in titanium alloys immersed in acidic fluoride solutions". *J. Alloys and Compounds* 396, 2005, pp. 269-274

[3] C.L. Briant, Z.F.Wang, N. Chollocoop, "Hydrogen embrittlement of commercial purity titanium". *Corrosion Science* 44, 2002, pp. 1875-1888

WATER CHEMISTRY AND CORROSION ISSUES OF CONTROL ROD AND PROTECTION SYSTEM IN RUSSIAN LWGRS

Evgeny Yurmanov, Victor Yurmanov (NIKIET), Russia

Light water cooled graphite moderated reactors (LWGRs) named RBMK (Reactor Bolshoi Moshchnosti Kipyashchiy) were designed in 1960-70s by N.A.Dollezhal Research and Development Institute of Power Engineering (NIKIET), Moscow, Russia. 15 of power units RBMK-1000 with rated electric power of 1 GWt were built and are still operating at three of nuclear power plants (NPPs) in Russia (Leningrad, Kursk and Smolensk NPPs) and Chernobyl NPP (Ukraine). Two RBMK-1500 units with rated electric power 1.5 GWt were built and operated in Lithuania (Ignalina NPP), Chernobyl and Ignalina NPPs were finally shut down. Nowadays 11 of RBMK-1000 power units are still in operation in Russia. Comprehensive modernizations were implemented at all RBMK plants taking into account experience of accident at unit 4 at Chernobyl NPP in 1986.

One of the most important improvements of RBMK reactors after Chernobyl accident was related to control and protection system (CPS). Namely CPS deficiency was one of the causes of the above catastrophe. In view of this RBMK designer (NIKIET) developed CPS modernizations aimed at safe RBMKs operation.

In the end of 1980s NIKIET designed new rapid emergency protection system (REPS) with reduced time of fast scram rod insertion into reactor core from 20 seconds to about 2 seconds. From 21 to 33 FSR at each RBMK-1000 are moving in gaseous phase as compared to water filled channels in case of as-design CPS.

Since early 2000s new cluster type CPS (CCPS) were implemented at RBMKs to improve their reliability and safe operation. Cluster type control rods are moved in air within long hermetic cases located within special reactor channels cooled by water coolant of RBMK auxiliary cooling system (SVO-3) aimed at cooling of special channels of RBMK, including channels of CPS.

The above modernizations of CPS at RBMKs were assisted with an intensification of radiation-chemical processes in the water within reactor channels with control rods. These processes led to increased rate of acidic radiolysis products formation in the water of CPS cooling system. Chemical quality changes of water in CPS cooling system impact corrosion of control rod elements made from aluminium alloy.

Water chemistry mode at above mentioned RBMK auxiliary cooling system (SVO-3) at RBMK plants was improved to reduce corrosion of aluminium alloy used for manufacturing of some control rod elements, namely flow displacers in RCPS and as-designed CPS or cases in CCPS. Aluminium content in the above water depends from corrosion of cases and purification of CPS cooling system. Corrosion rate of cases depends from water quality of CPS cooling system, primarily from pH values.

Powdex process was implemented for water coolant purification in CPS to facilitate removal of nitric acid produced in course of CPS cooling water radiolysis. Protective coating on aluminium case surfaces could be promising solution to solve the above corrosion problems.

This paper highlights water chemistry and corrosion issues of control rod and protection system in Russian LWGRS named RBMKs. This paper demonstrates that implementing of some modernizations at nuclear reactor systems should take into account possible increase of water coolant corrosion activity. The countermeasures to improve water chemistry control could prevent potential negative consequences of such modernizations of nuclear reactor systems with water coolant.

Sensitisation and IGSCC in type 321 SS NPP manifold welds

K.I. Shutko,

Research and development institute of power engineering (NIKIET), Moscow, Russia

This work is aimed to research after sensitisation development in heat-affected zones (HAZ) of multipass welds damaged by intergranular stress corrosion cracking (IGSCC) under operating in high-purity water at high temperatures. Cracked welds service time varied significantly. Grain-boundary sensitisation developed in narrow zones that are located adjacently to weld joints fusion lines and orientated lengthwisely to them. In cases investigated sensitization did not reach the outer manifold surface starting from the inner surface. Commonly, circular cracking occurred within the sensitized regions. Material sensitized conditions coupling with residual weld stresses and working load provided weld joints susceptible to IGSCC. Fracture mode is revealed predominantly as intergranular with some transgranular patches. However, corrosion fatigue was detected on the fracture surface under load cycling.

It is also found that initial cracks on the inner weld surface joined one to another forming the main crack. The notches produced with welding could promote the cracking initiation. Weld joint served for approx 23 years intact IGSCC also considered in comparison. As revealed, welding did not induce sensitisation.

This research employed both double-loop electrochemical potentiokinetic reactivation (DL-EPR) and oxalic acid etch techniques for quantitative and qualitative degree of sensitization (DOS) assessment. Material DOS in cracking vicinity is determined as beyond of well-known Strauss test sensitivity.

Influence of high-temperature heat treatment on DOS in weld HAZ was investigated using DL-EPR technique. High-temperature heat treatment is proposed as the possible remedy against welds IGSCC susceptibility as leading to both material desensitisation and stress improvement.

Key words: welds, sensitisation, heat treatment, IGSCC, DL-EPR

Behaviour of steam generator tube at different temperatures and levels of chloride

*Mônica M. A. M. Schvartzman; Fábio A. Mansur; Pedro H. B. O. Nogueira
Centro de Desenvolvimento da Tecnologia Nuclear; Belo Horizonte/Brazil*

The pitting resistance and pitting morphology of the nuclear grade alloy 800NG in the PWR secondary water environment at 250 °C were studied by electrochemical techniques. Anomalous conditions, considering the unintentional chloride contamination of the water cooling system as a result of condenser leakage were also investigated. The effect of chloride concentration in the range of 250 ppb to 50 ppm was examined. Immunity to pitting corrosion was evident at chloride levels below 1 ppm. The morphology of the localized attack observed on alloy 800NG was strongly dependent on chloride concentration. At a chloride concentration of 1 ppm, small corroded areas were observed on the specimen surface after the potentiodynamic tests, isolated and irregularly localized attacks were found in a few regions, and EDS analysis indicates some chromium enrichment inside of them. A high density of widespread pits filled with Cr-rich corrosion products was observed, at chloride concentrations higher than 10 ppm. In this case, pits became smaller and with a more regular shape. Potentiodynamic anodic curves showed that higher chloride concentrations shifts the pitting potential of alloy 800NG to lower values, probably due to the deleterious effect of chloride ion on the passive film.

Oxidation behavior and Spallation of oxide scales after T91 oxidation in water vapor environment

Marie Christine DEMIZIEUX^a, Clara DESGRANGES^a, Jérôme FAVERGEON^b, Laure MARTINELLI^a,

^a CEA, DEN, DANS, DPC, SCCME, Laboratoire d'Etude de la Corrosion Non Aqueuse, F-91191 Gif-sur-Yvette, France.

^b Université Technologique de Compiègne, Laboratoire Roberval, Département Mécanique, F-60200 Compiègne, France.

This study takes place in the framework of Generation IV reactors and in particular in the new Sodium Fast Reactor project in which the Fe-9Cr martensitic steel T91 is considered as structural material for steam generator.

Oxidation of T91 in steam leads to the formation of spinel type duplex oxide scale, possibly –depending on equivalent oxygen partial pressure- topped by a hematite layer. Stresses resulting from the oxide growth can lead to cracking and failure of the oxide, leading to spallation of the oxide layer and then to a loss of its protective properties and a possible increase of oxidation kinetics. The aim of this study was to investigate the growth kinetic of the oxide scale, the T91 oxidation mechanism and the major strains and stresses affecting the scale until its spallation under water vapor at 550°C.

In this context, two kinds of experiments are performed. One permits to assess *in situ* the stresses developed in the oxide scale as a function of time and temperature and in the subjacent steel during oxidation in Ar/H₂/H₂O mixture or in air. These experiments were performed in a deflection apparatus with various water vapor partial pressures and gas compositions. The other enabled to determine *in situ* mass gain of samples in a thermobalance performed in the exact same conditions as the deflection tests except in the use of D₂O instead of H₂O. Analyses of deuterium content performed by GD-OES on oxidized samples in the oxide scale and in the steel allow to determine deuterium localization in the oxide scale and at the substrate/oxide interface.

All the results performed in these two experiments were interpreted according to oxidation mechanisms, models of growth kinetic and mechanisms of failure of the oxide scale under water vapor beforehand developed. Various elastic and viscoplastic models were used to determine quantitatively and qualitatively all kind of strains and stresses generated during the oxidation cycle. It turned out that predominant growth strains were probably one of sources responsible of delamination and spallation of the oxide scale. The influence of pores and cavities – especially in the magnetite scale- on the oxide scale buckling was also investigated. Finally, a global mechanism is proposed taking into account the role of hydrogen on stress relaxation and the role of oxide scale failure on the oxidation mechanism.

Hydrogen production by iron corrosion under gamma-irradiation

STAMMOSE Denise, OSMOND Mélanie, BARKER Evelyne, WITTEBROODT Charles

IRSN, France

Abstract:

In geological disposal repositories for radioactive waste, one important source of gas will likely be generated by anoxic corrosion of metals, which produces hydrogen. Although gas generation rates for metals have been studied for several years, few studies focused on the influence of radiation on these rates. Exposed to ionizing radiation, water decomposes to yield a range of products like hydrogen and chemically reactive species (oxidizing and reducing) that can strongly impact the aqueous redox conditions and influence metal corrosion kinetics. This study aims at assessing the influence of gamma irradiation on hydrogen production rate through the anoxic corrosion of iron process.

A given mass of iron (powder or pieces) was added to pure water with low oxygen content ($< 4 \cdot 10^{-7} \text{ mol.L}^{-1}$) in a stainless steel cell. Anoxic conditions were maintained through a continuous bubbling of the system with helium. The mixture of flushed gas (H_2 , O_2 , N_2) was regularly sampled and analysed by gas chromatography. After a duration that allowed to reach a constant hydrogen production (pseudo-stationary state), the cell was submitted to continuous irradiation by gamma sources (^{60}Co) in the IRMA facility (CEA- Saclay), with dose rates ranging from 11 to 100 Gy h^{-1} . At the end of each experiment, the cell was dismantled for both solid and solution analyses.

The corrosion rates of iron deduced from the first step (corrosion without irradiation) of these experiments are in agreement with those presented in literature ($\sim 0.1 - 3 \mu\text{m.y}^{-1}$). Under irradiation, opposite effects are observed: an increase in production of hydrogen ($\times 10$) for the two higher dose rates (50 and 100 Gy.h^{-1}) and a decrease for the lower dose rate (11 Gy.h^{-1}). Furthermore, the increase in hydrogen production continued when irradiation ceased. Different mechanisms were investigated to explain these results. Oxygen content in the solution appears as a key parameter as it controls the type of corrosion layer and in turn the hydrogen production rate due to corrosion. Then, molecular radiolytical species like hydrogen peroxide were probably involved in direct or indirect oxidation reactions towards iron or corrosion layer and initiate corrosion mechanisms which carry on beyond the irradiation period. A kinetic model incorporating a reaction data set combining water radiolysis and corrosion reactions was finally developed to test different mechanisms and to evaluate the influence of a set of parameters.

Evaluating the Pit-Crack Transition in an Offshore Pipeline Steel

Christopher Evans, Robert Akid,

Corrosion and Protection Centre, University of Manchester, Manchester, UK

Corrosion fatigue plays a dominant role in the failure of offshore riser systems. This presents many performance issues during deep-water exploration in the oil & gas industry. The API-5L X65 pipeline steel often used to construct the riser systems is known to have good fatigue strength when operating in air. However, under the synergistic effect of cyclic stress and a corrosive environment, the fatigue resistance is greatly diminished. There are a number of models for prediction of fatigue life in air that have been accepted, however there are currently none that accurately predict the lifetime of a component under corrosion fatigue conditions. Stress-Number of cycles to failure diagrams (S-N curves) that contain integrated level of conservatism are often used. Crack growth models have adopted a dual-stage approach incorporating a pit growth stage and a long crack stage that is based on calculations using Linear Elastic Fracture Mechanics^[1]. This type of approach is acknowledged to have substantial limitations for predicting the lifetime of components when defects do not already exist in the material^[2].

The pit-crack transition stage of corrosion fatigue is investigated in this study, with the aim to evaluate the relationship between the stress and pit geometry during crack initiation from a corrosion pit. Single, artificial corrosion pits were created using a micro-electrochemical cell, which allowed geometrical control to be established. This method enables the effect of a single corrosion pit on fatigue lifetime to be studied. Artificial pits were then created in the surface of fatigue specimens manufactured from API-5L X65 (0.08 wt% C).

2D Digital Image Correlation (DIC) was used to examine the evolution of strain around corrosion pits as a function of fatigue cycling. In order to do this, interrupt testing was carried out in air using pre-pitted fatigue specimens.

References

1. Hoepfner, D. W., Taylor, A. M. H., Invited Chapter 13, "Modelling Pitting Corrosion Fatigue: Pit Growth and Pit/Crack Transition Issues" in *AVT-140 Corrosion Fatigue and Environmentally Assisted Cracking in Aging Military Vehicles*, NATO, RTO, NATO, France: **2011**
2. Akid, R.; Dmytrakh, I.; Gonzalez-Sanchez, J., Fatigue damage accumulation: aspects of environmental interaction. *Materials Science* **2006**, 42 (1), 42-53.

Critical analysis of the role of ferrite content in the environment- sensitive cracking of duplex stainless steels

*Rachel Pettersson, Jernkontoret, Box 1721, 111 87 Stockholm, Sweden
Sten Wessman, Swerea KIMAB, Box 7047, 164 07 Kista, Sweden*

Abstract

Duplex stainless steels have an attractive property profile of corrosion resistance in combination with a higher strength than the corresponding austenitic grades. This is achieved by a delicate balance between the component austenite and ferrite phases. In the wrought or cast state the phase ratio is often around 50-50 and numerous concerns over the years have been expressed that property degradation will result if the phase balance deviates too greatly from this level. In particular there is a fear that a ferrite-dominated microstructure might be susceptible to hydrogen embrittlement while an austenite-dominated structure may suffer anodic stress corrosion cracking. This has led to numerous standards such as NORSOK M-630 and NACE MR 0175 / ISO 15156-3 placing restrictions on the acceptable levels of ferrite (or austenite).

This paper presents a thorough analysis of the available literature data concerning the role of phase ratio on the corrosion properties of duplex stainless steels, in order to assess how strongly the basis is for restricting the ferrite content. Results are described for stress corrosion cracking and hydrogen embrittlement, but also include pitting corrosion which has been the subject of numerous investigations. The conclusion is that there is relatively sparse evidence for strict limits on ferrite content, also that the actual techniques of measuring ferrite contents have intrinsic inaccuracies which can lead to rejection of functional material, with associated expense.

The corrosion properties are dependent on how the different phase ratios are achieved in duplex stainless steels – whether it is by overalloying with certain elements, varying the heat treatment temperature, cooling too rapidly etc. A theoretical analysis is included to illustrate the way in which different processing may be expected to affect the composition and thereby the corrosion resistance of the austenite and ferrite phases and that of the alloy as a whole.

Influence of nitrate ions concentration, pH and applied potential on the susceptibility to corrosion and stress corrosion cracking of α - β brass in NaNO_3 solutions

Clément Berne^{(a) (b)}, Eric Andrieu^(a), Jean Reby^(b), Jean-Michel Sobrino^(c),
Christine Blanc^(a)

(a) Université de Toulouse, CIRIMAT, UPS / INPT / CNRS, Equipe MEMO ENSIACET, 4, allée Emile Monso BP 44362, 31 030 Toulouse Cedex 4, France

(b) CETIM, « Matériaux Métalliques et Surface »
74, route de la Jonelière BP 82617, 44 326 Nantes Cedex 3, France

(c) CETIM, « Matériaux Métalliques et Surface »
52, Avenue Félix Louat BP 80067, 60 304 Senlis Cedex, France

Stress corrosion cracking (SCC) is believed to be the principal cause for the cracks observed in brass components used in gas distribution network. In this framework, it is of interest to develop accelerated tests to determine the SCC susceptibility of the brass used in the gas transfer valves. This requires to understand the mechanisms explaining the observed damage. The present study aimed to contribute to a better understanding of the corrosion and SCC behaviour of alpha-beta brass.

The specimens, made of alpha-beta brass CuZn40Pb2 (CW617N), were machined from stamping rods used to manufacture gas transfer valves. The accelerated tests were performed in NaNO_3 solution selected with reference to research on alpha brass (1). Two types of objectives were aimed at; the first corresponded to the determination of the dissolution and dezincification kinetics from immersion tests at constant potential, and the second was the evaluation of SCC behaviour from tests performed at constant load and potential.

Results obtained over a wide range of conditions (potential, pH, nitrate ions concentration) were analyzed by measuring the dissolution/dezincification depth and the weight loss, performing chemical analyses of surfaces and corrosion products (Inductively Coupled Plasma, Energy-dispersive X-ray spectroscopy, X Ray Diffraction). Furthermore, SCC results were compared on the basis of time to failure, fractography analyses (Scanning Electron Microscope) and crack path characterizations. The discussion focuses on understanding the dezincification/dissolution processes and the SCC mechanism. Concerning the SCC mechanism, previous studies on similar materials (2) (3) and models often proposed in the literature (adsorption of damaging species, discontinuous cleavage-like mechanism) are discussed. First results have shown the need to take into account in the models both, the significant influence of the NaNO_3 concentration and pH on SCC behaviour and the evolution of the surface properties with the formation of Cu_2O and/or dezincified layers after immersion tests.

Metallurgy – Stress corrosion cracking – Brass – Dezincification

1. Fernandez, S.A. and Alvarez, M.G. Passivity breakdown and stress corrosion cracking of alpha-brass in sodium nitrate solution. *Corrosion Science*. Elsevier, 2011, Vol. 53, pp. 82-88.
2. Hintz, M.B.; Nettleton, L.J.; Heldt, L.A. Stress corrosion cracking of alpha-beta brass in distilled water and sodium sulfate solutions. *Metallurgical Transactions A*. May 1985, Vol. 16A, pp. 971-978.
3. Hintz, M.B.; Blanchard, W.K.; Brindley, P.K.; Heldt, L.A. Further observations of SCC in alpha-beta brass: Considerations regarding the appearance of crack arrest markings during SCC. *Metallurgical Transactions A*. June 1986, Vol. 17A, pp. 1081-1086.

MECHANISTIC INVESTIGATION OF STRESS CORROSION CRAKING OF PIPELINE STEEL IN NEAR-NEUTRAL PH ENVIRONMENT

R.I. Bogdanov, A.I. Marshakov and V.E. Ignatenko

Institute of Physical Chemistry and Electrochemistry of Russian Academy of Sciences, Moscow, Russian Federation

Stress corrosion cracking (SCC) has been identified as one of the primary reasons for failures in high-pressure buried pipelines [1-2]. Today, most researchers agree that SCC of pipeline steels in environments at near-neutral pH results from the synergistic effects of mechanical straining, local anodic dissolution, and hydrogen absorption [3-6]. However, it is not clear the primary mechanism of SCC in the various composition of the soil electrolyte at the various type and values of mechanical loading. This work explores the effect of corrosive compounds on the crack growth rate in X-70 pipeline steel under cyclic mechanical tensions to determine the primary mechanism of near-neutral pH SCC.

The crack growth rate was determined using X-70 steel specimens. A mixture of NS4 solution with a borate buffer (pH 7.0) were used as background solutions. Various compounds that affect steel dissolution and hydrogen absorption rates were added to the solutions.

The cyclic crack resistance of pipe steel in NS4 buffer solution at pH 7.0 is mainly determined by the regularities of the corrosion fatigue. Adding an anodic dissolution stimulator (sulphide ions) or a hydrogen absorption promoter (iodide ions) nearly does not affect the crack growth at high amplitudes of the stress intensity factor (ΔK). The rate of crack growth depends on the presence of a corrosive medium only at small amplitudes of loading ($\Delta K \sim 5 \text{ MPa}\cdot\text{m}^{0.5}$). The crack growth is accelerated in the presence of sulphide and thiourea; these species act as metal dissolution activators, and are hindered after adding a corrosion inhibitor (Catamin AB) to a sulphide-containing medium. The cathodic polarization of pipeline steel inhibits crack growth at low ΔK values. Therefore, the local anodic dissolution of the metal is the primary crack growth mechanism in X-70 pipeline steel in NS4 buffer solution at small amplitudes of loading.

References

1. National Energy Board, Report of Public Inquiry Concerning Stress Corrosion Cracking on Canadian Oil and Gas Pipeline Steels, MH-2-95. 1996
2. Stress corrosion cracking of gas transmission pipes. Reference book. Eds. A.B. Arabey and Z. Knoshinsky, Nauka, Moscow, 2006.
3. X. Tang, Y.F. Cheng, Corros. Sci. 53 (2011) 2927-2933
4. B.T. Lu, J.L. Luo, P.R. Norton, Corros. Sci. 52 (2010) 1787-1795
5. W. Chen, R. Kania, R. Worthingham, G. Van Boven, Acta Materialia 57 (2009) No 20 6200-6214.
6. A.B. Arabey, R. I. Bogdanov, V. E. Ignatenko, T. A. Nenasheva, A. I. Marshakov, Protection of Metals and Physical Chemistry of Surfaces 47 (2011) 236-245.

The Relationships Between Microstructure and Sulfide Stress Cracking Resistance of High Strength, Low Alloy OCTG Steels

Wei Ji Huang¹, Fang Cao², Adam Aylor¹, and Wei Sun¹

¹ExxonMobil Development Company, Houston, TX, USA

²ExxonMobil Research and Engineering Company, Clinton, NJ, USA

Abstract

Many HPHT (high pressure high temperature) wells are originally designed for sweet service, but are exposed to mild sour service environment either due to unexpected natural souring or reservoir souring. In the past decade, industry has developed proprietary high strength low alloy 125 ksi grade OCTG to withstand the mild sour service environment. However, the correlations of microstructure with the sulphide stress cracking (SSC) resistance are not fully understood. In this study, two proprietary C125 along with a P110 OCTG were selected for investigation. The SSC resistances of the materials were determined using NACE TM0177 Method D testing. The baseline microstructure and cracking morphology of the materials were characterized using scanning electron microscopy, electron backscattered diffraction, and transmission electron microscopy. Analysis of trapping sites was performed through thermal desorption spectroscopy and hydrogen permeation tests. An attempt was made to develop fundamental understanding of the factors governing SSC susceptibility by correlating the microstructure features with the measured diffusible hydrogen content.

Cathodic charging during hydrogen embrittlement testing

Qian Liu, Andrej Atrens

The University of Queensland, Materials Engin, St Lucia, Qld, Australia 4072

Andrejs.Atrens@uq.edu.au

Cathodic charging is a common method by which to introduce hydrogen during hydrogen embrittlement research. This work reviews our recent research at UQ into the evaluation of the equivalent hydrogen pressure under conditions of constant applied electrochemical potential. Included are the following: (i) theoretical evaluation of the thermodynamic relationship between pressure and cathodic charging parameters, (ii) measurement of the key quantities, (iii) influence of surface condition, and (iv) influence of solution composition. This review includes typical evaluations from our recent research.

The Kelvin Probe: towards rapid, in-situ evaluation of HISC susceptibility and undercoating corrosion

E. F. Turcu, Christian Michelsen Research AS, Bergen / Norway; M. Rohwerder, Max-Planck-Institut für Eisenforschung GmbH, Düsseldorf / Germany

Metallic materials ranging from mild to high strength steels are prone to mechanic fractures when certain combinations of environmental characteristics, intrinsic material properties and tensile stresses are simultaneously present. The typical failure mode resulting from such a set of parameters, generally referred to as environmentally induced cracking, is common to apparently dissimilar industries such as oil and gas, maritime, automotive or aviation.

Maritime environments are known to offer the environmental conditions that often induce cracking. As active corrosion processes and cathodic protection generate atomic hydrogen on the metallic surfaces, hydrogen induced cracking poses a major concern for offshore operators. Subsea installations are particularly affected by undetected early-stage corrosion and hydrogen embrittlement resulting from on-going corrosion and cathodic protection. With increasing technological complexity and material diversity, such degradations would occur more often and could rapidly lead, depending on environmental conditions, to significant material-, and eventually to system- failures.

Current non-destructive corrosion inspection and monitoring overlooks early-stage corrosion (i.e. before any wall-loss is measurable) and neglects hydrogen charging. This is different for steel and automotive industries where novel techniques such as Scanning Kelvin Probe (SKP) are increasingly gaining importance for corrosion monitoring. SKP recently was shown to be applicable even to residual hydrogen detection on steel components. The contactless measurement of the corrosion potential of any coated metal is accomplished via a vibrating capacitive probe placed at a certain distance over the object of interest. Via nulling of the sinusoidal displacement current the corrosion potential underneath a coating can be readily obtained.

Recent developments make the Kelvin Probe applicable for various field conditions as well to subsea equipment. SKP's main strengths in subsea applications are: 1) the ability to sense corrosion through protective coatings; 2) unmatched capacity to detect ultra-low (sub-ppm) amounts of hydrogen in metals.

Consequently, hydrogen embrittlement risk could be evaluated: i) before deployment the equipment or component (residual H₂), ii) during regular inspections / recertification of equipment, iii) during service.

Considering that sub-ppm hydrogen-levels can result in metal embrittlement, the practical importance of these detection possibilities are obvious.

The presentation will describe SKP's operating principle and will exemplify corrosion and hydrogen detection with recent test results and will touch upon potential benefits for maritime and automotive, and how the current standard SKP can be adapted for robust performance in the field.

Hydrogen induced stress cracking tests for offshore wind farm monopile foundations

D. Bangsgaard, T. Mathiesen, C. Christensen, FORCE Technology, Brøndby/Denmark

Development of test methods based on an assessment of the current issues in the offshore wind industry

Focus is on reducing the cost of renewable energy at present. In the case of offshore wind farms significant costs are related to maintenance and repair. Implementing corrosion monitoring will ease the process of defining a specific lifetime, and further aid assessing the service life of the wind turbine foundations. However, test of materials and components before manufacturing and installation in order to ensure that the best choices possible are made, is a crucial part of reducing costs, since it will help avoid repair and replacement of components.

Through a comprehensive survey of offshore wind farm monopile foundations the issue of mud zone corrosion has been identified and the risk of hydrogen induced stress cracking (HISC) discussed. Internal cathodic protection, the presence of sulphide rich environments and increased hardness increase the risk of HISC, as has been previously observed with spud cans in the oil & gas industry. These critical factors may all be present in offshore wind farm foundations. As ongoing research introduces new materials and welding procedures to optimize design and production in order to reduce cost, the need for relevant test methods is present.

A HISC test setup has been developed. Tests for comparison between compact tension specimens (CTS) and Charpy V specimens to determine a correlation between these two types of specimens are to be conducted. This study is driven by the overall motivation to reduce cost of the test method. Since Charpy V specimens are already manufactured for qualification of welding procedures they are both less time consuming and less costly to the manufacturer. The combination of stronger materials like high strength steels and new welding procedures such as the laser-hybrid welding method under development at FORCE Technology introduce new challenges. This requires test methods being adapted to the materials and processes of future offshore wind farms. The paper presents a review of the survey on HISC test together with the initial results of the established HISC test.

Investigation on Nickel base superalloy steam turbine bolts, fractured at high temperatures, a case history

G. Lovicu, Università di Pisa, Pisa, Italy;

R. Ishak, Università di Pisa, Pisa, Italy;

L. Rolla, CTS Centro tecnologico Sperimentale Srl, Ceparana, Italy;

C. Dellabiancia, Centro tecnologico Sperimentale Srl, Ceparana, Italy;

Mechanical, chemical, microstructural analysis on fractured refractaloy 26 steam turbine bolts after 30000 hours service.

Ni-base superalloys have been often used as material for bolts of the steam turbine valves and of the steam admission areas of the turbine casings, thanks to their high-temperature resistance properties. In order to withstand high creep and fatigue loading these alloys are strengthened by γ' and/or γ'' precipitates.

Among them, the most used are Incoloy 901, Refractalloy 26, Inconel X750, Nimonic 80A and Nimonic 90 (PER 2 B). Although these alloys are designed specifically for employing in high temperature applications (up to 600 °C) some brittle intergranular cracking have been observed to be a consequence of high temperature exposure and high tensile loads. Moreover, due to their high strength, Ni-base superalloys are prone to oxygen induced brittle cracking, either during rapid quenching from the solution – heat treatment temperature or during dwell times in-service conditions.

In the present paper a case study on some fractured Refractalloy 26 bolts, after about 30.000 h service at 600°C has been reported.

Mechanical and microstructural analysis have been performed on fractured, as-received and exercised (not fractured) bolts. Fractographic analysis have shown an intergranular brittle fracture in all the fracture surface. SEM observations of secondary cracks have revealed an oxides penetration at grain boundary without evidence of impurities from the environment other than oxygen. A moderate microstructural degradation of used and fractured bolts have been highlighted by the presence of “eta” phase. Nevertheless, this kind of microstructural degradation seems not to be responsible of the observed fracture both because the tensile tests on as-received and exercised samples have not shown significant differences and because the eta phase has not been observed in the region close to the cracks.

Moreover, no creep-induced microstructural damages (such as grain boundaries microcavoids) have been observed in failed and serviced samples.

From all the experimental evidence, the most probable governing failure mechanism is the Stress Accelerated Grain Boundary Oxidation (SAGBO), the only one compatible with the intergranular brittle appearance of fracture surface and the presence of oxygen penetration at grain boundaries in regions close to the fracture surface.

Artificial Neural Network analysis of coupled Electrochemical Noise and Acoustic Emission data applied to chloride stress corrosion cracking

Luigi Calabrese¹, Filippo Cappuccini², Domenico Di Pietro², Massimiliano Galeano¹, Edoardo Proverbio¹

1 Department of Electronic Engineering, Industrial Chemistry and Engineering
University of Messina, Contrada di Dio, 98166 Messina, Italy

2 GE Oil & Gas, Via F.Matteucci 2, 50127 Firenze, Italy

Abstract

The use of new investigation methods which can be effective aids in recognition of corrosion damage evolution is an issue of major importance in the oil and gas industrial sector.

Acoustic Emission (AE) is a technique well suited to real-time control of damaging phenomena. Also the Electrochemical Noise (EN) technique appears to be very useful for these purposes, being easy to be applied and characterized by low invasiveness.

In the present work, stress-corrosion cracking on 17-4 PH (UNS S17400) stainless steel specimens was monitored simultaneously by acoustic emission and electrochemical noise techniques. Samples were tested in aqueous solution containing 30% by weight of magnesium chloride (according to ASTM G36) with a constant tensile load of 90% AYS.

For the acoustic emission monitoring two acoustic sensors were located at the ends of the specimen. A third sensor was also used to discriminate background noise from corrosion signals. The Electrochemical Noise was measured in free system (without external supply of current or voltage) by using a ZRA configuration cell with three stainless steel 17-4 PH electrodes (one of which consisting in the stressed sample) connected to a potentiostat.

The AE and EN data were pre-processed to extract a set of variables useful in the subsequent multivariate analysis, to characterize the corrosive phenomena both in temporal and in frequency domain.

Through the use of multivariable statistical analysis (Principal Component Analysis - PCA, Self-Organising Map SOM), information about SCC related damage mechanisms (such as activation, growth and propagation of cracks) have been obtained. Furthermore by correlation between univariate and multivariate statistical analysis of AE and EN parameters it was possible either to better understand the corrosion evolution phenomena and to relate each damage stage with specific cluster parameters.

Keywords:

Acoustic emission, Electrochemical noise, signal processing, self-organising map, stress corrosion cracking,

Liquid metal embrittlement of the T91 steel in Lead Bismuth Eutectic: effect of the loading rate and the oxygen content

Ingrid Proriol Serre, Unité Matériaux et Transformations UMR CNRS 8207 – Université Lille 1, 59650 Villeneuve d'Ascq/France; Changqing Ye, Unité Matériaux et Transformations UMR CNRS 8207 – Université Lille 1, 59650 Villeneuve d'Ascq/France; Jean-Bernard Vogt, Unité Matériaux et Transformations UMR CNRS 8207 – Université Lille 1, 59650 Villeneuve d'Ascq/France

The use of liquid lead bismuth eutectic (LBE) as spallation target and coolant in Accelerating Driven Systems or coolant in future Lead-cooled Fast Reactor (LFR) rises the question of the reliability of structural materials, such as T91 martensitic steel, in terms of liquid metal assisted damage and corrosion.

In this study, the mechanical behaviour of the T91 martensitic steel has been studied in liquid lead-bismuth eutectic (LBE) and in inert atmosphere. Several conditions were considered to point out the most sensitive embrittling factor. The Small Punch Test technique has been employed by using smooth specimens at different temperatures and different loading rates. Tests were performed in air, Ar-3.5% H_2 gas, in oxygen saturated LBE. To take into account the corrosion effect in low oxygen content LBE, experimentation was adapted: purification of LBE by Ar3.5% H_2 to decrease the oxygen content in LBE, measurement of oxygen content in LBE, mechanical tests low oxygen LBE.

In this standard heat treatment, T91 appeared in general as a ductile material, and became brittle in the considered conditions only at least if the test was performed in LBE. It turns out that the loading rate appeared as a critical parameter for the occurrence of LME of the T91 steel in LBE. Loading the T91 very slowly instead of rapidly in oxygen saturated LBE resulted in brittle fracture. Furthermore, low oxygen content in LBE and an increasing in temperature promote this LME. Scanning Electron Microscopy (SEM) and Secondary Ion Mass Spectroscopy (SIMS) are performed to explain the mechanism of the embrittlement of the T91 steel in LBE and the role of the oxygen content in LBE.

The Effects of Sulfide and Flow Rate on Corrosion Behavior of Duplex Steel 1.4462 in the Artificial Molasse Basin Fluid

Joana Sobetzki, Ralph Bäßler, Alicja Boduch

BAM - Federal Institute for Materials Research and Testing,
Unter den Eichen 87, 12205 Berlin, Germany

Within the last years the use of geothermal energy as feasible energy source has risen and is going to replace fossil fuel supply more and more. Nevertheless, service conditions in geothermal facilities are due to the chemical composition of hydrothermal fluids and temperatures, in many cases, extreme in terms of corrosion. Since the construction of geothermal power plants shall be economical with maximum life service, materials selection based on preliminary material qualification is essential to guarantee a secure and reliable operation of those facilities.

The materials selection depends on several terms like the chemical composition of the produced aquifer fluid as well as service conditions like pressure, temperature and flow rate etc. The duplex steel, this contribution deals with, is often used as all-round solution, because of its combination of good mechanical and corrosion properties and its lower costs compared to other highly alloyed materials. In the case of the artificial geothermal fluid of Molasse Basin which is a low saline, slightly alkaline water, this contribution shall illustrate the effects of sulfides (present as $(\text{NH}_4)_2\text{S}$ in Molasse Basin aquifer) and flowing respectively stagnating water as it can be found during maintenance or downtime of a power plant.

The duplex steel 1.4462 in the artificial Molasse Basin fluid shows an excellent corrosion resistance against pitting and uniform corrosion. Nevertheless, there are effects on its corrosion behavior caused by sulfide and flow rate of the fluid as shown in the figure below.

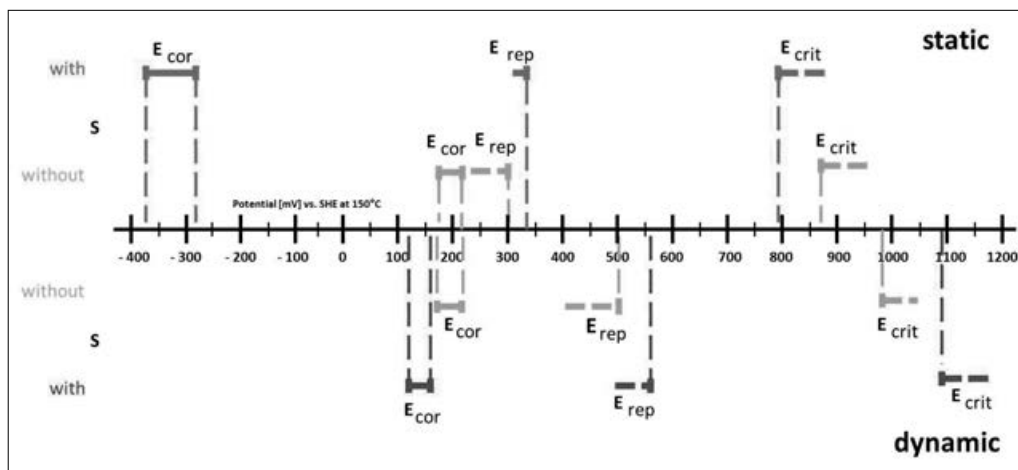


Fig.1: Different critical potentials determined electrochemically on duplex steel 1.4462 in flowing and static artificial Molasse Basin fluid with and without sulfide

Keywords: localized corrosion, duplex steel, geothermal energy

Influence of testing parameters on type of damage under cyclic loading

A. Visser, G. Mori, CD Laboratory of Localized Corrosion, Montanuniversitaet Leoben, Franz Josef Strasse 18, 8700 Leoben, Austria

H. Leitner, M. Kapp, R. Fluch, Böhler Edelstahl GmbH & Co KG, Mariazeller Strasse 25, 8605 Kapfenberg, Austria

B. Holper, Schoeller Bleckmann Oilfield Technology GmbH, Hauptstrasse 2, 2630 Ternitz, Austria

M. Panzenböck, Department of Physical Metallurgy and Materials Testing, Montanuniversitaet Leoben, Franz Josef Strasse 18, 8700 Leoben, Austria

Abstract

Corrosion fatigue cracks are initiated by different types of damage, such as dissolved slip-steps in pure corrosion fatigue (CF), stress corrosion cracking (SCC) and pitting corrosion. The type of crack initiation depends on the aggressiveness of the electrolyte and the mechanical properties of steel.

In this work two cold worked austenitic stainless steels have been tested in two different corrosive electrolytes: one mild medium (13.2 wt-% NaCl, 80 °C) and one aggressive medium (43 wt-% CaCl₂, 120 °C).

S-N curves have been compiled in both electrolytes as well as under inert condition in glycerine. Fracture surfaces were analysed using a scanning electron microscope (SEM). Additional immersion tests free from external loads have been performed in order to observe the type of attack and the presence of residual stresses that may derive from the cold working process or specimen fabrication.

The correlation of occurring types of damage in different corrosion systems is described.

Key words: Corrosion fatigue cracking, Stress corrosion cracking, Pitting, Austenitic stainless steels, Chloride solutions

CS-AFM study on the localized corrosion of 2507 duplex stainless steel

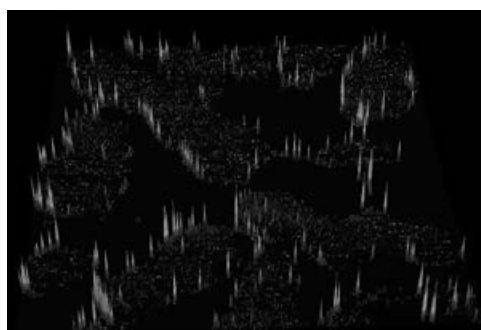
Lijie Qiao, Meichao Lin, Liqui Guo

Corrosion and Protection Center, Key Laboratory for Environmental Fracture (MOE)
University of Science and Technology Beijing, Beijing 100083, P. R. China

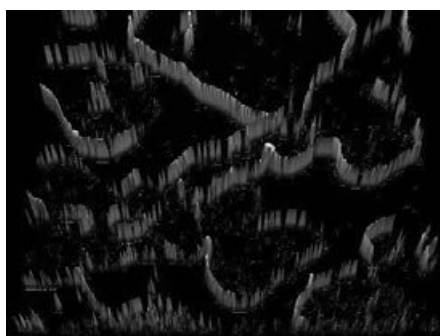
lqiao@ustb.edu.cn

Keywords: stainless steels, passive film, corrosion, pitting.

Abstract: The resistance to corrosion of stainless steels depends on the passive film formed on the surface in air or solutions. However, localized corruptions, such as pitting, crevice corrosion, grain boundary corrosion and stress corrosion cracking often occurred. This may be due to the inhomogeneous of the passive film. It was found that most of pitting occurred in austenite or grain/phase boundary in duplex stainless steel. The electric property of passive film on duplex stainless steel was investigated by current sensing atomic force microscopy (CS-AFM) and x-ray photoelectron spectroscopy (XPS). The electric resistance of the film formed on austenite, ferrite and the boundaries is different. The resistance of the film formed on the austenite is lower than that on the ferrite and it is lowest near the boundaries. This explained why pitting occurred in boundary and austenite phase. I-V curves show that the passive film is p-type semiconductor.



(a)



(b)

The map of current distribution along grain boundaries and in the phases of austenite and ferrite at 0.8V bias voltage (almost no current in the ferrite)

(a) film formed in air at room temperature; (b) film formed at 0 VSCE in 0.1M Na₂B₄O₇·10H₂O

The transition between Sulfide Stress Cracking and Stress Corrosion Cracking of the 2304 DSS as a function of T and pH in H₂S environment.

F. Ruel¹, S. Saedlou¹, S. Le Manchet², C. Lojewski², K. Wolski³

¹ Aperam R&D, Stainless Europe Research Center, 62330 Isbergues, France

² Industeel (ArcelorMittal group), 71201 Le Creusot, France

³ Ecole des Mines de Saint-Etienne, UMR 5307 LCG, Centre SMS, 42023 Saint Etienne, France

Depending on the experimental conditions (composition, microstructure, stress, temperature, pH, chloride content, H₂S partial pressure ...) Duplex Stainless Steels (DSS) may suffer from general corrosion and/or from local corrosion processes that involve the selective dissolution of the ferritic phase or the austenitic phase. These various corrosion phenomena can generate Sulfide Stress Cracking (SSC) or Stress Corrosion Cracking (SCC). The intent of this paper is first to delimit the domain of susceptibility corresponding to these two different forms of Environmentally Assisted Cracking (EAC). The second objective is to discuss the parameters affecting the transition from SSC to SCC.

Specimens of UNS S32304 Lean DSS plate have been tested by means of slow strain rate technique in solutions containing 50 g L⁻¹ NaCl, 5 g L⁻¹ NaCH₃COO and under a pressure of 14.5 psi (1 bar) of H₂S. Four pH – 2.8, 3.5, 4.5 and 6 – and three temperatures – 68 °F (20 °C), 122 °F (50 °C) and 194 °F (90 °C) – have been considered.

At pH 2.8 and 68 °F (20 °C) SSC occurs due to the general corrosion of the ferritic phase. At 122 °F (50 °C) the S32304 Lean DSS is sensitive to SCC. At this temperature, selective dissolution of the austenitic phase can be observed along the cracking paths and dissolution of the ferritic phase occurs at different points of the specimen. At 194 °F (90 °C) an “exfoliation corrosion” phenomenon appears and causes SSC.

At pH 3.5 and 68 °F (20 °C) SCC occurs associated to some selective dissolution of the austenitic phase along the cracking path. At 122 °F (50 °C) specimens are sensitive to SCC initiated by pitting corrosion and at 194 °F (90 °C) “exfoliation corrosion” phenomena of the ferritic phase appears once more and causes SSC. At higher pH SCC initiated by pitting corrosion occurs at 68 °F (20 °C) and 122 °F (50 °C) whereas only “exfoliation” corrosion of the ferritic phase without cracking appears at 194 °F (90 °C).

The different forms of EAC can be distinguished according to the cause of the dissolution and to its local character. From that distinction, delimitations of SSC / SCC susceptibility domains are deduced. Discussion on the transition between the two phenomena is done in terms of difference of depassivation pH between the austenite phase and the ferrite phase and of change in dissolution of H₂S in water and difference of depassivation pH between the austenite phase and the ferrite phase.

Key-words: UNS S32304, stress corrosion cracking, sulfide stress cracking, H₂S

Critical Factors in Corrosion and Biocompatibility of Biodegradable Mg Alloys

Sannakaisa Virtanen, *University of Erlangen-Nürnberg, LKO, Erlangen, Germany*

In recent years, the interest of exploiting Mg alloy corrosion for the use of these materials in biodegradable biomedical devices has found tremendously increasing research interest. For successful applications, detailed knowledge on the corrosion rate and mode in the biomedical application is of course required. Moreover, interactions between the corroding Mg surfaces and the biological environment need to be studied in detail. The challenges for successful applications are probably greater than expected, as in spite of the non-toxic nature of Mg ions, the side effects of Mg dissolution such as H₂ gas evolution or alkalization are of concern in view of the biocompatibility. In addition, many conventional Mg alloys seem to show too high corrosion rates in the biological environment (even though it should be mentioned that the desired corrosion rate of course very strongly depends on the targeted application).

Mg alloy corrosion has been studied *in vitro* in different types of simulated body solutions. Drastically different behaviors can be found between different formulations of solutions; in many cases the complex media used for these studies makes it challenging to attribute the specific corrosion behavior observed to a single parameter in the electrolyte. The presentation will discuss some critical factors influencing the observed corrosion rates, such as presence of proteins in the electrolyte.

As many conventional Mg alloys seem to show too high corrosion rates in the biological environment, various pathways to tailor the degradation rate of Mg alloys have been proposed, including development of novel alloys as well as various surface modification approaches. Recent developments in surface modification will be presented, in view of optimizing both the corrosion and the biological performance. This includes functionalization of Mg surfaces with organic molecules or protein adsorption layers, as well as coating Mg alloys with degradable polymers.

The presentation will further show results on the influence of Mg corrosion and surface modification on the biological performance, studied by cell culture experiments. In addition, influence of cell adhesion layers on the corrosion behavior is being studied by electrochemical impedance spectroscopy.

Application of Time-of-Flight Secondary Ions Mass Spectrometry (ToF-SIMS) to Corrosion Research

Philippe Marcus, Antoine Seyeux

*Institut de Recherche de Chimie Paris
CNRS-Chimie ParisTech, Paris, France*

ToF-SIMS (Time of Flight Secondary Ions Mass Spectrometry) is a powerful surface chemical analysis technique. It allows one to identify corrosion products on surfaces with extreme sensitivity ($< \text{ppm}$), high mass resolution ($M/\Delta M \sim 10\,000$). Using a dual beam system (Bi^+ ion beam for analysis and Cs^+ ion beam for sputtering) in depth composition profiles are obtained with high depth resolution (~ 1 monolayer). Surface chemical mapping can also be performed, using the primary ion beam, with a lateral resolution of the order of 150nm .

Selected examples of applications to corrosion research will be presented :

- Oxidation/passivation of stainless steel (316L) and nickel based alloys (Alloy 690) exposed to high temperature water (under conditions representative of pressurized water reactors of nuclear power plants). Oxide penetration at grain boundaries is revealed.
- Corrosion of carbon steel by naphthenic acids in the refinery industry. The nature of corrosion products is elucidated, which allows us to discuss the corrosion mechanisms.
- Effect of bacteria on passive films (stainless steel and Ti) in the early stages of biofilm formation. The data demonstrate the presence of a passive film at the bacteria/metal interface, the composition of which is modified.

Multiscale Corrosion Modelling

Johan Deconinck, Olga Dolgikh, Andrei Demeter, Simillion Hans, Nils Van den Steen

*Research Group Electrochemical and Surface Engineering (SURF)
Vrije Universiteit Brussel, Pleinlaan 2, B-1050 Brussel, Belgium*

Corrosion modelling has been done for several years with the aim to provide practical information to corrosion engineers in view of lifetime prediction.

The first models were based on relatively simple fitted correlations with little or no physical background. The increased knowledge on corrosion and mainly corrosion mechanisms allows now to perform better and to take into account the different aspects that finally lead to corrosion: composition of electrolyte and electrode composition, galvanic coupling of different materials, oxygen, film thickness, etc. Simultaneously the increasing computing power enables considering in more detail the mentioned aspects in more detail by considering for instance transport processes. Nevertheless for practical use models need to be simplified. It is impossible to consider all details in all dimensions. As a logical consequence, corrosion modelling needs to be multi-scalar and is also becoming a multi-physics problem such that for instance the role of film thickness variations due to temperature and humidity variations can be taken into account

In this contribution we give an overview of available models and modelling approaches. We start with models that only consider current density distributions due to competing reactions (e.g. oxygen reduction/metal oxidation) or galvanic coupling. They are particularly important for large scale corrosion systems. Then models that consider in detail transport of ions and that are mainly made to obtain quantified mechanistic understanding are presented.

Finally it will be explained how we see an integration of these models together with film variation modelling in view of reaching stepwise improved atmospheric corrosion models.

References

- (1) D. Deconinck, S. Van Damme, & J. Deconinck, *Electrochim. Acta* 60 (2012) 321–328
- (2) L.C. Abodi, J.A. DeRose, S. Van Damme, A. Demeter, T. Suter, & J. Deconinck, *Electrochim. Acta* 63 (2011) 169–178
- (3) V. Topa, A. Demeter, L. Hotoiu, D. Deconinck, & J. Deconinck, *Electrochim. Acta* 77 (2012) 339–347

Localised Corrosion Mechanisms of Magnesium in Methanol

*H.N.McMurray, J.E. Board and G. Williams, Swansea University, Swansea, UK
Email: h.n.mcmurray@swan.ac.uk*

It is well known that methanol is aggressively corrosive to light metals such as magnesium and that this can present a problem when methanol is present in cleaning solutions, fuel mixtures and coolant streams. However, the high electrical resistivity of methanol and (salt-free) methanol/water mixtures makes conventional electrochemical measurements involving polarisation difficult to perform. Consequently, whenever electrochemical studies of methanolic corrosion have been carried out they have typically been so in electrolyte mixtures comprising methanol, water and dissolved salt. Here we show that the scanning vibrating electrode technique (SVET) is capable of providing quantitative information on the intensity and localisation of electrochemical corrosion reactions as they occur on commercially pure magnesium immersed in pure methanol and salt-free methanol/water mixtures. As such it has been possible to determine more exactly the kinetics and mechanism of methanolic attack. It has been also possible to show that both water and oxygen actually inhibit methanolic corrosion and that, in the case of water, this inhibition can be profound. In the current paper SVET data are supported throughout with independent measurements of: hydrogen evolution rate and weight loss under conditions of known water activity and controlled oxygen partial pressure.

Magnesium foil (2mm thick, 99.9% purity, temper as rolled) was obtained from Goodfellow Metals (nominal iron impurity level 280ppm). Methanol (ACS Reagent Grade, 99.8% purity) was obtained from Sigma Aldrich Ltd. The electrical conductivity of the as-received Methanol was measured to be $1.170 \mu\text{S}/\text{cm}$. Fig. 1a shows pitting corrosion of magnesium, induced by immersion in methanol in contact with room air and Fig1b shows a corresponding SVET-derived current density map. The SVET data show evidence of cathodic activation, in which initially anodic areas switch to cathodic activity as a result of transition metal impurities (mainly iron) accumulating at the dissolving magnesium surface.

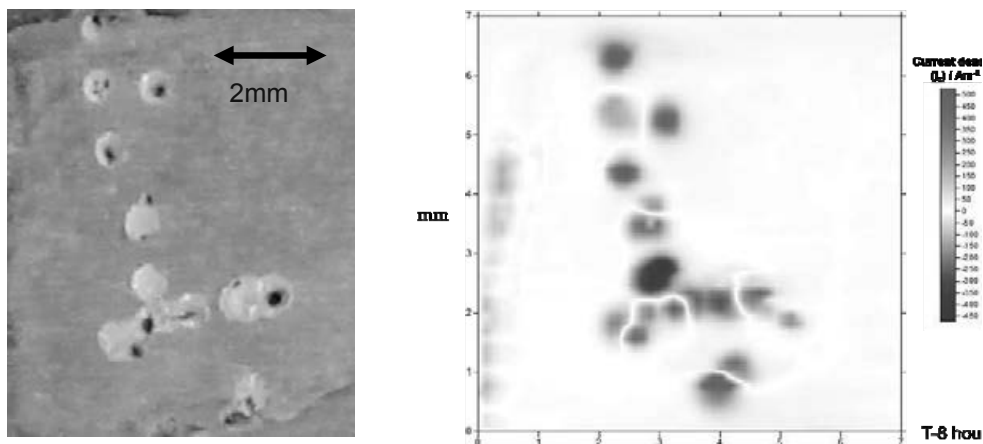


Figure 1: a) Photographic image of magnesium surface after immersion in Methanol for 20 hours. b) SVET derived current density map obtained from the same sample in methanol after 8 hours immersion.

Effect of Si on formation of Fe-rich particles in pure Mg and its influence on corrosion

Lei Yang^{a}, Xiaorong Zhou^a, Songmao Liang^b, Rainer Schmid-Fetzer^b, Teruo Hashimoto^a, Hong Liu^a, Xiangli Zhong^a, Joseph Robson^a, Zhongyun Fan^c, Geoff Scamans^d, George Thompson^a*

^a School of Materials, University of Manchester, Manchester, M13 9PL, UK

^b Institute of Metallurgy, Clausthal University of Technology, Clausthal-Zellerfeld, Germany

^c Brunel Centre for Advanced Solidification Technology (BCAST), Brunel University, Uxbridge, Middlesex, UB8 3PH, UK

^d Innoval Technology Ltd., Beaumont Close, Banbury, Oxon, OX16 1TQ, UK

* email: lei.yang@manchester.ac.uk, Tel: +441613064866

The tolerance limit of Fe in pure Mg is reported to be 170 ppm [1], and this is explained by using the calculated binary Mg-Fe phase diagram [2]. However, it is also reported that the corrosion rate of pure Mg can be high even when the Fe concentration is below 50 ppm [3, 4]. Reasons for this behaviour are still unclear, which makes the corrosion behaviour of Mg appear to be unpredictable. In this work, pure Mg with 25 ppm Fe, which displays a high corrosion rate (100 mm/year), was used to explore the corrosion behaviour of pure Mg. The microstructure was examined using conventional and 3D scanning electron microscopy (SEM) equipped with energy dispersive spectroscopy (EDS). The solidification behaviour was simulated using Pandat software to calculate the relevant phase diagrams. The corrosion behaviour was investigated using the hydrogen evolution method, together with in-situ image recording and the scanning vibration electrode technique. Fe-rich particles are observed even when the Fe concentration is only 25 ppm, and it is found that Si is always contained in the Fe-rich particles. Based on the calculated phase diagram, Si (even only at the low ppm level) can introduce a solidification interval and result in the formation of BCC_B2 particles (Fe particles with dissolved Si). The Fe-Si particles can act as strong cathodes to promote galvanic corrosion with the magnesium matrix and accelerate the corrosion rate. The corrosion initiates from one or multi-points and propagates across the macroscopic surface from the initiation points. The SVET shows the area after corrosion acts as a cathode and the interface of corroded/non-corroded area acts as the anode. The detailed mechanism of Fe-Si particles formation and the corrosion initiation and propagation behaviour are discussed.

Reference

- [1] J.D. Hanawalt, C.E. Nelson, J.A. Peloubet, Transactions of the American Institute of Mining and Metallurgical Engineers, 147 (1942) 273-298.
- [2] M. Liu, P.J. Uggowitzer, A.V. Nagasekhar, P. Schmutz, M. Easton, G.-L. Song, A. Atrens, Corrosion Science, 51 (2009) 602-619.
- [3] Z. Qiao, Z. Shi, N. Hort, N.I. Zainal Abidin, A. Atrens, Corrosion Science, 61 (2012) 185-207.
- [4] N. Birbilis, G. Williams, K. Gusieva, A. Samaniego, M. Gibson, H. McMurray, Electrochemistry Communications, 34 (2013) 295-298.

Corrosion of AZ31 Mg alloy in the presence of ammonium ion

*D. Buggio, M. Trueba, S.P. Trasatti
Università degli Studi di Milano, Italy*

The corrosion behaviour of AZ31 Mg alloy was studied in different electrolytes, namely NH_4Cl , $(\text{NH}_4)_2\text{SO}_4$, Na_2SO_4 , NaCl , NaClO_3 , and their mixtures, as well as dilute Harrison solution (DHS). DHS is constituted by a mixture of the commonly occurring atmospheric salts, $(\text{NH}_4)_2\text{SO}_4$ and NaCl . Its spray at ambient temperature corresponds closely to natural weathering. Corrosion potential and solution pH were monitored with time. The concentration of Mg^{2+} and hydrogen gas produced were also determined. Electrochemical experiments such as impedance spectroscopy, potentiodynamic and potentiostatic measurements, were conducted. In the presence of NH_4^+ , the formation of a black deposit on the surface with concomitant vigorous evolution of hydrogen is greatly favoured. XRD analysis of the deposits indicated the presence of a crystalline phase, identified as $\text{Mg}(\text{AlH}_4)_2$. The corrosion potential shifts to much less negative values and solution pH increases less markedly than in typical solutions of NaCl and Na_2SO_4 . The amount of Mg^{2+} released by the surface and of evolved hydrogen were much higher as well. Electrochemical experiments have provided confirmation of highly reactive Mg/NH_4^+ system. In particular, potentiodynamic polarization showed a purely ohmic behaviour, whereas a passive film breakdown was obtained in the absence of NH_4^+ . Low resistance to charge transfer was also observed in DHS. The results indicate different mechanism of Mg corrosion in the presence of NH_4^+ . The dissociation of NH_4^+ as the pH increases at the metal/solution interface promotes the replenishment of local acidity which favours the formation of a very reactive Mg hydride rather than precipitation of $\text{Mg}(\text{OH})_2$.

The dissolution of magnesium investigated with a microelectrochemical flow system

Lisa Rossrucker^a, Nick Birbilis^b, Gerald S. Frankel^c, Karl J.J. Mayrhofer^a

^a Max-Planck-Institut für Eisenforschung GmbH, Düsseldorf, Germany

^b Department of Materials Engineering, Monash University, Clayton, VIC, Australia

^c Department of Materials Science and Engineering, The Ohio State University, Columbus, OH, USA

Magnesium is a highly promising element for a large range of technical applications where weight reduction is beneficial, but unfortunately the use of magnesium and its alloys is limited by their low corrosion resistance. Therefore understanding the dissolution characteristics of magnesium remains an important research topic, especially as there is no conformity about the mechanism of its dissolution in aqueous solutions in literature [1-2]. Several studies conclude that the anodic dissolution of magnesium involves the unipositive Mg^+ ion [3,4], using the Mg^+ theory to also account for the so called 'negative difference effect' (NDE), which describes an increase of the hydrogen evolution with anodic polarization. However, there is no proof of the existence of Mg^+ and recent studies [5-7] reveal a dissolution stoichiometry of Mg^{2+} and additionally indicate that the NDE results from cathodic activation with increasing anodic magnesium dissolution.

The system presented in this study combines a microelectrochemical scanning flow cell (SFC) with online analytics via ICP-MS. This method allows for quantification of the magnesium dissolution during anodic and cathodic polarization and furthermore facilitates the determination of the dissolution directly at the free corrosion potential, which is not accessible by electrochemical techniques [2]. Further advantages are the low requirements for sample geometry and the fully automated change of sample position, which significantly reduces the time demand for measurements.

In this study we investigate the dissolution of magnesium at the free corrosion potential and during cathodic and anodic polarization utilizing the SFC and element-resolved analysis. The relationship between the applied current density and the dissolved magnesium will be discussed.

- [1] G. Song, *Advanced Engineering Materials*, 7 (2005) 563.
- [2] L. Rossrucker et al., *Journal of the Electrochemical Society* 161 (2014) C115.
- [3] R.L. Petty et al., *Journal of the American Chemical Society*, 76 (1954) 363.
- [4] Z. Shi et al., *Corrosion Science* 60 (2012) 296.
- [5] G.S. Frankel et al., *Corrosion Science* 70 (2013) 104.
- [6] J. Swiatowska et al., *Corrosion Science* 52 (2010) 2372.
- [7] G. Williams, *Proc. Conf. Corrosion and Prevention* (2012) Plenary 5.

Corrosion Behaviour of Magnesium Electrodes Investigated by Real-Time Hydrogen measurement

M. Curioni, Corrosion and Protection Centre, The University of Manchester, Manchester, M13 9PL, United Kingdom

A simple experimental setup to obtain real-time measurement of the hydrogen evolved from the surface of magnesium electrodes during electrochemical corrosion testing is presented. The setup comprises a plastic container, open at the bottom and closed at the top, placed above the corroding magnesium electrode, used for the collection of the evolved hydrogen. Both the electrode and the container are completely immersed in the corrosive electrolyte and mounted with an adequate support on the plate of a laboratory scale. The air in the plastic container is removed such as the container is completely filled by the electrolyte at the beginning of the test. When hydrogen is evolved from the magnesium surface, it is collected from the submerged cylinder. As a result, a volume of electrolyte corresponding to the volume of evolved hydrogen exits the cylinder from the open bottom. Thus, a hydrostatic force given by the volume of the evolved hydrogen multiplied by the density of the electrolyte develops and can be measured in real time by the laboratory scale. By using Faraday's law, the current associated to the evolved hydrogen can be calculated in real-time. For example, a corrosion current of 1 mA produces a variation in weight of 0.126 mg s^{-1} (or 7.6 mg min^{-1}), that can be easily detected by a common laboratory scale.

By using the proposed setup, the behaviour of magnesium is investigated both during free corrosion and during anodic and cathodic potentiodynamic polarization. The findings provide further insight into the phenomenon of the 'negative difference effect' and on the correlation between the corrosion current estimated by electrochemical techniques and the corrosion current directly measured from the evolved hydrogen.

Concerning the negative difference effect, it was found that the anodic reaction produces dark regions on the electrode surface that progressively propagate and such regions sustain a high cathodic activity. Anodic polarization increases the propagation rate of the dark regions and therefore increases the cathodic activity. This process is, thus, responsible for the observed 'negative difference effect'.

Regarding electrochemical measurements, it was found that Tafel extrapolation to the corrosion potential of the linear region of a cathodic potentiodynamic polarization initiated at the corrosion potential provides a reasonably accurate estimation of the corrosion current. On the contrary, anodic polarization initiated at the corrosion potential or a polarization initiated below the corrosion potential (cathodic) towards more positive potentials (anodic) does not provide a reliable estimation of the corrosion current.

Influence of plastic deformation on the corrosion resistance of TiAl6V4 and TiMo10Zr4 alloys in aqueous solution containing chloride ions

Halina Krawiec¹, Joanna Loch¹, Alicja Łukaszczyk¹, Vincent Vignal²

¹ AGH University of Science and Technology, Ul. Reymonta 23, 30-059 Krakow,
Poland

² ICB, UMR 6303 CNRS-Université de Bourgogne, BP 47870, 21078 Dijon, France

Abstract

TiAl6V4 is the most commonly used titanium alloy in the biomedical sector. It has a heterogeneous microstructure composed of two metallic phases (α and β with a content of β between 5 and 20 %). Recently, the cytotoxic response of titanium alloys have been studied and alloying elements like Nb, Ta and Zr have been selected as the safest elements to human bodies. Hence, new titanium alloys containing non-toxic elements have been developed like TiMo10Zr4.

The role of alloying elements and the microstructure on the micro-electrochemical behaviour and the pitting corrosion susceptibility of TiAl6V4 and TiMo10Zr4 alloys have been investigated in 10 g/L NaCl and Ringer's solutions using the electrochemical microcell technique. The influence of plastic strain on the electrochemical response and pitting corrosion susceptibility of the alloy has also been investigated using tensile specimens. Experiments were carried out at the meso- and microscale using the electrochemical microcell technique. Different strain levels were considered.

Local electrochemical measurements have revealed that both the increase of surface roughness and the increase of dislocation density have impact on the electrochemical behaviour of titanium alloys after plastic deformation. It has been shown the surface roughness induced by slip band emergence is the predominant parameter responsible for the increase of the cathodic current. It has also been shown that cathodic reactions occur preferentially at surface defects (α/β interfaces, slip bands, for example). The presence of aluminium oxide in the passive film hindered cathodic reactions.

Non-uniformity of Anodized Titanium Surface under UV-light Irradiation Observed by Ellipso-microscopy

K. Fushimi, K. Kurauchi, T. Nakanishi, Y. Hasegawa, M. Ueda, T. Ohtsuka
Faculty of Engineering, Hokkaido University, Sapporo, Japan

Titanium surface shows an excellent corrosion resistance even in highly chloride ion containing solution due to formation of a chemically stable oxide film. However, under the irradiation of UV-light, the surface allows to flow photo-electrochemical current because of its n-type semi-conductive property. Ohtsuka et. al reported the photo-corrosion of titanium surface induced by UV-light irradiation [1]. Ellipsometry has been an effective method for *in-situ* analysis of a passive film and used in the determination of thickness and optical properties of the film. The authors reported the growth and degradation of polycrystalline titanium surface anodized in sulfuric acid by using an ellipso-microscopy [2]. Here, the ellipso-microscopic observation of titanium surface anodized in sulfuric acid was carried out under UV-irradiation.

A laser light (532 nm) was used with an incident angle of 60°. The null ellipsometric condition of polarizer-compensator-sample-analyzer (PCSA) optics was fixed before the following anodization. The sample surface of polycrystalline titanium was anodically polarized in 0.05 mol dm⁻³ sulfuric acid solution with or without potassium bromide and irradiated by another laser light (325 nm) with the incident angle of 0°. Light passed through the PCSA optics was monitored by the microscope with a CCD camera and a 4X macro-lens.

During the dynamic polarization of sample surface, the initial null-condition of PCSA optics was gradually unadapted due to the formation of anodic oxide film on the surface. The film growth rate was dependent on the crystallographic orientation of the substrate as well as polarization potential. An *ex-situ* identification using electro backscatter diffraction patterning revealed that a special grain grew the thicker film than any other grains. The breakdown of the film with flowing a significant increase in anodic current was induced by addition of bromide ions to the solution. Prior to the film breakdown, however, an *in-situ* observation by ellipso-microscopy revealed that the surface was partially regressed the null-condition with flowing a slightly large anodic current. It was indicated that the film degradation commenced electrochemically and progressed chemically. The formation of dissolvable products such as bromoxide was suggested from a series of images and current transient. The film degradation tended to occur at the surface covered with a thinner oxide film rather than that covered with the thicker film. The irradiation of UV-light on the anodized titanium surface induced the change in the ellipso-microscopic image. Non-uniform image basically depending on the metallographic texture of the substrate was turned to dark and then bright. The irradiation time for the turning image decreased with increasing applied potential. It was suggested that the anodic oxide film was modified or reduced by photon energy of UV-light, depending on the substrate texture.

References

1. T. Ohtsuka, T. Otsuki, J. Electroanal. Chem., 473(1-2) 272-278 (1999).
2. K. Fushimi, K. Kurauchi, T. Nakanishi, Y. Hasegawa, T. Ohtsuka, EUROCORN2013, 1095.pdf (2013).

pH at zinc and magnesium surfaces during atmospheric corrosion

Claes Taxén, Swerea-Kimab, Stockholm/Sweden and Dominique Thierry, Institute de la Corrosion, Brest/France

Galvanic effects during atmospheric corrosion of zinc and magnesium are considered in a simulation study. Changes in the composition of a 10 μm thin liquid layer containing 1 M NaCl are calculated during electrochemical corrosion of a small part of the surface supported by a much larger cathode where oxygen reduction takes place. The imbalance current between anodic and cathodic regions is gradually increased in order to study the local solution compositions and precipitated solids. For a zinc anode, the first solid corrosion products to form are ZnO(s) and $\text{Zn}_5(\text{OH})_8\text{Cl}_2$. At slightly higher imbalance currents the solution becomes supersaturated also with respect to $\text{Zn}_5(\text{OH})_6(\text{CO}_3)_2$. The cathodic region attains pH-values higher than pH 10 also at moderate imbalance currents ($\sim 1 \text{ A/m}^2$ anodic current density). CO_2 from the atmosphere is taken up and gradually converted to carbonic acid H_2CO_3 which to some extent counteracts the high pH-values at the cathodic regions. Diffusion, mainly, carries carbonate species towards the anode. The carbonate form changes from mainly CO_3^{2-} to HCO_3^- and finally partly to H_2CO_3 according to the local pH values encountered. H_2CO_3 at the most acidic regions ($\sim \text{pH } 6.3$) produces CO_2 in excess of the level predicted by atmospheric equilibrium. CO_2 thus leaves the solution and is returned to the atmosphere.

This cycle of carbonate from the atmosphere at the cathode and back to the atmosphere at the anode is interrupted at an imbalance current density of about 10 A/m^2 anodic current density. At this point CO_2 from the atmosphere at the cathode is instead converted to $\text{Zn}_5(\text{OH})_6(\text{CO}_3)_2$. The main solid corrosion products are however ZnO(s) and $\text{Zn}_5(\text{OH})_8\text{Cl}_2$. The continued removal of chloride from the solution, in the form of $\text{Zn}_5(\text{OH})_8\text{Cl}_2$, eventually causes an alkalization of the whole liquid volume. Charge balance requires that the chloride ions be replaced by hydroxide ions and the initial NaCl solution gradually becomes a mixture of NaCl and NaOH. The model predicts pH-values higher than pH 13 for the conditions studied.

The behavior of magnesium as a local anode resembles that of zinc with one important difference. There is no sparingly soluble magnesium compound and all the initial chloride is predicted to remain dissolved. A pH value around pH 12 is predicted at the cathode, mainly due to the relatively high solubility of the hydroxide, Mg(OH)_2 .

The development of a mechanistic model towards the simulation of atmospheric corrosion

Simillion Hans, Olga Dolgikh, Herman Terryn, Johan Deconinck

*Research Group Electrochemical and Surface Engineering (SURF)
Vrije Universiteit Brussel, Pleinlaan 2, B-1050 Brussel, Belgium*

Corrosion predictions are usually based on empirical or historical data. The fitted parameters, that come out of the experimental exposure tests, provide an estimation of corrosion rates in general. However this estimation is very coarse, since the test conditions do not reflect the real corrosion rate of a specific system.

In this work a model based on transport equations is developed - the Multi-Ion Transport and Reaction model (MITReM)- that considers in more detail the underlying physicochemical properties of the system. It has been applied for electrochemical machining⁽¹⁾, pitting corrosion⁽²⁾ and galvanic corrosion⁽³⁾ simulations. The model takes into account relevant species in the electrolyte, together with electrode reactions and corrosion product formation. Next, potential and concentration distributions are calculated. This approach offers much more insight in the underlying mechanisms, but it also allows parametric sweeping and “what if” scenario testing. Previous work showed that these mechanistic models are a great step forward, towards the prediction of corrosion^(2,3). Also the time dependency and kinetics as well as the influence of corrosion products over time should be taken into account.

However such models are applied on a small scale only and are often too confined to anticipate long-term atmospheric corrosion of real structures. This highlights the need for a model that is computationally less complex, while covering the essential aspects of the corrosion processes.

We developed a model to simulate the corrosion processes on an electrode covered with thin aqueous electrolyte films. Averaging theorems are applied to reduce the amount of unknowns, significantly lowering the simulation cost. The details of the model are explained in this work, together with examples of a corroding zinc sample. Comparison of the reduced model and full model shows whether (or when) the loss in accuracy is acceptable in comparison to the gain in computational time.

References

- (1) D. Deconinck, S. Van Damme, & J. Deconinck, *Electrochim. Acta* 60 (2012) 321–328
- (2) L.C. Abodi, J.A. De Rose, S. Van Damme, A. Demeter, T. Suter, & J. Deconinck, *Electrochim. Acta* 63 (2011) 169–178
- (3) V. Topa, A. Demeter, L. Hotoiu, D. Deconinck, & J. Deconinck, *Electrochim. Acta* 77 (2012) 339–347

Role of pH on the *L*-cysteine action on zinc in 3 w/w % NaCl

*Presenting V. Shkirskiy**, Co-authors *P. Volovitch**, *K. Ogle**, *F. Leroux***,
*T. Stimpfling***, *P. Keil****, *H. Hintze-Bruening****

*Institut de Recherche de Chimie Paris, CNRS – Chimie ParisTech, 11 rue Pierre et Marie Curie, 75005 Paris, France (viacheslav.shkirskiy@chimie-paristech.fr)

**Clermont Université, Université Blaise Pascal, Institut de Chimie de Clermont-Ferrand (ICCF, UMR-CNRS 6296), BP 80026, F-63171 Aubière, France

***BASF Coatings GmbH, Glasuritstraße 1, 48165 Münster, Germany

In this work, we investigate the inhibitive action of *L*-cysteine which has been proposed as a possible “green” inhibitor on zinc substrates. We have used the *atomic emission spectroelectrochemistry* (AESEC) technique [1] to measure directly and *in situ* the spontaneous corrosion rate of Zn at the open circuit potential in 3 w/w % NaCl as a function of *L*-cysteine concentration and pH. A clear inhibitive effect was observed between 10^{-4} M and 10^{-3} M *L*-cysteine while an accelerating effect was observed for 10^{-2} M *L*-cysteine independent of pH.

In the concentration range where inhibition was observed, the inhibition efficiency decreased with pH: for 10^{-3} M *L*-cysteine it drops from 62 ± 5 % (at pH 4) to 27 ± 5 % (at pH 12) and for 10^{-4} M from 36 ± 5 % (at pH 4) to 16 ± 5 % at pH 12. The effect is explained by a rise of spontaneous *L*-cysteine dimerization to *L*-cystine with increasing pH. Experiments with pure *L*-cystine were performed as a confirmation.

The stability of the *L*-cysteine film formed at different solution concentrations was further investigated by a novel coupling of the AESEC technique and *electrochemical impedance spectroscopy* (EIS). This coupling allows us to directly monitor the effect of the AC perturbation on the elemental dissolution rate of Zn (Fig. 1). The comparison between the zinc dissolution current and the total current gives supplementary information about the film structure and corrosion mechanisms.

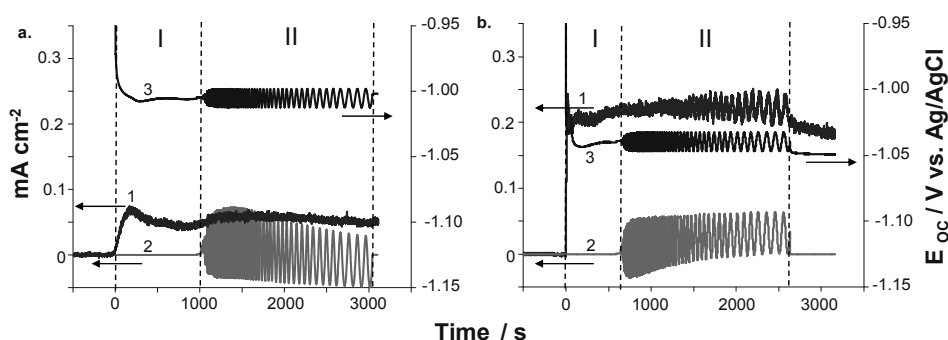


Fig. 1. Evolution of (1) zinc dissolution rate, (2) total current, and (3) potential at initial pH 6 (a) without and (b) with 10^{-2} M *L*-cysteine. Zone (I) shows the open circuit zinc corrosion rate; zone (II) shows the EIS experiment.

Finally, a 24 h immersion test under conditions of maximum inhibition demonstrated a 2 hours passivation period followed by activation indicating that the initially formed protective surface layer is destabilized with time.

In-situ Atmospheric Corrosion Monitoring using Resistometry

Kazuhisa Azumi, Hokkaido University, Sapporo, Japan

Introduction: Resistometry is one of useful corrosion monitoring tools which does not need electrochemical operation and thus applicable to the atmospheric corrosion. Wheatstone bridge type resistometry has been used to compensate the influence of temperature fluctuation of corrosion environment on metal resistance. We developed temperature compensated resistometry using electronic circuit and have been applied it to various corrosion monitoring of metal in, for example, high temperature water, the flow system of freshwater, and soil. In this study, resistometry was applied to atmospheric corrosion of Zn in wet and dry cycling test.

Experimental: Two Zn foils (Thickness: 25 or 50 μm , Length: 50 mm, Width: 2 mm) was embedded in laminate sheet. One foil (R_{corr}) was exposed to wet and dry corrosion environment (Wet: 25 $^{\circ}\text{C}$, RH90%, 3.6 ks, Dry: 60 $^{\circ}\text{C}$, RH30%, 3.6 ks, Transition time between them: 3.6 ks) with dropping NaCl solution and the other foil (R_{ref}) was placed in a same condition but sealed completely to be protected from corrosion and was used as a reference resistance for temperature compensation. The resistance of these two foils were measured by using an one chip impedance analyzer (Analog Devices Co., AD5933). The resistance of corroding Zn foil (R_{corr}) was divided by the resistance of protected Zn foil (R_{ref}) to compensate the temperature effect. Ag/AgCl paint was put beside the R_{corr} to measure the electrode potential of corroding Zn.

Results and Discussion: Fig.1 shows example of measurement parameters of Zn specimen changing in the wet and dry test. Electrode potential of corroding Zn was available only in the wet cycle and was about -0.6 V. Fluctuation in resistance of two Zn foil (R_{corr} and R_{ref}) with temperature (30 $^{\circ}\text{C}$ / 60 $^{\circ}\text{C}$) was ca. 0.2% while that of $R_{\text{corr}}/R_{\text{ref}}$ was less than 0.1 %. From the time transition of $R_{\text{corr}}/R_{\text{ref}}$, corrosion loss was estimated as shown in Fig. 2 where the total corrosion loss was about 0.1 μm for initial 400 ks of corrosion test.

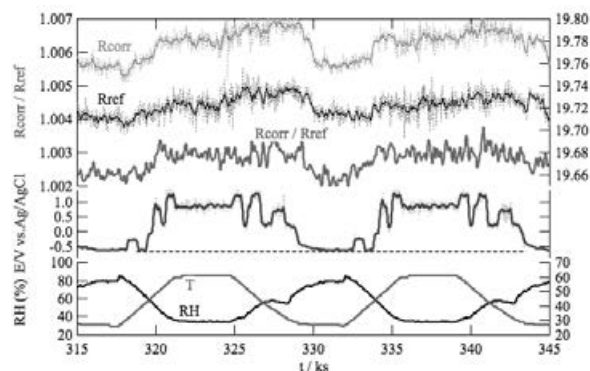


Fig.1. Change in resistance of two Zn foil (R_{corr} , R_{ref}), ratio of them ($R_{\text{corr}}/R_{\text{ref}}$), potential of R_{corr} , temperature (T) and relative humidity (RH) during the wet and dry cycling test.

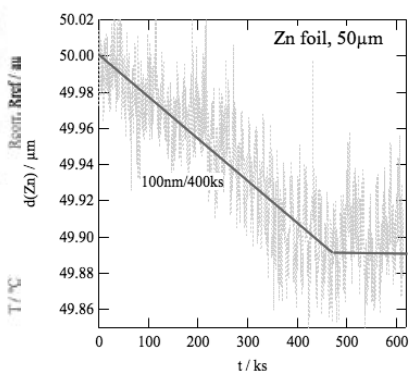


Fig.2. Time variation of corrosion loss of Zn foil during wet and dry test calculated from resistance change.

Corrosion performances of plasma electrolytic oxidized implant metals and alloys

*S.L. Sinebryukhov, S.V. Gnedenkov, O.A. Khisanfova, A.V. Puz', V.S. Egorkin,
A.G. Zavidnaya*

*Institute of Chemistry, Far East Branch, Russian Academy of Sciences, Vladivostok,
Russia*

Plasma electrolytic oxidation (PEO) technique provides an environmentally-friendly process to form well adhered coatings on titanium and magnesium alloys with high anticorrosion properties. PEO allows obtaining bioactive or bioinert implant surfaces depending on the composition of the used electrolyte.

PEO-coatings on nickel-titanium alloys demonstrate high anticorrosion properties in chloride containing electrolytes. Such layers decreasing the nickel ions release from the substrate prevent the harmful effect of nickel accumulation in human tissues. In spite of the presence heterogenous layer at the surface the details from alloy with PEO-coating save the shape memory effect. This point was confirmed by differential scanning calorimetry and differential thermo-analysis methods. Use of the superdispersed polytetrafluorethylene (SPTFE) in the coatings composition allows increasing the anticorrosion properties of the nickel-titanium alloys. After the processing of the PEO-coated sample with SPTFE powder, the modulus of impedance increases significantly. Its value is of an order of magnitude higher than for the sample without coating. This fact confirms the contention that processing with SPTFE powder allows the filling of pores in the coating with the polymer on the surface and, therefore, forming an additional barrier layer that will hinder the release of metal ions into the solution.

The approach to hydroxyapatite (HA) formation in the coatings composition during PEO on titanium and magnesium alloys has been developed. In this case the Ca/P ratio is equal or close to that of the human bone tissue. The porous HA-containing layer formed by the PEO method has prospects in medical applications. The experiment confirmed the bioactivity of these calcium phosphate layers. The HA-coatings obtained on magnesium alloys can be used for anticorrosion protection of biodegradable implants in order to slow down the corrosion rate of the substrate. The development of the corrosion process on the HA-coated specimens was evaluated in a Hank's and SBF solutions at 37 °C with uncoated specimens as a control using the potentiodynamic polarization, electrochemical impedance spectroscopy and hydrogen evolution measurement techniques. It was established the HA coating on magnesium alloys reduces the corrosion rate more than twofold as compared with unprotected specimen. Moreover, in SBF solution at 37 °C this coating possesses a high bioactivity due to their chemical composition.

Effect of Microstructure on the Morphology of Atmospheric Corrosion Pits in 304L and 316L Stainless Steel

Haval Mohammed-Ali, Liya Guo, Steven Street, Andrew du Plessis, Trevor Rayment¹, Moataz Attallah, Alison J. Davenport

University of Birmingham, School of Metallurgy and Materials, Edgbaston, Birmingham, UK ¹Diamond Light Source Ltd., Didcot, UK

Atmospheric corrosion of stainless steel is of concern for intermediate level nuclear waste (ILW) containers. Chloride ions present in atmospheric aerosols may deposit on containers during above ground storage and cause atmospheric pitting corrosion [1-5]. The effect of microstructure on the morphology of atmospheric corrosion pits in 304L and 316L stainless steel plate was investigated on the three orthogonal planes. The top surface (LT) of the plate shows ring-like structures for 304L but dish like pits for 316L. The plate edges (LS and ST) show a striped morphology for both 304L and 316L stainless steel. In situ X-ray tomography of 304L stainless steel pins shows the presence of similar striped attack. Scanning electron microscopy and etching revealed the presence of parallel bands along the rolling direction. EDX line scans across these bands indicated a local increase in the Cr/Ni ratio consistent with the presence of ferrite. TEM and Vibrating Sample Magnetometer (VSM) analyses were carried out to identify the phases. XRD and EBSD measurements were used to quantify the amount of ferrite. The morphology of atmospheric corrosion pits grown under droplets of $MgCl_2$ was found to be influenced by the presence of ferrite bands and non-metallic inclusions in the microstructure. Figure 1 shows the pit morphologies on the three orthogonal planes of the plate, (a) LT plane with pit showing narrowing ring like morphology, (b) LS plane and (c) ST plane exhibit a striped morphology associated with the rolling direction of the plate. This striped morphology has been attributed to the embedded bands of ferrite aligned to the rolling direction [6].

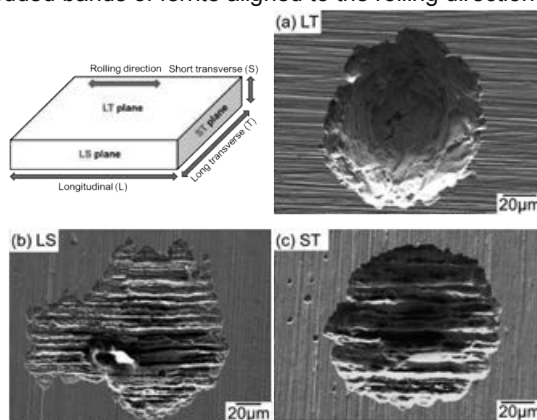


Figure 1 – Pit morphology observed for the three orthogonal planes of 304L plate exposed to a simulated atmosphere of ~35% RH at 30°C for 1 week, under a droplet of $MgCl_2$ solution with initial $[Cl^-]$ deposition density of 1000 $\mu g/cm^2$ (a) LT plane, (b) LS plane and (c) ST plane.

References:

- [1] Y. Tsutsumi, A. Nishikata, and T. Tsuru, Pitting corrosion mechanism of Type 304 stainless steel under a droplet of chloride solutions. *Corrosion Science*, 2007. 49(3): p. 1394.
- [2] B. Maier, and G.S. Frankel, Pitting corrosion of bare stainless steel 304 under chloride solution droplets. *Journal of the Electrochemical Society*, 2010. 157(10): p. C302.
- [3] B. Maier, and G.S. Frankel, Pitting Corrosion of Silica-Coated Type 304 Stainless Steel Under Thin Electrolyte Layers. *Corrosion*, 2011. 67(3): p. 035004-1.
- [4] Y. Wang, W. Wang, Y. Liu, L. Zhong, J. Wang, Study of localized corrosion of 304 stainless steel under chloride solution droplets using the wire beam electrode. *Corrosion Science*, 2011. 53(9): p. 2963.
- [5] S.M. Ghahari, A.J. Davenport, T. Rayment, T. Suter, J.P. Tinnes, C. Padovani, J.A. Hammons, M. Stampanoni, F. Marone, and R. Mokso, In situ synchrotron X-ray micro-tomography study of pitting corrosion in stainless steel, *Corrosion Science* 2011, 53(9): p.2684.
- [6] C.J. Donohoe, G.O.H. Whillock, and P.J. Apps, Localized Corrosion of Stainless Steel in a Nuclear Waste Cooling Water System—Part 2: Plant Inspection Findings. *Corrosion*, 2012. 68(9): pp. 844-852.

Nanostructure and local properties of oxide layers grown in simulated pressurized water reactor environment

*Vincent Maurice, Toni Massoud, Lorena H. Klein, Antoine Seyeux, Philippe Marcus
Institut de Recherche de Chimie Paris, CNRS - Chimie ParisTech (UMR 8247),
Paris, France*

One of the major materials challenge for continued safe, reliable and cost-effective utilisation of water-cooled nuclear reactors for electricity production is to develop the understanding of the fundamental mechanisms responsible for corrosion and stress corrosion cracking degradation of austenitic steels and nickel base alloys. Numerous studies of oxide films formed on these substrates in high temperature water focused on the thickness, composition, morphology and crystallographic structure of the oxide films.

In this work, Atomic Force Microscopy (AFM) and Conductive-AFM (Resiscope) have been applied to study oxide films formed by interaction of 316L stainless steel and Inconel Alloy 690 with simulated PWR primary water at 325 °C. The objective was to characterize the nanometer scale morphology of the oxide films providing corrosion resistance to the substrates and to get new knowledge on the relationship between nanostructure and local properties (i.e. electrical resistance) of oxide films of complex composition, which is a key aspect for local failure of the protection.

The results have been rationalized in terms of local variation of the composition of the duplex passive film and thus local resistivity of the oxide film. On 316L stainless steel, the data show that the oxide films present a nanogranular morphology that becomes increasingly inhomogeneous with oxidation time due to uneven local 3D growth of the outer oxide layer at nanometre scale. Electrical resistance maps measured at the nanoscale for the grain and grain boundaries of the passive films shows that the measured resistance ranges between $\sim 10^8$ and $\sim 10^{11.5}$ Ω at room temperature and the oxide film resistivity ranges between $\sim 10^1$ and $\sim 10^{4.5}$ $\Omega\cdot\text{cm}$. The large majority of the oxide films has local resistance variations spread over ~ 1 order of magnitude with larger variations, reaching 2-3 orders of magnitude, observed locally. These variations are assigned to the composition of the inner layer of the oxide film varying from unmixed Cr(III) (Cr_2O_3) in the zones of higher resistivity to Cr(III) mixed with Fe(II) (FeCr_2O_4) in the zones of lower resistivity. The higher electrical resistance measured at the grain boundaries of the outer layer is assigned to the depletion of the inner layer in Fe(II) and formation of unmixed Cr_2O_3 phase promoted by faster Fe(II) diffusion through the outer layer. Data obtained on the nickel base Alloy 690 will also be discussed.

About point defects formation in Cr_2O_3 passive films

B. Malki^{1,2}, A. Pasturel², B. Baroux²

¹ *Simorg system, 28 rue Jules Guesde 38600 Fontaine, France.*

² *Laboratoire Science et Ingénierie des Matériaux et Procédés (SIMAP), Grenoble INP, CNRS, 38402 Saint Martin d'Hères, France.*

We carry out density functional theory calculations (DFT) to assess the thermodynamics stability of the intrinsic and extrinsic point defects possibly present in a Cr_2O_3 based passive film formed on a stainless steel in aqueous environment. We first focus on the formation energy of native defects (vacancies or interstitials), then of extrinsic ones (hydrogen and chloride interstitials) and finally of some more complex defects such as: $V_{\text{O+Cl}}$, $V_{\text{Cr+H}}$ etc... These defects are considered both in their neutral and charged states. The chemical potentials in the aqueous environment and the Fermi level in the oxide are assumed to be the main controlling variables. All calculations are carried out with the Vienna ab initio simulation package (VASP) using projector augmented wave (PAW) method and supercell technique.

Close to the metal-film interface (reducing conditions) most of the studied defects have formation energies greater than 2 eV whatever the applied potential and are then not stable, (including interstitial chloride). The only stable defects, having small or even negative formation energies, are oxygen vacancy based defects (V_{O} , V_{OH} , $V_{\text{O+Cl}}$ and related charged species) and, to a lesser extent, chromium vacancies, (V_{Cr} , $V_{\text{Cr+H}}$, $V_{\text{Cr+Cl}}$ and related charged species). When the electrode potential is increased, i.e. in more favorable conditions for the localized corrosion, the formation energies of these defects decrease making plausible a passive film breakdown scenario as suggested by the PDM model.

At the film water interface (oxidizing conditions) one observes a positive shift in the formation energies, reflecting the need of a driving force for the vacancies to migrate toward the inner interface, which was not taken into account in this study (no more than the out of equilibrium reactions at the interfaces). It is also worthy to notice the possible role of hydrogen or proton inserted inside the film, since the energy formation of these defects remains small at the two interfaces.

In a second part, of the study we applied the method to the possible incorporation in the film of the alloying elements present in the underlying steel (Fe, Ni, Mo, N, etc...), It was found that in usual conditions Nickel cannot enter the passive film neither in reducing or oxidizing conditions. At the opposite, Fe and Mn can easily pass in chromium oxide and exhibit a rather strong tendency to segregate at the outer interface (oxidizing conditions), other elements, such as Mo and Nb are expected to segregate at the metal film interface and a co-dopage with nitrogen (Mo+N) is shown to reinforce the Mo segregation. All these predictions can be verified experimentally (using for instance XPS analysis), which deeply entrust us in the validity of the model.

Kelvin Probe Force Microscopy and Atmospheric Corrosion of Cold-rolled Grade 2205 Duplex Stainless Steel

C. Örnek & D.L. Engelberg

Corrosion and Protection Centre, University of Manchester, Sackville Street, M13 9PL, UK

Abstract

Modern duplex stainless steel microstructures are optimised for application in critical environment. In order to satisfy the production of low-wall thickness components, strain hardening by cold deformation can be used. The balanced ferrite to austenite ratio of the duplex microstructure provides superior corrosion resistance compared to most common austenitic and ferritic stainless steel grades. However, the effect of cold deformation on the likelihood of duplex stainless steels corrosion and the nucleation of stress corrosion cracking is not fully clear.

In this paper we report the effect of cold-roll deformations of up to 40% reduction on grade 2205 microstructure as a function of process orientations. The deformation heterogeneity and microstructure after cold-rolling in rolling (RD), transverse (TD), and normal (ND) directions has been analysed by electron backscatter diffraction (EBSD). Individual microstructure sites were then investigated using Kelvin Probe Force Microscopy (KPFM) and subsequently targeted with MgCl_2 salt-laden deposits ($100\text{--}1000\text{ }\mu\text{g}/\text{cm}^2$) to test their corrosion performance in controlled atmospheric environment at 50°C and 30% relative humidity.

The ferrite phase was preferentially corroded in the as-received microstructure condition, whilst the austenitic microstructure became more susceptible to localised corrosion under atmospheric exposure with increasing degree of cold deformation. Interestingly, Volta potential differences measured between a Pt-probe and the surface drastically changed with the degree of cold deformation, with significant differences observed in all three process orientations. Volta potential hot-spots determined by KPFM seemed to be influenced by strain hot spots after cold rolling.

Relative Humidity for Onsets of Pitting Corrosion and Repassivation of Stainless Steels under Wet-dry Cyclic Conditions Containing Chloride

*Atsushi Nishikata, Hiroyuki Nakamura, Tran Van Nam, Eiji Tada,
Tokyo Institute of Technology,
2-12-1 Meguro-ku, Ookayama, Tokyo, Japan*

When stainless steel (SS) is exposed to a marine atmospheric environment, airborne sea salts deposits on the surface and absorbs moisture from the air. The concentration of chloride ion in the formed solution film is very high, depending on relative humidity (RH). For instance, in case of NaCl salt deposits, the chloride concentration becomes approximately 5 M at the deliquescent RH (75 %). In case of MgCl_2 salt, chloride concentration rises to about 9.5 M. Even at 95 %RH, the equilibrium chloride concentration is about 2 M [1]. Passive films on stainless steel are exposed to very concentrated chloride solution films in marine atmospheric environments. Accordingly, breakdown and repassivation of the passive films may occur by a daily wet-dry cycle. In this study, RHs for onsets of pitting corrosion and passivation are clarified under wet-dry cyclic conditions.

Two different stainless steels, 304SS and 430SS, were employed as specimen. Eight specimens (6 X 6 mm) were embedded in epoxy resin, together with a silver plate that acted as a reference electrode. The surface was polished to #2000 with SiC paper and ultrasonically cleaned in distilled water. A 1.0 M MgCl_2 solution was placed on the surface and horizontally set in a programmable RH- and temperature-chamber. At 300 K, RH was lowered from 95 % to 45 % (or 60%) and then raised to 95 %. The RH cycle was repeated 7 times. RH was changed at a constant rate of 5 %/h, where the equilibrium between water molecule in solution film and water vapour in the air. The chloride concentration was estimated from the RH [1]. The onsets of pitting corrosion and repassivation were monitored by continuous measurement of corrosion potential E_{corr} with respect to Ag/AgCl electrode embedded.

The E_{corr} rapidly shifted in negative direction at the commencement of pitting corrosion during lowering RH and quickly shifted positively at repassivation during raising RH. The RH for onset of pitting corrosion was determined to be approximately 55 % for 304SS and 65 % for 430SS. From the critical RHs, critical chloride concentration of onset of pitting corrosion is 7.5 M for 304 SS and 6 M for 430SS. On the other hand, RH for repassivation was approximately 70-75 % for 304SS and 85 %RH for 430SS. From the above results, pitting corrosion of 304SS and 430SS can progress below 55 %RH and 65 % RH, respectively. The repassivation can occur above 75 %RH for 304SS and 85 %RH for 430SS.

Reference

[1] Y. Tsutsumi, A. Nishikata, T. Tsuru, *J. Electrochem. Soc.* 152,[9], p.B358-B363(2005).

Electrochemical AFM Study of Corrosion Behavior of a 2507 Super Duplex Stainless Steel: Influence of Precipitated Chromium Nitrides

Eleonora Bettini², Ulf Kivisäkk², Christofer Leygraf¹, Jinshan Pan¹

¹KTH Royal Institute of Technology, School of Chemical Science and Engineering, Division of Surface and Corrosion Science, SE-100 44 Stockholm, Sweden

²Sandvik Materials Technology, SE-811 81 Sandviken, Sweden

Abstract

Precipitation of different types of chromium nitrides may occur during processing of super duplex stainless steels (SDSS), affecting the properties of the material. In this study, by using specially heat treated samples, the influence of quenched-in and isothermal types of nitrides on the corrosion behavior of a 2507 super duplex stainless steel has been investigated, by a combination of microstructure characterization, electrochemical polarization at room temperature and at 90 °C in 1 M NaCl solution, in-situ electrochemical AFM measurements at room temperature and post-analysis of the corroded samples.

The microstructure, including precipitated nitrides, has been characterized by scanning electron microscopy and magnetic force microscopy. The isothermal nitrides particles (ca. 80-230 nm in size) precipitated along the α/γ boundaries, exhibiting higher Volta potential than the ferrite and austenite, while a local Volta potential drop was observed at the α/γ boundaries. The Volta potential difference of the nano-sized quenched-in nitride particles (ca. 50-100 nm in size) finely dispersed in the ferrite could not be resolved by the Volta potential mapping due to their very small size.

In-situ electrochemical AFM measurements of the samples in 1 M NaCl solution at room temperature show stable surfaces for a wide range of applied potentials. The nano-sized quenched-in or isothermal nitrides and a small amount of sigma phase in the 2507 SDSS didn't cause passivity breakdown of the material. During transpassive dissolution at 1.2 $V_{Ag/AgCl}$, the ferrite matrix with quenched-in nitrides dissolved preferentially, and the α/γ boundaries with isothermal nitrides and sigma phase started to corrode. The nano-sized quenched-in nitrides finely dispersed in the ferrite of the 2507 SDSS have little influence on the corrosion resistance. In the transpassive region, isothermal nitrides appear to be slightly more deleterious than quenched-in nitrides.

At 90 °C (above the critical pitting temperature) in 1 M NaCl solution, the isothermal nitrides and a small amount of sigma phase largely reduce the corrosion resistance of the austenite phase. The passivity is lost and fast corrosion of the austenite occurred, probably due to depletion of Cr, N and Mo in the austenite phase caused by precipitation of the isothermal nitrides and sigma phase along the α/γ phase boundaries. In contrast, the finely dispersed quenched-in nitrides reduce the corrosion resistance of the material to a much lesser extent. The results suggest that the isothermal nitrides are more detrimental than the quenched-in nitrides for the corrosion resistance of the 2507 SDSS at elevated exposure temperatures. The different formation mechanisms, sizes and distributions of the quenched-in and isothermal nitrides cause different situations of alloying element depletion, and thus have different effects on the corrosion behavior of the material.

Acknowledgement: AB Sandvik Materials Technology, Sweden, is acknowledged for the financial support of this study.

Influence of heat treatment on corrosion resistance of martensitic stainless steels 1.4034 and 1.4021

P. Rosemann¹, M. Babutzka¹, A. Heyn^{1,2}, T. Halle¹

¹Otto-von-Guericke-University Magdeburg, Institute of Materials and Joining Technology, PF4120, 39016 Magdeburg, Germany

²BAM Federal Institute for Materials Research and Testing, Unter den Eichen 87, 12205 Berlin, Germany

Abstract

In the last years, new approaches for the evaluation of the corrosion resistance of stainless steels were developed which allow short term corrosion testing with increased information content. This work analyses the extensive influence of heat treatment on microstructure and the resulting corrosion resistance of the martensitic stainless steels 1.4034 and 1.4021 with advanced methods. Different heat treatments at various austenitization temperatures up to 1100°C and the effect of different cooling rates were evaluated; the last has not yet been studied in literature at all. The resulting corrosion behaviour in relation to the different carbon content in the two used alloys and the applied heat treatment will be presented and discussed. The applied methods of investigation were conventional evaluation of the critical pitting corrosion potential (PP), modified electrochemical potentiodynamic reactivation (mEPR) and the "KorroPad" (KP) technique. The performance of modified EPR and its interpretation were optimized to provide additional information about the general passivation ability and the extent of chromium depletion as result of applied heat treatment. The aim using PP and KP was the correlation between the parameters of the mEPR with the changes in the pitting corrosion resistance. Furthermore the results will demonstrate the functionality and usability of the short term corrosion test methods mEPR and KP in order to increase their acceptance within the scientific community. The results indicate a surprisingly large influence of both austenitization temperature and cooling rate on the corrosion resistance within all three used test methods, which can explain the different corrosion behaviour of martensitic stainless steels in earlier investigations [1].

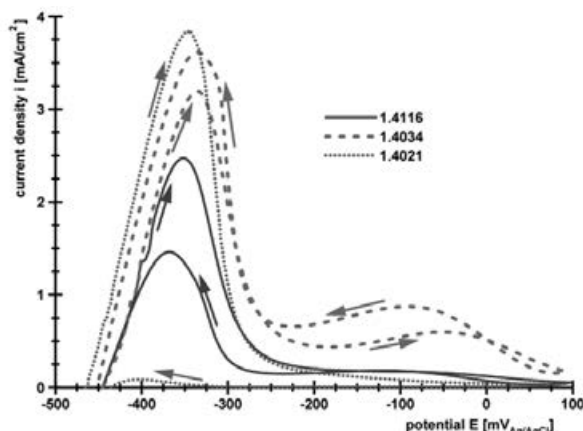


Fig. 1: Modified EPR curves of alloy 1.4116, 1.4021 and 1.4034 stainless knife steels with manufacturers heat treatment in 0.1 M H₂SO₄ according to [1]

[1] Rosemann, P., Müller, Th., Babutzka, M. and Heyn, A. (2013), Materials and Corrosion. doi: 10.1002/maco.201307276

Stress corrosion cracking at room temperature of austenitic stainless steels in marine areas: the case of fixed guards for climbing

F. Deflorian, M. Dalvit, S. Rossi, C. Zanella, M. Fedel, Department of Industrial Engineering, University of Trento, Via Mesiano 77, Trento (Italy)

Abstract

This work studies the particular mechanism of environmental Stress Corrosion Cracking (SCC) that has been described to interest stainless steel products, like climbing anchors, installed in sea areas.

The failure analysis of several broken anchors was carried out. The samples were coming from in service failure and they were collected in different parts of the world, always from climbing structures close to the sea.

The analysis confirmed the stress corrosion mechanism of degradation, giving also important information about the specific environments causing the metal fracture. These results are in agreement with a few previous works about this subject [1], and are in the frame of the larger topic of stress corrosion cracking of austenitic stainless steel at room temperature [2, 3].

Moreover, some corrosion tests were carried out on stainless steel samples simulating the operation conditions. Several U-Bend tests produced from AISI 304L and AISI 3016L steel were exposed to different environments, at different relative humidity, after contamination with electrolytes at different concentration. The tests are performed in order to better understand the degradation mechanism and to evaluate the influence of some environmental parameters over the susceptibility to SCC.

Finally, some electrochemical measurements were carried out in specific solutions in order to compare the electrochemical behaviour of the materials with the corrosion tests results obtained after exposure.

With these experimental data, a possible interpretation model has been proposed together with some reasonable solutions for the material selection process, considering the problem's characteristics and the multiple alternatives available nowadays for climbing materials.

[1] Sjong A.; Eiselstein L. "Marine Atmospheric SCC of Unsensitized Stainless Steel Rock Climbing Protection", *Journal of Failure Analysis and Prevention*, 8(5), (2008) 410–418.

[2] Prosek T.; Iversen A.; Taxen C.; Thierry D. "Low-temperature stress corrosion cracking of stainless steels in the atmosphere in the presence of chloride deposits" *Corrosion*, 65(2) (2009) 105–117.

[3] Shoji S.; Ohnaka N. (1989). *Effects of Relative Humidity and Kinds of Chlorides on Atmospheric Corrosion Cracking of Stainless Steels at Room Temperature*. *Boshoku Gijutsu*, 38, (1989) 92–97.

Passivity and corrosion behavior of duplex stainless steels after various surface preparations

Vincent VIGNAL, ICB, UMR 6303 CNRS-Université de Bourgogne, BP 47870, 21078 Dijon Cedex, France

Halina KRAWIEC, AGH University of science and Technology, Ul. Reymonta 23, 30-059 Krakow, Poland

Sandra LE MANCHET, ArcelorMittal, Global R&D Le Creusot, Industeel, BP 19, 71201 Le Creusot Cedex, France

The influence of different surface preparation methods (mechanical procedure, electropolishing and etching) on the passivity and corrosion behavior of a duplex stainless steel (UNS S32202) was studied using Auger spectroscopy and the electrochemical microcell technique.

Surface analysis showed that the thickness of the passive film was affected by the presence of the cold-worked layer induced by the mechanical procedure (passive film thinner in the presence of a thick cold-worked layer) and by performing etching (passive film thinner than after the mechanical procedure or after electropolishing).

The ratio Cr/Fe in the passive film was strongly affected by the surface preparation. It increased according to the following order: mechanical procedure (values around 0.3), electropolishing (values around 0.5) and etching (values between 0.6 and 0.7). Roughly the same values were found in both phases.

After electropolishing and after etching, nitrogen was detected at the inner interface and a residual quantity of chloride was incorporated in the passive film (outer and inner parts)

Etched samples were found to be more resistant to pitting corrosion than polished ones. The negative influence of the presence of the residual chloride ions in the passive film was then balanced by the positive influence of the high value of Cr/Fe in the passive film. The increase of the corrosion resistance of the etched samples was attributed to the increase of the ratio Cr/Fe in the passive film.

An oxidation peak was observed at the onset of the anodic domain of polarisation curves in the presence of the cold-worked layer (polished samples), corresponding certainly to the preferential dissolution of iron species. In addition, a second oxidation peak related to the transition from Cr^{3+} to CrO_4^{2-} was observed on samples with a high Cr/Fe value (etched samples).

Stable and metastable pitting corrosion susceptibilities from physical properties of passive films.

Benoît Ter-Ovanessian, Bernard Normand

Université de Lyon, INSA-Lyon, MATEIS CNRS UMR5510,

Bât. L. de VINCI, 21, avenue Jean Capelle 69621 Villeurbanne Cedex France

Ni-Cr alloys with high nickel content are widely used in the chemical or nuclear industry due to their good ability to form a passive film in different aqueous environments. The Chromium oxide passive film grown on these alloys is effectively known to provide them excellent corrosion resistance. However, in presence of chloride ions, this passive film may be sensitive to chemically induced breakdown, like pitting corrosion. Pitting corrosion is the deleterious result of the nucleation and the growth of stable pits due to the adsorption of chloride ions at the passive film/electrolyte interface concomitant with local destabilizations of the passive film. As adsorption of chloride ions is the first step of the pitting process, the determination of the key factors governing this phenomenon seems required in order to optimise the pitting corrosion resistance.

In the present work, the passive films grown on pure Ni, pure Cr and different Ni-Cr alloys (with 16, 20, 24 and 28 wt% Cr) have been firstly characterized by electrochemical impedance spectroscopy (EIS) and Mott-Schottky analysis to assess their physical properties according to their chemical composition. Secondly, for all these materials, the pitting corrosion resistance has been investigated by polarisation studies in terms of metastable pitting and stable pitting to apprehend the mechanism and the kinetics of pit initiation.

The main result of this study is that the Nickel content incorporated into the passive film affects, as expected its physicochemical properties, and also the chloride adsorption process. Then, focussing on the oxide electronic properties and the physicochemical characterisation of the passive film/electrolyte interface, the relation between metastable pitting susceptibility, stable pitting occurrence and the passive film properties is also discussed.

Chemical composition and nanostructure of passive films formed on FeCrNiMo austenitic stainless steel

Hao Peng, Vincent Maurice, Lorena H. Klein, Antoine Seyeux, Sandrine Zanna, and Philippe Marcus
Institut de Recherche de Chimie Paris,
CNRS-Chimie ParisTech (UMR 8247), Paris, France

Molybdenum is considered as one of the principal alloying elements in stainless steels and its beneficial effect on corrosion resistance has been most thoroughly investigated. It is well known that Mo enhances the resistance to pitting corrosion. But, controversy also exists when the chemical composition of the passive films is discussed. Moreover, the explanation for the effect of Mo on the corrosion resistance is still a subject of discussion.

In the present work, air-formed native oxide films and anodic passive films formed at +500 mV/SHE in 0.05 M H₂SO₄ (aq) on (100)-oriented Fe-17Cr-14.5Ni-2.3Mo single crystal stainless steel surfaces were investigated.

X-ray Photoelectron Spectroscopy (XPS) and Time-of-Flight Secondary Ion Mass Spectrometry (ToF-SIMS) were combined to investigate the thickness, chemical composition and the composition profiles of air-formed native oxide films and passive films. Anodic passivation results in a thickening of oxide layer and increases the Cr enrichment. Aging from 2h to 20h involves further enrichment in Cr. Ni was not detected in the passive films by XPS, but the first metallic layers underneath the films were found to be enriched in Ni. Mo was enriched in the passive films with respect to the concentration in the alloy and in the native oxide films.

Scanning Tunneling Microscopy (STM) and Scanning Tunneling Spectroscopy (STS) were used to investigate the nanoscale morphology and local electronic properties of air-formed native oxide films and anodic passive films. The results show that anodic polarization in the passive domain does not destroy the typical as-prepared substrate topography but modifies the nanogranular morphology of air-formed native oxide film initially covering the surface. The electronic gap increases in width after anodic polarization in the passive domain. Aging from 2h to 20h does not change significantly the electronic gap of the passive films. Meanwhile, inhomogeneity of electronic properties of the passive films was identified by STS. Supplemental to STM investigations, Atomic Force Microscopy (AFM) was used and allowed to exclude that electronic effects affect the topography measured by STM.

All the results were then compared with those previously obtained on (100)-oriented Fe-18Cr-13Ni single crystal stainless steel surfaces passivated in the same conditions. This allows addressing the effect of the addition of Mo on the corrosion properties.

POLARIZATION BEHAVIOUR OF NEW ALUMINIUM ALLOYS (AA2139 and AA2198) IN NEUTRAL MEDIA

A. Balbo, V. Grassi, A. Frignani, F. Zucchi
Corrosion & Metallurgy Study Centre “A. Daccò”, University of Ferrara
v. Saragat 4a, 44122 Ferrara (I)

ABSTRACT

This research investigates the electrochemical behaviour of recent aluminium alloys (AA2198 and AA2139) in various neutral aerated electrolyte solutions. AA2198 is a Li-containing aluminium alloy, while AA2139 is an age-hardenable quaternary Al-Cu-Mg-Ag alloy.

In electrolyte solutions, both alloys were initially subjected to a fast potential activation for the dissolution of the natural air formed aluminium oxide, followed by a potential ennoblement for the copper enrichment process due to very active element selective de-alloying of intermetallic (IM) precipitates. In this situation Li presence rendered the corrosion potential (E_{CORR}) of AA2198 more negative than that of AA2139. However, after a sufficiently long immersion time, the corrosion process led to a stable passive state, which was hampered by chloride anions. While in various chlorides solutions the cathodic polarization curves of the two alloys were almost the same, AA2139 displayed more negative E_{CORR} values, more elevated anodic and passive currents, more negative E_{BR} values. Such behaviour has been related to the amount of IM precipitates in the two alloys and in the related Cu-depleted zones around these particles.

In the present research the tendency to of both alloys to attain a passive condition is studied by fast and slow potentiodynamic polarization curves recorded in diluted, neutral, aerated sodium sulphate and sodium chloride solutions, implemented by some impedance measurements. In every case, AA2139 showed a lesser tendency than AA2198 to attain a stable passive condition.

Finally, a comparison is made with the behaviour of a common 2xxx aluminium alloy (AA 2024).

Mechanisms of scale dissolution on non alloyed and silicon alloyed steels

A. Alaoui Mouayd^{a,b,c}, E. Sutter^{a,b}, B. Tribollet^{a,b}, A. Koltsov^c,

^aCNRS, UMR 8235, Laboratoire Interfaces et Systèmes Electrochimiques, F-75005 Paris, France,

^bUPMC Univ Paris 06, UMR 8235, LISE, 4 place Jussieu, F-75005 Paris, France

^cArcelorMittal Maizières Research, voie Romaine, F-57280, Maizières-lès-Metz, France

An accurate understanding of the mechanism of pickling and over-pickling of scales on steel is necessary for a good control of the overall process of surface treatment. But such a study in real industrial conditions is difficult to be performed, since the pickling treatments on a mild steel fabrication line is very rapid, usually less than one minute.

To allow measurements at a reasonable time scale, a 1 molar hydrochloric acid solution was used as pickling solution in the present work, and all the experiments were performed at 20°C, assuming that a temperature increase does not modify the mechanisms, but only the rate of the reactions. Model scales were synthesized in a furnace, in order to reproduce the industrial scale composition, i.e. continuous parallel sub-layers deposited on the substrate and made of wüstite (FeO), magnetite (Fe₃O₄) and hematite (Fe₂O₃) in the case of non-alloyed steel. For the silicon-alloyed steel, an additional phase made of fayalite (FeSiO₄) was present at the wüstite/steel interface as grains or continuous layer.

In-situ Inductively Coupled Plasma Optical Emission Spectrometry (ICP-OES) measurements of pickling solutions were performed on scales in a flow-cell and the results were compared to electrochemical dissolution rates determined by potentiodynamic and impedance measurements on similar scales in static solutions, in order to estimate the contribution of the electrochemical mechanism to the overall dissolution reaction.

It appeared that dissolution of hematite is mainly of chemical nature, whereas the dissolution of magnetite and wüstite is both chemical and electrochemical. Initially, chemical dissolution of the scale dominated. The electrochemical reactions included oxidation of magnetite and wüstite and reduction of ferric ions formed by chemical dissolution. After the electrolyte reached the steel substrate, electrochemical dissolution of the iron became the main reaction (over-pickling step).

For silicon-alloyed steels, the insulating fayalite was liberated into the pickling solution after dissolution of the surrounding iron oxide or metal.

Simultaneously with the dissolution rate measurements, Electrochemical Impedance Spectroscopy (EIS) was used to follow the evolution of the scale characteristics at different pickling and over-pickling times. Accordingly, the capacitance of the insulation hematite outer layer was estimated from the measured CPE using a "power law" model, whereas a double layer capacitance was determined using Brug's law, at the conductive magnetite and wüstite. In the latter case, the huge value of the capacitance allowed estimating of the real surface of the porous scale.

Critical aspects of electrochemical noise-based corrosion monitoring

A.M. Homborg¹, T. Tinga², X. Zhang³, E.P.M. van Westing⁴, G.M. Ferrari³, J.H.W. de Wit⁵ and J.M.C. Mol⁵

¹Royal Netherlands Navy, Naval Maintenance and Sustainment Agency, Den Helder, The Netherlands, ²Netherlands Defence Academy, Den Helder, The Netherlands, ³Endures BV, Den Helder, The Netherlands, ⁴Tata Steel Research & Development, Velsen Noord, The Netherlands, ⁵Delft University of Technology, Delft, The Netherlands and Materials innovation institute (M2i), Delft, The Netherlands

The monitoring of corrosion should ideally be performed with a minimum perturbation of the spontaneously occurring processes. For this purpose, electrochemical noise measurements (ENM) are potentially interesting. The present work aims to illustrate the most important issues concerning the use of ENM for the monitoring of (localized) corrosion processes. The appropriateness of ENM for this purpose largely depends on practical data acquisition aspects and proper interpretation of the acquired electrochemical noise (EN) signal. This work provides a brief, yet critical, consideration of some recent developments in the practical configuration of ENM. After the measurement has been performed, a first and important step prior to analysis of the EN signal is definition and removal of the direct current (DC) drift component¹. Finally, the information about the kinetics of the reactions occurring at the electrochemical interface should be extracted from the resulting component of the EN signal. This requires the ability to distinguish between different corrosion characteristics without the need for subjective preliminary limitations or assumptions concerning the nature of the process under investigation, or the precondition of stationarity or linearity. These requirements, together with the ability to provide frequency characteristics of the physico-chemical processes while still maintaining time-resolved information (i.e. analysis in both time and frequency simultaneously), are met by characterization using Hilbert spectra^{2,3,4}. This principle will be shown based on the characterization of microbiologically influenced corrosion on carbon steel.

¹ A.M. Homborg, T. Tinga, X. Zhang, E.P.M. van Westing, P.J. Oonincx, J.H.W. de Wit, J.M.C. Mol, *Electrochim. Acta*, 70 (2012) 199-209

² A.M. Homborg, E.P.M. van Westing, T. Tinga, X. Zhang, P.J. Oonincx, G.M. Ferrari, J.H.W. de Wit, J.M.C. Mol, *Corros. Sci.*, 66 (2013) 97-110

³ A.M. Homborg, T. Tinga, X. Zhang, E.P.M. van Westing, P.J. Oonincx, G.M. Ferrari, J.H.W. de Wit, J.M.C. Mol, *Electrochim. Acta*, 104 (2013) 84-93

⁴ A.M. Homborg, E.P.M. van Westing, T. Tinga, G.M. Ferrari, X. Zhang, J.H.W. de Wit, J.M.C. Mol, *Electrochim. Acta*, 116 (2014) 355-365

A review on electrochemical noise measurement as a tool for evaluation of organic coatings and recent developments

Sina S. Jamali, Douglas J. Mills*

*School of Science and Technology, University of Northampton, St George's Avenue,
Northampton, NN2 6JD, UK.*

Tel 0044 1604 893005/3213

E-mail: douglas.mills@Northampton.ac.uk

Abstract

Electrochemical noise measurement (ENM) in corrosion science is often described as simultaneous measurement of current and potential fluctuations generated by electrochemical corrosion process. ENM is proved to be a non-destructive and effective way of obtaining quantitative and mechanistic information about corrosion behaviour of metal in aqueous media. The method and its capabilities in studying corrosion of an uncoated metal has been emphasised and reviewed in the literature elsewhere [1–3]. However it may have not fully received the attention it deserves as a tool for studying organic coatings.

Despite the usefulness and a long history in corrosion research, ENM was not introduced to the field of organic coatings until 1986. Eden, Hoffman and Skerry, used ENM for the first time to monitor anti-corrosion performance of two identical painted steel during an immersion test. ENM has since found increasing use as an effective way of assessing the protection afforded by organic coatings on metals. It has been shown frequently that the noise resistance conforms with the protection level afforded as measured by other well-established techniques such as EIS [4, 5] and linear polarization resistance (LPR) [6]. Noise resistance has been also used as equal to polarization resistance, both practically [7] and theoretically [8], to calculate the corrosion rate. The usefulness and simplicity of the ENM technique plus the relatively quick measurement and inexpensive instrumentation makes the method potentially ideal for in-situ corrosion assessments.

In this article, applications of electrochemical noise measurement as an assessment tool for organic coatings are reviewed. Also developments made on data processing and alternative set-up for data acquisition are explored. The later includes some of the recent studies on developing effective ways to implement ENM on-site for examining their protective properties.

[1] R.A. Cottis, corrosion, 57 (2001) 265–285.

[2] C. Loto, Int. J. Electrochem. Sci, 7 (2012) 9248–9270.

[3] S. Giriga *et al.*, Corros. Rev., 23 (2005) 107–170.

[4] S.J. Mabbutt *et al.*, Prog. Org. Coat., 59 (2007) 192–196.

[5] Q. Le Thu *et al.*, Prog. Org. Coat., 42 (2001) 179–187.

[6] G. Gusmano *et al.*, in: Corrosion 96, NACE International, Denver, 1996, paper No. 336.

[7] B. Lengyel *et al.*, Prog. Org. Coat., 36 (1999) 11–14.

[8] J.E. Chen *et al.*, Corros. Sci., 37 (1995) 1839–1842.

Study of the relation between microstructure and corrosion properties of polycrystalline copper

Esther Martinez-Lombardia¹, Linsey Lapeire², Vincent Maurice³, Iris De Graeve¹, Lorena Klein³, Philippe Marcus³, Kim Verbeken², Leo Kestens², Herman Terryn¹

¹Vrije Universiteit Brussel. Research Group Electrochemical and Surface Engineering, Pleinlaan 2 B-1050 Brussels, Belgium.

²Ghent University . Department of Materials Science and Engineering, Technologiepark 903 B-9052 Zwijnaarde (Ghent), Belgium.

³CNRS - Chimie ParisTech (UMR 8247). Institut de Recherche de Chimie Paris, 11 rue Pierre et Marie Curie, F-75005 Paris, France

Despite all the efforts to understand the corrosion behaviour of metals, few studies have been done to understand how the microstructure of polycrystalline metals, having certain grain sizes, grain orientations, and grain boundary characteristics, can influence the corrosion resistance. The aim of this work is to better understand the relation between the corrosion behaviour of a metal and its microstructural and crystallographic features. Electrolytic Tough Pitch (ETP) Cu is used as material because of its well-known electrochemistry as compared to other less noble common metals such as Fe, Al and Mg

Amongst other methods, Atomic force microscopy (AFM) [1], Scanning electrochemical microscopy (SECM) [2] and Electrochemical scanning tunneling microscopy (ECSTM)[3] in combination with Electron backscatter diffraction (EBSD) were used. Consequently, correlations between grain orientation and grain boundary characteristics, on the one hand, and the corrosion behavior, on the other hand, could be identified.

We could conclude that not only does the grain orientation itself have an influence on the corrosion behavior but also that the orientations of the neighboring grains seem to play a decisive role on the dissolution rate of the metal [1,2]. Regarding intergranular corrosion, we demonstrate that only coherent twin boundaries seem to be resistant against corrosion, which can be explained by the low energy of this special kind of grain boundary [3-5].

[1] L. Lapeire, E. Martinez-Lombardia, K. Verbeken, I. De Graeve, L.A.I. Kestens, H. Terryn. *Corrosion Science* 67 (2013) 179-183.

[2] E. Martinez-Lombardia, Y. Gonzalez-Garcia, L. Lapeire, I. De Graeve, K. Verbeken, L. Kestens, J.M.C Mol, H. Terryn. *Electrochimica Acta* 116 (2014) 89–96.

[3] E. Martinez-Lombardia, L. Lapeire, V.Maurice, I. De Graeve, K. Verbeken, L.H Klein, L.A.I Kestens, P. Marcus, H. Terryn. *Electrochemistry Communications (in press)*

[4] R. Gaggiano, E. Martinez-Lombardia, I. De Graeve, L. Lapeire, K. Verbeken, L.A.I. Kestens, H. Terryn. *Electrochemistry Communications* 24 (2012) 97-99

[5] L. Lapeire, E. Martinez-Lombardia, K. Verbeken, I. De Graeve, H. Terryn, L. A. I. Kestens. *Journal of Materials Science* (2013) DOI: 10.1007/s10853-013-7939-8.

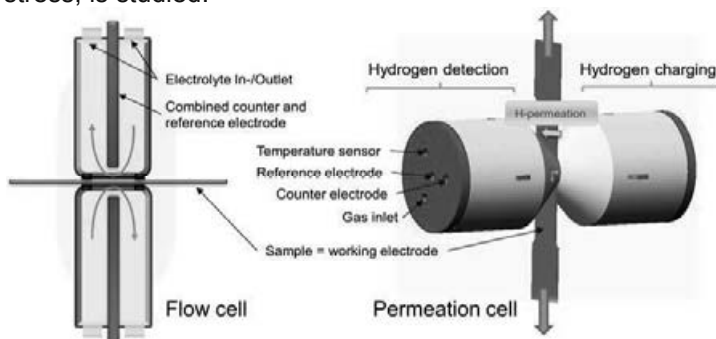
3D printed (flow) cells – A new approach in hydrogen embrittlement studies

G. Schimo^{1,2}, A.W. Hassel^{1,2}

1) Institute for Chemical Technology of Inorganic Materials, Johannes Kepler University Linz, Linz/Austria

2) CEST Competence Centre for Electrochemical Surface Technology, Wiener Neustadt/Austria

The study of hydrogen embrittlement is a constantly growing field in corrosion research, especially because of its importance for the steel industry. Numerous experimental procedures have been developed to study interaction between metals and hydrogen. Especially methods, which combine electrochemical and mechanical techniques, represent an auspicious approach, as they deliver insights not only into the mechanisms of metal-hydrogen interaction, but reveal direct consequences for the material's mechanical properties. 3D printing offers the possibility of producing various cell types for electrochemical experiments in an accurate and rapid manner, which can be designed for a large number of applications. Employing this production method, two types of cells are constructed: One type is characterized by a static electrolyte and is able to investigate sample areas of about 1 cm². The second type is designed as V- or U-type flow cell, through which electrolyte is pumped, offering the possibility of investigating even smaller sample areas without risking a surface blockage by generated gas bubbles. Taking two pieces of each cell and mounting it on both sides of a flat sample allows performing hydrogen permeation measurements. The first cell type resembles and offers the same functionalities as a standard Devanathan-Stachurski cell. Using a flow cell frequently occurring problems, like inadequate agitation of electrolyte and entrapment of gas bubbles, which are often due to the geometry of the cells, can be avoided by the strong convection of electrolyte through the cell. One of the most important advantages of both cell types is that due to their design they can be easily used for conducting permeation measurements or hydrogen charging during a tensile test. Both cell types are tested with and without application of tensile stress to the sample and results are compared. In all experiments, hydrogen charging is done in acidic or alkaline solution by cathodic polarization of the sample. In hydrogen permeation measurements, diffusible hydrogen, which has permeated through the sample, is detected by recording the hydrogen oxidation current under potentiostatic control. From the measured permeation transients, hydrogen diffusion coefficients are determined. Moreover, process of hydrogen entry, transport and trapping, also under applied mechanical stress, is studied.



Corrosion of iron and steel: occurrence of iron(II) hydroxysalts

Céline Rémazeilles, Ilanith Azoulay, Marc Jeannin, René Sabot, Philippe Refait, Laboratoire des Sciences de l'Ingénieur pour l'Environnement (LaSIE), UMR 7356 CNRS-Univ. La Rochelle, Bât. Marie Curie, Av. Michel Crépeau, F-17042 La Rochelle cedex 01, France.

Iron(II) hydroxysalts are mineral phases occurring in anoxic conditions on corroding ferrous metals. Iron(II) hydroxide $\text{Fe}(\text{OH})_2$ is always mentioned as the precursor of iron(III) rust compounds. However, natural environments contain chlorides, carbonates, sulphates, etc., which promote the formation of iron(II) hydroxysalts, instead of $\text{Fe}(\text{OH})_2$, when they are present in significant amounts. The formula of such compounds is $\text{Fe}(\text{OH})_{(2-nx)}\text{A}_x$, where A^{n-} is the anionic specie. Although their existence was theoretically predicted since the 1960's [1], iron(II) hydroxysalts were rarely studied so far. Actually, they were rarely detected in corrosion products layers. The difficulty of identifying such compounds is mainly due to their reactivity towards O_2 . After sampling and/or analysis under air, only their oxidation product can be characterised, although the iron(II) hydroxysalts could have occurred *in situ*.

One of the first studies identifying clearly an iron(II) hydroxysalt as a corrosion product dates from 1976 and deals with an iron(II) hydroxycarbonate ($\text{Fe}_2(\text{OH})_2\text{CO}_3$) [2]. However, iron(II) hydroxysalts became a real research topic only in the early 2000's. During the last decade, a thorough study of these peculiar compounds was launched at the LaSIE laboratory (University of La Rochelle) [3-5]. Because of important technological progresses in micro-analysis and increasing interest in micro-investigations between these two periods, iron(II) hydroxysalts can be more easily detected. They were indeed largely identified on ferrous archaeological objects extracted from seawater and soils and sometimes revealed on contemporary ferrous materials. Studies revealed that an iron(II) hydroxychloride $\beta\text{-Fe}_2(\text{OH})_3\text{Cl}$ occurs in rust layers of objects and structured aged in marine media [6]. Besides, the iron(II) hydroxycarbonate $\text{Fe}_2(\text{OH})_2\text{CO}_3$ (chukanovite) is often detected on ferrous materials extracted from soils [7] or in contact with groundwater and drinking water.

As their presence in corrosion systems is demonstrated, their role in the corrosion mechanisms of iron and steel cannot be neglected anymore. However there is a lack of data about them limiting the efficiency of corrosion modelling. In this presentation we propose to deal with iron(II) hydroxysalts considering their formation mechanisms on ferrous metals, their synthesis in laboratory, their spectral and structural characteristics, their thermodynamic stability and reactivity in natural environments. So far, chukanovite and the hydroxychloride $\beta\text{-Fe}_2(\text{OH})_3\text{Cl}$ were the more studied iron(II) hydroxyl-salts but some recent results about iron(II) hydroxysulfates will be presented.

- [1] W. Stumm, G.F. Lee, Schweizerische Zeitschrift für Hydrology XXII (1960) 95-139.
- [2] E. Erdős, H. Altörfer, Werkstoffe und Korrosion 27, 304-312 (1976).
- [3] C. Rémazeilles, Ph. Refait, Corrosion Science, 50 (2008) 856-864.
- [4] C. Rémazeilles, Ph. Refait, Polyhedron, 28 (2009) 749-756.
- [5] I. Azoulay, C. Rémazeilles, Ph. Refait, Corrosion Science, 58 (2012) 229-236.
- [6] C. Rémazeilles, D. Neff, F. Kergourlay, E. Foy, E. Conforto, E. Guilminot, S. Reguer, Ph. Refait, Ph. Dillmann, Corrosion Science, 51 (2009) 2932-2941.
- [7] M. Saheb, D. Neff, P. Dillmann, H. Matthiesen, E. Foy, J. Nuclear Mat. 379 (2008) 118-123.

Electrochemical characterization of corrosion behaviour of different metals in hot molten salt for solar thermal power plants

Dagmar Rückle, Stefanie Kaesche, MPA University Stuttgart, Germany

Harald Garrecht, IWB University Stuttgart, Germany

Sannakaisa Virtanen, LKO University Erlangen-Nürnberg, Germany

Abstract

Generation of electrical energy from solar radiation represents, especially for regions with a high level of incident solar radiation, an important opportunity for producing environmentally friendly energy. Hot molten salts are by now mainly used as a heat storage medium in solar power plants, but in future they should also act as heat transfer media in piping systems at temperatures up to 600°C. The used molten salt mixtures of alkali metal nitrates and/or alkaline earth metal nitrates represent from a corrosion point of view an electrolyte constituting a corrosion system in combination with metals. But unlike aqueous systems, only little knowledge about corrosion mechanisms in hot molten salts exists.

Within the framework of a research project at the MPA University of Stuttgart basic research work in this, by now, little studied field of corrosion science, was started. A new laboratory suitable for heat exposure tests and electrochemical measurements in molten salts at temperatures up to 600°C was installed. The performed research work aims to identify suitable construction materials with high corrosion resistance and to understand the basic corrosion phenomena.

For electrochemical measurements in hot molten salts it is necessary to assign standard methods to these special conditions. For instance, no standard reference electrode is applicable; hence an appropriate reference electrode needs to be developed. By the performance of electrochemical techniques, i.e. OCP determination and I/E-curves, information about corrosion rates, passivation behaviour, nature of oxide layers, and the solubility of single alloying components will be evaluated. Results gained by these characterization techniques will be presented. One point of major interest is the comparison of corrosion phenomena of samples after long time exposure in the furnaces and such of samples subjected to electrochemical measurements in dependence of the choice of parameters, e.g. exposure time and electrochemical parameters.

First results show severe differences in corrosion resistance and mechanisms for several pre-chosen materials in terms of the constitution and thickness of oxide layers and mass loss. DIN 1.5415 has shown strongly shallow pitting corrosion and a mass loss of 6.7% after 1 week exposure at 560°C in nitrate molten salts, while DIN 1.4301 stainless steel showed intergranular attack and 0.5% mass loss. The stainless steel DIN 1.4404 showed no attack and a minimal mass loss of 0.1%. A variety of further steels will be included in the investigation. First experiments showed a partial solubility of chromium in the melt after exposure at 560°C. This observation was confirmed by SEM- and X-ray analyses of the melt after steel exposure.

Effect of HNO_3 and Cl^- on Corrosion Behaviour of AISI 304 and Cr-Mn Austenitic Stainless Steels

Nilay N. Khobragade, Research Scholar, Department of Metallurgical and Materials Engineering, Visvesvaraya National Institute of Technology, Nagpur, India
Awanikumar P. Patil, Professor, Department of Metallurgical and Materials Engineering, Visvesvaraya National Institute of Technology, Nagpur, India

Abstract

Due to rising cost of Ni, there is interest in low cost Ni-free (Cr-Mn) austenitic stainless steels vis-à-vis AISI 304 (SS304) for a few industrial applications. The present work deals with studying effect of HNO_3/Cl^- ratio on corrosion behaviour of Cr-Mn austenitic stainless steel (Cr-Mn ASS) in comparison with that of SS304. Test methods used were potentiodynamic polarisation (PDP), electrochemical impedance spectroscopy (EIS) and Mott-Schottky analysis. Test solutions were 1000 ppm Cl^- , 0.01M HNO_3 +1000 ppm Cl^- , 0.1M HNO_3 +1000 ppm Cl^- and 1M HNO_3 + 1000 ppm Cl^- . From PDP plots it was found that SS304 exhibited active corrosion in 1000 ppm Cl^- and 0.01M HNO_3 +1000 ppm Cl^- solutions, and passivity in 0.1M HNO_3 +1000 ppm Cl^- and 1M HNO_3 + 1000 ppm Cl^- . Cr-Mn ASS exhibited active corrosion in 1000 ppm Cl^- and passivity in HNO_3 containing test solutions. From EIS results it was found that polarisation resistance (R_p) decreased on addition of HNO_3 for the both the steels. This is attributed to effect of pH on stability of Cr_2O_3 film. The film of Cr_2O_3 is a p-type semiconductor and has vacancies in cation sub-lattice. When Cl^- is incorporated in anion sub-lattice in sets in Schottky pair reaction by which anion vacancies are created. These vacancies allow migration of cations from metal-film interface to film-solution interface and anions in reverse direction by vacancy aided diffusion process. Therefore, the film forming on test alloys were characterised by Mott-Schottky analysis to find out cation and anion defect densities of passivating film in 1000 ppm Cl^- and 0.1M HNO_3 +1000 ppm Cl^- solutions. It was found that density of the cation vacancies in the film forming on SS304 and Cr-Mn ASS in 1000 ppm Cl^- solution was 7.95×10^{20} per cm^3 and 12.6×10^{20} per cm^3 , respectively and increased to 78.1×10^{20} per cm^3 and 87.5×10^{20} per cm^3 on addition of HNO_3 . This explains the role of HNO_3 addition. It was also found that the density of oxygen (anion) vacancies for both the test steels was almost same (approximately 13×10^{20} per cm^3) in 1000 ppm Cl^- solution and increased to 18.2×10^{20} per cm^3 for SS304 and 29.6×10^{20} per cm^3 for Cr-Mn ASS. The rise in defect densities is attributed to drop in pH on addition of HNO_3 .

Grain-dependency of passive oxide film formed on iron in sulphuric acid

Y. Takabatake¹, K. Fushimi², T. Nakanishi², Y. Hasegawa²

¹ *Graduate School of Chemical Sciences and Engineering, Hokkaido University*

² *Faculty of Engineering, Hokkaido University
Sapporo, Japan*

Introduction

The crystallographic orientation of a metal surface has not negligible effects on the corrosion behaviour of metallic materials. Most of metallic materials used in various fields of industry are polycrystalline and non-uniform corrosion occurs on it, reflecting the metal texture of the surface. However, the detailed mechanism of the non-uniform corrosion has been unclear. In order to elucidate how the metal texture affects corrosion reaction, precise analyses on electrochemical behaviours of metals from the view point of the crystallography of the metal surface are necessary. In this paper the authors investigate a grain-dependent passivity of pure iron in sulphuric acid using a micro-capillary-cell (MCC).

Experiments

The metal specimen was an annealed iron plate (purity: 99.99 %). After mechanical polishing and chemical etching, surface orientations of the specimen were identified with electron backscatter diffraction patterning. Single grains with lower Millar indices of $\{0\ 0\ 1\}$, $\{1\ 0\ 1\}$ and $\{1\ 1\ 1\}$ were used for electrochemical measurements with the MCC. After the potentiostatic polarisation of the single grain surface for 3.6 ks, electrochemical impedance spectroscopy (EIS) and galvanostatic polarisation were performed for evaluation of characteristics of the oxide film.

Results and discussion

Initially much the same anodic current flowed on the iron single grains during the potentiostatic polarisation. However, current-time transients showed different behaviours after 500 s depending on the orientation. The value of j_f the current density at 3.6 ks became larger in the order of $\{0\ 0\ 1\} > \{1\ 1\ 1\} > \{1\ 0\ 1\}$. Moreover, EIS measurements revealed that R_{ct} the charge transfer resistance of the oxide film depended on the orientation in the order of $\{1\ 0\ 1\} > \{1\ 1\ 1\} > \{0\ 0\ 1\}$. These results indicate that an oxide film forms on the $\{1\ 0\ 1\}$ grain is the most protective among the three single grains. On the other hand, the charge density consumed by the reduction of the passive oxide film under the galvanostatic polarisation increased in the reverse order of R_{ct} . It represents that the substrate orientation affects not only thickness but also structure and/or composition of the oxide film. Our results of micro-electrochemical measurements on the iron single grains suggest that the dissolution rate of substrate iron and/or the formation rate of oxide film depend on the crystallographic orientation. Therefore, grain-dependency was observed in the structure of the passive oxide film.

Predictive modelling of the corrosion rate of carbon steel focusing on the effect of the precipitation of corrosion products

A.Marion, B.Vuillemin, R.Oltra, D.Crusset *

Laboratoire ICB, Equipe EIC UMR 6303 CNRS – Université de Bourgogne, Dijon , France

** ANDRA, Direction de la Recherche et Développement, Châtenay-Malabry France*

It can be reasonably expected that C-steels selected by ANDRA for nuclear waste storage in a deep geological repository would be mainly affected by general aqueous corrosion. Until now, only short-term and interrupted tests (less than few years) have been performed to validate the average corrosion rates deduced from the study of archaeological analogues. Consequently there is a strong need to develop long term simulation to estimate the corrosion rate evolution, and then the thickness of the containers intended to maintain the confinement of nuclear wastes for several centuries.

The aim of the presented work was to demonstrate that it is possible to design numerical modelling at the engineering scale using the finite element method solving the Nernst-Planck equation in free potential conditions.

The basic electrochemical model was defined from parametric studies to check the influence of electrochemical kinetic constants, the values of the kinetic constants dealing with chemical reactions, the effect of temperature. The input data for the boundary conditions, more especially the electrochemical reaction rate laws, have been selected comparing results from a laboratory experiment with the outputs of the numerical calculations.

Following this approach a long term prediction 1D reactive-transport model was defined considering some realistic changes occurring in the electrolyte, i.e. the deaeration and the precipitation of the corrosion products. This latter was implemented into the numerical calculation by varying the porosity of the electrolytic medium.

The robustness of the model-based simulations was evaluated by comparing the calculated corrosion rate to an experimental one obtained for a short term underground experiment (3 years). The advantage of the numerical simulation is to focus on the transition between the different corrosion regimes and to demonstrate that the corrosion rate is controlled by the fractional coverage of the surface due to the precipitation of the selected corrosion products (magnetite, siderite). It confirms that at long term, the decrease of the total porosity can be identified as a key parameter in the reduction of the corrosion rate.

Acknowledgements: the authors would like to thank the ANDRA consultants, J-M Gras and P. Combrade, for fruitful discussions.

Development of a Liquid-phase Sulfide Ion Gun for Localized Sulfidation of Metal Surfaces

J.-S. Lee, K. Fushimi**, T. Nakanishi**, Y. Hasegawa***

**Graduate School of Chemical Sciences and Engineering, Hokkaido University,
Sapporo, Japan*

***Faculty of Engineering, Hokkaido University, Sapporo, Japan*

The sulfidation reactions on the surface of iron and iron-based materials are of particular interests of practical application such as sulfide-induced corrosion reaction in crude oil and gas wells (the sour environment) [1] and fundamental researches such as precursor reactions of localized corrosion initiated from metal sulfide inclusions [2,3]. However, it is very dangerous to utilize various electrochemical experiments in sulfide ion-containing environments, because sulfide ions can release very toxic hydrogen sulfide gas. It is necessary to establish safe experimental systems for handling the risk factors that should be limited to release the small amount of sulfide ions. Liquid-phase ion gun (LPIG) is a powerful tool for controlling very small amount of aggressive anions from a microelectrode [4]. In this study, the localized sulfidation reaction on copper and iron surfaces was carried out using a safe liquid-phase sulfide ion gun.

A silver wire with a diameter of several hundreds micrometers was embedded in a glass capillary with an epoxy resin for preparation of the microelectrode. Cyclic voltammetry of the microelectrode was carried out in $0.1 \text{ mol dm}^{-3} \text{ Na}_2\text{S}$ solution in the three-electrodes electrochemical cell with a platinum counter electrode and a reference electrode (Ag/AgCl/sat. KCl; SSE). After the microelectrode was polarized at -0.6 V (SSE) in $0.1 \text{ mol dm}^{-3} \text{ Na}_2\text{S}$ solution for 1.8 ks, the microelectrode was positioned in the vicinity of a copper or iron plate in $0.05 \text{ mol dm}^{-3} \text{ Na}_2\text{SO}_4$ solution and polarized at -1.0 V (SSE).

In the CV of silver microelectrode in Na_2S solution, the anodic and the cathodic current peaks were observed at about -0.6 and -1.0 V (SSE), respectively. The electric charges consumed in these peaks were almost same. They correspond to the formation and reduction of silver sulfide, respectively. It means that the cathodic polarization of the sulfide microelectrode at potentials lower than -0.8 V (SSE) can be used as a liquid-phase sulfide ion gun, that is LPSIG to generate sulfide ions. It was also confirmed since the application of LPSIG to copper plate was successfully induced to form sulfidated-copper locally on the plate.

References

1. T. A Ramanarayanan, S. N Smith, *Corrosion*, 46 (1990) 66.
2. S. E. Lott, R. C. Alkire, *J. Electrochem. Soc.*, 136 (1989) 973.
3. T. Suter, H. Böhn, *Electrochim. Acta*, 47 (2001) 191.
4. K. Fushimi, K. Azumi, M. Seo, *J. Electrochem. Soc.*, 147 (2000) 552.

Development of a sensor for interfacial pH measurements during pitting corrosion in situ observed by temporal series of micrographs

Alexsandro Mendes Zimer*, Marina Medina da Silva, Lucia Helena Mascaro, Ernesto Chaves Pereira. *Federal University of São Carlos (UFSCar), São Carlos – SP/Brazil. *amzimer@gmail.com*

Abstract

The pitting corrosion is one of the most dangerous forms of corrosion and its mechanism is not yet fully understood. The existence of stable pits when the pitting corrosion occurs in dissolved CO_2 environments can be attributed to precipitation of FeCO_3 which precipitates inside the pits and induces the acidification of the electrolyte. Consequently, Cl^- ions tend to accumulate at the interfacial pit boundary to counterbalance the H^+ produced during the formation of siderite film and, as a consequence, pits grow on the metal surface. Therefore, changes in interfacial pH are directly related to the processes of nucleation, growth, passivation and stabilization of pit. In this context, this work presents the development of a ring-shaped sensor built around a steel sample to determine the interfacial pH changes during the pitting corrosion. The AISI 1020 steel is the constituent material of the disc, in the center of the electrode, surrounded by a ring of IrO_2 , a sensitive material to pH variations. The Pechini method was employed to generate the ring on a glass tube (the phase separator between the ring and the disc). A disc area of $680 \mu\text{m} \times 544 \mu\text{m}$ (steel sample) was observed in situ by temporal series of micrographs (TSM) [1] with an optical microscope. At the same time, the sensor detected the interfacial pH changes during the initiation of pitting corrosion, its evolution and during the pit passivation. The study of pitting corrosion of carbon steel was performed in $0.1 \text{ mol dm}^{-3} \text{ Na}_2\text{HCO}_3$ (pH 8.3) with Cl^- ions during the open circuit potential (OCP), polarization curves (PC) and chronoamperometric measurements (CA). The TSM obtained was quantified using the ImageJ software. Gathering the ring potential (E_{ring}) of IrO_2 , interfacial pH changes were observed at the initiation and growth of pits. Fig.1a shows the PC performed with a sweep rate of 0.5 mV s^{-1} and a ΔE of 0.5 V in order to demonstrate such results. The surface passivation can be observed at the start of CP (see "1" and "2", Fig.1a). The beginning of the passivity breakdown occurred after 400 s with the nucleation of several pits over the metal surface, Fig 1c. A small variation in the E_{ring} is observed in Fig. 1b ("2" and "3"). During the onset in current density ("3", "4" and "5", Fig.1a) a stable pit grow on the surface (see micrographs from insets "4" and "5"). At this time, the greatest variation in E_{ring} ("3" to "5", Fig.1b) was recorded due to the anolyte which is released from the observed pit and from the unobserved ones on the metal surface during the anodic polarization.

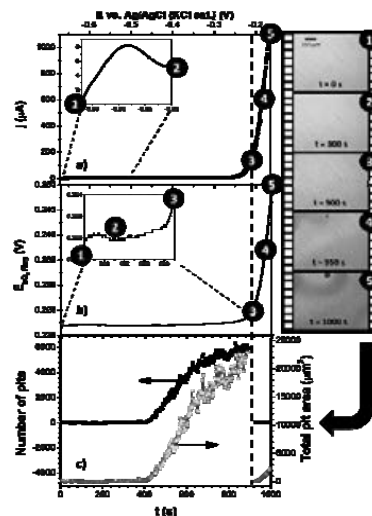


Fig. 1 – PC (a), ring potential of IrO_2 vs. time (b) and, number of pits vs. time (c). In situ micrographs (insets).

References

- [1] A.M. Zimer, M.A. Carra, L.H. Mascaro, E.C. Pereira, *Electrochem. Acta* (2013) (accepted).

Markov chain model to predict localised corrosion of stainless steels

A. Brenna, M. Ormellese, L. Lazzari

Politecnico di Milano, Dipartimento di Chimica, Materiali e Ingegneria Chimica "Giulio Natta", Milan, Italy

Abstract

Pitting, crevice and stress corrosion cracking are the most damaging corrosion forms of stainless steels in industrial applications. Pitting and crevice are unpredictable regarding the initiation time and the corrosion propagation, which occurs unfortunately with high corrosion rate due to the unfavourable cathodic-to-anodic surface ratio.

Generally, pitting and crevice susceptibility depends on a variety of factors related to the metal (chemical composition, differences in the metallurgical structure, inclusions), the environment (chloride content, pH, temperature, differential aeration) and the geometry of the system. Due to their unpredictable occurrence, localized corrosion events cannot be explained without using a proper statistical method.

In this work, a probabilistic approach based on Markov chains for the assessment of pitting and crevice corrosion initiation is proposed.

Formally, a Markov chain is a stochastic process characterized by a set of states and a transition probability matrix, which defines the probabilities to evolve from one state to another through a finite number of possible states, until a so-called "absorbing state" from which the system has no tendency to evolve is attained. Pitting and crevice corrosion may be represented as a Markov process with two absorbing states: pitting, characterized by the formation of corrosion attacks, and the passive state with negligible corrosion rate. A Markovian process is a "without memory process": the state of the system at fixed time depends only on the state immediately before and not on the sequence of events preceding it. In other words, the chain has no memory of the past.

The model presented in this work calculates the occurrence of pitting corrosion of stainless steel involving a large number of operating parameters related to both metal and environment. Experimental tests were carried out to validate the model, which requires more accurate investigations.

Keywords: stainless steel, pitting, localized corrosion, probabilistic model, Markov chain.

Mechanistic Study of Degradation of Coil Coated Steel

Y. Liu¹, X. Zhou¹, G.E. Thompson¹, S.B. Lyon¹, T. Hashimoto¹, G. Smith², S. Gibbon², D. Francis², A. Gholinia¹, X. Zhong¹

- 1. Corrosion and Protection Centre, School of Materials, The University of Manchester, Manchester M13 9PL, England, UK.*
- 2. AkzoNobel, Stoneygate Lane, Felling, Gateshead, NE10 0JY*

Zinc and zinc-containing alloys are used widely to protect steel from corrosion in the automotive and building industries. The zinc coated steel materials, which are often supplied with organic primers on the back face and organic primers with top coatings on the front face, also termed coil coated steel. The organic primers contain corrosion inhibitive pigments, barrier fillers, colour reflective pigment and a pH buffer. The commonly used zinc alloys include Galfan and Galvalume, with 5wt.% and 55 wt.% aluminium respectively. The microstructure of the Galfan coating is generally characterized by a two-phase structure, comprising a zinc-rich proeutectoid phase (<5 wt.% Al/(Al + Zn)) surrounded by a eutectic phase (5–10 wt.% Al/(Al + Zn)) consisting of beta (β) aluminium (5–25 wt.% Al) and eta (η) zinc lamellas (<5 wt.% Al) [2,3]. Conversely, the microstructure of galvalume contains beta (β) aluminum dendrites, Zn-rich interdendritic regions and a fine dispersion of Si particles. The aluminium dendrites contain approximately 18 wt% Zn and up to 1.8 wt% Si.

In the present study, the degradation of coil coated steel with Galfan and Galvalume in sodium chloride solution has been investigated using a combination of electrochemical and electron optical approaches. Scanning and transmission electron microscopies and 3D electron images (Figure 1) were employed to visualise the progression of damage within the organic coating, metallic coating and the steel substrate. These various observations and analyses have assisted in a fully mechanistic study of the degradation process of the coil coated steel systems. A degradation model is proposed from the results of the investigation.

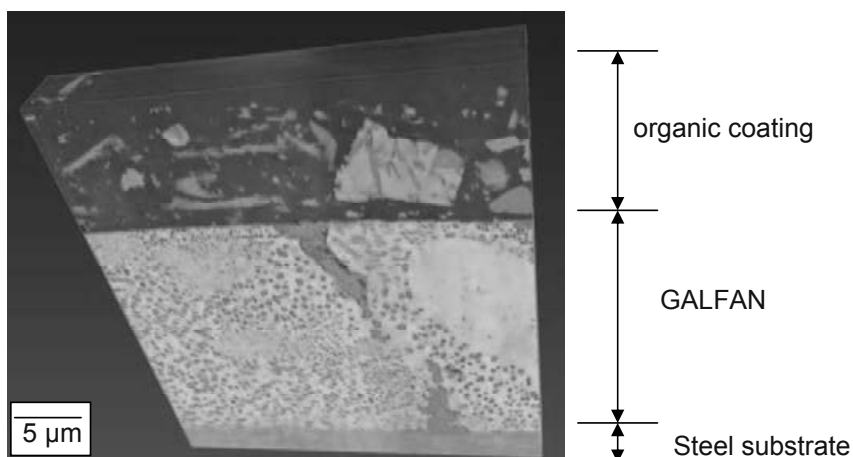


Figure 1: a 3D electron image of coil coated steel after corrosion test

Finely distributed anodic and cathodic centers underneath organic coatings – characterization and effects on the delamination mechanism

Markus Pichler¹, Martin Fleischanderl², Michael Wolpers³, Günter Faflek^{1,4}

¹*CEST Competence Center for Electrochemical Surface Technology GmbH, Viktor-Kaplan-Strasse 2 2700 Wr. Neustadt, Austria*

²*voestalpine Stahl GmbH, Research & Development, voestalpine-Strasse 3
4021 Linz, Austria*

³*Henkel AG & Co KGaA, Henkelstrasse 67 40589 Düsseldorf, Germany*

⁴*Vienna University of Technology, Institute of Chemical Technologies and Analytics,
Getreidemarkt 9/164EC 1060 Vienna, Austria*

Increasing demand for longevity of steel parts in various industries calls for ongoing enhancements in corrosion protection systems. Well established strategies are of course galvanizing and subsequent organic coating of the metal surface. The metal-polymer interface is in most cases additionally stabilized by pretreatments, which form a conversion layer on a nanometer scale that hampers delamination processes in case of physical damages to the organic coating.

This work focuses on the mechanisms behind polymer delamination processes at the polymer-metal interface and suggests that in fact a controlled distribution of anodic and cathodic centers can stabilize the interface. While well-established pretreatment systems mostly take influence on the cathodic reaction (that means suppression of the oxygen reduction reaction), the delamination rate can be additionally lowered by finely distributed cathodic centers which stabilize a pH-value corresponding to a low corrosion rate. The most straightforward approach is the precipitation of iron at the galvanized surface prior to organic coating. The precipitated iron significantly reduces overvoltage of the hydrogen evolution reaction (HER), and therefore promotes an additional counter reaction to zinc oxidation, which furthermore increases the pH-value at the delamination front (what in return lowers the zinc oxidation rate).

Besides iron other metals are taken into account for these mechanistic considerations. The effect of different pretreatments on the interface are studied with several electrochemical methods (e.g. cyclic voltammetry) and polymer delamination processes are furthermore studied with a Scanning Kelvin Probe. Furthermore, results of industrially established corrosion tests for selected sample systems are taken into account.

Mechanism of corrosion protection of zinc-magnesium coatings on steel studied by electrochemical depth profiling

J. Rodriguez¹, M. Mouanga¹, A. Lanzutti², F. Andreatta², L. Fedrizzi², M.-G. Olivier¹

*¹ University of Mons - UMONS, Faculty of Engineering Materials Science
Department, Place du Parc, 20 - 7000 Mons, Belgium*

*² University of Udine, Department of Chemistry Physics and Environment, Via del
Cotonificio, 108-33100 Udine, Italy*

In automotive industry, zinc coated steel is largely used thanks to its high corrosion resistance and sacrificial protection. However, zinc layer must be thick to assure a good protection. As a consequence, consumption of zinc is very intensive and coating prices are increasing. A large number of new coated steel formulations have consequently been studied for many years in order to reduce the consumption of zinc and its cost in coatings. Several studies have shown that the addition of magnesium into the metallic coating allows to improve corrosion resistance without increasing coating thickness.

The mechanism of corrosion protection is based on a coupling galvanic protection between magnesium which is less noble than zinc, which is itself less noble than iron. Nevertheless, protection mechanism understanding is not entirely complete. The aim of this work is to understand if each layer of the metallic coating is able to cathodically protect the underlying layer. Thus, the electrochemical behavior of zinc-magnesium coating on steel as a function of the in-depth structure and composition was studied. To achieve this objective, progressive glow discharge optical emission spectroscopy (GDOES) sputtering was used to create craters reaching the different sublayers. The microstructure of each layer was analysed using the scanning electron microscopy in combination with energy dispersive X-ray spectroscopy (SEM/EDX). The electrochemical analyses were carried out in NaCl 0.02 M using a micro-capillary three-electrode microcell and the scanning vibrating electrode technique (SVET).

Anodic and cathodic polarization curves at different depths using microcell allow to understand the corrosion behaviour of each layer. SVET measurements were carried out in order to understand the formation of galvanic coupling between each sublayer of the zinc-magnesium coating.

A novel method to study corrosion resistance of galvanised steel against corrosive dropping electrolytes

S. Ziebermayr¹, M. Fleischanderl¹, G. Haslehner¹, K.H. Stellnberger¹, A.W. Hassel²

¹*voestalpine Stahl GmbH, Research & Development, voestalpine-Strasse 3
4021 Linz, Austria*

²*Johannes-Kepler University, Institute for Chemical Technology of Inorganic
Materials, Altenberger Straße 69, 4040 Linz, Austria*

Hot-dip galvanised steel is widely used for automotive purposes and also for steel carrier constructions to carry e.g. photovoltaic modules. Because of its outdoor use galvanised steel can be exposed to particular corrosive stress resulting from rain or condensed water which aggregates on the modules and drops on one specific spot of the carrier construction. Compared to atmospheric corrosion, experience has shown that the effects of corrosion occur in a much shorter period of time.

The aim of our work was to simulate this corrosive stress in the laboratory and therefore a dropping-device was developed and conditions for a standardised test method were specified.

This device provides the possibility to vary parameters such as the dropping velocity, the droplet size, the drop height, as also the angle between steel and drops. To measure their influence on corrosion, the loss of mass was found to be a suitable determinant. The removal was done in accordance to ISO 8407 (Table A.1 – C.9.1). The study showed that the removal has to be done twice, immediately after the test and no signs of red rust should be traceable. The latter was assessed by scanning electron microscopy of prepared cross-sections.

With the aid of our device we were able to undergo various tests where the influence of preventative oil, cyclic corrosive stress and selected beforehand mentioned parameters on mass loss could be measured.

A study under standardised conditions showed differences between several metallic corrosion protection layers. It could be demonstrated, that a higher content of Al leads to a lower loss of mass.

Nanoscopic view on the initial stages of corrosion of hot dip galvanized Zn-Mg-Al coatings

J. Duchoslav¹, M. Arndt¹, T. Keppert², G. Luckeneder², K. H. Stellnberger², J. Hagler²,
C. K. Riener², G. Angeli², D. Stifter¹

¹Christian Doppler Laboratory for Microscopic and Spectroscopic Material Characterization, Center for Surface and Nanoanalytics, Johannes Kepler University Linz, Altenberger Straße 69, 4040 Linz, Austria

²voestalpine Stahl GmbH, voestalpine-Straße 3, 4031 Linz, Austria

The onset and very early progress of the atmospheric corrosion of ternary alloyed Zn-Mg-Al coatings induced by a chlorine rich environment was studied in detail by means of surface sensitive techniques, X-ray photoelectron spectroscopy (XPS) and Auger electron spectroscopy (AES). The experimental strategy – performing the analysis prior and after the corrosion treatment exactly in the same positions/regions on the sample – allowed a direct comparison of the appearance, structure and elemental composition of appearing corrosion features. The obtained experimental results lead, at first, to a clear identification of processes associated with a chemically and electrochemically preferential dissolution of the surface constituents, as well as helped to track anodic and cathodic surface activities, as depicted in Fig. 1. Furthermore, the observed processes were correlated to the phase microstructure of the coatings and lead to a model and probable explanation of the observed initial corrosion stages on Zn-Mg-Al coatings.

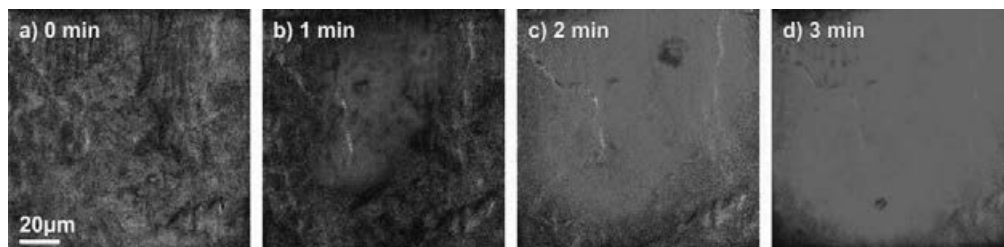


Figure 1. AES elemental mappings (Zn: red, Mg: green, Al: blue) illustrating the formation and growth anodic cracks/holes surrounded by an expanding circular spot of zinc corrosion products at cathodic regions as a function of corrosion time.

The Effects of Oxygen Concentration and pH on the Galvanic Protection of Tin

S. Geary, H. N. McMurray, A. C. A. de Vooys, N. Wint

Sustainable Product Engineering Centre for Innovative Functional Industrial Coatings (SPECIFIC)

Baglan Bay Innovation Centre, Central Avenue, Baglan Energy Park, Baglan, Port Talbot, SA12 7AX. United Kingdom

SVET is used to investigate rapid detinning processes affecting commercial tinplate (produced by TATA steel) in the malic acid solutions, commonly found in tinned food products. In malic acid concentrations $\geq 0.1 \text{ mol dm}^{-3}$ tin was found to become sacrificial with respect to iron, reversing the polarity predictions on the basis of tabulated E_o values. The tin dissolution mechanism in aerated solutions is shown to be cathodically controlled by the mass transport of oxygen to the exposed steel cathode. The sweeping removal of the tin coating is represented in Figure 1 which shows SVET-derived current density maps, the localised anodic dissolution of tin intensifies with an increasing cathodic steel surface area supporting the oxygen reduction reaction.

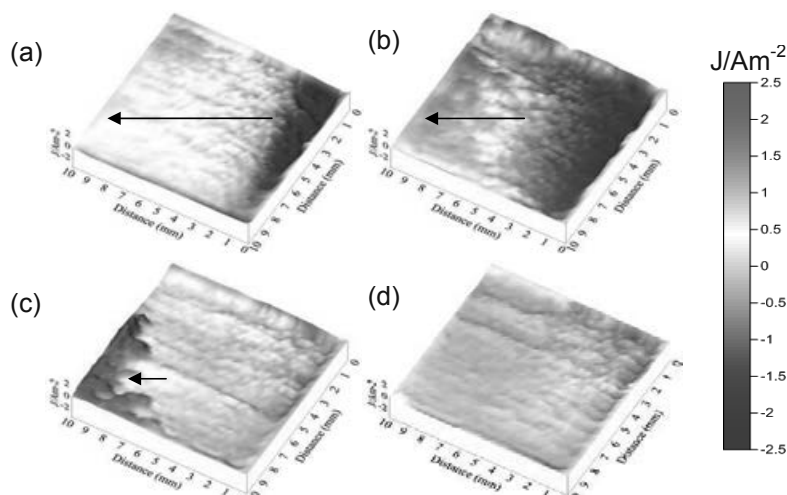


Figure 1. 3D SVET-derived maps showing the distribution of normal current density J above a detinning 2.5 gm^{-2} non-reflowed tinplate sample in 0.1 mol dm^{-3} malic acid at (a) 3 hours, (b) 3.9 hours and (c) 4.8 hours and (d) 5.1 hours of immersion.

Particular emphasis is given to the effects in low partial pressures of oxygen replicating the conditions occurring inside a food can. A novel, Environmentally controlled Scanning Vibrating Electrode Technique (E-SVET) is described which allows the measurement of localised corrosion current flux under conditions of controlled oxygen partial pressure. Experiments undertaken using the E-SVET show that reducing the oxygen partial pressure significantly reduces the detinning rate due to the limited oxygen supply for the cathodic oxygen reduction reaction. Polarity reversal and oxygen reduction kinetics are confirmed using global electrochemical techniques such as RDE and OCP.

Investigation of passive layers on SiC-based ceramics by Electrochemical Impedance Spectroscopy

M. Schneider, K. Kremmer, K. Sempf, M. Herrmann

Fraunhofer Institute for Ceramic Technologies and Systems Dresden, FRG

Depending on their chemical composition and resistivity, SiC-based ceramics can undergo electrochemical corrosion. However, the formation of a passive layer on the surface limits the corrosion rate as a rule in acidic and neutral electrolytes. The properties and the behaviour of the passive layers are again depending on the chemical composition and the microstructure of the materials. The electrochemical impedance spectroscopy (EIS) is a useful and well-established tool to characterize passive layers under corrosion conditions [1].

The authors investigate the properties and the electrochemical behaviour of passive layers formed on various SiC-based ceramics in sulphuric acid (pH 0.5) and a borate buffered solution (pH 5.9). The investigation mainly bases on EIS at open circuit potential. On selected samples additionally, the EIS is carried out at different polarization potentials. Since the relative high resistivity of all used SiC-based ceramics in comparison with metals, the impedance of the working electrode cannot be neglected. According to the circumstances, the solid-state impedance dominates the impedance spectra. This fact is a challenge in view of the measurement procedure and, moreover, the reasonable interpretation of spectra. The authors discuss the problems based on different equivalent circuits.

The passive layers by itself particularly consist of silicon dioxide. However, the results also show different passive layer thicknesses and properties due to the different composition and microstructure of the used ceramic materials.

The electrochemical measurements are completed by material analytic investigations especially SEM/EDX. The results verify the electrochemical investigations and allow a clear correlation between the microstructure of the ceramic materials and their electrochemical behaviour.

- [1] J.R. Macdonald (Ed.): *Impedance Spectroscopy*, John Wiley & Sons 1987;

Corrosion features of the PEO-coated magnesium alloys

A.S. Gnedenkov^{1,2}, S.L. Sinebryukhov¹, D.V. Mashtalyar^{1,2}, S.V. Gnedenkov^{1,2}

¹*Institute of Chemistry, pr. 100-letiya Vladivostoka 159, Vladivostok 690022, Russia*

²*Far Eastern Federal University, 8 Sukhanova St., Vladivostok, 690950, Russia*

The influence of the protective properties of the various composite coatings on the corrosion activity of magnesium alloys in the chloride-containing media was investigated by several independent methods.

The perspective application of the corrosion inhibitor embedded in the porous part of the coatings formed by the plasma electrolytic oxidation (PEO) method has been established in the present work. The results show a considerable decreasing of the corrosion rate values and the electrochemical properties improvement of the magnesium alloy with PEO-coating after inhibitor treatment of the surface in comparison with base PEO-coating in the corrosion-active media.

Influence of the corrosion inhibitor (8-Hydroxyquinoline) on the magnesium alloys corrosion rate were estimated by modern electrochemical methods in combine with volumetry. Special treatment of the PEO-coated magnesium alloys by inhibitor decreased the corrosion rate values in 10 times, the current density values were decreased by more than 3 orders of magnitude in comparison with bare alloy.

The difference in the corrosion mechanisms of the MA8 (Mg–Mn–Ce) alloy as compared to that of VMD10 (Mg–Zn–Zr–Y) magnesium alloy has been established. The stages and the kinetics of the magnesium alloy corrosion process have been also revealed and demonstrated using the scanning vibrating electrode technique (SVET) as well as the conventional methods of optical microscopy, gravimetry, and volumetry.

It has been established that the crucial factor of the corrosion activity of the samples under study consists in the occurrence of microgalvanic couples at the sample surface. The MA8 alloy contains lower amounts of the secondary phases in comparison with VMD10 that results in rapid dissolution of the VMD10 alloy in contrast to MA8 alloy.

The corrosion rate of the samples with PEO-coatings and composite polymer-containing coatings at the surface of various magnesium alloys has been investigated. The corrosion rate significantly decreased upon filling of pores by the inert compound – superdispersed polytetrafluoroethylene. Upon filling the PEO-coating pores by SPTFE followed by special heat treatment, no hydrogen in chloride-containing media was released at all. The corrosion rate (P_H) values for both types of the magnesium alloys (MA8 and VMD10) were about 0 mm per year after exposure of the samples to the 3% NaCl solution for 7 days [1].

This work was supported by the Russian Federation Government (Grant #02.G25.31.0035), Scientific Fund FEFU (#12-03-13001-07).

References

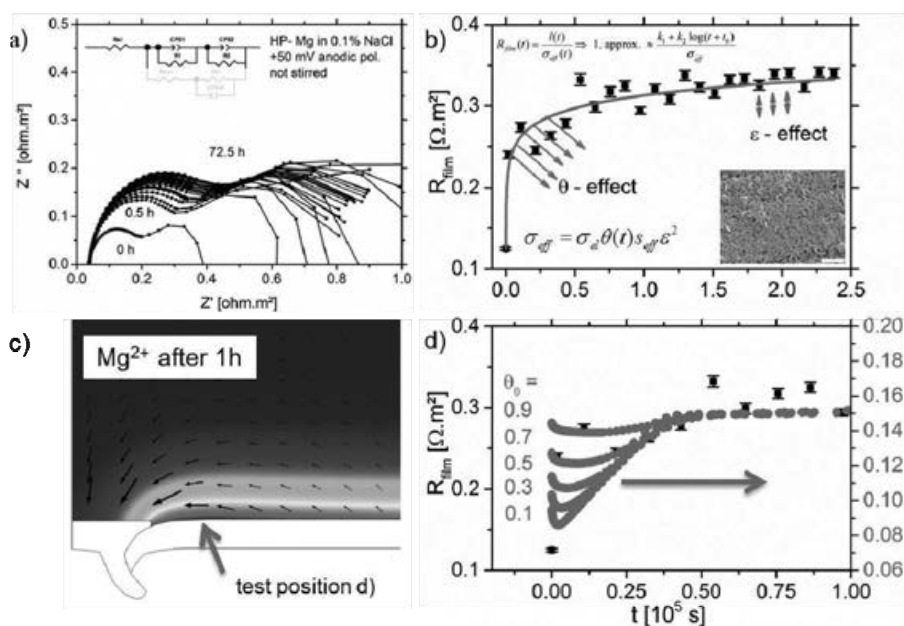
- [1] Gnedenkov, A.S.; Sinebryukhov, S.L.; Mashtalyar, D.V.; Gnedenkov, S.V. *Surf. Coat. Technol.* **2013**, *225*, 112-118.

Corrosion layer growth on Magnesium galvanic coupled to Aluminium simulated by FEM

Dr. Daniel Höche, Helmholtz-Zentrum Geesthacht, Germany

Galvanic corrosion of magnesium alloy based components coupled to more noble materials is a known problem. This work presents a simulation based study for predicting corrosion of pure magnesium galvanic coupled to aluminium including corrosion layer formation due to $\text{Mg}(\text{OH})_2$ precipitation. It includes studies on the involved mechanisms and discusses aspects like the porosity, the surface coverage by reaction products and the time dependent varying electrochemical electrode response.

The analysis via computer offers the possibility to study the corrosion performance and can be utilized for virtual studies of various process parameters. At the end future requests and challenges on modelling corrosion will be listed.



a) Nyquist plot of HP-Mg in unstirred 0.1% NaCl solution at +50 mV constant anodic polarization for 3 days. b) Film resistance measured at the shown surface and its fit (line) according to the standard layer growth model. c) Simulated Mg^{2+} ion distribution after 1 h immersion (marker on a test position). d) Simulated film resistance (red) for different initial surface coverage values θ_0 qualitative compared to the experiment.

Hydrogen Diffusion Mechanism in Nickel Base Alloy 718

Olesya Golenishcheva, Georg Andersohn, Matthias Oechsner; MPA IfW, Darmstadt/Germany; Jutta Kloewer, Ali Aghajani*, *Outokumpu VDM, Altena/Germany*

Nickel base alloy 718 (UNS N07718) is a precipitation hardened material. Due to its outstanding mechanical properties combined with a good corrosion resistance, alloy 718 is a widely used material in the oil and gas industry. During the operating phase in the oil field, the material is often exposed to corrosive hydrogen-containing environments at temperatures up to about 200 °C.

Some authors report the susceptibility of alloy 718 to hydrogen embrittlement [1,2,3], assuming this to be one of the several possible mechanisms of component failure in the field. Therefore the knowledge of the hydrogen transport processes is essential for improvement of the material utilization.

Earlier investigations of hydrogen diffusion in nickel and nickel base alloys revealed diffusion coefficients in the range of 10^{-12} cm²/s [4,5,6]. Also, it was observed that the hydrogen bulk diffusion in nickel is about 40 times lower than the diffusion along the grain boundaries [7].

The aim of the present work is to investigate the influence of the grain size and certain secondary phase precipitates (delta and gamma double prime) on the hydrogen diffusion in alloy 718.

First experimental results, obtained by electrochemical permeation experiments via the Devanathan and Stachursky method [8], revealed distinct differences between the material variations with different amounts on delta phase precipitates. Observed permeation current transients were higher for the material with lower delta phase content. This could be an indicator for the higher binding energy of the delta phase precipitates.

References:

- [1] K. Sadananda, A. Vasudevan, *Review of Environmentally Assisted Cracking*, Metallurgical and Material Transactions A, 42A (2), S. 279-293, 2011
- [2] F. Foct et al., *Stress corrosion cracking mechanisms of alloy 600 polycrystals and single crystals in primary water – Influence of Hydrogen*, Metallurgical and Materials Transactions A, 31 (8), S. 2025-2036, 2000
- [3] P. Hicks, C. Altstetter, *Hydrogen-Enhanced Cracking of Superalloys*, Metallurgical Transactions A, 23 (1), S. 237-249, 1992
- [4] J. Xu, X.K. Sun, Q.Q. Liu, W.X. Chen, *Hydrogen Permeation Behavior in IN718 and GH761*, Metallurgical and Material Transactions A, 25 (3), S. 539-544, 1994

- [5] W.M. Robertson, *Hydrogen Permeation and Diffusion in Inconel 718 and Incoloy 903*, Metallurgical Transactions A, 8A (11), S. 1709-1712, 1977
- [6] A. Turnbull et al., *Hydrogen Transport in Nickel-Base Alloys*, Metallurgical Transactions A, 23 A, S. 3231-3244, 1992
- [7] Harris, R. Latanision, *Grain Boundary Diffusion of Hydrogen in Nickel*, Metallurgical Transactions A, 22 (2), S. 351-355 [1991]
- [8] M.A.V. Devanathan, Z. Stachurski, *A Technique for the Evaluation of Hydrogen Embrittlement Characteristics of Electroplating Baths*, Journal of the Electrochemical Society, 110 8, 1963

Application of ENM to investigate the effect of different materials and methods of preparation of coating on anti-corrosion quality of ZRP

B. Eremias¹⁾, L. Mindos¹⁾, L. Turek¹⁾, L. Hochmannova²⁾

¹⁾ SVÚOM Ltd., U Mestanskeho pivovaru 934/4, 170 00 Prague, Czech Republic

²⁾ SYNPO Inc., Pardubice, Czech Republic

Abstract

Partial substitution of zinc by using of conductive fillers of different types and combinations as well as possible improvement of zinc rich paints by addition of nanoparticulate zinc has been investigated by means of EN measurements performed in 0,05 M NaCl solution. The motivation for doing this was the fact that EN measurements provide a set of parameters which can be used for fast assessment of the effect of different materials and methods of preparation of coating on anti-corrosion quality of modified ZRP. This multiparameter assessment (analysis of EN data in both time and frequency domains) permits to evaluate this effect in different stages of anti-corrosion performance of tested ZRP. Possibility of use of EN data in combination with single frequency (1 kHz) impedance test results to provide a rapid ranking of studied coatings corrosion control performance has also been discussed.

Corrosion Resistance of Cold Worked CrNi and CrNiMnN Metastable Austenites in Defined Strain States

*M.Eng. P. Seemann, WITg, Taegerwilen/Switzerland, p.seemann@witg.ch
Prof. Dr.-Ing. Dr. h.c. P. Guempel, HTWG Constance, University of Applied Sciences,
Constance/Germany, guempel@htwg-konstanz.de*

The application of strain-hardened austenitic stainless steels is constantly rising. Thereby the strength-increasing impact of deformation induced martensite is increasingly utilized. This lattice modification may result in a change of corrosion behaviour. Especially for new developed manganese alloyed steel grades (AISI 200-series) the corrosion behaviour is still not settled conclusively.

The present study depicts the corrosion behaviour of strain-hardened steels in relation to true strain, phase fraction and stress state. Three well established nickel alloyed steel grades (AISI 300-series) officiate as reference to the new manganese alloyed steel grades (AISI 200-series) to investigate the localized corrosion behaviour, as well as the influence of important alloying elements, such as Ni, Mn, or N, in combination with a cold forming process.

The investigated steels were strain hardened by means of a constant extension rate testing machine that was constructed for this purpose. Therefore, specifically designed tensile specimens with a large, continuous radius were deformed with various testing speeds. The radius effects differing lattice conditions in terms of phase fraction stress state etc. With the help of micro etchings defined measuring points were created alongside the longitudinal axis. Each measuring point was characterized in respect of lattice condition (phase fraction, stress state etc.) and its localized corrosion behaviour.

First, the deformation behaviour of the different steels was characterized with a mathematical approach that considers also the different lattice volumes of α' -martensite and γ -austenite. Second, potentiodynamic polarisation tests using an electrochemical microcell were conducted to investigate the influence of cold working on the localized corrosion behaviour. For these tests the investigated steels were strain hardened by cold rolling.

The results of this work could substantiate a negative impact of a cold forming process on the pitting resistance of metastable austenitic stainless steels.

In this regard, the alloying concepts CrNi and CrNiMnN revealed substantial differences in respect of the deformation behaviour and the corrosion resistance. The main reason for the reduction of the pitting resistance could be determined to be the increased number of lattice defects as a result of the cold forming process. These follow from a combined effect of increased number of lattice defects in the cold formed austenite, the formation of α' -martensite and the increased stress state in the lattice that origins from the differing volumes of the present phases. In the cold formed austenitic lattice of the CrNi-alloys, this can be attributed especially to the present dislocations and for the CrNiMnN-alloy to the formed twinning structures. Thereby a negative influence of the mentioned lattice defects could be verified with and without α' -fractions.

The conducted XPS measurements could identify a chemically induced weakening of the passive layer as a result of a cold forming process.

Nanoscale oxide growth on Nickel studied by reactive molecular dynamics

O. ASSOWE, L. Van Brutzel and A. Chartier

CEA DEN/DANS/DPC/SCCME/LM2T, Laboratoire de modélisation de thermodynamique et de thermochimie, CEA Saclay, 91191 Gif-sur-Yvette, France

Oxidation of metal and metal alloy surfaces are an important problem in physical chemistry and of potential importance in energy applications. In the nuclear industry, Nickel-based alloys are employed in gas turbine engines and in a whole other spectrum of relevant applications, such as high-pressure turbine disks. Ni-based alloys possess excellent corrosion resistance, which is largely due to the presence of dense ultrathin oxide/hydroxide films that protect the alloy surfaces in aqueous electrolytes or moist air. Therefore, understanding the corrosion behavior of Nickel and the growth of these passive films is of vital importance for both scientific research and engineering.

In this work, we are modelling at the atomic scale the first oxidation steps on Nickel low-index surfaces [(100), (110), and (111)] at different temperatures and constant gas pressure. We used molecular dynamics simulations with dynamic charge transfer between atoms where the interactions between atoms are described by Reactive force fields [1, 2]. We observe at the early stage of oxidation a dissociative chemisorption of the oxygen molecules on Ni(111) surface to form $p(2 \times 2)\text{-O}$ and $(\sqrt{3} \times \sqrt{3})R30^\circ\text{-O}$ overlayers, in agreement with experimental results [3]. We found that the growth mechanism of the oxide layer on the nickel surface is primarily attributed to the anion diffusion into interstitial sites of the metal substrate and nickel migration to the free surface. After few picoseconds, the structure of the first atomic layer at the Ni(111) surface is drastically perturbed while it is rather homogeneous inward forming almost a perfect NiO oxide structure. These observations are somewhat different than previous molecular dynamics simulations carried out with none reactive force fields [4]. However, the thickness of this oxide film is limited around 1.5 nm depending on the crystal orientation. We also, found that the oxide growth kinetics at 300 K under 1 ns timescale is the highest for the (110) surface and the lowest for the (100) surface. These oxidation rates increase with higher temperatures.

[1] A. C. T. van Duin, S. Dasgupta, F. Lorant, W.A. Goddard, *J. Phys. Chem. A*, 105 (2001) 9396-9409.

[2] O. Assowe, O. Politano, V. Vignal, P. Arnoux, B. Diawara, O. Verners and A. C. T. van Duin. *J. Phys. Chem. A*, 116 (2012) 11796-11805.

[3] T. Kamada, M. Sogo, M. Aoki and S. Masuda, *Surface Science* 602 (2008) 724-732

[4] S. Garruchet, O. Politano, P. Arnoux, V. Vignal. *Applied Surface Science*. 256 (2010) 5968-5972

Corrosion studies by depth profiling techniques

Célia Olivero, Patrick Chapon, Agnès Tempez, Sébastien Legendre

Horiba Jobin Yvon 16-18 rue du canal

91165 Longjumeau Cedex, France

RF GD OES and Plasma Profiling TOFMS provide direct measurement of the chemical composition of thin and thick layers as a function of depth with excellent depth resolution.

The techniques rely on the sputtering of a representative area of the material of interest (conductive or not) by a high density (10^{14}) and low energy plasma. All elements (and isotopes with MS) can be measured including H, O etc making them ideal tools for corrosion and diffusion studies.

Features and benefits will be illustrated by studies of aluminium with barrier- type oxide films, diffusion on stainless steels and Ni alloys and sol gel coatings on various substrates.

Influence of Surface Treatments on Localized Corrosion Behaviour of Welded AISI 316L Stainless Steel

M. Halamová[#], G. Fumagalli, T. Liptáková[#], F. Bolzoni**

**Politecnico di Milano, Dipartimento di Chimica, Materiali ed Ingegneria Chimica*

"Giulio Natta" Via Mancinelli, 7, Milano 20131, Italia

[#]University of Žilina, Strojnická Fakulta, Univerzitná 1, 010 26 Žilina, Slovakia

Stainless steels and similar alloys may suffer localised corrosion, such as pitting and crevice corrosion, in chloride containing oxidising environments. The behaviour of stainless steels vs pitting or crevice corrosion has been studied extensively by many authors over the last 50 years on the basis of different laboratory approaches.

Pitting and crevice initiation occur when chloride ions concentration in solution exceeds a critical value. This value depends principally on materials properties (composition, deformation degree, heat treatment, surface finishing) and environment properties (temperature, pH, presence of oxydising environment, flow regime).

Moreover, it is well known the negative influence on the localised corrosion behaviour of the "heat tinted oxides" formed on the surface and phases precipitated in the heat affected zone of the welded stainless steels.

In this work, influence of different surface treatments on corrosion behaviour of AISI 316L austenitic stainless steel welded by TIG method has been evaluated through potentiodynamic polarisation tests. Surfaces of the welded stainless steel were treated by mechanical methods (grinding, garnet blasting), chemical method (pickling) and combination of both methods. Potentiodynamic polarisation tests were carried out in sodium chloride (NaCl) solutions containing 100 to 3000 ppm Cl⁻ at room temperature. The surfaces of the specimens were examined using optical and scanning electron microscopy (SEM). Surface analysis by means of Glow Discharge Optical Emission Spectroscopy (GDOES) were carried out.

Comparitive corrosion resistance of dimensionally stable titanium based anodes and conventional lead alloy anodes in copper electrowinning

J.H. Potgieter^{a,b}, Z.S. Msindo^b, and V. Sibanda^b,

^a*Department of Chemical & Metallurgical Engineering, University of the Witwatersrand, Private Bag 3, Wits 2050, South Africa.*

School of Research, enterprise and Innovation, Manchester Metropolitan University, Oxford Road, Manchester, M1 5GD, UK

Abstract

The suitability of dimensionally stable anodes (DSA[®]s) in copper electrowinning of an industrial electrolyte was investigated and compared against the performance of a more conventional lead alloy anode. Two types of DSA[®] plate anodes and two types of DSA[®] mesh anodes of composition Ti-(70%) IrO₂/ (30%) Ta₂O₅, from 2 different sources, and a lead anode containing 6% antimony were tested. Cell voltage was monitored against time for over a period of 150 hours for each anode type. Surface morphology of the resultant copper deposits were analysed using optical microscopy while crystallographic orientation and composition were analysed using x-ray diffractometry. A basic economic evaluation based on the performance of each anode was done. Results showed that DSA[®] mesh anodes had the highest energy consumption per kilogramme of copper produced while the DSA[®] 1 plate anode had the lowest energy consumption per kilogramme of copper produced. The results also demonstrated that not all DSA[®] anodes will exhibit an expected anode characteristic of low over-potential compared to the lead anodes.

Scanning Vibrating Electrode Technique as a Tool for Investigating Corrosion Activities on Coated Mild Steel in NaCl Solutions

W. Shi, S.B. Lyon

*Corrosion and Protection Centre, School of Materials, University of Manchester,
Manchester, M13 9PL, UK*

The long term protection of metal structures exposed to a marine environment is a problem which needs to be approached from many different points of view. Early studies of continuous steel strips, steel sheet piling and also closely spaced individual, electrically isolated or electrically connected coupons in the marine tidal zone show severe corrosion losses, although the corrosion profiles were very different. There are indications that even under conditions of cathodic protection, levels of corrosion observed around the mean high tide level are slightly greater than those in the low tide to mid tide region.

Scanning Vibrating Electrode Technique (SVET) employs a mechanical vibrating probe and a lock-in amplifier to enhance signal recovery, performing a measurement that could be more sensitive than bulk electrochemical corrosion measurement. The SVET allows for the resolution and sensitivity to investigate local anode current density, cathodic active area, and the corresponding changes with time. Here we present the effect of cathodic protection on epoxy coated or calcareous film covered steel and the localised current distribution of corrosion reactions occurring in thin electrolyte layer when immersed in sodium chloride solution.

The work also investigates corrosion sample obtained by external simulated tidal instrument after different exposure time, in order to study the interaction between cathodic protection and coating in this environment.

Techniques used to understand the performance have included optical photography, together with Scanning Electron Microscopy (SEM). Furthermore, electrochemical analytical methods, for example localised electrochemical impedance spectroscopy (LEIS), are also used in this study to evaluate the effect of calcareous deposits, coating defects etc.

Qualification of stress and test methods for use in combined fatigue algorithms for riveted joints

Gehrke, Joerg, Institut für Korrosionsschutz Dresden GmbH, Dresden/Germany;

Introduction

This poster presents results of a cluster project "Combined mechanical and environmental stress of riveted joints", sub-project "Qualification of stress and test methods for use of combined fatigue algorithms. This project was developed by cooperation of three application-oriented AiF and two DFG-research institutions.

The ability of a combined mechanical-environmental aging for riveted joints was investigated in this project in the laboratory compared with the corrosion processes in the accelerated weathering.

Examined rivet joints

The investigation of the corrosion mechanisms was carried out on self-pierce riveting joints between carbon fiber reinforced plastic (CFRP) and aluminum plus blind rivet joints between steel and aluminum. The load tests were carried out according to VDA 621-415 and during the condensation variation load an overlapping with a mechanical fatigue loading occurred, see Figure 1.

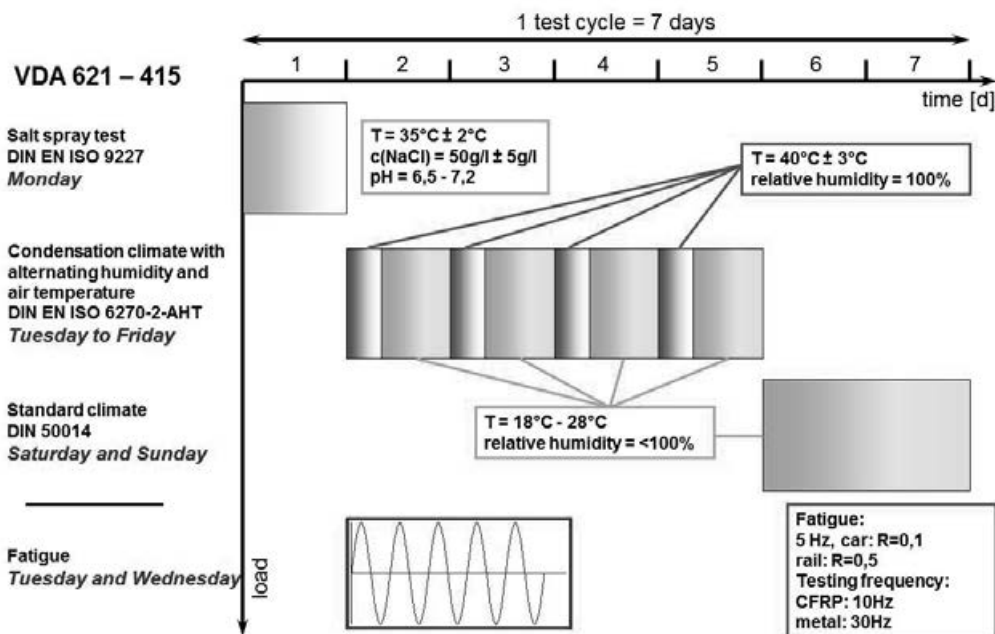


Figure 1: combined fatigue algorithms

Visual assessment of riveted joints

After visual evaluation of loaded riveted joints was found out, that the CFRP-aluminum self-pierce riveting joints 1 year accelerated weathering, sufficiently is adequate to 6 cycles VDA 621-415. The combined mechanical- environmental fatigue considered by the experimental program was compared to conventional serial load. Reinforced corrosion phenomena were found in both kinds of rivet joints by combined fatigue. In the CFRP aluminum rivet joints pitting was frequently found on aluminum, especially in the contact area to the carbon fiber reinforced plastic. After a short loading period the rivet elements showed partly corrosion depending on the rivet coating.

Electrochemical noise investigation

The method of electrochemical noise analysis was used to assess the rivet coating. The results of the electrochemical noise studies accord with both the visually encountered corrosion as well as with the analytical studies of the project partners. Electrochemical noise measurement is a method to assess the corrosion resistance of a rivet element in a very short measuring time. The poster includes the results of electrochemical noise measurements of the two riveted joints.

Pitting potential of materials during potentiodynamic polarization in a NaCl Solution

Yongsun Yi, Khalifa University, UAE

Mohammed Al Ameri, Khalifa University, UAE

Sara Al Saadi, FANR, UAE

Pyungyeon Cho, Khalifa University, UAE

Changheui Jang, KAIST, Korea

This paper discusses the pitting potential, E_{pit} , of materials determined by the potentiodynamic polarization in a NaCl solution. The pitting potential has been regarded as a potential above which stable pitting occurs on materials. Being determined using the potentiodynamic polarization technique, the values of E_{pit} are strongly dependent on the potential scan rate, which means that a value of E_{pit} cannot be uniquely determined by the technique. To investigate the factors governing E_{pit} , potentiodynamic polarization measurements were made on a 316 stainless steel in 3.5% NaCl solution at different scan rates from 0.01 to 50 mV/sec. The findings from the measurements are:

- Apparent E_{pit} values were increasing with the scan rate;
- The magnitudes of the passive current densities increased proportionally with the scan rate;
- Noticeable current fluctuations indicating metastable pitting were recorded at potentials close to E_{pit} ;
- Simple analysis on the current density fluctuations showed that the metastable pits formed near E_{pit} would be a few micrometers deep;
- Cumulative charge densities, Q_p , determined by integrating the current densities with respect to time appeared to be independent on the scan rate.

Metastable pitting has been known to be related to the chloride uptake by oxide films, which is responsible for passive film breakdown. A number of studies have proposed that there should be a critical condition for the transition from the metastable to stable pitting in terms of metastable pit geometry and electrochemical reaction rates. The cumulative charge densities which turned out to be independent on the scan rate in the potentiodynamic polarization measurements are interpreted as a total amount of electric charge required for sufficient chloride entry for the meatstable pitting and the critical condition for the stable pitting, which determines E_{pit} of materials during the potentiodynamic polarization.

"Effect of microstructure of X-65 in bioethanol and its implications for pipelines"

M.A. Lucio-García a, J.G. González-Rodríguez a, S. Serna a, A. Torres-Islas a.
a UAEM-CIICAP, Av. Universidad 1001, Col. Chamilpa, 62209-Cuernavaca,
Morelos, México,

Fuel grade ethanol, (FGE) is attracted much attention due the increasing demand for fossil fuel alternatives and reducing carbon oxide emissions. Although the occurrence of ethanol SCC thus far has not caused major problems, extensive pipeline transport of ethanol in the future requires sufficient understanding of the phenomenon to resolve this concern. Tensile test employed to study effects of kinetics of X-65 steel. Recent phenomenological studies have identified several constituents that significantly affect corrosion and Stress Corrosion Cracking (SCC) susceptibility in this alternative fuel. As well steel corrosion in FGE was investigated by electrochemical measurements on electrodes, as polarization curves, linear polarization resistance (LPR) and Electrochemical Impedance Spectroscopy (EIS). SCC has been evaluate by slow strain rate testing to evaluate hydrogen embrittlement under cathodic protection, reduction in area and percent age elongation of tensile specimens to asses the degree of embrittlement. Before testing, the specimens were abraded longitudinally with 600-grade emery paper, degreased, and masked, with the exception of the gauge length. Specimens were subjected to conventional, monotonic slow strain rate tensile (SSRT) testing in dry air as an inert environment, and in 0.1, 0.5, 0.01 M Sulphidric acid (H_2S) solutions with pH = 7.0, at room temperature and 50 °C at a strain rate of $1.36 \times 10^{-6} s^{-1}$.

Polarization curves were recorded at a constant sweep rate of 1 mV/s at a -300 to +300 mV interval respect to open circuit potential (E_{corr}). Measurements were obtained by using a conventional three electrode glass cell with two graphite electrodes symmetrically distributed and a saturated calomel electrode (SCE) as reference with a Lugging capillary bridge. Corrosion current density values, I_{corr} , were calculated by using the Tafel extrapolation method and by taking an extrapolation interval of ± 250 mV around the E_{corr} value once stable. The R_p values were obtained from the LPR measurements. LPR measurements were carried out by polarizing the specimen from +10 to -10 mV in respect to E_{corr} , at a scanning rate of 1 mV/s during 24 h. Electrochemical impedance spectroscopy tests were carried out at E_{corr} by using a signal with an amplitude of 10 mV in a frequency range of 100 mHz–30000 Hz. An ACM potentiostat controlled by a desk top computer was used for the LPR tests and polarization curves; whereas for EIS measurements, a model PC4 300 Gamry potentiostat was used.

The purpose of the present study was to understand better the effects of metallurgical factors in bioethanol on X-45 and identified that dissolved oxygen and corrosion potential are the critical factors contributing in pipeline steel, in conjunction with the effect of electrochemical potential on the external SCC in diluted H_2S solutions using the slow strain rate testing (SSRT) technique. However, impurities and additives can promote tendencies toward localized corrosion with low levels of water contamination. The corrosion rate of carbon steels in FEG is rather low, partly because of its low conductivity.

Corrosion performance of TiO_2 nanostructures synthesized at low voltage applying electrochemical techniques

¹H. Herrera-Gutiérrez, ¹C. Cuevas Arteaga, ²Ebelia del Ángel Meraz, ¹Facultad de Ciencias Químicas e Ingeniería/Centro de Investigación en Ingeniería y Ciencias Aplicadas, Universidad Autónoma del Estado de Morelos, Cuernavaca, Mor., México, ²División académica de ingeniería y arquitectura, Universidad Juárez de Tabasco, México.

In order to determine the electrochemical stability of TiO_2 nanostructures obtained through electrochemical potentiostatic text (anodization), corrosion study has been made using some electrochemical techniques named polarization curves (PC), electrochemical noise (EN) and electrochemical impedance spectroscopy (EIS). The synthesis of TiO_2 nanostructures was carried out exposing titanium foils in an aqueous solution 1 M H_3PO_4 adding 3 (wt. %) HF and applying a low voltage of 3V during the anodization. Anodization of Ti foils was made using a Teflon cell of three electrodes: one working electrode (0.27 m, 1 cm² titanium foil), a Ag/AgCl reference electrode and a mesh of platinum as auxiliary electrode. For polarization curves and EIS, the electrochemical cell was the same than that for anodization, whereas for EN, two identical electrodes (two TiO_2 nanostructures films) and one Pt mesh reference electrode was used. The corrosive solution was 1 M Na_2SO_4 . All the experiments were made at room temperature. For comparison, the corrosion study was made for a Ti pure foil, Ti foil with a planar TiO_2 obtained applying a galvanostatic test, an amorphous TiO_2 nanostructure film, and a crystallized TiO_2 nanostructure film.

Through the corrosion characterization in the determination of electrochemical stability, it was possible to state that the amorphous and specially the crystallized TiO_2 nanostructure films develop a passive layer even after 5 days of exposure. Both nanostructures films kept its original surface. This behaviour was in accordance with the results from the three electrochemical tests. With respect to pure titanium, pitting attack was seen, and the dissolution of the Ti foil with a planar TiO_2 by the effect of the corrosive solution. EIS technique showed that the TiO_2 nanoporous presented a minor charge transfer resistance and minor diffusive effects; so that it concludes that through these films the electron transfer is good, especially for the crystallized TiO_2 nanostructure films.

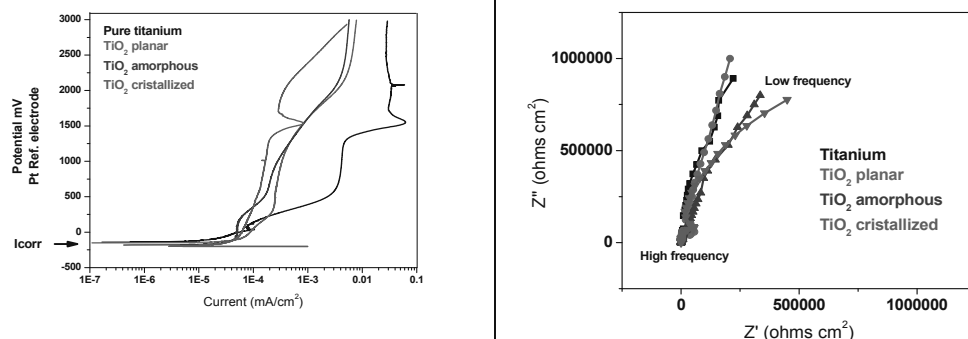


Fig. 1. Polarization curves and Nyquist diagrams of the different studied films exposed to 1 M Na_2SO_4 .

Corrosion Resistance of Zr 2.5Nb as Material for Permanent Implants

Silvia B. Farina, Comisión Nacional de Energía Atómica (CNEA) - Comisión Nacional de Investigaciones Científicas y Técnicas (CONICET) - Univ. de San Martín (UNSAM), Av. Gral Paz 1499 (1650) San Martín, Argentina

Andrea Gomez Sanchez, SIFIMAC, Servicios de Ingeniería, Formación e Inspección en Materiales Compuestos, Av. C. Tejedor 2281, (7600) Mar del Plata, Argentina

Silvia Ceré, División corrosión - INTEMA, Universidad Nacional del Mar del Plata - CONICET, Juan B. Justo 4302 (7600) Mar del Plata, Argentina.

Increasing bioactivity while keeping low corrosion rates is one of the main objectives of most of the research being performed on metallic materials for permanent implant applications. It has been extensively proved that the success or failure of the osseointegration process is determined by surface characteristics in different space length scales, and those materials where osseointegration occurs, have a lower implant replacement rate.

Zirconium is a potential material for permanent implants. In particular, surface modification induced by anodisation has proved to be effective to improve corrosion resistance while keeping good osseointegration. The combination of zirconium with niobium is supposed to develop a structure that presents a high corrosion resistance and continues having the mechanical resistance necessary for implants. The aim of the present work is to determine the viability of using anodised Zr-2.5Nb as implant material, and compare it with pure zirconium. The electrochemical in vitro response of anodised samples was studied in order to determine the effect of the surface modification process on the corrosion resistance of these two candidate materials. A simulated body fluid (SBF) solution was selected from literature to investigate the resistance to corrosion. In this study we have assessed the corrosion resistance of the metals using anodic polarisation tests and electrochemical impedance measurements. The presence of Ca-P rich compounds, believed to increase the apatite formation capability in vivo, was also investigated in the as-received and anodised samples after immersion in the SBF solution.

Monoclinic zirconium oxide was identified as the main crystallographic phase in the anodised samples of both materials (zirconium and Zr-2.5Nb). Zirconium pyrophosphates, which may be beneficial for further apatite growing in vivo, were also observed. Electrochemical tests performed in the anodizing solution and in the SBF solution revealed that by anodising the materials a higher corrosion resistance is obtained. The improvement on the corrosion resistance is particularly noticeable in the case of the pure metal after a short period immersed in the simulated biological solution. But, after a long period of immersion, the alloy shows better performance. Ca-P compounds were detected only on zirconium anodised at 30 V. Although the presence of these compounds may be beneficial for a good in vivo bone bioactivity of the material, their existence is not mandatory. Thus, as this study has shown the potentiality of using anodised zirconium and Zr-2.5Nb as implant materials from the corrosion point of view, in vivo tests are worth performing in the future to compare the bioactivity of the pure metal with the alloy.

Comparative Corrosion Behaviour of Different Sn-based Solder Alloys

Silvia B. Farina, Comisión Nacional de Energía Atómica (CNEA) - Comisión Nacional de Investigaciones Científicas y Técnicas (CONICET) - Univ. de San Martín (UNSAM), Av. Gral Paz 1499 (1650) San Martín, Argentina
Carina Morando, Instituto de Física de Materiales Tandil (IFIMAT, UNCPBA, CICPBA, MT) Centro de Investigaciones en Física e Ingeniería del Centro de la Provincia de Buenos Aires (CIFICEN-UNCPBA), Consejo de Investigaciones Científicas y Tecnológicas (CONICET), Pinto 399 (B7000GHG) Tandil, Argentina

The aim of the present work is to evaluate and compare the corrosion susceptibility of different tin alloys and pure tin. The corrosion properties of Sn-Ag, Sn-Cu, Sn-Ag-Cu, Sn-Zn and Sn-Bi solders were investigated. The results were compared with those of the eutectic Sn-Pb solder and pure Sn. The results obtained may be used as a guide for choosing solder materials for electronic devices when Sn-Pb solders must be replaced by a lead free one. These materials may undergo atmospheric corrosion in the presence of air and moisture at high temperatures, and electrochemical corrosion in aqueous solutions containing certain acids or particularly aggressive species, such as chloride ions. In fact, aqueous chloride solutions are the most studied ones not only for their aggressiveness but also for being chloride one of the most abundant species in nature.

The corrosion behaviour of five Pb-free solders was studied in a 0.1 M NaCl aqueous solution by means of polarization measurements (corrosion potential measurements, potentiodynamic polarization curves and linear polarization resistance tests), and compare to that of a conventional Sn-Pb solder and pure Sn. The results show that the Sn-3.5%Ag-0.9%Cu, Sn-3.5%Ag and Sn-0.7%Cu solders have the best resistance to localized as well as to general corrosion, similar to that obtained for the Sn-37%Pb solder and pure Sn. Their use is possible, even in the presence of high contamination with chloride ions because corrosion rates are low (less than 0.1 mm.year⁻¹). The Sn-57%Bi solder has poorer corrosion properties but its behaviour is still acceptable, because it passivates and shows a relatively low corrosion rate. In all these cases the corrosion resistance is good due to the content of noble elements (Ag, Cu, Pb and Bi) in the alloys. On the other hand, the Sn-9%Zn is definitely the one that exhibits the worst behaviour, not only to localized but also to general corrosion, due to the addition of a less noble material to the Sn matrix.

Scanning electron microscopy (SEM) was used to investigate the morphology of the alloy surface after the electrochemical tests. The SEM images were compared to the optical microscope images of the original microstructures. In most cases it was found that the Sn-rich phase corrodes selectively. The corrosion products found have a platelet-like shape and are distributed on the surface with different orientations. It is assumed that the corrosion product is SnCl₂.

Miniaturized cell for localized electrochemical measurements. Concept and examples of application

Massimiliano Bestetti¹, Antonello Vincenzo¹, Silvia Franz¹, Giacomo Puricelli¹ and Carlo Borioli²

¹. *Politecnico di Milano, Dipartimento di Chimica Materiali e Ingegneria Chimica, "G. Natta", Milano (Italia)*

². *Nanomaterials.it Srl, Milano (Italia)*

The use of miniaturized portable and low cost measuring instruments may encourage the spread of electrochemical science and technology. In general, potentiostats for research purposes are extremely expensive, although in recent years we are experiencing the development of portable instruments having small and very small sizes. Portable and low cost devices are useful in at least two cases: for classes of high school and university students and for field measurements.

Even the design of the electrochemical cells must follow this trend. In the paper we present the features of a newly developed miniaturized instrument, useful to perform localized electrochemical measurements. It is a miniaturized cell having the size and the shape of a pen. The cell consists of a hollow cylindrical body which allows the movement of the fluid in the vicinity of the working electrode by means of an external recirculation pump. The working area is circular and has the diameter in the order of millimeter. The device incorporates the reference electrode and the counterelectrode. The examples given in this paper report about several types of application ranging from the coulometric measurements of the thickness of galvanic coatings to the potentiodynamic polarization measurements on metals for the assessment of the corrosion behaviour.



Fig. 1. Drawing of the cell.



Fig. 2. OCP measurement
on a complex shape.

Dew-point corrosion resistance of alloys in geothermal fluids containing acid chloride

*M. Cabrini, S. Lorenzi, T. Pastore, Università di Bergamo, Bergamo, Italia
M. Favilla, R. Perini, B. Tarquini, Enel, Larderello, Italia*

Abstract

The presence of acid chlorides, mainly hydrogen chloride (HCl) and ammonium chloride (NH₄Cl), in steam was recognized to induce corrosion problem in geothermal power plants. In the vapour-dominated systems of Larderello, a risk of localized corrosion and stress corrosion cracking arise on corrosion resisting alloys blades of the wet section of steam turbines. Severe general corrosion can be induced on cold zones of on carbon steel pipelines conveying steam from wells to turbines.

At the dew point, that usually is in the range 150-200°C at the operational pressure of plants, the early stage of condensation promotes the formation of a layer of very aggressive saline solution with acid pH ranging between 2 and 4. Very high chloride concentrations reaching 20000 ppm were estimated, depending on the chloride content in the vapour phase, with relevant concentration of ammonium ion and boric acid.

Nowadays, corrosion mitigation is mainly achieved through steam scrubbing systems, by chloride abatement with alkaline sodium hydroxide solution. However, this treatment reduces the fluid temperature and, besides an increase in operating costs, it leads to a loss of power estimated around 0.5 MW on 15 MW turbines. Thus, the use of corrosion resistant alloys (CRA) can be a convenient alternative solution.

The paper shows the result of tests performed in order to evaluate the behaviour of a wide number of CRAs in conditions promoting dew point corrosion.

A number of tests were carried out in experimental devices placed in different production sites.

The testing section operated with continuous vapour flux directly extracted from the production line. In order to achieve vapour condensation, the temperature and pressure were adjusted in the range 150-156 °C and 4-5 bar respectively, depending on steam composition. U-bend and unloaded specimens were exposed for 1 month. After exposure, the specimens were removed in order to evidence stress corrosion cracking, localised corrosion forms and weight loss.

Different materials were tested in a wide range of corrosion resistance: 3 carbon steel/low alloyed steels, 9 martensitic stainless steels, 1 precipitation hardening stainless steel with martensitic structure, 2 ferritic extra low interstitials (ELI) stainless steels, 4 duplex stainless steels, 5 traditional austenitic and superaustenitic stainless steels, 6 nickel-chromium and nickel-chromium-molybdenum alloys, 4 titanium alloys. The results were discussed as a function of PREN index and nickel content. Experimental data were summarised in maps of susceptibility to the different corrosion forms evidenced on specimens after testing.

Corrosion resistance of ternary Ni-Ti alloys in 0.9% NaCl solution

Barros, CDR; Ponciano Gomes, JAC

*Federal University of Rio de Janeiro / Departament of Metallurgy and Materials -
LabCorr , Rio de Janeiro / Brazil*

Abstract

NiTi shape memory alloys are usually used as biomaterials because of the proprieties of memory effect, pseudoelasticity and good biocompatibility. The literature mentions that ternary elements have been added in order to adjust mechanical and physical properties, such as hysteresis, transformation temperatures and radiopacity for different reasons. However, these chemical composition changes can affect these materials's corrosion resistance. This study aims to evaluate the corrosion resistance of binary and ternary alloys NiTi, NiTiCo, NiTiCr and NiTiCu in a simulated physiological environment. The obtained results permit to compare the corrosion behavior of these alloys. Electrochemical impedance spectroscopy and anodic polarization measurements were performed in a 0.9% NaCl solution. The electrochemical impedances spectroscopy were measured at OCP within the frequency range of 10 kHz to 10m Hz and with potential amplitude of 10 mV. The anodic polarization tests were performed in a range of 800mV above the corrosion potential using 20 mV/ min scan rate. The parameters used to evaluate the corrosion resistance were the values of the polarization resistance and the passive range, defined as the potential difference between breakdown and open circuit potentials (OCP). Passive current densities within the passive range were considered. The results showed that the binary alloy showed higher corrosion resistance then ternary alloys, with higher values of R_p and higher ΔE . However, the passive current densities were not significantly increased by the third elements additions. The decrease of resistance to polarization, as well as the decrease in ΔE values can be explained by the changes of passive film composition when a third element is added. These results show that any positive effects of the third element addition must consider their adverse influence on corrosion resistance in simulated physiological environment.

Electrochemical induced dissolution of silver points in sodium fluoride solution

*Amaral,CCF, Ormiga, F, Ponciano, JAC, Federal University of Rio de Janeiro /
Departament of Metallurgy and Materials, Rio de Janeiro / Brazil.*

Abstract

The removal of silver points from inside the root canal has been a clinical concern to endodontists during endodontic retreatment. Several methods have been described for removing fractured instruments from root canals, however, these methods show different success rates. The aim of this study was to investigate the effectiveness of the dissolution process of silver points in a sodium fluoride solution. We evaluated the anodic polarization curves of the silver flat electrode and the redox curves of the solution NaF 12g/L at pH=5.0. After the tests silver points with size 30 were submitted to anodic polarization at $+0.5 V_{SCE}$ in the solution test for 4 minutes. The mass and length of each silver point were calculated before and after the tests. The morphological alterations of the tested silver points were evaluated by optical microscopy. The redox curve showed a current density of 0.4 mA/cm^2 until an anodic potential of approximately $+1.05 V_{SCE}$. Through the redox curve we observed that the material presented active dissolution below the oxidation potential of the solution, which indicated the oxidation of silver without occurrence of side electrochemical reactions. The anodic polarization curves showed current values of $+0.5 V_{SCE}$ near to the corrosion potential and current values of potential between $+0.2$ and $+0.4 V_{SCE}$, from which a significant increase of current, indicating generalized dissolution of silver in NaF 12g/L solution. In the amperometry tests it was observed that the initial anodic current reached was about 1000 mA, and after 1 minute of testing, the current drops sharply and becomes constant until 4 minutes, indicating an active dissolution of the silver point in 1 minute. The results of this study demonstrated that the concept for the removal of silver points in the root canals by electrochemical process can be used to remove silver fragments during an endodontic retreatment.

EIS Studies of As-cast Monotectic Al-Pb and Al-Bi Alloys in a 0.5 M NaCl Solution

Emmanuelle S. Freitas^a; Wislei R. Osório^b, Adrina Paixão Silva^c, José Eduardo Spinelli^d and Amauri Garcia^a

^a *Department of Materials Engineering, University of Campinas - UNICAMP, Campinas, SP, Brazil*

^b *School of Applied Sciences / FCA, University of Campinas - UNICAMP, Campus Limeira, SP, Brazil*

^c *School of Mechanical Engineering, Federal University of Pará - UFPA, Belém, PA, Brazil*

^d *Department of Materials Engineering, Federal University of São Carlos - UFSCar, São Carlos, SP, Brazil*

A series of monotectic Al-rich binary alloys having limited solubility in the solid state have been pointed up as desirable for many industrial applications, among them self-lubricated bearings, electronic materials and superconductors. However, it is important to note that monotectic alloys undergone an invariant reaction at the monotectic temperature, at which a liquid phase, $L1$, is decomposed in a solid phase $S1$ and a liquid phase $L2$. The competition between the growth of the minority phase and solidification velocity ahead of the solid-liquid interface will determine whether the morphology prevailing microstructure is characterized by fibers or droplets. The aim of this experimental study is to evaluate the electrochemical behavior of hypomonotectic Al-1.2 wt.% Pb and monotectic Al-3.2 wt.% Bi alloys as a function of the resulting microstructure array. The alloys were obtained by directional solidification apparatus, of which were retained samples for the study. Electrochemical impedance spectroscopy (EIS) plots and an equivalent circuit analysis were used to evaluate the corrosion resistance of Al-Pb and Al-Bi alloys samples in a 0.5 M NaCl solution at 25°C. It was found that the microstructure characterized by Pb and Bi dispersed into the Al-matrix, and the interphase spacing plays a significant role on the corrosion resistance.

Effect of Thermal Treatments on the Localized Corrosion Behaviour of Alloy 718

Mauricio Rincon Ortiz,¹ Mariano Iannuzzi,² Mariano A. Kappes,³

Martin A. Rodriguez,³ and Raul B. Rebak⁴

¹The University of Akron, Akron, OH 44304, USA

²GE Oil & Gas, Sandvika, Norway

³Instituto Sabato, Buenos Aires, Argentina

⁴GE Global Research, Schenectady, NY 12309, USA

Nickel (Ni) based Alloy 718 (UNS N07718) is used extensively for Oil & Gas sour applications, mainly in the heat treated high strength condition for down hole and wellhead accessories and other components. In general, the resistance to localized corrosion and environmentally assisted cracking (EAC) in high temperature sour environments containing high concentration of chloride increases as the amount of Ni, chromium (Cr) and molybdenum (Mo) in the alloy increases. The pitting resistance equivalent (PRE) of N07718 is approximately 29 based on the formula $PRE = \%Cr + 3.3\%Mo + 16\%N = \sim 29$. N07718 is a precipitation hardenable alloy that can be heat treated to increase its mechanical properties due to the precipitation of secondary phases containing aluminium, titanium and niobium. NACE MR0175 / ISO 15156 allows for a maximum hardness of HRC = 40 for heat treated Alloy 718. In general, N07718 has not been fully characterized regarding its general corrosion and localized corrosion resistance in wet environments like other corrosion resistant alloys (CRA) such as N06625 and N10276. For example, the ASTM G 48 defined critical crevice and critical pitting temperatures (CCT and CPT, respectively) of annealed and heat treated N07718 are difficult to find. The objective of the current research is to gain more knowledge on the resistance to corrosion of N07718 both in the annealed and thermally heat treated condition, especially in environments that could be relevant to downstream oil and gas applications. Immersion and electrochemical techniques such as ASTM G 61 and G 106 were used. Results will be presented to compare the behaviour of N07718 with other iron and nickel based alloys of similar PRE values. Tests were conducted both in 3.5% NaCl solutions at near neutral pH and in NACE TM0177 Solution A (5% NaCl + 0.5% Acetic Acid, No H₂S) at ambient temperatures.

Repassivation mechanism of Al alloys

D. Cicolin, E. Melilli, M. Pogliana, D. Guastaferro, M. Trueba, S.P. Trasatti
Università degli Studi di Milano, Italy

This work discusses the validity of single-cycle anodic polarization in investigating localized corrosion of Al alloys [1-3]. In particular, the electrochemical behaviour during polarization into the active region, mostly overlooked, provides an indication of the type of localized corrosion other than classical pitting, through the occurrence of an inflection in the reverse curve. More importantly, the analysis of the electrochemical parameters at the inflection such as pit transition potential and related current density, provides information about the thermodynamics and kinetics of the localized attack reactivation due to limited simultaneous repassivation of all corroded sites. In addition, the polarization behaviour after the inflection allows a quantification of the localized attack propagation for a given alloy. The effect of different experimental factors, such as solution composition, pH, time effects (scan rate and surface pre-conditioning), working area, cell geometry, and metallurgical condition (thermal treatment, artificial aging) will be presented for different Al alloys. Overall, elaboration of quantitative data leads to empirical laws for probing well-accepted concepts in localized corrosion, but also knowledge on still debated critical potentials and propagation rates. This electrochemical methodology should be addressed as a tool for evaluating relationships between composition/microstructure and properties. Limited understanding of these relationships directly affects mechanistic modeling and life-prediction analysis, hindered by uncertainties associated with local cell processes.

- [1] D. Cicolin, M. Trueba, S.P. Trasatti, *Electrochim. Acta* (2013) (<http://dx.doi.org/10.1016/j.electacta.2013.09.003>).
- [2] I. Comotti, M. Trueba, S.P. Trasatti, *Surf. Interf. Anal.* 45 (2013) 1575.
- [3] M. Trueba, S.P. Trasatti, *Mater. Chem. Phys.* 121 (2010) 523.

The modified phosphate conversion coating on Zn-Mg alloy coated steel for corrosion protection

Young Jin Kwak¹, Tae Yeob Kim¹, Dong Yoeul Lee¹, Kyung Hoon Nam¹,
Yong Hwa Jung¹, Woo Sung Jung¹, Mun Jong Eom¹, Seok Jun Hong¹
Jaekyu Min², Hong-Kyun Sohn²,

¹POSCO Technical Research Laboratories, 699, Gumho-dong, Gwangyang, Jeonnam,
545-090, Korea

²POMIA (Pohang Institute of Metal Industry Advancement), 166-5, Jigok-dong, Pohang,
Gyeongbuk, 790-834, Korea

Abstracts

Zinc phosphate conversion coatings have been widely used industrially as an undercoating for paint to improve the adhesion of the paint and to improve corrosion resistance. Tri-cation type phosphating bath consisting of Zn, Mn and Ni ions have been developed in order to increase the properties such as corrosion resistance, alkaline stability and paint adhesion. The modified phosphate conversion coatings were formed on Zn-Mg alloy coated steel which was manufactured with the Electro Magnetic Levitation-Physical Vapour deposition (EML-PVD) process in order to increase the corrosion resistance of coating layer. The characteristic changes and corrosion resistance of coatings were investigated with varying concentrations of Mo & Ni in phosphating solution. Surface morphology and crystal size were observed by SEM. Salt spray test, potentiodynamic polarization and electrochemical impedance spectroscopy were used to evaluate the corrosion resistance.

LOCAL ACTIVATION OF IRON IN WEAKLY ALKALINE MEDIAS CONTAINING HALIDE-IONS

S.A. Kaluzhina*, N.G. Nafikova**

*Voronezh State University, 394006 University Sq. 1

**Center for Quality Assurance and Certification medicines, 394051 Writer Marshak 1
Voronezh, Russia
e-mail: kaluzhina@vmail.ru

Local activation (LA) [1] of passive iron decreases its corrosion resistance. At the same time, the intensity of this process and nature of the metal surface destruction essentially depend on the activator concentration in the solution and experiment conditions. At the present work, the action of the indicated factors is analyzed under evaluation of the influence of aggressive halide- ions content and potential scan rate on the LA of the iron in a standard borate buffer electrolyte.

The experiments were performed with stationary electrode from ARMCO iron in a classic three electrode cell at 20 ± 2 °C in a borate buffer solution (pH = 8,4) with free air access using a combination of electrochemical methods, optical and scanning electron microscopy, and energy dispersion analysis (EDA) [2]. The concentration of the activating additive in the form of NaCl and NaBr varied in the range $C(\text{NaCl}) = 5,0 \times 10^{-4} \div 1,5 \times 10^{-3}$ M and $C(\text{NaBr}) = 1,0 \times 10^{-3} \div 6,0 \times 10^{-3}$ M, potential scan rate - $v_p = 3 - 50$ mV/sec.

The results of the investigation have shown that the passive state of the iron in a borate buffer solution is broken, and it undergoes LA at all studied concentrations of Cl^- - and Br^- -ions. The LA potential (E_{LA}) decreases linearly as the concentration of the activator increases according to equation: $E_{\text{LA}} = a - b \lg C$, with $b = 0,26 - 0,30$ B (for borate- chloride and borate- bromide medias, respectively), and a formal kinetic order of pitting initiation reaction (PT) – according to halide- ions ($n_{\text{Hal}^-} \rightarrow 1$). This fact permits to establish that LA process has complicated mechanism [3] with limiting stage of formation of $[\text{FeHalOH}]_{\text{ads}}^-$ adsorbed complex able to transfer into the solution volume later.

Studies of potential scan rate influence on the kinetics of LA of iron have shown that processes of PT initiation and development are faster than their repassivation. The discovered effect exhibits itself most distinctly at $v_p = 50$ mV/sec, what can be stipulated by formation of more defective passive film in these conditions, stimulating development of LA of iron. As a result, under the effect of halide ions passivity of the metal is locally destroyed on those areas where the structure or thickness of the passive film are altered due to dominant formation of soluble halide complexes.

References

1. Revi R. W., Ulig H.H. Corrosion and Corrosion Control. Introduction to Corrosion Science and Engineering. Published by John Wiley & Sons, Inc., Hoboken New Jersey, 2008. 479 p.
2. Kaluzhina S.A., N.G.Nafikova. Passive State of Iron in Weak-Basic Borate Solution // EUROCORR 2013 for a blue sky; European corrosion congress: book of abstract, 1-5 september 2013. Estoril (Portugal), 2013. P. 228.
3. Sukhotin A.M. Physical Chemistry of Passivating Films on Iron. L.: Chemistry, 1989. 390 p.

BROMIDE-IONS ADDITIVES EFFECT ON ALUMINUM ANODIC BEHAVIOR IN BORATE BUFFER SOLUTION

Kaluzhina S.A., Minakova T.A., Popova T.A., Chikova A.T.

Voronezh State University, Voronezh, Russia

In the present work was analyzed aluminum (Al 99.99 %) anodic behavior in borate background solution (0.2 M H_3BO_3 + 0.05 M $\text{Na}_2\text{B}_4\text{O}$ (pH 8.4)) with additives of bromide-ions ($C_{\text{Br}^-} = 10^{-3} \dots 6 \cdot 10^{-3}$ M). Reliability of experimental results was defined by use of a complex of independent physic-chemical methods (voltammetry, chronoamperometry, optical microscopy (MBS-2 (x7) and MIM-7 (x500)), scanning electronic microscopy (SEM, x1000) with JEOL-6380LV and energy-dispersive X-ray analysis (EDXA) with INCA Energy-250). It is known, that many metals (such as Fe, Bi), exposed to anodic polarization in borate buffer media, are in a passive state. Experimental results [1,2] have confirmed this fact for Al in investigated borate background solutions. At the same time passive state of Al is broken under bromide-ions introduction in system. In the presence of $C_{\text{Br}^-} \geq 10^{-3}$ M on metal surface are observed pitting corrosion. Under this depth ($h = 3 \dots 18 \mu\text{m}$) and diameter ($d = 10 \dots 25 \mu\text{m}$) of pits increase with aggressive anion concentration growth. On the basis of electrochemical data (voltammetric and chronoamperometric) and at parallel morphology observation of metal surface by optical and scanning electronic microscopic methods, quantitative characteristics of process pit formation (PF) have been defined. It was established, that PF potential (E_{PF}) shift to more negative values with growth of Br^- - ions concentration ($E_{\text{PF}} = 0.50 \dots -0.04$ V (NHE)) simultaneously with decrease of aluminum stability to local destruction and strengthening of its intensity. Comparison the obtained experimental and literature data has allowed to establish the associative mechanism (according to formal kinetics analysis) of the studied processes of Al depassivation in weakly alkaline solution under bromides-ions influence. The yielded fact is confirmed by results of SEM and EDXA results and interpreted on the basis of modern theories of competitive adsorption, complexing and nucleophilic substitution [3]. Thus PF on Al under the influence of bromide-ions (pH 8.4) represents reaction of nucleophilic substitution of associative type.

1. Minakova T.A., Kaluzhina S.A., Sokolov Yu.V. // 224th ECS Meeting. - 2013. - №1712.
2. Kaluzhina S., Minakova T., Chikova A., Sokolov Yu. // EUROCORR 2013. - 2013. - Page 222.
3. Kuznetsov Yu.I. // Protection of metals. - 1994. - V. 30, № 4. Page 341-351.

Application of micro-indentation techniques for investigation of seasonal corrosivity of Black Sea maritime atmosphere

Startsev O.V., Medvedev I.M.

Akimov Gelendzhik climatic testing center, Gelendzhik, Russia

Seasonal corrosivity of marine atmosphere at the Black Sea shore was investigated at Akimov Gelendzhik climatic testing center; a branch of the All-Russian scientific research institute of aviation materials. Corrosivity of the atmosphere in the area of testing is classified as C3, according to ISO 9223. Meteorological data has been collected to evaluate seasonal corrosivity as well as time of wetness measurements according to both ISO 9223 and the Davis leaf wetness sensor. Also, the chloride deposition rate was measured. All parameters of seasonal corrosivity were observed for five years. Tests were conducted on widely used St3 carbon steel. The influence of seasonal variations on the corrosion rate and micro-mechanical properties of samples was investigated during 4 seasons of the year 2012. ASTM E2546 indentation testing was used to determine the micro-mechanical properties of the samples by load-displacement diagrams. To achieve good reproducibility and accuracy of testing, 500 measurements of indentation hardness and elastic modulus per sample were performed. The distributions of indentation hardness and elastic modulus were fitted using Generalized Lambda Distributions. The parameters of distribution were estimated to provide additional information about surface hardness. Seasonal variations in marine atmosphere corrosivity of the Black Sea coast were revealed by analyzing the time of wetness, the chloride deposition rate, the corrosion rate, and the micro-mechanical properties of the samples. Research proves that micro-mechanical properties may be a useful tool for studying atmosphere corrosivity.

DESIGN CRITERIA OF RELIABILITY AND SAFETY IN THE DESIGN OF CORROSION PROTECTION OF STRUCTURAL STEEL

*Korolov V. *, Vysotsky Y. **, Filatov Y. ***, Gibalenko A. *****

**Priazovsky State Technical University*

7, Universitetskaya Str., Mariupol, 87500, Ukraine

*** Donetsk National Technical University*

58, Artyoma Str., Donetsk, 83001, Ukraine

**** PrSC «Donetsksteel» - Metallurgical Plant»*

174, Chelyuskintsev Str., Donetsk, 83001, Ukraine

***** OJSC «V.Shimanovsky UkrRDISteelconstruction»*

44, Fontannaya Str., Makeyevka, Ukraine

The article presents a methodological approach to the formation of limit state criteria that allows choosing means and methods of corrosion protection taking into account requirements of structural reliability and safety assurance. Design of corrosion protection for given design cases implies the use of partial reliability factors, which determine serviceability of the structure in normal service during the specified service life. Formulated is the problem of conformity of the design indices of corrosion impacts, primary and secondary protection means, as well as geometric parameters of the design model to the requirements of bearing capacity, serviceability and durability of steel structures. Presented is a logistical structure of constant, temporary and emergency design cases based on corrosion hazard indicators. Performed is a systematized description of standard (basic, characteristic) impacts and representative values of corrosiveness negative factors. Design characteristics of corrosion resistance, durability and serviceability of structures and their protective coatings are determined based on experimental data in accordance with the specified procedure of accelerated and bench tests. In the course of structural design, the level of facility corrosion hazard, classification features of structures and their protective coatings based on criticality rating are taken into account. It is proposed to substantiate design indices of structural durability using the developed procedure, taking into account reliability and availability factors of corrosion protection. Reliability factors of primary and secondary protection take into consideration uncertainty of design models of corrosion hazard in structures and installations. Availability factor of structural steel is taken as a complex index of reparability for analyzing alternatives of structural and process measures of primary and secondary protection. Results of theoretical and experimental substantiation of corrosion hazard criteria are used for developing a system of measures for quality control and safety assurance of steel structures in service.

Electrochemical induced dissolution of silver points in sodium fluoride solution

*Amaral, CCF, Ormiga, F, Ponciano, JAC, Federal University of Rio de Janeiro /
Departament of Metallurgy and Materials, Rio de Janeiro / Brazil.*

Introduction: The removal of silver points from inside the root canal has been a clinical concern to endodontists during endodontic retreatment. Several methods have been described for removing fractured instruments from root canals, however, these methods show different success rates.

Objective: The aim this study was to investigate the effectiveness of the dissolution process of silver points in a sodium fluoride solution.

Materials and Method: We evaluated the anodic polarization curves of the silver flat electrode and the redox curves of the solution NaF 12g/L at pH=5.0. After the tests silver points with size 30 were submitted to anodic polarization at $+0.5 V_{SCE}$ in the solution test for 4 minutes. The mass and length of each silver points were calculated before and after the tests. The morphological alterations of the tested silver points were evaluated by optical microscopy.

Results: The redox curve showed a current density of 0.4 mA/cm^2 until an anodic potential of approximately $+1.05 V_{SCE}$. Through the redox curve we observed that the material presented active dissolution below the oxidation potential of the solution, which indicated the oxidation silver without occurrence of side electrochemical reactions. The anodic polarization curves showed current values of $+0.5 V_{SCE}$ near to the corrosion potential and current values of potential between $+0.2$ and $+0.4 V_{SCE}$, from which a significant increase of current, indicating generalized dissolution of silver in NaF 12g/L solution. In the amperometry tests it was observed that the initial anodic current reached was about 1000 mA, and after 1 minute of testing, the current drops sharply and becomes constant until 4 minutes, indicating an active dissolution of the silver point in 1 minute.

Conclusion: The results of this study demonstrated that the concept for the removal of silver points in the root canals by electrochemical process can be used to remove silver fragments during an endodontic retreatment.

Corrosion resistance of ternary Ni-Ti alloys in 0.9% NaCl solution

Barros, CDR; Ponciano Gomes, JAC

*Federal University of Rio de Janeiro / Departament of Metallurgy and Materials -
LabCorr , Rio de Janeiro / Brazil*

Introduction NiTi shape memory alloys are usually used as biomaterials because of the proprieties of memory effect, pseudoelasticity and good biocompatibility. The literature mentions that ternary elements have been added in order to adjust mechanical and physical properties, such as hysteresis, transformation temperatures and radiopacity for different reasons. However, these chemical composition changes can affect these materials's corrosion resistance. **Objective** This study aims to evaluate the corrosion resistance of binary and ternary alloys NiTi, NiTiCo, NiTiCr and NiTiCu in a simulated physiological environment. The obtained results permit to compare the corrosion behavior of these alloys. **Materials and Methods** Electrochemical impedance spectroscopy and anodic polarization measurements were performed in a 0.9% NaCl solution on NiTi, NiTiCo, NiTiCr and NiTiCu alloys. The electrochemical impedances spectroscopy were measured at OCP within the frequency range of 10 kHz to 10m Hz and with potential amplitude of 10 mV. The anodic polarization tests were performed in a range of 800mV above the corrosion potential using 20 mV/ min scan rate. The parameters used to evaluate the corrosion resistance were the values of the polarization resistance and the passive range, defined as the potential difference between breakdown and open circuit potentials (OCP). Passive current densities within the passive range were considered. **Results** The results showed that the binary alloy showed higher corrosion resistance then ternary alloys, with higher values of R_p and higher ΔE . However, the passive current densities were not significantly increased by the third elements additions. The decrease of resistance to polarization, as well as the decrease in ΔE values can be explained by the changes of passive film composition when a third element is added. **Conclusion** These results show that any positive effects of the third element addition must consider their adverse influence on corrosion resistance in simulated physiological environment.

Thermogravimetric study of hydrogen uptake and desorption in titanium alloys

Vincent DUQUESNES, Université de Bourgogne - ICB, Dijon – France

Nicolas CRETON, Université de Bourgogne - ICB, Dijon – France

Tony MONTESIN, Université de Bourgogne - ICB, Dijon – France

Elise DELOYE, Vallourec Heat Exchanger Tubes, Venarey-les-Laumes – France

Keywords: thermogravimetric analysis, titanium hydrides, hydrogen diffusion, XRD

Over recent years, titanium has been increasingly used in several industrial fields, such as biomedical implants, structural material in aeronautics, production of energy, chemicals, military applications, luxury products... thanks to a good resistance to corrosion -even in severe conditions- and a low density leading to high specific strength.

Enlargement of the use of titanium and its alloys have highlighted new industrial issues and new technological challenges, especially given the sensitivity of titanium to the diffusion of interstitial light elements, which can cause hardening and embrittlement of the material, even at low contents.

At room temperature, pure titanium shows an alpha hexagonal close-packed crystal structure which transforms into a beta body-centered cubic structure above 882°C. This transition temperature can be increased or lowered with alloying elements. As an alloying element, hydrogen can be described as a beta-promoting element, meaning that hydrogen solubility is higher in beta than in alpha phase and the alpha-beta transus temperature decreases as the hydrogen level increases.

Below 100°C, hydrogen absorption and diffusion in titanium is considered as negligible and has no significant influence on the behaviour of the material. Beyond this temperature, hydrogen absorption can happen and depends on many parameters: temperature, pressure, surface strains and dislocations, properties of the passive layer.

This study deals with commercially pure titanium, especially the Ti40 grade, and the determination of the kinetics of hydrogen absorption, diffusion and desorption between 200 and 350°C. Hydrogen uptake has been followed by thermogravimetric analysis (TGA) with different atmospheres and hydrogen partial pressures, and the formation of titanium hydrides has been verified by XRD and XPS analyses. SEM has also been performed to characterize hydridated titanium microstructure.

Corrosion behavior of 18Cr-18Mn hot forging steel

A.Torres-Islas^a, R.Reyes-Hernandez^b, S.Serna^b A.Bedolla^c Lucio-GarciaM.A^b and J.Colin^a,

^aUniversidad Autónoma del Estado de Morelos (UAEM), Facultad de Ciencias Químicas e Ingeniería, PE. Ing. Mecánica, Av. Universidad 1001, Col. Chamilpa, 62209 Cuernavaca, Morelos, México

^bUAEM, Centro de Investigación en Ingeniería y Ciencias aplicadas (CIICAP) Av. Universidad 1001, Col. Chamilpa, 62209 Cuernavaca, Morelos, México

^c Instituto de Investigaciones metalúrgicas Universidad Michoacana de San Nicolas de Hidalgo Gral.Francisco J. Mugica S/N Felicitas del Rio 58030 Morelia Michoacan, México.

Abstract

A new 18Cr-18Mn alloy steel was developed by induction furnace melting process in accordance with requirements of industry of energy turbogenerator manufacturing. The steel were developed to increase corrosion and mechanical resistance of retaining rings. Their corrosion behavior were assessed by potentiodynamic polarization, electrochemical impedance spectroscopy and electrochemical noise techniques. In addition, nitrogen effect on corrosion resistance was study by inoculated via plasma. The highest corrosion resistant, were attributed to the nitrogen content and steel composition. Their corrosion, properties were due to chemical stability, high lattice order, structural state of the passive film and the ability to prevent diffusion of metal ions. Also, the nitrides in surface tend to prevent the corrosive pits from growing up.

Evaluation of the pitting corrosion on an AISI 304 using Scanning Electrochemical Microscopy

R. Sánchez-Tovar, R. Fernández-Domene, J. García-Antón

Ingeniería Electroquímica y Corrosión. Departamento de Ingeniería Química y Nuclear. Universitat Politècnica de València, C/ Camino de Vera s/n, 46022 Spain

Pitting corrosion is a localized type of corrosion commonly observed on stainless steels due to the presence of aggressive ions, such as chlorides. Scanning electrochemical microscopy (SECM) has become a powerful technique for quantitative investigations of interfacial physicochemical processes, in a wide variety of areas. In particular, SECM permits studying the formation and evolution of stable pits by monitoring the currents arising from them.

In this work, the evolution of pits formed on AISI 304 stainless steel has been evaluated. Pits were generated on a passivated AISI 304 surface by applying an anodic potential of 350 mV_{Ag/AgCl} in a 0.2 M sodium chloride solution. The faradic current was measured while a 25 μm -platinum tip scanned over the stainless steel surface. Oxygen was used as intermediate.

Figure 1 shows an image obtained in situ by SECM of the pit formed on the stainless steel surface. According to the results, currents obtained by SECM vary due to the pit evolution (Figure 2).

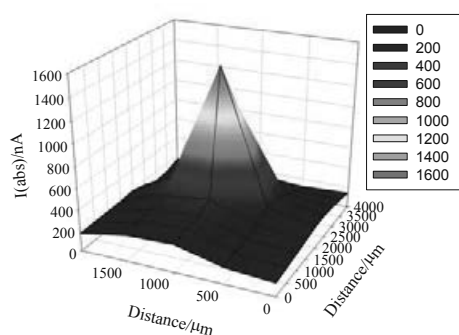


Figure 1. Image of a pit formation on the AISI 304 characterized using SECM.

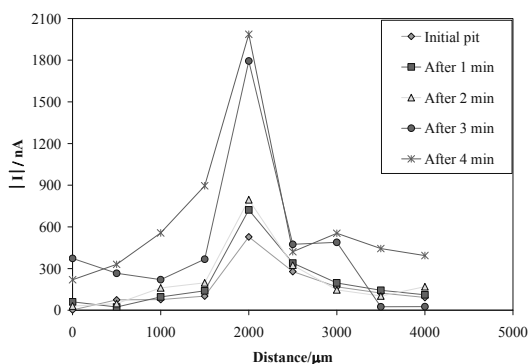


Figure 2. Evolution with time of a pit formed on the AISI 304 characterized using SECM.

Acknowledgements. We wish to express our gratitude to the Generalitat Valenciana for its help in the SECM acquisition (PPC/2011/013) and to Dr. Asunción Jaime.

Influence of submarine emissions from El Hierro volcano (Spain) on the corrosion resistance of stainless steels

R.M. Fernández-Domene, R. Sánchez-Tovar, C. Escrivà-Cerdán, R. Leiva-García, J. García-Antón, *Ingeniería Electroquímica y Corrosión (IEC), Universidad Politécnica de Valencia, C/ Camino de Vera s/n, 46022 Valencia, Spain (e-mail. jgarciaa@iqn.upv.es).*

Last 10th of October of 2011 a volcano erupted in the Atlantic Ocean near the island of El Hierro (Canary Islands, Spain). When a volcano erupts in the sea, it releases solids, thermal water emissions and gases, CO₂ being the main gas (90 %). This could cause a decrease of the seawater pH value and modify the behavior of the materials which are in contact with this medium. This work studies the corrosion behaviour of three different stainless steels (AISI 316, AISI 316L and Alloy 900, a duplex stainless steel) in two different seawater solutions at 25° C: non-polluted and polluted, collected from the El Hierro volcano. Potentiodynamic polarisation curves and impedance measurements (EIS) at open circuit potential (OCP) were performed.

Polarisation results (**Figure 1**) show that the samples immersed in the polluted seawater present higher current density values than those in the non-polluted seawater.

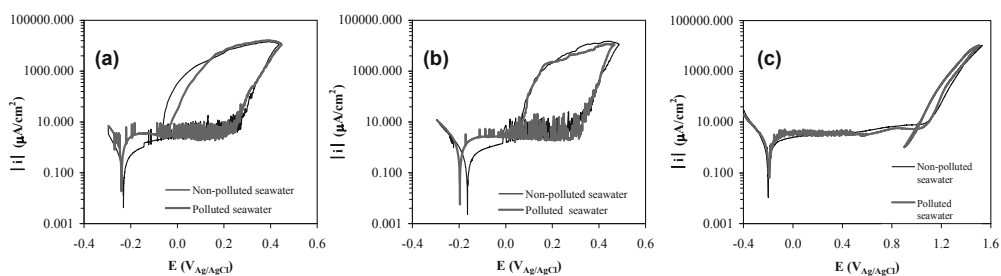


Figure 1. Polarisation curves of (a) AISI 316, (b) AISI 316L and (c) Alloy 900 in non-polluted and polluted seawater.

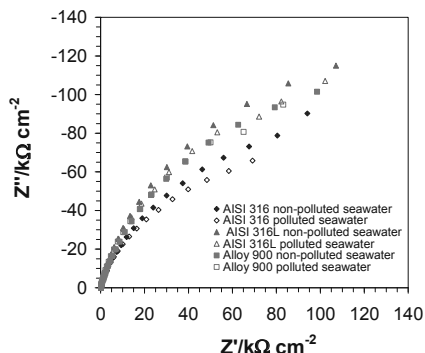


Figure 2. Nyquist plots for the three stainless steels in non-polluted and polluted seawater, obtained at OCP.

From EIS diagrams (Nyquist plots) at OCP (**Figure 2**), it can be observed that the samples immersed in the non-polluted seawater have higher impedance values than the electrodes immersed in the polluted seawater. This indicates worse protective properties of passive films formed spontaneously in the polluted seawater.

Acknowledgements. We wish to express our gratitude to Prof. Dr. Aurora Santos López, Dr. Rosario Lunar Hernández, Dr. Jose Arnoso Sampedro, Dr. Carmen López Moreno, Mr. Humberto Gutiérrez García and Mr. Alejandro Ramos Fernández for their help in supplying both non-polluted and polluted seawater samples, and to Dr. M. Asunción Jaime.

Data processing and data mining applied to Electrochemical Noise technique for Stress Corrosion Cracking recognition

Lucio Bonaccorsi¹, Luigi Calabrese¹, Domenico Di Pietro², Massimiliano Galeano¹,
Edoardo Proverbio¹

*1 Department of Electronic Engineering, Industrial Chemistry and Engineering
University of Messina, Contrada di Dio, 98166 Messina, Italy*

2 GE Oil & Gas, Via F. Matteucci 2, 50127 Firenze, Italy

Abstract

The susceptibility to damage, related to the synergistic action of a stress state and an aggressive environment, is usually assessed, in industrial practice, by means of standard tests that require the use of solutions usually more critical than the expected service conditions. Approaches based on the evaluation of the time to failure, threshold stress or by analyzing the fracture surfaces of the specimens is often insufficient to evaluate the damage steps or to discriminate the activation and propagation processes. The purpose of this work is to help to reduce this lack of knowledge through the use of the electrochemical noise (EN) technique. In particular stress corrosion cracking mechanisms of a precipitation hardening martensitic stainless steel in chloride environment have been studied.

The EN voltage and current trends have been processed both in time and in frequency domain to extract a set of variables useful to characterize the corrosive phenomena. Various processing algorithms have been used for this purpose, in particular by combining FFT, Wavelet, PSD, Hilbert - Huang transform important information about the corrosion progress was obtained. The results were verified by fractographic investigation. A data mining algorithm was finally utilized to extract the useful set of variables that significantly discriminated corrosion progress. So far EN resulted a very powerful technique to recognize corrosive phenomena in a non-invasive way with low computational load.

Keywords:

Electrochemical noise, signal processing, frequency analysis, Hilbert-Huang, Wavelet.

FEM analysis of H-Trapping Diffusion Model in Pipeline Steels

E. Fallahmohammadi, F. Bolzoni, G. Fumagalli, G. Re, L. Lazzari

*Politecnico di Milano. Dipartimento di Chimica, Materiali ed Ingegneria Chimica
"Giulio Natta" Via Mancinelli 7, Milano 20131, Italy*

The permeation of hydrogen into X65 and F22 pipeline steels under different metallurgical microstructure has been investigated in our previous publication [1]. To understand better the hydrogen trapping mechanism of industrial metal and alloys the attempt has been made to uncover the effect of different trapping parameters on hydrogen characteristic permeation curves based upon the obtained experimental results. The mathematical modeling of diffusion plus trapping has been established in past by other authors, however, still prediction of experimental results with the available analytical models is under ambiguity. To born this out, we have built a Finite Element (FEM) analysis of diffusion plus trapping model using the COMSOL Multiphysics 4.3a software. The reversible and irreversible mathematical model of MacNabb and Foster is introduced to the Transport of Diluted Species interface under a time dependent simulation. Then the experimental results were compared with the theoretical one to estimate both the reversible and irreversible trapping parameters.

Keyword: Pipelines, Hydrogen diffusion, Permeation transients, FEM analysis of Hydrogen trapping,

Reference:

- [1] E. Fallahmohammadi, F. Bolzoni, G. Re. G. Fumagalli, L. Lazzari, "Interaction of hydrogen with different microstructure of pipeline steels", Proceeding of EUROCORR2013, Estroil, Portugal 1-5 Sep.2013

Sustainable water and facility management in the steel industry: influence of saline streams on pipeline corrosion

*D. de la Fuente and M. Morcillo, National Centre for Metallurgical Research
(CENIM/CSIC), Madrid, Spain*

P. Ivashechkin, VDEh-Betriebsforschungsinstitut (BFI), Düsseldorf, Germany

V. Colla and T. A. Branca, Scuola Superiore Sant'Anna, Pisa, Italy

M. De Sanctis, Pisa University, Pisa, Italy

B. P. Vivas and M. Cabañas, ArcelorMittal España, Aviles, Spain

A. Rassow, Outokumpu Nirosta GmbH (OTKN), Düsseldorf Germany

C. Lucca, (ILVA S.p.A), Taranto, Italy

Several streams with increased salt concentration can be identified in the steel plants: cleaning waters from blast furnace and basic oxygen furnace, cooling water in hot rolling and continuous casting, process water from pickling lines, etc. These high concentrations of salts represent a considerable problem for the environment and effective operation of cooling circuits and the sewer system.

Therefore, the development of innovative concepts for sustainable water and facility management, on basis of selective salt elimination techniques with integrated salt valorisation is an important goal for the European Steel Industry and it has been the main objective of the SELSA project, carried out with a financial grant of the Research Programme of the Research Fund for Coal and Steel (RFCS).

These innovative concepts aim to reduce steel industry impact on workers health and the aquatic environment, save natural resources, reduce fresh water costs and waste water discharge costs by process water reuse and, of course also, to prolong pipes service life, reducing corrosion and scaling, because besides negative effects on the environment, salts in process waters can cause corrosion of equipment, defects on the product surface, reduction of pipe service life, etc.

In this way, a laboratory study to evaluate the effect of different saline streams on pipeline corrosion has been carried out. Both, process waters (gas cleaning from blast furnace and basic oxygen furnace and cooling water from hot rolling) supplied by different steel companies, as well as, artificially prepared waters with different saline compositions, have been tested in a set of closed circuits. Corrosion rates on carbon steel pipe samples after different exposure times have been measured by gravimetric mass losses. The effect of different parameters, such as, dissolved oxygen content, exposure time, flow rate, temperature, application of different water treatments for salt elimination, etc. has been also assessed. Additionally, different anticorrosion and protection methods (cathodic protection, additions of antiscaling agents and corrosion inhibitors) have been also evaluated. Surface and in cross-section characterization (Optical Microscopy, Scanning Electron Microscopy with X-ray microanalysis and X-Ray Diffraction) of exposed steel pipe pieces has been also carried out.

The results show that the $[Ca^{2+}]$ and $[HCO_3^-]$ content seems to have more influence in decreasing the corrosion rate, due to the formation of protective scales, than the expected increase produced by raising $[Cl^-]$ or $[SO_4^{2-}]$ content. Therefore, after the application of a salt reduction treatment, such as, ion exchange, reverse osmosis, etc. and specially in the case of a fresh steel pipe, without a protective previous scale, the $[Ca^{2+}]$ and $[HCO_3^-]$ should be increased or a corrosion inhibitor agent should be added in order to avoid high corrosion rates on the fresh steel.

Corrosion behavior of tungsten heavy alloys in different aqueous solutions

Z. Abdel Hamid¹ and H. B. Hassan²

¹Corrosion Control and Surface Protection Laboratory, Central Metallurgical R&D Institute, CMRDI, Helwan, Cairo, Egypt

²Faculty of Science, Department of Chemistry, Cairo University, Giza, Egypt

ABSTRACT

Tungsten heavy alloys (WHAs) are kind of composite materials; these alloys provide a unique combination of properties such as high density, excellent mechanical properties and good corrosion resistance that making them increasingly attractive in many practical applications. In this work, the corrosion behavior of the investigated tungsten heavy alloys with the composition of (95% W–3.5% Ni–1.5% Fe), (93% W–4.5% Ni–1.0% Fe–1.5% Co) and (90% W–6% Ni–4% Cu) fabricated by either chemical or mechanical technique has been evaluated through potentiodynamic polarization measurements in different aqueous solutions of 0.6M NaCl, 0.1M HCl and 0.1M NaOH. The extent of the corrosion has been illustrated by examining the surfaces of WHAs before and after the corrosion test using SEM. It includes general dissolution, localized attack of the binder phase and tungsten grain loss, where the extent of each of these depends on the fabrication technique and the alloy composition as well as the pH of the medium.

Influence of intermetallic phase content and microstructure on pitting potential of a duplex stainless steel

Daniella Caluscio dos Santos, Rodrigo Magnabosco, FEI, São Bernardo do Campo/Brazil

This work analyses the influence of the intermetallic phase content (sigma and chi phases) and the related microstructures on the pitting potential of a UNS S31803 duplex stainless steel (DSS). The as received material, solution-treated for 30 min at 1175°C and presenting 57% ferrite and 43% austenite phases, was aged at 750°C, 850°C and 950°C for periods up to 360 h, in order to achieve different amounts of sigma and chi phases, with distinguished morphologies in different temperatures, since intermetallic phases developed a lamellar structure at lower aging temperatures and massive morphology at 950°C.

Volume fraction of intermetallic phases was determined through quantitative stereology over backscattered electron images obtained in a scanning electron microscope, and pitting potential (Epit) was determined after cyclic potentiodynamic polarisation in 3.5% sodium chloride (NaCl) solution, using a saturated calomel electrode as reference electrode, a platinum wire as counter-electrode and polished samples of the DSS in the different heat treatment conditions.

It was found that large amounts of intermetallic phase (higher than 15% volume fraction) leads to reduction of Epit, and very small amounts of intermetallic phase formed at 750°C also leads to significant Epit reduction, as shown in Figure 1. However, at 950°C and 850°C, intermetallic phase formation lower than 10% volume fraction did not promote significant Epit reduction, and this is probably associated to the possibility of Cr and Mo redistribution in higher temperatures.

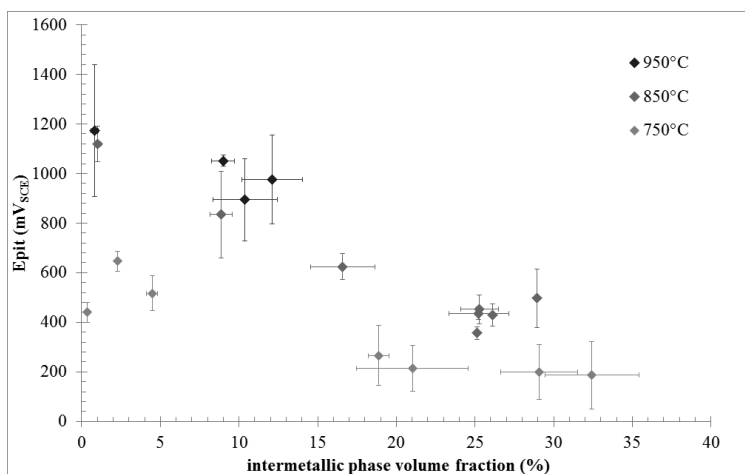


Figure 1. Pitting potential in 3.5% NaCl solution as a function of intermetallic phase volume fraction in the studied steel.

Evaluation of elemental sulfur role on brittle failure in sour brine environment

Marco Anselmi², Lucio Bonaccorsi¹, Luigi Calabrese¹, Filippo Cappuccini², Angela Capri¹, Angelo Donato², Edoardo Proverbio¹

*1 Department of Electronic Engineering, Industrial Chemistry and Engineering
University of Messina, Contrada di Dio, 98166 Messina, Italy*

2 GE Oil & Gas, Via F.Matteucci 2, 50127 Firenze, Italy

Abstract

In the recent years the formation of the so-called elemental sulfur deposits, coming from high pressure-temperature sour (H₂S containing) gas, on oil & gas mechanical components (pipeline, valves and other facilities), has become quite widespread. This event has been considered as the cause of unexpected brittle failures of stressed components, whose material had been regarded as resistant to sour condition, having passed sulphide stress corrosion cracking (SSC) test, performed in declared working conditions.

Aim of this work was to define a set-up for SSC test with elemental sulfur addition to sour brine solution in accordance with National Association of Corrosion Engineers (NACE) specifications. The design of this test will be useful to evaluate the behavior of corrosion resistant alloys (CRAs) used in oil & gas applications where elemental sulfur presence has been observed.

Exposition tests were performed and on the basis of obtained results a sour corrosion mechanism in presence of sulfur was proposed (consulting also literature information on this issue).

Keywords:

elemental sulfur, sour gas, sulphide stress corrosion cracking, mechanisms, corrosion-resistant alloys

Quantum Chemical Study of Adsorption of Organic Inhibitors of Corrosion of Al on Al₂O₃ and Al(OH)₃ Surfaces

Georgiy S. Beloglazov*, Sergey M. Beloglazov

Baltic Federal university. Kaliningrad, Russia;

*The University of Dodoma. Dodoma, Tansania, drgeorge59s@gmail.com

Seven organic inhibitors (Inh, see Table 1) were studied using quantum chemistry [1] MNDO computations of (a) their free isolated molecules (FIMs), (b) model clusters containing each of the FIMs + Al₂O₃ finite fragment (in fact represented by "Al₈O₁₂" that was found to be geometrically sufficient for the "flat" oxide area coverage by an Inh molecule), and (c) model clusters containing one (each) of the FIMs + Al(OH)₃ fragment.

Table 1

Studied Inh	Angle between the vector of modified dipole moment of the adsorbed molecule and the perpendicular to the model plain $\alpha, ^\circ$		Change of the module of dipolar moment of the Inh molecule on its adsorption on the model fragment $\Delta p_{ad} = p' - p_0, D$
	QCD1: $\alpha, ^\circ$ (Al ₂ O ₃ plain)	QCD2: $\alpha, ^\circ$ (Al(OH) ₃ plain)	QCD3: Δp_{ad} for Al ₂ O ₃ surface
Phenol	83.2	80.9	1.203
Paracetamol	46.2	46.3	1.251
o-nitrophenol	71.9	96.0	0.697
α -dinitrophenol	74.5	71.2	0.218
Oxyphenyldiantipilmethane	56.8	54.7	57
Salicylic acid (stimulator)	128.4	124.1	-0.401
Phenolphthalein	74.5	67.6	3.682

Apart from the data given above, other Quantum Chemical Data (QCD) have been tested such as ΔQ_{ad} (net charge sum appearing on the whole of the adsorbed Inh molecule) and $\Delta q(O)_{ad}$ (algebraic changes of the charges on the oxygen atom of the adsorbed Inh molecules) but the corresponding values of correlation coefficients r were also insignificant ($|r| < 0.5$) for both Al₂O₃ and Al(OH)₃ (as in the case of Δp_{ad}):

Table 2

Correlation coefficients between QCD and experimentally measured corrosion Inh efficiencies (IEC) at concentrations, mMol/L:	QCD1: α for Al ₂ O ₃ surface	QCD2: α for Al(OH) ₃ surface	QCD3: Δp_{ad} for Al ₂ O ₃ surface
1	-55 %	-46 %	0 %
5	-67 %	-58 %	21 %
10	-68 %	-67 %	30 %
15	-74 %	-73 %	37 %

However the correlation between the change of the module of dipolar moment of the Inh molecule on its adsorption on Al₂₀ model fragment and IEC was found to be significant for the case of quantum chemical cluster study of adsorption of the same 7 species on "pure" Al₂₀ model fragment. The dipolar moment of Inh FIM itself (and some other QCD) also strongly correlates with Corrosion Inhibiting Efficiencies (IEC) [2] measured experimentally for "D16" Al alloy exposed to Postgate B media under the presence of sulfate reducing bacteria.

References: [1] Gaussian 94 // Revision E3 / M.J. Frisch, G.W. Trucks e.a., Gaussian, Inc., Pittsburgh PA. 1995. [2] G. Beloglazov. Organic inhibitors of corrosion of metals and hydrogen absorption by steel: quantum chemical approach to explaining their adsorption and protective action // Saarbrücken: Lambert Academic Publishing. ISBN 978-3-659-39656-4. 2013. – 67 p.

A probabilistic model for localized corrosion on a metallic pipe under D.C. stray current influence

Giovanni Lucca, SIRT I S.p.A, Via Stamira d'Ancona 9, 20127 Milano, Italy

E-mail: G.Lucca@sirti.it

Purpose of the paper is to present a model of localized corrosion attack on a metallic pipe under the influence of D.C. stray current typically produced by electrified traction lines (railway, subway, etc.).

The model, that is focused only on the corrosion produced by stray current, can be used in order to estimate the perforation time of the pipe wall; the knowledge of such a result can be helpful, especially at the design stage, of new D.C. traction lines and/or new pipelines.

We suppose that the corrosion process occurs and starts at the location of a holiday in the insulating coating of the pipe and evolves along the surface of a cone having the base given by the holiday area A and height H growing with the time. See Fig.1.

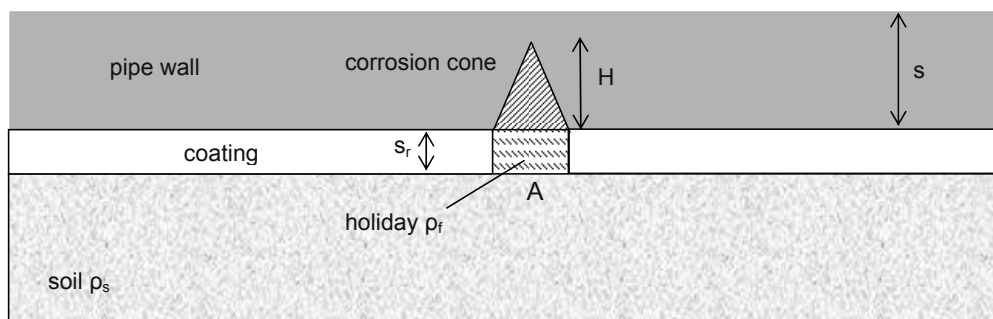


Fig.1: Sketch of the holiday inside the coating and of the corrosion cone in the pipe wall.

The corroded mass is shown to be related to the pipe-soil potential shift produced by the stray current and to geometrical and physical parameters like soil resistivity ρ_s , pipe thickness s , magnitude of holiday area A and others; in particular, a formula relating the height of the cone H with the time t is proposed. From such a formula, one can deduce the corrosion velocity by considering the time derivative of H with respect to the time.

As far as the holiday area A is concerned, we have to remark that it strongly influences the corrosion time and the corrosion velocity as well; nevertheless, such a quantity has, without any doubt, the characteristics of a random quantity; thus, the corrosion time and the corrosion velocity have random characteristic too.

Starting from experimental data coming from the field that are at our disposal, we showed, in a previous work [1], that the probability density distribution of the holiday area A can be approximated by a log-normal distribution. Consequently, we can

deduce analytical formulas for the probability distributions of the corrosion time and of the corrosion velocity. Figs.2 and 3 show examples of such distributions for different values of the potential shift ΔU produced by the stray current.

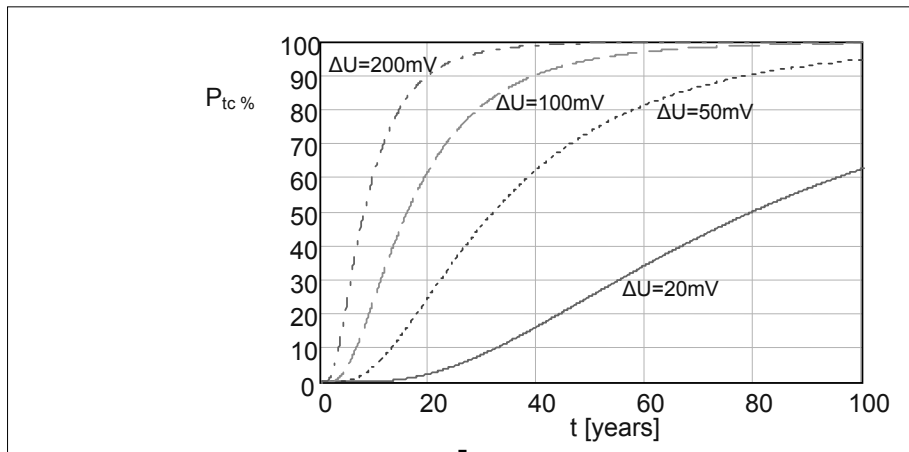


Fig.2: Probability of having a corrosion time less than the value shown in abscissa for different values of pipe-soil potential shift.

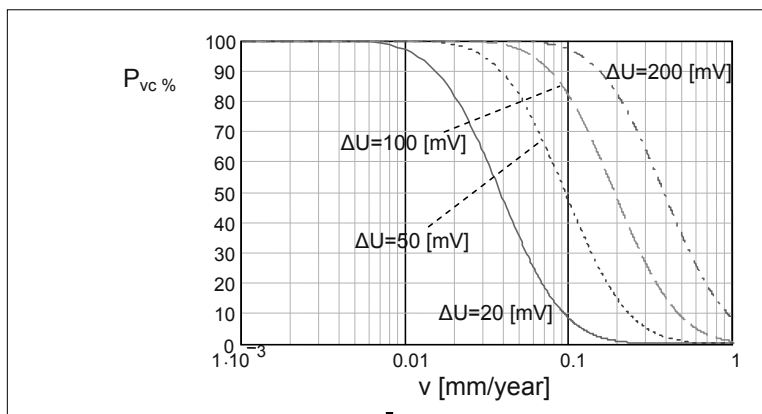


Fig.2: Probability of having a corrosion velocity exceeding the value shown in abscissa for different values of pipe-soil potential shift.

Results like the ones shown in Figs. 2 and 3 can be useful in assessing the D.C. stray current impact on pipes located in proximity of electrified traction lines or other sources of D.C. electric field in the soil.

- [1] G. Lucca, L. Di Biase, M. Moro: "A. C. corrosion on buried pipelines: a probabilistic approach", Proc. of 6th CEOCOR Int. Cong. Giardini Naxos (Messina), Italy, 2003.

The kinetic during atmospheric corrosion of a nickel cathode

Stefan Wibiha, CEST, Wr. Neustadt/Austria

The passivity of the nickel electrode was widely studied over the last century. After chromium it is the second most important alloying agent with an amount of 8% up to 25% in most stainless steel types and nickel plating is often used to increase the corrosion resistance of a substrate.

The Ni/Ni²⁺ redox couple has a standard electrode potential of -0.23 V vs. SHE which is relatively noble especially compared to the Fe/Fe²⁺ redox couple (-0.41 V) or the Cr/Cr²⁺ redox couple (-0.91 V). For this reason and according to mixed potential theory it can be assumed that nickel acts mainly as a cathode when it is in contact with less noble materials (for example iron or chromium on a stainless steel surface).

The main cathodic reactions in atmospheric corrosion are the oxygen reduction (ORR) and the hydrogen evolution (HER). Under neutral conditions the hydrogen evolution does not depend on the mass transport and can be described by a simple Tafel equation. The oxygen reduction on the other hand is a much more complex reaction. Prior to reduction the oxygen must be transported to the nickel surface where it can then be reduced to hydrogen peroxide or hydroxide. The increase of the pH near the surface further complicates the clarification of the mechanism. For these reasons a rotating ring disc electrode was used. By this method the mass transport can be controlled and the reaction products can be detected by the ring. Measurements at a nickel disc combined with a platinum ring electrode at different rotation rates between 100 rpm (63 μ m diffusion layer) and 2000 rpm (14 μ m diffusion layer) were carried out. As electrolyte a 0.1 mol L⁻¹ and a 0.6 mol L⁻¹ sodium chloride solution saturated with air and deaerated with nitrogen were used.

The kinetic data were determined using the Tafel and the Levich equation. The whole polarization curves of the disc electrode were modelled by a modified Butler-Volmer equation including the diffusion limiting current.

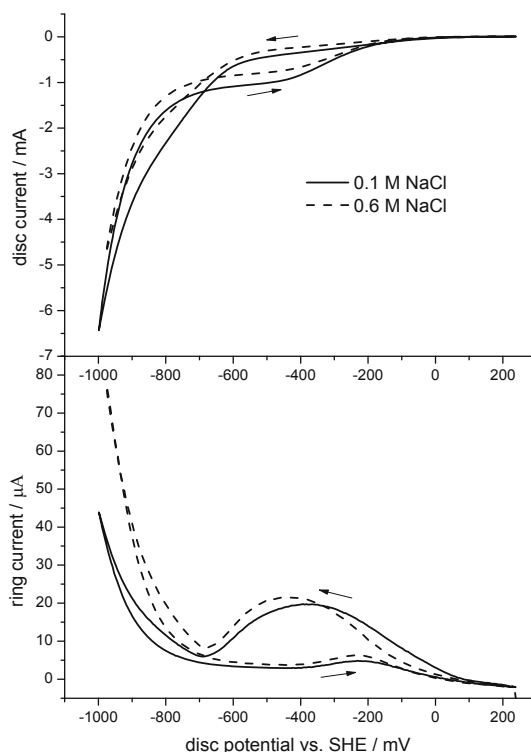


Figure 1: RRDE measurements on a Ni-disc at 1000 rpm in 0.1 M NaCl (solid lines) and 0.6 M NaCl (dashed lines) and a Pt-ring at +550mV vs. SHE

Hlfabar as effective environmentally friendly corrosion inhibitor for zinc metal in different aqueous solutions

O. A. Abdullatef, Pharos University, Alexandria/Egypt

B. A. Abd-El-Naby, Alexandria University, Alexandria/Egypt

Abstract

The inhibitive effect of Hlfabar extract on the corrosion of zinc in aqueous solution of 0.5 M NaCl, NaOH and H₂SO₄ were investigated at 30 °C by potentiodynamic polarization and electrochemical impedance spectroscopy (EIS) techniques. Potentiodynamic polarization curves indicated that hlfabar act as mixed type inhibitor in neutral medium, cathodic in alkaline medium and anodic in acidic medium. EIS measurements showed that the total resistance and consequently the inhibition efficiency increase with increasing concentration of hlfabar indicating the inhibitive effect of this extract on zinc corrosion in different media. The inhibition of the extract was assumed to occur via adsorption of active ingredients on the metal surface. Theoretical fitting of different isotherms, Langumir, Florry-Huggins and the Kinetic-Thermodynamic model were tested to clarify the nature of adsorption.

Study of the influence of the different percentages of sigma phase in the resistance to pitting corrosion of a duplex stainless steel

Gorka Argandoña, Cemitec, Pamplona/España; María Biezma, Universidad de Cantabria, Santander/España; Carlos Berlanga, Universidad Pública de Navarra, Pamplona/España; P. Linhardt, Vienna University of Technology, Vienna/ Austria

Duplex stainless steels are increasingly used in various industrial sectors such the petrochemical and offshore, due to its excellent mechanical and corrosion resistance.

Due to the presence of high alloy content, the duplex stainless steels tend to form numerous phases and intermetallic compounds, being the sigma phase one of the most relevant, whose range of nucleation and growth is found at high temperatures (600 - 900 ° C). This phase is very harmful since decrease critically the localized corrosion resistance.

So far, there have been numerous studies focused on analyse the influence of elevated percentages of sigma phase with the localized corrosion resistance of stainless steels duplex, but few studies that have examined in detail how the presence of low percentages of sigma phase affects that property.

In this work, it has been thermally treated seamless tubes super duplex UNS S32760 to induce the formation of different percentages of such sigma phase (0 - 20%). Samples with and without sigma phase have been tested using electrochemical and immersion techniques in order to evaluate the localized corrosion resistance. Thus, the objective has been to relate the influence of different percentages of sigma phase with resistance to pitting corrosion in the super duplex UNS S32760.

Corrosion awareness education a key for a better environment.

A. Eliezer, G. Hays, E.H. Han, E. Leining, W. Burns

World Corrosion Organization, P.O.B. 2544, New-York. U.S.A

Corrosion affects the lives of every person, often significantly. If not controlled, the consequences of corrosion can be disastrous for human health and safety and the environment. The key to addressing corrosion is, in fact, to increase awareness of the issue. As long as modern life develops, corrosion costs will exist; therefore, the main challenges are to increase the awareness of corrosion costs among governments, define international corrosion standards, promote corrosion prevention world-wide, and incentivise corrosion prevention activities by government agencies, corporations and research organisations. For example to achieve longer-term cost savings there has also been growing use of assessment tools to predict maintenance schedules based on past performance. “Previously, paint on bridges, for example, was automatically done at a set period of time and all parts were coated. Today, owners are looking to paint assets on a schedule that prevents significant corrosion, and if corrosion occurs, to target the repair of only the sites that require repainting. In order to achieve such goals corrosion education awareness suggested program should be applied within high school students and especially focus on undergraduate students. The program also suggests including innovative thinking skills and entrepreneurship education due to the need of creative innovative tools and systems in order to apply advanced corrosion prevention technology.

Corrosion Education: Present and Future

Alec Groysman

Israeli Society of Chemical Engineers & Chemists, Tel Aviv, Israel

Technion, Haifa, Israel

E-mail: alecgroysman@gmail.com

Background: What will be in shortage in the near future? Skilled knowledgeable specialists! There is need for knowledge transfer. One can see the aging of the workforce in any country. The number of elderly experts after the age of 60 is increasing while the influx of young people (at the age of 25-30) who would have to become experts is decreasing. The interest of young people to study technical subjects is reduced. What is the place of (corrosion) engineer in our society? How the engineer must be tomorrow? How can engineers use art, history and philosophy in their inspiration and creativity? Thus we should explain how humanitarian aspects can be used in engineering education. We speak about interdisciplinary and humanitarian thinking of engineers.

Aim: To show how humanitarian aspects and interdisciplinary communication can help in corrosion engineering education. The philosophy of my work is establishing of interrelationships between humanitarian aspects, corrosion engineering and science, studying new inspirations and creativity in corrosion engineering, in order to show the young generation of engineers and educators how learning, education and our very existence may be interesting, fascinating, creative, productive, exciting, attractive, rich, and as a result beautiful.

Methodology: The examples of use of different humanitarian disciplines (art: music, painting, literature, poetry, sculpture; history; philosophy) in curricula of corrosion science and engineering, are shown. Interdisciplinary communication between exact sciences as well between corrosion engineering and humanitarian disciplines were used. Analogies, interrelations, metaphors, comparison, logics and intuition, common aspects and differences between humanitarian and engineering disciplines are used in corrosion engineering education for students.

Results: Students and young engineers who received explanations of corrosion engineering in interaction and communication with humanitarian aspects showed more creativity and satisfaction in their job, progress, further studying, and life. They have another approach to apprehending of engineering disciplines and very existence which is now seems beautiful.

Conclusions: Humanitarian aspects and interdisciplinary communication should be more and more included in corrosion engineering education, namely we can talk about "beautifying" engineering. Learning and education of students and educators using humanitarian disciplines results in attractiveness of corrosion engineering, their beauty, inspirations and creativity of young generation of corrosion engineers. We should strive to educate polyfunctional, diversified and multiform cultural corrosion engineer. The results are summarized in the books "*Corrosion for Everybody*" and "*Corrosion in Systems for Transportation and Storage of Petroleum Products and Biofuels*" published by Springer.

Keywords: corrosion education, humanitarian aspects, interdisciplinary communication.

Corrosion Education in the framework of Knowledge Management

Giovanna Gabetta, Eni E&P, Italy

ABSTRACT

With the increase both in quality and in quantity of the information systems and tools, the amount of information available to scientists and engineers is increasing at a speed that was not conceived until a few years ago. The complexity of the scenario makes quite difficult to take all the possible advantages of the increasing amount of knowledge available. Organizations and companies worldwide are facing with:

- (a) increasing amount of information available;
- (b) increasing number of people with high education,
- (c) increasing complexity of the problems to be solved.

The necessity of knowing and processing such a complex of data and problems is in conflict with the ability of a single human brain. There is a need for exploiting the existing knowledge with Information and Communication Technology (ICT) tools to support team work and networking, taking advantage of people's experience and worldwide cooperation. There is also a need of a big cultural change to promote a better use of all the intangible resources. The complete process can be defined in the frame of a Knowledge Management system.

As a consequence, the author of this presentation will try to figure out the way forward for corrosion education, taking into account the new scenario of knowledge. Not only the basic knowledge of corrosion processes is necessary, but the use of advanced tools and how to take advantage of them is of paramount importance. Basic notions must be at hand, and networks of data and tools and people shall be exploited. The challenge is very big, and the feeling is that our ability to work profitably and reliably is now under test.

The way to teaching corrosion based on visual inspection:
student's opinions

Maria Victoria Biezma¹, Sonia Braunstein Faldini²

¹*Universidad de Cantabria, Santander, Spain.*

²*Universidade Presbiteriana Mackenzie, São Paulo, Brazil*

This paper collected the student's opinions about practical lectures that point out visual observation of corrosion problems in real conditions, attending the particular topic of corrosion in Engineering courses, as Grade, Master as PhD. In order to impart the practical lectures, two methodologies of looking at a problem of corrosion were applied: the first one is a teacher-student interaction during walking aimed at the discovery in situ of corroded metallic structures and a discussion regarding to it and the second one is exclusively directed to the student, who will identify situations of corrosion in the workplace, at home or on the street; the student works alone and had to defend his opinion suggesting what kind and the potential causes of corrosion observed. The student also proposes solutions to minimize corrosion and finally argues with the teacher. The high level of participation has provide the choice to establish a representative idea of the learning method based of the use of this sense: visual inspection. The possibility to define a short and clear survey has helped to obtain high level of participation and excellent successful learning process for our students, all related to Materials and Engineering Science, i. e. Chemist Engineering, Mechanical Engineering, Marine Engineering, etc. They also comment that this type of class allowed a better understanding of the corrosion theory.

Corrosion test rig for the amelioration of the service life of industrial components

Manuela Franchi - Tetra Pak Packaging Solutions, Modena (Italy)

Ranieri Cigna - Isproma, Rome (Italy)

Osvaldo Fumei - Isproma, Rome (Italy)

Pietro Pranovi - Ecor Research, Schio (Vicenza)

Corrosion tests should be performed in an environment that reproduces actual working conditions; therefore, a test rig has been designed and built for studying and increasing the service life of a sophisticate filling machine for food products.

The corrosion test rig is composed of three sections, each consisting of a loop, containing corrosion specimens and measuring devices, where the fluids, fed by metering pumps, can be circulated, sprayed or dripped by means of a suitable systems. The first section is devoted to the study of the influence of the hydrogen peroxide concentration and temperature.

The second section is devoted to the study of the influence of the cleaning solutions (acid and alkaline), of the temperature and of the mains water characteristics (in particular chlorides and hardness) used for the dilution of the chemicals.

The third section is devoted to the study of the influence of the detergent agent, of temperature and of mains water characteristics.

The influence of the various parameters on the crevice and pitting corrosion behavior of the metallic materials to be tested will be evaluated by visual examination and local corrosion potential measurement. The generalized corrosion rate will be measured by the polarization resistance technique.

The operation of all loops is controlled by a computer where switches and components icons on screen allow the operator to maneuver and manually select the desired operation.

Potential ennoblement of stainless steel in tropical seawaters

D. Thierry¹, N. Larché¹, Sudesh L. Wijesingue² and S. Teo³

French Corrosion Institute, Brest, France

SIMTECH, Singapore

NUS, Singapore

Abstract

Stainless steels are widely used for different applications in seawater in the oil and gas and desalination industry. It is well known that the corrosion potential of stainless steel shifts to the noble direction (ennoblement) when exposed to natural seawater. The other significant effect of the biofilm on metallic surfaces is a dramatic increase of the cathodic efficiency (e. g. cathodic reduction of dissolved oxygen), promoting the corrosion reactions and increasing the rate of corrosion propagation. Although, this has been widely studied in cold and temperate natural seawater, very little is known for tropical seawater. In this work, potential measurements have been performed on different stainless steels in Singapore. The crevice corrosion susceptibility of different stainless steel has also been determined. Measurements have been completed by biofilm analyses performed on stainless steel surfaces during potential ennoblement. Finally the temperature limit of potential ennoblement has been determined in the tropical seawater of Singapore.

Effect of residual chlorine on the spontaneous potential of stainless steels in seawater

*Hiroshi Yakuwa, Matsuho Miyasaka, Ebara Corporation, Fujisawa/Japan;
Nobuyasu Shinoda, Yoshiro Kuriki, JFE Techno-Research Corp., Yokohama/Japan;
and
Jun'ichi Sakai, Waseda University, Tokyo/Japan*

Background

Spontaneous potential (E_{sp}) of stainless steels in raw seawater becomes noble by influences of aerobic microorganisms. Therefore the possibility of crevice corrosion and pitting corrosion becomes high in raw seawater compared to in artificial seawater. However, it is said that it is difficult to reproduce ennoblement of the spontaneous potential by laboratory testing even if transported seawater is used. On the other hand, usual industrial plants using seawater as cooling water or processing water often adopt chlorine treatment to avoid attaching shellfishes or marine creatures to the equipment in the plants. The residual chlorine has an effect of reducing the activity of microorganisms. At the same time, it also has an effect of accelerating corrosion because of an oxidant. In this paper, the experimental method was examined to reproduce ennoblement of the spontaneous potential of stainless steels in a laboratory. Further, change of the spontaneous potential of stainless steels was also studied by adding the residual chlorine in seawater.

Summary

Biofilms grew on the surface of stainless steels and the spontaneous potential became noble by immersing in transported seawater which includes sea creatures like crabs for a long term. Though the spontaneous potential of stainless steels became less noble by adding the residual chlorine of 0.2 mg/L (Figure 1), it became noble followed by the chlorine concentration when adding more than 2.0 mg/L (Figure 2). It is indicated that ennoblement of the spontaneous potential of stainless steels and the possibility of crevice corrosion and pitting corrosion can be reduced by adding residual chlorine with appropriate concentration in raw seawater.

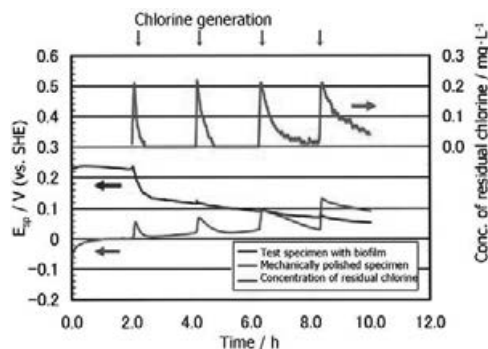


Figure 1 Changes of E_{sp} of a stainless steel by adding chlorine of 0.2 mg/l in transported seawater.

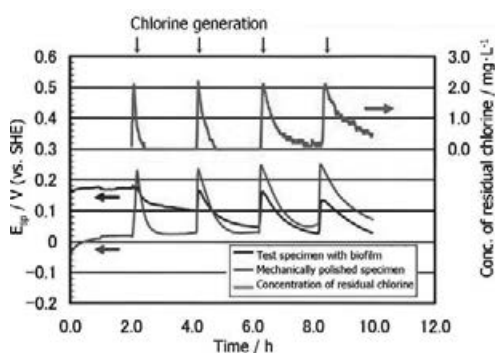


Figure 2 Changes of E_{sp} of a stainless steel by adding chlorine of 2.0 mg/l in transported seawater.

Electrochemical monitoring of damaged thermally sprayed aluminium coatings on steel in a simulated marine immersion environment

S. Paul and C. Gomez, TWI, Cambridge, UK;

Thermally sprayed aluminium (TSA) and aluminium alloys are more reactive than carbon steel according to the galvanic series and hence when sprayed onto steel provide sacrificed protection in seawater. In seawater immersion service, such coatings may suffer mechanical damage and the underlying steel may be exposed to the corrosive environment. Understanding the corrosion behaviour of damaged coating thus forms an important objective.

In this paper the corrosion behaviour of damaged thermally sprayed coatings is presented. Al and Al-5Mg were sprayed onto carbon steel substrates and exposed to synthetic seawater at 5°C for six months. Prior to exposure defects were generated to expose 5% area of the substrate. The samples were left at their free mixed corrosion potential and the corrosion rate was monitored using linear polarisation resistance (LPR) technique. Once the tests were completed the samples were sectioned and microstructural characterisation was carried out. It was observed that the potential decreased from -700mV vs standard calomel electrode (SCE) at the start to a steady value of -1000mV SCE after three months of testing. This reduction in the potential was accompanied by a reduction in corrosion rate. The corrosion rate decreased from an initial high value of $>100\mu\text{m/y}$ to $<10\mu\text{m/y}$ after 3 months. Microstructural examination revealed a thin layer of calcareous deposit on the exposed steel surface. This calcareous deposit had two-layer structure with $\text{Mg}(\text{OH})_2$ close to the substrate and CaCO_3 away from it. This calcareous layer seems to have provided a barrier and protected the steel from further corrosion. Thus, defects in the sacrificial coating, in contrast to noble coating material, are not a great issue as coating can partially cathodically protect the base steel.

Corrosion and cathodic protection of carbon steel in the tidal zone: Products, mechanisms and kinetics

Ph. Refait^a, R. Sabot^a, M. Jeannin^a, A. Antony^b, S. Pineau^c,

*^a Laboratoire des Sciences de l'Ingénieur pour l'Environnement (LaSIE),
UMR 7356 CNRS-Univ. La Rochelle, Bât. Marie Curie, Av. Michel Crépeau,
F-17042 La Rochelle cedex 01, France.*

*^b Corrodys, 145 chemin de la Crespinière, BP 48, 50130 Cherbourg-Octeville,
France.*

*^c Accoast SAS, Espace Atlantis, 7 Parc d'Activité Doaren Molac, 56610 Arradon,
France.*

Carbon steel coupons were set in the tidal zone of a French seaport (Le Havre). The layers of corrosion products covering the coupons after 6 months, 12 months and 7 years of exposure to the marine medium were thoroughly characterized by X-ray diffraction and μ -Raman spectroscopy. The results obtained for short immersion times (6 and 12 months) reveal a general process leading mainly to magnetite Fe_3O_4 , a typical product of atmospheric corrosion favored by wet/dry cycles, and Fe(III) oxyhydroxides FeOOH . The sulfate green rust $\text{GR}(\text{SO}_4^{2-})$, a typical product of marine corrosion [1,2], is also identified locally on the steel surface underneath magnetite. For longer exposure times (7 years), the layer of corrosion products is rather similar to that resulting from atmospheric corrosion, i.e. made of magnetite and Fe(III) oxyhydroxides. The average corrosion rate, estimated from residual thickness measurements, is $\sim 90 \mu\text{m/yr}$.

Other carbon steel coupons were set in the tidal zone for 7 years with a cathodic protection applied permanently, stopped after 6 years or applied only the last year. Permanently protected steel coupons are characterized by corrosion rates ($\sim 9 \mu\text{m/yr}$) ten times smaller than those measured for unprotected coupons. The products of the residual corrosion process, similar to those observed at the open circuit potential, form a thin layer on the steel surface under the calcareous deposit. The calcareous deposit is characterised in any case by an important proportion of brucite $\text{Mg}(\text{OH})_2$. Pyroaurite, a Mg(II)-Fe(III) hydroxycarbonate, is also frequently identified. This compound, formed from Mg^{2+} and Fe^{3+} cations, may be considered as a result of the residual corrosion of steel or as a component of the calcareous deposit as well. Stopping cathodic protection after 6 years induces a re-acceleration of the degradation, as revealed by the accumulation of the usual corrosion products. This confirms that cathodic protection has mainly a moderating effect on the kinetics of a process basically unchanged. Finally, the delayed application of cathodic protection to previously corroded coupons seems to induce a partial reduction of Fe(III) oxyhydroxides into magnetite.

References:

- [1] S. Pineau, R. Sabot, L. Quillet, M. Jeannin, Ch. Caplat, I. Dupont-Morral, Ph. Refait, *Corros. Sci.* 50 (2008) 1099.
- [2] Ph. Refait, D. D. Nguyen, M. Jeannin, S. Sablé, M. Langumier, R. Sabot, *Electrochim. Acta* 56 (2011) 6481.

SEM/EDX-investigation of rust scales formed on an aluminium-steel friction weld under marine atmosphere

M. Schneider¹, U. Langklotz², U. Gierth¹,

¹Fraunhofer Institute for Ceramic Technologies and Systems Dresden, FRG

²TU Dresden Institute of Materials Dresden, FRG

Aluminium-steel friction welds (FW) are established in automotive industry for many years [1]. Friction welding allows the joining of dissimilar material with different properties (e.g. different melting points). This great advantage in view of construction design can be a critical considering the corrosion behaviour. In the present work AlMgSi0.5-C35 FW were exposed in marine atmosphere on Helgoland over two years. In marine atmosphere tree types of corrosion of AlMgSi0.5-C35 FW were identified as recently reported by Schneider et al. [2]:

- (i) Pitting corrosion on aluminium parent material induced by chlorides.
- (ii) Galvanic corrosion with aluminium as scarified anode close to the welding zone
- (iii) Strong intrinsic corrosion in the parent zone of C35

The intrinsic corrosion of the C35 under marine atmosphere under natural exposition tests over two years leads to thick rust scales of approximately 0.1mm. The present work focus on the investigation of these rust scales across the interface steel/rust/electrolyte by SEM/EDX investigations. This investigation of the rust layer was carried out depending on the distance of the welding plane. It can be shown that the rust scale (morphology, microstructure) reflects the type of corrosion and the transition from the bi-metallic corrosion between Al-alloy and steel to the intrinsic corrosion of C35. FTIR-measurements complements the investigation and identify the different iron oxides into the rust scale.

[1] D. Schober, L. Appel, H. Horn, J. dos Santos, P. Wiesner, H.-J. Winkel:
Schweissen & Schneiden, 54 (2002) 502

[2] M. Schneider, U. Langklotz, M. Labus, B. Arnold, A. Michaelis:
Corr.Eng.Sci.Technol. 47 (2012) 312

Use of nanostructured materials in marine corrosion protection: an integrated approach

J. Tedim, F. Maia, A. Kuznetsova, A. P. Silva, R. Martins, A. Cunha, A. Almeida, S. Loureiro, R. Freitas, A.M.V.M. Soares, M.L. Zheludkevich, M.G.S. Ferreira
University of Aveiro, Aveiro, Portugal

Abstract

The application of coatings for protection of metallic structures in offshore structures deals with two main, inter-related issues: corrosion and (bio)fouling. One of the most recent strategies to impart anticorrosion functionality to organic coatings has consisted of encapsulation/intercalation of corrosion inhibitors and biocides into the so-called “smart” micro and nanocontainers, structures that store the active species and release them under certain stimuli [1].

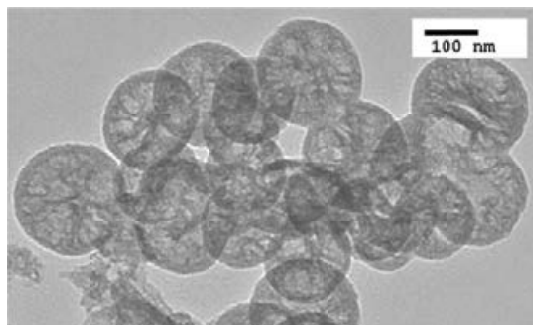


Figure 1 – Silica nanocapsules [2]

In this work, we synthesized and characterized different nanostructured inorganic materials (Figure 1) containing an organic corrosion inhibitor also known for its biological activity, 2-mercaptobenzothiazole (MBT) [2]. The corrosion protection of these systems was investigated by electrochemical techniques and the biological activity assessed using a bioluminescent assay [3].

The safety of nanomaterials and its life cycle is also a relevant aspect when including novel additives into commercial products. Therefore, the toxicity of these materials was assessed using the edible Manila clam (*Venerupis philippinarum*), throughout a wide set of physiological and biochemical parameters [4].

The main objective is to obtain an integrated overview of the performance provided by MBT-loaded nanocontainers and to assess the impact of these materials in the marine ecosystem.

References:

- [1] – M.L. Zheludkevich, J. Tedim, M.G.S. Ferreira, *Electrochim. Acta*, 82 (2012) 314.
- [2] - F. Maia, J. Tedim, A. Lisenkov, A. Salak, M.L. Zheludkevich, M.G.S. Ferreira, *Nanoscale* 4 (2012) 1287.
- [3] – E. Alves, C.M.B. Carvalho, J.P.C. Tomé, M.A.F. Faustino, M.G.P.M.S. Neves, A.C. Tomé, J.A.S. Cavaleiro, A. Cunha, S. Mendo, A. Almeida, *J Ind Microbiol Biotechnol* 35 (2008) 1447.
- [4] – J. Nilin, J.L.T. Pestana, N.G. Ferreira, S. Loureiro, L.V. Costa-Lotufo, A.M.V. Soares, *Sci Total Environ* 435 (2012) 44.

The use of composite patches to repair ship structures: an electrochemical approach

A. Collazo, X.R. Nóvoa, C. Pérez
ENCOMAT Group, EEI, Univeristy of Vigo,
Campus Universitario As Lagoas-Marcosende; 36310 Vigo (Spain);
presenting author: cperez@uvigo.es

Abstract

Corrosion is one of the most relevant causes for marine casualties in aging ships. Different techniques have been developed to repair the structural damages, including welding and attachment of steel splice plates, currently the most employed solutions [1]. However, the use of hybrid composite patches has increased in the recent years, mainly in the aerospace engineering. Although in the shipbuilding industry the implementation of this solution is more recent, its cost-effectiveness makes patching practice is being rapidly widespread [2].

The present study evaluates the water uptake process, and so, the durability of an adhesively bonded composite patch to a naval steel. The laminated composite has an epoxy matrix (35% w/w) with fibre carbon reinforcement (65%, w/w). This is bonded to the steel by an epoxy-based adhesive. The system (composite + adhesive) has a thickness of about 400 μm (see figure 1). Electrochemical Impedance Spectroscopy (EIS) was employed to characterize the composite patch. The results indicate that discrimination between the composite's response, at higher frequencies, and that of the adhesive, at lower frequencies is possible.

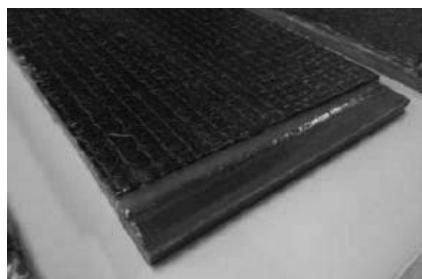


Figure 1. Optical image of the composite patch applied over naval mild steel

Acknowledgment

This study is carrying out in the framework of the FEDER-INTERCONECTA program for the Galician Region financed by the Technology Fund (CDTI), ref. ITC-20133012.

¹ Recommendation N° 47, Shipbuilding and Repair Quality Standard, International Association of Classification Societies Ltd.

² R.C. Allan, J. Bird, J.D. Clarke, "Use of adhesives in repair of cracks in ship structures", Materials Science and Technology, 4 (1988) 853.

The hydrogen permeation characteristics of high strength steel during splash zone corrosion process*

*Huang Yanliang***, Qu Wenjuan and Yu Xiuming

Key Laboratory of Marine Environment Corrosion and Marine Fouling, Institute of Oceanology, Qingdao 266071, P. R. China

Abstract The structure materials used in marine environment are mainly medium or low strength steels, but the far and deep sea explorations put forward the new request to marine engineering materials. High strength steel has the advantages of saving material, making the structure light in weight and other advantages, meeting the requirements of deep sea engineering materials. Its use has become the development trend of ocean engineering structure materials. But the high strength steel has the disadvantage of stress corrosion and hydrogen embrittlement sensitivity that needs to be overcome or proper protection. Therefore a better understanding of the marine splash zone hydrogen permeation characteristics has an important reference value for the development of stress corrosion and hydrogen embrittlement inhibition or protection technology. Study shows that the splash zone exhibits not only the high corrosion rate, but also large hydrogen permeation current. Splash zone is still in a wet state even during low tide time due to the high air humidity effect and high flying sea water foam, especially after the formation of corrosion products. Hydrolysis can always maintain in the corrosion products under this condition. The low pH value beneath the rust layer facilitates the reducing of H^+ .

Key Words hydrogen permeation; splash zone; stress corrosion cracking

* This work was financially supported by the national science foundation of China, No.41276087 and Jiangsu Provincial Natural Science Foundation No.BK2012649.

** hyl@qdio.ac.cn

Marine corrosion of SS 316L in Persian Gulf and protective coating

Mohammad Najmi, Daryoush Masouri, Pars Oil & Gas Co., Tehran/Iran;

Stainless steels are well known corrosion resistant materials in most onshore atmospheres.

But applications of stainless steels have some limitations in marine structures and corrosion investigations of this type of materials in marine environments have been reported.

In this issue corrosion of SS 316L in the Persian Gulf atmosphere are studied and proper protective coatings are discussed. Special attention on surface preparation and protective coatings for SS 316L are involved.

Keywords: Marine atmosphere, SS 316L, Atmospheric corrosion, Persian Gulf.

Study on copper release from an antifouling coating and its influence on corrosion of aluminum alloy substrate

Jingyi Cao*, Naval Coatings Analysis and Test Center, Beijing 102442, P.R.China

Jie Sun, Yuming Tang, Yu Zuo*, Faculty of Materials Science and Engineering, Beijing University of Chemical Technology, Beijing 100029, P.R. China

Corresponding author: caojy_22@yahoo.com.cn, zuoyu@mail.buct.edu.cn

Abstract: The copper release process and the alteration of organic functional groups in a self-polishing antifouling coating containing Cu_2O were studied using XPS and FT-IR methods. The results show that during the immersion period in 3.5% NaCl solution the pigment Cu_2O in antifouling coating could react with chloride ions and oxygen in the solution to produce Cu^{2+} , and with the hydrolysis of the acrylic resin in the paint Cu^{2+} would be released into solution gradually, thus provides a good antifouling effect. For an aluminium alloy/anticorrosive primer/intermediate coating/ antifouling coating system, the distributions of copper ions in different layers were analyzed by EDS measurement. It is found that Cu^{2+} could penetrate into the intermediate coating and the anticorrosive primer, and the concentration of copper ions in each layer increases linearly with the immersion time. The weight loss and electrochemical tests results show that when the Cu^{2+} concentration reaches a critical value the corrosion rate of the aluminum alloy substrate under the coating system will be increased. So, if the coating system is damaged or its shielding property decreases, the release of copper ions from antifouling coating would accelerate corrosion of the aluminum alloy substrate under the anticorrosive antifouling coating system.

Keywords: antifouling coating; cuprous oxide; copper release; corrosion; aluminium alloy

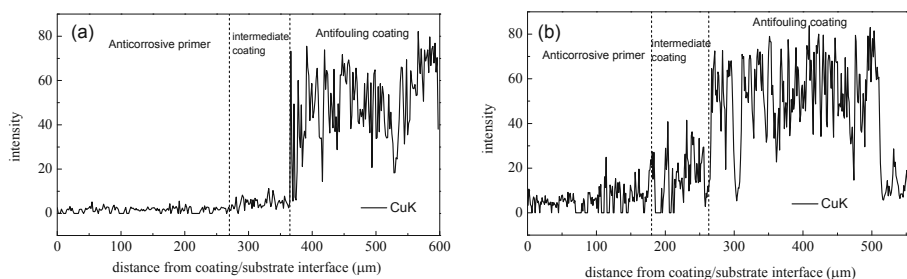


Figure Copper distributions in the coating system after immersion in 3.5% NaCl solution for 22d (a) and 200d (b). The regions from left to right are the anticorrosive primer, the intermediate coating and the antifouling coating respectively.

Corrosion resistance in multipass welding of thick UNS S31304 lean duplex stainless steel plates welded using SMAW, GMAW and FCAW processes

*Carla Soares Souza¹, Vanessa de Freitas Cunha Lins², Dalila Moreira da Silveira²,
Cintia Gonçalves Fonseca Costa², Ronaldo Cardoso Junior³, Frederico Rodrigues
Campos⁴, Alexandre Queiroz Bracarense⁴*

1 Fiat Automobile S.A., Materials Science Technology Center, Betim, Brazil

2 Federal University of Minas Gerais, Chemistry Engineering Department, Belo Horizonte, Brazil

3 ESAB Industry and Trade LTD, Contagem, Brasli;

4 Federal University of Minas Gerais, Mechanical Engineering Department, Belo Horizonte, Brasil

The UNS S32304 lean duplex stainless steel presents a lower cost compared to other duplex steels due to the partial substitution of nickel by nitrogen as an element that stabilizes austenite. During the welding of duplex stainless steels, the desired material properties can be radically altered by a process which locally melts and recasts the steel. In this work, samples of the lean duplex stainless steel welded using GMAW, SMAW and FCAW processes and two types of consumable, 2209 (22% wt Cr, 9% wt Ni and 3% wt Mo) and 2307 (23% wt Cr and 7% wt Ni) were analyzed by electrochemical impedance spectroscopy and potentiodynamic anodic polarization to evaluate the corrosion resistance of the material and in NaCl 3.5% m/v aqueous solution. The electrochemical impedance spectroscopy results showed that the top of the weld had a higher corrosion resistance in saline solution than the root of the weld, except for the welded joint using the GMAW process and the consumable 2209. The welded joint using the GMAW process and the 2209 consumable showed the highest corrosion resistance in NaCl aqueous solution. Electrochemical processes with two time constants were obtained for the samples welded using the GMAW and FCAW process with the two consumables, and for the samples welded using the SMAW process with the 2209 consumable. One capacitive arc in the Nyquist diagram, and one time constant in the Bode diagram, was observed for the samples welded using the SMAW process with the 2307 consumable. The anodic potentiodynamic polarization indicated that the welded joints using the GMAW process showed a higher breakdown potential and a lower passivation current density than the samples welded using the SMAW and FCAW processes, for the two types of consumable. After the polarization tests, all samples exhibited the highest degree of corrosion in the heat affected zone.

Behaviour of anti-corrosion coatings: comparison of the ageing in real environment in 2 different exposition sites

Marta Tejero¹, Jean-Baptiste Jorcin¹, Antoni Prieto², Tomás Alhambra², Joaquim Ferreiro²

¹ Tecnalia Research & Innovation, Parque Tecnológico de San Sebastián, Mikeletegi Pasealekua, 2, E-20009 Donostia-San Sebastián, Spain

² Hempel R&D, C/Sentmenat, 108, 08213 Polinya, Spain

The marine environment is considered as one of the most aggressive natural environment. The complexity of this environment allows various possible interactions leading to the degradation of materials. The sea water itself is aggressive, because of its content in ions and in particular in chloride which is known to promote localized corrosion and autocatalytic reactions on metallic materials, and also because of the presence of microorganisms. Microorganisms such as bacteria are forming biofilms which may increase the degradation rate of materials and moreover these biofilms are the initial step for the formation of bio-fouling which can also lead to corrosion, mainly by differential aeration phenomena.

The exposition zone is also very important as the degradation mechanisms are different if the materials are fully immersed, placed in the tidal/splash zone, or just expose to a marine atmosphere.

In this context, metallic materials are very sensitive to corrosion and should be protected. One of the most efficient ways to achieve it is using anti-corrosion coating.

The purpose of this study is to observe the behaviour of the anti-corrosion coatings provided by Hempel in 2 different real conditions:

- Offshore conditions: samples were exposed in the Helgoland highland (North Sea, Germany) in the Fraunhofer IWES facilities accessible to the FP7 shared infrastructure project (European project) MariNet.
- Port condition: samples were exposed in the port of Pasaia (Cantabrian Sea, Spain)

These coatings were applied on a carbon steel substrate, and half of the samples were artificially damaged to investigate a possible delamination of the coating.

The main point is to compare the behaviour of the coating in offshore and port condition where the fouling is drastically different and there is the presence of pollution.

Role of green rusts in corrosion and biocorrosion of carbon steel in marine environment

Ph. Refait^a, R. Sabot^a, M. Jeannin^a, S. Sable^b, I. Lanneluc^b,

*^a Laboratoire des Sciences de l'Ingénieur pour l'Environnement (LaSIE),
UMR 7356 CNRS-Univ. La Rochelle, Bât. Marie Curie, Av. Michel Crépeau,
F-17042 La Rochelle cedex 01, France.*

*^b Littoral, Environnement et Sociétés (LIENSs), UMR 7266 CNRS-Univ. La Rochelle,
2 rue Olympe de Gouges, F-17000 La Rochelle, France.*

The corrosion products of steel in seawater are associated with micro-organisms, extracellular polymeric substances and other species of organic origin. When steel is immersed in seawater, the sulfated green rust $\text{GR}(\text{SO}_4^{2-})$ with composition $\text{Fe}^{\text{II}}_4\text{Fe}^{\text{III}}_2(\text{OH})_{12}\text{SO}_4 \cdot 8\text{H}_2\text{O}$, is the first corrosion product that forms. During the initial aerated period of the corrosion process, $\text{GR}(\text{SO}_4^{2-})$ is oxidized by dissolved O_2 into lepidocrocite $\gamma\text{-FeOOH}$ (mainly), goethite and magnetite. The corrosion product layers are thus made of two strata, an inner one mainly composed of $\text{GR}(\text{SO}_4^{2-})$, growing on the metal surface, and an outer one, mainly composed of lepidocrocite, resulting of the oxidation of the GR. Microbiological analysis of this layer shows that numerous bacterial species are associated with the corrosion products. Sulfate reducing bacteria (SRB) were identified on coupons left only one month in seawater. In agreement, FeS could be detected locally on the same coupons. This shows that at that time, SRB have already begun to grow in the most deaerated zones.

After some time (>6 months), FeS is a major corrosion product, associated with $\text{GR}(\text{SO}_4^{2-})$ and SRB in the inner part of the rust layer [1]. This shows that in most cases the corrosion process remains rather uniform because the whole steel surface, placed in anoxic conditions, can finally be colonized by SRB. The behavior of steel in anoxic conditions was then studied in the laboratory using seawater-like electrolytes [2]. Carbon steel electrodes were polarized anodically at a potential ~ 100 mV higher than the open circuit potential, in an electrolyte continuously de-aerated by an argon flow. X-ray diffraction and μ -Raman analysis performed after 23 h of polarization demonstrated that a layer mainly composed of $\text{GR}(\text{SO}_4^{2-})$ had grown on the steel surface. In parallel, carbon steel coupons immersed for 11 years in the harbor of La Rochelle (Atlantic coast) were removed from seawater for analysis. The inner part of the rust layer (7-8 mm thick) proved to be mainly composed of magnetite, $\text{GR}(\text{SO}_4^{2-})$ and iron sulfide FeS [2]. This definitively confirms that $\text{GR}(\text{SO}_4^{2-})$, as Fe_3O_4 and FeS, can also form from steel during the anaerobic period of the corrosion process.

Laboratory studies finally demonstrated that SRB could grow using the sulfate species coming from $\text{GR}(\text{SO}_4^{2-})$, thus using the GR as a source of sulfates. The consumption of sulfate induces the transformation of the GR and the formation of mackinawite FeS [3]. This suggests that the ratio $\text{FeS}/\text{GR}(\text{SO}_4^{2-})$ can measure the importance of the influence of SRB on the corrosion process.

References:

- [1] S. Pineau, R. Sabot, L. Quillet, M. Jeannin, Ch. Caplat, I. Dupont-Morrall, Ph. Refait, *Corros. Sci.* 50 (2008) 1099.
- [2] Ph. Refait, D. D. Nguyen, M. Jeannin, S. Sablé, M. Langumier, R. Sabot, *Electrochim. Acta* 56 (2011) 6481.
- [3] M. Langumier, R. Sabot, R. Obame-Ndong, M. Jeannin, S. Sablé, Ph. Refait, *Corros. Sci.* 51 (2009) 2694.

**Microbial corrosion of steel in argillite:
complementarity of surface characterization (μ RamanS and FESEM)
and of microbiological approach**

F. Mercier-Bion^{1*}, Y. Léon¹, D. Neff¹, C. Wittebroodt³, L. Urios², A. Perez¹, F. Marsal⁴,
M. Flachet⁴, M. Magot², J. P. Gallien¹, P. Dillmann¹

1. DSM/IRAMIS/NIMBE/LAPA, CEA/CNRS UMR3299, 91191 Gif-sur-Yvette, France

2. UPPA, IPREM UMR 5254, IBEAS, F-64013 PAU, France

3. IRSN, PRP-DGE/SRTG/LETIS, B.P. 17, 92262 Fontenay aux Roses, France

4. IRSN, PRP-DGE/SEDRA/BERIS, B.P. 17, 92262 Fontenay aux Roses, France

The French design for deep geological disposal of high-level radioactive waste, involves carbon steel overpacks emplaced in a clayey medium. These overpacks have to ensure containment for several thousand years, and it is of primary importance to understand the short and long-term corrosion mechanisms of iron in oxic and anoxic conditions respectively in presence of Toarcian argillite and microorganisms present in deep geological media (sulphate-reducing bacteria SRB, iron-reducing bacteria IRB,...).

An original study has been launched on steel coupons placed in an argillite core sample from the Tournemire Underground Research Laboratory in contact with a synthetic solution representative of the pore water percolating through the set-up, in absence and in presence of a mix of different bacterial strains. Several environmental conditions are tested: two temperatures (25°C and 50°C), anoxic or oxic atmosphere, and contact times from one to nine months. The mix of bacteria representative of those encountered in deep geological media (Urios *et al.*, 2012) includes SRB, sulfur-oxidizing bacteria (SOB), IRB, and biofilm forming strains. This mix has been chosen to follow the synergy between the different types of bacterial strains and their relative effect to the steel corrosion. After their corrosion, the coupons (surface and polished transverse sections) are studied with FESEM at 5 kV to evidence the surface biofilms morphology, and by μ Raman spectroscopy and XRD to identify the corrosion products. A characterization of the bacterial diversity on coupons and in the outgoing solution is realized using quantitative-Polymerase Chain Reaction (qPCR). Analyses of outgoing solution (pH, concentrations of ions) indicate the microbial metabolisms occurring in the cell.

FESEM and μ RamanS permit to evidence the presence of bacteria on the external surface of the corrosion products formed on the steel surfaces. Indeed, corrosion product growth already occurs for one month experiments concomitantly to the presence of bacteria and increases for four months with the localized apparition of bacterial morphologies and surface biofilms evidenced on the corrosion product surface. Moreover, the nature of the corrosion products are typical of each medium: for the aerated one, lepidocrocite γ -FeOOH, goethite α -FeOOH and magnetite Fe_3O_4 are evidenced whereas for deaerated conditions, siderite FeCO_3 , chukanovite $\text{Fe}_2\text{CO}_3(\text{OH})_2$ and magnetite are observed. Coupons contacted for one and four months in aerated conditions show the predominance of magnetite when bacteria are added, whereas the same coupons contacted without bacteria only evidence lepidocrocite and goethite.

Evaluation of pH under-deposit using the dual-cell technique in flow conditions - The case of CuNi 70:30 in high bacteria contaminated freshwater

Maria Leonor Carvalho^a, Edoardo Guerrini^b, Stefano Trasatti^b, Pierangela Cristiani^a, Mirna Urquidi-Macdonald^c

^aRSE SpA, Ricerca sul Sistema Energetico, Dipartimento Ambiente e Sviluppo Sostenibile, Via Rubattino 54, 20134 Milan, Italy

^bUniversità degli Studi di Milano, Department of Chemistry, Via Celoria 19, Milan, Italy.

^cSabrina's Technology, Fort Myers, FL; Emeritus Professor at The Pennsylvania State University, University Park, PA 16802, U.S. and A. Professor at KFUPM, Center of Research Excellence in Corrosion, Dhahran, Saudi Arabia

Abstract

Copper alloys are widely used in cooling circuits due to their corrosion resistance, mechanical workability, and excellent electrical and thermal conductivity. Copper was believed to be immune to microbial corrosion because its toxicity to the biological organisms, but it is well known that this material suffers of this kind of corrosion.

Biofilms modifies the local environment at the biofilm/alloy interface; the local environment can be radically different from that of the bulk medium in terms of pH, dissolved oxygen, and different ions concentrations that build at the interface coming from the metal and/or the electrolyte as a direct action of the bacteria.

We investigate the effect of pH changes on CuNi 70:30 samples clean and covered with a biofilm. Experiments were carried out in a hydraulic circuit built in a wastewater treatment plant, after the depurative process and before the sanitization treatment. The methodology consisted in measuring the coupling current between two copper alloy samples (electrodes), one covered by biofilm and other clean (no biofilm); both immersed in the hydraulic loop and with the same electrolyte characteristics. A current, measured with a zero resistance ammeter, will be detected between the two electrodes (biofouled vs. clean sample). Our hypothesis is: if the current is prevalently due to a lower pH under the biofouled interface (biofouled sample vs clean one), it will become gradually smaller as the pH in the cell compartment with the clean sample is decreased. The results showed that, decreasing the pH in the cell compartment containing the clean sample has a significant impact on the coupling current, as it is expected. The measurement performed indicated that a zero current between the two electrodes cannot be reached at pH higher than 4. This may indicate that CuNi passive film, under the biofilm samples, may change not solely due to the pH changes; *i.e.* pH is not the only variable affecting the corrosion formed under biofilm. The possible complex role of the pH on the cathodic and anodic reactions is discussed.

Acknowledgements

This work has been financed by the Research Fund for the Italian Electrical System under the Contract Agreement between RSE S.p.A. (formerly known as ERSE) and the Ministry of Economic Development - General Directorate for Nuclear Energy, Renewable Energy and Energy Efficiency stipulated on July 29, 2009 in compliance with the Decree of March 19, 2009.

Electrochemical corrosion behavior of carbon steel exposed to low concentration agar with and without nutrients

Amy Spark, RMIT University & CSIRO, Melbourne Australia; Liam Ward, RMIT University, Melbourne Australia; Ivan Cole, CSIRO, Melbourne Australia; Donavan Marney, CSIRO, Melbourne Australia; David Law, RMIT University, Melbourne Australia.

A novel technique for the study of microbial corrosion in soil is currently being developed. This technique uses microbiologically graded agar to simulate more closely the conditions experienced in soil than is possible with an aqueous solution. Traditionally, most soil based corrosion testing is conducted in the laboratory with solutions made to mimic the chemical composition of soil. This does not take into account the physical structure of soil and resultant electrochemical interactions between the soil, steel and microbes. Agar is commonly used as a solidly setting gelling agent. However, in lower concentrations it forms a sludge like consistency, similar to the consistency of saturated soil.

Utilizing low concentration agar in an electrochemical cell, the corrosion behavior of carbon steel has been investigated under varying nutrient conditions. Potentiodynamic scans, potential hold measurements, optical microscopy and SEM imaging were used to monitor the steel surface both during and after exposure of the steel to the agar. These measurements will make the basis of a control for later experiments when the response of *Pseudomonas* to nutrient changes under a range of potentials when in an electrochemical set up will be investigated.

This work is part of a continuing investigation into the mechanisms of microbial corrosion at the soil-steel interface of buried potable water pipes.

Influence of Fe-S clusters of hydrogenase on mild steel corrosion

Ingrid ROUVRE, Charles GAUQUELIN, Isabelle MEYNIAL-SALLES, Régine BASSEGUY, Laboratoire de Génie chimique, CNRS-UNIVERSITE de Toulouse (INP, UPS), 4 allée Emile Monso, BP 84234, 31432 Toulouse, France

Anaerobic microbiologically influenced corrosion (MIC) is a problem that affects materials used in many industrial fields. This is the acceleration of the degradation of conductive materials in the presence of microorganisms that adhere to and grow on the surface of materials. It is now commonly agreed that sulphate-reducing bacteria (SRB) and thiosulfate reducing bacteria (TRB) are the main causes of anaerobic MIC [1], [2]. Hydrogenases, which are either present in bacteria (such as SRB) or free in solution, have also been identified as a key protein of MIC [3], [4].

In the present work, the influence of [Fe]-hydrogenase from *Clostridium acetobutylicum* is studied on the anaerobic corrosion of mild steel (S235JR) according to the oxidation state, the number and/or the position of Fe-S clusters contained in the protein. The approach is to study the catalysis of proton reduction by hydrogenase (cathodic corrosion motor), and analyse the coupled phenomena at different scales.

For this purpose, different types of [Fe]-hydrogenases are used: native or specific mutant types. The specific mutant hydrogenases are constructed by site-directed mutagenesis at the molecular level, overexpressed and produced in *Clostridium acetobutylicum*. The modification types studied in this work are:

- the removal of accessory Fe-S clusters, only the catalytic domain remains,
- the destabilization of a Fe-S cluster (Cysteine substituted by Alanine), a S atom is in less,
- the reformation of a Fe-S cluster (Histidine substituted by Cysteine) a S atom is in addition.

Native or mutant type hydrogenases are extracted and purified from *Clostridium acetobutylicum* cells cultured at regulated pH in fermenters. [Fe]-hydrogenases are purified by affinity chromatography on streptactin-, using a tag (Strep-tag II) specifically fused at the C-terminal of the protein [5], [6]. Native and specific mutant of hydrogenases are, first, biochemically characterized and, secondly, used under their active or deactivated form for corrosion tests. Among deactivation techniques, denaturation of the enzyme by heating was proved to have the greatest impact on the corrosion of steel due to the release of Fe-S clusters.

The electrochemical methods used to characterize the behaviour of the S235JR steel in the presence of hydrogenases are the monitoring of corrosion potential, linear polarization, impedance measurement coupled with surface analyses (SEM, EDX, XPS). The effects of [Fe]-hydrogenases are compared taking a same protein concentration, or a same Fe-S concentration.

[1] C. Xu, Y. Zhang, G. Cheng, and W. Zhu, *Materials Science and Engineering: A*, vol. 443, no. 1–2, pp. 235–241, Jan. 2007.

[2] R. Javaherdashti, R. K. Singh Raman, C. Panter, and E. V. Pereloma, *International Biodeterioration & Biodegradation*, vol. 58, no. 1, pp. 27–35, Jul. 2006.

[3] M. Mehanna, R. Basseguy, M.-L. Delia, L. Girbal, M. Demuez, and A. Bergel, *Electrochimica Acta*, vol. 54, no. 1, pp. 140–147, Dec. 2008.

[4] S. Da Silva, R. Basséguy, and A. Bergel, *Journal of Electroanalytical Chemistry*, vol. 561, no. 0, pp. 93–102, Jan. 2004.

[5] L. Girbal, G. von Abendorff, M. Winkler, P. M. C. Benton, I. Meynial-Salles, C. Croux, J. W. Peters, T. Happe, and P. Soucaille, *Applied and Environmental Microbiology*, vol. 71, no. 5, pp. 2777–2781, Jan. 2005.

[6] T. Lautier, P. Ezanno, C. Baffert, V. Fourmond, L. Cournac, J. C. Fontecilla-Camps, P. Soucaille, P. Bertrand, I. Meynial-Salles, and C. Léger, *Faraday discussions*, vol. 148, pp. 385–407, 2011.

Outer membrane associated redox active components in lithotrophic SRB trigger direct electron transfer during anaerobic electrical MIC

Pascal F. Beese-Vasbender^a, Julia Garrelfs^b, Simantini Nayak^a, Andreas Erbe^a,
Karl J.J. Mayrhofer^a, Martin Stratmann^a & Friedrich Widdel^b

¹ Max-Planck-Institut für Eisenforschung GmbH,
Max-Planck-Straße 1, 40237 Düsseldorf, Deutschland

² Max-Planck-Institut für Marine Mikrobiologie, Celsiusstraße 1, 28359 Bremen

Session: Microbial Corrosion (WP10)

Previous studies have apparently shown the astounding ability of marine corrosive δ -proteobacterial SRB, in particular *Desulfopila corrodens* strain IS4, to directly utilize electrons from pure iron (Fe^0) serving as the sole electron source, to reduce sulfate to sulfide much faster than conventional H_2 -scavenging SRB during MIC (1–4). This observation led to the consideration whether reduced electrodes other than iron may serve as the sole electron donor for sulfate reduction in cultures of strain IS4. Direct electron transfer at cathodes was first discovered in *Geobacter* species that accepted electrons from graphite electrodes for anaerobic respiration (5). Hitherto only a few pure cultures were found to possess the ability to directly accept electrons from polarized electrodes for the reduction of a terminal electron acceptor (6, 7), which demands at least one outer membrane associated redox active component to accomplish the entry of electrons into intracellular electron transfer mechanisms (8, 9). Here we report on the ability of strain IS4, representing highly corrosive SRB, to directly take up electrons from graphite and germanium electrodes for sulfate reduction. Besides electrochemical measurements, observations with *in-situ* ATR-FTIR spectroscopy and environmental SEM have been performed to demonstrate interactions of strain IS4 at the bacteria/electrode interface.

1. H. T. Dinh *et al.*, *Nature* **427**, 829–832 (2004).
2. D. Enning *et al.*, *Environ. Microbiol.* **14**, 1772–1787 (2012).
3. H. Venzlaff *et al.*, *Corros. Sci.* (2012), doi:10.1016/j.corsci.2012.09.006.
4. P. Beese *et al.*, *Electrochimica Acta* **105**, 239–247 (2013).
5. K. B. Gregory, D. R. Bond, D. R. Lovley, *Environ. Microbiol.* **6**, 596–604 (2004).
6. D. R. Lovley, *Environ. Microbiol. Rep.* **3**, 27–35 (2011).
7. J. C. Thrash, J. D. Coates, *Environ. Sci. Technol.* **42**, 3921–3931 (2008).
8. F. Van Ommen Kloeke, *Anaerobe* **1**, 351–358 (1995).
9. M. Rosenbaum, F. Aulenta, M. Villano, L. T. Angenent, *Bioresour. Technol.* **102**, 324–333 (2011).

Biofilm impact on the stainless steel passive film.

Audrey Allion¹, Sandrine Zanna², Antoine Seyeux², Marie-Hélène Berger³, Philippe Marcus²

¹Aperam Isbergues, Corrosion & Surface Dept., BP 15, F-62330 Isbergues, France

²Laboratoire de Physico-Chimie des Surfaces, CNRS/ENSCP (UMR 7045), Chimie ParisTech, 11 rue Pierre et Marie Curie, F-75005 Paris, France

³MINES-ParisTech, Centre des Matériaux, CNRS UMR 7633, BP 87 91003 Evry Cedex, France

Microbial corrosion

For micro-organisms, the preferred living state is adhering to surfaces that lead to the development of a biofilm. It is well known that the material chemical composition and its topography affect microbial colonization ⁽¹⁾. Furthermore, adhesion to surfaces and growing inside biofilm modify microbial metabolism ⁽²⁾. The secreted products by adhering cells will modify their local environment in terms of pH, RedOx. Thus, biofilm can affect surface properties of materials.

In aqueous environment, materials are mainly chosen for their corrosion resistance property. For stainless steels, the corrosion resistance is due to the formation of a thin passive chromium and iron oxide/hydroxide ^(3,4). The passive film modification in presence of bacteria is a key issue for the integrity and reliability of metallic materials. The purpose of the present work is to study the modifications of the passive film on stainless steel after initial adhesion of *E. coli* K12 (1h) and in the early stage of biofilm formation (24h).

Observations performed by TEM (Transmission Electronic Microscopy) confirmed the presence of the passive layer under the bacterial cells. XPS (X-Ray Photoelectron Spectroscopy) was used to define chemical composition of the passive layer near and under *E. coli* cells. The *E. coli* cells were removed by sputtering to define the oxide layer composition under bacteria. The work evidence that the passive film formed after *E. coli* adhesion is enriched in Cr compared to the passive film not exposed to bacteria. The enrichment in Cr is observed in the oxide film under bacteria as well as in the oxide film not covered by bacteria (next to the bacteria). The longer the exposure time, the richer in chromium is the passive film.

¹ Mafu, A.A., D. Roy, J. Goulet, and P. Magny (1990) Attachment of *Listeria monocytogenes* to stainless steel, glass, polypropylene and rubber surfaces after short contact times. J. Food Prot. 53:742-746.

² Archer N.K. et al. (2011) *Staphylococcus aureus* biofilms Properties, regulation and roles in human disease. Virulence 2:5, 445-459.

³ Baroux B., Béranger G. and Lemaitre C. (1990) Passivité et rupture de la passivité des aciers inoxydables. Ed Lacombe, Baroux, Béranger In les aciers inoxydables p161

⁴ H.S. Strehblow, P. Marcus, X-ray Photoelectron Spectroscopy in Corrosion Research in Analytical Methods in corrosion science and engineering, p. 1- 38, edited by Philippe Marcus, Florian Mansfeld, Taylor and Francis, 2006

Experimental study of wear and corrosion interaction in steel chains under working conditions

Amin Lotfollahi Yaghin, University of Newcastle, Australia

Amin.Lotfollahiyaghin@uon.edu.au

Robert E. Melchers, Centre for infrastructure performance and reliability, University of Newcastle, Australia

Rob.Melchers@newcastle.edu.au

Steel chains are used for maritime floating structures like floating production storage and offloading platforms (FPSOs), ship mooring buoys, navigation signal buoys and etc. However, the mooring systems may be damaged by storm waves and by material deterioration. A main cause of the damage is the breakage of the mooring chain of the system due to impulsive tension which is produced by large buoy motion and the abrasion between the chain links. Corrosion of the mooring chain has been linked to severe localized corrosion attributed, to date, mainly to microbiological corrosion. This paper reviews this background and then reports on a project that aims to study the effect and interaction of wear and corrosion on the remaining lifetime of a chain under working conditions. A specially-designed laboratory test rig is used to cause wear on realistic chains, both corroded and un-corroded. The corroded chains were subject to marine corrosion for different periods of time. The wear experimental study involves using the test rig to produce wear on the two types of chains by wearing the adjacent surfaces of the inter-link zones of 5-link chain sets against each other under a static axial load. The original chain metal diameter and the link height were 16mm and 96mm respectively. Measurements include the reduction in weight and in the diameter of the chain links and also the reduction in maximum load capacity. The chains are worn under different tensile forces (which are produced by static dead loads) for various numbers of cycles, up to 250,000. A mathematical model is proposed that is capable of predicting the remaining lifetime of steel chains under different conditions. The effect of initial corrosion on the amount of wear is also presented. The results show that tensile force has a significant effect on the abrasion of links and the wear rate is higher in corroded compared to un-corroded chains.

Keywords: steel chains, marine corrosion, microbiological corrosion, wear, tribocorrosion, remaining lifetime

A microelectrodes study for anaerobiosis profiles in biofilms

Edoardo Guerrini^a, Matteo Grattieri^b, Pierangela Cristiani^c, Stefano Trasatti^a.

^a Università degli Studi di Milano, dept. of Chemistry, Via Golgi 19, 20133 Milan, Italy.

^b Politecnico di Milano, Department of Chemical-Engineering and Materials, Piazza Leonardo Da Vinci, 32, 20133 Milan, Italy.

^c Ricerca sul Sistema Energetico s.p.a.(RSE), Via Rubattino 54, 20134 Milan, Italy.

The potentiality of self-made microelectrodes to measure crucial parameters (redox potential, pH, conductivity, sulphides concentration) inside anaerobic biofilms is presented. Advantages and limitations of the use of a single chamber microbial fuel cell (MFC) as device to study anaerobic biofilms and microbial corrosion of AISI 304 SS is highlighted, in comparison with the dual-cell method. The physico-chemical profiles and trends of microelectrodes, suitably located in the cathodic biofilm, were analyzed at different operating power of single chamber MFCs. The biofilm activity was correlated to the changes in chemistry and power production of MFCs.

pH profiles allow to demonstrate that a proton gradient is established within the cathodic biofilm of operating MFCs, with an increasing acidity near the electrode.

Conductivity increases inside the biofilm, proving low diffusion and enhanced ion concentration.

Redox profiles provide a significant insight in the understanding of the biochemical equilibrium inside and outside the biofilm, explaining the role of bacteria in the redox potential establishment.

Sulphide variations emphasize a role of the sulphur cycle in the MFC productivity.

Diffusion is the key-factor for the development of a biofilm. Under the biofilm, many factors may cause an indirect biologically-assisted increase in corrosion rates: 1) dramatic pH-drop, 2) increase in solution conductivity and 3) presence of sulphides.

The central role of residual oxygen concentrations in the electrolyte outside the anaerobic biofilm was demonstrated in different experiments with microbial fuel cells equipped with AISI 304 SS. A completely anaerobic environment prevents MIC 304SS corrosion, even in long-term MFC operation. At the opposite, the presence of residual oxygen traces causes the formation of pits, compatible with the typical Sulphate Reducing Bacteria (SRB) corrosion damage.

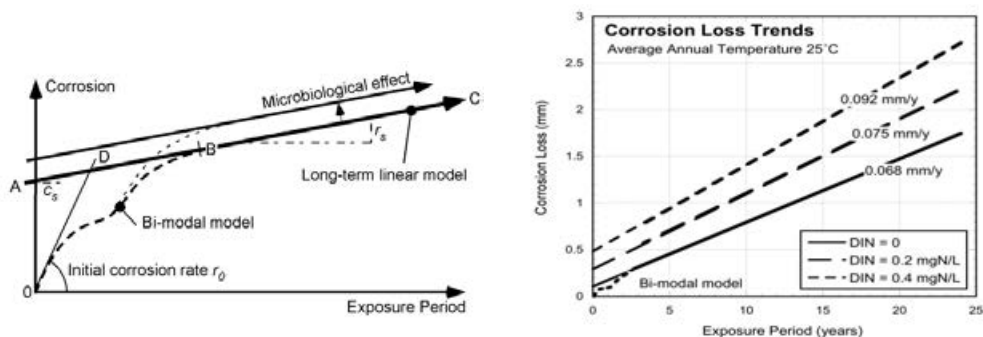
Microelectrodes were employed for the determination of the oxygen gradient, from the solution surface, down to the bottom of the cell. These profiles demonstrate the presence of an oxygen gradient, developing with time and cell current production. Two different wastewaters will be used as media for developing anaerobic condition: a) wastewater from municipal wastewater treatment plant and b) wastewater post-digestate from anaerobic bio-gas production plants. Great differences are connected with the capability of the digestate to quickly develop a biofilm and solution environment completely free of oxygen.

Long-term corrosion of steels and steel piling in seawaters with elevated nutrient concentration

Robert E Melchers & Robert J Jeffrey, Centre for Infrastructure Performance and Reliability, The University of Newcastle, Australia

Previously it has been demonstrated that accelerated low water corrosion (ALWC) of steel piling in many seawater harbours is correlated strongly with elevated levels of dissolved inorganic nitrogen (DIN) in sea and brackish waters. This has led to the inference that this is responsible for microbiologically influenced corrosion (MIC) and in particular for additional corrosion in the low tide zone. The studies used field data from a number of Australian experimental sites, US naval sites and some severe sites in Norway, Japan and the UK. However, these findings could not explain (1) the highly localized corrosion often associated only with the webs of U and Z profile sheet piling rather than more generally at any given elevation and (2) the increased corrosion in the immersion zone. Recent investigations have shown that the localized horizontal effect is most likely the result of local material differences, including localised centreline segregation, porosity and composition differences. These stem from the steel making process and are likely to be less severe for modern steels. These results are reviewed and shown to explain most of the observations for actual steel piling in various harbours, both vertically and horizontally (i.e. for U and Z and other pile profile types). The increased corrosion in immersion zone exposures was considered by using data from a variety of field exposure programs show that long term marine immersion corrosion of steel can be approximated as asymptoting the long-term part of the previously proposed bi-modal corrosion loss model. This asymptote correlates with elevated concentrations of dissolved inorganic nitrogen (DIN). This allows the model to be calibrated and used for predicting long-term corrosion loss in nutrient polluted waters of known average temperature. An example application shows that anthropological pollution of seawater potentially is a major hazard for corrosion of steel infrastructure.

Keywords: Steel, seawater, corrosion, microbiological corrosion, nutrients, modelling.



Corresponding author: rob.melchers@newcastle.edu.au

Introducing a Corrosion Management Approach to MIC Assessment, Control and Monitoring in the Oil and Gas Industry

Torben Lund Skovhus
Hans-Erik Berge
Richard Eckert
Gerry Koch
DNV GL

The corrosion management process is based on the assessment of corrosion threats; the identification of mitigation or barriers to those threats; and monitoring of barrier effectiveness. Assessment of Microbiologically Influenced Corrosion (MIC) can be incorporated within these fundamental corrosion management processes; improving the operator's ability to manage MIC threats.

Historically, assessment of MIC in the oil and gas industry has focused on sulfate-reducing bacteria (SRB) using cultivation-based techniques. Today, the use of molecular microbiological methods (MMM) for investigation of troublesome microbes provides improved accuracy and timeliness of results.

While microorganisms abound in nearly every oil and gas production environment, determining their role in internal corrosion and identifying appropriate corrosion management strategies requires a consistent and methodical approach. Since microorganisms can influence corrosion in different ways, MIC diagnostics using MMM must be done in consideration of other factors that support corrosion such as operating history, the presence of scale and deposits, fluid composition, and mitigation history.

In this paper we describe several industry case studies that are used to illustrate the use of MIC diagnostics, control and monitoring in the context of supporting a corrosion management program. The paper also discusses the implementation and applicability of the newly published NACE standard TM0212-2012 for operating companies.

Key words: Industry Case Stories, Oil and Gas, MIC Diagnostics, Molecular Microbiological Methods (MMM), Mitigation, Corrosion Management Framework, TM0212-2012.

A Numerical Model for Copper Biocorrosion

Diego Fischer¹, Carlos Galarce¹, Magdalena Walczak¹, Gonzalo Pizarro^{1,2} and Ignacio Vargas^{1,2}

¹School of Engineering, Pontificia Universidad Católica, Santiago, Chile

²Centro de Desarrollo Urbano Sustentable Santiago, Chile.

Biocorrosion of copper is a particular type of corrosion induced by microbial organisms that has reportedly proved disastrous in consequences in many pipe systems around the world. Once the microorganisms induce biocorrosion, not only the pipe material is damaged but also the transported water is spoiled by copper released in form of ions and particles causing potential harm to the users. The complexity of the problem is due to the high number of the involved variables, including water composition, temperature, presence of copper resistant bacteria, stagnation time and flux conditions.

This study aims at developing a model of copper biocorrosion that would help understanding how the conditions generated by the presence of bacteria at micro scale affects both failure of the material and release of dissolved and particulate copper. The model takes into account the key water parameters, dissolved oxygen and pH, as well as electrochemical reactions occurring at the pipe surface, chemical reactions in the water and growth of the biofilm. Flux, diffusion and migration of each of the involved chemical and electrochemical species are determined by means of Nernst-Planck equation with boundary conditions determined by heterogeneous reactions. Homogeneous reactions in the bulk represent precipitation of solid species and activity of the biofilm. The model is developed in transient mode in order to understand the conditions set after the water is flushed from the plumbing system.

Biofilm growth and decay is modeled with a time discrete-continuous approach. The discrete part of the model is used for the distribution of new cell growth and the representation of 3D structures associated with the biofilm. The continuous part of the model is used for computing substrate utilization, diffusion and migration of dissolved species, as well as growth of the biomass.

Finally, the model is calibrated using the data collected from experiments in our laboratory.

Corrosion behaviour of titanium in the presence of *Streptococcus Sanguinis*

Fei Yu^a, Owen Addison^b, and Alison Davenport^a

^aSchool of Metallurgy and Materials, University of Birmingham, B15 2TT, UK

^bSchool of Dentistry, University of Birmingham, St Chad's Queensway, B4 6NN, UK

Because of their biocompatibility, suitable mechanical properties and good corrosion resistance, Ti and its alloys have been routinely used in the manufacture of biomedical implanted devices since the 1950s. However, some corrosion-related failures of Ti implants have been observed [1] and Ti corrosion products have been found in human tissues from around retrieved implants [2]. The corrosion products can induce pain, cause adverse cellular responses, and peri-implant inflammation, which in turn may lead to failure of Ti implants.

Implanted devices that penetrate skin or oral mucosa are likely to have surface biofilms, which may drive the peri-implant inflammatory response. *Streptococcus Sanguinis* (*S. Sanguinis*) is Gram-positive aerobic bacteria species which is found in dental biofilms and may be of particular interest [3]. This bacterium usually serves as an early colonizer which facilitates adhesion of later species onto the surface of the biomaterial.

In this study, three grades of titanium with two types of surface finish were prepared to mimic the surface of the dental implants. The corrosion behaviour of titanium and its alloy have been investigated in the presence of *S. Sanguinis* in artificial saliva by measuring the released ions and using scanning electron microscopy. These results suggest that the presence of the bacteria destabilise the protective oxide film on the surface, which means it promotes corrosion of titanium.

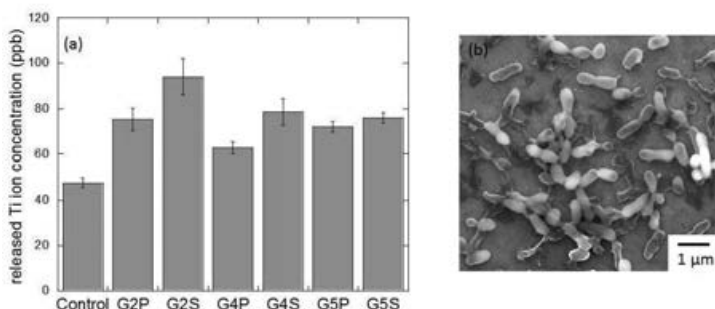


Figure 1 (a) Ti ion release of three grades of titanium with two types of surface finish; mirror polished commercial pure titanium grade 2 (G2P), mirror polished commercial pure titanium grade 4 (G4P), mirror polished Ti6Al4V (G5P), sandblasted-acid-etched (SLA) commercial pure titanium grade 2 (G2S), SLA commercial pure titanium grade 4 (G4S) and SLA Ti6Al4V (G5S) in the presence of *S. Sanguinis* in artificial saliva at 37°C; (b) SEM image of G2P in the presence of *S. Sanguinis* after 30 days incubation

References

1. Thomas, S.R. et al., *Journal of Bone and Joint Surgery-British Volume*, 2004. 86B(7): p. 974-978.
2. Addison, O., A. J. Davenport, et al., *J. R. Soc. Interface.*, 2012 9(76): p. 3161-3164
3. Zheng, L., Z. Chen, et al. *Journal of Bacteriology*, 2011. 193(2): p. 516-526.

Acknowledgements

This work has been funded in part by University of Birmingham and China Scholarship Council.

Effect of marine *Pseudoalteromonas* sp. on the microstructure and corrosion behaviour of 2205 Duplex stainless steel

Masoumeh Moradi, Zhenlun Song

Surface protection research group, Surface Department, Ningbo Institute of Materials Technology and Engineering, Chinese Academy of Sciences, 519 Zhuangshi Road, Ningbo315201, China

Abstract:

A new generation of Fe-based alloys, such as duplex stainless steels (DSS), has been applied in marine environment because of their high corrosion resistance. This property is attributed to the high alloy contents of chromium, nickel and molybdenum. When exposed to oxygen; these elements allow the formation of a passive film on the surface of alloys, protecting it from aggressive chemical species, such as chlorides in marine environments. However, these alloys suffer from localized corrosion like microbiologically influenced corrosion (MIC). Antony et al. studied the behaviour of 2205 duplex stainless steel in the presence of sulphate-reducing bacteria (SRB) and found that SRB can modify passive film and depolarize cathodic reactions. Also, it is reported the formation of a biofilm on the surface has an important influence on the initiation of localized corrosion; while there is no report about the effect of aerobic bacteria on the corrosion mechanism of these alloys. In this work, the effects of marine isolated bacterium *Pseudoalteromonas* sp. on the microstructure and corrosion behaviour of 2205 duplex stainless steel was investigated using electrochemical and surface analysis methods. This bacterium is an aerobic, Gram-negative which isolated from East Sea (China). Electrochemical studies showed that E_{OCP} shifted to a negative direction in the presence of bacteria, indicating the activation of the metal surface because of chloride ions and metabolic by-products. The corrosion current density increased and charge transfer resistance decreased in the presence of *Pseudoalteromonas* sp. by exposure time which confirmed the corrosivity of this bacterium on 2205 DSS. Anodic current density also greatly increased in the presence of the bacteria after 30 days and induced a localized attack on the metal surface. EDS results showed a high concentration of chloride ions in the biofilm structure and a decrease in Cr content beneath the biofilm layer and near cracks. Indeed, the adhesion of bacteria and the formation of the porous biofilm on the metal surface resulted in chloride ion accumulation on the metal surface and induced the localized corrosion. In addition, the process of bacterial attachment on the metal surfaces at different exposure times was studied by FESEM technique.

Influence of sterilization methods on corrosion behavior of stainless steel in simulated cooling water containing Sulfate reducing bacteria

Hong-Hua Ge, Xue-Juan Wang, Min Zhang, Xin-Jing Meng
Shanghai University of Electric Power, Shanghai Engineering Research
Center of Energy-Saving in Heat Exchange Systems, Shanghai Key
Laboratory of Colleges and Universities for Corrosion Control in Electric
Power System and Applied Electrochemistry, Shanghai 200090, China*

Abstract

Microbiologically induced corrosion (MIC) especially caused by sulfate reducing bacteria (SRB) is frequently occurred in cooling water system in power plants. The corrosion behavior of sulfate reducing bacteria on stainless steel with and without sterilization such as using microbicide glutaraldehyde, polyhexamethylene guanidine, and electromagnetic treatment has been investigated by using electrochemical impedance spectroscopy (EIS), potentiodynamic polarization, scanning electron microscope (SEM), energy dispersive x-ray spectroscopy (EDS) and theoretical adhesive work. It was shown that the impedance of stainless steel was significantly reduced while the passive current density increased more than an order of magnitude in presence of SRB, compared with aseptic system. The results of SEM/EDS analysis illustrated the formation of an uneven biofilm on the surface of stainless steel and the concentration of sulfide tested through solution analysis was found quite high in this system. The impedance value increased and the passive current density of stainless steel reduced with the time of electromagnetic and polyhexamethylene guanidine treatment in the bacteria system. The analysis of surface thermodynamics also revealed the theoretical work of adhesion between biofilm and stainless steel in water was reduced after electromagnetic and polyhexamethylene guanidine treatment, which means the adhesiveness of the biofilm on the surface of the stainless steel was decreased by the electromagnetic and polyhexamethylene guanidine treatment. Most of the biofilm stripped from the surface of stainless steel after electromagnetic and polyhexamethylene guanidine treatment, which was confirmed by the results of SEM/EDS analysis. In contrast, the anti-corrosion performance of glutaraldehyde to stainless steel in solution with SRB is poor although glutaraldehyde appears better bactericidal efficiency. The main reason may be due to the fact that the biofilm on stainless steel surface can hardly be stripped in this system because of its higher theoretical work of adhesion between biofilm and stainless steel in water.

Keywords: *sulfate reducing bacteria; stainless steel; electromagnetic treatment; glutaraldehyde; Polyhexamethylene guanidine; corrosion inhibition*

Concrete deterioration by bacteriogenically induced sulfuric acid attack

Cyrrill Grengg, Andre Baldermann and Martin Dietzel, Institute of Applied Geosciences, Graz University of Technology, Rechbauerstraße 12, 8010, Graz, Austria

Florian Mittermayr, Institute of Technology and Testing of Building Materials, Graz University of Technology, Inffeldgasse 24, 8010, Graz, Austria

Michael E. Böttcher, Leibniz Institute for Baltic Sea Research (IOW), Seestraße 15, D-18119 Warnemünde, Germany

Albrecht Leis, RESOURCES – Institute for Water, Energy and Sustainability, Joanneum Research, Elisabethstraße 18/2, 8010, Graz, Austria

Abstract

In this study we analysed severe corrosion and concrete damage in an Austrian sewage system, which is urgently due for restoration. Understanding the underlying reaction mechanisms leading to the deterioration by bacteriogenically induced sulfuric acid attack of concrete structures is highly complex and often not fully understood. The aim of this study is to contribute to a deeper understanding by introducing a novel approach that comprises a range of mineralogical methods, as well as hydro-geochemical analyses, analyses of gases, hydro-geochemical modelling, microbiology and stable isotope geochemistry. An overview of the field site and analytical results will be presented. Actual causes for concrete deterioration and countermeasures will be discussed.

Microbiologically Induced Corrosion on Tin Bronze samples simulating uncommon Archaeological corrosion

G. Ghiara¹⁻², P. Piccardo¹⁻², M. Stauder³, C. Pruzzo³

¹*Department of Chemistry and Industrial Chemistry (DCCI), University of Genoa
Via Dodecaneso 31, 16146 Genova (ITALY)*

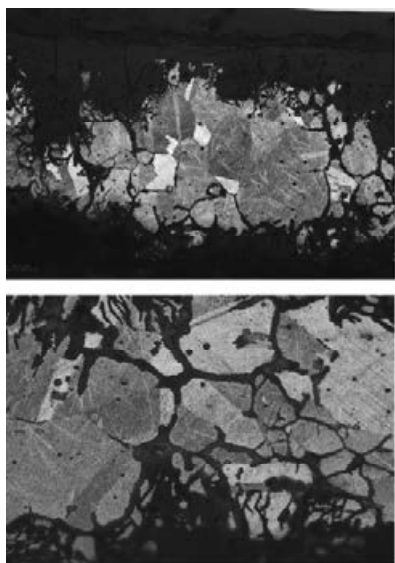
²*Consorzio Interuniversitario Nazionale per la Scienza e la Tecnologia dei Materiali
(INSTM), Via G. Giusti 9, 50121 Firenze (ITALY)*

³*Department of Earth, Environment and Life Sciences (DISTAV), University of Genoa
Corso Europa 26, 16132 Genova (ITALY)
Email: giorgia.ghiara@gmail.com*

Archaeological corrosion does not always show common morphological features when peculiar factors – foreign agents such as microorganisms – are involved [1,2]. It is well known that copper acts as a biocide for any type of organism; but it is also true that some of them – mostly microorganisms – may develop a tolerance towards copper ions. In this case corrosion mechanisms are induced by microbial agents – so called Microbiologically Induced or Influenced Corrosion (also called MIC) [3]. Researches on copper based alloys linked to microbial colonization are usually connected to sanitary problems: seawater piping system exposed to estuarine and seawater or weld and heat affected zones usually provide ideal conditions for the colonization of different kinds of bacteria [4]. Few Tin-bronze materials under microbial attack have however been analysed, being the only alloy studied so far copper- nickel, brass and aluminum brass [5].

The detection of a specific and seldom documented penetrating corrosion, called 'tentacle-like' by its peculiar shape once observed in cross section was noted on several Tin-bronze objects dated Bronze Age during a research carried out by Piccardo et al [6]. The morphology as well as the composition differed so much from classical models that it was not possible to simply classify it amongst the variety of known corrosion mechanisms for archaeological bronze objects. Also some morphological and chemical aspects suggested the intervention of corrosive agents never considered before. This type of corrosion effectively penetrated the metallic matrix forming 1-1.5 μm wide tunnel shaped structures, not following any microstructural features as grain or twinning boundaries, or slip bands due to cold deformation. Moreover the detection inside the tentacles of anomalous concentration of silicon, phosphor and even aluminum, manganese and iron lead to formulate the hypothesis related to the presence of MIC [7].

This research focuses on the reproduction of such features by experimental sessions using a specifically selected strain of *Pseudomonas fluorescens*. Procedure was carried out following literature data [8]. Analyses were



later performed by Light Optical Microscopy, Scanning Electron Microscopy coupled with Energy Dispersive X-Ray Spectroscopy and MicroRaman Spectroscopy in order to verify the correlations between archaeological and laboratory morphologies and corrosion products.

References

1. D. Nercessian, F. B. Duville, M. Desimone, S. Simison, and J. P. Busalmen, *Water Res.* **44**, 2592 (2010).
2. Z. Dwidjosiswojo, J. Richard, M. M. Moritz, E. Dopp, H.-C. Flemming, and J. Wingender, *Int. J. Hyg. Environ. Health* **214**, 485 (2011).
3. A. Reyes, M. V. Letelier, R. De la Iglesia, B. González, and G. Lagos, *Int. Biodeterior. Biodegradation* **61**, 135 (2008).
4. S. J. Yuan, A. M. F. Choong, and S. O. Pehkonen, *Corros. Sci.* **49**, 4352 (2007).
5. B. J. Little and J. S. Lee, Wiley (2007).
6. P. Piccardo, M. Mödler, G. Ghiara, S. Campodonico and V. Bongiorno, *Appl. Phys. A* (2013).
7. B. Little, *Biofouling* **9**, 251 (1996).
8. M. B. Valcarce, S. R. de Sánchez, and M. Vázquez, *Corros. Sci.* **47**, 795 (2005).

MIC on bridge-building carbon steel in a tropical/Amazonian environment

M. Vastra, P. Salvin, C. Roos, Laboratoire des matériaux et molécules en milieux amazonien, Université des Antilles et de la Guyane, UAG-UMR ECOFOG, F-97337 Cayenne, Guyane Française.

Microbiologically influenced corrosion (MIC) is a phenomenon that occurs in natural water and soil when a metallic component is immersed. Once in the water, the metallic surface is covered by a natural biofilm which is responsible for this corrosion [1]. The Larivot Bridge in French Guiana was built in the 1970's and was recently closed (2009) because of pier failure. This bridge is the only link between the East and the West economic zones. The corrosion mainly takes place at the low water level, which can suggest MIC[2]. The bridge was built over the estuary of the Cayenne, an Amazonian brackish River very rich in nutrients. There, air and water temperatures are constant year-round, around 26°C. This study aimed to prove the occurrence of MIC. To do so, *in situ* and *in vitro* tests were performed on the same carbon steel that was used for the bridge construction (S355). The corrosion was electrochemically described by impedance spectrometry and linear polarization at three levels of immersion. These measurements allowed to identify the phenomena happening on the surface and to get the corrosion speed after a month in water. To complete the study, the corrosion speed was also measured by gravimetry. The *in situ* results were compared with *in vitro* ones carrying out the same measurements and using natural water fresh and sterilized. Alongside, the biofilm microbiological diversity of bacteria, Archaea and phytoplankton, were determined with PCR-DGGE. The *in situ* results confirmed the faster low water corrosion and this is correlated with a greater microbial diversity.

[1] W. H. Dickinson and Z. Lewandowski, "Electrochemical concepts and techniques in the study of stainless steel ennoblement." *Biodegradation*, vol. 9, no. 1, pp. 11–21, 1998.

[2] I. B. Beech and S. A. Campbell, "Accelerated low water corrosion of carbon steel in the presence of a biofilm harbouring sulphate-reducing and sulphur-oxidising bacteria recovered from a marine sediment," *Electrochimica Acta*, vol. 54, no. 1, pp. 14 – 21, 2008, special Issue BIOCORROSION OF MATERIALS Selection of papers from the International Conference (BIOCORYS 2007) 14-17 June 2007, Paris, France. [Online]. Available: <http://www.sciencedirect.com/science/article/pii/S0013468608007330>

Meromictic lakes as field laboratory for corrosion studies in aerobic and anaerobic conditions

Guerrini Edoardo^{a,b}, Pierangela Cristiani^b, Stefano P.M. Trasatti^a, Maria Leonor Carvalho^b, Gildo Storni^b

^a Department of Chemistry, Università degli Studi di Milano, Via Celoria 19, Milan, (Italy)

^b RSE - Ricerca sul Sistema Elettrico S.p.A., Environment and Sustainable Development Department, via Rubattino 54, Milan, (Italy)

^c Politecnico di Milano, Dept. Of Chemistry, Materials and Chemical Engineering "G. Natta", via Mancinelli 7, Milan, (Italy)

Idro lake is a meromictic southern deep alpine lake located in the Northern part of Italy. The presence of a superficial layer of aerobic water and of a deep constant layer under anaerobiosis makes it a unique environment for microbial corrosion studies.

The glacial origin of the lake, together with the steep walls of the basin and the depth of 120 m, led in the last century to the evolution of a *meromictic* condition. A first 50 m layer of water is continuously recirculated and oxygenated; a second layer is characterized by the depletion of oxygen; the final layer is constituted of stationary water.

Stratifications of different species, especially manganese compounds in a carbonatic matrix and sulfur from gypsum deposits, characterizing the rocks around the lake, is observed.

Physico-chemical features of the different layers along the lake depth profile are herein described.

Based on home-built sensors, oxygen and sulphide content, pH, conductivity, and temperature profiles were obtained. Unique correlations between the above parameters and electrochemical characteristics (free corrosion potential and polarization resistance R_p) of CuNi70/30 specimens placed at different depths and for several exposure times were demonstrated.

The corrosion rates, as calculated from R_p values, showed a significant increase in the layer corresponding to the anoxic area, where the oxygen dissolved was below 0.2 mg/l. The rates falls down to negligible values below 50 m depth, as the anaerobic condition were well established. The lowest corrosion rates were detected at the aerated surface (1 m depth) and at the transition between the aerobic and anaerobic layer, in correspondence of a "white cloud", rich in reduced manganese compounds. The analysis of manganese lacustral concentrations, as well as of redox and pH variations in this zone, are reported.

SEM examination of CuNi 70/30 specimens and molecular analyses were performed in order to document corrosion morphology and microbiology operating in the Idro Lake.

Acknowledgements

This work has been financed by the Research Fund for the Italian Electrical System under the Contract Agreement between RSE S.p.A. (formerly known as ERSE) and the Ministry of Economic Development - General Directorate for Nuclear Energy, Renewable Energy and Energy Efficiency stipulated on July 29, 2009 in compliance with the Decree of March 19, 2009

Corrosion in Biogas plants

R. Feser, A. Krebs, University of Applied Sciences South Westfalen, Iserlohn, Germany

Abstract

For the realization of the energy turnaround in Germany, Biogas power plants have been built increasingly in the past years. In a research project, the typical corrosion damage that occurs in biogas plants has been systematically investigated. With this knowledge the materials and corrosion protection methods for biogas plants will be improved. In a second step, the corrosion processes in the typical media from these biogas plants will be examined. In this publication an overview of typical corrosion damages from biogas plants will be presented. The observed corrosion phenomena are ranging from pitting corrosion to stress corrosion cracking or shallow pit formation. The corrosion failures are due to different causes. The medium, to which the materials are exposed, is aggressive because of the microorganisms present. Moreover, it comes to corrosion in the gas chamber of the biogas plant due to condensation. Agitators are subject to a corrosion attack combined with mechanical stress, which leads to corrosion fatigue cracking. The corrosion failures are presented; SEM and metallographic investigation have been performed. The corrosion mechanisms will be discussed. On the basis of the determined corrosion mechanisms recommendations for the future use for an optimized material selection will be given.

Furthermore the results of corrosion experiments will be presented. On the one side results of the exposition of steel and stainless steel in biogas plants will be presented. On the other side results of electrochemical experiments will be shown. The influence of the media to the corrosion mechanisms will be discussed. The results of failure analysis and corrosion experiments provide the basis for optimizing the use of materials and thus increase the efficiency and stability of the biogas process.

FAILURE INVESTIGATION OF HEAT EXCHANGER TUBES IN CLOSED LOOP COOLING WATER SYSTEM

Saad Almaaesab, Dr. Hussain Al-Mahamedh,

SABIC Technology Centre, P.O. Box 11669, Jubail Indust. City 31961, Saudi Arabia

Failure investigation was conducted on two heat exchangers installed in 1997 as part of closed loop cooling water system. The inspection history of the heat exchangers indicated multiple failures due to heavy deposits, fouling, pitting and thickness reduction as a result of high corrosion rate. Two tube samples have been examined and analysed using Scanning Electron Microscopy (SEM) and Energy Dispersive X-ray (EDX). In addition, water samples have been collected from the heat exchangers to study pH, conductivity, Total Dissolved Solids (TDS), Total Suspended Solids (TSS), Hardness, Anions and Cations. After analysing the samples provided and the given data of the failure, it was concluded that a high percentage of nitrate is present in cooling water which is probably due to the presence of nitrifying bacteria that will convert nitrite to nitrate. In addition, under-deposit corrosion was initiated due to fouling and heavy deposits and it was accelerated by the presence of chloride ions. It was recommended that cooling water quality should be checked regularly to maintain the standard requirements and limits especially the chloride level, Total Suspended Solids (TSS) and Total Dissolved Solids (TDS). In addition, identify the source of existing microbe that can contribute in the corrosion process. Finally, chemical cleaning should be applied on both heat exchangers.

Electrochemical behavior of low-carbon steel within MIC-induced corrosion and cathodic protection

E.J. León¹, D.A. Koleva¹, H.M. Jonkers¹, J.M.C. Mol², K. van Breugel¹

¹*Delft University of Technology, Faculty of Civil Engineering and Geosciences, Department Materials & Environment, Stevinweg 1, 2628 CN Delft, The Netherlands*

²*Delft University of Technology, Faculty 3mE, Department Surfaces & Interfaces, Mekelweg 2, 2628 CD Delft, The Netherlands*

Microbiologically induced corrosion (MIC) is a challenge on many levels when steel corrosion and corrosion protection are of concern. The complexity of the process arises from the fact that electrochemical phenomena (steel corrosion) and viability and action of micro-organisms are simultaneously present and exert various difficulties within corrosion control. For example, well known is that although impressed current cathodic protection (CP) is recognised to be the only suitable method for corrosion control in highly aggressive environment, the sufficient protection of steel structures when MIC corrosion (especially anaerobic) is involved, is still a challenge for the engineering practice. Well recognised are the reasons behind the inability of the current practice to cope with the aforementioned issues e.g. standard levels for steel polarisation do not allow further cathodic polarization, which could reduce micro-organisms viability. On the other hand, steel ennoblement due to bio-films formation, but also contribution of hydrogen evolution (both from cathodic reactions and bacterial activity) enlarge even more the complexity within corrosion control.

This paper will discuss the preliminary investigation on MIC corrosion control, using a modified regime of CP, based on pulse technology. The initial studies involve monitoring MIC-induced corrosion, where both mixed and anaerobic only (SRB-induced) conditions apply. The experimental set-up is presented in Fig.1, depicting the relevant environment and positioning of the electrodes to account for varying medium. EIS was mainly employed as electrochemical technique for corrosion monitoring – Fig.1b) depicts R_p values derived from EIS. As can be observed, different from expected behaviour was recorded i.e. the highest R_p is relevant to the steel in SRB-containing sand i.e. electrodes 1. The reason is hypothesized to be related to either steel ennoblement due to bio-film formation, or inhibitive effects of the “food” (saccharine-based) for SRB activation. At this stage, it seems that the effect of “food” addition is determining steel resistance, which can be due to: either enhanced bacterial activity, more resistive bio-film formation and hence larger anodic shift, or anodic shift due to inhibitive effects of the “food”. These considerations are supported by OCP readings of steel electrodes conditioned separately in each relevant environment i.e. sea water only, sea water+ SRB-free sand, sea water + SRB sand and sea water +SRB+ food – Fig.1c). The most noble potentials are for steel in SRB+ food containing environment, whereas the most active state was observed for steel in SRB and no “food” additions containing environment. Further clarification is necessary through recording electrochemical behaviour of steel in sea water with “food” addition only.

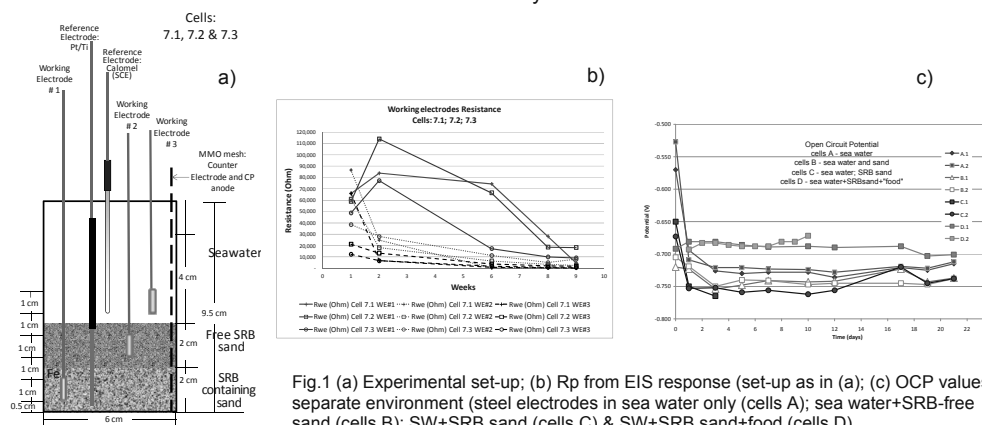


Fig.1 (a) Experimental set-up; (b) R_p from EIS response (set-up as in (a)); (c) OCP values separate environment (steel electrodes in sea water only (cells A); sea water+SRB-free sand (cells B); SW+SRB sand (cells C) & SW+SRB sand+food (cells D))

Further, the paper will discuss the response of the steel electrodes with CP application, where conventional (constant) and pulse DC current were applied at the level of 10 mA/m² for the former and cumulative 5 mA/m² for the latter case.

Accelerated souring test of crude oil under the anaerobic condition

*Yasunori Tanji, Ryo Hasegawa, Kazuya Tohyama, Kazuhiko Miyanaga
Graduate School of Bioscience and Biotechnology, Tokyo Institute of Technology,
4259-J2-15 Nagatsuta-cho, Midoriku, Yokohama 226-8501, Japan*

Seawater injection to the crude oil well is commonly used to increase oil recovery rate. However, biochemical reduction of the sulfate ion presents in seawater causes souring, production of sulfide. Sulfate reducing bacteria (SRB) involved in the souring. Microbial sulfate reduction is an important metabolic activity in many petroleum-hydrocarbon (PHC) contaminated aquifers as contamination with mono-aromatic PHC, e.g. benzene, toluene, ethylbenzene, is of regulatory concern due to their solubility and toxicity. Sulfate reduction can be coupled to the bacterial metabolism of mono-aromatic PHC, and thus has gathered increasing interest as an intrinsic remediation process. SRB are among the microorganisms present in oil fields that induce souring; most SRB belong to Deltaproteobacteria and Firmicutes. In order to control corrosion, steps are taken to remove oxygen from injected water, but this provides an environment conducive to the growth of SRB that are obligate anaerobes. Seawater contains sulfate (approximately 28 mM). SRB derive energy for growth by coupling the oxidation of organic electron donors to the reduction of sulfate to sulfide. The electron donors most commonly used by SRB in oil fields are volatile fatty acids (VFAs). VFAs in oil-field water (OFW) are produced by microbial degradation of crude-oil components. Putative hydrocarbon metabolites have been detected in production water taken from oilfields. OFW was sampled from the Yabashi crude oil well in Akita, north part of Honshu-island of Japan. The OFW contained volatile fatty acids (acetate-540, lactate-183, propionate-154 and i-butyrate-48 in mg/L). Crude oil and alkane mixture were incubated for 190 days with the seawater supplemented with the microbes separated and concentrated from the OFW under the anaerobic, and microaerobic condition, respectively. Sulfide production was observed when the crude oil was incubated. Microaerobic condition did not promote souring. Drastic change of microbial consortia was observed when the crude oil and alkane mixture was incubated with the seawater. However difference of the consortia among the two substrates was small. Main components of crude oil responsible for the souring were identified.

Accelerated biological souring test

Sulfate-reducing bacteria induced the corrosion of copper

Dun Zhang, Shiqiang Chen, Peng Wang, Institute of Oceanology, Chinese Academy of Sciences, Qingdao, China,

Sulfate-reducing bacteria (SRB) induced corrosion behavior of copper was investigated by surface analysis and electrochemical measurements in seawater. It is demonstrated that SRB can adhere onto copper surface to form biofilm, and resulting corrosion product is mainly composed of cuprous sulfide. In SRB growth cycle, corrosion rate is related to metabolic activity. Especially in exponential growth and stationary phases, SRB metabolic process can decrease anodic zone area and promote localized corrosion of copper.

The Effects of Ag-Cu Ions on the Microbial Corrosion of 316L Stainless Steel in the Presence of *Desulfovibrio* sp.

Tuba UNSAL^a, Simge ARKAN^a, Esra ILHAN-SUNGUR^a, Nurhan CANSEVER^b

^a Istanbul University, Faculty of Science, Department of Biology, 34134 Vezneciler, Istanbul-Turkey

^b Yıldız Technical University, Faculty of Chemistry-Metallurgy, Metallurgical and Materials Engineering Department, 34210 Esenler, Istanbul-Turkey

Abstract

316L stainless steel is the most preferred material in cooling tower systems especially in areas where water accumulates, such as the cold water basin, owing to its high corrosion resistance, durability feature and resistance to chloride- containing environments. However some studies reported that the cooling water conditions may cause severe corrosion resulting in structural failures which are attributed to microbial activity. Sulfate reducing bacteria (SRB) are considered as the major bacterial group involved in microbiologically influenced corrosion (MIC). Especially, *Desulfovibrio* sp. is one of the most abundant and dominant genus of SRB in the cooling tower water. As a result of their ability to generate H₂S, SRB cause corrosion of various metals seriously in cooling towers which are the essential part of industrial systems. Although the excellent corrosion resistance of stainless steel, it is susceptible to localized corrosion by reduced sulfur compounds and chloride ions. In recent years, Ag-Cu ionization system is used as an alternative to biocides for preventing both of microbial corrosion and the formation of biofilms in order to improve water systems. However, there are limited studies about the effects of Ag-Cu ions on the growth of SRB and corrosion behavior of stainless steel where Ag-Cu ionization systems were used.

The aims of this study were to determine the microbial corrosion of 316L stainless steel and the inhibitor effects of Ag-Cu ions on the MIC of 316L stainless steel in the presence of *Desulfovibrio* sp. Electrochemical tests were carried out in sterile Postgate's C (PC) medium, PC medium containing Ag-Cu ions, PC medium containing *Desulfovibrio* sp., PC medium containing *Desulfovibrio* sp. and Ag-Cu ions. Potentiodynamic polarization and Open circuit potential (OCP) methods were used to analyze the corrosion behavior of 316L stainless steel. The biofilm, corrosion products and Ag-Cu ions on the steel surfaces were investigated by using Scanning Electron Microscopy (SEM), Energy Dispersive X-ray Spectrometry (EDS) and elemental mapping.

It was observed that the corrosion potential values of 316L stainless steel exposed to the *Desulfovibrio* sp. culture changed with time when compared to the sterile PC medium. The results indicated that pitting was developed with the breakdown of passive surface layer by *Desulfovibrio* sp.. Also, the addition of Ag-Cu ions to the *Desulfovibrio* sp. culture decreased the values of current density that was related to the inhibitor effect on corrosion of 316L stainless steel.

Keywords: 316L stainless steel, Microbiologically influenced corrosion (MIC), *Desulfovibrio* sp., Electrochemical tests, Ag-Cu ions.

INFLUENCE OF BIOFILM WITH MIXED CULTURE IN CORROSION RATE OF CARBON STEEL

Sara H. Oliveira, UFPE, Recife/Brasil; Magda R. S. Vieira, UFPE, Recife/Brasil; Diniz R. Lima Junior, UFPE, Recife/Brasil; Maria Alice G. Andrade Lima, UFPE, Recife/Brasil; Severino L. Urtiga Filho, UFPE, Recife/Brasil.

At the instant at which a metal surface is immersed in water, starts the formation of biofilm. A biofilm is a microbial mass composed of water, micro-organisms, extracellular polymeric substances (EPS), dissolved substances and retained and adsorbed particles. The micro-organisms tend to adhere to the surfaces where they find a greater availability of nutrients and develop there. Alterations occur as a result of electrochemical conditions at the interface metal / solution, leading to an intensification of the corrosion process. In this study were evaluated differences in cell concentrations and corrosion rates of carbon steel coupons immersed in bioreactors with seawater, and different sterilization conditions. The carbon steel used was SAE 1010, with dimensions 30mm x 10mm x 2.5mm. The seawater used was from the Port Complex SUAPE - Ipojuca-PE, Brazil. The bioreactors with the means remained for 720h. The biofilms formed on the surface of the coupons were characterized using the techniques of surface analysis, X-ray Diffraction (XRD) and Scanning Electron Microscopy (SEM). The results showed that the system where the bioreactor and the coupons were sterile, bacterial colonization and the corrosion rate of the coupons were lower than the system where the bioreactor, coupons and seawater, were not sterile. The XRD analysis of the coupons revealed that the system where the coupons were sterile found less corrosion compounds.

Effect of electromagnetic field on the corrosion behaviour of 2205 Duplex stainless steel in the presence of *Pseudoalteromonas* sp.

Zhenlun Song, Masoumeh Moradi

Surface protection research group, Surface Department, Ningbo Institute of Materials Technology and Engineering, Chinese Academy of Sciences, 519 Zhuangshi Road, Ningbo315201, China

Abstract:

The control of microbial growth is necessary in many practical situations. The international debate on the problem of the possible biological effects of electromagnetic fields, led us to test the possibility that such fields could be used as low-cost and easy-handling agents with which to inhibit microbial growth in marine environment. The effects of magnetic fields (MFs) in metal corrosion also have been extensively studied in recent years and it is found that Corrosion rates of stainless steel and copper significantly reduced in the presence of a magnetic field. The present research was aimed at exploring the effects of MFs on the MIC of 2205 Duplex stainless steel (DSS) caused by aerobic marine isolated bacterium, namely *Pseudoalteramonas* sp. in terms of bacteria growth, corrosion extent, and corrosion products. Different electrochemical and surface analysis methods have been used in this study. The results showed 0.4T is the optimum magnetic field to control of this bacterium growth; however it didn't show the MBC effect; so the bacteria grew again in the absence of MFs. Different electrochemical behaviour of DSS in the presence and absence of magnetic field was observed due to antifouling and anticorrosion effect of MFs. FESEM images showed the presence of bacteria and their metabolic by-products in the absence of magnetic field; while in the presence of the MFs, there were no bacteria on the surface. Furthermore, the structure of the biofilm was even found to be different than what is commonly observed when there is no magnetic field.

Long-term survival of reinforced concrete structures in marine environments

*Robert E Melchers & Igor Chaves, Centre for Infrastructure Performance and Reliability,
The University of Newcastle, Australia*

Corrosion damage in reinforced concrete structures in marine environments occurs sometimes already after only 20 years exposure. Usually this is attributed to chloride diffusion through the concrete to the reinforcing bars, sufficient to initiate corrosion and its progression and thus to structural damage. However, despite this conventional wisdom, there are many examples of RC structures that have survived for long periods (e.g. 60 or more years) in marine environments. In most cases there is little evidence of reinforcement corrosion, such as rust stains, concrete cracking or concrete spalling, even though chloride concentrations at the reinforcement usually are much higher than conventionally permitted. Many were made with seawater as mixing water and others have only thin concrete cover to the reinforcement. Several examples are given reviewed, briefly, together with a study that included more than 300 similar cases extracted from the literature. It showed concretes with calcium carbonate aggregates (limestone or seashells or non-reactive dolomites) to have longer times both to commencement of corrosion initiation and to active corrosion. The results were not particularly sensitive to chloride concentration. They suggest that high concrete alkalinity (pH buffering capacity) is an important factor in delaying reinforcement corrosion.

The main part of the paper reports results from a 10y study of the corrosion of 6mm diam. reinforcing bars centrally placed in 40x40x160mm concrete specimens made with seawater as mixing water. Some were made using calcium carbonate aggregates and other alkalis. All were exposed in a fog-room. Similar tests by Shalon & Raphael (1959) also using calcium carbonate aggregates showed serious corrosion after only 3-4 years exposure. No such corrosion was observed in the new experiments even after 10 years.

The reasons for the differing observations are explored by careful examination of the initiation of corrosion where it did occur, of the pH patterns in the concrete samples and of the concrete diffusion characteristics. This shows that concretes (1) made with high cement contents (and therefore high alkalinity) and (2) which were also very well compacted show no evidence of reinforcement corrosion, irrespective of the high concentrations of chlorides. This is consistent with field observations and some other, shorter, test programs. Conversely, those concretes with poor compaction, low cement content and/or high aggregate contents showed irregular, patchy and localized corrosion initiation on the bars. These are attributed to the inadequate achievement of the crucial intimate physical and chemical contact required between all parts of the surfaces of steel reinforcement and the enveloping cement paste and alkaline aggregates. If the latter is not achieved the steel is exposed wholly or in part essentially to natural seawater. The corresponding corrosion-time behaviour is then exactly that observed in the 1959 tests. The results have obvious and important implications for industry.

References:

- R. Shalon & M. Raphael (1959) Influence of seawater on corrosion of reinforcement, J.ACI, 30(12) 1251-1268.
- Melchers RE and Li, CQ (2006) Phenomenological Modelling of Corrosion Loss of Steel Reinforcement in Marine Environments, ACI Materials Journal, 103(1) 25-32.
- Melchers RE, Li CQ Li and Davison MA (2009) Observations and analysis of a 63-year old reinforced concrete promenade railing exposed to the North Sea, Magazine of Concrete Research 61(4) 233-243.
- Melchers RE (2010) Carbonates, carbonation and the durability of reinforced concrete marine structures, Aust J Struct Engrg 10(3) 215-226.
- R.E. Melchers and T. M. Papé (2011) Aspects of long-term durability of reinforced concrete structures in marine environments, European Journal of Environmental and Civil Engineering, 15(7) 969-980.

Corrosion behaviour of steel in fly-ash geopolymer mortars exposed to chloride solutions

C. Monticelli^{1,2}, M. Abbottoni¹, S. Manzi^{3,4}, C. Chiavari⁴, A. Balbo^{1,2}, F. Zanotto^{1,5}, M.E. Natali³, M.C. Bignozzi^{3,4}

¹ *Centro Studi Corrosione e Metallurgia "A. Daccò", Università di Ferrara, Italia*

² *Teknehub, Università di Ferrara, Italia*

³ *DICAM (Dipartimento di Ingegneria Civile, Chimica, Ambientale e dei Materiali), Università di Bologna, Italia*

⁴ *C.I.R.I. (Centro Interdipartimentale di Ricerca Industriale) Meccanica Avanzata e Materiali, Università di Bologna, Italia*

⁵ *Terra & Acqua Tech, Università di Ferrara, Italia*

Nowadays, the environmental impact of Portland cement (OPC) production and the construction industry in general has prompted a search for alternative materials. Fly ash geopolymers can represent new choices as concrete binders, making clear the urge to consolidate and widen the current state of understanding the physical-mechanical properties and the degradation mechanisms of the new corresponding concrete materials.

In this research different fly ash geopolymer mortars were prepared by varying the sodium oxide/silicon oxide ratios in the activating solutions. At decreasing ratios from 0.16 to 0.12, the porosity decreased, though always remaining higher than that in the OPC mortar prepared with the same liquid to solid ratio. Reinforced slabs obtained with geopolymer and OPC mortars were continuously exposed to either distilled water or 3.5% NaCl solution. Under the latter conditions, chlorides penetrated by a combination of capillary suction and diffusion.

Corrosion was monitored by periodic corrosion potential and polarization resistance measurements and less frequently by Electrochemical Impedance Spectra recording. Chloride content at the rebar level was measured on unreinforced slabs exposed to the same environmental conditions. The results showed that a quick chloride penetration occurred and corrosion started within one day in the OPC mortar and in the geopolymer mortar with the highest sodium oxide/silicon oxide ratio and the highest porosity. On the contrary, corrosion took one month to start in the other more compact geopolymer mortars. The results were interpreted by taking into consideration the mortar pH values and the total chloride concentrations at the rebar levels.

Study of reinforcing bar corrosion in solution simulating bacteria metabolites

*Matteo Stefanoni, Enrico Volpi, Stefano Trasatti
Università degli Studi di Milano, Italy*

Reinforced concrete deterioration is recognised as a serious problem, resulting in significant economic loss, safety concerns and reduction of durability and service life of civil structures. Among the different causes of reinforced concrete structure damages, the corrosion of steel reinforcing bars is one of the most studied, frequently occurring in chloride contaminated environments. Much less studied is concrete degradation and steel rebar corrosion due to microbial activity, although it is a significant issue occurring in sewer systems, waste water treatment plants, animal housing and concrete manure tanks. In such environments the deterioration mechanism is mainly related to bacteria involved in the sulphur cycle, i.e., Sulfate Reducing Bacteria (SRB) and Sulphur Oxidizing Bacteria (SOB).

The preparation of significantly reinforced mortar samples is extremely complicated and time consuming, which does not allow multivariable study. For this reason the use of simulated concrete pore solution results to be the most convenient initial option.

Samples of B450C mild steel were naturally passivated in saturated Ca(OH)_2 solution, then exposed to Na_2S and H_2SO_4 environments to simulate the metabolic products of SRB and SOB, respectively.

The corrosion due to different concentrations of aggressive species was monitored electrochemically by means of anodic polarization and cyclic voltammetry, which highlighted completely different behaviours and attacks. Different corrosion morphologies were confirmed by SEM images, while corrosion products were analysed by XRD.

Once the behaviour of steel in the simpler system of simulated concrete pore solution was clarified, it was possible to move to the more complicated system of the steel rebars embedded in mortar samples.

As above mentioned, reinforced mortar samples were exposed to solutions simulating bacteria metabolites, and the corrosion of reinforcing bars was monitored by non destructive measurements such as OCP and linear polarization resistance (LPR). In the latter tests attention was also focused on the degradation of the cementitious matrix of the mortar sample, evaluated by weight loss measurements besides microscopic and spectroscopic techniques.

Investigations of chloride diffusion for reinforced geopolymer mortar

C. Monticelli^{1,2}, M. Abbottoni¹, S. Manzi^{3,4}, C. Chiavari⁴, A. Balbo^{1,2}, F. Zanotto^{1,5},
M.E. Natali³, M.C. Bignozzi^{3,4}

¹ Centro Studi Corrosione e Metallurgia "A. Daccò", Università di Ferrara, Italia

² Teknehub, Università di Ferrara, Italia

³ DICAM (Dipartimento di Ingegneria Civile, Chimica, Ambientale e dei Materiali),
Università di Bologna, Italia

⁴ C.I.R.I. (Centro Interdipartimentale di Ricerca Industriale) Meccanica Avanzata e
Materiali, Università di Bologna, Italia

⁵ Terra & Acqua Tech, Università di Ferrara, Italia

Alkali activated materials and geopolymers are receiving particular attention as new binders for mortar and concrete preparation. Their potential use in civil engineering field can be considered as a sustainable alternative to traditional Portland cement if the raw materials used for alkali activation come from recycling process. So far, granulated blast furnace slag, carbon fly-ash, municipal solid waste ash, ceramic residues, etc. have been activated by means of alkaline solutions with different concentrations in order to obtain solid products with adequate mechanical properties. However, if alkali activated materials and geopolymers have to substitute Portland cement in mortar and concrete preparation, then it is necessary that the precursors are available in large amount, the mixes are safe to handle and able to consolidate at room temperature in a proper time.

For this reason the research has been recently focused on geopolymers obtained by carbon fly-ash, a type of waste already well known by traditional concrete and cement producers. In last years a lot of investigations on the alkali activation of carbon fly-ash in order to produce building materials have been performed, however durability issues are still scarcely studied.

This work aims at investigating the corrosion behaviour of steel reinforcements in carbon fly-ash geopolymers exposed to artificial marine environment. So different geopolymer mortars were prepared by modifying the sodium oxide/silicon oxide ratios in the activating solutions and were used to produce reinforced mortar cylinders. Their corrosion behaviour was compared to that of samples prepared with traditional ordinary Portland cement.

Corrosion was monitored by electrochemical tests and the mortars were characterized by assessing chemical and physical parameters (chloride % and pH) as well as pore size distributions. In particular, the chloride concentration profiles were measured in order to determine the critical chloride content for the onset of steel corrosion in the different geopolymer mixes and to make a useful comparison with the well-known behaviour of traditional cement based materials.

Chloride Treshold Level for Steel in Concrete – Development of Research Efforts

Dipl.-Ing. Marc Kosalla, Prof. Dr.-Ing. Michael Raupach, RWTH Aachen University, Aachen/Germany

Abstract (400 words)

At the Institute of Building Materials Research (RWTH Aachen University) a new research project regarding the critical chloride content was started in 2013. This project investigates the chloride threshold level including a differentiation of the type of binding material and the quality of the interface (contact zone) of steel and concrete, which is depending on the orientation of the rebar in relation to the direction of concrete casting. Moreover the project is aimed at being the basis for developing a test method, which potentially could gain a wide acceptance for being implemented as standard test method.

In the first two parallel test series of the project, currently the influence of electrochemical polarisation in the test method and the actual existing polarisation of the reinforcement in construction elements with practical geometries are investigated. On the one hand small cubic concrete specimens with a rebar inside were exposed to NaCl-solution at the surface, while the potential vs. a reference electrode and the current flow to a grid of titanium mixed oxide serving as cathode are monitored. Reference and cathode are placed in the salt solution and the polarisation is varied gradually between resting potential and an anodic polarisation of ca. +560 mV. In the parallel series two column bases and four plane specimens with practical geometries were fabricated. The reinforcement in each specimen is segmented in ten separate sections with variable sizes, which are electrically decoupled. The measurement of potentials both between the sections and vs. a reference electrode is possible for all combinations. The results deliver information about available polarisations in practice. In both series an OPC and a BFS cement composition are used.

A critical analysis of proposed test methods for measuring the chloride threshold value in reinforced concrete

U. Angst, B. Elsener

ETH Zurich, Institute for Building Materials, CH-8093 Zurich, Switzerland

The chloride content at which reinforcement corrosion initiates in concrete is usually referred to as “chloride threshold value” or “critical chloride content” (C_{crit}). As has been shown in a recent review [1], many aspects of chloride induced reinforcement corrosion in concrete are still incompletely understood and huge differences from virtually 0 to more than 3% chloride by cement weight are reported for C_{crit} in the literature. There are various reasons for this, such as experimental inaccuracies (limited measurement precision, sampling methods, etc.) or localized corrosion initiation being a stochastic phenomenon. Nevertheless, also the numerous types of experimental procedures and setups being used by different laboratories are considered a major factor contributing to the scatter of literature values for C_{crit} . This involves parameters such as specimen geometry, specimen preparation, concrete mix design, curing, methods to accelerate chloride ingress, electrochemical methods to detect corrosion initiation, sampling procedures, etc. This situation led in 2009 to the formation of a RILEM Technical Committee (TC 235-CTC) with the aim of proposing a realistic and feasible test procedure. Preliminary results of a round-robin test carried out with a test procedure selected on the basis of a careful state of the art report revealed that a few more challenges need to be addressed.

Thus an additional effort has to be made in developing a standardized test method for the determination of C_{crit} . The outcome of the mentioned RILEM Technical Committee will provide a sound basis for this. It may be combined with new insights gained over the last years such as probabilistic aspects related to specimen size [2] or challenges with corrosion initiation detection with certain binders such as slag, e.g. Ref. [3]. Also the currently running research project funded by the Swiss Federal Roads Office that aims at determining C_{crit} in samples taken from field structures (rather than laboratory made samples) will provide useful experience.

In this paper, advantages and disadvantages of the numerous test methods for measuring C_{crit} proposed in the literature are discussed e.g. with respect to practice-relationship, experimental time / acceleration of real-world processes, applicability to different cement types, and relevance of the obtained results. The discussion also relates this to the different objectives that determining C_{crit} may have, viz. if input parameters for service life modeling are the desired output or if the method is applied for comparative purposes only, e.g. for ranking materials (steel types, binders, etc.).

References

- [1] U. Angst et al. Critical chloride content in reinforced concrete – A review, *Cem Concr Res*, 39 (2009) 1122-1138.
- [2] U. Angst et al. Probabilistic considerations on the effect of specimen size on the critical chloride content in reinforced concrete, *Corros. Sci.*, 53 (2011) 177-187.
- [3] V. Garcia, Contribution à l'étude du taux de chlorures pour l'amorçage de la corrosion des armatures du béton armé, doctoral thesis, University of Toulouse, 2013. (in French)

Chloride threshold for corrosion initiation in reinforced concrete: the applicability of Ag/AgCl sensors revisited

F. Pargar¹, D.A. Koleva¹, P. Taheri², J.M.C. Mol², E.A.B. Koenders¹, K. van Breugel¹

¹Delft University of Technology, Faculty of Civil Engineering and Geosciences, Department Materials & Environment, Stevinweg 1, 2628 CN Delft, The Netherlands

²Delft University of Technology, Faculty 3mE, Department Surfaces & Interfaces, Mekelweg 2, 2628 CD Delft, The Netherlands

The need of accurate determination of chloride thresholds for Cl^- -induced corrosion initiation in reinforced concrete has long been recognised; numerous investigations and reports on the subject are available. Yet, chloride thresholds have always been and are still debatable on a larger scale. The challenge of course is related to many factors, among which: cement type, steel surface properties, accuracy of free vs chemically bound chloride determination, drawbacks of sensor technologies, fundamental considerations regarding passivity breakdown and/or re-passivation, etc. Additionally, the durability of commonly used sensors and their reliable performance within the service life of a reinforced concrete structure needs firmer justification, together with sensors' stability and "sensitivity" in the originally high pH environment of the concrete pore water.

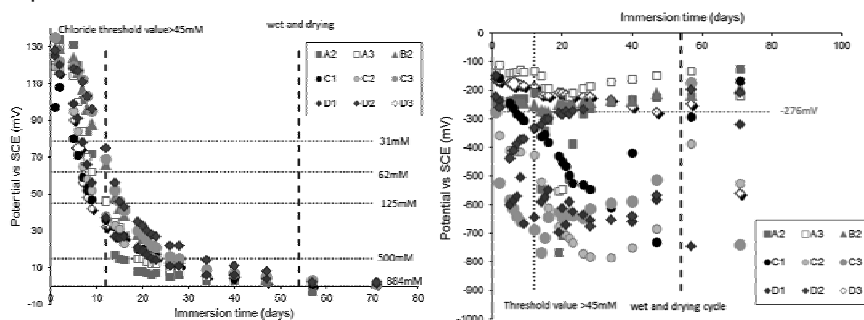


Fig.1 OCP readings for Ag/AgCl sensors (left) and steel rods (right)

This work will discuss the importance of the AgCl layer properties and the effect of the AgCl|cement paste interface on the performance of commonly applied Ag/AgCl sensors for quantification of Cl⁻ levels in reinforced concrete. Further, the paper correlates the sensor's and embedded steel electrochemical behaviour, recorded simultaneously in one and the same environmental medium: Ag/AgCl electrodes (sensors) and steel rods were embedded and monitored in cement paste cylinders, which after 30-days curing in sealed condition were immersed in simulated pore water, containing 5% NaCl. The sensors were initially prepared at different anodisation regimes (0.5, 2 and 4 mA/cm² in 0.1 M HCl) in order to account for a desired variation of AgCl layers' thickness, morphology/porosity, aiming to identify the optimum layer characteristics towards stability and sensitivity of the sensors. The aim was also to evaluate the dependence of the sensor readings' accuracy on the sensors' and sensor/cement paste interface characteristics. The electrochemical response of both sensors and steel were monitored over a period of >120 days via OCP readings (Fig.1), EIS and LPR techniques. For the sensors prepared at lower level current densities (e.g. 0.5 mA/m², specimens A2, Fig.1), the results show a good correlation of sensor and steel electrochemical response i.e. Cl content as approximated from sensors' OCP readings corresponds well to indication of corrosion initiation from steel OCP records. On the other hand, discrepancies were observed for sensors prepared at currents of > 2 mA/cm², e.g. specimens C1, C2, D3, Fig.1. EIS results for both sensors and steel substantiate the observed behaviour through the recorded best fit parameters for surface layer properties, including cement matrix properties (high frequency domain) and charge transfer (or diffusion limitations) characteristics (low frequency domain). EIS best fit parameters further clarify the phenomena behind the observed behaviour, accounting for the importance of the AgCl layer properties and bulk matrix microstructural characteristics and their effect on sensors' readings and recorded chloride thresholds, respectively.

Effect of concrete pore solution composition on the electrochemical behaviour of C15 steel reinforcement

S. Chakri^{1,2}, E. Sutter^{1,2}, B. Tribollet^{1,2}, V. Vivier^{1,2}, I. Frateur^{1,2}

1- CNRS, UMR 8235, *Laboratoire Interfaces et Systèmes Electrochimiques*, F-75005, Paris, France

2- Sorbonne Universités, UPMC Univ Paris 06, UMR 8235, LISE, F-75005, Paris, France

The passivity of reinforcing steel in concrete is generally attributed to the formation of a protective oxide layer on the steel surface. This process is related to the high alkalinity of the surrounding pore solution (at pH values higher than 12) due to the release of calcium hydroxide, Ca(OH)_2 , during the hydration process of cement. Although pore solutions of ordinary Portland cement concrete are saturated with Ca(OH)_2 , they also contain different auxiliary ions depending on the type of cement and supplementary cementing materials (e.g. fly ash, high furnace slag and silica fume). The major ionic species include cations such as Ca^{2+} , Na^+ and K^+ and anions such as OH^- and $(\text{SO}_4)^{2-}$. Sodium and potassium ions originate from alkali oxides, such as Na_2O and K_2O , that exist in cement; sulphate ions can come from gypsum ($\text{CaSO}_4 \cdot 2\text{H}_2\text{O}$) added during cement production, or from contaminated aggregates or mixing water. All of these ions may play a role in the corrosion processes of reinforcing steel.

The objective of this work was to study the influence of the chemical composition of pore solutions on the electrochemical behaviour of C15 mild steel, used for reinforcement of building concrete. For that purpose, electrochemical measurements (monitoring of the corrosion potential E_{corr} as a function of immersion time, polarization curves, and electrochemical impedance spectroscopy) were performed in various simulated electrolytes representative of concrete pore solutions extracted from different concrete mixtures and at different times after mixing (fresh and mature concretes). The pH of the synthetic pore solutions was adjusted to 13. The results were compared to those obtained in the 0.1 M NaOH reference solution. Under anodic polarization, it was shown that the steady-state passive current density j_{ss} is reached within several tens of hours; therefore, the steady-state anodic polarization curves must be plotted point by point, and not using a scan rate even as low as 0.1 mV/s [1,2]. For example, j_{ss} is two decades lower compared to the passive current density recorded at 0.5 mV/s. Another main result is that pH is not the single determining parameter to predict the electrochemical behaviour of steel: at constant pH, the corrosion current and the polarisation resistance at E_{corr} are very different from one solution to another.

[1] A. Carnot, I. Frateur, P. Marcus, B. Tribollet, J. Appl. Electrochem. 32 (2002) 865-869.

[2] P. Ghods, O.B. Isgor, G. McRae, T. Miller, Cement & Concrete Composites 31 (2009) 2-11.

Potentiostatic evaluation of the critical chloride threshold of 1.4362 stainless steel in concrete with mixed-in chloride

M. Gastaldi, F. Lollini, L. Bertolini

*Department of Chemistry, Materials and Chemical Engineering "G. Natta",
Politecnico di Milano, Milan (Italy)*

Different stainless steel grades are commercially available as reinforcement, characterised by different chemical composition, microstructure and surface conditions. Experiences reported in literature show that their corrosion resistance can be significantly different. Indeed, the chloride threshold is a property of any specific stainless steel; furthermore it also depends on concrete characteristics (e.g. pH), potential and temperature.

The knowledge of the critical chloride threshold is essential to make a proper choice of what stainless steel type can be used to guarantee the durability target of a concrete structure, in a specific environment.

To assess the chloride threshold of stainless steel in concrete different tests have been proposed. Due to the high value of the chloride threshold for stainless steels, often tests with mixed-in chloride and potentiostatic polarization have been considered. Nevertheless the results of such type of tests need to be evaluated, in order to assess its applicability to both the simple comparison of different stainless steel (e.g. for ranking purpose) and use in service life modelling.

In this paper, results of a study for evaluating the corrosion resistance of duplex stainless steel reinforcement type 1.4362 in concrete as a function of polarization conditions are reported. Different amounts of chlorides (from 2% to 5% of chloride by cement mass) were mixed in concrete reinforced specimens and potentiostatic anodic polarisation test at different potentials were performed; polarisation was maintained constant for different time intervals. Every test was performed on, set of 10-15 specimens to take in account results variability. Results showed that the experimental procedure significantly affects the results of the test and these cannot be used directly in service life modelling.

Investigation of chloride-induced pitting corrosion of steel in concrete by a combination of electrochemical methods with X-ray tomography

Gino Ebell, Jürgen Mietz, Andreas Burkert; BAM – Federal Institute for Material Research and Testing, Berlin/Germany

Steel in concrete is protected by the alkaline pore water environment and the resulting formation of a protective passive layer against corrosion. Adverse environmental conditions due to carbonation or chloride ingress can destroy the passive layer on the steel surface. Corrosion processes starting in those areas lead to uniform corrosion or local corrosion like pitting corrosion. In comparison to uniform corrosion pitting corrosion is a form of increased local corrosion and thus leads to a progressive reduction in cross-section of the reinforcing steel. The corrosion products are first absorbed by the pores of the concrete matrix, without causing visible external changes at the concrete surface.

Due to the concrete cover the steel surface is not visually accessible, so that the proportion of the corroded surface can only be determined by a destruction of the samples. In order to get a reliable basis for modelling the corrosion progress it requires a large number of specimens to do systematic laboratory studies on the effect of several parameters [1]. As chlorides penetrate only slowly into the concrete, for laboratory investigations the chlorides are usually added directly to the mixing water. A part of the chloride is bound in the cement matrix and is no longer effective for corrosion [2]. Hence, the damage mechanism differs from practical situations. At the BAM electrochemical corrosion tests were performed on specially designed specimens (fig. 1) where chlorides are able to reach the steel surface within short time. In combination with novel investigation methods, the main disadvantages of the existing test procedure could thus be eliminated [3, 4]. By using a combination of electrochemical investigations and X-ray tomography, a reference surface of the determined characteristic values without destroying the specimens is possible, so that quantitative information on the progress of corrosion, at various points in measuring time, can be obtained.

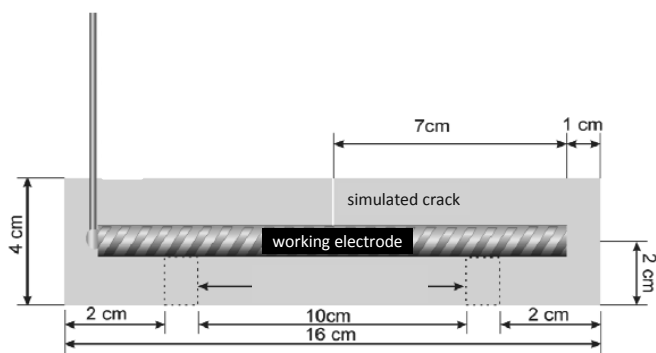


Fig. 1: Schematic representation of the specimen

In the development of the specimen, the main focus laid on the simulation of a cracked reinforced concrete component. The crack was designed as a 400 microns wide crevice. In the area of the simulated crack an injection with a defined amount of chlorides was carried out. To initiate pitting corrosion under defined parameters, the specimens were subjected to potentiostatic holding test.

- [1] Beck, M., Isecke, B., Lehmann, J., *Modelling of reinforcement corrosion – Influence of concrete technology on corrosion development*, In: Materials and Corrosion 2006, 57, 914-919
- [2] Breit, W., *Kritischer korrosionsauslösender Chloridgehalt – Untersuchungen an Mörtелеlektroden in chloridhaltigen alkalischen Lösungen*, In: Materials and Corrosion 2003, 54, 430-439
- [3] Beck, M., Goebbels, J., Burkert, A., *Application of X-ray tomography for the verification of corrosion processes in chloride contaminated mortar*, In: Materials and Corrosion 2007, 58, 207-210
- [4] Beck, M., Goebbels, J., Burkert, A., Isecke, B., Bäßler, R., *Monitoring of corrosion processes in chloride contaminated mortar by electrochemical measurements and X-ray tomography*, In: Materials and Corrosion 2010, 61, 475-479

Geo-polymeric and cementitious mortars with the same strength class: corrosion behaviour of steel and galvanized steel reinforcements.

*T. Bellezze, A. Mobili, G. Roventi, F. Tittarelli
Department SIMAU, Polytechnic University of Marche,
Via Breccia Bianche, 60131 Ancona, Italy*

Geo-polymeric and cementitious mortars with the same strength class and workability were studied and compared in terms of mechanical and corrosion behaviour of possible reinforcements. To this aim, three different geo-polymeric and cement mixtures were manufactured in order to obtain mortars belonging to $R1 \geq 10\text{MPa}$, $R2 \geq 15\text{MPa}$ and $R3 \geq 25\text{MPa}$ strength class.

In particular, mortars based on geo-polymer binder were prepared with fly ash, aluminous cement, a solution of sodium silicate/sodium hydroxide ratio of 1:1, with different concentration of NaOH, and a sand/binder ratio of 3:1, by weight. The respective three cementitious mortar mixtures were prepared with different proportion of ordinary Portland cement and hydraulic lime as binders, different water/binder ratio by weight and the same sand/binder ratio (3:1 by weight).

The corrosion resistance of embedded steel and galvanized steel reinforcements was investigated by free corrosion potential, polarization resistance measurements and metallographic analysis.

The results showed that the galvanized steel reinforcements are particularly susceptible to corrosion in geo-polymer mixtures due to their high alkalinity. However, after few days of curing, they become passive, even if the passivation process is slower than that of same reinforcements in cementitious mixtures. On the other hand, in geo-polymer matrix, the steel reinforcements show a lower corrosion rate, if compared with galvanized steel reinforcements, and their corrosion behaviour do not change significantly with the type of binder.

Stress corrosion cracking behaviour of the prestressing steel: influence of steel microstructure

Ioan Pепенar, ICECON Group-Research Centre CERTINCON, Bucharest, Romania

The paper presents the results of the laboratory tests on the stress corrosion cracking behaviour of two types of high-strength steel used as tendons for prestressed concrete: cold-drawn steel with pearlitic microstructure and thermally treated (quenched and tempered) steel with martensitic microstructure.

The prestressing steel specimens were subjected to 75% of the ultimate tensile strength, by tensioning in rigid frames. The corrosion tests have been performed by immersing the stressed specimens in two main types of corrosive solutions:

- Solutions susceptible to induce the cracking of the specimens by selective dissolution of the anodic areas (active path corrosion), the stress corrosion cracks (SCC) progressing by an anodic mechanism: NH_4NO_3 solution;
- Solutions susceptible to induce the cracking of the specimens by the embrittlement effect of the hydrogen (Hydrogen-Induced Stress Corrosion Cracking-HISCC), resulting by the cathodic reaction: H_2S saturated water, H_2S saturated H_2SO_4 solution, H_2SO_4 solution, NH_4SCN solution.

In order to accelerate the corrosion process, some of the stressed specimens immersed in corrosive solutions have been subjected to an electrochemical polarization (anodic or cathodic), at a constant current density.

The assessment criteria for the resistance to SCC and HISCC of the stressed specimens were based on measuring: (a) the time until the specimen failure, (b) their failure type and (c) the variation of the electrode potential of specimen, during the stress corrosion test. After each corrosion test, the steel specimens were examined visually and microscopically/metallographic.

The influence of the microstructure of the steel specimens on the stress corrosion cracking behaviour has been studied.

The results and conclusions of this comparative research showed that the cold-drawn prestressing steel with pearlitic microstructure had significantly better corrosion behaviour than thermally treated prestressing steel with martensitic microstructure.

SIMPLE CONCRETE LIFE EXTENSION

Alexis Borderon Specialist, Stainless steel reinforcements Valbruna Spa , Viale della Scienza, 25 - 36100 Vicenza – Italy Mobile : +45 22222 791 - e-mail : alexis.borderon@valbruna.it webpage : www.reval-stainless-steel.com

Keywords: Corrosion, stainless steel, durability, maintenance, sustainability.

Abstract.

Concrete life is submitted to the influence of climate and time. Much is done to design mix to ensure the durability of concrete, as well as preventing its collapse through the use of many different coating solutions. Every process insitu is manual and therefore subject to failure. Those errors will demand maintenance in time to prevent concrete disintegration.

Using stainless steel reinforcement on exposed zones secure extended lifetime and no maintenance, as corrosion is no longer an issue. The simplicity of this solution is obvious thus very much unfamiliar to most engineers as knowledge and references they do not access. By eliminating all risks of corrosion on the bearing structure, the success of the construction does no longer depend on the skills of the people involved.

Many solutions are today available to increase service life; coatings of the rebars or the concrete surface, composite materials as reinforcements, galvanized steel, cathodic protection.. although none can ensure durability without maintenance nor can be executed and produced by any contractor. All these solutions require skills when stainless steel don't: It can be processed as regular mild steel.

Simple concrete life extension is a pragmatic guideline based on leading engineers design methods to achieve durability and therefore sustainability of the structures, meeting their clients wishes to reduce maintenance costs over time. Using stainless steel where needed only; in joints, edges, splash and tidal zones, The remaining costs represent merely 1% of the reinforcement volume.

The inner qualities of stainless steels; equal tensile and fatigue strengths , sustainability, low magnetism, non corrosive , meet the increasing demand of sustainable solutions for concrete durability.

Smart Controlled Release Corrosion Inhibitors for Steel Reinforced Concrete

D. M. Bastidas¹, I. Aguirre¹, S. Fajardo¹, E. Medina², I. Llorente¹, V. La Iglesia¹, V. González³, J.M. Rodríguez⁴, N. Birbilis⁵, C. Monticelli⁶, A. Balbo⁶, V. J. Gelling⁷.

¹ *National Centre for Metallurgical Research (CENIM), CSIC, Ave. Gregorio del Amo 8, 28040 Madrid, Spain*

² *Department of Architectural Works and Construction Control, School of Building Construction (ETSEM-UPM), Universidad Politécnica de Madrid, Ave. Juan de Herrera 6, 28040 Madrid, Spain*

³ *Department of Chemistry and Agricultural Analysis, School of Agricultural Engineering (ETSIA-UPM), Universidad Politécnica de Madrid, Ave. Complutense, 3, 28040 Madrid, Spain*

⁴ *Building Engineering Area, ETSICCP, University of Granada, C/Severo Ochoa s/n, 18071 Granada, Spain*

⁵ *ARC Centre of Excellence for Design in Light Metals, Department of Materials Engineering, Monash University, Clayton, VIC. 3800, Australia*

⁶ *Corrosion Study Centre A. Dacco, University of Ferrara, Via Saragat 4a, 44122 Ferrara, Italy*

⁷ *Department of Coatings and Polymeric Materials, North Dakota State University (NDSU), 1735 NDSU Research Park Drive, Fargo, ND 58105, United States*

david.bastidas@cenim.csic.es

ABSTRACT

Deterioration of reinforced concrete structures (RCS) is a costly problem, with an estimated cost of three to four percent of the gross national product (for direct and indirect costs) in developed countries due to maintenance and repair operations. The main cause of RCS degradation is the corrosion of steel reinforcement, due to a pH reduction arising from the concrete carbonation process or the penetration of chlorides leading to depassivation of steel.

The aim of this research is to explore the delivery of controlled release corrosion inhibitors as a smart rehabilitation method to prevent corrosion propagation of RCS. This method of inhibition allows a controlled delivery within the concrete or by incorporation into a steel conversion layer, thus enabling a slow and gradual release of the inhibitor compound as a function of environment pH. Selectively of release may also be possible depending on the type of corrosion, whether due to chlorides or carbonation. We report the study of calcium nitrite (as a reference inhibitor) encapsulated in natural resins via the double micro-emulsion method, as a candidate for controlled release corrosion inhibition.

Investigation of sodium molybdate's effect on the passive film of steel rebars in different simulated concrete pore solution environments

Tan Yong Teck, NUS Graduate School for Integrative Sciences & Engineering, Centre for Life Sciences (CeLS), #05-01, 28 Medical Drive, Singapore 117456;
Sudesh L. Wijesinghe, SIMTech, 71 Nanyang Drive, Singapore 638075;
Daniel J. Blackwood, National University of Singapore, 9 Engineering Drive 1, Singapore 117576

This research was carried out to investigate the effectiveness of sodium molybdate as a corrosion inhibitor for the two main causes (chloride ingress and carbonation resulting in pH drop) of corrosion of carbon steel rebars in reinforced concrete. Open-circuit potential (OCP) measurements, potentiodynamic tests, linear polarization resistance (LPR) experiments, electrochemical impedance spectroscopy (EIS) and scanning vibrating electrode technique (SVET) experiments were conducted on carbon steel (AISI 1020) to characterize the corrosion behaviour of the carbon steel under different aggressive conditions. SEM and EDX were performed on samples to characterize the steel surface before and after corrosion.

New results

A series of experiments were conducted to determine the effectiveness of Na_2MoO_4 at protecting AISI 1020 carbon steel in simulated concrete pore solution (saturated calcium hydroxide solution with a pH of 12.5) in the presence of Cl (4000 ppm Cl and 20000 ppm Cl). Carbonation was simulated by reducing the pH of the pore water via the addition of NaHCO_3 to produce a pore solution of pH 9.

It was found that Na_2MoO_4 was effective at increasing both the polarization resistance and the pitting potential of the carbon steel, especially at the lower chloride level (4000 ppm Cl). Based on the experiments conducted, Na_2MoO_4 extended the potential range of the passive region. This suggests competitive adsorption of molybdate with chloride. EDX carried out on pits detected the presence of Mo, which is an indication of support for the hypothesis of pore-plugging mechanism in which molybdate precipitates out in the anodic sites and helps to repair the damaged passive film.

Long duration OCP experiments (~20 hours) were carried out. LPR and EIS were conducted during the OCP measurement at certain intervals, allowing for the characterization of the change in polarization resistance over time and also with respect to the OCP. This set of experiments showed the effectiveness of Na_2MoO_4 in increasing the polarization resistance in Cl-polluted pore water and also in carbonated pore water. Mott-Schottky analysis was also done to analyse the properties of the passive film present on the steel surface under different conditions.

SVET experiments provided appealing visual images of the effect of Na_2MoO_4 in reducing the current density of a previously corroding area. SVET experiments indicate that this technique can be used to monitor changes in corrosion rate and the extent of corroded area over time in a simple manner.

Application of Gamma-Ray radiography and gravimetric measurements after accelerated corrosion tests of steel embedded in mortar

Gustavo Duffó, CNEA, CONICET, UNSAM, Buenos Aires, Argentina
Natalia Gaillard, Instituto Sabato, CNEA-UNSAM, Buenos Aires, Argentina
Mario Mariscotti, THASA, Buenos Aires, Argentina
Marcelo Ruffolo, THASA, Buenos Aires, Argentina

The corrosion of steel bars is the major cause of premature deterioration of reinforced concrete structures. Initially, due to the high alkalinity of the solution contained in the pores of the concrete ($\text{pH} > 13$), steel bars are passivated by the presence of a protective oxide film. However, under certain circumstances, this protection is broken by destruction of the passive film due to the presence of aggressive ions (chloride, for example) or by the acidification of the medium in the vicinity of the steel rods (carbonation). Under natural conditions, the corrosion process of reinforcing bars is very slow and usually the first signs of deterioration appear after many years of exposure, so the tests require long exposure times. Therefore, there is a tendency to perform what is called "accelerated corrosion tests", in order to obtain results in the short term. The accelerated corrosion by the impressed current technique is widely used in studies of concrete durability since it has the advantage that tests can be carried out within reasonable periods of time. On the other hand, for the inspection of the state of reinforced concrete structures, the use of non-destructive testing is relatively new probably because, unlike steel, concrete is a highly non-homogeneous composite material with varying composition and different raw materials. Among the new non-destructive techniques, Gamma-Ray radiography (as well as Gamma-Ray tomography), lets the inspection and diagnosis of reinforced concrete structures allowing detailed visualization of the interior of structural elements and information about the positions and dimensions of the reinforcements, defective grouting, identification of piping and obstructions, etc.

In the present work, through the implementation of accelerated corrosion tests on reinforced mortar, the relationship between the applied current density and the resulting damage on the reinforcing steel by applying optical microscopy, scanning electron microscopy, gamma-radiography and gravimetric measurements was studied. The results show that the efficiency of the applied current is between 1 and 77%, regardless of the applied current density, the water/cement ratio and the mortar cover of the specimens. Furthermore, it was found that chloride content present in the cement plus the amount coming from the sand, was sufficient to generate localized corrosion of the steel embedded in the mortar. This fact was justified by analysing the Pourbaix diagram for the system $\text{Fe}/\text{Cl}^-/\text{H}_2\text{O}$ and because the major corrosion product identified was *akaganeite*, which only forms in the presence of Cl^- . Finally, using the Gamma-Ray radiography –with a detection limit under the experimental conditions of about $90\text{ }\mu\text{m}$ – it was possible to determine that, the relationship between the depth of localized attack and generalized attack is about 3. The results show the applicability of the Gamma-Ray radiography technique to detect corrosion of steel rebars.

Long Term Performance of Migrating Corrosion Inhibitors to Protect Reinforced Concrete Structures in Aggressive Environments

Behzad Bavarian and Lisa Reiner

Dept. of Manufacturing Systems Engineering & Management
College of Engineering and Computer Science
California State University, Northridge, USA 91330

Abstract

Corrosion creates long term reliability issues for reinforced concrete structures. Billions of dollars have been spent on corrosion protection of concrete and steel bridges, highways, and reinforced concrete buildings. Among the commercial technologies available today, migrating corrosion inhibitors (MCIs) show versatility as admixtures, surface treatments, and in rehabilitation programs. The effectiveness of the MCIs (mixture of amine carboxylates and amino alcohols) on reinforced concrete was evaluated throughout this project. Corrosion test results conducted over five years (1800 days), 240 cycles per ASTM G109 using immersion and ponding in 3.5% NaCl solutions. The results have indicated that polarization resistance (R_p) for the MCI coated concrete was higher (60-80 kohms-cm² with increasing trends) than non-coated concrete. The untreated concrete samples not only had lower R_p values, but also demonstrated decreasing trends. Examination of the embedded steel rebar after corrosion tests showed no corrosion attack for the MCI treated concrete samples, while non-treated concrete showed corrosion. X-ray photoelectron spectroscopy (XPS) and depth profiling confirmed that the inhibitor had reached the rebar surface in less than 150 days. XPS depth profiling showed an amine-rich compound on the rebar surface that corresponded with the increase in R_p and improved corrosion protection for the MCI treated steel rebar even in the presence of chloride ions. Based on measured corrosion rate the life expectancy of a concrete reinforced structure can be improved by more than 40 years.

The use of corrosion resistant steel reinforcement in chlorides contaminated concrete

Nina Gartner, Tadeja Kosec, Andraž Legat, Slovenian National Building and Civil Engineering Institute, Ljubljana / Slovenia

From experiences and many examples from real life it is obvious that the problem of corrosion in reinforced concrete structures is still being unsolved. Despite numerous anticorrosion protection methods that are based on prevention of electrochemical processes (i.e. cathodic protection, corrosion inhibitors, etc.), the use of stainless steel reinforcement is considered as one of the best methods for protection of reinforced structures exposed to aggressive environments.

The main problems concerning the use of stainless steel reinforcement in concrete structures are: 1) insufficient knowledge about basic corrosion mechanisms of stainless steel in concrete and lack of experiences from real life implementation; 2) much higher price of stainless steel reinforcements (especially high-Ni alloyed steels), compared to carbon i.e. black steel reinforcement.

To address both of these problems, the corrosion resistance of 6 different types of corrosion resistant steel reinforcements (ferritic TOP12 – 1.4003, austenitic low-Ni 204Cu – 1.4597, austenitic AISI 304 – 1.4301 and 304L – 1.4306, duplex SAE/UNS S3 2205 – 1.4462 and UGIGRIP 4362 – 1.4362) were tested in simulated concrete pore solution (carbonated and non-carbonated, with different additions of Cl^-) and embedded in small laboratory concrete specimens (cyclically wetted with NaCl solution). Next to laboratory results, concrete columns were prepared and exposed to real marine environment. During 4-year exposure of columns at the coastal area, frequent measurements were performed on embedded reinforced steel: galvanostatic pulse measurements, Electrical Resistance (ER) probes measurements and Electrochemical Noise sensors (EN measurements). After 4 years, concrete columns were transported to laboratory, where final (visual, microscopy, CT, etc.) inspection of embedded steel, different probes and concrete itself was performed. Results of non-destructive measurements were compared to final (destructive) examination.

The preliminary results show that ferritic stainless steel (TOP12) does not seem to be more suitable for the use in chloride contaminated environment than black steel. On the contrary, low-Ni austenitic stainless steel (204Cu) show relatively good corrosion resistance when compared to more expensive austenitic AISI 304, 304L and both duplex steels (duplex SAE/UNS S3 2205 and UGIGRIP 4362 – 1.436).

Lessons learned from first test site were used to establish new test site in marine environment, where carbon steel reinforcement, austenitic low-Ni (204Cu – 1.4597) and austenitic (AISI 304 – 1.4301) stainless steel reinforcements were embedded in two different types of concrete. Beside steel reinforcement, the exposed columns have embedded sensors for EN measurements and improved ER probes for continuous data acquisition. The purpose of the new test site is to compare different options for non-destructive detection of corrosion in real concrete structures and to establish new smart corrosion system.

The synergetic effect of molybdenum and nitrogen alloying elements on austenitic stainless steels pitting resistance

V. Roche¹, I.N. Viçosa¹, R.P. Nogueira¹, E. Chauveau², M. Mantel^{2,3}, T.J. Mesquita²

¹ LEPMI - UMR5279 CNRS – Grenoble INP – Université de Savoie – Université Joseph Fourier, 1130, rue de la piscine, BP 75 - 38402 Saint Martin d'Hères, France

² CRU Ugitech, Av Paul Girod 73400 Ugine, France

³ SIMAP - UMR5279 CNRS – Grenoble INP – Université de Savoie – Université Joseph Fourier, 1130, rue de la piscine, BP 75 - 38402 Saint Martin d'Hères, France

Corresponding author : virginie.roche@lepmi.grenoble-inp.fr

Stainless steels exhibit good resistance to oxidation and corrosion in many natural and synthetic environments; however, it is important to select the suitable grade of stainless steel (SS) for a specific application. It is well known [1] that molybdenum, when used as an alloying element in SS, increases the pitting corrosion resistance in acidic and neutral environments containing chlorides. Likewise, the addition of nitrogen in the alloy composition can also improve the corrosion resistance of SS [2]. However, the possible interaction of N and Mo as alloying elements in the same grade is not clearly understood. In this work, an eventual synergy Mo/N was investigated from acid to alkaline media in the presence of Cl^- by electrochemical cyclic polarization for several laboratory austenitic heats (18Cr12Ni, 18Cr12Ni3Mo, 18Cr12Ni0.1N and 18Cr12Ni3Mo0.1N). This synergetic effect was observed on the pitting corrosion potential as clearly demonstrated in Figure 1.

In addition, the passive layer electrochemical properties of each laboratory grade were evaluated by electrochemical impedance spectroscopy EIS. The effect of aging time (up to 3 weeks) on passive layer was also pointed out by EIS results. Finally, the composition of the passive layer was characterized by X-ray photoelectron spectroscopy.

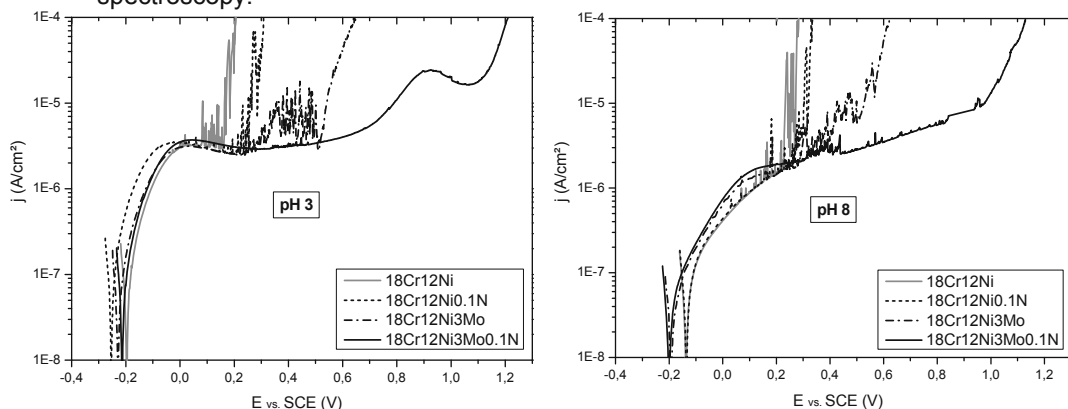


Fig. 1. Polarization curves obtained for laboratory alloys in different pH.

Reference

[1] Thiago J. Mesquita, Eric Chauveau, Marc Mantel, N. Kinsman and Ricardo P. Nogueira. *Materials Chemistry and Physics*, 126 (2011)

[2] K.H. Lo, C.H. Shek, J.K.L. Lai. *Materials Science and Engineering R* 65 (2009)

Influence of the type of reinforcement on load bearing capacity of corroded reinforced concrete structures

*Antonio Bossio¹, Gian Piero Lignola², Tullio Monetta¹, Andrea Prota², Francesco Bellucci¹,
Edoardo Cosenza², Gaetano Manfredi², University of Naples “Federico II”, Naples;*

¹ Dept. of Chemical Engineering, Materials and Industrial Production, Italy

² Dept. of Structures for Engineering and Architecture, Italy

antonio.bossio@unina.it

Corrosion of steel in concrete is a worldwide economical, social and safety problem. In order to investigate about influence of type of reinforcement, 48 specimens have been exposed to 3.5% wt sodium chloride solution and corrosion current has been imposed. After about one year, they have been tested in order to evaluate the loss of bearing capacity. Reinforcement bar diameter loss has been evaluated by performing gravimetric measurement. Three different kinds of bar have been used: non-ribbed bars, ribbed bars and ribbed galvanized bars in order to simulate “old structures”, “nowadays structures” and a possible way to build “more durable” structures, respectively.

Design, Installation and Performance of Cathodic Protection Systems on Langeland Bridge, Denmark.

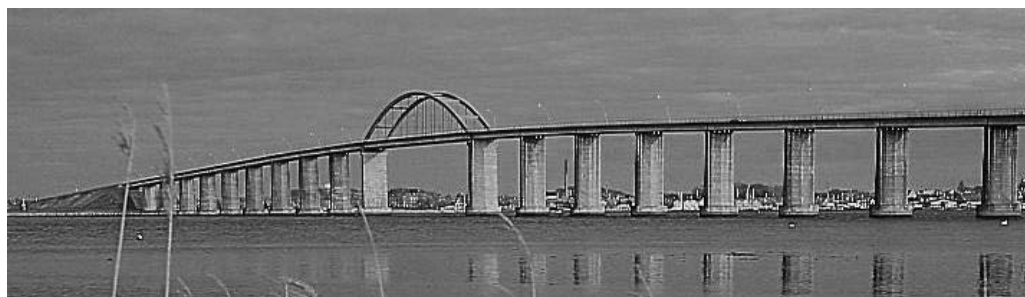
*Ruth Elise Sørensen and Jonas Kok, COWI A/S, Kgs. Lyngby, Denmark
Kirsten Riis, Danish Road Directorate, Copenhagen, Denmark
Franck Villumsen, Krüger Aquacare A/S, Glostrup, Denmark*

The Langeland Bridge was constructed during the period 1960-62 as a high bridge with an overall length of 774 meter. The substructure consists of 20 reinforced concrete piers in water and the superstructure comprises a pre-stressed concrete box girder with 5 boxes.

The concrete quality was varying with porous areas, and the chloride ingress soon caused reinforcement corrosion in the piers. During the period 1977-1984, the bridge piers were repaired with traditional concrete repairs, however special inspections of the piers in years 2000 and 2002 revealed that new corrosion had initiated.

In order to find a technical and economical feasible repair strategy for the bridge piers, a trial cathodic protection installation was installed on one of the piers. Based on among others this trial, cathodic protection was selected as repair method, and 2 cathodic protection systems were installed on the piers during the period 2008-2013.

During the installation works for the cathodic protection systems a requirement for repair of the pre-stressed concrete box girder was found. After performing trial cathodic protection systems on the box girder as well, cathodic protection was also chosen as repair method for these areas. A cathodic protection system was installed on the most damaged parts of the box girder's bottom plate during the period 2011-2013.



This paper presents the considerations taken into account, regarding cathodic protection designs, the challenges during installation and evaluation of the performance of cathodic protection system seen from the Bridge Owner's, the Consultant's and the Contractor's point of view.

Altered cement hydration and subsequently modified porosity, permeability and compressive strength of mortar specimens due to the influence of electrical current

A. Susanto, D.A. Koleva, K. van Breugel

Delft University of Technology, Faculty of Civil Engineering and Geosciences, Department Materials & Environment, Stevinweg 1, 2628 CN Delft, The Netherlands

In the fields of steel corrosion, cement-based materials science and performance of reinforced concrete structures in general, the effect of electrical current on materials properties (both steel and concrete) is commonly considered only when steel corrosion is of concern e.g. stray current effects on steel corrosion initiation in close-by or remote structures that appear to be in the way of low resistive underground path-ways. Stray current is a current leakage e.g. from rail transit systems. Except stray currents, electrical current due to the application of impressed current Cathodic Protection (CP) also flows through reinforced concrete or steel structures. Whereas stray current can be non-stable and of significantly larger scales, the current (DC only) within CP applications is generally in the range of mA/m² steel (concrete) surface. Similarly to stray current effects, the DC current with CP applications is only monitored in terms of sufficiency in order to assure proper polarization (protection) from steel corrosion. However, all types of electrical current flowing through a reinforced (or not) civil structure, would pass through the concrete bulk matrix as well. The related effects (positive or negative) are normally not subject to investigation. Considering that a concrete bulk matrix is a porous medium with relevant humidity and ionic strength of the pore solution, logically any type of electrical current flow will exert alterations in ion/water migration and will consequently affect the bulk matrix properties.

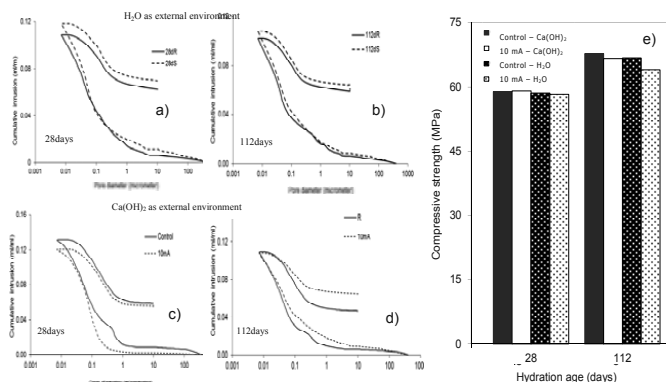


Fig.1 Porosity and compressive strength of mortar cubes in H₂O and Ca(OH)₂ as external environment

This paper presents the effect of electrical current flow at the level of 10 mA/m², as commonly used for CP applications, on cement-based matrix properties. Mortar cubes were cast and after 24h immersed in H₂O & Ca(OH)₂ environment. Electrical current was applied (via metallic conductors in the medium) as a simulation of stray current. The effect of current flow was investigated in conditions where leaching was possible (H₂O medium) and compared to such where leaching was avoided (Ca(OH)₂). The results show a larger effect on porosity and mechanical properties when leaching was involved and also accelerated by the el. current flow, whereas these effects were less pronounced in Ca(OH)₂ medium. For the former case, coarser pore structure and lower compressive strength were observed (Fig.1a,b,e) under current conditions. For the latter case, enhanced water and ion transport lead to apparently enhanced cement hydration and densification of the pore structure (Fig.1c) at earlier stages (24h to 84 days). However, after 112 days, although the total porosity for under current and control regimes is similar, alterations are relevant to the "ink bottle" and "effective" porosity for the stray current regime (Fig.1d). The paper will further discuss electrical properties of the specimens with time of treatment, pore size, pore connectivity and permeability and will link those to the observed alterations in mechanical properties, cement hydration and chemical composition of the external environment. The results support the hypothesis for the effect of electrical current flow on microstructural properties of cement-based materials and justify the need for further investigation and/or specification of threshold levels for electrical (incl. stray) current densities, expected to bring about negative alteration in (reinforced) concrete structures.

Monitoring steel corrosion in reinforced concrete beams with variable crack widths under sustained load

A. Blagojević, D.A. Koleva, J.C. Walraven, Delft University of Technology, Faculty of Civil Engineering and Geosciences, the Netherlands

Steel corrosion in reinforced concrete is well recognised to be the major cause for structures' degradation. For a good quality concrete and within the absence of detrimental external influence, the steel reinforcement is in a passive state. Passivity is maintained as long as the concrete bulk matrix maintains high alkalinity (i.e. buffer to corrosion initiation) and performs as a sound physical barrier against penetration of aggressive substances. On the other hand, concrete is a porous material and depending on pore network permeability and connectivity, corrosion-accelerators, as chloride ions, can initiate steel corrosion even at high pH (12.9 – 13.5) of the surrounding medium. Logically, the process of chloride-induced corrosion would have a faster onset and will be further more pronounced when except porosity, concrete cracking is at hand. Cracks are unavoidable in civil structures, ranging from micro to macro level. Therefore, standards are applicable for permissible crack width within engineering applications. Numerous works exist on the topic, however, a systematic approach considering standards for crack width/concrete cover, but also taking into account mechanisms related to steel electrochemical response, including micro-cell versus macro-cell corrosion dependence on crack width, crack pattern and loading, is still under discussion with respect to standards and criteria.

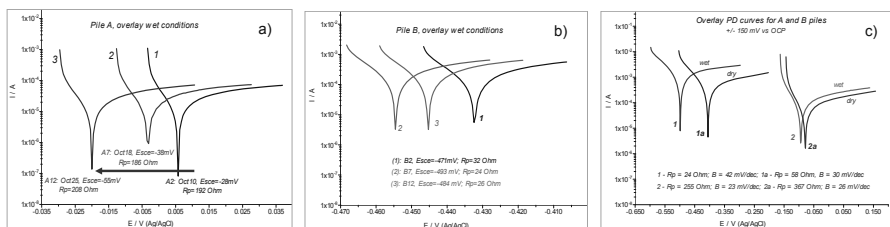


Fig.1 LPR response (a,b) and potention-dynamic curves (c) for control and corroding cases (wet conditions)

This paper will discuss monitoring of steel corrosion in reinforced concrete beams of 1000 mm in length, where variable crack widths were induced by 4-point bending under sustained load. The beams were subjected to wetting (5 % NaCl for corroding cases and tap water for control ones) and drying cycles. Steel corrosion initiation and propagation was monitored via OCP measurements (local “wet spot” records over various cracks and “whole bar” readings using external Ag/AgCl reference cells) and LPR tests. Preliminary EIS and PD measurements were also conducted in order to justify the suitability and reliability of these techniques for larger scale experiment and applicability when various crack widths and crack patterns are concerned. Within the wetting cycles, a cathodic shift of corrosion potential (E_{corr}) for the control cases (beam A) was observed (Fig.1a). For the corroding beam B, a cathodic shift of E_{corr} is relevant within wetting (Fig.1b), already with a contribution from Cl-penetration. Wetting cycles increase corrosion currents and anodic current densities in both corroding and control conditions, more pronounced for beam B (Fig.1c), where the effect of chlorides is governing corrosion behavior. As expected, current densities for the control beams are at least one order of magnitude lower (wet conditions). EIS response further elucidates the dependence of electrical properties on microstructural alterations, RH and O_2 availability, along with maintained stability of the passive layer for control conditions and activity/ennoblement for corroding conditions.

Active corrosion time affecting visual corrosion damage in carbonated concrete facades

*Arto Köliö, Tampere University of Technology, Tampere/Finland; Jukka Lahdensivu
Tampere University of Technology, Tampere/Finland*

Concrete facades and balconies have been widely used in Finland since mid-1960s. Totally there is approximately 44 million m² of concrete facades and almost a million balconies. Despite the rather young age of the Finnish concrete building stock, several problems have been encountered in their maintenance and repair. The structures have deteriorated due to several different deterioration mechanisms whose progress depends on many structural, exposure and material factors. The most common degradation mechanisms causing the need to repair concrete facades and balconies in Finland, and concrete structures in general, are carbonation induced corrosion of reinforcement as well as inadequate frost resistance concrete, which leads to, for instance, frost damage.

In many service life models corrosion time is divided to initiation period (carbonation) and propagation period (active corrosion). This study consists of a statistical study on the actual observed corrosion damage and active corrosion of reinforcement on concrete facades and balconies in Nordic climate.

The research data consist of data gathered from 947 condition assessment reports. The concrete buildings were built in 1960-1996. Visually seen damage was seen totally 811 buildings, which 59 % suffered local or extensive corrosion damage.

Active corrosion was examined in this study by calculating backwards the age of the building and the initiation time by carbonation which is thoroughly examined in condition assessment. The information required to make the calculation was collected from condition assessment reports of concrete facades and balconies from assessments conducted in 1992–2006. The earliest corrosion damage was observed in condition assessment already after 10 – 17 years from construction. Carbonation of concrete achieves small cover depths (< 10 mm) within the first 15 years in most of cases. Probability for the active corrosion time in carbonated concrete was calculated using statistical simulation. According to calculation, the active corrosion period is 0.6-1.4 years when adopting a 5 % safety level, which is commonly used in reliability analyses. As the effects of corrosion of facades and balconies are mainly visual defects, a safety level of 50 % could be applied, which means 6-12 years active corrosion time.

Cross-border research for corrosion control in civil structures: recent research lines and novel approaches, employing electrochemistry, concrete materials science and nano-technology

D. A. Koleva

*Delft University of Technology, Faculty of Civil Engineering & Geosciences,
Department Materials & Environment, Stevinweg 1, 2628 CN, Delft, The Netherlands*

Corrosion-related materials' degradation adversely affects the reliability of civil structures. Presently, materials' degradation is a multi-billion issue for the EU, of which 60% is corrosion-related. For the civil engineering sector, 90% of costs (direct and in-direct) are due to corrosion. Although, durability issues with the above respect are already recognised and more and more public concern is expressed, the engineering field still lacks feasible solutions.

Despite the various corrosion protection approaches, including standard and conventional ones (as blended cements or cathodic protection) or more novel ones (as self-healing concrete), an optimal solution, including considerations for sustainability, or originating from different scientific backgrounds is not yet available. The reason is the commonly fragmented approach i.e. civil-engineering oriented only or corrosion-engineering oriented only, and hence the restriction of the applied methods and technology to either steel or concrete. Therefore, the barrier to achieve durable and sustainable built environment and significantly reduced corrosion costs in the civil engineering sector is the absence of a simultaneous recognition of the involved materials and the still lacking thorough fundamental understanding of their interconnected behaviour, especially within the increasingly challenging bio- and climate-diversity.

This paper will discuss the importance of a multidisciplinary approach when steel corrosion or corrosion protection in reinforced concrete are concerned. An overview of recent and on-going research will be presented with respect to novel and more conventional research lines, aiming sustainability and safe service life of our built infrastructure. More recent results for wastes, nano-technology utilization and self-healing of corrosion damage will be also discussed. The paper aims to provide an overview of recent research and forthcoming approaches for the field of steel corrosion in civil engineering.

Performance of Conductive Coatings Used for Cathodic Protection of Reinforced Concrete Structures under Consideration of Durability Issues

*Christian Helm, Michael Raupach, Institute of Building Materials Research,
RWTH Aachen University*

Abstract

Carbon-based conductive coatings can serve as anode systems for cathodic protection (CP) of reinforced concrete structures. Due to their comparably low material costs, negligible weight and thickness as well as their easy application they form efficient solutions for numerous applications. However, the limited current output and durability issues prevent these systems from a wider spread.

Therefore, an industrial research project led by the Institute of Building Materials and Research, RWTH-Aachen University (ibac), and the Federal Institute for Materials Research and Testing, Berlin (BAM), was established in order to develop a model for reliable lifetime prediction of conductive coatings serving as CP anodes.

Within this paper, the resulting polarisation of three commercially available products is determined for varying operating parameters such as geometry (concrete and rebar), protection current, distribution of primary anodes, climate and concrete properties (binder, chloride content, carbonation, etc..) by means of numerical calculations.

Subsequently the durability of the CP-system will be derived by comparing the results with the limits of applicability determined by our research partners at BAM.

THE USE OF CATHODIC PROTECTION FOR LIFE ENHANCEMENT OF IMMERSED REINFORCED CONCRETE STRUCTURES

Paul Chess, FORCE Technology, City/Country: 37A Victory Road, CO5 8LX, England

Oskar Klinghoffer, FORCE Technology, Park Alle 345, DK- 2605 Brøndby, Denmark

Frits Grønvold, FORCE Technology, Gissselfeldvej 4, DK-2665 Vallensbæk, Denmark

Peter Vagn Nygaard, FORCE Technology, Gissselfeldvej 4, DK-2665 Vallensbæk, Denmark

Abstract

Many years ago the majority of professionals in civil engineering were of the opinion that reinforced concrete structures were maintenance free. With more diverse use of this building material it became obvious in exposed structures that there was staining, cracking of the concrete and corrosion of the underlying steel reinforcement. This led to greater cover depths, improved concrete but this did not take the problem away.

Reinforced concrete structures in the ground or water were not considered to be particularly at risk though some research was directed at it. The main focus of concern was on bridge decks and other exposed structures. What changed was in Saudi Arabia and other parts of the Middle East very large levels of damage were found in coastal areas on reinforced concrete chambers built in the ground. Severe corrosion was occurring within ten years. This was found to be replicated on many structures in the region where there was saline ground water, high temperatures and the inside of the structure was dry (later it was found to be damaging reinforced concrete without these dry surfaces). For these structures CP was implemented on new foundations or other below ground level structures to prevent further corrosion and enhanced measures were taken to monitor this problem.

Also in Europe cathodic protection was implemented or prepared for installation in structures submerged below water. In the late 80's and 90-'s two big construction projects were built in Denmark namely Great Belt link connecting island of Zealand and Funen and Øresund link connecting Denmark with Sweden.

Now around the world large reinforced structures which are being buried and expected to last a long period of time are starting to be assessed according to the likely corrosion threat, ways of monitoring the corrosion risk as the structure deteriorates and finally means of simplifying the application of cathodic protection when required. This paper discusses a structured approach to this life enhancement engineering, including the challenges and experiences gained from the mentioned applications. The available results of these analyses shall be utilized in new projects such as the Fehmarn Fixed Link, Denmark to Germany, where cathodic protection is being considered in the preliminary design phase.

Study the effect of Heat and LASER Treatments on the corrosion behaviour of microalloyed carbon steels.

F. M. Sayed^a, M. M. Hegazy^a, G. A. El-Mahdy^a, M. M. Eissa^b, and A. M. Fathy^b

^a Chemistry Department, Faculty of Science, Helwan University, Cairo, Egypt.

^b Central Metallurgical Research & Development Institute (CMRDI).

ABSTRACT

The influence of heat and LASER treatments on the corrosion behaviour of reinforced Carbon steel was investigated in saturated Calcium Hydroxide solution using weight loss, Potentiodynamic Polarization, X-ray Diffraction (XRD) measurements and Scanning Electron Microscope (SEM) examination. Heat and LASER surface treatments play an important role for improvement of the mechanical properties and corrosion resistance of the reinforced Carbon steel. The corrosion rate of LASER alloyed sample is very close to that of the sample treated with low heat treatment at 900°C and is lower than that experienced for the sample treated at higher one at 1200°C. The results may be attributed to uneven distribution of Titanium, Vanadium microalloying elements throughout the surface and low grain refinement for treated sample at high heat treatment at 1200°C.

KEYWORDS: Heat treatment, LASER, Microalloyed steel, Titanium, Vanadium, Polarization, X-ray Diffraction (XRD) and Scanning Electron Microscope (SEM).

Corrosion resistance of several metallic materials in contact with mortar

Gustavo S. Duffó, CNEA, CONICET, UNSAM, Buenos Aires, Argentina

Silvia B. Farina, CNEA, CONICET, UNSAM, Buenos Aires, Argentina

Fátima M. Schulz Rodriguez, CONICET, UNSAM, Buenos Aires, Argentina

In structural engineering, different metals such as carbon steel, stainless steel, aluminium, copper, zinc and lead get into contact with very different mineral building materials, and those produced with cement, play an important role. Besides, several formulations made with cements are frequently used in the immobilization of Intermediate Level Radioactive Waste containing some of these metals. In general, building materials do not attack metals, and a corrosive attack only is possible if the material contains free water, chloride and/or a decrease in the pH value due to a carbonation process has occurred. In spite of the fact that the corrosion of carbon steel in cementitious materials has been largely studied, few data concerning the corrosion behaviour of other metals in contact with concrete or mortar has been published. The aim of the present work is to compare the corrosion susceptibility of several metallic materials: copper, lead, aluminium, zinc, AISI 304 stainless steel and SAE 1040 carbon steel, when they are in contact with mortar, with and without the presence of aggressive species. The specimens used in the tests are mortar prisms where bars of metals under study were embedded. In addition, these specimens were contaminated with chloride ions in different concentrations and exposed to different conditions: immersed in a solution of 3.5 wt.% NaCl; laboratory environment with a relative humidity (RH) of 45% and curing chamber (98% RH). The electrochemical parameters normally used to characterize the corrosion behaviour of reinforcing steel in concrete were monitored periodically for 3.4 years. These parameters are the corrosion potential, the polarization resistance and the electrical resistivity of mortar. After the exposure time, weight loss determinations were performed to compare the real corrosion rate of the metals with the electrochemical results in order to obtain the constant "B" of the Stern-Geary equation. The results indicate that aluminium shows the major corrosion attack in all the systems studied and that stainless steel exhibits the best performance in all conditions tested. Specimens that contained aluminium bars and were contaminated with chloride ion presented cracks and partial mortar cover detachment due to the effect of voluminous aluminium corrosion products (Figure 1).



Figure 1.- Aspect of the mortar specimen contaminated with chloride ion(1% wt/cement) containing aluminium bars, after 2 months exposure.

FTIR study on the amorphous corrosion products of galvanized steel in carbonated concrete

G. Roventi, T. Bellezze, R. Fratesi

*Department of Materials, Environmental Sciences and Urban Planning,
Polytechnic University of Marche, Ancona, Italy*

Hot-dip galvanizing has been used since the 1930s for corrosion protection of steel reinforcements in concrete structures. Corrosion protection offered by these steel coatings is determined by zinc passivation process, which is spontaneous in concrete, due to the formation of a compact and protective layer of calcium hydroxyzincate $\text{Ca}[\text{Zn}(\text{OH})_3]_2 \cdot 2\text{H}_2\text{O}$ (CHZ). In previous works, it was found that the carbonation leads to the CHZ layer destruction. Corrosion potential and corrosion rate measurements showed that, despite the disappearance of the protective CHZ layer, zinc remains in the passive state also after carbonation. These results indicate that new passivating products are formed, but their identification was not possible by means of XRD, because they are not well crystallized. A study performed on pure zinc immersed in $\text{Ca}(\text{OH})_2$ solution, showed that carbonation leads to the formation of $\text{Zn}_5(\text{CO}_3)_2(\text{OH})_6$ (hydrozincite, HZ). The present research was performed on steel sheets galvanized in a pure zinc bath embedded in cubic concrete specimens. After 39 days of air curing, the specimens were placed in a carbonation chamber and then were submitted to wet-dry cycles in tap water. After different periods of time, some concrete specimens were broken and the sheets were removed and submitted to Fourier transform infrared spectroscopy (FTIR), scanning electron microscopy (SEM) and energy dispersive X-ray analysis (EDX). The results confirm that concrete carbonation leads to the destruction of CHZ; FTIR spectra indicate that after concrete carbonation both HZ and ZnCO_3 are present on zinc surface, with a prevailing presence of the latter. Corrosion rate measurements and SEM observations of the coating cross-sections confirmed that zinc remains passive after concrete carbonation. The same tests indicated that the exposure to 19 wet-dry cycles in tap water after carbonation leads only to a slight decrease of the amount of the corrosion products on the coating surface, without significantly increase in corrosion rate with respect to that measured in not carbonated concrete.

Adsorption and inhibition corrosion of the biopolymer on carbon steel in simulated pores concrete solution

Manoel Martins S. Filho¹, Josealdo Tonholo²; Silvia B. B. Uchoa²

¹ *Federal Institute of Alagoas, Brazil, e-mail: manoelmartins1998@hotmail.com*

² *Universidade Federal de Alagoas, UFAL, Brazil*

ABSTRACT

This work presents the investigation of the effect of biopolymer [1] on the inhibition of corrosion of carbon steel in saturated solution of $\text{Ca}(\text{OH})_2$ simulating the environment of the concrete. Corrosion studies were performed by potentiodynamic measurements and cyclic voltammetry in a three electrode electrochemical cell containing a carbon steel working electrode with a 0.28 cm^2 surface area, a platinum auxiliary and Hg/HgO as reference electrode, in Milli-Q standard water medium. Tafel plots were obtained by scanning at a scan rate of 1 mVs^{-1} , going from initial potential of -250 mV vs. OCP (open circuit potential) to $+250 \text{ mV}$ vs. OCP. The results indicated that biopolymer acted as mixed-type inhibitor predominantly anodic and the inhibitory efficiency depends on its the concentration. Results obtained revealed that composition containing biopolymer acted excellently as a corrosion inhibitor for carbon steel in solution hydroxide of calcium saturated and its efficiency is more than 65 %. There are no significant changes in Tafel slopes indicating that compound inhibited the anodic dissolution and hydrogen evolution reaction on steel surface without changing the reaction mechanism. The free energy of adsorption of carbon steel was found to be $-11.13 \text{ kJmol}^{-1}$ indicating that adsorption is a spontaneous process and that the inhibitor adsorbs to the surface by physisorption. The adsorption model of biopolymer followed the Langmuir isotherm, with a correlation coefficient close to unity. The values of activation energies for the solutions do not inhibited and inhibited, are respectively, 28.92 kJmol^{-1} and 23.80 kJmol^{-1} . These results reveal that the whole process is controlled by the reaction of the surface. The inhibitor acts by reducing the rates of both cathodic and anodic reactions. The cyclic voltamograma in the presence of the inhibitor also showed a reduction in anodic and cathodic current, suggesting the inhibitor effect on the surface, with blocking active sites by adsorption, directly proportional to the concentration of the inhibitor. The results also showed a decrease in anodic load with the concentration. [1] PI 1003149-9-BR

Characterization and processing digital series obtained from electrochemical monitoring of reinforcing steel

R. Camacho-Chab¹, T. Pérez², B. Escobar-Morales³

¹Instituto Tecnológico de Campeche, Carretera Campeche-Escárcega, Lerma Campeche, México.

²Centro de Investigación en Corrosión (CICORR) - Universidad Autónoma de Campeche, Av. Agustín Melgar s/n, C.P. 24030, San Francisco de Campeche, Campeche, México.

³Instituto Tecnológico de Cancún, Av. Kabáh, Km 3. C.P. 77500, Cancún, Quintana Roo, México.

This paper shows the results of characterization and digital signal processing (DSP) obtained from the electrochemical monitoring of corrosion of reinforcing steel embedded in concrete specimens exposed in a tropical marine environment. The characterization was carried out on samples with the addition of NaCl, Benzotriazol and without addition of salts in the mixing water simultaneously using the time series obtained as noise electrochemical technique, both in potential and current¹ as well as by applying filters low and high frequency². Finally, were performed the analysis of the data sets obtained from the recursive digital processing using graphics as a tool for analysis of time series, which shows an indirect relationship between behavior patterns and graphics processed as recursive obtained respect to the original signal.

Adsorption and inhibition corrosion of the biopolymer on carbon steel in simulated pores concrete solution

Manoel Martins S. Filho¹, Josealdo Tonholo²; Silvia B. B. Uchoa²

¹ *Federal Institute of Alagoas, Brazil, e-mail: manoelmartins1998@hotmail.com*

² *Universidade Federal de Alagoas, UFAL, Brazil*

ABSTRACT

This work presents the investigation of the effect of biopolymer [1] on the inhibition of corrosion of carbon steel in saturated solution of $\text{Ca}(\text{OH})_2$ simulating the environment of the concrete. Corrosion studies were performed by potentiodynamic measurements and cyclic voltammetry in a three electrode electrochemical cell containing a carbon steel working electrode with a 0.28 cm^2 surface area, a platinum auxiliary and Hg/HgO as reference electrode, in Milli-Q standard water medium. Tafel plots were obtained by scanning at a scan rate of 1 mVs^{-1} , going from initial potential of -250 mV vs. OCP (open circuit potential) to $+250 \text{ mV}$ vs. OCP. The results indicated that biopolymer acted as mixed-type inhibitor predominantly anodic and the inhibitory efficiency depends on its the concentration. Results obtained revealed that composition containing biopolymer acted excellently as a corrosion inhibitor for carbon steel in solution hydroxide of calcium saturated and its efficiency is more than 65 %. There are no significant changes in Tafel slopes indicating that compound inhibited the anodic dissolution and hydrogen evolution reaction on steel surface without changing the reaction mechanism. The free energy of adsorption of carbon steel was found to be $-11.13 \text{ kJmol}^{-1}$ indicating that adsorption is a spontaneous process and that the inhibitor adsorbs to the surface by physisorption. The adsorption model of biopolymer followed the Langmuir isotherm, with a correlation coefficient close to unity. The values of activation energies for the solutions do not inhibited and inhibited, are respectively, 28.92 kJmol^{-1} and 23.80 kJmol^{-1} . These results reveal that the whole process is controlled by the reaction of the surface. The inhibitor acts by reducing the rates of both cathodic and anodic reactions. The cyclic voltamograma in the presence of the inhibitor also showed a reduction in anodic and cathodic current, suggesting the inhibitor effect on the surface, with blocking active sites by adsorption, directly proportional to the concentration of the inhibitor. The results also showed a decrease in anodic load with the concentration. [1] PI 1003149-9-BR

Improving Durability of Reinforced Concrete Structures using Migrating Corrosion Inhibitors

Behzad Bavarian¹, Lisa Reiner¹ and Jessi J. Meyer²
Dept. of Manufacturing Systems Engineering & Management
College of Engineering and Computer Science
California State University, Northridge, USA 91330¹
Cortec Corporation
4119 White Bear Parkway
St. Paul, MN 55110²

Abstract

Concrete durability based on the performance concepts is a more realistic approach on the life predication. The performance concepts are based on quantitative predications for service life from exposure to environmental service conditions and concrete measured materials properties. The performance approach supports innovation in new materials technology, and allow explore new concrete formulation by moving away from restrictive material composition and construction practices.

Corrosion creates long term reliability issues for reinforced concrete structures. Traditional design and prescriptive concepts based on the cover depth, simple concrete mix parameters, water/cement ratio, and minimum chloride content are not sufficient to ensure concrete durability and satisfying required service life. Billions of dollars have been spent on corrosion protection of concrete and steel bridges, highways, and reinforced concrete buildings. Among the commercial technologies available today, migrating corrosion inhibitors (MCIs) show versatility as admixtures, surface treatments, and in rehabilitation programs. The effectiveness of the MCIs (mixture of amine carboxylates and amino alcohols) on reinforced concrete was evaluated throughout this project. Corrosion test results conducted over five years (1800 days), 240 cycles per ASTM G109 using immersion and ponding in 3.5% NaCl solutions. The results have indicated that polarization resistance (R_p) for the MCI coated concrete was higher (60-80 kohms-cm² with increasing trends) than non-coated concrete. The untreated concrete samples not only had lower R_p values, but also demonstrated decreasing trends. Examination of the embedded steel rebar after corrosion tests showed no corrosion attack for the MCI treated concrete samples, while non-treated concrete showed corrosion. X-ray photoelectron spectroscopy (XPS) and depth profiling confirmed that the inhibitor had reached the rebar surface in less than 150 days. XPS depth profiling showed an amine-rich compound on the rebar surface that corresponded with the increase in R_p and improved corrosion protection for the MCI treated steel rebar even in the presence of chloride ions. Based on measured corrosion rate the life expectancy of a concrete reinforced structure can be improved by more than 50 years.

Comparison of Martensitic Stainless Steels threshold properties in Stress Corrosion Cracking phenomena

Arianna Scatena, PontLab S.r.l., Pontedera Italy;

Marco Anselmi, GE Oil&Gas, Firenze Italy;

Filippo Cappuccini, GE Oil&Gas, Firenze Italy;

Domenico Di Pietro, GE Oil&Gas, Firenze Italy;

Arianna Scatena

Martensitic stainless steels (MSS) have been used widely for producing and transporting Oil and Gas process fluids because of their high strength and acceptable corrosion resistance in mid sour gas applications. In this review, the behavior of martensitic stainless steels are tested for their resistance to stress corrosion cracking (SCC) in aqueous environments containing chlorides, and in environments containing hydrogen sulfide (H₂S). Several testing environments are used in order to simulate service applications.

Investigations on the stress corrosion cracking of martensitic stainless steel have been documented, but important aspects are still unclear: whether threshold must reach a critical level and whether the threshold, if it exists, can be quantified, particularly as it relates to the chloride concentrations and H₂S content.

Significant factors on steel corrosion were investigated. SCC of several martensitic stainless steels were tested in accordance with ASTM G123 in chloride environment stressing U-bend test specimens.

These data were compared to the results of corrosion tests carried out using four point loaded specimens with the aim to obtain different load conditions, in accordance with ASTM G39 in the same environmental conditions of ASTM G123. The applied stress was determined from the size of the specimen and the bending deflection. The tests were duplicated with different stress levels.

The alloys performances were compared with respect to resistance to cracking failure and the effects of temperature and chloride concentrations are examined.

Martensitic Stainless Steels specimens were also tested for resistance to cracking failure under the combined action of tensile stress and corrosion in aqueous environments containing H₂S according to NACE TM0177, Method A in solution A.

The overall resistance of each MSS is outlined. Furthermore, within the same class of alloys, the differences were described with respect to stress corrosion cracking resistance.

Effect of acetic acid on corrosion behaviour of modified martensitic stainless steels in high temperature sour environments

Toshiyuki Sunaba^{1,2}, Shinji Okazaki² Yasuyoshi Tomoe¹ and Susumu Hirano¹

¹ INPEX CORPORATION, Tokyo/JAPAN

² Yokohama National University, Kanagawa/Japan

Organic acids such as acetic acid (CH_3COOH) present in some oil and natural gas production fluids. Corrosion behaviour of some grades of steels is often influenced significantly by the presence of organic acids in CO_2 corrosion environments. Presence of organic acids affects not only to decrease the solution pH but also to weaken the stability of passive films on 13%Cr and Super Martensitic Stainless Steels (SMSS) such as modified 13Cr SS (13Cr-5Ni-2Mo). However, effects of organic acids on film formation and deterioration of modified martensitic stainless steels have not been investigated in high temperature sour environments.

Behaviour of passive films and corrosion products film formation was investigated on conventional L80-13%Cr and SMSS in NaCl solutions pressurized with mixed H_2S and CO_2 gas in the presence of acetic acid. Immersion tests and electrochemical measurements were carried out, as well as surface analysis.

An immersion test was carried out in a static autoclave and the test duration was 40 days. Test temperature was 180°C and chloride ion concentration was 20,000ppm. Acetic acid concentrations were 0, 600ppm and 0.5vol.%. Test solution was pressurized by 1bar H_2S and 1bar CO_2 gas at room temperature. Polarization curves at high temperatures were measured in the static autoclave using an External Pressure Balanced Reference Electrode (Ag/AgCl, 0.1mol KCl) system and the potential sweep speed was 10mV/min.

Acetic acid affects formation and deterioration of corrosion product film on SMSS.

Martensite-based stainless steel OCTG of 15Cr-based and 17Cr-based material for sweet and mild sour condition.

*Yasuhide Ishiguro, Takeshi Suzuki, Kenichiro Eguchi, Tetsu Nakahashi
and Hideo Sato : JFE Steel Corporation, Handa, JAPAN.*

This report mentions the concept of the alloy design and the updated corrosion data about martensite-based stainless steel materials of 15Cr (generic 15Cr-6Ni-2Mo) and 17Cr (generic 17Cr-4Ni-2.5Mo-Cu-W).

Targeted corrosion environment

15Cr-based and 17Cr-based stainless steel OCTG materials targets at sweet and mild sour environment application, mainly for severer conditions in HPHT oil and gas wells. These materials aim at the corrosion environment between modified-13Cr stainless steel OCTGs (generic 13Cr-4Ni-1Mo and 13Cr-5Ni-2Mo) and duplex stainless steel OCTG of 22Cr and 25Cr, and are also expected to expand the application area even to the milder corrosion environment region of duplex-stainless-targeting area. It is positioned as the upper grade of Modified-13Cr, and also as alternatives partially for duplex-stainless-targeting area.

Alloy-design concept and strength grade

The concept is based mainly on two things. One is to enhance the stability of passivation film in these stainless steels to improve corrosion properties by adding corrosion-resistant alloy elements. The other is to keep martensite as main phase, because high-temperature strength shows better performance when strength is based mainly on martensite but not on cold-drawn-strain strengthening. Therefore, the alloy-design does not mean that alloy elements are added monotonically to Regular-13Cr (API-specified L80-13Cr and higher-strength-version of the same chemistry) and/or Modified-13Cr. Alloy elements are categorized as ferrite-stabilizing-elements and austenite-stabilizing-elements, and these two groups of elements are added to keep martensite as main phase. 15Cr-based stainless steel is composed of 15Cr-6Ni-2Mo chemistry, and is based mainly on martensite. 17Cr-based stainless steel is composed of 17Cr-4Ni-2.5Mo-Cu-W chemistry, and is based mainly on martensite and ferrite. Yield strength in 15Cr is 125ksi-grade (861MPa-grade), and in 17Cr is 110ksi and 125ksi-grade (758MPa and 861MPa-grade).

Corrosion-resistant properties and mechanical properties

The corrosion-resistant properties of SSC, corrosion rate under sweet condition and SSC are mentioned. The upper limit and the domain map in 15Cr and 17Cr at each corrosion-resistant property are mentioned and updated. For example, in terms of H₂S-free CO₂ corrosion, the application limit temperature in 15Cr and 17Cr are below 200 deg.C and below 230 deg.C, respectively, under 10MPa of CO₂ environment judging by the criterion of 0.127mm/year (5mils/year). The details will be presented and discussed, and mechanical properties as well.

Hydrogen stress cracking susceptibility of super duplex stainless steel 2507 in natural sea water

Flavien Vucko, Nicolas Larché, Dominique Thierry,

French Corrosion Institute, 220 Rue Pierre Rivoalon, 29200 Brest, France

Super duplex stainless steels are widely use in offshore applications. These steels offer high strength, toughness and excellent corrosion resistance. They are characterized by high chromium content and a mixed microstructure of austenite and ferrite in equal amount. These steels may be sensitive to hydrogen stress cracking when exposed to cathodic protection in natural seawater. This sensitivity could induce a detrimental effect reducing the fatigue resistance of such materials under cyclic loading conditions.

The aim of this study is to evaluate the high cycle fatigue resistance of the steel under cathodic protection in natural seawater by performing stress vs. number of cycles (S-N) curves. For this purpose fatigue tests under four point bending are performed in seawater on Sandvik SAF 2507 (UNS S32750) seamless tubes with a small austenite spacing (about 2 μm). These tests were performed in air, at the open circuit potential and under cathodic protection at -1100 mV/SCE (vs. saturated calomel electrode). Different load ratios, temperatures and frequencies are investigated to estimate the sensitivity of the steel to hydrogen embrittlement.

At room temperature and a load ratio of 0.1, no detrimental effect of cathodic protection is noticed comparing to open circuit potential. The fatigue lifetime is even enhanced by cathodic protection in these particular conditions, and frequency has no noticeable impact. Hydrogen pre-charging tends to reduce the difference of fatigue resistance under cathodic protection and open circuit potential.

Influence of thermal treatments between 650 and 850°C on the pitting corrosion behaviour of 2304 duplex stainless steel

F. Zucchi, F. Zanotto, V. Grassi, M. Merlin, A. Balbo

*Corrosion and Metallurgy Study Centre "A. Daccò" / Terra&AcquaTech Laboratory,
University of Ferrara, Italy*

Since its introduction in the worldwide market, the lean duplex family has been proposed as substitute for the 304 and 316 austenitic stainless steels and also for carbon steels in applications where maintenance costs are significant. Conventional duplex stainless steels (DSS) show a high decrease in localized corrosion resistance and fracture toughness after aging between 300 and 1000°C. This behavior is determined by the precipitation of secondary phases such as carbides ($M_{23}C_6$) and nitrides (CrN and Cr_2N) and the chi (χ) and sigma (σ) phases, depending on the temperature and time of treatment.

The 2304 duplex stainless steel (DSS) has been the first "lean" duplex grade developed. It is characterized by a low molybdenum content, which significantly reduces or inhibits the precipitation of the deleterious χ and σ phases. However, several studies showed that in the lean duplex the precipitation of carbides and nitrides is still possible after aging, at the α/α and α/γ grain boundaries.

In this research the effect of thermal treatments, performed in the range from 650 to 850°C, on the pitting corrosion behaviour of a DSS 2304 was investigated.

The DSS 2304 was treated for 5, 10 and 60 minutes at 650, 750 and 850°C. The pitting resistance of the treated samples was estimated in 0.1 M NaCl solution by the anodic polarization curve recording to determine the pitting potential (E_{pitt}) and by the potentiostatic critical temperature (CPT) technique.

The results showed that the DSS 2304 resistance to pitting corrosion decreased by increasing the treatment time and by decreasing the treatment temperature. The most critical conditions were the longest treatment time (60 min) at 650 and 750°C.

Optical and scanning electron microscopy (OM and SEM) observations, were used to correlate the effects of thermal treatments on the microstructure and on the pitting resistance.

Optimisation of the Corrosion Resistance of Pipe Butt Welds in Super Duplex Stainless Steels (SDSS)

G. Byrne (Rolled Alloys), G. Warburton (NeoNickel), R. Francis (RF Materials),
Z. Schulz (Rolled Alloys)

ABSTRACT

Because of the need to meet G48 Method A Ferric Chloride corrosion test requirements for SDSS joints in many fabrication specifications and the difficulty fabricators have experienced in meeting these requirements, butt welds in thin walled super duplex stainless steel pipe work systems have been described as “the most challenging joint facing the oil and gas fabrication industry”. This paper describes and discusses the reasons behind this statement and the fabricator experience in developing WPS/PQR’s to pass G48 Method A requirements using conventional techniques and methods. The paper considers what is and is not achievable for Ferric Chloride testing of welds under these circumstances and compares this with the results of potentiostatic electrochemical CPT tests in simulated chlorinated seawater. Results are presented showing the effect of different shielding and backing gas welding combinations on performance of welds in ferric chloride solution and electrochemical CPT testing. This data also covers the effects of weld heat input and inter pass temperature for each of the gas combinations considered. These results are correlated with the changes in weld metal microstructure. The paper identifies the welding parameters required to significantly enhance and consistently maintain the corrosion resistance of welds in both Ferric Chloride solution and in the electrochemical CPT test.

**Stress Corrosion Cracking of Solution Annealed and Cold Worked UNS S31603
Stainless Steel in H₂S Containing Production Environments**

Thierry Cassagne
Total
Avenue Larribau
64018 Pau Cedex
France

Cécile Plennevaux
Institut de la Corrosion
ZA du parc
42490 Fraisses
France

Claude Duret
Institut de la Corrosion
ZA du parc
42490 Fraisses
France

Low grade stainless steels of the AISI 300 series are extensively used in Oil and Gas production. They are often used for piping and various other process components, such as valves, pumps, or vessel internals. For larger equipment such as vessels or pipelines they are normally used as clad or weld overlay. In many instances 316L stainless steel is the first choice not only for such components but also for small bore lines where cold work is not uncommon. In the presence of H₂S it is important that such low grade corrosion resistant alloy is used appropriately and with caution. Indeed UNS S31603 stainless steel is very susceptible to pitting and/or stress corrosion cracking in the presence of chlorides and H₂S, particularly when the temperature increases. In order to assess safe limits of use constant load tests were carried out on as-received alloy pipe and cold worked components including plate and bar materials with hardness close to 22 HRC. Results indicate that constant load testing leads to tighter limits of use on solution annealed material compared to the new balloted limits in NACE MR0175/ISO 15156. The influence of cold work appears to increase the susceptibility to cracking at temperatures below 60°C and 1 bar H₂S partial pressure in the presence of 50,000 ppm chlorides. No adverse influence was observed at higher temperatures under the conditions tested.

Assessment of the crevice corrosion oxygen and temperature limits of CRAs for waste water injection wells

Marc E. Wilms, Sean Fletcher, William Grimes and Johan Smit, Shell Global Solutions International B.V., Amsterdam, The Netherlands

Max Klein, Sobhan Abolghasemi, Nederlandse Aardolie Maatschappij, Assen, The Netherlands

In oil and gas production, water injection of produced water for disposal is often necessary. Further, injection of water from a number of sources – produced fluids, surface water, seawater – often occurs to enhance oil field production and recovery. An important aspect of material selection for injection wells is the crevice corrosion resistance of the candidate materials – especially for corrosion resistant alloys (CRAs). This corrosion issue is particularly relevant in cases where the oxygen is not completely removed or fully oxygenated water is injected.

In this paper, an advanced, accelerated test method to qualify CRAs for use in oxygen contaminated saline injection waters basis their resistance to crevice corrosion is presented. The Test method combines stepwise polarisation of test specimens and use of PTFE crevice formers, in accordance with the methodologies defined in the European CREVCOR project. Details of this test method will be described, as well as the resulting safe application limits of four tested CRA materials. Safe application limits were determined with respect to combinations of the maximum allowable temperature and limits of oxygen concentration. The test program compared results using both actual and simulated field brines.

Failure Investigation: Produced Water Re-Injection Tubing and Equipment

Henrik Rese, Sr. Engineer Material Technology, Statoil ASA, Stavanger Norway
Perry Ian Nice, Sr. Specialist Material Technology, Statoil ASA, Stavanger Norway
Adriaen Nelemans, Sr. Engineer Ops Intervention, Statoil, Trondheim Norway

A tubing to annulus leak was registered in a produced water re-injection (PWRI) well on the Norwegian Continental Shelf, after approximately 10 years in operation. It was established that the leakage was located at the side pocket mandrel (SPM), resulting in a decision to re-complete the well. This well was constructed using ISO 11960 grade L80 carbon steel tubing alloyed with 1 wt.% chromium. The associated well equipment was manufactured in AISI 4130 with a 25Cr super duplex down hole safety valve (DHSV).

In the planning phase of the recompletion it was decided to perform an extensive failure investigation of the well tubing and equipment. The investigation included a thorough review on the injected water quality and the platform's chemical treatment systems. Earlier well interventions had shown that a black tar like substance, referred to as "Black Sticky Stuff" (BSS), was lining the internal surface of the well tubing and equipment. It was decided to take offshore samples of the BSS and corrosion products for further detailed analysis.

During the well workover tubing joints were extracted at various depths, as well as SPM were then shipped onshore for further analysis. One of the pulled tubing joints had collapsed during a pressure test of the A-annulus. This joint was found to be heavily internally corroded and was included into the investigation program.

This paper describes the process, tests and conclusions from the conducted failure analysis investigation.

Galvanic effects in drilling equipment – challenges and solutions of corrosion resistance

Sergey Kolesov, Weatherford International, St Petersburg, Russia

Robert Badrak, Weatherford International, Houston, Texas, USA

Valery Chizhikov, Weatherford International, St Petersburg, Russia

Aleksandr Kharkov, Saint-Petersburg State University, Russia

Alexey Alkhimenko, Saint-Petersburg State University, Russia

Effective design solutions are often achieved with use of dissimilar metals or alloys in structures. The potential problem with mixing metallurgies is galvanic or crevice corrosion in drilling or production return fluids that may be corrosive. This localized corrosion could be a considerable factor which reduces the operational life of structures.

Methods of the galvanic corrosion control are studied in the present work including application of protection coatings on contact pairs and application of electrical isolation coating between two contacted metals. Here the classical contact pair aluminum-steel has been investigated. The full electrical isolation between aluminum and steel leads to elimination of galvanic corrosion effects. The effect of different coating resistance values on the corrosion behavior of aluminum-steel pairs have been investigated and reported herein.

In-situ Surface Strain Mapping of Pitting Corrosion in a High Strength Carbon Steel

P.E. Barnes^{1,2}, S.B. Lyon³, D.L. Engelberg^{2,3}

1 Intertek, Bainbridge House, London Road, Manchester, UK

2 Advanced Metallic Systems CDT, The University of Manchester, UK

3 Corrosion & Protection Centre, School of Materials, The University of Manchester, UK

High strength carbon steel wires are used in flexible risers to act as pressure and tensile armours for the fatigue loads and pressures sustained by the riser. The armours are contained within an annular space where the presence of condensed water and gases such as CO₂, H₂S and CH₄ maintain a corrosive environment. Consequently, the high strength steel wires can suffer from corrosion fatigue under cyclic loading conditions. Previous work has shown that fatigue cracks initiate from corrosion pits that form on the surface of the carbon steel wire [1].

Digital Image Correlation has been used to explore the formation and development of local surface strain fields around localised corrosion pits of high strength steel wire in a seawater environment. This technique has not been used before on steel exposed to seawater and successful application therefore required the development of a suitable corrosion scale on the surface to optimise imaging conditions. Corrosion pits have been grown on the surface of the steel using chrono-amperometry and chrono-potentiometry.

The effect of pit size and population on the localised strain development of a high strength carbon steel sample under tensile loading has been explored. This has been achieved by growing single pits of different diameter and multiple pits in different size areas.

Statistical analysis of the DIC results demonstrates that there is an increase in localised strain for the multiple pitted areas than for the single pits. This validates that multiple corrosion pits increase the localised strain field on the steel surface.

- [1] P. E. Barnes, S. B. Lyon, T. McLaughlin, and D. L. Engelberg, "Corrosion Fatigue Cracking of High Strength Carbon Steel Wires in CO₂-Saturated Seawater Environment," in *Eurocorr 2013*, 2013.

Sour corrosion – Investigation of iron sulfide layer growth in saturated H₂S solutions

Georgi Genchev¹, Karsten Cox¹, Adnan Sarfraz¹, Christoph Bosch², Michael Spiegel², Andreas Erbe¹

¹ Max-Planck-Institut für Eisenforschung GmbH, Max-Planck-Str. 1, 40237 Duesseldorf, Germany – email: g.genchev@mpie.de

² Salzgitter Mannesmann Forschung GmbH, Ehringer Str. 200, 47259 Duisburg, Germany

Crude oil and gas usually contain water but may also contain relevant amounts of hydrogen sulfide and/or carbon dioxide [1]. The presence of these compounds has been shown to promote the corrosion process, wherein the reaction conditions, e.g. pressure, temperature, and flow velocities, are of great importance [2]. To date, there is debate concerning the exact mechanism of the (electro)chemical process(es) during the H₂S-triggered corrosion of iron or steel. Therefore, the properties of the formed sulfide layers have been examined in detail by electrochemical methods and subsequent analysis, e.g. by X-ray diffraction (XRD), scanning electron microscopy (SEM), X-ray photoelectron spectroscopy (XPS), IR and Raman spectroscopy.

Tafel plots have been engendered from linear sweep experiments, conducted in N₂ purged solutions without and with H₂S saturation. The presence of H₂S results in a negative shift of the corrosion potential (E_{corr}), indicating the more active corrosion of the metal under these conditions. Furthermore, anodic polarization experiments have shown no decrease of the current density over time, suggesting a non-protective nature of the formed iron sulfide layers. The black color of the precipitate is a clear indication that it is not a high band gap insulator. Optical transmission measurements in the mid and far infrared regions have shown very high absorption of the investigated material, showing that if the corrosion products possess a band gap it must be <0.03 eV. Moreover, the conductive properties of the iron sulfide layers compared to iron oxide have been verified using electrochemical impedance spectroscopy (EIS). Theoretical studies indicate a metallic behavior for at least one spin channel [3,4].

The loose and brittle character of the corrosion product scales has been unambiguously identified by means of XRD. The scales consist of the mineral mackinawite (tetragonal FeS) without any further detectable impurities. Furthermore, additional information about the layer thickness and preferred orientation of the crystallites has been obtained from the diffraction patterns. The Raman spectra of the electrochemically formed films clearly prove the presence of the above mentioned compound. The most intensive Raman bands appear at around 210 cm⁻¹ and 280 cm⁻¹ and correspond to the lattice mode and the symmetric stretching mode of FeS, respectively [5].

References:

- [1] C. Ren, D. Liu, Z. Bai, T. Li, Mater. Chem. Phys. 93, 2005, 305; [2] S. Netic, Corros. Sci., 49, 2007, 4308; [3] A. Devey, R. Grau-Crespo, N. de Leeuw, J. Phys. Chem. C, 112, 2008, 10960; [4] K. Kwon, K. Refson, S. Bone, R. Qiao, W. Yang, Z. Liu, G. Sposito, Phys. Rev. B 83, 064402, 2011, 1; [5] J.-A. Bourdoiseau, M. Jeannin, R. Sabot, C. Remazeilles, P. Refait, Corros. Sci., 50, 2008, 3247.

Electrochemical noise analysis on modified 13%Cr stainless steels in sour environments under stress

*M. Sakairi, J. Tatehara and Y. Mizukami, Hokkaido University, Sapporo/Japan
S. Hashizume, TenarisNKK Tubes, Kawasaki/Japan*

Because of oil and gas fields are severe corrosive environments, high corrosion resistant stainless steels are widely used. It is, however, well known that HE, SCC, and SSC are severe corrosion problems of these materials in the fields. Therefore, there are many papers have been published. It is also awaited to predict initiation or propagation of pitting events, which is lead to SCC or SSC. One of the possible techniques is electrochemical noise analysis. it is also try to clarify the relationship between features of PSD and initiation of crack or pitting corrosion during immersion corrosion tests by using consecutive PSD calculation technique.

An 110 ksi grade 0.02 %C -13 %Cr – 2%Mo martensitic stainless steel was used as samples. Before the test, specimens were polished with SiC papers and then cleaned with ethanol and doubly distilled water. Two solutions (1) 20 mass% NaCl + 0.4 gdm⁻³ CH₃COONa (pH=4.5) solution with 5 % H₂S-CO₂ balance and (2) 1.6 mass% NaCl + 0.4 gdm⁻³ CH₃COONa (pH=3.5) solution with 10% H₂S-CO₂ balance were used. Rest potential under 90 % AYS in different solutions were measured with sampling interval of 5 s. The rest potential changes were processed calculating the power spectrum density (PSD) consecutively by the Fast Fourier Transform (FFT) method with 1024 data points (5120 s), and average value of PSD from 0.8 mHz to 5 mHz (average PSD) were calculated as one feature of the PSD.

Figure 1 shows typical example of PSD (left), and average PSD and rest potential as a function of time(right) at 90% AYS in 20% NaCl + 0.4 g/L CH₃COONa (pH=4.5) solution with 5% H₂S-CO₂ balance. The rest potential shows fluctuations, and three large slow positive shift and then sudden decrease are observed. No failure of the specimen was observed after 720 hours, while a pit was observed at 336 hours corresponds to first potential drop. Crack-like localized corrosion observation at 552 hours corresponds to second potential drop. The peaks of average PSD are in good agreement with rest potential change and localize events. From the result, using optimized feature of PSD makes it possible to monitoring initiation of pitting corrosion or cracks

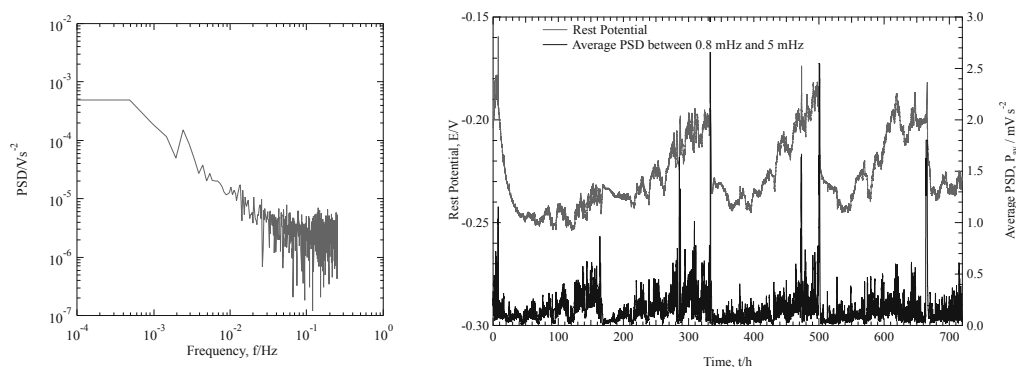


Fig.1 Typical example of PSD (left), and average PSD and rest potential as a function of time (right) at 90% AYS in 20% NaCl + 0.4 g/L CH₃COONa (pH=4.5) solution with 5% H₂S-CO₂ balance.

Localised corrosion attack of pipeline steel associated with weldments in CO₂ containing environments

A.A. Abdurrahim

Libyan Petroleum Institute, Gergarish St., Km 7, Tripoli-Libyan Arab Jamahiriya

Abstract

In this work the corrosion behaviours and metallurgical characterisation of the different weld regions such as parent metal (PM), heat affected zone (HAZ) and weld metal (WM) of X70 grade pipeline carbon steel is reported. Electrochemical techniques such as corrosion potential monitoring, polarisation resistance technique and galvanic current measurements were employed to evaluate the corrosion behavior of the material in a 3.5% NaCl solution saturated with CO₂ at ambient temperature, where the pH of the system ranges from 3.9 to 4.3 under static and flow conditions. Optical microscopy was used for the metallurgical characterisations and the main morphological phases found in the WM and HAZ were bainite, martensite and acicular ferrite structures. Conversely, ferrite and pearlite phases were observed in the PM. Galvanic current measurements for the coupled weld regions under static conditions showed that selective weld corrosion attack were minimised either in the WM or the HAZ relative to the adjacent region of the PM. However, under flow condition of speed 2000 rpm weld attack was found to be also reduced in the HAZ and after a round of 15 hours of immersion it reduced slightly in the WM rather than large area of the PM. In general galvanic corrosion tests for coupled weld regions indicated that weld corrosion attack was reduced in the HAZ while a slight decrease in the corrosion current was observed in the WM rather than the large area of the PM. Galvanic corrosion test between three weld regions indicated that localised weld corrosion occurred in the PM rather than HAZ or WM. This is a promising solution for the oil and gas industries as the weld corrosion attack was spread over the large area of the pipeline steel. Moreover, the immersion test at ambient temperature was shown to be effective to reduce the corrosion rate penetration in the pipeline steel welds.

Key words: Welded steel X70, Weld attack, Galvanic tests, CO₂ corrosion.

Pipeline Pigging and CP Specialised Electrical Surveys:

A unique integral strategy for Pipeline Integrity

Lucio Di Biase, Osvaldo Fumei – ISPRONA Srl – Roma - Italy

Giovanni Fumei – New York University

Pigging is an integral and critical aspect of pipeline maintenance and operation.

In-Line Inspection (ILI) with various inspection methods such as Magnetic Flux Leakage (MFL) or Ultrasonic Technology (UT) has become standard in pipeline integrity assessment worldwide.

This paper will discuss different aspects of pipeline pigging, the advantages and disadvantages of competing technologies, the defects that intelligent pigs currently do not detect or size well and the attributes of manual and automated data analysis processes.

Magnetic Flux Leakage (MFL) Pig and Ultrasonic Pig (UT) for metal loss, axial defects detection, pipeline defects and analysis, data handling, reporting and repairs will also be illustrated.

Some experiences show how Pipeline Pigging Data and Specialised Electrical Survey comparison results could be used to figure out the corrosion conditions and how to deal with similar pipelines which cannot actually be pigged.

Protective ability of iron sulphides in sour corrosion

*Morten Tjelta and Jon Kvarekvål, Institute for Energy Technology (IFE),
Kjeller/Norway; Morten Tjelta*

Iron sulphide, frequently found on carbon steel under sour conditions, is under certain conditions expected to act as a (large area) cathode thereby increasing the corrosion rate of the underlying steel through galvanic coupling. In the present work electrochemical reactions taking place at iron sulphide (FeS) in the presence of acetic acid and carbonic acid have been studied using potentiodynamic measurements. Both the weak acid systems were found to increase the cathodic currents at iron sulphide electrodes compared to the supporting electrolyte alone.

CI-SCC Attack in SS 316L Branch Connection Welding

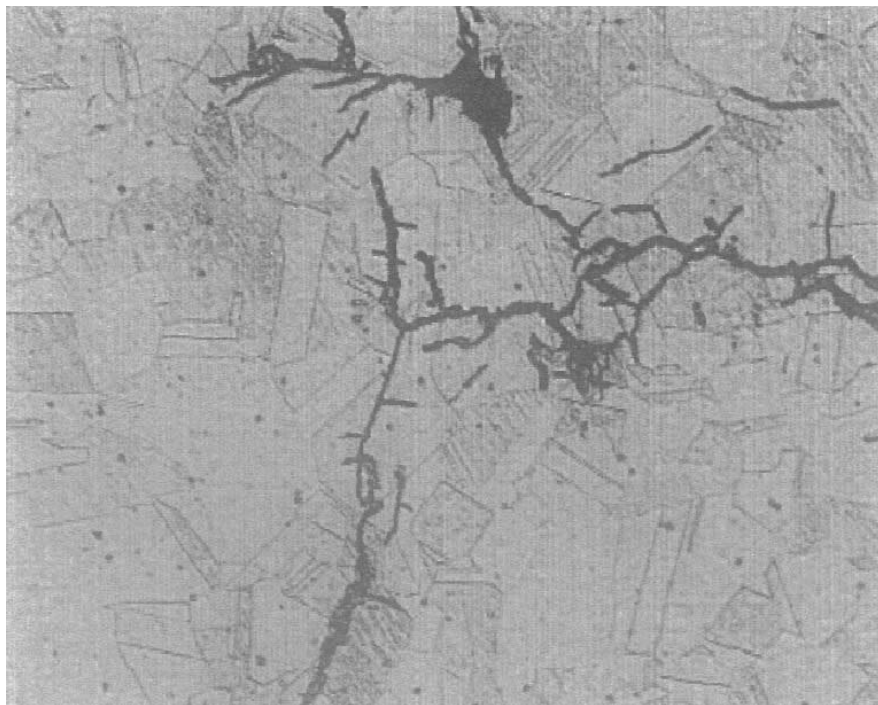
Munther Al-Hammad, Saudi Aramco, Saudi Arabia

After seven (7) years in service, a failure occurred in an austenitic stainless steel (316L) pipe transferring feed sour gas separated by three phase separator. The gas leak was observed in the vertical relief valve branch connection. Failure analysis confirmed the reason of leak was several cracks developed near the welding joint.

The cracks were identified to be chloride stress corrosion cracking CI-SCC. Although the routine collected sampled from the fed gas streams revealed very low chloride concentrations, the collected sample from the failed spool shown a high concentration up to 300 ppm.

The result from a Risk Based Inspection (RBI) assessment for the feed gas stream showed an in-crease in the potential risk in SS 316L piping with increasing the chloride percentage.

Several action plans were evaluated to prevent reoccurrence starting with inspecting all welding joint in the system. The inspection faced difficulty in branch connections where more plans were stated including coating the piping and upgrading the piping material more resistance metal. Inconel 825 was elected to replace SS 316L in the branch connections to insure immune to chloride attacks material. All preventing methods were discussed in this work including the feasibility and cost estimate for each plan.



Pittings occurrence in coupons of weight loss for corrosion monitoring in pipelines.

Neusvaldo Lira de Almeida, Instituto de Pesquisas Tecnológicas de São Paulo, São Paulo/Brazil

Lorena Cristina de Oliveira Tiroel, Petrobras Transportes S.A, São Paulo/Brazil
Vanessa Yumi Nagayassu, Instituto de Pesquisas Tecnológicas de São Paulo, São Paulo/Brazil

Rômolo Hernandez de Moraes, Instituto de Pesquisas Tecnológicas de São Paulo, São Paulo/Brazil

Weight loss coupons used for monitoring internal corrosion has shown pitting consistently. Some pipelines, however, have no history of occurrence of pitting. That is why it was hypothesized that this phenomenon was related to the characteristics of the coupons and not to the aggressiveness of the product transported by pipeline. To identify the causes of the pitting formation, coupons of three origins were initially submitted to characterization test, immersion tests, electrochemical tests, and SEM and subsequently coupons were installed in the duct in real operating conditions. This study showed that the occurrence of pitting was associated with the manufacturing process the material, which generated MnS inclusions elongated shape of the coupons. These inclusions are cathodic in relation to carbon steel. When the coupons are installed in the ducts, the inclusions are perpendicular to the flow direction and in contact with the corrosive medium, there is dissolution of the steel surrounding the inclusion, forming small crevice that trap the electrolyte accelerating the corrosion process. Some cavities type "tunnels" are formed with pullout full inclusion. These cavities, in turn, trap the electrolyte and further accelerate the corrosion process inside.

Effects of high flow rate on corrosion of carbon steel in high pressure CO₂ environment by means of linear polarization resistance

*F. Todesco*¹; *M.E. Gennaro*¹; *S. Sgorlon*¹; *L. Torri*²;

¹ *Venezia Tecnologie s.p.a., via delle industrie, 39, Porto Marghera, Venezia, 30175,*

² *eni E&P, via Emilia, 1, San Donato Milanese, 20097*

The effects of high flow rate on X65 carbon steel corrosion in carbon dioxide (CO₂) environment were studied using an autoclave mini-loop apparatus. The corrosion process was monitored both in static and in high flow rate conditions (5m/s) by means of linear polarization resistance (LPR) tests. Tests were performed at 180 bar and 90°C, with a gas mixture of 0.1% (molar) CO₂ in nitrogen and 0.5% (weight) NaCl brine. High flow conditions were achieved pumping the brine through the LPR test section of a mini loop. Both the loop and the rotary pump were totally immersed in the brine. Static and dynamic tests were performed respectively for 720h (30 days) and 480h (20 days) in order to obtain a significant prediction of the average corrosion rate. In both cases, after several days a progressive drop of cathodic and anodic reactions was noticed, which indicates the growth of a corrosion product layer (FeCO₃) which could have offered a certain degree of protection against general corrosion. However, diffused pits were observed both in static and dynamic conditions. Despite these similarities, the comparison of the corrosion rates in the two hydrodynamic regimes indicates that high shear stresses, due to flow, can enhance corrosion rate by ten times. Moreover, it was experimented that local turbulence may cause detachment of the carbonate film.

Translating Oilfield Material Exposures into Laboratory Tests

William D. Grimes and Marc E. Wilms, Shell Global Solutions International B.V., Amsterdam, Netherlands

Material use in oil and gas fields are usually characterized by a broad range of exposure conditions, e.g., varying total pressures, carbon dioxide content, hydrogen sulphide content, water chemistries, flow rates, flow regimes, stress condition. More often, a material chosen for use in an oilfield (oil or gas) project is expected to last the life of the field – a strategy of limited replacement as lifecycle conditions change. This strategy is especially true for materials chosen for sour projects. However, when testing materials there is sometimes a simplified assumption that the worst exposure condition is the sum of the more severe conditions – which may not be true. Translation of field exposures into a realistic testing plan requires a full assessment of expected exposures over the full field life cycle. This criticality assessment should include potential field operating modes, physical and chemical exposures, and an understanding, by proposed material type, of the material's potential failure modes and the critical corrosion and mechanical contributors to a material's multiple modes of failure.

Once critical field operating environments are identified, to qualify materials it is necessary to translate these field exposures into laboratory tests. The challenge of this process is to assure that all critical aspects of the mechanical and physical chemistry exposure are addressed in the laboratory testing. This is usually further challenged by the fact that laboratory capabilities may not reach or match those in actual field service, e.g., total pressure, flow. Thus translating the critical field exposures requires that one understands both critical physical chemistry exposures and material modes of failure. The reality is thus that proper simulation of some modes of failure may require use of non-standard test approaches.

Discussed will be a protocol for identification of critical field conditions by material type and translation of field exposure conditions into relevant laboratory tests. The focus will be on sour cracking modes of failure and some modes of corrosion failure.

Corrosion Fatigue of aluminium drilling pipes: case study

L. Alleva, Centro Sviluppo Materiali, Rome, Italy; R. Porta, Centro Sviluppo Materiali, Rome, Italy; G. Hoxha, ENI, Milan, Italy

Long drill strings made of tubular elements are used for oil drilling operations. Carbon steel pipes are generally used but in some conditions the use of Aluminium alloys is more convenient due to the light weight and the lower stiffness. Aluminium drill pipes (ADP) are connected through tool joints made in carbon steel. Recently during drilling operations, failures occurred on aluminium drill pipes close to the pin and boxes connections. Metallographic Investigations have been carried out on base materials and close to the failures, and fracture surfaces have been analyzed to highlight the cause for premature damaging. A 3D FEM model has been built for a steel box to Aluminium Drilling Pipe (ADP) joint, with the aim of investigating the stress fields during drilling process and to understand possible causes of ADP failures. A damaging mechanism has been proposed based on results from both metallographic analysis and FEM simulations.

An Innovative Design for Top-of Line Corrosion Assessment in Laboratory

*Hesham Mahmoud, Anne Neville, Xinming Hu University of Leeds/WoodGroup
Kenny, Leeds/United Kingdom*

Abstract:

This research work represents a study of Top of the Line Corrosion (TLC) on carbon steels X52 in presence of carbon dioxide and acetic acid. The special case of Top of the Line corrosion will be considered in detail. Designing a new experimental model used to compare between Top of the Line Corrosion (TLC) and Bottom of the Line Corrosion (BLC). The lid model is designed by using solid works software and manufactured by using 3D printing machine. The model is designed to measure the corrosion rate at same time for both TLC and BLC. Linear polarization resistance method is used to measure the corrosion rate for BLC samples, while weight loss method is used to measure TLC samples. Special TLC samples were designed (half pipe section). The influence of different parameters such as acetic acid concentration, condensation rate and bulk temperature will be studied. The free acetic acid concentration will be varied from 0 to 1000 ppm (0-250-500-1000 ppm), with three different sets of temperature 50 C°, 70 C° and 90 C°. CO₂ partial pressure is constant on all experiments. Twelve tests is done for each acetic acid concentration with each temperature, each test runs for 24 hours. At the bottom of the line, the corrosion rate is always greater than at the top of the line in order of magnitude. By Comparing the corrosion rate between Top of the line and Bottom of the line, it is found that BLC = 1/10 TLC. There is directly proportional relationship between acetic acid concentration and the corrosion rate on both BLC and TLC. When acetic acid is added in the presence of CO₂ corrosion, it will lead to increase in the general corrosion rate. Regarding the top of the line corrosion, same observation as bottom of the line corrosion is expected. The condensation rate will be varied according to the bulk temperature (Low-Medium-High), it has a great influence on TLC, while it is difficult to examine the results of condensation rate on bottom of line, due to gravity forces where the condensate goes and accumulates downside at the electrolyte. At low condensation rate (50 C°), a protective black film formed on the surface of the sample which shows lower corrosion rates compared to medium and high condensation rates 70 C° and 90 C° respectively. Localized corrosion is found at the bottom of the line. The corrosion on top of the line is uniform.

Effect of Plastic Deformation on Hydrogen Permeation of API 5L X65 Steel Pipeline

E. Fallahmohammadi, F. Bolzoni, G. Fumagalli, G. Re, L. Lazzari

This paper deals with the effect of different levels of plastic deformation on hydrogen permeation of cold rolled or tensile specimen of X65 pipeline steel. Diffusion of hydrogen are evaluated using the three techniques: Subsequent Transients (method of ISO 17081), Partial transients and desorption technique. Results are compared with our previous results concerning the effect of different steel microstructures on diffusivity of hydrogen on the same steel [1].

Fatigue testing was also carried out in the same smooth flat API 5L X65 specimen continuously charged with hydrogen to study the effect of low frequency fatigue load on hydrogen permeation characteristic curve and diffusion coefficient of hydrogen.

Keywords: Pipeline, Hydrogen Diffusion, Plastic Deformation, Fatigue.

References:

- [1] E. Fallahmohammadi, F. Bolzoni, G. Re, G. Fumagalli, L. Lazzari, "Interaction of hydrogen with different microstructure of pipeline steels", Proceeding of EUROCORR2013, Estroil, Portugal 1-5 Sep. 2013

Effective Assessment of Crude Oil Sourness for the Material Selection of Refinery Feeder Pipeline

Javad Khosravi, NIORDC-NIOEC, Tehran/Iran; Javad Khosravi

Doubtless, in the oil and gas industries, H_2S presence is the main cause for so-called sour services corrosion. NACE standard MR 0175/ISO 15156 provides the guideline to determine the degree of sourness of gas, liquid or multi-phases services and the material required. The sour service aspects may differ from a process engineer to a material engineer and it is sometimes due to the different concepts about dissolved H_2S concentration. The worst possible operating conditions include maximum temperature and H_2S partial pressure in the gas phase and crude oil composition usually use for evaluation of the sourness level. The present work comprises the investigations carried out on crude oil and provides the results obtained from the analysis of major parameters influencing the crude oil sourness. It should be noted that although the mentioned crude oil is fed into an oil refinery but the present study has its focus on material selection of transmission pipeline and the relevant facilities.

Assessment of ionic liquids corrosivity: preliminary results

M.V. Diamanti¹; U. Velardi¹; A. Mele¹; MP. Pedferri¹; M. Ormellese¹

¹ *Politecnico di Milano, Milan, Italy*

CO₂ is one of the most important greenhouse gases, which absorb infrared energy radiated from the Earth resulting in an increase of the temperature of the troposphere. Nowadays, the most used CO₂ Capture and Storage (CSS) process is the post-combustion absorption with alkanolamine solvents^{1,2}, but it still presents some drawbacks such as high energy consumption for solvent regeneration, limited cyclic CO₂ loading capacity and especially corrosivity, which prevent their use on industrial scale.

Ionic Liquids (ILs), with their special properties of tunability of chemical structure – and therefore of their properties, non-volatility and, above all, negligible vapour pressure can succeed in lowering the energy consumption in the CO₂ stripping and in the subsequent solvent regeneration compared to amine absorption³. Yet, corrosivity of ILs cannot be predicted and, although some preliminary studies were conducted and showed a potential compatibility between the steels considered and some ILs, further information on this topic is still needed^{4,5}.

The aim of this work is to investigate the corrosion behaviour of stainless steel AISI 316 and carbon steel in contact with several ILs, changing alternatively cation and anion to evidence possible dependence of the corrosion behaviour of steels on one, or both, relevant groups. ILs examined were those with 1-Butyl-3-methylimidazolium (b-mim) cation, combined with four different anions: tetrafluoroborate (BF₄), hexafluorophosphate (PF₆), chloride(Cl), and bis(trifluoromethylsulfonyl)imide (TFSI). Furthermore, investigations concerned the effect of cation alkyl chain length combined with the anion TFSI: 1-Ethyl-3-methylimidazolium, 1-Butyl-3-methylimidazolium, 1-Hexyl-3-methylimidazolium, 1-Methyl-3-octylimidazolium.

Tests consisted in potentiodynamic polarization performed in all ILs considered and in a 35 g/l NaCl solution as reference, conducted in a specially designed small volume cell (5 ml). Tests were performed at 60°C in order to approach industrial application conditions of CCS, as well as to reduce ILs viscosity. Moreover, different ILs preparation conditions were considered: after purging in N₂, i.e., with reduced content of oxygen and water, and after exposure to the atmosphere to restore their natural humidity and oxygen content.

References

1. H.H. Khoo, R.B.H. Tan, Environ. Sci. Technol. 40, 2006, 4016–4024.
2. D.M. D'Alessandro, B. Smit, J.R. Long, Angew. Chem. Int. 49, 2010, 6058 – 6082.
3. X. Zhang, X. Zhang, H. Dong, Z. Zhao, S. Zhang, Y. Huang, Energy Environ. Sci. 5, 2012, 6668.
4. I. Perissi, U. Bardi, S. Caporali, A. Fossati, A. Lavacchi, F. Vizza, Russian J. Electrochem. 48, 2012, 434-441.
5. L. Pisarova, C. Gabler, N. Dörr, E. Pittenauer, G. Allmaier, Tribol. Int. 46, 2012, 73-83.

An alternative to H₂S in NACE corrosion test for Sulphide and Hydrogen-Induced Cracking risk assessment

C. Colombo, S. Corsinovi, G. Lovicu, R. Valentini

*Department of Civil and Industrial Engineering, Largo L. Lazzarino 1, 56122
University of Pisa (Italy), email: costanza.colombo@for.unipi.it, s.corsinovi@alice.it,
g.lovicu@diccism.unipi.it, r.valentini@diccism.unipi.it*

Abstract

Sulphide Stress Cracking (SSC) and Stress Corrosion Cracking (SCC) have always been great concerns for pipeline steels operating in H₂S environments. Sulphides presence may enhance hydrogen uptake in steels and promote Hydrogen-Induced Cracking (HIC). The resistance to these detrimental phenomena is usually evaluated by standard corrosion tests based on the use of solutions containing H₂S. For environmental and safety reasons, the use of the abovementioned acid is likely to be reduced in the future, thus traditional standards have to be reconsidered. Due to the general commitment towards the replacement of H₂S, the present work aims to propose a convenient alternative to recreate the sour environment typical of standard tests (such as NACE TM 0177). Sodium thiosulfate (Na₂S₂O₃·5H₂O) was selected as one of the most promising options to be added to the NACE A solution, thanks to its ability to promote hydrogen absorption. The material chosen for the study is an HSLA low carbon steel largely used in the Oil&Gas industry. The steel was preliminary characterized as regards hydrogen diffusivity and mechanical strength. Hydrogen permeation tests were carried out, varying the Na₂S₂O₃·5H₂O concentration. A campaign of Slow Strain Rate Tensile (SSRT) tests and Thermal Desorption Analysis (TDA), was performed on specimens, after immersion in the selected solutions, in order to evaluate their hydrogenation ability. Results confirmed that it is possible to achieve an optimum concentration for Na₂S₂O₃·5H₂O in order to maximize hydrogen flux permeating. TDA results demonstrated that the proposed solution causes a consistent hydrogenation and so may be successfully used for further investigation on HIC.

Examination of line pipe strength and toughness in arctic environments combined with severe sour service

A. Smith, Centro Sviluppo Materiali, Rome, Italy; G. Mortali, Centro Sviluppo Materiali, Rome, Italy; G. Melis, Centro Sviluppo Materiali, Rome, Italy; O. Albores, TenarisTamsa, Veracruz, Mexico; E. Garcia, TenarisTamsa, Veracruz, Mexico

The oil and gas transport pipelines in arctic fields e.g. Kashagan and Karachaganak, nominally operate at temperatures of 100°C or higher. In addition, for these fields, large quantities of H₂S will be present during pipeline operation i.e. 5 to 20%. These high concentrations represent a significant risk of hydrogen ingress during pipeline operation. Furthermore, during pipeline shutdown in winter time, temperatures can reach very low levels e.g. -40°C. In the presence of previously introduced hydrogen from the operation phase, the low temperature strength and toughness of the pipeline may be impaired. Thus during restart operations when there is an increase of internal pressure, the pipeline integrity could be at risk. From these considerations there is a need for assessing line pipe materials at H₂S partial pressures much higher than the usual 1 bar imposed for standard qualification tests.

The present work aimed to simulate the above pipeline operation and shut down conditions by first exposing line pipe materials to high temperatures and H₂S pressures in autoclaves. After exposure samples were subjected to mechanical tests at low temperatures simulating the shut-down phase. Line pipe materials strength and ductility were assessed via low temperature tensile tests. Low temperature toughness was also evaluated. The degradation of line pipe materials properties was then examined by comparing to tests performed without autoclave exposure. Finally, the results obtained have been discussed with respect to the different hydrogen damage mechanisms that may be operative during the mechanical tests.

Reducing Sour Corrosion Using New, Thermally Stable Hydrogen Sulfide Scavengers

Scott Lehrer, Vladimir Jovancicevic, Sunder Ramachandran
Baker Hughes

Abstract

Safe transport of sour gas and crude oil from offshore and land-based wells involves using metallurgy resistant to hydrogen sulfide- (H_2S) induced localized corrosion (sulfide corrosion cracking). The use of corrosion-resistant metallurgy usually increases equipment cost. Consequently, in some instances it is more economical to remove H_2S from the production fluid by applying an H_2S scavenger. The scavenger enables the use of less-expensive materials and reduces environmental and safety concerns.

Conventional hydrogen sulfide scavengers such as triazines have been used to mitigate the effect of H_2S in gas and oil production facilities. However, triazines exhibit a high scaling tendency, low thermal stability, and performance reduction under high-temperature conditions. Non-nitrogen-based scavengers have been used with success, but can cause corrosion, exhibit slow kinetics, and show reduced effectiveness at elevated temperatures.

A research program was initiated to meet the market need for an effective, fast-acting hydrogen sulfide scavenger suitable for elevated temperature applications. A new test procedure was developed to evaluate hydrogen sulfide scavenger candidates and understand the critical parameters that control the scavenger efficiency and kinetics in various applications and conditions.

The result of the research is new, non-triazine-based scavengers with high-temperature stability and fast kinetics for use in gas, oil, or mixed production applications. The improved kinetics of the new scavengers makes them especially useful for situations where the system residence time is low. Field test results of the new scavenger compared to triazines or other conventional scavengers are shown for gas and mixed production applications.

About the correspondence of test conditions with field conditions in materials selection

G. Gabetta, S. Correr, eni e&p Division, Italy; S. Sgorlon, VeneziaTecnologie, Italy; S. Trasatti, Milano University, Italy

It is well known that the presence of acid gases, CO₂, H₂S and/or Sulfur in production fluids can be responsible for both general and localized corrosion, acting with different mechanisms which depend on chemical and physical properties of the produced fluids.

Materials selection for plants handling such fluids is performed by combining experience with suggestions from standards and regulations. A good deal of knowledge is available to predict corrosion rates for CO₂ containing hydrocarbons, but the effect of high H₂S pressure is less known, mainly due to the difficulty of performing laboratory tests in such challenging conditions. The so-called Nace Solution to assess SSC (Sulfide Stress Cracking) susceptibility of steels is a water-based solution simulating production fluids in equilibrium with one bar bubbling H₂S gas. This solution does not simulate situations where high pressure of gas is present; moreover, it does not take into account the corrosive properties of Sulfur and its compounds that may deposit in such conditions. Properties of high pressure gases are intermediate between those of a gas and those of a typical organic liquid; high pressure gases have superior wetting properties and better penetration in small pores with respect to liquids. These features can enhance and accelerate the corrosion; unfortunately, such conditions are likely to be present in many production fields.

Corrosion behaviour of metals and alloys in high pressure gases and in presence of different production fluid components is not fully understood. The analysis of such complex environments requires the knowledge of phase equilibria in wet acid gas mixtures, containing, in addition to H₂S and CO₂, light hydrocarbons (methane, ethane, propane), sulphur compounds and water. Their phase equilibria are difficult to predict, and the corrosion resistance of materials in such fluids is not well known. To predict corrosion and damage risks in different locations along a pipeline, moreover, the behaviour of fluids needs to be modelled taking into account the full composition.

This paper will try to point out a few challenges of dealing with high pressure gases, to suggest that, for materials selection in sour service, a better correspondence of test conditions with the real field conditions shall be pursued.

Methanesulfonic acid (MSA) as an acid used in the well stimulation procedure and corrosion of 22Cr

*Jennifer Jackson, BASF SE, Corrosion and Production Chemicals, Global Oilfield Solution, Carl-Bosch Strasse 38, 67056 Ludwigshafen, Germany
Matjaž Finšgar, University of Maribor, Faculty of Chemistry and Chemical Engineering, Smetanova ulica 17, 2000 Maribor, Slovenia*

A very important step in the oil, gas, and geothermal water drilling industry is the well acidizing procedure, which is a rock reservoir (the origin of the natural resource or water – a geological subterranean formation) stimulation technique used to improve productivity. In the well acidizing procedure different acids are employed depending on the underground reservoir characteristics.

Acids frequently represent a potential danger for drilling crews and the environment. For drilling crews it is particularly important that fluids do not cause health problems, i.e. dermal toxicity, eye irritation, skin sensitisation, and mutagenicity. However, conventional acids frequently cause these problems (e.g. HCl, HF, HCOOH, CH₃COOH). Moreover, inhibitors for conventional acids are frequently effective only at high concentrations and are extremely toxic, causing handling and waste disposal problems, and producing toxic vapours under acidizing process conditions.

Due to the above listed potential problems and disadvantages of using conventional acids, safer, environmentally more acceptable and less corrosive alternatives are currently being sought. A standalone acid such as methanesulfonic acid (MSA) could be a solution to address some of these challenges. From the environmental perspective, MSA is usually described as a “green acid” and frequently environmentally and human health hazard much more acceptable compared with some conventional acids.

In this work we will show that MSA could be an alternative to the conventional acids currently employed in the well acidizing procedures. The great compatibility of non-inhibited MSA with 22Cr steel (material used for the well construction) at elevated temperature in terms of general and pitting corrosion will be explored. We will demonstrate the use of MSA without inhibitor can be a viable option for acidizing well application that are constructed from 22Cr steel.

Deposits effect on corrosion behavior of carbon steel in sour environments

Nayef M. Alanazi, A. M. El-Sherik, A.H. Rasheed, Saleh H. Amar, and
Moayyad N. Alneemai

Research & Development Center, Saudi Aramco, Saudi Arabia
Box 62, Dhahran 31311

Abstract

Effect of deposits on corrosion behavior of carbon steel in sour environments was investigated. Clean sand, sand with 4wt% sulfur, sand with 8wt% sulfur, and filed-collected sludge deposits were used to study under-deposit corrosion (UDC). Two different field brines and sour gas compositions were included in this work to simulate field environments in order to investigate the effect of TDS and H_2S contents on the UDC mechanism. UDC activities were assessed underneath of these deposits by means of linear polarization resistance, zero ampere resistance using coupled multi-electrode array system (CMAS) and weight loss coupons. The results showed that the clean sand deposit inhibits the UDC and the general corrosion rate was lower than that obtained from on-deposit test. No localized corrosion was noticed on coupons inserted under no-deposit and clean sand deposit. It was also observed that low H_2S/CO_2 gas ratio and high total dissolved sale brine increased the corrosion rate under all mentioned deposits. Severe localized corrosion was observed only on coupons inserted under field-collected sludge deposit and under sand with sulphur contents.

Keywords: Under-deposit corrosion, sour environments, filed-collected sludge deposit, coupled multi-electrode array system, and linear polarization resistance.

Improving Oil and Gas Production infrastructure and equipment durability with active thermal sprayed coatings

Fred van Rodijnen, Oerlikon Metco, Kelsterbach, Germany;

Fred van Rodijnen

Ferrum corrumpitur, Corrosion is a natural process capable of degrading man made structural steel components, like used in oil and gas production systems, in the shortest possible time. In order to preserve these structures, the thermal spray technology contributes to extend the service life.

Zinc, Aluminium and their alloys used as a sacrificial coating preserving oil and gas production systems against corrosion

Thermal spray coatings have been used for corrosion protection since their invention in the early 20th century. The paper addresses the needs and a solution package for the oil and gas production industry, to combat their biggest enemy — corrosion. A metallic coating of Zinc, Zinc/Aluminum or Aluminum provides long-lasting active corrosion protection with little or no maintenance or repair for its 20 to 50 years of protective life.



Pictures Courtesy from Ogramac Brazil

Failure of corrosion barriers in integrity management of subsea production systems; - a statistical overview

*Brit Graver
Felix Saint-Victor
Kari Lønvik
Bente Leinum
DNV GL
Høvik/Norway*

For subsea production systems (well, pipelines and subsea equipment) a robust process and corrosion control management system is important for maintaining their integrity (INTEGRITY CONTROL). Loss of integrity which can lead in loss of containment can be due to material degradation such as corrosion, erosion and ageing caused by inadequate control of the produced medium in terms of e.g. fluid composition, temperature etc. Integrity control is a vital part of an integrity management system. Material degradation (e.g. corrosion) is one of the threats that may result in loss of containment. Typically, an integrity management system consists of a continuous integrity improvement process with supporting management processes, - often explained as a plan, do, check, act -process.

Barriers can be any kind of measure put in place to prevent a leakage (preventive barriers) and any measure that breaks the chain of events to prevent or minimize consequence escalation should the leakage take place (reactive barriers). The barriers can be physical/technical and/or non-physical (human/operational/organisational). Barriers can be illustrated in a bow-tie diagram. DNV GL has defined four barrier groups to represent four lines of defence against reaching a material degradation, where each of these barrier groups have been further broken down to more detailed barrier elements/systems.

DNV GL has performed a mapping of failures related to material degradation in order to show which of the four barriers that has failed. This work will include in-house experience from well, pipelines and subsea equipment. The industrial examples will be mapped towards defined barriers in the bow tie diagram in order to identify which barrier that has been violated. The results will highlight where the oil and gas operators should pay more attention, especially related to interface management between different parts of the operational organization. These studies also show what type of material degradation relevant to which type of equipment that has been identified.

Key words: Corrosion, material degradation, bow tie, preventive barriers

Protective Effect of Molybdenum Added to Nickel Based Alloy in $\text{H}_2\text{S}\text{-Cl}^-$ Environment

Akiko Tomio^a, Masayuki Sagara^a, Takashi Doi^a, Hisashi Amaya^b, Nobuo Otsuka^a and Takeo Kudo

Nippon Steel & Sumitomo Metal Corporation, Technical Research & Development Bureau, 1-8 Fuso-Cho, Amagasaki, Hyogo, 660-0891 Japan^a

Nippon Steel & Sumitomo Metal Corporation, Wakayama Works, 1850 Minato, Wakayama City, Wakayama, 640-8555 Japan^b

Introduction

Ni based alloys containing Mo have been used for $\text{H}_2\text{S}\text{-Cl}^-$ environment such as oil and gas wells because of their high corrosion resistance. The authors have suggested that the alloying Mo resulted in the enhanced formation of protective chromium oxide film¹⁾, but the exact role of alloying Mo have unclarified. Therefore, the present work further investigated the role of alloying Mo in the $\text{H}_2\text{S}\text{-Cl}^-$ environment, using a model alloy which does not contain chromium.

Experimental Procedures

For the fundamental investigation of the effect of alloying Mo on the corrosion resistance, the alloy which consisted of 60%Ni-0%Cr-16%Mo-Fe (Alloy A, mass %) was used. The electrochemical test was carried out in a glass cell at 70 °C. The test solutions consisted of 25 mass % NaCl with 0.5 mass % CH_3COOH and the gas phase was 0.1MPa N_2 or 0.1 MPa H_2S . Anodic polarization curves were obtained potentiodynamically from corrosion potential at a sweep rate of 20 mV min^{-1} with a potentiostat. Saturated Calomel Electrode (SCE) was used for a reference electrode and platinum electrode was used for a counter electrode.

Results

Figure 1 shows the anodic polarization curves of Alloy A obtained in the $\text{N}_2\text{-Cl}^-$ environment and the $\text{H}_2\text{S}\text{-Cl}^-$ environment. Alloy A did not passivate in the $\text{N}_2\text{-Cl}^-$ environment. The 60Ni-0Cr-16Mo alloy was suffered general corrosion in this environment. In contrast, the Alloy A passivated in the $\text{H}_2\text{S}\text{-Cl}^-$ environment from -0.45 V vs. SCE to -0.2 V vs. SCE and remarkable increase of the current density at around -0.05 V vs. SCE was noticed. The increase would correspond to occurrence of pitting because pitting was found on the specimen polarized until -0.05 V vs. SCE in the $\text{H}_2\text{S}\text{-Cl}^-$ environment. Therefore, these results suggest that the alloying Mo would be able to act like a protective film in the presence of dissolved H_2S .

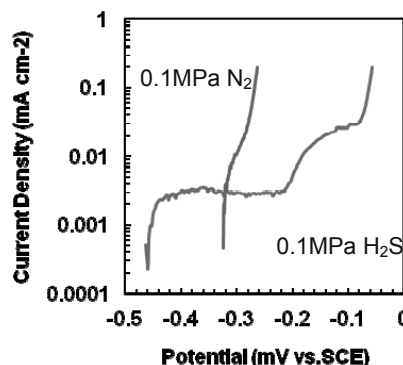


Figure 1 Anodic polarization curves of Alloy A.

(25 mass% NaCl + 0.5 mass % CH_3COOH , 70 °C)

Reference

1) A. Tomio, M. Sagara, T. Doi, H. Amaya, N. Otsuka and T. Kudo, EuroCorr2013, 1507 (2012)

Wireline failures in oil & gas wells – case studies

Daryoush Masouri, Pars Oil and Gas Company, Tehran/Iran

Mehdi Askari, Pars Oil and Gas Company, Tehran/Iran

Sahar Afroukhteh, Pars Oil and Gas Company, Tehran/Iran

Abstract

A wireline operation is a technique for deployment of various electrical or mechanical downhole tools (logging tools, plugs, packers, perforating guns, shifting tools, pulling tools etc.) on electrical cables, braided cables or slick line. The operations are performed in pressurized wells or in dead wells.

The development of the surface equipment for solid wireline operations has been thoroughly associated with new methods and tools for use in well completions, remedial measures and workovers. In connection with oil and gas well drilling, wirelines have been in use since the early days of the industry.

The main purpose of this paper is to report some studies regarding to common failures taken place for oil and gas wells wirelines. The probable causes and relevant mechanisms in different working conditions have been fully discussed by figures and site records and as conclusion the safe working procedures have been finally proposed.

Corrosion Mitigation and Inspection Strategy for Protection of Assets in Oil and Gas Production Facilities: An Experience of Nafoora Oilfield

Dr. Iftikhar Ahmad
Arabian Gulf Oil Company (AGOCO)
Benghazi (Libya)
Email: ahmadift@yahoo.com

The nature of petroleum industry recognizes the potential human, environmental and financial consequences that can result from failing to maintain the integrity of wellheads, vessels, tanks, pipelines and other assets. The importance of effective asset integrity management increases as the industry infrastructure continues to age. The primary objective of assets integrity management (AIM) is to maintain assets in a fit-for-service condition while extending their remaining life in the most reliable, safe and cost effective manner. A successful assets integrity management program incorporates aspects of design, material selection, operations, maintenance, corrosion mitigation, monitoring and inspection, risk evaluation and communication concepts to maximize the return from assets. These concepts are interlinked. Corrosion mitigation management of assets in oilfield is discussed in this paper.

Nafoora oilfield is one of the biggest oilfields in North Africa. It produced oil from five reservoirs and it has large network of oil and gas production facilities. This paper presents the experience of management of oil and gas production facilities through corrosion mitigation, corrosion monitoring and inspection strategies in Nafoora oilfield. The assets of the oilfield can be divided into five following categories namely: (i) Well bore and wellheads; (ii) Vessels such as separators, desalters, and gas processing facilities; (iii) Pipelines including all flow lines, trunk lines and shipping lines; (iv) tanks; (v) Other assets such as turbines and compressors, etc. External corrosion on pipelines, well bores, buried assets and bottoms of tanks is controlled with a combination of coatings and cathodic protection while external corrosion on surface equipment, wellheads and storage tanks is controlled by coatings. Internal corrosion is controlled with a combination of chemical inhibitors, periodic cleaning and process control. The monitoring and inspection techniques provide a way to measure the effectiveness of corrosion control systems and provide an early warning when changing conditions may be causing a corrosion problem. This paper describes corrosion management system used in Nafoora oilfield for its oil and gas production facilities based on standard practices of corrosion mitigation and inspection.

The influence of temperature on corrosion behavior of chromium steels in CO₂-containing environments

I. Yu. Pyshmintsev*, I. V. Kostitsyna*, V. P. Parshukov*, A. G. Tyurin**

*The Russian Research Institute for the Tube&Pipe industries, Novorossiyskaya str. 30, 454139 Chelyabinsk, Russia

**Chelyabinsk State University, Br. Kashirnyh str. 129, 454001 Chelyabinsk, Russia

The problem of CO₂-corrosion has become an increasing importance because of development of deep wells with high temperatures, pressures and CO₂ content. For such cases the use of usual carbon steels as the material of tubing is limited by high corrosivity of produced fluid.

The present work was carried out to study corrosion behavior of steels with different chromium content (1, 5 and 13%) in flow loop autoclave at high temperatures (100, 150, 200 °C). It has been shown, that corrosion rate of steels with 1 and 5% Cr decreases with increasing temperature and the highest rate of corrosion for these steel is observed at the test temperature of 100 °C. Corrosion rate for steel with 13% Cr practically is not dependent on test temperature.

According the data of X-ray diffraction analysis various films of corrosion products formed on the surface of steels at different temperatures. At the same time there has been increasing their protective properties with increasing temperature. At 100 °C on the steel surface film formed mainly friable iron carbonate (FeCO₃), not having protective properties, at higher temperatures phase Fe₃O₄ and/or Fe₂O₃ generated. Magnetite (Fe₂O₃) with its cubic lattice of spinel type, has good size and structure compliance to the surface and form thin film with high adhesion to the steel surface. This layer has a low permeability and exhibits protective properties.

The results for corrosion rate are confirmed by calculated thermodynamic diagram E-pH Fe - CO₂ - H₂O for 100, 150, and 200 °C, P (CO₂) 3 MPa and activity of iron ions in solution $a_i = 10^{-6} - 1$ mol/l. It is noted that the formation area of FeCO₃ decreases with increasing temperature, and apparently at temperatures above 100 °C under these conditions a dense oxide film mainly composed of oxides of iron is formed on the surface, which prevents the further dissolution of the metal.

Key words: CO₂-corrosion, chromium steels, E-pH diagram, corrosion films

Hydrogen induced cracking of austenitic-ferritic stainless steels SAF 2205 and SAF 2507

Samara Cruz da Silva¹, José Antônio C. Ponciano Gomes¹,

¹Federal University of Rio de Janeiro - LabCorr, Rio de Janeiro/Brazil

Abstract

The duplex stainless steels are ternary Fe-Cr-Ni alloys and present austenitic-ferritic microstructure. The high content of chromium and molybdenum provide to these alloys a high resistance to localized corrosion, such as pitting, crevice and stress corrosion cracking in environments containing chloride. However under cathodic conditions or sulfide environments adverse hydrogen effects must be taken into account. The use of duplex stainless steels has increased in chemical and petrochemical industries. In this work a comparative study of hydrogen effects on SAF 2205 and SAF 2507 duplex stainless steels was carried on. Hydrogen permeation and slow strain rate testing (SSRT) were used. These tests were conducted using sodium thiosulphate solutions and synthetic sea water. The results showed that both the steels did not present hydrogen permeation currents in both solutions. In the slow strain rate testing under the same cathodic potentials conditions the steels showed a clear reduction of ductility. This effect was due to the hydrogen induced cracking mechanism.

Corrosion process of API 5L X52 in production water from oil well

Octavio Olivares-Xometl¹, Mónica Corrales-Luna², Natalya V. Likhanova³, J. Manuel Hallen², Irina V. Lijanova⁴

¹Facultad de Ingeniería Química, Benemérita Universidad Autónoma de Puebla, Av. San Claudio, Ciudad Universitaria. Col. San Manuel, Puebla, Pue. 72570, México,

²Instituto Politécnico Nacional, ESIQIE-DIM, Av. Instituto Politécnico Nacional S/N Col. Lindavista, México D.F. 07300, México

³Instituto Mexicano del Petróleo, Programa de Investigación y Posgrado, Eje Central Lázaro Cárdenas No. 152, Col. San Bartolo Atepehuacán, México D.F. 07730, México

⁴Instituto Politécnico Nacional, CIITEC, Cerrada Cecati S/N, Colonia Santa Catarina, Azcapotzalco, México D.F. 02250, México

Abstract

Nowadays, the Oil Industry is facing new challenges due to the fact that most oil wells are at an advanced exploitation stage, where oil is being extracted along with water, which contains high concentrations of organic and inorganic pollutants. These compounds, when in contact with other aggressive media, promote the corrosion of the metallic parts of the transport pipelines. This situation has triggered the necessity of eliciting the corrosion mechanism of the API 5L X52 steel that is contact with natural production water coming from the oil well so that the Oil Industry can act accordingly. The corrosion process was studied by using different electrochemical techniques: polarization resistance (R_p), Tafel slopes and electrochemical impedance spectroscopy. The evaluations were carried out with exposure times of 90, 180 and 270 days at 25 °C and 45 °C with and without oxygen. The metal surface exposed to the corrosive media was analyzed by using scanning electron microscopy and X-ray photoelectron spectroscopy. The corrosion products were removed from the metal surface and aqueous medium in order to be analyzed by the Mössbauer technique, X-ray diffraction and ultraviolet-visible spectroscopy (UV-vis). The results show that there is more damage of the metal surface of the samples exposed to the oxygen-free medium; in addition, it was found that the corrosion process is a function of time. The corresponding results confirmed the formation of deposits on the metal surface in the form of salts such as sodium chloride, calcium and iron, where the iron and oxygen quantities in the steel sample without oxygen are lower than those obtained for the oxygen-exposed sample. The corresponding results confirmed the formation of lepidocrocite, which supports the information obtained from previous characterization techniques.

Assessment of Localized Corrosion Resistance of 13Cr, 15Cr and 17Cr Stainless Steels in high chloride and CO₂ environments

E. V. Senatore, J. A. C. Ponciano Gomes

Federal University of Rio de Janeiro-LabCorr, Rio de Janeiro/Brazil

Abstract

The supermartensitic stainless steels are Fe-Cr-Ni-Mo alloys with low carbon content, besides addition of Ni (4 to 6%) and Mo (to 2,5%), presenting better mechanical properties, corrosion resistance and weldability than the conventional martensitic stainless steels. Their main applications are in oil and gas industry as a practical and economical alternative to be selected as structural materials. Therefore, this study aims to make a comparative analysis of the behavior of supermartensitic stainless steels of different Cr contents such as 13Cr, 15Cr and 17Cr in environments with high chloride (150000ppm) and CO₂, at temperatures within 25°C and 85°C. Anodic polarization and electrochemical impedance spectroscopy (EIS) and a modified method to determine the critical pitting temperature (CPT) were used. The results showed that, at 25°C, all the studied steels presented a stable passive range, characteristic of forming a protective film on the material surface. The 17Cr steel presented the highest passivation range at 25°C. With increasing temperature, only the 17Cr steel presented a stable passivation range. The 13Cr and 15Cr steels showed higher anodic currents at lower anodic potentials, suggesting an active to passive transition, and higher current densities within their passive range when compared with the same values obtained with the 17Cr stainless steels.

Corrosion resistance of rolled and rerolled supermartensitic steel in media containing chlorides and hydrogen sulfide

Renata Braga Soares, Daniela Cristina de Sousa Garcia, Marília Mendonça Lima, Maria das Mercês Reis de Castro, Vanessa de Freitas Cunha Lins, Federal University of Minas Gerais, Belo Horizonte/Brazil;

Abstract

The supermartensitic stainless steels have been widely used in the oil and gas industry due to their good mechanical properties, good weldability and corrosion resistance acceptable in environments containing chlorides, CO₂ and H₂S. Thus supermartensitic steels have increasingly replaced the duplex stainless steel that has a high cost of production in many onshore and offshore applications. In the oil and gas industry, supermatensitic steels have been used primarily in the manufacture of seamless steel pipe for use in drilling oil and gas.

Compared to conventional martensitic stainless steels, the supermartensitic steel contains up to 3% (w/w) higher in molybdenum (Mo) content and up to 6% (w/w) over nickel (Ni) content. Molybdenum is added to improve corrosion resistance of steel, while Ni is added to stabilize austenite (γ) at elevated temperatures while avoiding the formation of δ -ferrite. Levels of carbon (C) reduced to 0.01% (w/w) contribute to improve the weldability.

The objective of the present work is to evaluate the corrosion resistance of rolled and rerolled supermartensitic steels in electrolytes of aqueous solution of NaCl 35 g/L, and aqueous solution of NaCl 120 g/L, sodium acetate 0.4 g/L, with pH 4.5 adjusted with acetic acid, saturated and unsaturated with H₂S, simulating the service conditions of petroleum industry in the pre-salt operation. For this evaluation, the electrochemical tests used are measurement of the open circuit potential, electrochemical impedance spectroscopy, potentiodynamic polarization test, and cyclic polarization test. The characterization techniques used are optical microscopy, scanning electron microscopy (SEM) and energy dispersive spectroscopy (EDS). In media of standard solution saturated with H₂S, the rerolled steel showed a higher corrosion resistance than the rolled steel, showing the highest corrosion potential and pitting potential. In this medium, the repassivation of steels was not observed. Already in the standard solution, the rolled steel showed a higher corrosion potential and a higher pitting potential than the rerolled steel. However, in this solution, only the rerolled steel presented a repassivation process with a potential protection of - 393mV (Ag / AgCl). In NaCl solution, the highest pitting potential was observed for the rerolled steel, which showed the highest value of polarization resistance, according to the electrochemical impedance spectroscopy results. In NaCl solution saturated with H₂S, the rolled steel showed the highest pitting potential.

In aqueous solution of NaCl, the rolled and rerolled steels showed pitting diameter of 140 μ m and 100 μ m, respectively.

IMPROVEMENT OF 9% NICKEL STEEL FOR CO₂ REINJECTION IN FSPOS AND ITS CORROSION RESISTANCE IN BRAZILIAN PRÉ-SALT CONDITIONS - SSC AND HIC

KALUME, R / Vallourec Tubos do Brasil / Belo Horizonte / Brazil; LIMA, L. I. L / Vallourec Tubos do Brasil / Rio de Janeiro / Brazil; Ferreira, M.C / Vallourec Tubos do Brasil / Belo Horizonte / Brazil; Palmieri B. ,I. / Petrobras S.A. / Rio de Janeiro / Brazil; G. Silva, V. / Petrobras S.A. / Rio de Janeiro / Brazil; D'Ávila, C. R. / Petrobras S.A. / Rio de Janeiro / Brazil; C. Velasco, J. A. / Instituto Nacional de Tecnologia / Rio de Janeiro / Brazil; V. Landim, R./ Instituto Nacional de Tecnologia / Rio de Janeiro / Brazil; C. de Souza, S. M. / Instituto Nacional de Tecnologia / Rio de Janeiro / Brazil.

In CO₂ reinjection plant of FPSO the selected steel need to have high toughness in lower temperature due to Joule Thomson effect in a suddenly. To answer the ductile-fragile transition problem, Vallourec improved ASTM A333 Grade 8 Steel according to additional requirements of operating conditions in the FPSOS. The result was a modified 9% Nickel steel, which provided better toughness at cryogenic temperatures.

As the process of CO₂ reinjection could contain low H₂S concentration, which would dissolve in the condensed water, and causes Sulphide Stress Corrosion Cracking (SSC). Thus, SSC and Hydrogen Induced Cracking (HIC) tests were carried out to understanding this corrosion phenomenon and evaluated the integrity of this material in CO₂ reinjection that will be used in the Brazilian Pre-Salt Area.

Influence of molybdenum on UNS S32304 and UNS S31803 duplex stainless steels corrosion resistance

Adolfo Kalergis N. Viana¹, Tarcisio R. Oliveira¹, Oscar R. Mattos², Kioshy S. Assis²

¹ Aperam South America Research Center, Timóteo/Brazil

² Universidade Federal do Rio de Janeiro, Rio de Janeiro/Brazil

Abstract

After pre-salt layer discovery and oil & gas sector expansion in Brazil, the production of Duplex Stainless Steels (DSS) has been significantly driven. In Brazil the main application of DSS are flexible pipes. In this way, the mechanical and corrosion resistance properties are very important to avoid any failure risk. The molybdenum (Mo) as Chromium (Cr) and Nitrogen (N) has an already known beneficial effect in corrosion resistance.

Samples used were the Aperam UNS S32304 (Mo=0.3 wt%) and an experimental Aperam UNS S31803 (Mo=3.0 wt%) with less nitrogen (N) than normal. This N adjustment in S31803 was designed to equalize as much as possible the chemical composition in order to highlight the Mo effect. Two conditions were carried out: Condition 1 (C1) the samples were hot rolled in the lab from 16 to 8 mm-thick in 5 passes at 1000°C, heat treated (HT) at 1000°C for 30 minutes and water quenched; Condition 2 (C2) the samples after the C1 were HT at 700°C for 60 minutes and water quenched. Thermocalc simulation software was used to define the HT temperatures and also to calculate the PREN by phase.

After the C1, the phase balance of δ/γ measured was 54.8/45.2 to S31803 and 57.5/42.5 to S32304. After the C2, the phase balance of δ/γ /nitride has been 56.2/42.9/0.9 to S31803 and 58.8/40.6/0.6 to S32304. After C2 σ was not identified.

Two techniques were used, the DL-EPR with 2M HCl solution, 0.56 mV/s scanning rate to evaluate passive layer stability and the NACE 0177 standard with solution "a" (NaCl 5%+Acetic Acid 0.5%, saturated with H₂S) loaded with 72% of yield strength for 30 days to evaluate the sulphide stress cracking resistance (SSC).

The results in samples after C1 have shown more pronounced reactivation in S32304 with Qr/Qa 0.74 compared with Qr/Qa 0.16 to S31803. This was already expected due to the beneficial role of the Mo. The DL-EPR has shown γ preferentially attacked in both grades agreeing with PREN by phase simulation. There were no failure in the NACE 0177 but nevertheless the test has evidenced the superior corrosion resistance of S31803 without any surface attack after the test while S32304 was visibly corroded. A SEM/EDS analysis has shown in S32304 δ phase preferential corrosion. The DL-EPR technique cannot be used in C2 samples due to no passivation of both DSS, evidencing how nitrides precipitations impact the passive layer formation and consequently the corrosion resistance. The NACE 0177 in C2 samples of S31803 have failed and in S32304 samples have presented a similar preferential δ phase attack without failures as in C1 samples. The Mo has improved the corrosion resistance in C1 samples but in C2 samples due to nitride precipitation the S31803, with more Mo, failed.

Effect of AC frequency on stress corrosion cracking behavior of X80 pipeline steel in carbonate/bicarbonate solution

Cuiwei Du, University of Science and Technology Beijing, Beijing

Min Zhu, University of Science and Technology Beijing, Beijing

Xiaogang Li, University of Science and Technology Beijing, Beijing

Zhiyong Liu, University of Science and Technology Beijing, Beijing

With rapid development of electricity, petroleum and transportation industry, more and more pipelines are buried in parallel with electric power lines or electrified railways due to the limitation of available space to construct these facilities. On such pipelines, AC current would transfer between soil and pipeline at the coating defects, leading to AC corrosion. It is reported that, AC could induce pitting corrosion on pipeline steel. It is well known that SCC cracks can be easily initiated at the pitting (or localized corrosion). Thus, AC corrosion may induce and facilitate the occurrence of SCC failures of pipeline steels, which constitutes a vital threat to safe operation of buried oil/gas pipelines. However, there has been no report on the related research at present. Consequently, it is necessary to investigate the effect of AC on the SCC behavior and mechanism of pipeline steels in concentrated carbonate/bicarbonate solution. X80 pipeline steel is a low carbon, micro-alloyed high-grade steel and has been a fairly new steel used worldwide as a pipeline material. It has a huge potential to be used widely for building the oil/gas transmission pipelines in the 21st century, because of its high strength and high toughness

Herein, in this paper, the effect of AC frequency on stress corrosion cracking behavior of X80 steel was investigated in concentrated carbonate/bicarbonate solution by electrochemical measurements, immersion tests and slow strain rate tensile tests. The results show that the decreasing AC frequency negatively shifts the corrosion potential and increases the corrosion rate of steel, as well as corrosion pits occur more readily. At low AC frequency, there is a significant negative shift of corrosion potential, and an obvious damage to the passive film, as well as the increased corrosion rates. In contrast, high frequency AC results in a small negative shift of corrosion potential and a slower increase in the corrosion rates. Under the short term effect of AC interference, the fracture mode is intergranular, and the mechanism can be attributed to anodic dissolution, which is the same as steel without AC application. The SCC susceptibility of the steel increases with decreasing AC frequency. The steel has high susceptibility to SCC at a low AC frequency of 30Hz, whereas AC current with high frequency shows little effect on the SCC susceptibility.

Influence of heat treatment on the stress corrosion cracking resistance of Inconel 718

L.C.M. Valle, Petrobras, Rio de Janeiro/Brazil

A.I.C. Santana, UEZO, Rio de Janeiro/Brazil

L.H. de Almeida, UFRJ, Rio de Janeiro/Brazil

O.R. Mattos, UFRJ, Rio de Janeiro/Brazil

Abstract

Inconel 718 superalloy is widely used in oil and gas applications, where superior properties are required. The work evaluate the influence of the presence of the γ' , γ'' and δ phases on the stress corrosion cracking of alloy 718. To obtain different grain sizes and amounts of δ phase, this alloy was subjected to solution heat treatments at 1050°C for 5 minutes and 1 hour followed by water quenching. Subsequently, an 800°C isothermal aging heat treatment was performed for 24 hours followed by water quenching, based on API specification (UNS N07718). For the microstructural characterization, optical microscopy (OM), scanning electron microscopy (SEM) and transmission electron microscopy (MET) were used. For the stress corrosion cracking study, tests were performed in offshore environment based on NACE TM 0177. The results were interpreted according to the microstructure.

A study by in situ Raman spectroscopy of carbon steel corrosion in CO₂ and H₂S environment

O. Delpoux, J. Kittel, F. Grosjean, IFP Energies nouvelles, Rond-Point de l'échangeur de Solaize BP3, 69360 Solaize, France

S. Joiret, CNRS, UPR15, Laboratoire Interfaces et Systèmes Electrochimiques, F-75005 Paris, France

N. Desamais, C. Taravel-Condat, Technip, rue Jean Huré, 76580 Le Trait, France

Abstract

Corrosion products formed in oil and gas environments are very often composed of iron carbonate and / or iron sulfide. The perturbation of corrosion process by such scales highly depends on the chemical nature of the layer. In some cases the corrosion rate can be significantly reduced. A classical rule-of-thumb considers a dividing line between CO₂ and H₂S corrosion where the ratio of CO₂ and H₂S partial pressure is 500. However, a recent review of thermodynamic calculations showed that the error band for the calculation of this ratio threshold was extremely large [1], and that iron sulfide scale might slowly evolve with time from mackinawite to pyrrhotite [2], the latter forming preferentially at higher temperature and high P_{H₂S}. Raman spectroscopy is a technique which is more and more used to study the corrosion products thanks to its high sensitivity to the crystalline structure of iron species. Nevertheless, it is still hardly used to characterize the corrosion products with CO₂ or H₂S whereas it permits to identify iron carbonates and many types of iron sulfides such as pyrite, mackinawite or greigite [3,4]. Besides it can be easily used *in situ*, without removing the steel specimen from the test solution, so as to protect the system from oxygen contamination. In the present paper, *in situ* Raman spectroscopy was used to analyse corrosion scales formed on low alloy steel in both CO₂ and H₂S environments. As a first step, the *in situ* device was validated by analyzing corrosion products formed in a test solution containing only dissolved CO₂ or H₂S. Then, the competition of the corrosion process between CO₂ and H₂S was studied by carrying out experiments with different CO₂ / H₂S ratios. The results show that the nature and the beginning of the formation of iron sulfides and carbonates strongly depends on this ratio.

References

- [1] S.N. Smith, Discussion of the history and relevance of the CO₂/H₂S ratio, Corrosion/2011 paper no065, NACE International (2011)
- [2] S.N. Smith, B. Brown, W. Sun, Corrosion at higher H₂S concentrations and moderate temperatures, Corrosion/2011 paper no081, NACE International (2011)
- [3] J.A. Bourdoiseau, M. Jeannin, C. Rémazeilles, R. Sabot, and P. Refait, Journal of Raman Spectroscopy, **2011**, 42, 496-504
- [4] Bernard, S. Duval, S. Joiret, M. Keddami, F. Ropital, and H. Takenouti, Progress in Organic Coatings, **2002**, 45, 399-404

Inhibitory protection of the installations of the oil-refining enterprises from corrosion

V.M.Abbasov, L.I.Alieva, T.A.Ismailov

Yu.G.Mamedaliev Institute of Petrochemical Processes of National Academy of Sciences of

Azerbaijan, AZ 1025, Baku, Khojaly ave, 30

e-mail:leylufer-ipcp@rambler.ru

The results of the scientific researches that conducted in IPCP in the field of synthesis, developments of the technologies of production and application of chemical reagents of multifunctional actions are analyzing. In the creating of inhibitors the much attention was paid to the reagents and composite compositions with complex protective properties. Besides application of water- and oil-soluble composite compositions showing simultaneously bactericide and inhibitory actions from corrosion, salt- and paraffin-deposition, also demulsifying property that would increase the efficiency of extraction and field preparation of oil and gas, reduce the costs on well maintenance and the other technological equipment.

Corrosion monitoring of NPP equipment and pipelines by high-temperature on-line sensors

*Sof'in M.V., Nikolaev F.V., Kritsky V.G., Styazhkin P.S.
Concern «Rosatom», JSC «Leading institute «VNIPIET»
St.Petersburg, Russian Federation*

Presented is a new approach to the arrangement and technical solution for a continuous corrosion monitoring of the VVER NPP equipment and pipelines. Discussed are procedures to determine corrosion potential of alloys to be monitored relative to the standard hydrogen electrode. Noted is that monitoring of uniform corrosion based on the analysis of transient processes of the electrochemical system response to an external excitation is a sufficiently valuable procedure allowing to perform a substantiate diagnosis and prediction of NPP equipment structural material status and coolant corrosion activity. Presented is a corrosion monitoring system with a simultaneous use of polarization resistance sensors and electrochemical corrosion potential allowing to determine the mechanism of corrosion process and its dynamics.

Galvanizability and Corrosion Properties of Zn-Mg-Al Hot-dip Coating with Shot Blasting Pre-treatment

Tae Chul Kim, Sang Heon Kim, Su Young Kim, Min Suk Oh, Jong Sang Kim
Surface Technology Research Group, POSCO Technical Research Lab
Pohang, Korea

In recent, we have developed the hot-dip alloyed steel sheet having the coating composition of Zn-3.0wt%Mg-2.5wt%Al. It has a higher corrosion resistance than galvanized steel sheet due to having both the sacrificial ability of Zn and the passive property of Al. Especially, when we have produced the hot-dip coated Zn-Mg-Al sheets, we used the shot blasting pre-treatment as a role of removing scale before continuous pickling process on hot-rolled strip.

We have investigated the effects of the shot blasting wheel speed on galvanizability and corrosion properties of Zn-Mg-Al alloy coated steel sheet by using FE-SEM, GDS, EDS, XRD, Surface profiler and Salt Spray Test. The hot-rolled coils from endless rolling as substrate are continuously transferred to the shot blasting machines, so the mill scale is removed about 50% of the total amounts of scale. After that the strip is passing through two short chambers filled with HCl. The fresh surface of steel sheets is annealed in the reduction furnace and subsequently put into the bath with the melt consisting of Zn-3.0wt%Mg-2.5wt%Al. Finally, the strip is cooled down and post-coated with Chromate or Cr-free functional materials on Zn-Mg-Al alloy coated steel sheet.

There are several advantages of shot blasting pre-treatments. First of all, the impact of shot balls can induce a compressive stress on the strip surface. The compressive stress enhances reactivity between strip and molten metal in the pot. Therefore, the sheet has an excellent adhesion property and good surface appearances. Beside the shot blasting influences on the morphology of steel strip surface. There are covered with numerous dimple-like shaped structures which have a positive effect on the corrosion resistance because the steel sheets are having Zn-Mg-Al metals into dimples as a reservoir. After galvanizing process, the average surface roughness of the pre-treated sheet is higher than non-treated one. The rough structure plays an important role of pocket containing of the post-treated coating materials. Thus, we can manufacture Zn-Mg-Al coated steel sheets with having a superior corrosion resistance and these sheets would be promising materials for construction and buildings.

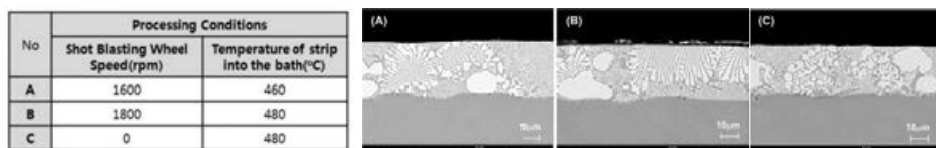


Fig 1. Microstructures of hot-dip galvanized Zn-Mg-Al steel sheets with varying conditions

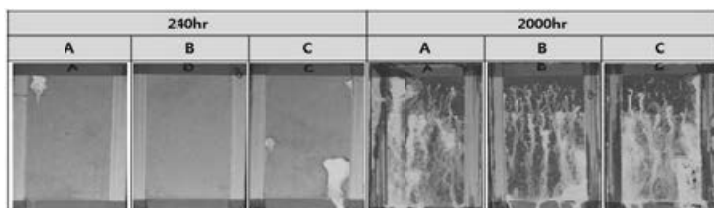


Fig 2. Salt Spray Test results of hot-dip galvanized Zn-Mg-Al sheets with varying conditions

Corrosion and microstructure study of new ZnAlMg galvanized steel by single dip technology.

Ana Alvarez Pampliega, METALogic N.V., Heverlee/Belgium

Erik Thomas, METALogic N.V., Heverlee/Belgium

Alexander Tomandl, HILTI Aktiengesellschaft, Schaan/Liechtenstein

Caroline Masquelier, Galvapower Group N.V., Hasselt/Belgium

Julien Balduyck, Galvapower Group N.V., Hasselt/Belgium

Thomas Pinger, Galvapower Group N.V., Hasselt/Belgium

Christine Buelens, METALogic N.V., Heverlee/Belgium

Abstract

The use of steel for offshore applications implies serious consideration on the way to improve corrosion performance when the expected product lifetime is 20 years or longer. This challenge comes to a higher level when considering the protection of joining elements i.e. bolts, screws or anchors, which are commonly hot dip galvanized in a centrifuge hot dip galvanizing process. This traditional technology leads to limited corrosion protection performance: firstly, the corrosion resistance per micron zinc layer is largely a given value and secondly, the thickness of the zinc layer must match in tight dimensional tolerances and is thus not arbitrarily expandable to increase the corrosion protection.

To solve this dilemma the use of innovative zinc alloys in the spinning HDG process is investigated. At present many galvanizing alloys are available in the market where Al and Mg are added to the zinc bath to improve corrosion resistance at lower thicknesses. Batch HDG with ZnAlMg as single dip technology requires the development of a specific pre-treatment to ensure the proper wetting of the steel surface by the zinc alloy, strongly depending on steel grade and Zn-alloy composition. Further challenges occur if batch HDG with ZnAlMg as single dip technology is combined with spinning operation. The major problem relates to the behaviour of the thin film grown during dipping, due to inhibited formation of ZnFe phases, which does not withstand spinning without being almost totally removed from some parts of the surface.

This work aims to study the effect of the microstructure on the corrosion behaviour of ZnAlMg alloys formed by single dip galvanizing in combination with spinning technology. In this work Mg additions up to 4% wt. were considered. Intercrystalline corrosion, corrosion resistance of the coatings and the electrochemical behaviour of the coating were evaluated in terms of standardized bending tests, neutral salt spray and cyclic corrosion testing and by local electrochemical techniques. As output of this study, a link is established between the parameters of the galvanizing process, microstructure and corrosion behaviour of the coating.

Corrosion behaviour of ZnAlMg coatings in tropical and coastal environments

*Alexander Tomandl, Eckhard Labrenz, Anna Erni,
Hilti AG, Schaan, Liechtenstein*

In this work various ZnAlMg alloy coatings have been exposed to coastal environments in Mexico, China and Sweden for a period up to three years. The exposition included plates in freely exposed 45° position as well as in a 5° sheltered position. Additionally to the flat plates samples with certain features like scratches and bended edges were tested. Measurements of the corrosion rate and metallographic investigations (LOM, SEM) have been conducted.

All coatings show selective and preferential attack of certain phases (mainly Al-rich phases) as well as the formation of a stable layer of corrosion products. The corrosion rates in the first year determined by weight loss after pickling are at least two times lower compared to zinc coatings. Depending on the environment and coating composition the factor can even be higher. The exposition in the sheltered position usually causes higher corrosion rates. Due to the predominant role of the corrosion products and the selective attack, weight loss measurements after one year may deliver misleading results for predicting the long term behaviour. Investigations after three years give a better picture of the corrosion mechanism.

The results are correlated with the atmospheric parameters of the test locations. With the chloride deposition rate being comparable at all three locations, the mean annual temperature is the main factor in determining the corrosion attack. For the corrosion of zinc we got corrosion rates in good accordance with the calculated ones using the dose response function given in the ISO 9224:2012. The results are also compared to a cyclic corrosion test (ISO 16701).

The investigation allows an assessment of the practical corrosion protection of steel products by ZnAlMg coatings in a wide range of coastal environments. It takes the impact of typical manufacturing processes like forming or cutting into account.

The effect of Mg composition on corrosion protection of steel using PVD Zn-Mg coatings

J. Davies and G. Williams

*Sustainable Product Engineering Centre for Innovative Functional Industrial Coatings (SPECIFIC), College of Engineering, Swansea University,
Baglan Bay Innovation Centre, Central Avenue, Baglan Energy Park, Baglan, Port Talbot, SA12 7AX. United Kingdom*

There is significant current interest in using so-called “clean” coating technologies to replace traditional methods of depositing sacrificial metallic coatings on to industrial steel panels. Of the various technologies available, physical vapour deposition (PVD) is considered to be one of the most promising and economically viable methods of depositing thin coatings on an industrial scale. In this work corrosion protection of strip steel by a duplex PVD coating system, comprising an outer 1.5 μm Zn-Mg alloy layer and an inner pure Zn layer (ca. 0.25 μm) to provide improved adhesion to the steel surface, is characterised by a combination of conventional and advanced scanning electrochemical techniques. A cross section of a typical Zn-Mg PVD coating on steel, showing the Zn adhesion layer at the interface is given in Figure 1. The influence of Mg PVD layer content on corrosion behaviour upon immersion in aerated 1% w/v will be presented. Corrosion of Zn-Mg PVD coatings is characterised by a significant darkening of the surface and the onset of this phenomenon is shown to be a function of the Mg content. Time-dependent free corrosion potential (E_{corr}) measurements show that Zn-Mg coatings of $\leq 15\%$ Mg adopt E_{corr} values similar to Zn within a few minutes of immersion, but that higher Mg compositions sustain more negative E_{corr} values for significantly longer periods (see Figure 2). In-situ current density mapping using a scanning vibrating electrode technique (SVET) is employed to correlate localised corrosion behaviour with the phenomenon of surface darkening. It is demonstrated that all compositions of Zn-Mg coatings undergo significant localised corrosion, involving highly focal anodic regions coupling with lower intensity distributed cathodes. However, areas of the Zn-Mg surfaces which undergo darkening cannot be readily reconciled with localised activity, and from this it is concluded that the phenomenon is caused by general corrosion occurring over a length scale which cannot be resolved by SVET.

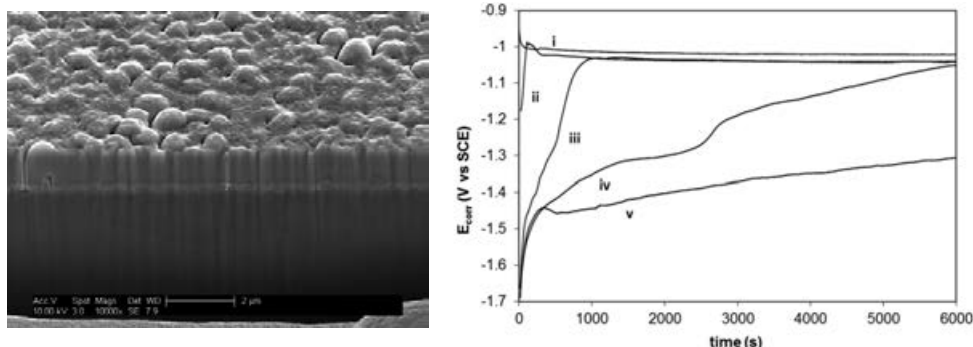


Figure 1: SEM image of typical cross section of ZnMg PVD coated steel. Figure 2. Free corrosion potential versus time profiles for PVD Zn-Mg coated steel specimens of various compositions immersed 1% w/v NaCl. Mg composition key: i. 0, ii. 10, iii. 12, iv. 15 and v. 20% w/w.

Influence of organic sealants on the corrosion protection of thermally sprayed ZnAl 15 coating

A. Mertke, R. Feser, University of Applied Sciences South Westphalia, Iserlohn, Germany

Abstract

Off-shore wind parks are increasingly planned as renewable energy sources. The corrosion conditions are very harsh in this marine environment. Thermal sprayed zinc and zinc-aluminum coatings have been proven to protect steel constructions under these conditions. To increase the corrosion resistance thick organic paint systems are applied over the thermally sprayed layer, sealers are used on top of the Zn or ZnAl 15 layer. Especially in the case where no further application of organic coatings to the thermal sprayed layers is possible, e.g. at bolted connections, the influence of sealers to corrosion resistance should be investigated. To improve the corrosion protection of thermally sprayed ZnAl 15 coating, without formation of a thick organic film, four organic sealants have been examined.

In the present work the corrosion behavior of thermally sprayed Zn, ZnAl 15 and ZnAl 15 coating plus sealer were investigated by accelerated corrosion test (salt spray chamber) and electrochemical measurements. Corrosion progress and changes in layer composition were examined by means of optical microscopy, scanning electron microscopy (SEM), energy dispersive X-ray microanalysis (EDX) and visual observations.

The investigations show, that by using organic sealants the corrosion resistance of thermally sprayed ZnAl 15 coatings is improved slightly. Only one sealant, which isolates the zinc-aluminum layer with a solid physical barrier from the aggressive environment, improved corrosion protection over a longer period of exposure has been found. ZnAl 15 coating and ZnAl 15 plus sealants demonstrate a much better corrosion resistance in comparison to Zn coating.

Zinc Flake Coatings vs. Zinc-Nickel Electroplating: New Trends and Developments

Holger Sahrhage, COVENTYA, Guetersloh/Germany; Michael Krumm, COVENTYA, Guetersloh/Germany; Alain Hill, COVENTYA, Paris/France

Zinc flake coatings are widely used to protect steel against corrosion. In some applications they compete against other technologies like electroplating of zinc or zinc alloys. Both technologies are based on the sacrificial properties of zinc against steel which leads to a cathodic corrosion protection.

With both - electroplated zinc-nickel and with zinc flake coatings - 720 or even more hours in the neutral salt spray test according to DIN EN ISO 9227 can be achieved without base metal corrosion. In the last years there is a big competition between both technologies especially for fasteners in the automotive industry. In view of the high nickel price the zinc flake coatings are generally cheaper. The topic hydrogen embrittlement caused by hydrogen evolution during the electroplating process is often given as a strong argument to favour the zinc flake coatings against zinc-nickel to protect high strength steel fasteners. Electroplated high strength steel parts still have to undergo a subsequent thermal treatment to release potential hydrogen from the steel although several studies in recent years have proved that no hydrogen embrittlement occurs for fasteners plated in modern alkaline zinc-nickel electrolytes for high-strength steel up to 1200 MPa.

On the other hand there are several reasons that favour the electroplating against zinc flake coatings. With modern alkaline zinc-nickel processes it is generally easier to achieve a homogenous coating thickness on complex shaped parts. The coating thickness in the thread of fasteners has to be within a narrow defined range. A minimum thickness is required to guarantee the corrosion resistance, but in the thread a too high thickness can affect the screwing properties. With conventional zinc flake coatings it is difficult to guarantee this dimensional accuracy since higher thicknesses are achieved in the valley of the thread. Latest developments have overcome this problem by modifying the rheology of the zinc flake system.

Finally there are environmental, health and safety considerations that influence the choice. This contribution shows the latest developments in both technologies, compares advantages and disadvantages and shows application examples.

XPS investigations of ZnCr coated steel after corrosion load

R. Steinberger¹, J. Duchoslav¹, M. Arndt¹, T. Steck²,
F. Lengwin³, J. Faderl² and D. Stifter¹

¹CDL-MS-MACH / ZONA, JKU Linz, Altenberger Straße 69, 4040 Linz, Austria

²voestalpine Stahl GmbH, 4031 Linz, Austria

³CEST GmbH, 2700 Wiener Neustadt, Austria

Besides conventional corrosion protection coatings based on hot-dip galvanized Zn layers, alternative concepts like hot-dip galvanizing with ZnMgAl [1] or electro-deposition of ZnCr layers [2] were recently developed and characterized for improved corrosion resistance at decreased layer thickness. In the scope of the current research ZnCr coated steel samples, treated by means of standardized salt spray tests, were therefore systematically investigated using X-ray photoelectron spectroscopy (XPS). The corrosion products, which were formed on the surface, as well as their depth distribution was studied in detail for varying parameters of the corrosion environment (*i.e.* variation of exposure time or NaCl content). Special attention was paid to the evolution of the Cr signal (revealing oxidic and metallic Cr contributions) and Zn peaks over depth: for depth profiling Ar⁺ ion etching was used in the XPS system. Since it is known that ion sputtering may cause serious damage to the investigated material (*e.g.* preferential sputtering, atomic mixing, ion implantation, chemical changes, etc.), and due to the lack of published data on the influence of sputtering on zinc based coatings, a range of high-purity reference materials of possible corrosion products were investigated at first during long time sputtering. Indeed, some of the studied compounds, like CrO₃ (Fig. 1), revealed a very unstable nature. However, not only ion etching influences the chemical properties: even standard XPS measurements performed on the surface affects the stability of corrosion products, which can form on coated steel surfaces. Especially Zn(OH)₂ was found to be rapidly converted to ZnO (Fig. 2), but also the stoichiometry of hydrozincite does not stay constant during usual acquisition times. Hence, dedicated reference samples were studied in order to illustrate and to identify the source of these degradation effects. All the new knowledge obtained from these investigations can now serve as basis for reliable data interpretation from corroded surfaces and depth profiles of real samples.

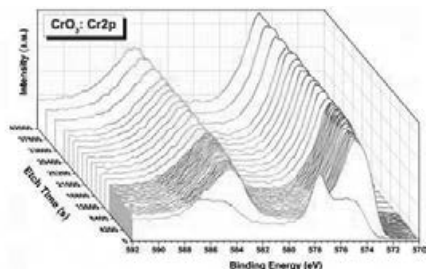


Fig. 1: long term ion sputtering of Cr(VI) oxide

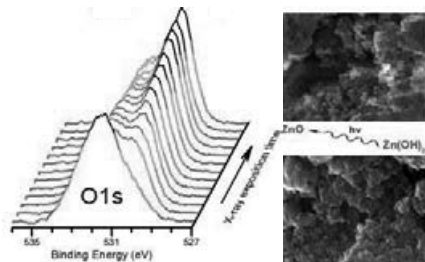


Fig. 2: Degradation of Zn(OH)₂ during X-ray exposure

[1] M. Arndt et al., Anal. Bioanal. Chem. 403, 651-661 (2012).

[2] H. Itani et al., Anal. Bioanal. Chem. 403, 663-673 (2012).

Electrocodeposition of Al-Zn alloy by using Double Counter Electrodes System

*Yusuke Sato and Kazuhisa Azumi
Hokkaido University, Sapporo Japan*

1. Introduction

For corrosion protective coating of steels, alloying of Zn with the other less-noble metal such as Al is required to improve the anticorrosion performance and to reduce the consumption of Zn resource. Electroplating has been examined to control the composition of alloy coatings by changing the deposition condition such as composition of plating bath and polarization potential. However, such simple strategy cannot achieve the desired composition because of kinetic limitation of electrodeposition reaction of Zn and Al in the given deposition condition. In this work, therefore, the Double Counter Electrodes system was developed to control more effectively the deposition rate of Al and Zn. In the system Zn and Al counter electrodes (CE) are switched alternately because the CE acts not only as a path for electricity but also as supply of metal ions to the bath. Because Zn electrodeposits preferentially from the bath containing Al(III) and Zn(II) ions, supplying Zn ions to the bath may determine the deposition rate of Zn in the codeposition of Al and Zn. Ionic liquid (IL) bath composed of AlCl_3 and 1-ethyl-3-methylimidazolium chloride (EMIC) was used as a bath because Al cannot be electrodeposited from aqueous solution.

2. Experimental

Electroplating bath was prepared by adding AlCl_3 slowly to IL (EMIC) at room temperature until a molar ratio reaching 2:1 and then Al plate (5N%) was immersed in the IL bath at ca. 90°C to remove residual water. Arrangement of electrochemical cell of the Double Counter Electrodes system is shown in Fig. 1. Galvanostatic pulse polarization was used ($i_{\text{on}} = -15 \text{ mA cm}^{-2}$, $t_{\text{on}} = t_{\text{off}} = 1 \text{ s}$, total charge $Q_{\text{C}} = 5 \text{ C cm}^{-2}$) for electrodeposition. Al and Zn CEs are switched alternately during electrodeposition with a ratio of pulse number, $N(\text{Al}):N(\text{Zn}) = 1:5$ or $5:1$. Surface morphology and elemental composition of electrodeposits were examined using SEM and EDX.

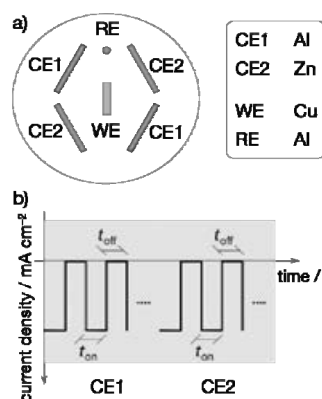


Fig. 1. (a) Arrangement of electrodes in the electrochemical cell, (b) current-pulse form used for electrocodeposition.

3. Result and discussion

SEM images of electrodeposits shown in Fig. 2 reveal that the particle of deposits was finer at lower ratio of $N(\text{Al}):N(\text{Zn})$. EDX results show that the Zn content was ca. 1 at% at $N(\text{Al}):N(\text{Zn})=5:1$ and ca. 2 at% at $N(\text{Al}):N(\text{Zn})=1:5$. These results confirm that the composition and structure of deposits were affected by the ratio of $N(\text{Al}):N(\text{Zn})$.

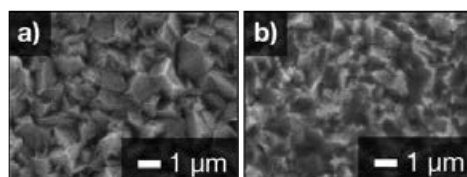


Fig. 2. SEM images of coatings electrodeposited with the ratio of $N(\text{Al}):N(\text{Zn})=1:5$ (a) and $5:1$ (b).

Development of Aluminum Magnesium Alloy Coating by New Mist Air and Nitrogen Cooled Thermal Spraying Gun

Yasuhiro Omori¹, Yusuke, Nishiura¹, Takashi Kumai¹ and Toshiharu Morimoto²

¹*Yoshikawa Kogyo, Surface Treatment Div, Okihama 2113-23 Aboshi-ku, Himeji, 671-1241, Japan*

²*Nakayama Amorphous, Technical Div, Funamachi 1-1-66 Taisho-ku, Osaka, 551-0022, Japan*

Abstract.

Using the cylindrical type thermal spraying gun with mist air and nitrogen, we have produced amorphous alloy films in ultra rapid cooling at the world first⁽¹⁻²⁾. However, as amorphous alloys such as zirconium, nickel are too expensive, they would not applied to huge constructions of our society for anti-corrosion. Thus, we are developing aluminum magnesium alloy coating by our original thermal spraying technique. Because aluminum magnesium alloys are thermally sprayed at ultra rapid cooling rate in reducing atmosphere, our aluminum magnesium coating films have no pores, no cracks, less oxide and higher standard electrode potential than conventional aluminum magnesium coating films. Further research showed our aluminum magnesium films have micro-structures and superior micro passivation layers, too. Then, in the continuous salt spraying test, they show less corrosion rate than conventional ones. We are going to adapt this aluminum magnesium coating to outer parts of windy generator in the offshore front. We hope this aluminum alloy spraying technique adapt to mechanical parts in automobile fields to reduce weight.

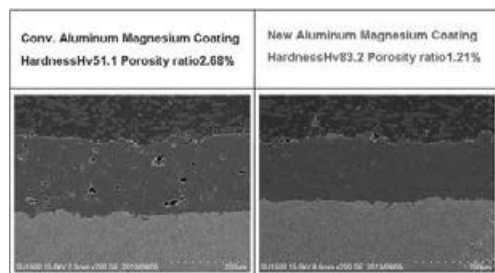


Fig.1 Al-5Mg spraycoating

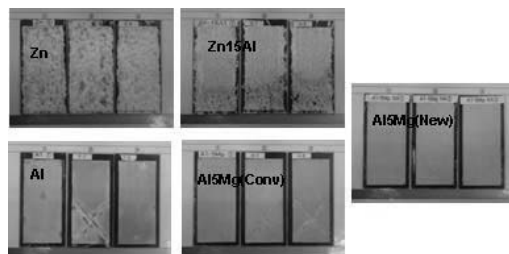


Fig.2 Appearance by 150cycles CCT

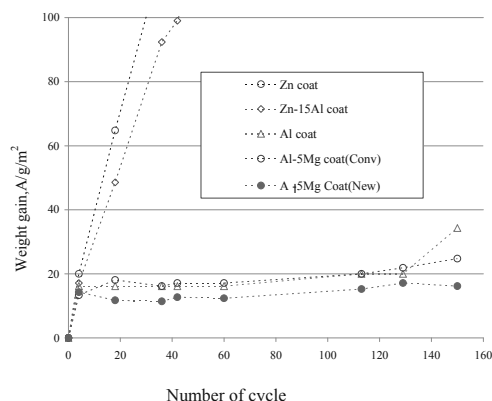


Fig.3 Weight gain by CCT

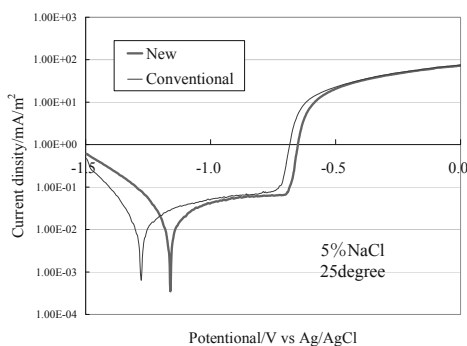


Fig.4 Polarization curve

1) R.Kurahashi, M.Komaki, N.Nagao, K.Hakomori, M. Kozaki, A.Yanagitani: Revue de Metallurgie 105 (2008) 575.

2) Kurahashi Ryuro, Takehara Junji, Yoshihisa Fukudome, Toshiharu Morimoto, Manabu Kiuchi: Revue de Metallurgie 110 (2013) 235.

Antibacterial and protective properties of Cr/Ag nanocomposite coatings obtained by electrochemical techniques

E. García-Lecina, B. García-Blanco, I. García-Urrutia, J.A. Díez, Surfaces Division, IK4-CIDETEC, San Sebastián/Spain; egarcia@cidetec.es

In the past few decades, cases involving bacteria that cannot be combated with antibiotics have become a growing problem in healthcare worldwide. Clothes and hands constitute the largest disease carriers. Studies show that multiresistant bacteria are often spread through surfaces (principally metallic and polymeric) that people frequently touch, such as door handles or light switches. For this reason, there is a great interest in the design and development of materials that provide biocidal activity.

Achieving these properties on a surface is possible by means of coatings and treatments where nanotechnology plays a key role. Most of these coatings acquire their capacity by incorporating specific nanoparticles. In this sense, it has been known that silver and its compounds have strong inhibitory and biocidal activity for bacteria, fungi, and virus. Thus, compared with other metals, silver exhibits higher toxicity to microorganisms while exhibiting lower toxicity to mammalian cells.

Taking into account Ag NPs properties, it would be expected that their codeposition in a metallic matrix (e.g. Ni or Cr) would lead to metallic surfaces with biocidal activity avoiding the growth of multiresistant bacteria that are often spread through surfaces that people frequently touch. However, few studies are described in the literature concerning the incorporation of Ag nanoparticles in metallic coatings.

To achieve this goal, in the present work, Cr/Ag nanocomposite coatings have been deposited on brass substrates by direct current electrodeposition process from suspensions of Ag nanoparticles ($\varnothing = 50$ nm) in commercial trivalent chromium electrolytes. The effect of Ag NPs concentration, agitation and surfactant addition on the codeposition of Ag was evaluated. Moreover, the antibacterial activity and protective properties (electrochemical corrosion tests and NSS accelerated tests) of these Cr/Ag nanocomposite coatings were evaluated and compared with that of pure metal.

Study of corrosion resistance of electroless duplex NiP/NiB coatings in different media by potentiodynamic polarisation and SEM observation.

*Author Véronique VITRY, François TOSAR, Fabienne DELAUNOIS,
Metallurgy Lab, University of Mons, Mons, Belgium*

Electroless nickel coatings are well known for their mechanical and tribological properties as well as their corrosion resistance. The 2 main kinds of electroless nickel coatings are reputed for different properties, Nickel-Phosphorous (ENP) is privileged when corrosion resistance is needed while Nickel-Boron (ENB) is more popular for mechanical and wear applications.

Duplex electroless nickel coatings (composed of 2 layers of electroless nickel) appear thus as a good compromise to get the best properties of both ENP and ENB.

Duplex electroless nickel coatings were synthesized on mild steel substrates: the ENP coating was synthesized with commercially products (Nicklad 767) and ENB was deposited with a lab-developed (with sodium borohydride as a reducing agent and lead tungstate as a stabilizer).

Several variations of the duplex coatings were studied: ENP/ENB; ENB/ENP, ENP/ENP and ENB/ENB and were compared to single coatings (ENP and ENB) of similar thickness.

In order to observe how deposits react in different corrosive media and evaluate the corrosion resistance in these environments, the corrosion resistance of the samples was investigated by potentiodynamic polarisation in 0.1 M sodium chloride, in 0.1 M sodium hydroxide and 0.1 M sulphuric acid with different pH values (6 and 1).

Friction and corrosion properties of electroless nickel nanocomposite coatings codeposited with MoS₂ or WS nanoparticles.

C. Zanella¹, M. Righetti¹, A. Gracco², F. Deflorian¹,

1. Department of Industrial Engineering, University of Trento, Trento (Italy)

2. NPSRR Department, University of Padova, Padova (Italy)

Abstract

Nanocomposite coatings have been a wide research field in the past decades, since the combination of different metal matrix and reinforcement particles can induce to novel surface properties as improved wear or corrosion resistance. Moreover electrochemical and electroless deposition are easy and industrially widely applied technique. Electroless nickel in particular is a supersaturated NiP alloy in the as deposited state that can reach 1000 HV in hardness when heat treated due to the precipitation of NiP₃.

In this work the effect of incorporation of solid lubricant nanoparticles on the electroless nickel coatings properties was studied. Lubricant particle were suspended in the electroless deposition bath and stabilized by 0.5 g/l of CTAB surfactant. The suspension was stirred overnight and treated by ultrasound for 1 hour before deposition in order to reduce particle agglomeration. By temperature increase the nickel alloy deposition was activated and the lubricant particles embedded in the metallic film. In order to considered the effect of matrix hardening, some samples have also been treated at 400 °C for 1 hour under nitrogen flux.

SEM observation and cross-sectional microstructure studies evidence how the presence of the solid particles induce a strong heterogeneity in the film thickness leading to a very rough surface. Particles result to be strongly agglomerated in the composite layer. Moreover EDX was applied to estimate the embedded quantity of lubricant particles.

Friction was tested by pin on disc test with a stainless steel counter body. If nickel shows usually a low friction coefficient and low wear if coupled to a hard surface, its behaviour is very poor when coupled to a soft material as stainless steel.

Solid lubricant particles could be very beneficial in this case.

Corrosion protection was verified by potentiodynamic polarization in chloride electrolyte.

Corrosion resistance of laser clad 304L stainless steel surfaces enriched with ruthenium additions exposed to sulphuric acid media

Josias van der Merwe, University of the Witwatersrand, /School of Chemical and Metallurgical Engineering/ DST/NRF Centre of Excellence in Strong Materials Johannesburg/ South Africa, Dominique Tharandt, / School of Chemical and Metallurgical Engineering/ Worley Parsons, Johannesburg/South Africa, and Poolo Masiu, University of the Witwatersrand/School of Chemical and Metallurgical Engineering/ Johannesburg/ South Africa

The corrosion behaviour of 304L stainless steel samples after these were laser surface clad with different compositions of ruthenium was evaluated by conducting a series of electrochemical tests including open circuit potential, and cyclic potentiodynamic polarisation. The laser clad samples were exposed to sulphuric acid solutions, with and without sodium chloride. The tests were conducted at 25°C and 45°C.

The 304L stainless steel samples were clad by using a 4.4 kW Rofin Sinar diode pumped Nd:YAG laser. A 304L stainless powder was used with five different ruthenium concentrations, namely: 1wt%, 2wt%, 3wt%, 4wt% and 5wt% ruthenium, and this yielded a clad coating of: 0.4wt%, 0.8wt%, 1.3wt%, 2.4wt% and 4.6wt%. This was determined with The metallurgical characteristics of the clad layer was evaluated by performing a cross sectional analysis with an optical microscope, micro Vickers hardness tester and a field emission scanning electron microscope equipped with an energy dispersive X-ray spectroscopy unit. The samples were sectioned and the clad layer was mounted in an epoxy resin for electrochemical tests. The microhardness of the samples did not show a significant dependence on the ruthenium concentration. The electrochemical characteristics of these mounted samples were analysed by performing a potentiodynamic test at a scan rate of 0.5 mV/s while the samples were freshly exposed to the environment and this was compared to a potentiodynamic scan after a 12 hour exposure. In addition the open circuit potential was monitored over a 12 hour exposure period.

It was found that after the immediate exposure of the samples the higher ruthenium concentration samples showed better results in terms of measured corrosion rates and passivation characteristics. The best results were achieved around 1.3wt% ruthenium. After the 12 hour exposure the corrosion potential increased and the passivation characteristics showed a significant improvement for the samples above 1wt% ruthenium. With the addition of sodium chloride a considerable improvement was only found on the 2.4wt% ruthenium sample. At the higher temperatures the improvement was not considerable. The open circuit potential values of the samples when exposed to only sulphuric acid were mostly above zero and showing an increasing trend as expected. However, with the chloride present the open circuit values were more active below zero, but an increasing trend was found.

Anticorrosion composite coatings obtained by of plasma electrolytic oxidation

S.V.Gnedenkov, S.L.Sinebryukhov Institute of Chemistry Far Eastern Branch of Russian Academy of Sciences, Vladivostok, Russia

Composite multifunction coatings having practically important properties (e.g., anticorrosive, antifriction, hydrophobic, superhydrophobic etc.) were obtained at the metals and alloys (titanium, aluminium, and magnesium as well as on steel) surfaces using unipolar or bipolar modes of the plasma electrolytic oxidation (PEO) in different aqueous electrolytes. The inclusion of nanosized polymer and inorganic compounds into the coatings compositions allows increasing their stability in corrosion-active media [ref. #1]. The developed approaches to the formation of composite polymer-containing PEO-pretreated coatings by using various low-molecular fractions of superdispersed polytetrafluoroethylene (SPTFE) have been summarized. A unique method for the formation of a composite polymer-containing coating at the surface of various metals and alloys has been suggested [ref. #2]. The anticorrosion properties of the composite coating significantly surpassed those of PEO coatings. After fivefold treatment by SPTFE the corrosion current is more than 4 orders of magnitude lower than those of the sample without coating and more than 280-fold lower than that of the base PEO-layer. Furthermore, the composite coating is characterized by practically important antifriction properties under dry sliding conditions caused by low friction coefficient (0.04) (as compared to the unmodified PEO-layer (0.2–0.4)). The formation methods of hydrophobic (HP) and superhydrophobic (SHP) nanocomposite coatings at the surface of titanium, magnesium alloys and steel pretreated using PEO were developed also [ref. #3]. For SHP coating, the values of the contact and rolling angles are $166^\circ \pm 3^\circ$ and $5^\circ \pm 3^\circ$, respectively. The impedance modulus ($|Z|_{f=0.005}$) value, which characterizes the anticorrosion properties, attains $2.5 \cdot 10^7 \Omega \text{ cm}^2$ for the SHP coating and $1.4 \cdot 10^6 \Omega \text{ cm}^2$ for the HP coating [ref. #1]. The developed composite layers are promising for various practical applications [ref. #4].

This work was supported by the Presidium of FEB RAS (Grant # 12-I-П8-07), and by the Russian Federation Government (Grant #02.G25.31.0035), Scientific Fund FEFU (#12-03-13001-07).

[1] Gnedenkov, A.S.; Sinebryukhov, S.L.; Mashtalyar, D.V.; Gnedenkov, S.V. *Surf. Coat. Technol.* **2013**, 225, 112–118.

[2] Gnedenkov, S.V., Sinebryukhov, S.L. *Composite Interfaces*. **2009**, 16, 4–6, 387–405.

[3] Boinovich, L.B., Gnedenkov, S.V., Alpysbaeva, D.A., Egorkin, V.S., Emelyanenko, A.M., Sinebryukhov S.L., Zaretskay A.K. *Corrosion Science*. **2012**, 55., 238–245.

[4] Gnedenkov, S.V., Egorkin, V.S., Sinebryukhov, S.L., Vyaliy, I.E., Pashinin, A.S., Emelyanenko, A.M., Boinovich, L.B. *Surf. Coat. Technol.* 2013,– **2013**, 232., 240–246.

Corrosion Protection Property of Corrosion Products of Zinc Galvanized Steels

Hideki KATAYAMA, Ryota MIYAHARA, Yoshinao HOSHI*,
Isao SHITANDA*, Masayuki ITAGAKI*
National Institute for Materials Science
1-2-1 Sengen, Tsukuba, Ibaraki, 305-0047 JAPAN
Tokyo University of Science*
2641 Yamazaki, Noda, Chiba, 278-8510 JAPAN*

Zinc galvanized steels have been widely used for many industrial fields such as automobiles, construction and appliances. The amount of zinc resource, however, might not be sufficient in the future since the zinc demand in China remarkably increases year by year. Therefore, it is important to conduct a research survey of alternative materials of zinc coatings for saving and effective utilization of zinc resource. Although some researchers have reported on the corrosion products, the corrosion behaviour and the corrosion mechanism, the corrosion protection property of corrosion products is still unclear. In this study, the corrosion protection property of corrosion products on zinc galvanized steels have been discussed as one of the guideline for development of alternative materials of zinc coatings.

A part of zinc coating was dissolved by immersion in HCl solution to prepare zinc galvanized steels with a macroscopic defect. A droplet of NaCl solution was added to the sample surface, and wet-dry cyclic corrosion test was carried out. After the corrosion test, the corrosion products were formed on the samples. Furthermore, the carbon steel samples covered with corrosion products were prepared by covering the sample surface with epoxy resin except for the macroscopic defect part. The corrosion protection property of the corrosion products was investigated with electrochemical methods.

The amount of corrosion products formed on the steel substrate obviously increased with the number of cycles. The obtained impedance characteristics were explained by the equivalent circuit which consists of the zinc corrosion products part and the interface part between steel substrate and the corrosion products. The 10mHz impedance of the steel substrate covered with corrosion products increased with an increase of wet-dry cycles, indicating that the zinc corrosion products inhibit the corrosion of the steel substrate. In addition, the polarization curves of the steel substrate covered with corrosion products showed that the anodic current density of the samples was much lower than that of the carbon steel. The anodic current density decreased with an increase of the number of cycles. This result indicates that the anodic reaction was greatly inhibited by the corrosion products.

Pd-In and Pd-Fe as new type of “Ni-free” top coatings for decorative applications

Stefano Caporali, Patrick Marcantelli, Ugo Bardi

Università di Firenze, Via della Lastruccia 3, 50019- Sesto Fiorentino(FI), Italy;

Nickel is the primary determinant of contact sensitization; therefore there is now a tendency to take nickel out of goods that are designed to be in contact with human skin [1]. However, its peculiar physical and chemical properties; i.e. very good corrosion resistance, white colour and lustrous shining, make its substitution a very challenging task, especially for jewellery goods and all the items requiring high aesthetical quality and durability.

Actually, the most diffused top finishing treatment for jewellery and fashion accessories is the electrodeposition (plating) of a thin layer of nickel alloyed with noble metals such as gold, rhodium and, mainly, palladium over a nickel intermediate layer. The presence of precious metals on top assures the required aesthetical characteristics and, more importantly the Ni-content available for leaching results reduced. However, these solutions do not solve the problem since nickel is still presents and eventually have to be substituted with properly Ni-free technologies.

The aim of this work is to characterize the corrosion resistance of really “Ni-free” coatings constituted by bronze intermediate layer and Pd-In and Pd-Fe top-coatings. The corrosion resistance of the systems were evaluated by means of electrochemical techniques, mainly electrochemical impedance spectroscopy and potentiodynamic polarization curves. The results evidenced good corrosion capability of these coatings respect the traditional Pd-Ni one.

Finally, comparative free corrosion tests were carried out in neutral saline environment and artificial sweat in order to evidence their capability to constitute an aesthetically valuable “Ni-free” technology suitable for jewellery and fashion applications.

[1] C. Liden, M. Bruze, T. Menné, Textbook of Contact Dermatitis, 2nd ed., eds. R.J.G. Rycroft, T. Menné, P.J. Frosch, J.P. Lepoittevin (Heidelberg, Germany: Springer-Verlag, 2001).

Thin film hot dip galvanizing – the innovative revival of a traditional process

*Dr. Thomas Pinger, Jürgen Tomaszewski, Fontaine Technologie GmbH,
Gelsenkirchen / Germany*

General hot dip galvanizing (HDG) is well known over more than 130 years as a robust and long lasting protection of iron and steel structures against corrosion. Even if the system is highly accepted in the market the shares of HDG are stagnating or decreasing. Against the background of increasing requirements in the market concerning the complexity of structures and materials, the performance and functionality during use as well as the recyclability at the end of the product life the need for high performing surface technology is obvious.

microZINQ® is an innovative, highly resource efficient corrosion protection technology combining the process-related advantages of hot dip galvanizing with the zinc alloy-related know-how of the continuous galvanizing process. This new technology offers great answers to the various demands of the market: high corrosion protection, high resistance against mechanical impact, thin zinc layers and thus weight reduction, applicable on high strength steels, very good behavior to downstream processing like forming, coating, adhesive bonding and welding.

In comparison to conventional galvanizing microZINQ®-layers are very thin with an average thickness of 10µm. Nevertheless a very high corrosion protection is provided by the use of a Zn5Al-alloy and the thereby increased passivity of the zinc surface. The results in relevant corrosion tests e.g. neutral salt spray test acc. ISO 9227 (1,200 hours) or climate alternating test VDA 621-415 (10 cycles) give proof of this behavior as well as convincing results in the field.

The microZINQ® technology benefits from the general advantages of the hot dip galvanizing process: firstly, the immersion of steel in the liquid molten zinc bath leads to a metallurgical bond between zinc and steel and thus to a characteristically high mechanical resistance. Secondly, the process of galvanizing after the production of the workpiece guarantees that the steel surfaces are completely covered by a closed zinc layer with no bare cutting edges or weld areas as they are unavoidable when using pre-galvanized steel sheets.

Further, the zinc layer offers a good surface for subsequent coating or adhesive bonding. Corrosion tests with powder coating and cathaphoretic painting show very good results: more than 2,000 hours in the salt spray test as well as in condensation water atmosphere acc. ISO 6270-2 CH for each system.

The microZINQ® technology won the Germany Resource Efficiency Award as well as the Materialica Award in 2013. It is successfully used since several years on underbody components in the automotive industry.

Influence of deposition techniques on properties of solar selective coatings on Cu and Al substrates

M. Shoeib¹ N. El-Mahallawy², and Y. Ali³.

¹Central Metallurgical Research & Development Institute, El tebbin, Helwan, Cairo, Egypt
mshoeib@yahoo.com

² Faculty of Engineering, Design and Production engineering Department, Ain Shams University, Abasia, Cairo, Egypt
n_mahalawy@yahoo.com

³ The German University in Cairo, New Cairo City - Al Tagamoa Al Khames, Cairo, Egypt
eng.yehia.ali@gmail.com

Corresponding author: Madiha A. Shoeib. Tel: +2 01006356373, Fax: +2 02 25011185

Abstract

The main part of solar thermal heaters is the absorber surface which must have a maximum absorption at short wave lengths in the UV range and minimum emission of solar radiation at long wave lengths in the IR range. This is achieved by application of selective coat on a conducting material.

In the present work, black nickel selective coating is applied on copper substrate using Ni electroplating technique and on aluminium substrate using Ni-P electroless plating. The Ni coating is then followed by blackening in a solution of nickel chloride and sodium chloride in a galvanic cell at 0.2 A/dm² for 7.5 minutes. Different deposition parameters are applied in both techniques in order to find the process parameters needed to give the maximum absorbstivity and the minimum emissivity, hence, maximum selectivity for the coating. The parameters for bright nickel electroplating include current density from 1 to 4 A/dm² and deposition time from 0.25 to 30 minutes and for electroless plating the deposition time was varied from 15 to 60 minutes. The effect of blackening on the coating characteristics was studied by varying the current density from 0.1 to 0.3A/dm² and time from 2 to 10 minutes. The optimum parameters resulted in a maximum absorption of 98% and very low emission less than 1% for both black nickel electroplated on copper and electroless plating on aluminum resulting in selectivity of 170 and 145 for copper and aluminium substrates respectively. These results are higher than those present in the literature. The surface topography was investigated using SEM and AFM.

Keywords: solar collectors, selective coat, emission, absorption, black nickel electroplating, electroless nickel plating.

Electrochemical Behaviour of Protective Coatings in Chloride Solutions

Guruprasad Sundararajan, and Raul B. Rebak
GE Global Research JWTC, Bangalore, 560066 India
GE Global Research, Schenectady, NY 12309, USA

This work explores the electrochemical and corrosion behaviour of several protective coatings that may be applied on alloy C450 (S45000) (Balance Fe, 14-16Cr, 5-7Ni, 0.5-1Mo, 1.25-1.75Cu, 2Mn) for corrosion, wear and/or antifouling service. Table 1 shows a list of the coatings investigated. Most of the tests were performed in aerated 5% NaCl solutions, pH 4 at 50°C. The electrochemical tests performed for different immersion times included monitoring of the corrosion potential, polarization resistance (ASTM G 59), electrochemical impedance spectroscopy (ASTM G 106) and galvanic corrosion current of coated and non-coated specimens. Results from the tests helped understand for example which coatings provided corrosion protection to the substrate. The electrochemical results correlated well with results from the exposure of coated coupons salt fog (ASTM B117).

Table 1
Coatings Investigated

Designation	Description
C450	Bare, non-coated
C450 + TiN	C450 coated with multiple layers (ML) titanium nitride
C450 + HVOF Al	C450 coated with high velocity air fuel aluminum
C450 + NiAl	C450 coated with nickel aluminide (NA)
C450 + HVOF + TiN	C450 coated with high velocity air fuel aluminum and then coated with ML titanium nitride
C450 + NiAl + TiN	C450 coated with nickel aluminide and then coated with ML titanium nitride

Electrodeposition of Ni-Mo-P Electrodes for direct alcohol fuel cell applications

Z. Abdel Hamid¹ and H. B. Hassan²

¹*Corrosion Control and Surface Protection Laboratory, Central Metallurgical R&D Institute, CMRDI, Helwan, Cairo, Egypt*

²*Faculty of Science, Department of Chemistry, Cairo University, Giza, Egypt*

Abstract

Ternary Ni-Mo-P thin films have been electrodeposited from citrate-based electrolyte onto carbon substrates for application as anode catalysts for ethanol electrooxidation. The operating deposition parameters were optimized to produce Ni-Mo-P alloy films of outstanding catalytic activity. The phase structure of the deposits was evaluated employing X-ray diffraction (XRD) technique. Morphology and chemical composition of the deposited alloy films were studied using scanning electron microscopy (SEM) and energy-dispersive X-ray (EDX) analysis, respectively. The results demonstrated that the rate of Ni-Mo-P deposition increases with increasing the ammonium molybdate concentration in the plating electrolyte up to 10 g L⁻¹. Also, the amount of Mo in the deposits increases with increasing the ammonium molybdate concentration up to 7.5 g L⁻¹ and the maximum Mo content in the film was 9.1 at.%. The catalytic activity of Ni-Mo-P/C alloy films has been evaluated towards electrooxidation of ethanol in 1.0 M NaOH solution by using cyclic voltammetry and chronoamperometry. The catalytic performance of the prepared anodes as a function of the amount of Mo was studied. The results showed an increase in the oxidation peak current density of ethanol with increasing the Mo at.% in the deposited alloy films. Additionally, Ni-Mo-P/C electrodes displayed significantly improved catalytic activity and stability towards electrooxidation of ethanol compared with that of Ni-P/C electrode.

Ternary Ni-Mo-P thin films have been electrodeposited from citrate-based electrolyte onto carbon substrates for application as anode catalysts for ethanol electrooxidation. The operating deposition parameters were optimized to produce Ni-Mo-P alloy films of outstanding catalytic activity. The phase structure of the deposits was evaluated employing X-ray diffraction (XRD) technique. Morphology and chemical composition of the deposited alloy films were studied using scanning electron microscopy (SEM) and energy-dispersive X-ray (EDX) analysis, respectively. The results demonstrated that the rate of Ni-Mo-P deposition increases with increasing the ammonium molybdate concentration in the plating electrolyte up to 10 g L⁻¹. Also, the amount of Mo in the deposits increases with increasing the ammonium molybdate concentration up to 7.5 g L⁻¹ and the maximum Mo content in the film was 9.1 at.%. The catalytic activity of Ni-Mo-P/C alloy films has been evaluated towards electrooxidation of ethanol in 1.0 M NaOH solution by using cyclic voltammetry and chronoamperometry. The catalytic performance of the prepared anodes as a function of the amount of Mo was studied. The results showed an increase in the oxidation peak current density of ethanol with increasing the Mo at.% in the deposited alloy films. Additionally, Ni-Mo-P/C electrodes displayed significantly improved catalytic activity and stability towards electrooxidation of ethanol compared with that of Ni-P/C electrode.

Characterizing the structure of ZnAlMg-coated steel sheet via FIB-tomography

M. Arndt¹, J. Duchoslav¹, C. K. Riener², G. Angeli², D. Stifter¹

¹*Christian Doppler Labor für mikroskopische und spektroskopische Materialcharakterisierung (CDL-MS-MACH) und Zentrum für Oberflächen- und Nanoanalytik (ZONA), Johannes Kepler Universität Linz, Altenbergerstraße 69, 4040 Linz, Österreich*

²*voestalpine Stahl GmbH, voestalpine-Straße 3, 4031 Linz, Österreich*

ZnAlMg (ZM) hot-dip galvanized coatings of steel show significant better corrosion protection in comparison with conventional Zn coatings (Z) in salt spray test as well as in natural exposure outdoor tests. Therefore, ZM-layers can be applied thinner and more cost efficient. In order to improve these layers further one has to understand first of all their inner structure. From other works it is known that the layer consists of several phases (Zn-dendrites, Al-phases, binary and ternary eutectic of MgZn₂-Zn and MgZn₂-Zn-Al phases). It is as well known that cross preparation of Zn-coated steel sheets by grinding and polishing leads to problems because Zn is significant softer than steel. Also other preparation methods as focused ion beam (FIB) or ion beam cross section polishing create artefacts like holes via re-deposition.

The aim of this analysis is therefore to show how to prepare such clean cross sections of ZM-layers (96% Zn, 2% Mg, 2% Al in the bath) via FIB in order to illustrate the distribution of Al in shape of dendrites in a 3 dimensional model by repeated ion milling and subsequent imaging of the secondary electrons. These FIB cuts where compared with results obtained from etching and subsequent energy dispersive X-ray analysis.

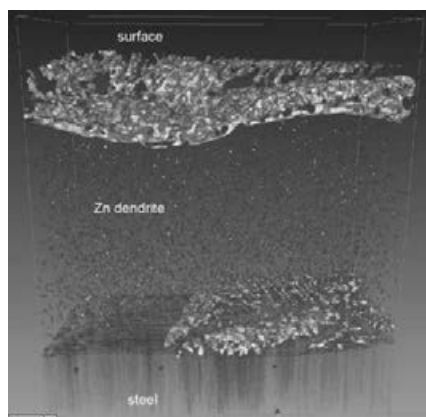


Figure 1 Al distribution in ZnAlMg coating obtained by FIB-tomography



Figure 2 Al dendrite prepared via selective etching

An Electrodeposition Process for Fabrication of Super-hydrophobic Nickel Film and Its Corrosion Resistance

S. Khorsand^{a,}, K. Raeissi^a, F. Ashrafizadeh^a, M.A. Arenas^b*

^a Department of Materials Engineering, Isfahan University of Technology, Isfahan 84156-83111, Iran

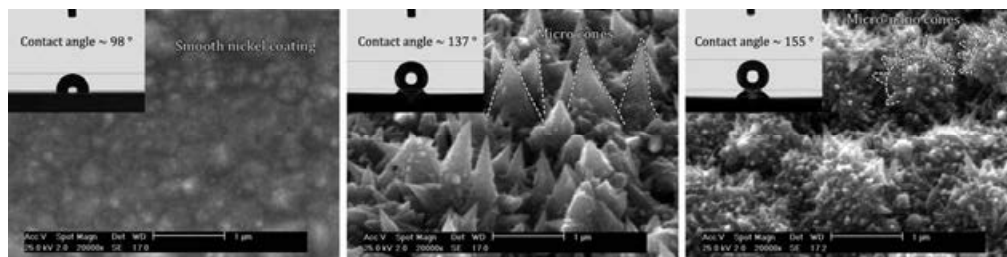
^b Department of Surface Engineering, Corrosion and Durability, National Center for Metallurgical Research (CENIM-CSIC), Avda. Gregorio del Amo, 8, 28040 Madrid, Spain

Email: s.khorsand@ma.iut.ac.ir, Tel. +34657022306

A super-hydrophobic nickel film with micro-nano structure was successfully fabricated by electrodeposition process. By controlling electrodeposition parameters and considering different storage times for the coatings in air, various nickel films with different wettability were fabricated. Surface morphology of nickel films were examined by means of scanning electron microscopy (SEM). The results showed that the micro-nano nickel film was well-crystallized and exhibited pine cone-like microstructure with nano-cone arrays randomly dispersed on each micro-protrusion. The wettability of the micro-nano nickel film varied from super-hydrophilicity to super-hydrophobicity by exposing the surface in air at room temperature. The corrosion resistance of the super-hydrophobic film was estimated by electrochemical impedance spectroscopy (EIS) and Tafel polarization measurements. The potentiodynamic curves revealed that the corrosion rate of superhydrophobic surface was only 0.16 % of the bare copper substrate. Moreover, EIS measurements and appropriate equivalent circuit models revealed that the corrosion resistance of nickel films considerably improved with an increase in the hydrophobicity. The superhydrophobic surface also exhibited an excellent long-term durability in neutral 3.5 wt.% NaCl solution.

Keywords: Nickel, Electrodeposition, Super-hydrophobic, Micro-nano structure, Corrosion resistance.

Graphical abstract:



The Effect of Texture and Surface Morphology on the Corrosion Resistance of Zinc electrodeposits

S.Khorsand, K.Raeissi, M.A. Golozar

*Department of Materials Engineering, Isfahan University of Technology, Isfahan
84156-83111, Iran*

Email: s.khorsand@ma.iut.ac.ir, Tel. +34657022306

Texture plays a major role in the corrosion resistance of zinc electrodeposits. This is because the grain dissolution rate depends on its orientation. In the present investigation, zinc coatings were electrodeposited from an acidic sulfate bath on carbon steel substrate. The effects of substrate surface preparation and additives of oxalate and Sn^{+2} ions on texture and surface morphology of deposits were evaluated. The corrosion behavior of zinc electrodeposited coatings was investigated in 5 wt.% NaCl solution. It was observed that the corrosion resistance of zinc electrodeposits is related to the crystallographic planes exposed to aggressive solution, and not only the planes of texture components. The findings highlight the role of surface morphology of the coatings in exchange current density of water reduction and its subsequent effect on corrosion resistance.

Keywords: Electrodeposition; Texture; Microstructure; Corrosion.

Anodic oxidation of galvanic Zn-Ni alloy coatings in the NaOH solutions

A. Maciej¹⁾, W. Simka¹⁾, J. Michalska¹⁾, T. Gorewoda²⁾, G. Dercz³⁾

¹⁾ Silesian University of Technology, Gliwice, Poland

²⁾ Institute of Non Ferrous Metals, Gliwice, Poland

³⁾ University of Silesia, Chorzów, Poland

Key-words: Zn-Ni coating, anodic oxidation, oxide coating, corrosion

Abstract: Ones of the most effective anodic coatings, which are used to corrosion protection of steel elements are zinc-base alloy coatings. One of them are the Zn-Ni type coatings, which are most often applied. Many reports indicate that zinc-nickel coatings consisting of 10 – 15 % Ni are very good protection of steel, which is comparable to the toxic cadmium coatings and much better than the zinc ones. In spite of the excellent anticorrosion properties of the Zn-Ni coatings, for the sake of a fact that they do not fulfill the industry (e.g. aircraft) requirements, a realization of additional treatment improving their corrosion properties is most often necessary. In order to significant improvement the corrosion properties of zinc-base alloy coatings, the conversion coating formation on their surface is realizable. One of the most effective, most popular and up to now most often using is chromate coatings. However, in the classic method of its formation the cancerigenic and mutagenic hexavalent chromium compounds are used. It's currently replaced by methods basing on trivalent chromium. The undertaken investigations applying to formation of conversion chromium-free coatings on Zn-Ni alloy galvanic coatings by anodic oxidation method.

The surface morphology (SEM), phase composition (XRD) and corrosion properties (LSV) of the formed coatings were carried out under the investigations. It was found that anodic treatment of galvanic Zn-Ni alloy in the NaOH solutions of a concentration of 10 – 50 g/dm³ allows to zinc oxide coating formation. In the range of the used parameters, the process lead to creation a cracked structure, which is dependent on the sodium hydroxide concentration. Despite of the cracks presence, the corrosion current density values of the samples (0,9 – 6,0 $\mu\text{A}/\text{cm}^2$) were similar to the one of the untreated Zn-Ni alloy coating (4,1 $\mu\text{A}/\text{cm}^2$) but in all of the cases a significant increase of corrosion potential as well as polarization resistance was observed.

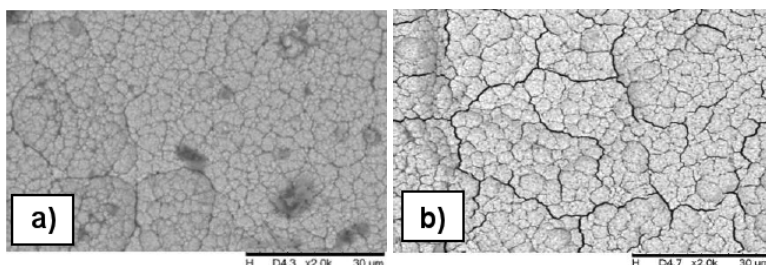


Fig.1. SEM images of Zn-Ni alloy coatings: a) untreated, b) after anodic oxidation

Acknowledgments: This work was supported by The National Centre for Research and Development under research project no. LIDER/009/433/L-4/12/NCBR/2013

Deposition of zinc powder on iron with cold spray application

*Antonio Bossio, Tullio Monetta, Ciro Bitondo, University of Naples "Federico II",
Naples;*

*Dept. of Chemical Engineering, Materials and Industrial Production, Italy
antonio.bossio@unina.it*

In this work we want to investigate a new method for deposition of a metallic coating, in particular we want to study the application of powders of zinc on a substrate of iron. It will be used the technique of Cold Spray (Dimet® Equipment), which provides for the application of zinc powder at supersonic speed and at temperatures below the melting temperature of zinc. The test was conducted by carrying out two powder mixtures: i) Zinc 80% and Al_2O_3 20%, ii) Zinc 70% and Al_2O_3 30%, the use of Al_2O_3 facilitates the anchoring of the zinc powder on the substrate. The metallographic observations (SEM with EDS analyses) show that the deposit is uniform and free of macroscopic porosity, the potentiodynamic polarization measurements confirm that the zinc deposit is compact. The measurements of electrochemical impedance spectroscopy (EIS) show that the coating increases its efficiency over time, the very few pores present is compacted completely with the products of corrosion.

Development of a bilayer superhydrophobic electrophoretic sol-gel coating on stainless steel

A. M. Simões, M. M. Lourenço, J.C.S. Fernandes*

*ICEMS & Instituto Superior Técnico, University of Lisbon,
Avenida Rovisco Pais, 1049-001, Lisbon, Portugal*

** alda.simoes@ist.utl.pt; Ph: +351-218417963*

The interest of novel coatings with well-tailored properties has been increasing, with the key idea of adjusting the surface characteristics of base materials while keeping the bulk properties. Sol-gel processes enable the production of bulk materials but also of coatings, with the great advantage of being produced under mild conditions.

Sol-gel technology has attracted a great deal of attention for the production of powders and fibers, but also for anti-corrosion coatings on metal substrates, replacing toxic chromate-based treatments. These coatings often use silanes as precursors and they are considered environmental friendly. Silica coatings can have specific interesting properties, like adhesion, hardness [2], oleophobicity or superhydrophobicity [3]. Silane coatings are most commonly applied by dip coating, but electrophoretic deposition is an interesting alternative, as it allows better tailoring of the silica films.

In this work a bilayer sol-gel coating was developed, using a stainless steel substrate and a sequence of electrophoretic deposition and dip-coating. TEOS (tetraethoxysilane) and APTES (3-amino-propyltriethoxysilane) were used as precursors in the bottom layer and were applied by electrophoresis, whereas the top layer, applied by dip-coating, used PhTMS (phenyltrimethoxysilane) as precursor. The system was characterized by Scanning Electron Microscopy (SEM), Electrochemical Impedance Spectroscopy (EIS) and contact angle measurements. Thicker and homogeneous coatings were obtained for more negative potentials and longer electrodeposition times, as monitored by the quartz crystal microbalance. The electrophoretic layer was hydrophilic and decreased the global impedance, whereas the two-layer film produced with -1.2V had strongly increased impedance and superhydrophobic, with contact angles up to 145°. This film was opaque, homogeneous, whitish and had a cauliflower morphology, with particles between 100 and 500 nm and hence with a high effective area. This coating revealed good stability in sodium chloride solution.

Keywords: corrosion, silica, coatings

1. J.R.V. Lakshmi, T. Bharathidasan, B.J. Basu, Superhydrophobic sol-gel nanocomposite coatings with enhanced hardness, *Appl. Surf. Sci.* 257 (2011) 10421–10426.
2. Y. Goto, H. Takashima, K. Takishita, H. Sawada, Creation of coating surfaces possessing superhydrophobic and superoleophobic characteristics with fluoroalkyl end-capped vinyltrimethoxysilane oligomeric nanocomposites having biphenylene segments, *J. Colloid Interface Sci.* 362 (2011) 375–381.

Sol-Gel Derived Protective Coatings to Prevent Microbial Induced Corrosion

Stefan Pfeifer¹, Alejandro Gutierrez², Edwin Kroke^{1*}

¹*TU Bergakademie Freiberg, Institut für Anorganische Chemie, Leipziger Str. 29, 09596 Freiberg, Germany, e-mail: kroke@tu-freiberg.de*

²*Van Loon Chemical Innovation, Science Park 408, 1098 XH Amsterdam, The Netherlands*

Microbial Induced Corrosion (MIC) is a very aggressive form of corrosion. To prevent this type of corrosion a novel coating system based on sol-gel chemistry was developed. Newly designed and synthesized as well as commercially available molecular precursors were used for the preparation of a green alternative to the coatings and solutions currently used up to protect large iron and steel infrastructures against damages caused by MIC.

The molecular precursors were comprehensively analyzed using FT-IR, ¹H, ¹³C and ²⁹Si NMR spectroscopy. The initial stages of hydrolysis and condensation reactions under acidic conditions were examined with solution ²⁹Si NMR spectroscopy. For the deposition of the different precursor systems we used dip-coating as well as painting. In addition to curing with conventional heating cabinets we used infrared emitters. The protection behavior of these coatings was studied as a function of coating material, thickness and curing method.

The performance of the coatings to protect against classical corrosion was verified using electrical impedance spectroscopy (EIS). In order to proof the protective behavior in a MIC environment sea water was used. Coating morphology was investigated by scanning electron microscopy (SEM). By use of CP/MAS ²⁹Si NMR the chemical structures of the coating materials were analyzed.

The EIS-tests proved that the obtained coatings provide very good protection against corrosion. The coating resistance after one month of immersion in saline water solution (3.5% NaCl) was $>>10^{10} \Omega \text{ cm}^2$. Besides, these coatings showed low water uptake.

Novel nanoparticle-based coatings for the oxidation protection of steel compounds during press-hardening

B. Tigges¹, S. Benfer¹, A. Tenié², C. Klesen², M. Yekehtaz¹, W. Bleck², W. Fürbeth¹

¹Dechema Forschungsinstitut,

Theodor-Heuss-Allee 25, D-60486 Frankfurt am Main, Germany

²Institut für Eisenhüttenkunde - Department of Ferrous Metallurgy

Intzestr. 1, D-52072 Aachen, Germany

New demand in automotive industries to reduce the CO₂ emission and fuel consumption have spread the use of high strength steel alloys. In order to increase the passenger's safety, these parts have to undergo a press hardening process before assembling into the cars. During this process, the objects will be heated up to 950 °C, and then quenched to room temperature to form a martensitic microstructure. The main problem in this process is the formation of an oxide layer which causes problems in further manufacturing and surface treatment processes.

Application of protective layers on the substrate can hinder the kinetics of oxidation at high temperatures, possibly providing additional temporary wet-corrosion protection. All systems (such as Zn plating, AlSi and organic-inorganic layers) that are in industrial use to increase the oxidation resistance of steel alloys, show significant disadvantages, i.e. burn-off of organic components at high temperatures, very slow heating rates and confined weldability. Therefore, further research in this field is required.

A novel way of oxidation protection is the deposition of sol-gel solutions on steel substrates resulting in thin films that can resist high temperatures of up to 1000 °C. However, measuring the oxidation rate of coated samples revealed that these films are only able to provide good protection up to 800 °C. At higher temperatures their ability to provide reasonable protection is decreasing due to the porous nature of the sol-gel film and poor adhesion properties.

To overcome these problems, several new strategies such as the use of pyrosil as adhesion promoting layer, use of additives to decrease the melting point of the sol deposited on the substrate and the use of commercial aqueous SiO₂-nanoparticle dispersions with higher solid contents are under investigation.

Characterization of conversion layers hexavalent chromium free applied in electrogalvanized steel

K. Provazi¹, C. R. Tomachuk¹, L. E.M. Palomino¹, C. M. Reis², I. Costa¹

¹ *Instituto de Pesquisas Energéticas e Nucleares (IPEN), São Paulo, SP, Brasil.*

² *Universidade Federal de São Paulo (UNIFESP), Diadema, SP, Brasil.*

Abstract

This work investigates the effect of zirconium based conversion coatings on galvanized steel. The conversion layers studied were prepared by dipping galvanized steel plates in solutions with zirconium salts and colloidal silica. Three types of colloidal silica were investigated with mean particles size corresponding to 10 nm, 14 nm or 20 nm. After surface treatments the samples were evaluated by electrochemical methods. The electrochemical tests showed that the best performance was associated to the colloidal silica with the smallest particle size (10 nm). This was related to a more homogeneous surface with better particles distribution in the layer leading to the choice of the silica with mean particles diameter corresponding to 10 nm. The effect of silica concentration on the characteristics of the layer formed was evaluated using two concentrations, specifically, 2 mL L⁻¹ and 5 mL L⁻¹. The corrosion resistance of the treated samples was investigated by electrochemical impedance spectroscopy in 0.1 M NaCl solution at increasing immersion periods, until 6 days of immersion. Potentiodynamic polarization tests were also carried out after 30 minutes of immersion in the sodium chloride solution. The results were compared to that of a surface with hexavalent chromate layer. The surface of the treated samples was investigated by Scanning Electron Microscopy Field Emission Gun (FEG) and X-ray Energy Dispersive Spectroscopy (EDS). The electrochemical results showed that for the whole period of immersion test, the surface layer obtained in the solution with both concentrations of colloidal silica presented high corrosion resistance which was superior to that associated to the hexavalent chromium conversion layer. Besides, surface observation after polarization showed that pitting was inhibited in the samples with the layer obtained in the solution with 5 mL L⁻¹ of colloidal silica. The polarization tests showed that passivation with zirconium in the presence of colloidal silica caused polarization of the anodic reaction protecting the surface of galvanized steel against corrosion.

Behavior of Alloying Elements during anodizing of Magnesium Alloys

A. Němcová¹, P. Skeldon¹, G.E. Thompson¹, C. Olivero², P. Chapon²

¹ Corrosion and Protection Group, School of Materials, The University of Manchester, Manchester M13 9PL, U.K.

² Horiba Jobin Yvon 16-18 rue du canal, 91165 Longjumeau Cedex, France

Recent work has shown the feasibility of forming uniform barrier-type anodic films on magnesium alloys by use of a glycerol-based electrolyte containing fluoride ions. The films contain significant amounts of oxide and fluoride species, as well as species derived from the alloy substrate. The formation of such films appears to give rise to the enrichment of certain alloy elements in an alloy layer located immediately beneath the anodic film. The enrichment process is possibly similar to that occurs during the formation of anodic films on aluminium alloys, which has been extensively studied. The enrichment of aluminium alloys can significantly affect the composition of the film and the film morphology. Further, enrichment occurs not only beneath anodic films of aluminium alloys but also beneath other types of film on the alloys, such as ones generated by etching and electropolishing, and the enrichment can subsequently affect the corrosion potential and behaviour of the alloy during conversion treatments. In contrast to aluminium alloys, enrichment of magnesium alloys has received comparatively little attention.

In the present work, the enrichment of alloying elements due to formation of anodic films on magnesium alloys is examined by glow discharge optical emission spectroscopy and ion beam analysis. The study focuses on the thickness of the enriched alloy layers, the rate of accumulation of the enriching element, and the behaviour of the alloying element once it is oxidized and incorporated into the anodic film.

Chemistry of Zr/Cr based solutions: application to sealing of anodized aluminium alloys

Najat Chahboun^{1,2}, Emmanuel Rocca¹, Delphine Veys-Renaux¹, Myriam Augros², Malik Boutoba³, Nancy Caldeira⁴

¹*Institut Jean Lamour, Université de Lorraine – CNRS, 54500 Vandoeuvre les Nancy, France.*

²*Messier-Bugatti-Dowty - 5 rue Antoine St Exupéry - 67129 Molsheim - France*

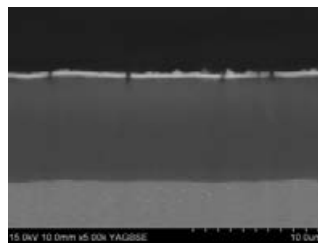
³*Eurocopter - Materials and Processes Laboratory*

Aéroport International Marseille Provence 13725 Marignane - France

⁴*Snecma - Rue Henri Auguste Desbruères - BP81- 91003 Evry Cedex France*

The protection against corrosion of aluminium alloys 2XXX and 7XXX, extensively used in the aircraft industry, is generally achieved by an anodizing process performed in a sulphuric acid medium followed by a “sealing” step. Within the framework of developing efficient and nontoxic sealing processes, new formulations based on Zr(IV) and Cr(III) salts are investigated to “seal” the nanoporosity.

Anodized and sealed aluminium oxides were characterized by scanning electron microscopy and energy dispersive x-ray spectroscopy. The sealing process actually induces the precipitation of a thin homogeneously covering overlayer, between 200 and 500 nm. The electrochemical interface was characterized by electrochemical impedance spectroscopy carried out in K_2SO_4 0.1M.



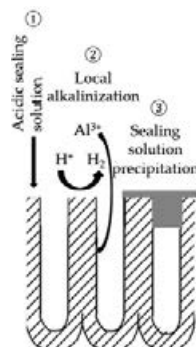
SEM micrograph of sealed anodized layer

Whatever the considered alloy, the appearance of a contribution at low frequency after sealing indicates a slowing-down of the diffusion processes through the coating and induces a reinforcing of anticorrosion properties.

In order to basically understand the formation of the sealing products, the precipitation of Zr(IV) salts, Cr(III) salts and mixture of both was investigated by titration.

The resulting precipitates were characterized by infrared spectroscopy, x-ray diffraction and thermogravimetric analysis coupled with mass spectrometry. The results show the formation of a mixed Cr/Zr hydroxide, that can be modified by Al(III) addition.

A sealing mechanism of anodized aluminium with Zr(IV)/Cr(III) solutions is proposed, comparable to the formation of a chemical conversion layer: a local alkalization of the interface induces the precipitation of Zr(IV) and Cr(III).



Sealing mechanism of anodized aluminium with Zr/Cr solution

Corrosion properties of PEO coatings obtained on Mg alloys with an electrolyte containing different concentrations of molybdate

Luca Pezzato^{}, Katya Brunelli^{*}, Maurizio Magrini^{*}, Manuele Dabalà^{*}*

^{*} Department of Industrial Engineering, University of Padua, Italy

The improvement of the corrosion resistance of magnesium and magnesium alloys is one of the main requirements to use these metals in a bigger range of applications, especially in automotive and aerospace sectors.

Plasma electrolytic oxidation (PEO) is a relatively new process that can be used to improve corrosion and tribological properties of lightweight metals, because during the treatment the formation of a thick, dense and hard oxide ceramic coating occurs. PEO technology is derived from conventional anodizing but uses environmental friendly solutions as electrolytes and the coatings exhibits improved wear and corrosion resistance.

The typical equipment for PEO treatment consist in a DC power supply colligated with a metallic tank, that work as cathode, and with the sample immersed in the electrolyte. During the process immediately an oxide film on the surface forms and when the potential exceeds the dielectric breakdown, the breakage of the weak parts of this film with the formation of micro-discharges occurs. These micro-discharges move randomly on the surface and produce the formation of the final coating.

The properties of the coating are strongly influenced by process parameters, such as current density, treatment time and electrolyte composition. Current density in particular influences the porosity and the thickness of the coatings, whereas the electrolyte composition conditions the structures the phase composition and the element distribution of the PEO coatings.

In this work PEO process was applied on commercially pure magnesium and AZ91 magnesium alloy using different solutions as electrolytes. In particular were used base alkaline solutions of silicates or phosphates with the addition of different concentrations of sodium molybdate. The effect of the addition of molybdate on the corrosion resistance of the coatings was studied with potentiodynamic polarization tests and electrochemical impedance spectroscopy (EIS) in chloride and sulphate environment. Also the effect of the variation of the current density in combination with the addition of molybdate was studied.

The differences of the morphology, phase and chemical composition of the various coatings were examined using a scanning electron microscope equipped with EDS, X-ray diffraction (XRD) and X-ray photoelectron spectroscopy (XPS).

The corrosion properties of the PEO coated samples are remarkably improved if compared with the uncoated samples. The addiction of sodium molybdate, in determinate conditions, seems to have a positive effect on the characteristics of the coatings in terms of corrosion resistance.

Electrochemical and surface analysis of corrosion properties of nanometre-thick alumina coatings prepared by ALD on copper

Shadi Mirhashemihaghighi^a, Jolanta Światowska^a, Vincent Maurice^a, Antoine Seyeux^a, Lorena H. Klein^a, Emma Härkönen^b, Mikko Ritala^b, Philippe Marcus^a

*^aInstitut de Recherche de Chimie Paris,
CNRS-Chimie ParisTech (UMR 8247), Paris, France*

*^bLaboratory of Inorganic Chemistry,
University of Helsinki, Finland*

Ultra-thin coatings gain more interest for corrosion protection of metals and alloys in small scale systems where precision is critical. Among different deposition methods used to produce coatings with precise thickness control, Atomic Layer Deposition (ALD) is an ideal candidate for growing films with high uniformity and conformity even on difficult surfaces [1-3]. Alumina is a good candidate for the coating material deposited by ALD due to its growth properties and amorphous structure which makes it free of grain boundaries and resulting defects, and it has been deposited on different substrates with promising corrosion protection properties [2,4-6].

In this work, the corrosion properties of ultra-thin (≤ 50 nm) alumina films deposited by ALD on copper at 250°C with trimethyl aluminium (TMA, $\text{Al}(\text{CH}_3)_3$) and water as precursors were studied in 0.5 M NaCl aqueous solution by combining electrochemical, microscopic and spectroscopic analytical methods. Linear Sweep Voltammetry (LSV) and Electrochemical Impedance Spectroscopy (EIS) showed a decrease in the current density and an increase in the charge transfer resistance reaching 4 orders of magnitude for 20 and 50 nm coated samples in comparison with bare copper substrates, yielding an uncoated surface fraction of 0.05%. Depth profiles analysis performed by Time-of-Flight Secondary Ion Mass Spectrometry (ToF-SIMS) revealed a homogenous in-depth composition of the alumina coating, its contamination by organic and hydroxyl precursor residues and the contamination of the interface with the Cu substrate by spurious oxide layers, organic residues, sulfur and phosphorus. Immersion tests combining *in situ* monitoring by EIS of the coating capacitance and resistance with *ex situ* ToF-SIMS depth profile analysis and Atomic Force Microscopy (AFM) surface analysis of the corrosion-induced chemical and morphological modifications will be discussed. They allow addressing the effect of the substrate preparation and coating thickness on the corrosion properties.

- [1] M. Ritala, M. Leskelä, Atomic layer deposition. In Handbook of Thin Film Materials; Nalwa, H. S., Ed.; Academic Press: San Diego, 2002; p 103-158.
- [2] S. M. George, Chem. Rev. 110 (2010) 111-131.
- [3] E. Marin, A. Lanzutti, F. Andreatta, M. Lekka, L. Guzman and L. Fedrizzi, Corros. Rev. 29 (2011) 191-208.
- [4] B.S. Lim, A. Rahtu, R.G. Gordon, Nat. Mater. 2 (2003) 749-754.
- [5] B. Díaz, E. Härkönen, V. Maurice, J. Swiatowska, A. Seyeux, M. Ritala, P. Marcus, Electrochim. Acta. 56 (2011) 9609-9618.
- [6] B. Díaz, E. Härkönen, J. Swiatowska, V. Maurice, A. Seyeux, P. Marcus, M. Ritala, Corros. Sci. 53 (2011) 2168-2175.

Experimental evaluation of the corrosion protection ability of PVD-Coatings

*U. Depner-Miller, G. Andersohn, M. Oechsner, Zentrum für Konstruktionswerkstoffe,
TU Darmstadt, 64283 Darmstadt, Germany
K. Bobzin, N. Bagcivan, T. Brögelmann, R. Weiss, IOT- Surface Engineering
Institute, RWTH Aachen University, 52072 Aachen, Germany*

In the past investigations on the corrosion protection capability of coatings, which are applied by means of physical vapor deposition (PVD), was performed by a variety of different characterization and evaluation methods. In most cases PVD coatings show a higher corrosion resistance compared to the substrate material and therefore the degradation of the substrate coating compound is dominated by coating defects. Especially, the numbers of pin-holes, which enable a direct penetration of the substrate material by the corrosive media, have an impact on the corrosion behaviour of the compound. Therefore the examination of the density of these defects is a common way to evaluate the corrosion resistance of the substrate coating compound. Generally, evaluation of this defect density can be done by electrochemical investigation like dynamic polarisation or impedance spectroscopy. But the results of those investigations can be affected by passive defects, such as clogged pin-holes by corrosion products.

In this work an optimized evaluation method is presented, which allows the identification of these phenomena. Besides the identification, the new method provides further a correction of these affecting results. The method is based on dynamic polarisation investigations and a determination of the porosity in the region of the open circuit potential of the substrate material compound. These results will be compared to a designated current density at higher potentials, characterizing the degradation of the substrate coating compound at a state of higher corrosion driving force.

The optimized evaluation method will be presented on several examples, to characterize the impact of the preparation of a nitrided low alloy steel as well as the impact of the layer architecture of a PVD multilayer coating system.

Environmentally Friendly CeCC for AA6060 aluminum alloy

L. Paussa¹, F. Andreatta¹, A. Gobessi¹, C. Cepek², L. Fedrizzi¹

¹ *Department of Chemistry, Physics and Environment, University of Udine, Italy*

² *Istituto Officina dei Materiali – CNR, Laboratorio TASC, Trieste, Italy*

Aluminium alloys like AA6060 are susceptible to severe corrosion attack in aggressive solutions (e.g. chlorides). Conversion coatings like chromate conversion coatings are usually applied in order to improve corrosion behaviour of aluminium alloys. Conversion coatings based on rare earth elements can be considered efficient alternatives to toxic chromate systems.

This work evaluates the behaviour of cerium based conversion coatings applied on AA6060 aluminum alloy. In order to improve the protection of the cerium conversion coating (CeCC), an additional sol-gel layer has been applied as a top layer.

Scanning Electron Microscopy was used for the characterization of the surface of AA6060 treated with CeCCs. Potentiodynamic Polarization Curves and Electrochemical Impedance Spectroscopy were used for determining the corrosion protection efficiency provided by the protection systems. Chemical composition profiles of CeCCs were evaluated by X-ray Photoelectron Spectroscopy and Glow Discharge Optical Emission Spectroscopy.

Aluminium alloys anodizing: effect of the composition and the microstructure

Najat Chahboun^{1,2}, Emmanuel Rocca¹, Delphine Veys-Renaux¹, Myriam Augros²,
Malik Boutoba³, Nancy Caldeira⁴

¹*Institut Jean Lamour, Université de Lorraine – CNRS, 54500 Vandoeuvre les Nancy, France.*

²*Messier-Bugatti-Dowty - 5 rue Antoine St Exupéry - 67129 Molsheim - France*

³*Eurocopter - Materials and Processes Laboratory*

Aéroport International Marseille Provence 13725 Marignane - France

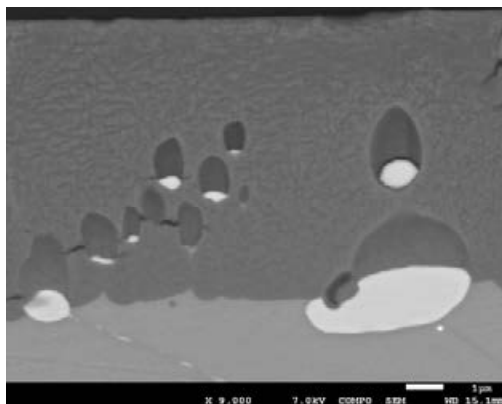
⁴*Snecma - Rue Henri Auguste Desbrières - BP81- 91003 Evry Cedex France*

The protection against corrosion of aluminium alloys 2XXX and 7XXX, extensively used in the aircraft industry, is generally achieved by an anodizing process performed in a sulphuric acid medium.

Despite the fact that the anodizing of different alloys in a same conditions (H_2SO_4 200 g/l, around 15 V) lead to nanometric pores in oxide with comparable size (10 to 20 nm), the electrochemical behaviour of the anodized layer can be very different. So in many cases, a “sealing” process” is necessary to improve the anticorrosion of the oxide layer after anodizing.

This study focuses on the growth of anodized layer on 2214, 2618 and 7050 alloys, and especially, on macroscopic defaults created by the presence of intermetallic phases in these aluminium alloys. Indeed, many cracks, heterogeneities, holes are present in anodized layers of these alloys.

Then, the electrochemical behavior, especially the barrier layer characteristics, was characterized by electrochemical impedance spectroscopy carried out in K_2SO_4 0.1M.



SEM micrography of anodized layer on 2618 alloy

Investigation on defect morphology and corrosion behaviour of TiMgN hard coatings on steel substrate

Thoralf Müller, BAM Federal Institute for Materials Research and Testing, Berlin/Germany; Andreas Heyn, BAM Federal Institute for Materials Research and Testing, Berlin/Germany; Martin Fenker, fem Research Institute, Schwäbisch Gmünd/Germany; Martin Balzer, fem Research Institute, Schwäbisch Gmünd/Germany

Nitride hard coatings, such as Titanium nitride and chromium nitride coatings are widely used for applications focussing on wear protection and decorative purposes. Also these coatings are often applied on low alloyed steel substrates. The inevitable contact of the coated components with the environment through pores and coating defects bears the danger of corrosion of the steel substrate followed by further delamination of the coating and a loss of function of the component. A new attempt to increase the corrosion behaviour of those physically deposited hard coating systems is the implementation of magnesium. The positive effect of magnesium could be verified already electrochemically. Performed experiments on TiMgN have shown that corrosion resistance could drastically improved with increasing Mg content of the TiMgN up to 30 at% compared to steel substrates with applied titanium nitride hard coatings.

Besides the clarification of the electrochemical and phenomenological effect of the magnesium on the corrosion behaviour, an additional aim of this work is the investigation of the coating defects, defect morphologies and their influence on the local corrosion behaviour.

For this the incorporation of the magnesium and its effects on the coating material, the influence of coating growth related defects and the effect of the coating structure on the corrosion behaviour should be experimental examined by using innovative surface and material analysis methods such as FIB and TEM. Furthermore the evolution of the coating defects should be investigated by combining confocal microscopy with a new developed exposure test method using the electrochemical indication test KorroPad. The function of the KorroPad test, which was developed and patented [1] at the BAM for the detection of corrosion sensitive steel surfaces by indicating dissolution of iron ions [1], allows the detection and identification of critical coating defects for further microscopic investigation. Additional to that the KorroPad test simulates an accelerated exposure test by simultaneous absence of the disadvantages of typical short time exposure test like salt spray tests. Thus it allows a monitoring and analysis of the evolution of the critical coating defects and their influence on the local corrosion behaviour and the overall corrosion mechanisms. The results of this work should contribute to the development of new hard coatings with improved corrosion protection properties and also to a better understanding of the corrosion mechanisms of coated steel substrates.

- [1] J. Lehmann , A. Burkert , U.-M. Steinhoff, German Patent Nr. DE102010037775A1: Overlay used in device for detecting corrosion of metal surfaces or corrosion sensitive metal surfaces, consists of base material containing bromide or chloride and potassium hexacyanoferrate; BAM Berlin, 2010, published 2012
- [2] Lehmann, J; Burkert, A.: Detection of corrosion sensitive surfaces of stainless steel by the fabricator; Final report of AiF research project 17136 N/1; published 2014

Performance and failure mode of Diamond-like carbon coatings in simulated oil and gas conditions

Ashley Broughton, Stuart B Lyon, University of Manchester, UK

Diamond-like Carbon coatings are a group of materials that can exhibit an impressive combination of properties that make them attractive for use in upstream oil and gas. These include; high hardness, low coefficient of friction and good corrosion resistance. Materials that are new to upstream oil and gas are being trialled to enable less favourable, more extreme well locations and geologies to be exploited.

This research was conducted in three parts: the first of these parts was to characterise Diamond-like carbon coatings produced by reactive PVD methods deposited on X65 steel. This was done by use of SEM, optical microscopy and AFM. The second part of the research concerned electrochemical impedance spectroscopy and potentiodynamic polarisation testing of the coating. Different combinations of organic inhibitor presence or absence, prior damage with ball bearing impact or undamaged coating and sweet or deoxygenated conditions were used. Scanning electrochemical microscopy (SECM) was also used to examine the coating and gain insight into the failure mode. After this, the third part of the research consisted of characterising the damage using microscopy.

There could be a considerable economic and safety benefit by using this material in upstream components such as transmission pipelines, valves and pumps. Therefore the goals of this research are to elucidate the performance characteristics and failure mechanisms.

Typical performance of these coatings under proposed service conditions is demonstrated including key failure modes. Such data will give greater confidence in the use of such materials in demanding applications.

Synthesis and Behavior of Nano Hard Anodized Layers

Z. Abdel Hamid¹, Malak T. Abou El-khair², M. Hassan Gomaa¹, Fatma A. Morsy³,
Nevien Abdel Atty khalifa³

¹*Corrosion Control and Surface Protection Laboratory, Central Metallurgical R&D
Institute, CMRDI, Helwan, Cairo, Egypt*

²*Composite Lab., Central Metallurgical Research & Development Institute (CMRDI),
Helwan, Cairo, Egypt*

³*Faculty of Science, Chemistry Department, Helwan University, Helwan, Egypt.*

ABSTRACT

The purpose of this study is to analyze the effect of chemical composition of aluminum substrate on the formation of nano hard anodized aluminum oxide layer (NHAAO) from sulfuric acid bath. The effect of bath operating conditions (temperature, time, and current density) and chemical composition of the Al substrate on the thickness, pore diameter, morphology, microhardness, abrasion resistance and corrosion resistance of the anodized layers have been investigated. The optimum growth conditions for the formation of NHAAO films were studied by field emission-scanning electron microscope (FE-SEM) and X-ray photoelectron spectroscopy (XPS), moreover, the mechanical properties were investigated using nano indentation machine. The results demonstrated that the substrate composition, anodizing temperature and current density have affected on the thickness and pore diameters of the anodic film, while the time had shown a positive effect on the coating thickness only. Moreover, the formation of thick and dense NHAAO layer on pure Al and 3004 Al alloy could be obtained using low temperature of (-2 °C) and low current densities (1 - 3 Adm²). XPS analysis illustrated that, the prepared film consists mainly of oxide. Additionally, it was found that the formation of NHAAO on pure Al or 3004 Al alloys improve the hardness, abrasion resistance and corrosion resistance comparing with unanodized substrates.

Effect of PTFE and Al_2O_3 Particles Variation on Corrosion and Wear Behavior of Ni-P-PTFE- Al_2O_3 Nanodispersion Coatings

A. K. Singh and Ankita Parashar,

*Department of Applied Science & Engineering
I.I.T. - Roorkee, Saharanpur Campus, Saharanpur, India*

Abstract

Nanodispersion coatings reinforced with hard ceramic particles (e.g., alumina Al_2O_3) and solid lubricant polytetrafluoroethylene (PTFE) are expected to be new coating materials where reduced coefficient of friction and wear loss with improved corrosion resistance are important. In the present study, coatings of Ni-P-PTFE- Al_2O_3 , with varying amounts of PTFE and Al_2O_3 , were developed through electroless process on mild steel substrate. It was observed that relative amount of PTFE and Al_2O_3 affects the deposition process. To investigate the effect of Al_2O_3 and PTFE in Ni-P matrix on corrosion and wear behavior, these coatings were tested for corrosion resistance, micro-hardness, wear and friction coefficient. Microstructure/composition and phase structure of the coatings were investigated by SEM/EDAX and XRD techniques. Vicker microhardness tester and Pin on Disc methods were used to study tribological properties (hardness, wear and friction coefficient) of the coatings. Electrochemical polarization tests and immersion tests were carried to analyze the corrosion resistance of the coatings. Results were compared with the singly incorporated Ni-P- Al_2O_3 and Ni-P-PTFE coatings. The results showed that Al_2O_3 and PTFE particles co-deposit with Ni-P homogeneously. Nanodispersion coatings showed intermediate hardness and friction coefficient in comparison to singly incorporated nanocomposite coatings. Ni-P- Al_2O_3 coating shows higher resistance against localized corrosion and lower corrosion rate as compared to Ni-P-PTFE and Ni-P-PTFE- Al_2O_3 coating. Among the different coatings, one with the combination of 6gm/l Al_2O_3 and 20ml/l PTFE was observed to provide better results. These changes have been tried to correlate with various physical and structural properties of the coating components.

Advanced environmentally friendly chemical surface treatments for cast magnesium helicopter transmission alloys preservation

*Fabiola Brusciotti, Usao Izagirre Etxeberria, Ainhoa Unzuurrungaza Iturbe
TECNALIA, Materials for Energy and Environment, Donostia-San Sebastián (Spain)*

The main objective of this work is the development of new eco-friendly chemical conversion technologies as an alternative to CrVI-based coatings, which provide an excellent corrosion protection but present health and environmental hazards. The aim is the protection of cast EV31A magnesium alloy used in the fabrication of helicopter transmission components as required by AgustaWestland (an Anglo-Italian helicopter company which supported the project) and the validation over other Mg alloys, hence fulfilling the demands of the aerospace industry.

The work was carried out starting from a Tecnalía own patented process for conversion coating of Mg alloys based on phosphates and permanganates chemistry (Spanish patent ES2178917A1). Three main steps have been carried out during the optimization process in order to improve the corrosion resistance of the coating:

- Pre-treatment selection: pre-treatment of the substrate is a fundamental step in the preparation route, as it directly affects the performance of the whole system.
- Incorporation of additives to the base conversion treatment in order to improve the corrosion protection (including self-healing capabilities) of the coating.
- Adjustment of operation conditions (pH, dipping time, temperature, etc.) and concentration of additives in order to achieve the best final performance of the coated part.

The optimization process has led to the selection of two different permanganate based treatments improved with the presence of rare earth additives in order to enhance the corrosion protection. The laboratory process was scaled-up and a 20 L pilot plant at TECNALIA was used for the production of the plates (Mg alloys EV31A as provided by AgustaWestland, AZ91 and AM60). After the newly developed treatment, the samples were coated with a primer and a resin (according to the requirements set by AgustaWestland), both chromium-free.

The specimens were then tested in terms of appearance, composition and morphology, mild environment (in climatic chamber) and salt spray fog corrosion resistance, resin and primer adhesion and evaluation of the chemical resistance of the component. All the requirements for the testing procedures were set and validated by AgustaWestland and are in agreement with the main standards and regulations set for the aeronautic industry.

The samples showed a remarkable corrosion resistance in both mild environment and salt spray fog, comparable or superior to the Cr-Mn reference samples.

The achievements of this work were developed within the framework of the Clean Sky Joint Technology Initiative (MAGNOLYA, project no. 307659).

The results of this work have a European patent application process pending (application number EP14382173, May 16th 2014).

BIOCERAMIC COATINGS ON Ti6Al4V, DEVELOPED BY ELECTROCHEMICAL PLASMA, LASER PRINTER WITH LOCALIZED STRIPPING AND DEPOSITION ELECTROPHORESIS

Laura Ramos R., Universidad de Colombia, Medellín/Colombia. Darío Yesid Peña B, Universidad Industrial de Santander, Bucaramanga/Colombia, Hugo A. Estupiñán D., Universidad Nacional, Medellín/Colombia

Coatings texturized of 45S5 bioglass and glass-ceramic materials grown on Ti6Al4V ELI (ASTM F136) anodized, were evaluated for use as improved bone anchoring surfaces that can be used in implants for some parts of the body. These were obtained in three stages. The first, by galvanostatic electrochemical anodized plasma at 8.8 mA/cm² in 0.5M H₃PO₄ electrolyte, the second by texturized laser printing to create a mask of ink and plating solution to create holes with controlled size and distances. The third step was to obtain bioglasses by electrophoretic deposition using a source of direct current at a constant voltage of 50 V for 5 minutes with particles of 45S5 Bioglass® (wt.%), particle size 5μm, concentration 0.5 g / L and 0.5 g / L and diluted with chitosan previously dissolved in ethanol and acetic acid. Glass ceramic coatings obtained by heat treatment of bioglasses obtained in an oven at 680°C for 15 minutes. Bioactivity, that is the ability of a material to react favorably with the physiological environment in the human body was evaluated in vitro by immersion in simulated body fluid (SBF) for 24 hours with stirring at 37°C, determining the ability to form apatite on the surface by SEM -EDS and electrochemical impedance spectroscopy EIS. Additionally, the ability to form extracellular matrix in these developed area by the adsorption of albumin dissolved in SBF than 1g/L, was assessed by EIS. The results showed better adsorption -ceramic coatings configuration.

Keywords: Bioglass, glass-ceramics, EIS, albumin, bioactivity, texturized bioceramic, Ti&Al4V.

Elaboration of silica hybrid coatings for corrosion protection of carbon steel: Electrochemical study

T.Phan, C. Jama, Unité Matériaux et Transformations (UMET), CNRS UMR 8207, ESNCL, 59652 Villeneuve d'Ascq Cedex, France

Nowadays hybrid sol-gel coatings with the presence of organic groups which can eliminate the drawbacks and limits of inorganic coatings are widely studied and considered to have varieties of application in the field of corrosion protection coatings. Good adhesion of sol-gel film is achieved by formation of chemical bonds $M-O-M'$ where M and M' are metallic ions in the films and substrate, respectively. Nevertheless, sol-gel film becomes less adherent when thicker since the coherent force within the film $M-O-M$ exceeds the adhering force $M-O-M'$.

In the aim of palliating this problem, a pre-treatment process by a phosphate conversion layer before sol-gel application is usually applied. A phosphating process can form, as a result of a chemical reaction between phosphoric acid and metallic substrate, insoluble phosphates which are contiguous and highly adherent to the underlying metal and are considerably more absorptive than the metal. Because metallic surface possess a certain roughness, phosphating reaction can't occur over the entire substrate; there are consequently unphosphated areas which becomes suspect corrosion. Thus, the idea of integrating phosphoric acid groups in polymer network is reported in several studies. It is demonstrated that the phosphate-containing structure increased adhesion of coatings to metallic substrate, likewise corrosion protection performance of materials.

This work reports the elaboration and characterization of silica hybrid coatings containing phosphate groups via sol-gel route to improve the corrosion resistance of carbon steel. Hybrid coatings were obtained by hydrolysing 3-[(methacryloyloxy) propyl] trimethoxysilane (MEMO) in acidic catalysis and copolymerizing with Bis [2-(methacryloyloxy) ethyl phosphate] (BMEP). The surface and the cross-section of obtained coatings on carbon steel were observed by Scanning Electron Microscopy (SEM), indicating that the hybrid coatings are free from cracks and have an approximate thickness of 27 to 30 μm . Fourier Transform Infrared Spectroscopy (FTIR) is used to study condensation and polymerization properties of hybrid network. The formation of Si-O-Si, P-O-P and Si-O-P linkages was confirmed using X-ray Photoelectron Spectroscopy (XPS). A visual observation after 35 days of immersion in NaCl 3% at 30°C shows that no corrosion product was present on the surface of coated steel. Anticorrosion performance of coated samples was investigated using potentiodynamic polarization and electrochemical impedance spectroscopy (EIS) techniques.

Influence of aluminium alloy type on the corrosion behaviour of formed alumina films

Ch. A. Girginov, S. V. Kozhukharov

*University of Chemical Technology and Metallurgy, 8 Kliment Ohridski blvd.,
1756 Sofia, Bulgaria*

The influence of the type of aluminum alloy (99.5% Al, 8006 and 8011) on its corrosion characteristics has been investigated. This study was performed by means of linear sweep voltammetry (LSV) and electrochemical impedance spectroscopy (EIS).

All experiments were carried out in a conventional three electrode cell, where the Al alloy served as a working electrode, a Pt mesh as a counter electrode and for reference electrode (Ag/AgCl/3M KCl) was used. The samples were anodized in 15 wt% H₂SO₄ in isothermal (20 °C) and galvanostatic (15 mA cm⁻²) regime, for 45 min. The formed oxides were immediately sealed in distilled water for 60 min. Under these conditions the anodic films have a thickness of 20 µm. The electrochemical tests were conducted in an unstirred, neutral 3.5 wt% NaCl at 20 °C.

LSV measurements and EIS spectra were employed to monitor the corrosion behavior of the alumina films, using Autolab PGSTAT 30, driven by GPES and FRA software (Eco Chemie, The Netherlands).

The LSV curves of the aluminum alloys were obtained with a potential sweep rate of 10 mVs⁻¹, from -600 mV to +600 mV, in respect to the open circuit potential (OCP).

EIS spectra of the specimens were measured before and after anodization. The tests were performed applying a perturbation signal of 40 mV in the frequency range from 10 mHz to 10 kHz. The obtained impedance spectra have been fitted to equivalent circuits, which are based on different physical models. Equivalent circuit parameters for the porous layers formed on three types of aluminum alloys were calculated.

It has been found a noticeable influence of the type of aluminum alloy on the corrosion resistance of the formed oxide films. The importance of the sealing process of the porous film on their protecting properties is also discussed.

Corrosion Behavior of Nanostructured Bioactive Apatite Coating on Ti6Al Alloys

Ahmed Alshamsi¹, Yaser E. Greish¹, Ahmed Aysh²

¹Department of Chemistry, ²Department of Physics, College of Science,
United Arab Emirates University, UAE

Bioinert Ti-6Al-4V alloys have been used for the past decades on total bone replacement applications. However, due to possible corrosion of these alloys, biomaterial scientists have been working on modifying surfaces of these alloys to minimize their corrosion in body media and enhance their bioactivity. In the current study, the corrosion behavior of coated and uncoated bioinert Ti-6Al-4V alloy with different surface roughness has been investigated in a phosphate buffered saline (PBS) solution at 37°C. A sputtering technique has been used to develop a 300 µm thick continuous bone-like apatite (calcium phosphate hydroxide) layer on the surfaces of the alloy of different degrees of surface roughness. Coatings were evaluated for their structure, morphology and durability in simulated body fluid (SBF) media using X-ray diffraction (XRD), X-ray photoelectron spectroscopy (XPS), and scanning electron microscopy (SEM) techniques. Corrosion techniques that have been employed included cyclic polarization measurements, polarization resistance (R_p) vs. time measurements, and EIS measurements. Surface analysis shows the formation of a stable, homogeneous, and nanostructured apatite layer with interconnected porosity. In SBF media, apatite coatings were underwent remodeling into bone-like apatite structure and morphology. Corrosion tests showed the coated samples have corrosion rates 2 to 3 orders of magnitude lower than the uncoated samples while the R_p values were 3 orders of magnitudes higher. Both the uncoated and coated samples showed no hysteresis in the reverse polarization scans signifying the absence of pitting. Finally, the current densities in the passive range were 2-3 orders of magnitude lower for the coated samples than the uncoated ones indicating the enhancement of the already existing protective film in the presence of coatings. These results, therefore, indicate the potential of bioactive apatite-coated Ti-6Al-4V alloys to be further evaluated as total bone replacement in load-bearing sites.

Microstructure and optical appearance of anodized friction stir processed Al- Metal oxide surface composites

Visweswara Gudla, Flemming Jensen, Kirill Bordo, Rajan Ambat, Department of Mechanical Engineering, Technical University of Denmark, DK-2800 Kgs. Lyngby, Denmark

Aude Simar, Université Catholique de Louvain – iMMC, 1348 Louvain-la-Neuve, Belgium

Rajashekhara Shabadi, Unité Matériaux et Transformations, Université Lille1, 59655 Villeneuve 'Ascq, France

Multiple-pass friction stir processing (FSP) was employed to impregnate Ti, Y and Ce oxide powders into the surface of an Aluminium alloy. The FSP processed surface composite was subsequently anodized with an aim to develop optical effects in the anodized layer owing to the presence of incorporated oxide particles which will influence the scattering of light. This paper presents the investigations on relation between microstructure of the FSP zone and optical appearance of the anodized layer due to incorporation of metal oxide particles and modification of the oxide particles due to the anodizing process. The effect of anodizing parameters on the optical appearance of the anodized surface was studied. Characterization was performed using SEM, FIB-SEM, TEM and GI-XRD. The surface appearance was analysed using photospectrometry technique which measures the diffuse and total reflectance of the surface. The appearance of the anodized surface changed from dark to bright upon increasing the anodizing voltage. Particles in the FSP zone were partially or completely modified during the anodizing process and modified the morphology of the surrounding anodized Al matrix which has a clear influence on the mechanism of light interaction like scattering and absorption from the anodized surface.

Keywords: Aluminium, TiO₂, Anodizing, Friction stir processing, Appearance, TEM

Electrochemical characterization of a zinc rich epoxy nano-coating primer on an X52 steel pipeline grade in flow conditions

Enrique Maya, Violeta Valencia and Homero Castaneda

Chemical and Biomolecular Engineering,

National Center for Research and Education in Corrosion,

The University of Akron

Akron, Ohio, USA

Todd Hawkins

Tesla NanoCoatings Inc.

Canton Ohio, USA

ABSTRACT

Internal corrosion protection of pipelines in oil and gas production includes chemical inhibitors that are added to the transported product. Although effective, some chemicals forming the inhibitor mixture might constitute an environmental hazard. Recently, environmental friendly solutions have been proposed as alternative route for corrosion prevention and protection, such as coatings.

This present research aims the characterization of a zinc-rich epoxy nano coating primer (ZREP) by electrochemical impedance spectroscopy (EIS) under rotating cylinder electrode (RCE) conditions. X52 API steel samples were tested at different rotational rates in chloride solution at room temperature. The behaviour of the nano structures is influenced when are exposed to saturated CO₂ and NaCl 3%wt. electrolytes. Electrochemical characterization of the nano structure architectures was performed by monitoring the coating/substrate/electrolyte interface in real time assuming steady state conditions. The electrochemical testing, high surface resolution techniques and characterization methods comprise the multi-scale theoretical tools that compare the performance of the substrate/coating interface with the physical characteristics (thickness and composition) of the primer layer.

Hybrid films modified with polyethylene glycol for corrosion protection of tin plate

Henrique Ribeiro Piaggio Cardoso, Universidade Federal do Rio Grande do Sul, Porto Alegre/Brazil; Sandra Raquel Kunst, Universidade Federal do Rio Grande do Sul, Porto Alegre/Brazil; Maria Rita Ortega Vega, Universidade Federal do Rio Grande do Sul, Porto Alegre/Brazil; Tiago Lemos Menezes, Universidade Federal do Rio Grande do Sul, Porto Alegre/Brazil; Célia de Fraga Malfatti, Universidade Federal do Rio Grande do Sul, Porto Alegre/Brazil.

The largest application of tinplate is in packaging food, being ideally suited for this purpose by virtue of it being non-toxic, light in weight, strong, and corrosion resistant. Currently, packings are submitted to a chromate-based surface treatment nevertheless, non-toxic pre-treatments have been developed to substitute the chromization process. Among those alternatives, hybrid organic-inorganic films, obtained by sol-gel process, have been used. Besides, to increase the barrier protection, plasticizers, such as poly(methyl methacrylate) or poly(ethylene glycol), have been added to the formulation of the sol to augment coating thickness, increase sol viscosity and improve the flexibility of the system to obtain uncracked films which can be subjected to mechanical deformation without failure.

Thermal curing contributes to the formation and performance of hybrid films. Thermal curing enhances barrier properties by reticular densification, which originates from a less porous layer and improves corrosion protection. Besides, the properties are further enhanced by increasing the number of deposited layers. Because of this enhancement, the deposition of bilayers on metallic substrates is recommended. The aim of this work is to coat a tin plate substrate, which is a substrate widely used in packing industry, by dip-coating process with monolayered and bilayered hybrid films modified with polyethylene glycol. The films were cured at different temperatures (60 and 90 °C) and the morphology of the obtained films were evaluated by SEM. FT-IR measurements were carried out in order to characterize the films. The coatings were characterized regarding their electrochemical behaviors by open circuit potential (E_{OC}) monitoring and electrochemical impedance spectroscopy (EIS). Preliminary results showed that the bilayered hybrid film obtained at 60 °C had a higher layer thickness and the best performance in the electrochemical assays (Figure 1), as well as the most hydrophobic character, related to the other samples studied.

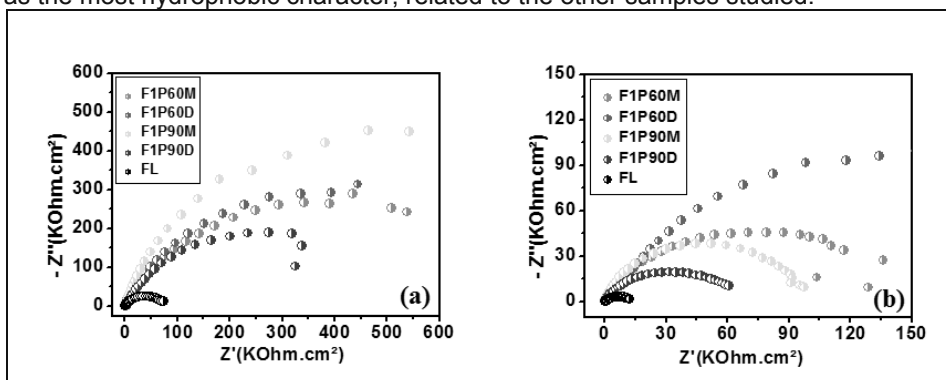


Figure 1. Nyquist plots obtained for hybrid film coated and uncoated tin plate in 0.05 M NaCl solution: (a) 24 and (b) 96 hours of immersion.

Electrochemical characterization of a $\text{H}_2\text{F}_6\text{Zr}$ film formed on SAE 1006 steel

J. dos Anjos Moraes¹, R. Sánchez-Tovar², R. Leiva-García², J. García-Antón², J. Zoppas-Ferreira¹

¹*Laboratorio de Corrosão e Proteção de Metais - PPGEM - Universidade Federal do Rioa Grande do Sul - Porto Alegre, RS, Brasil*

²*Ingeniería Electroquímica y Corrosión. Departamento de Ingeniería Química y Nuclear. Universitat Politècnica de València, Spain*

Commonly, metals and alloys are painted to enhance appearance and to provide protection from corrosion. The metal surface typically is modified by applying a pretreatment and, consequently, the resulting conversion coating improves paint adhesion and reduces the tendency for corrosion to occur beneath the paint. The desirable characteristics for the conversion coatings are that they should promote paint adhesion, inhibit corrosion, and be cost-effective.

Phosphating and chromium-based pretreatments have been widely and successfully used. However, the environmental concerns and health risks associated to these coatings contribute to an increase in the search of new eco-friendly conversion coatings. Conversion coatings based on zirconium and titanium have gained acceptance to any extend. This work studies the electrochemical stability and resistance of a new zirconium based conversion coating formed on SAE 1006 steel.

$\text{H}_2\text{F}_6\text{Zr}$ coatings have been formed on the steel and they were characterized at different times (Figure 1). Additionally, the pH of the electrolyte was varied. Electrochemical characterization of the formed coating was carried out by means of electrochemical impedance spectroscopy (EIS) and laser scanning confocal microscopy (LSCM) was used to evaluate the morphology of the coating. According to the results, it can be pointed out that the electrochemical resistance of the coating increases with time and as the pH value increases.

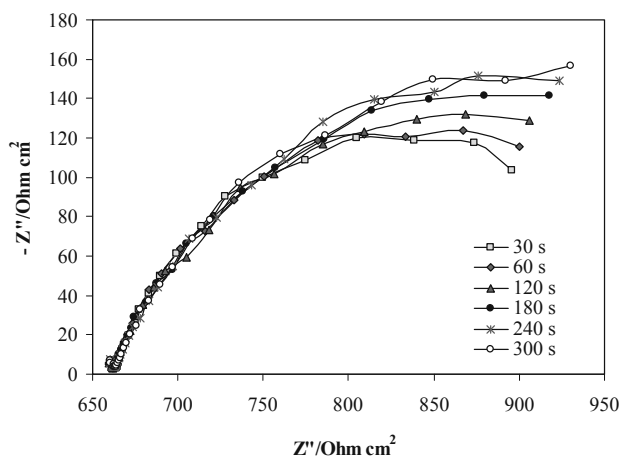


Figure 1. Nyquist diagrams during the $\text{H}_2\text{F}_6\text{Zr}$ formation at pH = 5.

Corrosion resistance of economical environmentally friendly anodization for Mg-3Zn-0.8Ca alloy

M.A.Shoeib¹ and H. Soliman¹

¹*Surface treatment & corrosion control dept., Central Metallurgical Research and Development Institute, CMRDI, P.O. Box: 87, Helwan, Cairo, Egypt

mshoeib@yahoo.com

Abstract.

Magnesium is a promising implant material for orthopedic applications due to its biodegradability and desirable mechanical properties. However, in order for Mg alloys to have clinical relevance that address the rapid degradation in physiological environments and permute increased bone-forming activity are necessary. The objective of this study was to develop an anodization process using economically environmentally friendly treatment that improves corrosion resistance of Mg alloy due to low voltages and low energy consumption. Mg-3%Zn-0.8Ca alloy was electrochemical anodized in 1 N NaOH according to the applied potential variation from 1-15V. The effects of applied potential on the surface morphology, composition and reaction process, especially the non-sparking discharge anodic film formation process, were investigated. The anodized samples were characterized by field electron emission (FEI), Energy dispersion X-ray spectroscopy (EDX) and X-ray diffraction (XRD). The corrosion resistances of anodized Mg alloys in simulated body fluid (SBF) were characterized by potentiodynamic polarization and electrochemical impedance (EIS) techniques. The electrochemical test reveals that the corrosion resistance of anodized Mg alloy at 3V increases by 2 order of magnitude. Higher voltages of anodization causes horizontal and vertical expansion of lamellar structure resulted in the formation of multi cracked layer structure with high corrosion rate. The high corrosion resistance of the anodized layer is mainly related to formation of MgO than Mg(OH)₂ phase.

Keywords: oxidation OF Mg alloy, anodization, corrosion resistance and SBF

Corrosion protection properties of the yttria stabilized sol-gel ZrO_2 thin film on 316L stainless steel

Ivana Bačić, Forensic Science Centre Ivan Vučetić, Zagreb/Croatia,

*Helena Otmačić Ćurković, Faculty of Chemical Engineering and Technology,
Zagreb/Croatia,*

*Lidija Ćurković, Faculty of Mechanical Engineering and Naval Architecture,
Zagreb/Croatia*

Abstract

In this paper, one layer and three layers of yttria stabilized sol-gel ZrO_2 thin films were deposited on the X2CrNiMo17-12-2 (AISI 316L) austenitic stainless steel by dip coating method. For the preparation of sol zirconium(IV) butoxide was used as precursor, i-propanol as a solvent with addition of nitric acid as a catalyst, acetylacetone as chelating agent and water for hydrolysis. Deposited films were calcined at the temperature of 400 °C.

Thickness of sol-gel ZrO_2 films deposited on stainless steel was determined by glow-discharge optical emission spectrometry (GD-OES). It was found that thickness of deposited films increases by increasing the number of layers.

Morphology of sol-gel ZrO_2 films was analysed by SEM-EDS.

Electrochemical impedance spectroscopy (EIS) in simulated marine environment (3.5 wt. % NaCl aqueous solution) was used to determine the corrosion behaviour of ZrO_2 coated stainless steel. The influence of ZrO_2 layers number on the degree of the protection was examined as well. It was found that the sol-gel ZrO_2 films are able to make an appreciable improvement in the corrosion resistance of stainless steel in the investigated corrosive medium.

Optical appearance of AC anodized Al/TiO₂ composite coatings

K. Bordo, V. Gudla, R. Ambat, Technical University of Denmark, Kgs. Lyngby, Denmark;

F. Jensen, Bang&Olufsen, Struer, Denmark

Anodization of aluminium is widely used in different fields of industry for corrosion protection and decoration. Decorative alumina films are commonly produced by direct current (DC) anodization of aluminium in sulphuric acid. The resulting anodic alumina films are usually transparent; however, their optical appearance depends on the anodization conditions as well as on the composition and surface morphology of the specimen being anodized. Different kinds of light-grey or white appearance can be obtained by introducing metal oxide nanoparticles into the anodic film. However, it was observed [1] that DC anodization of aluminium containing metal oxide nanoparticles can result in a dark tone which is unfavourable for decorative applications. It is expected that the microstructural issues responsible for such optical appearance can be avoided by employing alternating current (AC) anodization.

In the present work, AC anodization of Friction Stir Processed (FSP) surface composites of Al/TiO₂ was systematically investigated with an aim to understand the effect of the anodization parameters on the optical appearance of the anodic layer. FSP-treated Al samples were anodized at different conditions (composition and temperature of the electrolyte, frequency, and voltage amplitude). The microstructure and composition of the obtained anodic films were determined by scanning electron microscopy (SEM), energy-dispersive X-ray spectroscopy (EDX), transmission electron microscopy (TEM), glow discharge optical emission spectroscopy (GDOES), and grazing incidence X-ray diffraction (GIXRD) measurements. The optical appearance of the films was characterized by optical reflectance spectroscopy. The changes of the optical reflectance spectra were analysed and correlated to the microstructural features observed for the FSP-treated samples before and after anodization.

References

1. V. Gudla, F. Jensen, S. Canulescu, A. Simar, R. Shabadi, J. Schou, R. Ambat. "Microstructure and Optical Appearance of Friction Stir Processed and Anodized Al-TiO₂ Surface Composites". Paper presented at TMS 2014, San Diego.

Superficial patina: analytical interpretation of the ancient process of realization of Japanese *Shakudo* alloy.

Ferro D., Servidio D., De Filippo B., Loepp D., (Sapienza University of Rome, Italy)

Keywords: surface treatments, *shakudo*, patina, Japanese alloys, *irogane*, hot immersion colouring

Shakudo belongs to the group of traditional Japanese alloys called *irogane* ("colored-metal"); it is a copper alloy basically containing 1-10% of gold, which has a deep coppery color before the patination treatment (called *nikomi-chakushoku*). In striking contrast with pure copper, *shakudo* alloys develop a purple-black patina by hot immersion coloring in an aqueous solution containing different salts.

The aim of this work is to provide a better understanding of the chemical and physical reactions involved in the formation of *shakudo* patina, the peculiarity of its color and to attempt to develop a method with a scientific basis for its study and recognition. Different recipes for patina were reviewed, choosing one for its historical coherence and proven efficacy and using it for the patination of both a pure copper sheet and a Cu alloy containing 1 % Au, in order to compare the different features of the pure metal and the alloy. The patinas were then analyzed with EDXD and XRD to identify the surface compounds; the structure of the metal was observed with SEM-EDS to identify any morphological changes that may contribute to the patina's characteristic hues. Objects from the Pigorini museum collection of Japanese manufactures have been studied in order to compare their features with the experimental samples. XRD and EDXD analysis highlight the similarity of the spectra of pure copper and copper-gold alloy before and after the patination treatment. After treatment, on both the surfaces a layer of copper oxide(I) (cuprite) is formed. The difference between them is in the color: although the color due to cuprite tends to red, this color is observable only on pure copper sheet, while, as is observed visually and as showed in the colorimetric analysis carried out by other authors, *shakudo* surface appears black in color, with purple-blue shades.

On the bases of the analysis made and taking into account the reactants used it can be said that in patina formation different chemical species are involved, which, by reacting in solution in dynamic equilibrium, lead to the formation of cuprous oxide on the metal. From the SEM observation of the samples in section at high magnification irregularities are visible on the order of nanometers. This is consistent with the reaction mechanism presented: corrosion of metallic copper, precipitation of copper oxide(I). The color observed on *shakudo* appears to be due to three different factors: chemical, structural and morphological.



An object from the Pigorini Museum's collection: decorative element of a katana's handle with gold, copper and *shakudo* inlays.

Effect of Primer-Free Helical Inserts To Prevent Galvanic Corrosion

Dr. İng. Ali Erdem EKEN

*ASELSAN AS, Defense Systems Technologies Division, Mechanical Design
Department, Mehmet Akif Ersoy Mahallesi 296. Cadde No: 16, 06370 Ankara/Turkey*

M. Sc. Cemil YILMAZ

*ASELSAN AS, Defense Systems Technologies Division, Mechanical Design
Department, Mehmet Akif Ersoy Mahallesi 296. Cadde No: 16, 06370 Ankara/Turkey*

Dr. Evren TAN

*ASELSAN AS, Defense Systems Technologies Division, Mechanical Design
Department, Mehmet Akif Ersoy Mahallesi 296. Cadde No: 16, 06370 Ankara/Turkey*

In this paper we investigate the effects of primer-free helical inserts to prevent galvanic corrosion between dissimilar parent and thread materials.

In order to avoid galvanic corrosion, proper attention should be given to the material selection while designing a mechanical system. Particularly in military systems, it is often desired to use more than one type of metal for performance and operational reasons. For instance, aluminum alloy structures and stainless steel threads fastened together in a structure is the frequently used couple in military systems. In these systems galvanic couple formation is inevitable if moisture and contamination are present. If possible, completely insulating the system or insulating dissimilar metals wherever practical would solve this risk. Coatings may be used to insulate dissimilar metals by breaking the electrical connection in between or by reducing the potential for galvanic corrosion.

In this study, we seek a solution to overcome the galvanic corrosion problem between aluminum alloy and austenitic stainless steel threads using primer-free helical inserts. Electrical insulation performance of these inserts is compared with the uncoated stainless steel helical inserts and those installed using zinc primer. Furthermore, salt spray performances of these different systems are examined according to ASTM B 117 test. Results show that using primer-free helical inserts seems to be the best solution. Galvanic corrosion between insert and parent material can be prevented by using this type of inserts. Another advantage of using primer-free helical inserts is found to be the improvement in production process by eliminating human factor which may cause problems during installation via zinc primers.

Corrosion resistance of H₂F₆Zr coatings in NaCl

J. dos Anjos Moraes¹, R. Sánchez-Tovar², R. Leiva-García², J. García-Antón², J. Zoppas-Ferreira¹

¹*Laboratorio de Corrosão e Proteção de Metais - PPGEM - Universidade Federal do Rioa Grande do Sul - Porto Alegre, RS, Brasil*

²*Ingeniería Electroquímica y Corrosión. Departamento de Ingeniería Química y Nuclear. Universitat Politècnica de València, Spain*

The immersion of metals or alloys in a hexafluorozirconic acid (H₂F₆Zr) solution is a promising pretreatment technique that has emerged as a potential replacement for phosphating and chromium based coatings. The formed zirconium oxide film provides corrosion resistance and paint adherence to the material and it is widely used in so many industrial sectors, such as the automobile industry.

The main goal of this research is to study the corrosion resistance of different H₂F₆Zr conversion coatings formed on SAE 1006 steel in NaCl by means of electrochemical techniques. Polarization measurements and electrochemical impedance spectroscopy tests were carried out. The coatings were formed at different pH (from 3 to 5) of the H₂F₆Zr solution (0.86 g/L) during 60 seconds.

Figure 1 shows the polarization curves in NaCl for the samples coated with H₂F₆Zr at different pH and for the SAE 1006 steel without any coating. It can be observed that pH enhances the corrosion resistance of the H₂F₆Zr coatings formed on the steel.

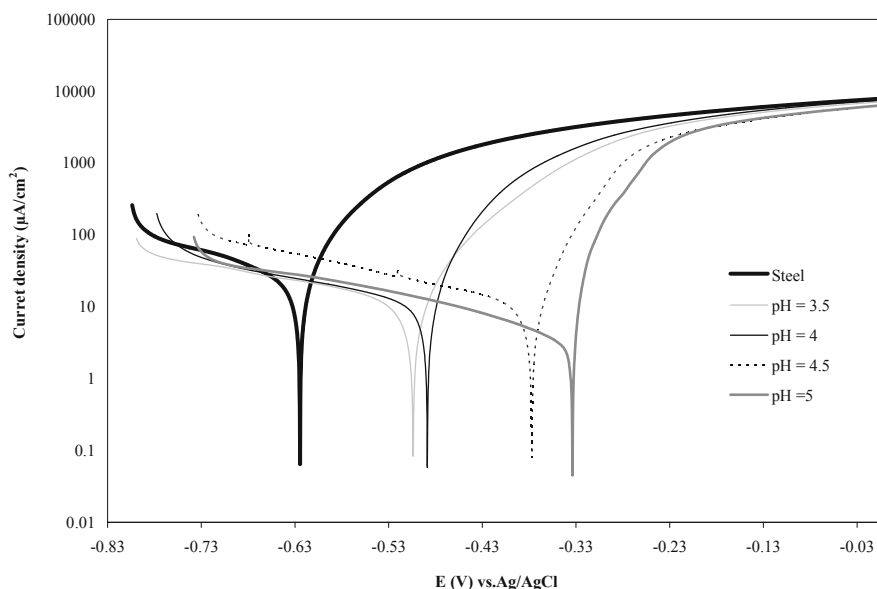


Figure 1. Polarization curves for the samples coated with H₂F₆Zr at different pH and for the steel without coating in 35 g/L NaCl.

Investigation of possibility to use glass-based layer to prevent internal corrosion of pipelines

*Martin Ronceray, Xinming Hu, Kabir Abiodun Raheem
Wood Group Kenny Ltd, Staines-upon-Thames, UK*

Internal corrosion of carbon manganese steel pipelines in the oil and gas industry is an ongoing issue with challenges encountered in several new and existing assets that see severe corrosion rates from the transported fluids.

Chemical corrosion inhibitors in combination with a corrosion allowance are often used in the design of pipelines to withstand service conditions and last the required life. This additional thickness due to corrosion allowance adds extra mass to the pipe, then there is the requirement for chemical injection facility, without mentioning the continuous supply of inhibitors and equipment maintenance during operation.

In other cases, internal anti-corrosion layers have been used in either metallic or plastic forms. Cladding and welding overlay of Corrosion Resistant Alloy (CRA) have been extensively used and the increase in capital expenditure made this solution restrained to short pipeline sections. Internal anti-corrosion coating systems have mainly been used to prevent corrosion of water transportation lines due to their permeability to gas, poor chemical compatibility with some crude oil products and limitation for high temperature services. In their plastic form these layers also have almost no resistance to abrasion in case sediments are transported by the pipeline.

The consideration of using internal anti-corrosion layer made of mineral material is not new. Silicon-based coatings are known to the industry, especially to provide external wet or dry thermal insulation. They are flexible and light, reasonably easy to apply by injection moulding system, and have a considerable wide range of temperature and chemical resistance for their utilisation. The application for internal corrosion prevention would be challenging; however this is not the subject of this paper, which is to focus on another silicon-based material: glass.

In everyday life glass is known to be in solid form, very strong and brittle at the same time. Nonetheless special chemical formulations can make glass a highly corrosion resistant, less brittle and still strong material, and a possible candidate for internal anti-corrosion layer of carbon manganese steel pipelines.

This paper identifies the possible process(es) to consider for internal glass coating application, their limitations, challenges to overtake and further developments required to make this anti-corrosion system of more interest to the industry. It also discusses the anticipated impacts on the steel pipe substrate as well as expected properties achieved with combination of such materials.

A new way for corrosion research in an artificially produced micro-climate between alloys and organic coatings

S. Walkner^{1,2}, A.W. Hassel^{1,2}

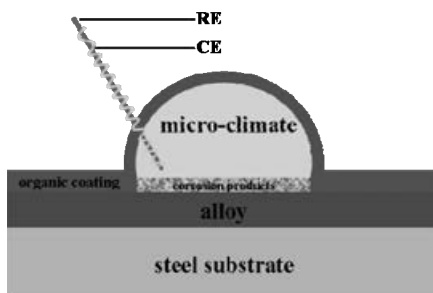
1) Institute for Chemical Technology of Inorganic Materials,

Johannes Kepler University Linz, Austria

2) Competence Centre for Electrochemical Surface Technology, Wiener

Neustadt, Austria

To improve stability of metal sheets, they are often coated with different kinds of alloys. Additionally, organic coatings are used to protect steel components from atmospheric corrosion and give them long term stability. Different ways of de-adhesion of organic coatings of a metal substrate are known like cathodic or anodic delamination, filliform corrosion and blister formation. This work focuses on the micro-climate that is developed within a blister. Once a blister is formed there are different ways of changing the climate inside the blister and investigations of the ongoing corrosion processes become possible. It is important to control the humidity outside the samples so that they are always filled with electrolyte. Dotting of the blisters and refilling them with selected electrolytes gives a variety of experimental chances. In this way the influence of different anions like sulphate, chloride and nitrate on the mechanism that takes place and appearance of the blisters can be investigated. It provides information if the presence of certain anions has an effect on their growth mechanism and on the formed corrosion products. Comparison of the corrosion behaviour in the artificially produced micro-climate and bulk samples is also important, as the developed surrounding can accelerate the damage of underlying alloys. Furthermore, electrolytes with different pH-values can be used to modify the environment in the blister. Changing of pH during a corrosion process often gives an evidence for formation of precipitates. In an alkaline pH-region hydroxide ions are consumed during film formation, which shifts the pH-value to more acidic values. Ion selective electrodes, more in detail pH-sensitive microelectrodes, are used to test pH-changes over certain time periods. Microelectrodes (RE, CE) are directly inserted into the micro-climate followed by sealing of the blisters with wax. The free metal surface in a blister acts as working electrode. All kind of electrochemical measurements are possible, like for example CV, OCP and even electrochemical impedance measurements (EIS). EIS is performed throughout a certain time period and provides information about the formation, structure and properties of the formed film. If the area of the free metal is well known even thickness of the formed corrosion products can be calculated.



Delamination kinetics of chemisorbed polymer coatings on nanostructured metal surfaces

A.Bashir, D.Iqbal, A.Erbe and M.Rohwerder, Max-Planck-Institut für Eisenforschung GmbH, Düsseldorf/Germany,

Keywords: Organic coatings, Copolymerization, Corrosion protection, Cathodic delamination

Abstract

Polymer coatings are the prerequisite materials for modern corrosion protection systems [1, 2]. The sustainable adhesion between metal/polymer interface is always a challenge, as de-adhesion of polymer coating from the metal/oxide substrate due to corrosive/electrochemical processes is a major problem which could lead to complete loss of desired material properties. High adhesion strength at a metal/polymer interface can be achieved by the formation of covalent bonds between metal surface and polymer.

Herein, we report a systematic study on the delamination kinetics of nanostructured zinc oxide (NSZ) by synthesizing ultrathin polymer films attached covalently to the metallic substrates. Initially, the NSZ surfaces were modified with silane coupling agent followed by thermally initiated polymerization reaction. Finally, polymerization was carried out in a solvent phase by adding methylmethacrylate (MMA) as a monomer, diacrylate as a crosslinker and azobisisobutyronitrile as a thermal initiator to yield thin layer of linear/crosslinked polymethylmethacrylate (PMMA). The stability of polymer coatings was explored by its delamination kinetics, measured by scanning Kelvin probe (SKP).

The covalently grafted PMMA coating exhibits lower delamination rate as compared to physisorbed PMMA film, as a result of strong chemical bond across the metal/polymer interface. The influence of crosslinking densities to the delamination rate of polymeric coating across the metal/polymer interface will be discussed in this talk.

1. de la Fuente, D., et al., *Methods for salt contamination of steel corrosion products: A characterization study*. Materials and Corrosion-Werkstoffe Und Korrosion, 2007. **58**(10): p. 781-788.
2. Grundmeier, G. and M. Stratmann, *Adhesion and De-adhesion mechanisms at polymer/metal interfaces: Mechanistic understanding based on in situ studies of buried interfaces*. Annual Review of Materials Research, 2005. **35**: p. 571-615.

Strain induced defect formation in ultra-thin protective films on TWIP steels

Chen-Ni Liu¹, Ozlem Ozcan¹, Thomas Niendorf², Florian Brenne², Guido Grundmeier¹

¹*Technical und Macromolecular Chemistry (TMC), University of Paderborn, Germany*

²*Materials Science (LWK), University of Paderborn, Germany*

Alloys with superior mechanical properties attracted great amount of industrial and scientific interest for applications in lightweight construction in automotive and aeronautics industry [1]. High manganese steels showing transformation-induced plasticity (TRIP) and twinning induced plasticity (TWIP) are very promising candidates for future applications due to their high strength and high ductility. For TWIP steels, ultimate strength values of about 1200 MPa and elongations to failure of more than 100 % have been reported in the literature [2]. However, their low corrosion resistance in aerated aqueous electrolytes results in severe material degradation, even in mildly corrosive environments. Novel surface treatments providing a temporary corrosion protection have to be developed to enable a wide utilization of TWIP steel as a lightweight construction material.

This paper focuses on the defect formation in thin, flexible polyelectrolyte films on TWIP steel induced by strain and the resulting changes in their barrier properties. Studied films consist of bilayers of polyacrylic acid (PAA) and polyallylamine hydrochloride (PAH) prepared by layer-by-layer technique (LBL) with dominating electrostatic interactions. In-situ testing employing a miniature load frame, confocal laser scanning microscopy (CLSM) and digital image correlation (DIC) was used to analyse the mechanical properties of the bilayer films on TWIP steel under mechanical load. It was shown that these films can withstand very high strains of up to 180 % without mechanical failure indicating a very good compatibility with the substrate material [3]. The investigations by means of electrochemical impedance spectroscopy (EIS) indicated a decrease in the barrier properties with increasing strain, which are assigned to the evolution of micro defects. The electrochemical investigations are supported by Field Emission – Scanning Electron Microscopy (FE-SEM) analysis to clarify the initiation of defect formation. Complementary in-situ water uptake measurements were performed by means of in-situ Fourier Transform Infra Red Reflection Absorption Spectroscopy (FT-IRRAS) to investigate the reorganisation of strained polyelectrolyte films under high humidity. The results will help to clarify the limits of temporary corrosion protection of TWIP steels by the application of polyelectrolyte films.

1. M. Naderi, V. Uthaisangsuk, U. Pahl, W. Bleck, *Steel Res. Int.* 79 (2008) 77-84.
2. O. Bouaziz, S. Allain, C.P. Scott, P. Cugy, D. Barbier, *Curr. Opin. Solid State Mater. Sci.* 15 (2011) 141-168.
3. T. Niendorf, F. Brenne, C-N. Liu, O. Ozcan, *Mater. Sci. Eng. A-* 566 (2013) 82-89.
4. J. Lackmann, R. Regenspurger, M. Maxisch, G. Grundmeier, H. J. Maier, *J. Mech. Behav. Biomed. Mater.* 3 (2010) 436-445

Effect of polymer structure and stress-state interactions on water diffusion processes in epoxy base coatings

*G. Bouvet, S. Cohendoz, X. Feaugas, S. Mallarino, S. Touzain,
Laboratoire des Sciences de l'Ingénieur pour l'Environnement (LaSIE) UMR 7356,
Université de La Rochelle, La Rochelle, France*

Organic coatings have been abundantly used to prevent metals from corrosion. Among them, epoxy-based paints are often industrially chosen, due to their low cost and their efficiency in corrosive medium like seawater. The degradation of these coatings is usually due to the action of environmental factors such as water, UV, oxygen, temperature and external mechanical stress. The durability under these factors is mainly governed by physic-chemical properties related to the polymer network structure. The objectives of this study are to highlight the effects of structure and external mechanical stresses on polymer coating during a hygrothermal ageing. In order to avoid the influence of pigments, adjuvants and other fillers, a DGEBA/DAMP model epoxy system was chosen to obtain the response of the sole polymer. This response is compared to a DGEBA/TETA model system response [1, 2] in order to highlight polymer structure effects.

Firstly, dry DGEBA/DAMP free films were mechanically studied by DMA using a loading–unloading recovery test. By varying the stress-strain state, the limits between the mechanical behaviour domains (elastic/visco-elastic and visco-elastic/visco-plastic) can be estimated [1, 3].

Secondly, the water absorption of free- stress systems was studied. The totally cured DGEBA/DAMP specimens were submitted to water immersion-desorption cycles, at several temperatures (30, 40, 50 and 60°C). The water uptake and diffusion coefficients were determined by gravimetry for non-bent free films. It is shown that the polymer network has a significant effect onto the water absorption processes.

In order to study effect of an external visco-elastic stress onto the performances of DGEBA-DAMP coating, non-bent and stressed coated panels (compressed and stretched sides) have been immersed in NaCl 3wt% solution at different temperatures and followed by Electrochemical Impedance Spectroscopy (EIS). Depending on the applied stress value (± 2 and ± 4 MPa), the water absorption parameters modification were discussed.

- [1] D. Nguyen Dang, S. Cohendoz, S. Mallarino, X. Feaugas, S. Touzain, Effects of curing program on mechanical behavior and water absorption of DGEBA/TETA epoxy network, *Journal of Applied Polymer Science*, 129 (2013) 2451-2463.
- [2] D. Nguyen Dang, B. Peraudeau, S. Cohendoz, S. Mallarino, X. Feaugas, S. Touzain, Effect of mechanical stresses on epoxy coating ageing approached by Electrochemical Impedance Spectroscopy measurements, *Electrochimica Acta*, (2013).
- [3] N. Fredj, S. Cohendoz, X. Feaugas, S. Touzain, Effect of mechanical stress on kinetics of degradation of marine coatings, *Progress in Organic Coatings*, 63 (2008) 316-322.

Anticorrosion atmospheric plasma coatings for metal protection

I. De Graeve *, *A. Kakaroglou* *, *G. Scheltjens* ‡, *B. Nisol* §, *G. Van Assche* ‡, *B. Van Mele* ‡, *F. Reniers* §, *H. Terryn* *

*Vrije Universiteit Brussel, * Research Group Electrochemical and Surface Engineering, ‡ Research Group Physical Chemistry and Polymer Science, Pleinlaan 2, 1050 Brussels, Belgium,*

§ Université Libre de Bruxelles, Faculty of Sciences - Analytical and Interfacial Chemistry, 1050 Brussels, Belgium

Plasma coatings based on allyl methacrylate (AMA) and containing corrosion inhibitors, deliberately located near the metal film interface [1], have been deposited on aluminium using a Dielectric Barrier Discharge atmospheric plasma reactor. Using various surface analysis techniques, such as FT-IR, XPS, AES, Solid State HNMR and VIS-SE, the full chemical characterisation and thickness analysis of the coatings was possible [2,3]; these features were seen to be dependent on the injected precursor flow rate, plasma power and deposition time. Furthermore, the presence of C=C double bonds of various reactivity in the precursor molecules played an essential role in the plasma deposition mechanism as compared to conventional polymerisation [2,4]. Additionally, DSC and TGA were used for the study of the thermal behavior, revealing significant residual reactivity in the plasma deposited material. To further elucidate the plasma deposition mechanism, in-situ Mass Spectrometry (MS) of the plasma gas phase was performed for AMA as well as for propyl isobutyrate (PiB), revealing different levels of fragmentation of the precursor depending on the number of double C=C bonds in the molecule, flow rate and plasma power [5]. For the corrosion protection properties, Electrochemical Impedance Spectroscopy (EIS) and the local Scanning Vibrating Electrode Technique (SVET) revealed the activity of the corrosion inhibitor when coated substrates of AA2024 were artificially scratched and exposed to an aggressive electrolyte [6].

[1] EP 12166997,2

[2] Kakaroglou, A.; Scheltjens, G.; Nisol, B.; De Graeve, I.; Van Assche, G.; Van Mele, B.; Willem, R.; Biesemans, M.; Reniers, F.; Terryn, H.; Deposition and Characterisation of Plasma Polymerised Allyl Methacrylate Based Coatings, *Plasma Processes and Polymers* 2012, 9 (8), 799-807.

[3] Nisol, B.; Batan, A.; Dabeux, F.; Kakaroglou, A.; De Graeve, I.; Van Assche, G.; Van Mele, B.; Terryn, H.; Reniers, F.; Surface Characterization of Atmospheric Pressure Plasma-Deposited Allyl Methacrylate and Acrylic Acid Based Coatings, *Plasma Processes and Polymers* 2013, 10 (6), 564-571.

[4] Batan, A.; Nisol, B.; Kakaroglou, A.; De Graeve, I.; Van Assche, G.; Van Mele, B.; Terryn, H.; Reniers, F.; The Impact of Double Bonds in the APPECVD of Acrylate-Like Precursors, *Plasma Processes and Polymers* 2013, 10 (10), 2013, 857-863.

[5] Nisol B.; Arnoult G.; Bieber T.; Kakaroglou A.; De Graeve I.; Van Assche G.; Van Mele B.; Terryn H.; Reniers F.; About the influence of double bonds in the APPECVD of acrylate-like precursors: a Mass Spectrometry study of the plasma phase, submitted for publication in *Plasma Processes and Polymers* (at time of abstract submission)

[6] Kakaroglou A.; Hauffman T.; Nisol B.; De Graeve I.; Reniers F.; Terryn H.; Incorporation of corrosion inhibitor in plasma polymerized allyl methacrylate coatings, submitted for publication in *Plasma Processes and Polymers* (at time of abstract submission)

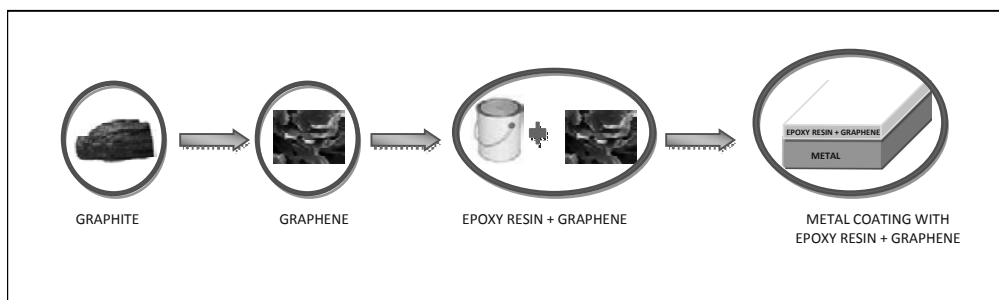
Electrochemical properties of graphene/epoxy coating

T. Monetta, A. Acquesta, F. Bellucci

University of Naples "Federico II", Dept. of Chemical Engineering, Materials and Industrial Production, Naples, Italy

In recent years graphene has attracted growing attention in both academic and industrial field owing to its exceptional thermal, mechanical, and electrical properties. In particular, the use of graphene as filler in the preparation of inorganic/polymer nanocomposites has involved increasing interest because show superior mechanical, thermal, gas barrier and electrical properties compared to the neat polymer. In addition, graphene is an ideal candidate to enhance anti-corrosion properties of the resin, since it absorbs most of the light and provides hydrophobicity for repelling water. The most important aspect of these nanocomposites is that all these improvements can be realized even at very low filler loadings in the polymer matrix. In this work, graphene nanoflakes were achieved by graphite exfoliation in various organic solutions and then, in different weight percentages, were incorporated into a water-soluble epoxy resin. Finally, the coating incorporating the nanoadditives was applied on a metal sample.

The identification of graphene nanoflakes was performed by Raman Spectroscopy SEM and XRD analysis. While, the concentration was carried out by UV-vis analysis. DSC and static contact angle measurements were performed to investigate the thermal and surface properties of the graphene-filled resin, respectively. The corrosion resistance of metal sample coating with graphene-filled resin was examined by Potentiodynamic Polarization test and by Electrochemical Impedance Spectroscopy (EIS).



Advanced Functional Ormosil coatings modified with conductive fillers for corrosion protection of Mg alloys

D. Snihirova¹, B. Martins¹, A. Zomorodian¹, Y. Morozov¹, S. Piçarra², M.F. Montemor¹

¹ ICEMS/DEQB, Instituto Superior Técnico, Technical University of Lisbon, Av. Rovisco Pais, 1049-001 Lisboa, Portugal

² Instituto Politécnico de Setúbal, Setúbal, Portugal
Corresponding author: mfmontemor@ist.utl.pt

The interest in magnesium alloys for various technological applications has increased during the last years mainly due to their interesting mechanical properties and decreased weight compared to other structural metals. However, the high corrosion susceptibility of Mg alloys requires application of corrosion protective coatings. Good barrier properties combined with addition of certain functionalities targeted for specific applications can be achieved by combining a silane modified epoxy with functional additives such as conductive fillers. The addition of these fillers is many times required for increased conductivity. However most of the systems loaded with conductive fillers present decreased barrier properties and therefore decreased corrosion resistance. In this work a novel functional Ormosil coating modified with conductive particles (Polyaniline particles, graphite and graphene oxide) is presented and its corrosion resistance evaluated. Moreover, an additional functionality was added to the coating that consists on the application of a superhydrophobic thin layer.

The corrosion protection ability of coated AZ31 panels was studied by Electrochemical Impedance Spectroscopy. Standard salt spray corrosion tests and standard adhesion measurements were performed as well. In addition the morphological features were evaluated by SEM.

The corrosion protection performance of the Ormosil coatings will be discussed and the effect of the various conductive fillers and superhydrophobic layers highlighted. The work addresses a new challenging field targeted for the functionalization of the surface of corrosion protective coatings for advanced applications.

Keywords: Magnesium alloys, Ormosil coating, electrochemical impedance spectroscopy, superhydrophobic

A New Composite Coating for Corrosion Protection of AZ31 and RZ5 Magnesium Alloys

*Ferreira, MC; Zomorodian, A; Montemor, MF; Fernandes, JCS
ICEMS / Instituto Superior Técnico, University of Lisbon, Lisbon, Portugal*

Biocompatible metallic materials represent the state of art for medical implants and an increasing interest in degradable alloys for biomedical devices is observed. A number of recent works have emphasized the use of magnesium alloys as a new class of bio-resorbable materials for orthopaedic implants. They combine multiple useful properties such as biocompatibility and osteoactive properties, low density, elastic modulus close to natural bones and the elimination of a second surgery for implant retrieval. However, some key issues still lack of a precise study and improvement. Problems such as in vivo reabsorption being too fast, localized and unpredictable and the fact that Mg corrosion produces hydrogen gas which may accumulate adjacent to the implant in the body still need to be overcome.

One of the most common and effective ways to control corrosion is the use of coatings and intensive research has been conducted in order to find a successful, practical and cheap process for coating magnesium alloys.

For the particular use of magnesium as orthopaedic biodegradable material, it should stand the corrosive physiological environment for the entire duration of the repair or healing of the injured bone tissue. Then, the implant should be gradually dissolved or absorbed in the human body. Thus, a good coating must protect the material during the healing process, allowing it to degrade afterwards.

In this work a new composite coating, involving an oxide layer followed by a second layer of organic nature, was tested on magnesium alloys AZ31 and RZ5. The first layer is obtained by anodizing in alkaline solution of sodium hydroxide, sodium silicate, sodium fluoride and glycerol, whereas the organic layer consists of a new formulation developed by the authors, based on polycaprolactone. This polymer has shown to efficiently protect Mg against corrosion but tends to degrade by hydrolysis in physiological conditions (such as in the human body), so this protection is lost after a certain period, allowing the material to slowly start to corrode, being assimilated back into the body, as required for a resorbable implant.

Electrochemical Impedance Spectroscopy was used to assess the behaviour of the composite coating during immersion in Hank's solution, showing a remarkable increase in the corrosion resistance, compared to the bare material, with initial impedance values in the range of 10^9 ohm.cm². After several weeks of immersion, the natural degradation of the polymer coating layer is reflected on a progressive increase in the corrosion rate of the magnesium alloy substrate, as expected.

Elaboration of bisphenol A polybenzoxazine coatings for barrier protection applications on aluminum substrate

Julien Escobar,^a Marc Poorteman,^a Ludovic Dumas,^{ab} Leïla Bonnaud,^b

Philippe Dubois,^b and Marie-Georges Olivier^a

^a Department of Materials Science, Materials Engineering Research Center (CRIM),
University of Mons, Place du Parc 20, B-7000 Mons, Belgium

^b Laboratory of Polymeric and Composite Materials, Center of Innovation and
Research in Materials and Polymers (CIRMAP), Materia Nova research Center &
University of Mons, Place du Parc 20, B-7000 Mons

Aluminum alloys are used in different fields such as aeronautics, automotive- or space applications because of their numerous advantages, amongst which their low weight. Nevertheless, these alloys are sensitive to corrosion and, therefore, need to be protected. Recently, polybenzoxazines have gained an increasing interest due to their potential of combining the excellent properties of traditional epoxy- or phenolic resins. This class of polymer offers highly attractive properties such as high glass transition temperatures, low absorption of water, near zero shrinkage [1], good dielectric properties [2].

In this work, a commercial bisphenol A benzoxazine was chosen to assess the barrier properties of an applied coating. Several solutions were prepared with different starting concentrations in benzoxazine, dissolved in acetone. The optimal solvent concentration of the solution was determined on basis of rheological behaviour. Thick coatings (from 5 to 20 microns) were obtained by dip coating on a 1050 aluminum substrate.

A heat treatment at 180°C followed by a step at 200°C was then performed to polymerize the benzoxazine. The structural transformation during thermal curing was followed by Fourier Transform Infrared spectroscopy (FT-IR) and the polymerization degree was calculated from data obtained by Differential Scanning Calorimetry (DSC). Dielectric Analysis (DEA) and Thermogravimetric Analysis (TGA) showed a particular behaviour related to a partial decomposition at 180°C and to the creation of intermediary ionic and volatile species. Moreover, during the consecutive curing step at 200 °C, an increase of the electrical insulation of the benzoxazine related to the polymerization was showed by DEA. Finally, the barrier protection was evaluated by electrochemical impedance spectroscopy (EIS) during 30 days in 0.5 M NaCl solution. The results showed an improvement of the impedance modulus from $10^4 \Omega \cdot \text{cm}^2$ for an uncoated aluminum to $10^9 \Omega \cdot \text{cm}^2$ with a 10 microns thick polybenzoxazine coating.

[1] H. Ishida, D. Allen - *Physical and Mechanical Characterization of Near-Zero Shrinkage Poly benzoxazines* - Journal of Polymer Science Part B: Polymer Physics – 34 (1996) 1019– 1030

[2] M.C. Tseng, Y.L. Liu - *Self-assembled benzoxazine-bridged polysilsesquioxanes exhibiting ultralow-dielectric constants and yellow-light photoluminescent emission* – Polymer – 51 (2010) 5567-5565

Poly(3,4-Ethylenedioxythiophene)-Poly(Styrene Sulfonate) as a Primer Coating for the Inhibition of Corrosion Driven Cathodic delamination and filiform corrosion on Iron

C.Glover, G. Williams

Sustainable Product Engineering Centre for Innovative Functional Industrial Coatings (SPECIFIC)

Baglan Bay Innovation Centre, Central Avenue, Baglan Energy Park, Baglan, Port Talbot, SA12 7AX. United Kingdom

Conducting polymers have been widely studied for corrosion protection on metals and the success of polypyrrole and polyaniline coatings for corrosion protection is well documented [1-2]. In this work the corrosion protection afforded by the conducting polymer Poly(3,4-Ethylenedioxythiophene)-Poly(Styrene Sulfonate) (PEDOT:PSS), applied to iron surfaces, is studied. The successful protection against corrosion, where PEDOT:PSS is present in a coating as an additive, has been reported previously. The mechanism by which PEDOT:PSS prevents corrosion is attributed to its electrochemical stability and high electrical conductivity [3]. However, few studies into this area currently exist.

The work investigates the effect of PEDOT:PSS as a primer-layer, over which a model organic polyvinyl butyral (PVB) coating is applied. Corrosion protection is evaluated under two different scenarios where:

1. PVB coating failure by cathodic delamination dominates.
2. the principal PVB coating failure mechanism is anodic disbondment in the form of filiform corrosion (FFC).

An in-situ Scanning Kelvin Probe (SKP) is used to study the corrosion potentials of the underfilm corrosion cell and measure the kinetics of coating failure. The delamination rate of PVB coatings applied over a PEDOT:PSS layer will be presented. Results indicate that a PEDOT:PSS layer acts to accelerate the cathodic delamination rate of a PVB coating. Such a result has been attributed to macroscopic percolation networks of the ICP leading to reduction of the ICP at an increased rate due to fast mobility of cations within the network. A further investigation of the inhibitory effects of PEDOT:PSS in its reduced form will be presented. FFC experiments are initiated using FeCl_2 added to a scribed defect where samples are held in a constant 95% r.h. atmosphere over a time period of several weeks. In contrast to cathodic delamination, FFC experiments show a considerable reduction in anodically driven filament initiation and propagation.

References

- [1] G. Paliwoda-Porebska, M. Stratmann, M. Rohwerder, K. Potje-Kamloth, Y. Lu, A. Z. Pich, and H.-J. Adler, *Corrosion Science*, vol. 47, no. 12, pp. 3216–3233, Dec. 2005.
- [2] E. Armelin, Á. Meneguzzi, C. A. Ferreira, and C. Alemán, *Surface and Coatings Technology*, vol. 203, no. 24, pp. 3763–3769, Sep. 2009.
- [3] C. Ocampo, E. Armelin, F. Liesa, C. Alemán, X. Ramis, and J. I. Iribarren, *Progress in Organic Coatings*, vol. 53, no. 3, pp. 217–224, Jul. 2005.

Structure property relationships in highly structured composite layers as corrosion protection coatings on mild steel

C. Becker-Willinger, S. Schmitz-Stoewe, M. Opsoelder, M. Jochum, S. Albayrak, E. Perre, INM – Leibniz-Institute for New Materials gGmbH, Saarbruecken / Germany

Newly developed highly structured composite coatings have been derived from epoxy resin matrix with finely dispersed platelet shaped SiO_2 type fillers with aspect ratio of about 30. These coatings show excellent gas diffusion barrier properties and corrosion protection up to 1000 h in the neutral salt spray test when applied with a coating thickness of about 50 μm on mild steel. In order to understand the mechanisms on the micro-scale causing the observed macroscopic behaviour the platelet filler concentration and the degree of alignment of the platelets has been varied systematically up to filler concentrations of 10 wt.-% using different types and concentrations of surface modifiers. The changes in composite morphology have been followed by metallographic analysis combined with scanning electron microscopy on cross-sections. The results showed that several types of composites with different morphology ranging from statistically oriented to almost perfectly aligned platelets could be achieved. Dielectric spectroscopy (DE-spectroscopy) has been used to investigate the influence of addition of cross-linkable hydrophobic co-monomer to the cured composite mixtures. It could be revealed that concentrations of < 1 wt.-% of co-monomer already have a pronounced effect on water up-take of the composites which correlates well with the corrosion results in the neutral salt spray test. The influence on the glass transition temperature of the polymer matrix and the interfacial interaction between polymer matrix and platelets could be followed as well. Infrared spectroscopy (FT-IR) on remaining hydroxyl group content supported the results from the DE-spectroscopy on the hydrophobic behaviour. Electrochemical impedance spectroscopy (EIS) showed that the platelet alignment and the hydrophobicity of the polymer matrix are important parameters besides cross-linking density of the polymer matrix to achieve appropriate barrier functionality. These parameters have to be balanced in certain ranges in order to achieve maximum barrier effect of the resulting composite coating. Localised corrosion processes have been followed on selected systems with statistically oriented and aligned platelets using scanning vibration electrode technique (SVET) and could be correlated with the morphological results.

Inorganic-organic hybrid(TiO_2 -MAPTS) coating on carbon steels for corrosion inhibition

*Wan Young Maeng, Geun Dong Song, Mun Hwan Kim, Jung June Noh, Mi Yoo
Korea Atomic Energy Research Institute, Daejeon/Korea*

We developed hybrid (inorganic-organic) coatings on carbon steel substrates for corrosion inhibition using sol-gel method. The hybrid coatings were made with various mixtures of TBOT(TetraButylOrthotitanate) and MAPTS(3-methacryloxypolytrimethoxysilane) catalysed with HCl addition. The ratio of TBOT:MAPTS was varied as 1:8, 1:4, 1:2, 1:1, 1:0.25, 1:0.125, and 1:0(Pure TBOT). After dip coating, the coated materials were heat treated at 100°C and 200°C in air. The properties of the coating materials were analysed with SEM, FIB, TEM and FTIR. Various homogeneous surfaces without cracks were developed on the coatings of the mixtures as shown in (a) of Figure 1 below. The thickness of the coatings was varied from 400nm to 6µm as to the ratio of TBOT to MAPTS. The coating layer was composed of carbon and the oxide of Ti, Si. The bonds of Si-O, Ti-O and Si-O-Ti were observed with FT-IT analysis of the coating. The coated specimens were tested with electrochemical polarization apparatus to evaluate the corrosion inhibition properties. The corrosion rate of coated specimen decreased, but the degree of corrosion inhibition effect of the coatings was varied with the ratio of TBOT and MAPTS and the heat treatment after dip coating.

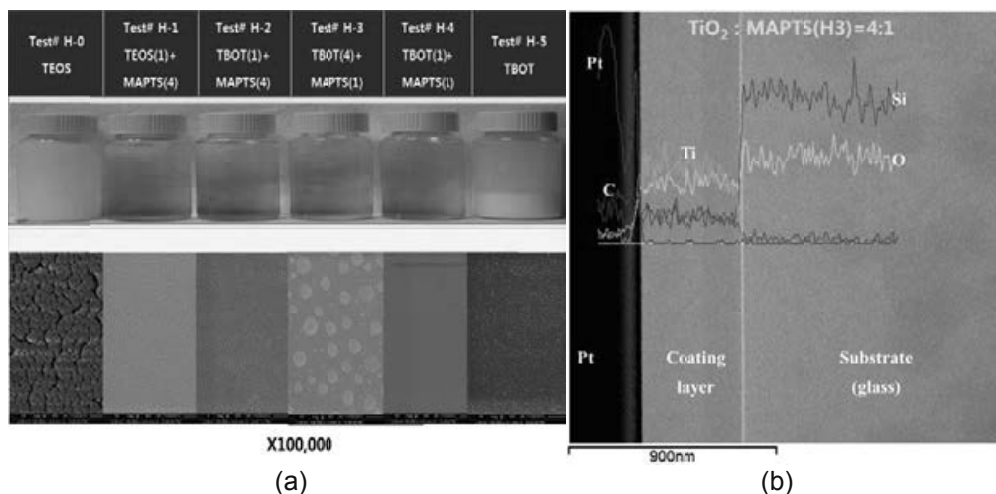


Fig. 1: Microstructures of the hybrid coatings of various mixtures.
(a) surface morphology, and (b) chemical composition of coating layer(TiO_2 :
MAPTS=4:1).

Posibilities of *ex situ* IR and *in situ* Raman spectroscopies for investigation of sol-gel anticorrosion coatings during anodic polarisation

Angela Šurca Vuk¹, Mirjana Rodošek¹, Aleksander Rauter¹, Lidija Slemenik Perše¹,
Darinka Kek Merl²,

¹National Institute of Chemistry, Hajdrihova 19, SI-1000 Ljubljana, Slovenia

²Institute Jožef Stefan, Jamova 39, SI-1000 Ljubljana, Slovenia

E-mail: angela.surca.vuk@ki.si

Organic-inorganic hybrid materials have been extensively investigated during recent years for various applications, among them also coatings for corrosion protection of various metals¹. In this study we prepared anticorrosion coatings from hydrophobic precursor 3-glycidoxypopyl terminated poly(dimethylsiloxane) (EP-PDMS-EP) and crosslinker (3-aminopropyl)trimethoxysilane (APTMS) for aluminium alloy AA 2024. To influence the mechanical hardness, thermal stability, chemical and scratching resistance the aminopropyl-heptaisooctyl-polyhedral oligomeric silsesquioxane was incorporated into the structure of the coatings^{2,3} through the reaction between amino and epoxy groups. The effect of POSS on thermal stability will also be evaluated. In order to obtain information about structural changes in material during their forced electrochemical treatment *in situ* and *ex situ* vibrational techniques were used. Namely the combination of vibrational spectroscopies, i.e., infrared reflection-absorption (IR RA) and Raman, provided complementary information. IR RA spectroscopy could give information about hydration of the coatings and changes in the siloxane and $\nu(\text{C-H})$ spectral region⁴. *Ex situ* IR RA measurements were performed under P-polarisation with near-grazing incidence angle 80°, giving the longitudinal optical (LO) modes as the result, which are blue-shifted with regard to the transversal optical (TO) modes recorded with absorbance IR technique. The LO-TO splitting results from long-range Coulombic interactions among vibrating dipoles.

With the aim of comparing *ex situ* IR RA measurements with the findings obtained from another vibrational technique a special *in situ* Raman spectroelectrochemical cell was constructed. The Pt grid and Ag/AgCl electrodes were used as counter and reference electrodes, while the anticorrosion coating on AA 2024 was mounted in horizontal position and charged chronocoulometrically in steps of +0.1 V from -0.8 V to 0.2 V for at last 240 s at each potential. Changes in Raman images revealed the lowering of the band intensities at the sites, at which the pitting corrosion was noted.

The anticorrosion properties of coatings were also evaluated using standard techniques like potentiodynamic polarisation technique, electrochemical impedance spectroscopy and exposure in salt chamber. SEM was used for evaluating the morphology of the coatings.

¹ M. Fir, B. Orel, A. Šurca Vuk, A. Vilčnik, R. Ješe, V. Francetič, Langmuir 23 (2007) 5505-5514.

² D. Sun, L. Hu, X. Zhang, Z. Lu, Coll. Surf. A: Physicochem. Eng. Aspects 313-314 (2008) 278-281.

³ Y. R. Liu, Y. D. Huang, L. Liu, Polymer Degrad. Stab. 91 (2006) 2731-2738.

⁴ A. Rauter, L. Slemenik Perše, B. Orel, B. Bengü, O. Sunetci, A. Šurca Vuk, J. of Electroanal. Chem. 703 (2013) 97-107.

Delamination of organic coatings on a zinc substrate investigated with a current measurement method

Stefan Wibiha, CEST, Wr. Neustadt/Austria; Günter Fafilek, Vienna University of Technology, Vienna/Austria; Martin Fleischanderl, voestalpine, Linz/Austria

Zinc has become the most important corrosion protection coating for steel and therefore the zinc/polymer interface is of vital interest for several industrial applications. During the last decades two methods have been established for the investigation of such organic coating/metal systems.

The electrochemical impedance spectroscopy (EIS) delivers data about the current state of the coating. Several parameters such as the pore resistance, the capacity of the organic coating or further inward the capacity of the double layer and the polarization resistance of the metal can be measured.

Using the scanning Kelvin probe (SKP) the potential distribution over such a surface can be determined. The potential reveals the distribution of cathodes and anodes and its value gives also a hint which reaction or equilibrium is in charge.

Both methods have been proven to be very useful to investigate the delamination but still neither provides information about the contribution of each zone to the corrosion of the substrate. This would only be achieved by measuring the galvanic current density distribution but since on a metal sheet the whole surface is short circuited no external current can be measured. To overcome this problem a device was developed at which the metal is separated into small, electrically isolated stripes. This was achieved by putting thin inert foils between zinc sheets. The painted cross sectional area represents the surface at which the delamination proceeds perpendicular to the stripes. Such an assembly is illustrated in Figure 1.

At idle mode all stripes are short circuited and the surface reacts like as a common metal sheet. By interconnecting a zero resistance ampere meter (ZRA) between a single stripe and the short circuited rest, the current contribution of each stripe can be measured. With this method it is possible to measure the time dependence of the current density distribution under the organic coating.

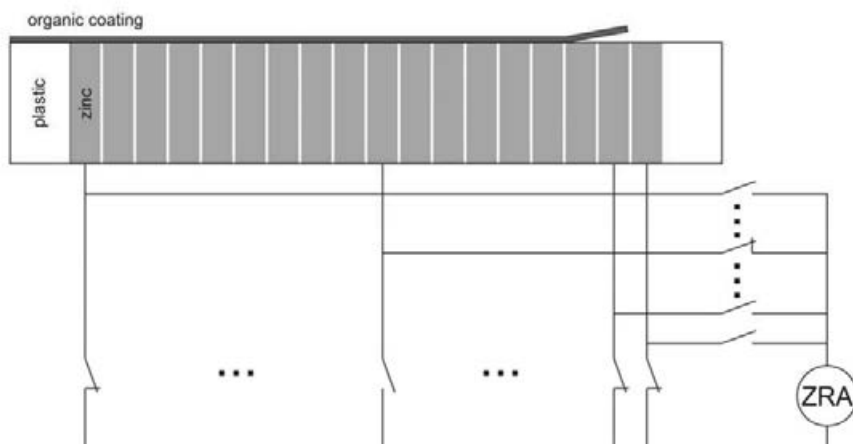


Figure 1: Zinc-Stack with organic coating

Raman spectroscopy as a tool for investigation of fluoropolymer coatings on electronic boards

Mirjana Rodošek¹, Lidija Slemenik Perše¹, Mohor Mihelčič¹, Matjaž Koželj¹, Boris Orel¹, Başak Bengü², Onder Sunetci², Pavel Pori³, Angela Šurca Vuk¹

¹National Institute of Chemistry, Hajdrihova 19, SI-1000 Ljubljana, Slovenia

²Arcelik R&D, 34950 Cayirova Campus-Tuzla/Istanbul, Turkey

³Chemcolor Sevnica, d.o.o., Dolje Brezovo 35, SI-8290 Sevnica, Slovenia

E-mail: mirjana.rodosek@ki.si; angela.surca.vuk@ki.si

Raman spectroscopy is a non-destructive technique and is a very useful tool for the investigation of materials in various fields and for providing the correctness of technological processes. Raman spectra show the energy shift of the excitation light (laser) as a product of inelastic scattering by sample molecules, resulting in information about their chemical structure.ⁱ In this work we used this vibrational technique for detecting the efficiency of the spray deposition process of anticorrosion coatings on electronic boards (EBs). We investigated various component pins on EBs to verify the presence of the sprayed protective coatings. An optical microscope and UV light were also used for searching the coverage of the most critical spots.

For EBs protection, also in harsh environments, e.g. humidity, unintended exposure to liquid water, pollutants, thermal and mechanical loads, conformal coatings (parylene, urethane, acrylic, epoxy...) are mostly applied.ⁱⁱ The application of conformal coatings on EBs is demanding because EBs surfaces are of uneven and composition of various materials (metal, plastic, soldering, conductive adhesives). In this study we investigated fluoropolymer conformal coatings with fluoroethylene and acryl vinyl ether segments, which provide exceptional UV stability, hydrophobic and oleophobic characteristics, superior abrasion and chemical resistance, cross-linking sites and solubility in common solvents. Fluoropolymer coatings are suitable also for decreasing the surface energy values, due to the high content of $-CF_2$ and $-CF_3$ groups, what we showed with contact angle measurements. The efficiency of fluoropolymer coating was improved by addition of TiO_2 nanoparticles. The coatings were first deposited using spray coating technique on model substrate, i.e. aluminium alloy AA 2024, and characterised with potentiodynamic polarisation technique. The cathodic current densities ranged from 10^{-9} – 10^{-10} A/cm² and became even lower for coatings with TiO_2 nanoparticles. The most optimal formulation was used for spraying of EBs and evaluation of the coverage of various elements. Morphological properties of chosen coatings were determined also with SEM microscopy.

ⁱ A. Rauter, M. Koželj, L. Slemenik Perše, A. Šurca Vuk, B. Orel, B. Bengü, O. Sunetci, Materials and technology 47 (2013) 2, 205–210.

ⁱⁱ J. J. Licari, Coating Materials for Electronic Applications, William Andrew Publishing, Noyes, (2003).

It's all Relative, When It Comes to Protective Coatings

D Ferguson & P Dove, GHD Pty. Ltd. Melbourne, Australia

The successful application of a protective coating can be dependent on many factors. One of the most critical is the environmental conditions at the time of application. The dew point of air is one of the key environmental parameters which must be measured. This is usually determined by measuring relative humidity.

Technical specifications and manufactures guidelines almost universally include a requirement for relative humidity levels during coating application. Depending on the nature of the coating, a high or low relative humidity may be required for the coating to cure. Additionally, long term performance of some coatings can be influenced by the environmental conditions at the time of application such as moisture on the substrate surface.

Unlike other standard testing required for quality control during the application of protective coatings, for which verification is readily achieved, the equipment used to assess environmental factors can be subject to operator variations or uncertainty in the calibration of the instruments used. Verification of the calibration of relative humidity meters while on site is not readily achieved.

This paper will review the science of relative humidity and its importance as a measured environmental condition during protective coating application. A review of European and International standards applicable to the field measurement of relative humidity will be discussed. Common methods of measuring the relative humidity will be identified and a comparison of the requirements, advertised accuracy and other points of difference, for each method of measurement will be made.

After reviewing the science of relative humidity, this paper will identify where errors can occur when determining relative humidity, and subsequently dew point, as well as the variation (or relative humidity accuracy) for common instruments used in the field. The paper will include an assessment of the practicality of using relative humidity tables and psychometric charts and other available methods.

Finally, the paper will explore ways in which relative humidity measurements can be verified on site and assess the sensitivity of different measurement techniques, and factors which may influence the measured value. Using basic experimental and theoretical science, a practical field test method to verify the calibration of relative humidity meters will be developed.

The Study on Failure Process of Acrylic Polyurethane Coating under Alternate Wetting and Drying Condition

*Zhigang Fang**, Naval Academy of Armament, Beijing 100161, P.R. China;
*Liang Zhang, Xuhui Zhao, Yu Zuo**, Faculty of Materials Science and Engineering,
Beijing University of Chemical Technology, Beijing 100029, P.R. China
Corresponding author: zhigangfang@263.net, zuoy@mail.buct.edu.cn

Abstract: The failure process of an acrylic polyurethane coating in simulated sea water under a wet-dry cyclic condition and immersion condition was studied with the methods of electrochemical impedance spectroscopy (EIS), Fourier transform infrared spectroscopy (FT-IR) and scanning electron microscope (SEM). The results show that the failure rate of acrylic polyurethane coating under the condition of wet-dry alternation is obviously greater than that under complete immersion. Under wet-dry condition both the porosity and the water absorptivity of the coating are also greater than those under complete immersion condition. However, the corrosion products formed under wet-dry alternation condition are more compact, and the electrochemical dissolution of the corrosion products is postponed in contrast to that under complete immersion. Owing to the physical effect of wet-dry alternation, the fillers in the coating surface layer may fall off and result in micro-pores, which could multiply the defects in the coating and accelerate the coating degradation. FT-IR analysis shows that the isocyanate group in the coating not only participates in the curing of coating, but also hydrolyzes with water molecule. The C-O bonds fracture partly due to hydrolysis of the main molecule chains, which is one reason of the coating failure. A failure mode for acrylic polyurethane coating under a wet-dry cyclic condition is suggested.

Key words: Acrylic polyurethane coating; wet-dry cycle; Failure; EIS; Mechanism

Improved corrosion protection of graphene oxide reinforced siloxane-PMMA hybrid coatings

Samarah Vargas Harb, Fábio C. dos Santos, Sandra H. Pulcinelli, Celso V. Santilli, Peter Hammer, Instituto de Química, UNESP-Univ. Estadual Paulista, 14800-900 Araraquara, SP, Brazil

Using the sol-gel process, organic-inorganic nanocomposite coatings were synthesized containing different concentrations of graphene oxide, to improve their mechanical strength, thermal resistance and passivation character. The siloxane-PMMA hybrids were prepared by radical polymerization of methyl methacrylate (MMA) with 3-methacryloxypropyltrimethoxysilane (MPTS) using the thermal initiator benzoyl peroxide (BPO), followed by acid catalyzed hydrolysis and condensation of tetraethoxysilane (TEOS) and then deposited by dip-coating on carbon steel substrates. Structural analysis of the coatings was performed by nuclear magnetic resonance, X-ray photoelectron spectroscopy and thermal analysis. The morphology was studied by atomic force microscopy and electrochemical impedance spectroscopy was used to evaluate the corrosion resistance in standard saline and saline/acid environments. The mechanical strength was investigated using traction test. The results have shown that the excellent dispersion of graphene oxide in the hybrid matrix contributed to the improvement of thermal stability and particularly to the mechanical resistance of the coatings. Structural results indicate the formation of covalent bonds between the graphene oxide nanoparticles and the siloxane phase resulting in crosslinked structure with high network connectivity. Electrochemical tests showed that the low roughness hybrids coatings ($R_{\text{RMS}} < 0,5 \text{ nm}$) act as a very efficient diffusion barrier with corrosion resistance of up to $10 \text{ G}\Omega$ after long-term exposure in aggressive environment. The impedance values are about six orders of magnitude higher than those of uncoated carbon steel.

Anodic protection produced by Smart Ink

*Rodrigo Sanchotene Silva, Vitor Maggi, Jane Ferreira Zoppas, Álvaro Meneguzzi
Federal University of Rio Grande do Sul, Porto Alegre/Brazil*

Currently the industries of paint have directed their efforts in manufacturing products that provide effective performance in corrosion protection of metallic materials. With that, this work search as an innovation, the introduction of a new organic coating alternative, without the presence of hazardous metals and replacement of commercial rectifiers used for protection of oxidized metals by anodic protection method. Then, was held the production of a Smart Ink (SI), composed basically of a Polyurethane Paint Commercial (PPC) mixed at a determined concentration of binder, consisting of the Intrinsically Conducting Polymer (ICP), constituted base emeraldine polyaniline (PAni EB) and the plasticizer chemically inert 4-chloro-3-methylphenol (CMF). The production of the binder PAni EB was performed with the aid of high-speed dispersion equipment Dispermat N1, already to training for the SI was used the ball mill equipment Dispermat SL, in order to homogenize the mixture of binder PAni EB and PPC. After the SI and PPC were applied to plates of AISI 1010 steel, with the use of dip coat technique and were submitted drying for 48 h. In order to investigate the protective capacity of SI produced relative to PPC, were performed electrochemical assays Cyclic Voltammetry (CV) and Open Circuit Potential (OCP) using the equipment potentiostat/galvanostat AUTOLAB PGSTAT302 Ecochemie, and the solution aqueous of $2 \text{ mol.L}^{-1} \text{ H}_2\text{SO}_4$. The assays of CV and OCP showed that the SI is capable of forming protective oxides within the passivation region AISI 1010 steel, for a determined period. And with that, we can say that the binder PAni EB binder can be an alternative of organic coatings that act effectively in corrosion inhibition, and also in replacement of electronic devices that provides anodic protection to the carbon steel. This coating seeks to maximize the performance of the PIC associated with the CMF, lets aggregate to PPC the ability to induce the formation or maintenance of protective oxides in oxidizable metals subjected to harsh environments, and thereby inhibit the corrosion process.

Protective compositions on base of wastes of vegetable oils production against atmospheric corrosion of steel goods

L.E. Tsygankova^a, V.I. Vigdorovich^b, A.A. Uryadnikov^a, N.V. Shel^c

^aDerzhavin State University, Tambov, Russia

^bRRITOP, Tambov, Russia

^cTambov State Technical University, Tambov, Russia

Protective coatings on base of wastes of vegetable oils production protect carbon steel against atmospheric corrosion with sufficiently high efficiency. In open site after 6 – 10 months exposition of the steel samples covered by these compositions, protective effect reaches 80%. Insertion of 20% of wastes to vegetable oils (colza and sunflower oils) allows an increase of the protective effect by 10 %.

Efficiency of the protective coatings was studied by the methods of gravimetric corrosion tests, linear polarisation resistance (LPR), potentiodynamic polarisation, spectroscopy of electrochemical impedance. Protective efficiency of coatings on base of the vegetable oils production wastes reaches 73 – 80 % in the salt sulphate solutions and the apparatus for heat and moisture treatment (one cycle includes exposure for 8 h at 40°C and 100% relative humidity and for 16 h at gradual cooling to room temperature in the switched off and closed reactor). Compositions of the wastes with zinc powder are characterized by a growth of protective efficiency by 10 %.

Retardation of steel corrosion is caused by slowing down anodic reaction at the coating presence. This fact is confirmed by data of the polarization measurements and the results of the impedance spectroscopy. The impedance measurements testify to porous structure of the oil coatings too.

The vegetable oils production wastes are the colloidal systems, in which the particle dimension increases with temperature decrease. They absorb some quantity of water forming emulsions of «water in oil» type. Protective efficiency of such emulsions is as near as the initial wastes. Therefore, the coatings on base of the vegetable oils production wastes will show the protective efficiency even in the conditions of heightened humidity when a formation of the emulsions is possible.

The coatings under study are high producible because they have small thickness (20 – 30 µm) and their putting on steel surface does not demand preheating (temperature is 20-25°C).

Fine textured polymer based composite materials as multifunctional low friction coatings with corrosion protection

*D. Bentz, S. Schmitz-Stöwe, M. Wild, C. Becker-Willinger,
INM - Leibniz-Institute for New Materials gGmbH Saarbruecken/Germany*

In many industrial fields like automotive, power generation e.g. a fast growing interest on capable and efficient multifunctional coatings is existing. Corrosion protection properties combined with low friction is typically put into practice by an approach using stacks of two or more layers. A new class of wear resistant composite coatings was developed combining corrosion protection abilities and low friction in a single coating layer by an appropriate combination of high aspect ratio platelet shaped pigments, ceramic hard particles and an inorganic solid lubricant in a polyimide based binder matrix. In the neutral salt spray test even after 1200 h no blistering or delamination of the coating was observed. Additionally no subsurface migration could be detected. Based on this materials concept a friction coefficient of 0.07 to 0.09 could be achieved over a sliding distance of 1000 m in the ball-on-disc tribology test. It is assumed that the remarkable corrosion protection ability may be caused by a barrier effect protecting the substrate surface against water vapour and corrosive gases. This barrier could be explained by a fine textured morphology of the high aspect ratio platelets together with the layered solid lubricant which extends the diffusion pathway through the polymer binder significantly.

To investigate the mutual dependency of the corrosion protection and low friction properties, different composite coating materials with varied content of platelet shaped pigments up to 15 wt% were synthesized and applied on mild steel substrates. Mechanical stress was applied to the coating layer by using a ball-on-disc tribometer with variations in distance of up to 1000 m and normal forces of 2 N and 5 N. The durability of the corrosion protection effect was investigated by subjecting the mechanically treated samples to the neutral salt spray test. The corrosion formation and the condition of the platelets at the mechanically induced track in the coating layer produced by the tribometer was investigated by optical and scanning electron microscopic methods. Additionally local corrosion investigations were carried out using Scanning vibrating electrode technique (SVET). It was found that even after applying mechanical stress over a distance of a 1000 m by the ball-on-disc test at these stressed areas the corrosion protection was not negatively influenced compared to the unloaded coating areas.

The Effects of the nano-TiO₂ on the interfacial corrosion behavior of immersed coatings

Jin Gao^{1)*}, *Hongxia Jiang*¹⁾, *Haiyan Qian*¹⁾, *Lin Lu*¹⁾, *Xiaogang Li*¹⁾

1) Corrosion and Protection Center, University of Science and Technology Beijing, Beijing 100083, China

*Jin Gao, E-mail: g.jin@163.com

ABSTRACT

As the economic and effective means of preventing the corrosion of metal, the organic coatings have been widely applied. But the organic coatings applied in actual environment are vulnerable to erosion by environment corrosion medium and to lose protective effects eventually. The factors include ultraviolet light, water, oxygen, et al. The effects of UV light and water are great. According to the status of organic coatings aged, those modified by nanometer anti-aged materials can be applied widely. While in fact the environment factors, especially the existence of water will cause the ignition and propagation of corrosion. Moreover it is unknown that the effects of nano-TiO₂ on the seeping of water. So it is very important to grasp the basic laws of coatings failure to take effective measures to alleviate or even prevent the failure process, which is essential for the long-term protection of organic coatings.

How to realize the real-time, dynamic observation of the interface corrosion behavior during the initiation stage is the key point and difficulty in this field. Electronic speckle pattern interferometry (ESPI) is a new non-destructive testing technology with the non-contact and high accuracy, which can be applied to observe the corrosion of metal. In addition, the changes of interface behavior will lead to the change of electrochemical behavior, which will change the corrosion morphology. Scanning electrochemical microscopy (SECM) can detect the corrosion morphology of the local area by the combination of the local electrochemical technology and the microstructure.

Thus based on the study of acrylic polyurethane coatings immersed in 3.5% (wt) NaCl solution, the interfacial corrosive behavior can be investigated dynamically by electronic speckle pattern interferometry (ESPI) and scanning electrochemical microscopy (SECM). Moreover, the effects of nano-TiO₂ on the interfacial behavior can be valued by the addition of nano-TiO₂. The results show that the interfacial variety during the beginning of coating failure can be detected by ESPI, which can get the same results combined with SECM. The addition of nano-TiO₂ slows down the interfacial variety, which reflects that the anti-corrosion properties of coatings can be improved.

Sources of funds: The National Nature Science Fund (No. 51071027 and 51133009).

Study of the corrosion behavior of electrogalvanised steel/Cr(III) and Zr conversion layer/paint system by electrochemical and visual methods

F.M. Queiróz¹, P.R. Seré², C.I. Elsner², A.R. Di Sarli², C.R. Tomachuk³, I. Costa¹,
¹Instituto de Pesquisas Energéticas e Nucleares, IPEN-CCTM, São Paulo-SP, Brazil,
mq_fernanda@yahoo.com.br, icosta@ipen.br

²Centro de Investigación y Desarrollo en Tecnología de Pinturas (CICPBA-
CONICET), La Plata, Argentina, anelpire@cidepint.gov.ar

³Escola de Engenharia de Lorena da Universidade de São Paulo, EEL-USP, Lorena,
São Paulo, Brazil, celiatomachuk@usp.br

Finding environmentally friendly conversion layers with the same performance of those previously existing has been the great challenge for researchers of the surface treatment field. Successful examples are the Cr(III)-based pretreatments, which used to replace the Cr(VI) ones are, so far, the best alternative. In the last years, studies in nanotechnology are increasing and nanoparticulate systems based on silica, titanium and zirconium have been evaluated. In this work, the corrosion behavior of an electrogalvanised-zirconium conversion treatment-paint system was characterized by evaluating not only the open corrosion potential (OCP) and electrochemical impedance spectroscopy (EIS) evolution as a function of the exposure time but also the samples performance subjected to accelerated corrosion tests. All the electrogalvanised steel sheets were obtained by using an alkaline free-cyanide bath. After this, they were immersed in a nanoparticulate system containing Cr(III)-based salts and zirconium. Finally, part of these samples was covered with a solvent-based paint, and the remaining with a waterborne-paint. After curing, the samples were exposed to salt spray or humid chamber. Periodic inspections for measuring the treated samples' OCP and EIS were performed. Moreover, visual observations to detect and photographically record the eventual appearance of corrosion and/or blistering were also carried out. In order to compare the corrosion performance of the new system, samples pretreated with trivalent chromium or hexavalent chromium were also evaluated. The experimental results allowed to infer that the electrogalvanised-nanoparticulate conversion layer-paint system afforded a corrosion protection higher than that of the Cr(III) or Cr(VI) pretreated and painted samples, and therefore, that the new pretreatment is a promising alternative to the Cr(VI) one.

Research into the Causal Effects and Development of Solutions to Pinholing of Powder Coated Galvanized Steel

*Alexander F Speakman, Glasgow Caledonian University,
Professor Colin Chisholm, Glasgow Caledonian University, Glasgow, UK*

Powder Coating of metal substrates is used to add corrosion protection and aesthetic quality. The process is widely utilised across a wide range of industries such as construction, automobile and domestic appliance manufacture. The technique dates back to the 1950s and was first established commercially in the 1970s, the current global market has a value of approximately \$6bn per annum. Powder coating can be used in combination with hot dip galvanizing to greatly improve the corrosion performance and aesthetics of steel.

Globally a range of defects on the surface of the powder coated galvanised steel have been reported, often described as pinholing and outgassing, which compromise corrosion protection as well as aesthetic quality and are thus unacceptable in a finished product. While many theories and mechanisms have been discussed and reported in articles and journals it is clear that to date a real understanding of the mechanisms has still to be established through systematic scientific investigation. While the metallurgy of zinc coated galvanised steel is well established and understood it is obvious that the behaviour of the composite of galvanised zinc coated steel with the polymer based coating needs further scientific research to understand the mechanisms leading to unacceptable surface defects and how to conduct processing to avoid such defects.

A collaborative research project between Glasgow Caledonian University and Highland Colour Coaters Limited based on a government grant known as a Knowledge Transfer Partnership has been carried out over a 30 month period. The project utilised University research facilities and industrial hot dip galvanizing and powder coating production facilities.

The research has scrutinised multivariables which have been presented in previous work as well as potential contributory factors highlighted within the collaborating production facility. The trending of defects through the duration of the project has allowed for the prioritising of these contributory factors as causal effects. Quality control, process control, contamination, use of primers, impact of the pretreatment process and effect of steel type are some of the factors examined and discussed. The research has allowed for the examination of the defect both as part of the industrial quality control check and to high levels of magnification utilising scanning electron microscopy.

This report will discuss the impact of the various causal effects and the process adjustments implemented which have had a positive impact on the reduction of defect within the production process.

Behaviour of coatings at the defect – scribing tools for investigations of coatings on steel

Roland Bentfeld, Institut fuer Korrosionsschutz Dresden GmbH, Dresden/Germany

The behaviour of coating systems at damages is an important quality criterion according to appropriate test regulations when loaded in corrosive media. This abstract describes the influence of different scribing tools on the behaviour of corrosion protection of coatings on steel.

In practice damages of a coating appear in different characteristics that can show the weak point of the coated material.

Typical pictures of damage are delamination of the coating and corrosion of the substrate under the coating starting from the border of the defect.

A galvanic cell develops from defects of coatings between the area of active metal dissolution (anode) and the nearly intact interface metal/coating (cathode).

The increase of pH value at the interface metal/coating is held responsible for loss of adhesion (cathodic delamination).

The coating is injured manually or mechanically down to the metal substrate by a scribing tool and afterwards exposed to loadings with influence of salt spray.

DIN EN ISO 4628-8 describes the under-rusted area as corrosion and the undermined area as delamination around the scratch.

Some standards and test regulations only assess the corrosion around the scratch and not the size of delamination as the weak point within the system.

Thereby the determination of mean values for corrosion resp. delamination should be preferred in principle instead of determination of maximum values.

Comparing investigations using different scribing tools showed that this leads to different width and depth of the scribes.

Following scribing tools and methods were used:

- 1) Cutting knife
- 2) Scribing graver Clemen (do-it-yourself)
- 3) Scribing graver Clemen (merchantable)
- 4) Scribing graver Van Laar
- 5) Scribing graver Sikkens
- 6) Tape 0.5 mm width
- 7) Milling tool with circular saw blade 0.5 mm width
- 8) Milling tool with cross tooth system 2.0 mm width

The evaluation was made according to DIN EN ISO 4628-8 after loading determining the width of the undermined area at several measuring points. A smaller width of the scribe leads to a smaller undermining.

During the loading undermining of the coating goes ahead. The performance of the artificial defect influences the behaviour of undermining of the coating (difference up to ca. 3 mm) caused by different scribing profiles.

Standards and test regulations provide many possibilities of the arrangement regarding the performance of artificial defects. Defined requirements and criteria often have to be complied exactly on the other hand. To modulate both sides in practice of corrosion protection tests for coatings more attention on this aspect should be drawn.

New Flange Corrosion Protection System

Kyle Flanagan, Belzona Polimerics Ltd., Harrogate/UK

Belzona, a global leader in the manufacture and supply of corrosion protection systems, is introducing another innovation, adding to their diverse offering. Belzona 3411 (Encapsulating Membrane) is an iso-cyanate free, moisture cured polymer coating designed to provide external corrosion protection to bolted equipment such as flanged pipe joints. This product can be easily peeled back for inspection or disassembly of the bolts before being easily resealed for continued protection. With the Belzona ethos in mind, this system is easy and safe to apply to complex geometries using simple tools.

Anti-corrosive conversion coating on Aluminium Alloys using high temperature steam with incorporated chemistries

Rameez Ud Din, Morten S. Jellesen, Rajan Ambat, Department of Mechanical Engineering, Technical University of Denmark, Kgs. Lyngby, Denmark rudin@mek.dtu.dk

Aluminium is extensively used as a structural material due to its excellent strength to weight ratio and corrosion resistance properties. Aluminium needs alloying of different elements to develop high strength. This decreases corrosion resistant properties provided by the native oxide layer of aluminium. The thin native oxide layer is formed on the surface when aluminium is exposed to air. The thickness of native oxide layer is 1-10nm, which depends on the alloy and surrounding conditions. However due to lower thickness, flaws and heterogeneity of native oxide layer does not provide long time corrosion resistance and adhesion of organic coating for a particular function in different environments. In order to enhance the corrosion resistance and adhesion of organic coating, the aluminium native oxide layer is treated to transform or convert to a functional conversion coating. In the last several decades chromate conversion coating (CrCCs) have been the most common conversion coatings used for aluminium alloys. Due to the toxicity of the hexavalent chrome, however, environmental friendly alternatives to CrCCs have been investigated extensively. Despite the intense research no equivalent substitute for (CrCCs) has been found. For these reasons, alternative conversion coatings are sought for substituting existing ones.

Aluminium alloys AA 1090, Peraluman 706, and AA 6060 were subjected to high pressure steam treatment and various chemistries based on pH and oxidizing capabilities. Treatment is carried out in an autoclave at a temperature of 110 – 112 °C and pressure of 5 psi for varying times. The growth and composition of the oxide layer was investigated in detail as a function of microstructure using GD-OES, FEG-SEM, EDX, FIB-SEM, XRD, and FTIR. Potentiodynamic polarization measurements and acid salt spray testing were used to study the corrosion behavior of the produced coatings. In average, thickness of the oxide layer formed was increased to ~1-1.5 µm with steam treatment and various chemistries, and the coverage on the surface was dependent on the microstructure of the alloy, particularly the composition of the intermetallics. Mechanism of the coating formation will be elucidated.

Keywords: steam, aluminium oxide, FEG-SEM, FIB-SEM

Comparative study between conventional tests and ACET technique for powder coatings used on steel with different phosphate pretreatments

J. Molina¹, J.J. Gracenea², J. Suay^{1,2}

¹PIMA Research Group. Universitat Jaume I. Castellón, Spain

²MEDCO S.L. Avda, Vicent Sos Baynat s/n, 12071 Castellón, Spain

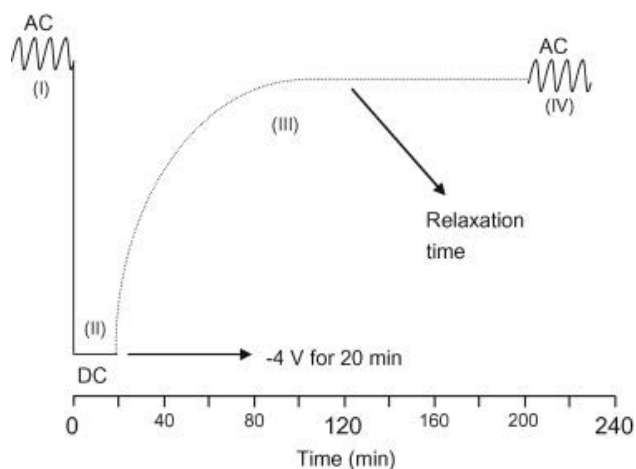
Companies producing organic coatings often need to test newly formulated products, which may have used different production or application parameters, to determine their actual behaviour before large-scale production. Proper choice of the test for this characterisation and the method of evaluation are critical. The results must be obtained in relatively short times so it is impracticable for manufacturers to wait for the completion of outdoor exposure tests. To reduce these times in the development process, the use of accelerated tests (such as salt spray resistance and EIS) to predict durability of the coating is essential. Yet, the time needed to perform such tests is usually weeks or months.

The aim of this study is to use ACET technique (which consists in a 24 hours test with a combination of impedance results, cathodic polarizations and relaxation steps) in order to correlate it with conventional tests and know beforehand the performance of the coating in the long term. The systems were five powder coatings (with different proportions of resin, anticorrosive pigment and the addition of salts of aromatic sulfonic acids supplied on a silica carrier, in order to make a differentiation on quality between them) used on steel with three different phosphated pretreatments (amorphous, microcrystalline, nanotechnological). The standard tests used were resistance, adherence, Salt spray fog and EIS finding an accurate correlation with ACET technique and its modeled parameters.

Physicochemical and electrochemical characterization of the anticorrosive pigment was carried out in order to predict the mechanism of action. The synergistic effect of the anticorrosive pigment and the salts of aromatic sulfonic acids supplied on a silica carrier was also studied isolated.

Description of ACET technique

ACET technique consists in a combination of DC and AC measurements. First, an AC test is applied to the sample under the same conditions as EIS. Following the first AC measurement, the test sample is treated for a short time with a constant cathodic voltage (-4 V) for 20 min (DC) and, after that, a relaxation time is applied to the sample until it again reaches a new steady state and the potential is once more stabilized. In this case, the relaxation time was of 3 h. During that time, a registration of the system's potential variation with time was performed. Finally, a new EIS measurement (AC) is applied to the sample in order to determine the new present state. The procedure is repeated in six cycles. A schematic representation of the ACET technique is shown.



The ACET technique is absolutely automated on PGSTAT 30 AUTOLAB equipment. Experimental results obtained in EIS measurements were modelled using an equivalent circuit.

References

- Garcia, S., and J. Suay. "A Comparative Study between the Results of Different Electrochemical Techniques (EIS and AC/DC/AC). Application to the Optimisation of the Cataphoretic and Curing Parameters of a Primer for the Automotive Industry." *Progress in Organic Coatings* 59.3 (2007): 251-58. Print.
- García, S.J., and J. Suay. "Optimization of Deposition Voltage of Cataphoretic Automotive Primers Assessed by EIS and AC/DC/AC." *Progress in Organic Coatings* 66.3 (2009): 306-13. Print.

The role of surface modification by phosphating in corrosion protection of sintered Nd-Fe-B magnets

*Elisa Isotahdon, Elina Huttunen-Saarivirta & Veli-Tapani Kuokkala,
Department of Materials Science, Tampere University of Technology, Tampere,
Finland*

The strongest permanent magnets yet discovered are based on the compounds of neodymium, iron and boron (Nd-Fe-B). The microstructure that is formed during sintering of the magnets consists of several phases. The multiphase structure together with the presence of highly active rare-earths make the Nd-Fe-B magnets vulnerable to corrosion. When the magnet is exposed to, e.g., humid environment, the presence of an anode (the Nd-rich phase), a cathode (the Nd₂Fe₁₄B-phase) and an electrolyte (humidity, water) rises the risk of galvanic corrosion. In the worst case, the active Nd-rich grain-boundary phase may corrode selectively, detaching the magnetic Nd₂Fe₁₄B grains. In consequence, the magnet pulverizes partly or totally, causing failure of the device. Hence, Nd-Fe-B magnets need to be corrosion protected in many service environments.

Nd-Fe-B –magnets are typically protected by alloying cobalt into the magnet, which decreases the potential difference between the phases and, thereby, hinders the galvanic corrosion. Also protective coatings are used for the purpose. In addition to these two methods, manufacturers use surface modification treatments. Typically, surface modification is made by treating the magnet with a phosphating solution, followed by glass-bead blasting. Phosphating treatment etches the Nd-rich areas in the magnet surface and thus prevents the formation of a corrosion cell by removing the active anodic phase. The effect is strengthened by blasting the magnet with glass beads so that the grains of the Nd₂Fe₁₄B phase on the surface are flattened.

In this study, one standard grade Nd-Fe-B magnet and one Co-alloyed grade magnet were studied. Both phosphated and non-phosphated surfaces of the magnets were exposed to various corrosion tests: highly accelerated stress test (HAST) and electrochemical measurements in NaCl solution. In HAST, the magnets were exposed to the temperature of 130°C and the relative humidity of 95 % for the standard 96 hours. Electrochemical measurements used in this study were open circuit potential monitoring and electrochemical impedance spectroscopy (EIS) that were recorded as a function of immersion time. The tested magnets were further studied with scanning electron microscopy.

In HAST tests, phosphating had a slight positive influence on the corrosion performance of the non-alloyed magnet grade. Electrochemical measurements showed that phosphated and non-phosphated surfaces behaved dissimilarly. Phosphating influenced the open circuit potential of the magnets primarily at the early stages of immersion. EIS measurements revealed formation of corrosion products on the magnet surfaces during immersion in NaCl. Explanations for the observations are provided and discussed.

Investigation of under film corrosion using pH sensitive microcapsules

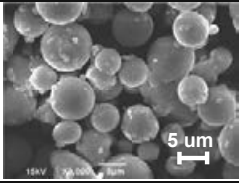
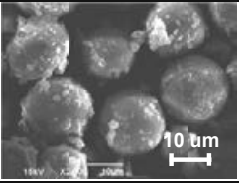
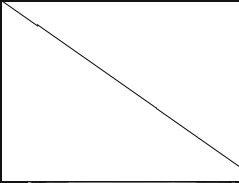
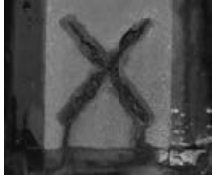


Takeshi Matsuda¹, Kiran. B. Kashi¹, Mark Jensen², Victoria. J. Gelling¹,

1. North Dakota States University, Fargo, USA

2. Concordia College, Moorhead, USA

Intelligent materials, also known as responsive materials, are an emerging area of study. Specifically, materials that can respond to a trigger, such as changes in pH, are of potential use in the fight against corrosion. During recent years, stimuli-responsive microcapsules are expected as new technology such as drug delivery, food preservation, self-healing materials. In the literature, microcapsules have been synthesized that act as an intelligent material by rupturing upon exposure to variations in pH. This is especially useful when one wishes to detect and respond in an intelligent manner in response to corrosion, as it is well known that corrosion reactions cause variations in pH at both the cathodic and anodic reaction sites on metal substrates. For example, in the cathodic reaction, pH of the electrolyte increases to rather basic levels due to the reduction reaction of oxygen. The aforementioned pH sensitive microcapsules can be designed to collapse by a hydrolysis reaction as the shell of the microcapsule may consist of cross-linked polyester. As a result, the core material can be released only when the corrosion reaction progresses.

In this study, pH sensitive microcapsules containing cerium nitrate (Ce-MC) were synthesized by water-in-oil emulsion polymerization. To investigate the effect of particle size to corrosion protection, Ce-MC having three different particle size were synthesized by adjusting the agitation speed. In the result, it was found that under film corrosion resistance around the artificial defect was improved by decreasing the particle size. Electrochemical analyses such as potentiodynamic polarization scan, electrochemical impedance spectroscopy, and scanning electrochemical microscope, were also utilized in the study and were able to provide important mechanistic information regarding the corrosion protection provided by the responsive microcapsules.

Agitation speed	2000 rpm	180 rpm	Control
Particle size	7.3 μm	17.5 μm	
SEM images			
Appearance of specimen after 986 hrs of SST	 Epoxy resin with 10 vol% of Ce-MC	 Epoxy resin with 10 vol% of Ce-MC	 Epoxy resin

Influence of different pretreatments of Mg4Y2Nd prior to NaF-coating on the electrochemical corrosion behaviour

C. Schille, E. Schweizer, J. Geis-Gerstorfer; University Hospital Tuebingen, Dental Clinic, Section Medical Materials & Technology, Tuebingen, Germany

Introduction

Coating can be an effective means to improve the corrosion resistance of magnesium alloys. Before coating different pretreatment protocols of the magnesium alloys are applied which customarily consists of (A) cooking in distilled water for 20 minutes to form a magnesium hydroxide layer; (B) after drying at air immersion in 0.5 M NaOH solution for 20 minutes to increase the hydroxide layer thickness; (C) after drying at air acid pickling for some seconds.

The aim of the study was, to investigate the influence of these three pretreatments itself (A, B, C) and furthermore their combinations (A+B, A+C, B+C, A+B+C) compared to the grinded surface as a reference on the electrochemical corrosion behaviour and surface characteristics of an experimental Mg4Y2Nd magnesium alloy.

Materials & Methods

With each surface condition 3-4 samples were prepared. After grinding and cleaning in ethanol, each pretreatment was done before starting the corrosion measurements. For pretreatment C 0.02% oxalic acid was used. With each sample and surface condition anodic polarization measurements were performed from -150 mV~E_{corr} to -1200 mV without delay and a feed rate of 1 mV/sec (PAR 273, Software M352, EG&G). As electrolyte PBS(minus) was used. The electrochemical cell was heated at 37°C. From each measurement the parameters i_{corr} , R_p , E_z and CR were calculated. Additionally, the Mg-release into the electrolytes was analyzed by ICP-OES (Optima 4300 DV, Perkin Elmer). For surface characterization microscopic images were taken before and after corrosion. From each pretreatment the surface topography was recorded and the surface roughness R_a was calculated.

Results

Pretreatment B showed the lowest i_{corr} ($51 \pm 11 \mu\text{A}/\text{cm}^2$) and highest R_p value ($1532 \pm 895 \text{ Ohm}\cdot\text{cm}^2$) followed by A ($62 \pm 8 \mu\text{A}/\text{cm}^2$, $1494 \pm 239 \text{ Ohm}\cdot\text{cm}^2$) and A+B ($85 \pm 26 \mu\text{A}/\text{cm}^2$, $1097 \pm 290 \text{ Ohm}\cdot\text{cm}^2$). The grinded surface showed similar i_{corr} values compared to A but R_p was reduced to the half. The pretreatment C showed the highest i_{corr} value ($470 \pm 106 \mu\text{A}/\text{cm}^2$) which could be reduced using the combinations B+C ($274 \pm 130 \mu\text{A}/\text{cm}^2$), A+C ($118 \pm 30 \mu\text{A}/\text{cm}^2$) and A+B+C ($80 \pm 19 \mu\text{A}/\text{cm}^2$), however, the R_p values were lower and ranged between 150 (C) and 600 $\text{Ohm}\cdot\text{cm}^2$ (A+B+C).

Conclusion

Compared to the grinded surface the pretreatments A, B and A+B improve the corrosion resistance significantly. Pickling (C) alone showed worst results, but in combination with A/B it revealed an additional corrosion protective effect.

Acknowledgement

Special thanks to Dr. N. Hort, Helmholtz-Center Geesthacht, for casting the specimens.

Employing Electro-deposition Technique for coating Nano-Bioactive ceramic coating on Dental Ti-alloy implant

Madiha M. Shoeib¹, Heba A. Shalaby², Mohamed S. Nassif³ and Ahmed M. Abdelrahman⁴

^{1*} Professor, surface treatment & corrosion control Dept., Central Metallurgical Research and Development Institute, Cairo, Egypt

mshoeib@yahoo.com

^{2*} Lecturer, Dental Biomaterial, Faculty of Oral and Dental Medicine, Beni-Suef University, Egypt

Hebashalabby_dental@yahoo.com

^{3*} Associate professor, Dental biomaterial, faculty of Oral and Dental Medicine, Ain Shams University, Cairo, Egypt

Biomaterials71@gmail.com

^{4*} Assistant Lecturer, Dental Biomaterial, Faculty of Oral and Dental Medicine, MTI University, Cairo, Egypt

Biointegration of orthopedic and dental implants is a prime request for their stability and accordingly adequate performance. This study **aimed to** employ electro-deposition technique for deposition of nano-active ceramic coating layer on dental Ti-alloy implants. Thirty six dental Ti alloy disks were used and divided equally into three groups (n=18). Nano-MgO ceramic layer was electrodeposited by using potentiostate galvanostate at different potentials in hydrated MgO solution (-1800 and -1200 mV) for a constant time (1600 sec) group II and III respectively. Group II and III were compared to native dental Ti-alloy disks represented group I. The different dental Ti-alloy disks were characterized by using XRD and SEM. Group II and I were Biomimetically immersed in SBF for 7 days. Bioactivity of nano-ceramic Ti coating were monitored by using XRD, FTIR and SEM. **Results of** XRD and SEM revealed the deposition of nano-ceramic coating occurred at -1800mV (group II). Biomimetic bioactivity testing indicated the formation of well developed nano-HA crystals with group II rather than group I. **The study Concluded that the** deposition of nano-ceramic MgO layer on dental Ti-alloy surfaces enhanced their bioactivity.

Key Words: Electro-deposit[ion Technique, potentiostate galvanostate, Nano-Bioactive ceramic coating, Dental, Ti-alloy implant, biomimetic. Bioactivity.

Establishment of a novel CV-method to measure real work pieces and comparison with the standard method

Jürgen Schodl, CEST Centre of Electrochemical Surface Technology, Viktor-Kaplan-Straße 2, 2700 Wiener Neustadt, Austria

Günter Fafilek, TU-Vienna, Institute for Chemical Technology and Analytics, Getreidemarkt 9/164ec, 1060 Vienna, Austria

Christoph Kleber, CEST Centre of Electrochemical Surface Technology, Viktor-Kaplan-Straße 2, 2700 Wiener Neustadt, Austria

* juergen.schodl@cest.at

The surface of hot-dip galvanized construction steel can be damaged by mechanical stress and thus the corrosion prevention properties of the native protective layer of the zinc-patina or even of an additional corrosion protection layer is reduced significantly and white rust will be formed. In this work, we present cyclic voltammetry (CV) studies of the corrosion protection properties of different commercial surface finishing systems. Samples with different types of corrosion protection systems (chromium (III)-, silica- and mineral oil-based) were prepared. The application of the corrosion protection systems was carried out by immersing or spraying.

CV measurements were carried out with a novel developed surface mounting technology, which also enables measurements at 3D geometries of the work piece such as in elbows or edgings. The average measurement area was approximately 0.08 cm^2 . The CV data were compared with the standard method DIN EN ISO 6270-2. Results of the CV measurements, as well as data from standard method showed improved corrosion prevention for all three corrosion protection systems. Thus a correlation between the two test methods could be established. Furthermore the investigations showed that with the application technique of immersing, a better corrosion protection effect was achievable in comparison to the spraying technique.

Highly ordered mesoporous silica loaded with dodecylamine for active anticorrosion coatings

J. M. Falcón¹, T. Sawczen¹, I. V. Aoki¹

¹Chemical Engineering Department – Polytechnic School – University of São Paulo
Av. Prof. Luciano Gualberto, travessa 3, nº. 380 - CEP 05508-010-São Paulo-Brazil
E-mail: idavaoki@usp.br

Abstract

The development of nanoscience and technology has drawn significant attention to studies on hollow particles. Among these materials, mesoporous silica nanoparticles have recently attracted much attention as potential nanocontainers due to their high stability, biocompatibility, large surface area, controllable pore diameter and easy surface functionalization. Mesoporous silica nanoparticles can uptake, store and release organic or inorganic molecules of various sizes, shapes and functionalities; hence they have been believed to be ideal nanocontainers for guest molecules. Furthermore, mesopores aligned perpendicular to the hollow cores is much more suitable for encapsulating the guest species and providing a fast diffusion path to the cores. The synthesis of nanoporous materials and more precisely mesoporous materials, which are defined by IUPAC as materials with pore sizes between 2 and 50 nm, is an active field of research. The aim of this work is to study the use of a mesoporous silica with hexagonally ordered tuneable uniform mesoporous (4-14 nm) for active corrosion protection of carbon steel. Mesoporous silica was characterized by X-ray diffraction, thermogravimetry (TGA), differential scanning calorimetry (DSC), transmission electron microscopy (TEM), nitrogen adsorption-desorption isotherms and particle size distribution measurements. Mesoporous silica structures were loaded with dodecylamine and embedded into an alkyd primer with a weight load ratio of 15 wt.% of mesoporous silica. Kinetics of dodecylamine release from mesoporous silica in an aerated 0.1 mol/L NaCl solution for different pH values (2, 9 and 6.2) was studied. The anticorrosive performance of the alkyd primer loaded with 15 wt% of mesoporous silica entrapped dodecylamine was tested on coated carbon steel by direct exposure of the coated samples with a provoked defect to 0.01 mol/L NaCl corrosive media using electrochemical techniques as EIS and scanning vibrating electrode technique (SVET). The results showed that this complex porous system provides high loading capacity and efficient inhibitor release on demand. In addition, due to the pH-stimulated release of inhibitor during the corrosion process, well-pronounced active anticorrosion properties and self-healing were provided and confirmed *in situ* via SVET and EIS measurements. Coated samples were also evaluated in a salt spray chamber and the self healing effect was also noticed.

Self healing organic coatings on aluminium alloy

Amin Firouzi, Alessandra Bianco, Giampiero Montesperelli

University of Rome – Tor Vergata, Department of Enterprise Engineering

INSTM RU, Rome Tor Vergata, Viale del Politecnico, 00133 Rome, Italy

Aluminium and its alloys represent one of the most cost-effective production class of materials because of their high specific strength-to-weight ratio. However, they can be seriously limited by corrosion attack, especially in aqueous electrolytes containing chlorides, which leads to huge economic losses. Therefore, there is a strong demand for surface treatments or coatings to provide long-lasting anticorrosion performance.

Several surface treatments or coatings have traditionally been adopted to improve the corrosion protection of metal alloys. Nowadays, the organic coatings are extensively used to impart corrosion resistance due to their good barrier characteristics, ability to include active anticorrosion pigments, like corrosion inhibitors, and low manufacturing costs.

Nevertheless, these organic coatings show weak mechanical properties compared to the metallic substrate that imply to be damaged by mechanical impacts and lose their protective features.

Hence, design and development of new organic coatings with autonomous self-healing properties have become an important target for many industries in the last years.

This work presents a novel and simple route to produce poly(vinyl alcohol) (PVA) fibrous coatings, loaded with two different cerium (III) inhibitors (i.e., cerium nitrate and cerium acetylacetonate), by means of conventional electrospinning technique onto 6082 aluminium alloy for corrosion protection in 3 wt% NaCl solution. PVA has received many attentions due to its cheapness, good film forming ability, good chemical resistance, interesting mechanical properties and biocompatibility. In order to avoid PVA dissolution in aqueous environment, several cross-linking procedures were assessed.

Collected mats were characterized by several analytical techniques. Electrochemical impedance spectroscopy (EIS) measurements showed that all the investigated coatings possess remarkable corrosion resistance. Self-healing effect has been observed only for artificially damaged coating loaded with cerium (III) acetylacetonate. Inductively coupled plasma mass spectrometry (ICP-MS) confirmed the release of cerium from broken fibers.

Assessment of corrosion performances of Cerium based Silane-Zeolite coatings on AA6061 substrate

Lucio Bonaccorsi¹, Luigi Calabrese¹, Angela Capri¹, Giuseppe Gulli¹, Edoardo Proverbio¹

¹Department of Electronic Engineering, Industrial Chemistry and Engineering
University of Messina, Contrada di Dio, 98166 Messina, Italy

Keywords: sol-gel; silane; zeolite; cerium nitrate; coatings.

Corrosion inhibitors based on cerium represent an interesting alternative to the use of chromates due to their certified toxicity. The presence of eco-friendly cerium ions favors the formation, in characteristic conditions, of protective films on the surface increasing the metal durability. Several research activities were carried out by using cerium based inhibitors with the purpose to investigate on new coatings with high durability and self-repairing properties [1].

In the present work we analyzed the anti-corrosive properties of sol-gel silane-zeolite hybrid coatings, doped with cerium nitrate ions as inhibitor, on AA6061. It was possible to highlight that zeolite coatings evidenced promising results in the field of anti-corrosion coatings [2]. Furthermore zeolites, thanks to their highly porous crystalline structures, can act as nanocontainers of inhibitors ensuring a controlled-release of cerium ions [3]. Three different types of composite coatings were prepared by using cerium doped zeolite and/or silane matrix. For each type, four formulations, varying the zeolite amount (in the range 60-90% wt), were tested.

Chemical-physical properties of the coating were evaluated by adhesion (pull-off and peeling) and wettability tests. The corrosion behavior of the composite coatings was studied during immersion in a 3.5% NaCl solution by electrochemical impedance spectroscopy and potentiodynamic polarization tests.

All composite coating evidenced a high homogeneity and good adhesion performances. Cerium addition in the coating formulation did not compromise the hydrophobic properties of the coating. Furthermore the addition of the cerium ions improved the anti-corrosion properties of the composite films inducing a significant stability of the electrochemical behavior.

References:

- [1] S. Thomas, N. Birbilis, M.S. Venkatraman, I.S. Cole. *Self-repairing oxides to protect zinc: Review, discussion and prospects*, Corrosion Science 69 (2013) pp. 11–22.
- [2] L. Calabrese, L. Bonaccorsi, E. Proverbio, Corrosion protection of aluminum 6061 in NaCl solution by silane–zeolite composite coatings, Journal of Coatings Technology and Research, 9 (5) (2012) pp 597-607
- [3] M.F. Montemor, D.V. Snihirova, M.G. Taryba, S.V. Lamaka, I.A. Kartsonakis, A.C. Balaskas, G.C. Kordas, J. Tedim, A. Kuznetsova, M.L. Zheludkevich, M.G.S. Ferreira. *Evaluation of self-healing ability in protective coatings modified with combinations of layered double hydroxides and cerium molybdate nanocontainers filled with corrosion inhibitors*, Electrochimica Acta 60 (2012) pp. 31–40

Numerical modelling as a tool for the design of self-healing dispersion coatings

Magdalena Walczak

School of Engineering, Pontificia Universidad Católica de Chile, Santiago, Chile

The continuous search for improved performance of protective coatings motivates the application of advanced materials and technologies in the coating formulation. In particular, the feature of enhancing the level of protection as a reaction to the less or more abrupt changes in the surrounding environment, i.e. the ability to self-heal, has been made available. One of the approaches is by incorporation of functional particles to the coating resulting thus in a dispersion coating. Upon the event of corrosion, the particles would enhance the protective function of the coating by acting as corrosion inhibitor or curing agent. The particles may possess this function on their own behalf or serve as carriers of functional agents.

The functioning of self-healing dispersion coatings has been hypothesized since long and the last decade has seen truly smart solutions including dispersion of various types of nanoparticles and/or nanocontainers in metallic, organic as well as inorganic type of coatings. The fabrication and testing of these novel coatings requires significant dedication of economic and human resources because improvement (or not) of the anti-corrosion function is hard to predict. Numerical modelling comes handy in the design of dispersion coatings as it allows reducing the number of experimental trials by rejecting geometrical configurations (coating's thickness, number of dispersed particles, etc.) that impossibly provide the self-healing effect.

In this work the methodology of numerical modelling of corrosion by means of finite element method is presented as applied to the problem a damaged (scratched) coating immersed in an aggressive electrolyte. In each point of the electrolyte, flux of each of the involved species is determined as resulting from diffusion, electromigration and, when corresponding, homogeneous reaction. Flux of species involved in the electrochemical reactions is described by means of the Butler-Volmer kinetics, whereas passivity results from precipitation of solid species at the surface. Applicability of the electroneutrality condition is discussed.

Applicability of the method to the design of a metallic dispersion coating is presented by demonstrating the effect of the geometrical parameters on the overall efficiency of the coating, with special account on the self-healing effect. In addition, the role of the type of the employed corrosion inhibitor as well as variables of the environment (pH, concentration of salts) are discussed. Finally, some general guidelines and limitations of the methodology are presented.

L-Cysteine intercalated layered double hydroxide as anticorrosive agent for organic coatings

Presenting: Thomas STIMPFLING, co-authors: Horst HINTZE-BRUENING**, Patrick KEIL**, Hubert THEIL**, Fabrice LEROUX**

* Institut de Chimie de Clermont-Ferrand, 24 avenue des landais 63171 AUBIERE, France.

** BASF Coatings GmbH, Glasuritstrasse 1, 48165 Muenster, Germany.

Because of its high toxicity, chromate-based anticorrosion pigments widely used in transport application, have been banished and alternatives are intensively investigated. An original and elegant concept is to host the substitute corrosion inhibitor (an amino acid, especially L-Cysteine) into an inorganic framework like layered double hydroxide (LDH) materials. LDH platelets have been chosen because of their ability to release the entrapped anticorrosive anion via exchange reaction (basic media) or inorganic framework dissolution (acidic media) allowing the protection of aluminium alloy 2024 when facing cathodic and anodic corrosion phenomena, respectively. The inhibition efficiency of L-Cysteine and chromate anions has been evaluated and compared by using electrochemical experiments performed in 0.005M NaCl solution. After 15 cycles of linear polarization, L-Cysteine presents an inhibition-efficiency close to that of chromates. Furthermore, L-Cysteine anions intercalated into a LDH host structure are found to be released during exposure to corrosive media. X-ray diffraction analysis proves that L-Cysteine may completely be leached out of the LDH platelets after short exposure time in corrosive media. When LDH/L-Cysteine pigments are dispersed into epoxy primer coating and directly applied to the AA 2024 substrate, a "self-healing"-type behaviour is demonstrated using electrochemical impedance spectroscopy experiments with long exposure times. The evolution of the coating resistance (R_c) and oxide layer resistance (R_{ox}) values during exposure time both indicate an enhancement of the barrier property as well as the corrosion inhibition effect due to the presence of LDH/L-Cysteine as a functional filler. Finally, tests provoking filiform corrosion reveal that the presence of LDH/L-Cysteine effectively decreases the corrosion propagation.

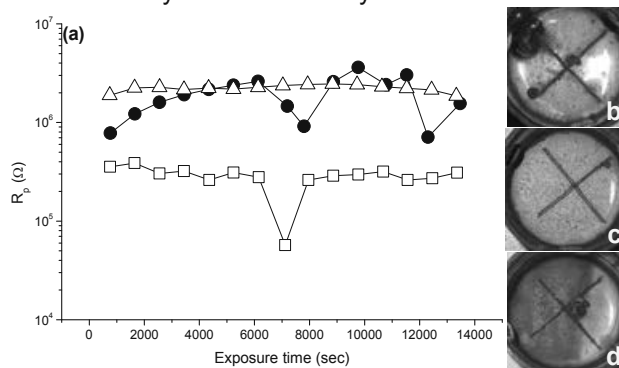


Fig. 1. a) Corrosimetry experiment performed in 0.005M NaCl (additive free \square , LDH/L-Cysteine \triangle and LDH/ CrO_4 \bullet additives, respectively) and visual observation performed on epoxy primer unfilled (b), filled with LDH/L-Cysteine (c) and LDH/ CrO_4 (d) as fillers after 72 days of exposure time in 0.005 M NaCl solution.

Micro-electrochemical study of organic corrosion inhibitors for AA2024

F. Andreatta¹, I. Recloux², L. Pausa¹, M. Mouanga², M. Olivier², L. Fedrizzi¹

¹ *Department of Chemistry, Physics and Environment, University of Udine, Italy*

² *University of Mons (UMONS), Materials Science Department, Belgium*

Inhibition mechanisms of active corrosion species are strongly related to microstructure in aluminium alloy AA2024. In particular, organic inhibitors might lead to the formation of insoluble compounds providing an inhibiting action on the substrate corrosion. As an example, triazole derivatives are well-known for their ability to reduce cathodic and anodic activities at the sites of intermetallics. Nevertheless, contradictory information is found in the literature about the ability of such compounds to form a protective film on the matrix.

The organic inhibitor selected for this work is benzotriazole. The micro-electrochemical behaviour of this organic corrosion inhibitor was investigated using the electrochemical micro-cell technique. This technique enables the investigation of small areas with resolution in the micrometer range by the use of glass capillaries to define the area of the working electrode. In particular, the paper focuses on the different behaviours of areas containing different types of intermetallics and areas without inclusions (matrix). Moreover, the deposition of benzotriazole was investigated by complementary surface analysis techniques in order to study the morphology and the chemical composition of adsorbed compounds on the substrate. EIS measurements and polarization curves were also carried out at the large scale in sodium chloride solution in order to quantify the inhibition effect with immersion time and the durability of the inhibitive layer and to help the interpretation of local electrochemical data obtained by micro-cell.

Coating self-healing effect by loading microcapsules with two-component epoxy film former

Fernando Cotting, Idalina Vieira Aoki.

Chemical Engineering Dept, Polytechnic School, University of São Paulo, São Paulo/Brazil

Abstract

Due to common defects presented in paint layers, systems capable of providing prolonged protection to the substrate should be developed. The encapsulation technique of repairing agents in polymeric microcapsules is an attractive alternative of self-healing systems. After the encapsulation of these substances in a polymeric wall, the microcapsules are doped in a primer and applied on a metal substrate. When the coating is damaged, the microcapsules are ruptured, releasing the protective agent.

The development of smart coatings by additivition of microcapsules in polymeric coatings is reported in literature. Several papers were published which after coating suffering a mechanical defect, corrosion inhibitors and even film formers were released from microcapsules for prolonged protection of the metal substrate. Nevertheless, these repair agents provide a short and low protection against corrosion as compared to an epoxy two-component system.

In this work, the two components of an epoxy resin – A epoxy resin and B curing agent - were separately encapsulated into urea formaldehyde microcapsules. Both microcapsules were doped into an epoxy coating on carbon steel, in order to evaluate the self-healing effect. By the images of optical microscopy, it was perceived the release of the epoxy resin components after crushing of the microcapsules. The morphology of the microcapsules was evaluated by scanning electron microscopy (SEM). The evaluation of performance was obtained by EIS and SVET electrochemical techniques and by accelerated corrosion tests in a salt spray chamber. Results showed that the two-component epoxy film former has an excellent self-healing effect and showed a better performance when compared to a self-healing system obtained from microcapsules containing a classic film former like linseed oil.

Keywords: self-healing coatings, polymeric microcapsules, epoxy two-component film former.

Non-destructive In-situ Characterization of Microcapsules and Self-healing Coatings using Confocal Raman Spectroscopy

Alexander Lutz^{a,b}, Iris De Graeve^a, Herman Terryn^a, ^aVrije Universiteit Brussel, Group of Electrochemical and Surface Engineering, Belgium, ^bvzw SIM Flanders, Belgium

At least since the paper of White et al.¹ the integration of microcapsules into coatings for corrosion protection is a topic of high interest in the corrosion community². Various groups have performed research on different kind of capsules or containers for different types of coatings. Self-healing coatings with extrinsic polymer repair mechanisms as well as corrosion inhibition mechanisms have been developed.

Most containers up to now have been characterized ex-situ in SEM and TEM when they were not in the coating or by taking cross-sections. However, the sample preparation for such analysis has disadvantages: Samples need to be broken in liquid nitrogen and are analyzed under high vacuum conditions, capsules fall out of the coating, etc. Moreover, capsules with a liquid content like monomers cannot be put into vacuum chambers for obvious reasons. Two other interesting points are the determination of the location of capsules in a coating as well as the question whether the capsule content actually survives the coating procedure.

Therefore a technique is necessary which can differentiate between different molecules. This needs to be done at a spatial resolution in the micrometer – preferably down to the nanometer – range. Just as well it needs to be able to record the information in depth and especially without altering the sample. Besides, it would be advantageous if the sample size would be without narrow constraints.

Confocal Raman Spectroscopy fulfills these requisites by recording Raman shift spectra of a point location where the laser is focused on in ambient environment. Filled microcapsules in a coating could be distinguished from empty ones and their location (x, y and z) in the coating could be identified by using Confocal Raman Spectroscopy. To the authors' knowledge there is no other straightforward technique to obtain these results at this scale.

These and further results will be presented in order to show and to discuss with the corrosion community and especially the coating community the advances which can be made with this technique.

- (1) White, S. R.; Sottos, N. R.; Geubelle, P. H.; Moore, J. S.; Kessler, M. R.; Sriram, S. R.; Brown, E. N.; Viswanathan, S. *Nature* **2001**, 409, 794–7.
- (2) Binder, W. *Self Healing Polymers*; Binder, W., Ed.; 2013.

Recent Developments on Microencapsulation for Autonomous Corrosion Protection

L.M. Calle,¹ W. Li,² J.W. Buhrow,² L. Fitzpatrick,² S.T. Jolley,² J.M. Surma,² B.P. Pearman,¹ and X. Zhang¹

¹NASA, Kennedy Space Center, FL 32899, United States

²ESC-QNA, Kennedy Space Center, FL 32899, United States

Abstract

The work presented on this paper concerns recent progress in the development of a multifunctional smart coating based on microencapsulation for the autonomous control of corrosion. Microencapsulation allows the incorporation of desired corrosion control functionalities, such as early corrosion detection and inhibition through corrosion controlled release of corrosion indicators and inhibitors, as well as self-healing agent release when mechanical damage occurs.

While proof-of-concept results have been reported previously, more recent efforts have been concentrated in technical developments to improve coating compatibility, synthesis procedure scalability, as well as fine tuning the release property of encapsulated active agents.

Development of Self Healing Polymer Coatings On Metals

A.Lutz, I. De Graeve, H.Terryn

Vrije Universiteit Brussel (VUB)

Research Group Electrochemical and Surface Engineering (SURF), Department
Materials and Chemistry, hterryn@vub.ac.be, www.vub.ac.be/SURF

The concept of self healing materials is currently a fast developing research area in materials science with a wide range of promising industrial applications. Self healing concepts are built in traditional materials such as concrete, metals, ceramics, and composites. Additionally development of new generations of coatings is considered with self repair capabilities. Several polymer synthesis [1] routes are explored making use of both non autonomous [2] (trigger is eg heat) as well as autonomous repair [3]. This polymer approach is combined with inhibitor selections making use of high throughput electrochemical investigations to tackle multi metal approaches [4]. To study in detail the combined working principles of the encapsulated inhibitor and the repair of the barrier polymer properties in a created defect we are making use of complementary advanced local electrochemistry set ups such as Scanning Electrochemical Microcopy [5], Scanning Vibrating Electrodes [6], Scanning Selective Ion Selective Electrodes [7] and a new developed EIS approach [8]. This information is complemented with several spectroscopic and electron microscopy analyses. The overall approach will be discussed in detail making use of a thermo reversible polymer [8] systems developed at VUB. This physically cross linked polymer system shows a self-healing ability based on the fracture and reformation of thermally reversible physical bonds in the polymer matrix. Because heat is necessary to trigger and assist the healing process, these materials are classified as non-autonomic healing polymers. Additionally inhibitors were added to the coating formulation. As such the feasibility was shown that a multiple action self-healing coating system on a metal was feasible to create.

Acknowledgements: SIM-Flemish partners of the project “NAPROM”, Vrije Universiteit Brussels, University of Ghent and University of Antwerp and of Tu Delft.

References

- 1) S.J. García, H.R. et al Progress in Organic Coatings 72 (2011) 211– 221
- 2) J.-B. Jorcin et al., Electrochimica Acta 55 (2010) 6195–6203
- 3) S.J. García, et al Prog. Org. Coat. 70 (2011) 142
- 4) S.J. García Surface and Interface Analysis (2011) 205-210
- 5) Y. González-García, et al. Electrochem.Comm 13 (2011) 169-173
- 6) Y Gonzalez-Garcia et al., Electrochimica Acta 56 (2011) 9619-9626
- 7) T. Breugelmans et al. Progress in Organic Coatings 69 (2011) 215-218
- 8) G. Scheltjens et al Journal of Thermal Analysis and Coulometry 105 (2011) 805-809

Design and Analysis of Multi-Layer Self-Healing Coatings tailored for Smart Corrosion Protection

T.H. Tran¹, A. Vimalanandan¹, J. Fickert², K. Landfester², D. Crespy², M. Rohwerder¹

¹ *Max-Planck Institut für Eisenforschung GmbH, Düsseldorf/Germany;*

² *Max-Planck Institut für Polymerforschung, Mainz/Germany*

Corrosion protection by application of coatings is often the best choice regarding economic and ecologic factors. Besides high barrier properties of the coatings, the addition of corrosion inhibitors can further improve the corrosion protection capability. One of the most effective and most used corrosion inhibitors are based on chromium (VI). Due to environmental- and health related concerns the use of chromium (VI) as a corrosion inhibitor has been restricted. As a consequence of its wide ranging restriction, smart corrosion protection concepts are subject of extensive research in order to find alternatives for achieving high end corrosion protection similarly to the one achieved with chromium (VI). Smart corrosion protection refers to an autonomous ability for a targeted delivery of corrosion inhibitors to a corrosion site only when this starts to actively corrode. Hence, a corrosion sensing trigger adjusted to the corrosion conditions of the particularly metallic element is necessary to initiate the corrosion inhibitor release and thereby the self-healing process. Possible release triggers are changes in pH-, ionic strength or the electrochemical potential [1].

The next conclusive step after successful corrosion inhibition is an actual site selective self-healing by forming a protective and insoluble polymeric barrier film isolating the inhibited metal surface from water and ions which cause corrosion. Ideally, the self-healing process should take place under ambient conditions. In this work the ring opening metathesis polymerization (ROMP) was selected as the self-healing reaction. The ROMP leads to the formation of a thin polymer film that seals off the defect and stops the further corrosion. For that purpose, a multi-layer self-healing coating system comprising a metal/nano-composite coating with electro-codeposited surface modified pH-responsive nano-container filled with catalyst and an organic top coating with embedded pH-responsive nano-container filled with self-healing agents are investigated. The storage of the catalyst in the metal coating ensures that it remains active even after month or years. The release of the self-healing agent and the catalyst is exclusively triggered by a pH-change to higher values during active corrosion. The characteristics and self-healing performance of the multi-layer self-healing coating system are investigated and discussed in detail via Scanning Kelvin Probe (SKP) and additional analytical methods.

References:

[1] a) A.Vimalanandan., L.P. Lv., T.H. Tran, K. Landfester, D. Crespy, M. Rohwerder, *Adv. Mater.* **2013**, DOI: 10.1002/adma.201302989. b) L.P. Lv, Y. Zhao, N. Vilbrandt, M. Gallei, A.Vimalanandan, M. Rohwerder, K. Landfester, D. Crespy, *J. Amer. Chem. Soc.* **2013**, 135, 14198 c) M. Rohwerder, S. Isik-Uppenkamp, C. A. Amarnath, *Electrochim. Acta* **2011**, 56, 1889. d) M. Rohwerder, A. Michalik, *Electrochim. Acta* **2007**, 53, 1300. e) J. Fickert, P. Rupper, R. Graf, K. Landfester, D. Crespy, *J. Mater. Chem.*, **2012**, 22, 2286.

Fundamental Investigation on the Mechanism of Capsule Based Redox-Responsive Self-Healing Coatings

Ashokanand Vimalanandan¹, Li-Ping Lv², The Hai Tran, Katharina Landfester²,
Daniel Crespy² and Michael Rohwerder¹

¹ Max-Planck-Institut für Eisenforschung GmbH, Max-Planck-Str. 1, 40237 Duesseldorf, Germany – e-mail: a.vimalanandan@mpie.de

² Max-Planck-Institut für Polymerforschung, Ackermannweg 10, 55128 Mainz, Germany

Autonomous self-healing coatings for corrosion protection of metals are the focus of intense academic and industrial research. In case of damage of the coating and exposure of the metal to corrosive environment, these coatings should provide active and case responsive corrosion protection mostly by release of corrosion inhibitors.

Release of inhibitors occurs by either mechanical damage of the coating or by utilizing triggers such as pH-change, ionic strength or the electrochemical potential change. Recently a new capsule based concept has been introduced for the electrochemical potential triggered release of corrosion inhibitors [1, 2]. For the first time the design and application of a smart coating based on conducting polymer has been achieved for the corrosion protection of galvanized steel. Even though remarkable results have been achieved with the concept, further fundamental questions have to be addressed before the idea can be transferred to an industrial relevant product.

Recent results unraveled that the cathodic delamination is a key factor for release of inhibitors, fast signal spreading and self-healing of a defect. The inter relation between the efficiency of the inhibitor and the design of the coating system (e.g. latex based coating system) on the self-healing performance are the focus of this work and advanced surface analytical and electrochemical methods have been used to strengthen the conclusions.

[1] A.Vimalanandan, L.-P. Lv, T.H. Tran, K. Landfester, D. Crespy, M. Rohwerder, *Adv. Mater.* **2013**, 25, 6980.

[2] L.-P. Lv, Y. Zhao, N. Vilbrandt, M. Gallei, A.Vimalanandan, M. Rohwerder, K. Landfester, D. Crespy, *J. Amer. Chem. Soc.* **2013**, 135, 14198.

Keywords : capsules - conducting polymers - miniemulsion technique - Scanning Kelvin Probe - smart coatings

Self-healing properties of Smart coating for hot dip galvanized steel

Wei-Jen Li, C.Y. Tsai, C.J. Lu

Industrial Technology Research Institute, Hsinchu/Taiwan

Hot-dip galvanized steel (GI steel) provides superior sacrificial cathodic protection for steel. To further protect GI steel against corrosion during transportation and storage, hexavalent Cr coating is generally applied onto the GI steel surface. Hexavalent Cr coating not only provide barrier layer protection, but also offers superior self-healing protection via the release of corrosion inhibitor from the coating. However, hexavalent Cr is highly toxic and its use has been strictly restricted according to international regulations such as RoHS and WEEE. Recently, a smart polymer coating with self-healing ability afforded by microencapsulation technology has been developed. Various corrosion inhibitors, such as cerium nitrate, molybdate have been encapsulated, and these microcapsules in the polymer coating can release healing agent to the damaged region of the coating. Vanadate is an effective corrosion inhibitor for Zn or Al alloy. This study developed a smart polymer coating with self-healing ability afforded by the incorporation of microcapsules containing vanadate as healing agent. The self-healing behaviour was evaluated by SEM analysis, EIS analysis and salt spray test, and the self-healing mechanism was further proposed and discussed.

“Green” encapsulation of corrosion inhibitors for smart coatings

Abdulrahman Altin^{1,a}, *Michael Rohwerder*^{1,b} and *Andreas Erbe*^{1,c}
¹ *Max-Planck-Institut für Eisenforschung GmbH, Düsseldorf/Germany,*
e-mail: ^aaltin@mpie.de, ^brohwerder@mpie.de, ^cerbe@mpie.de

Keywords: smart coatings, cyclodextrin, corrosion protection, self-healing, Scanning Kelvin Probe

Abstract

Corrosion of metal is a serious issue in all metal-processing industries. Despite the excellent performance of coatings containing chromium(IV) to protect metals against corrosion, its toxic and carcinogenic properties led to a legal ban. Hence, there is an urgent need for alternative concepts, which are economically and ecologically accepted.

We will show that cyclodextrin based organic coatings promise a “green” encapsulation concept of corrosion inhibitors for intelligent corrosion protection. Cyclodextrins are cyclic oligosaccharides produced from starch by means of enzymatic conversion. They are mainly used in the pharmaceutical industry for drug delivery, especially to increase the controlled release of poorly soluble pharmaceuticals in the human body. Furthermore it protects highly sensitive chemical agents against external influences such as oxidation or reduction. Additionally due to its hydrophilic shell, a better transport of high hydrophobic substances in aqueous solutions is enabled.

In this study, successful incorporation of different corrosion inhibiting agents with cyclodextrins is shown. Subsequently, the delamination kinetics of coatings containing the resulting complexes on different metals (Fe, Zn, Al) were investigated. The release of the inhibitors is triggered by increase in pH, initiated by the corrosion process of the metal. Controlled release and the effect on the delamination of the composite coatings were investigated with a number of different techniques, including Scanning Kelvin Probe and electrochemical impedance spectroscopy. The results suggest that cyclodextrins may play a role in smart and “green” encapsulation concepts for corrosion inhibitors to protect metals against corrosion.

Encapsulation of corrosion inhibitors in a self-healing polymeric coating

Hilke Verbruggen¹, Alexander Lutz^{1,2}, Herman Terryn¹, and Iris De Graeve¹

¹*Research Group Electrochemical and Surface Engineering (SURF)
Vrije Universiteit Brussel, Pleinlaan 2, B-1050 Brussel, Belgium*

²*SIM vzw Technologiepark 935, B-9052 Zwijnaarde, Belgium*

For the corrosion protection of metallic structures a new type of coating, which is in line with the general need for more sustainable materials, has been developed: self-healing polymeric coatings. Whereas the conventional organic coatings were designed only to prevent damage, these “smart” coatings – inspired on nature – are able to cope with possible damages. This grants them an extended lifetime.

In this work the concept of a multiple action self-healing coating is considered. This coating combines an active action of incorporated corrosion inhibitors for immediate metal passivation in case of local damages to the coating, with a defect repair mechanism of the polymeric matrix coating (thermally triggered) resulting in the recovery of the barrier properties.

The present work focusses on the encapsulation and leaching out of the corrosion inhibitors. The organic inhibitor 2-mercaptobenzothiazole (MBT) is encapsulated in two different ways: either in porous silica nano-spheres[1] or intercalated in layered double hydroxides [2]. These capsules are studied by means of electron microscopy, voltammetry, amperometry and (surface-enhanced) Raman spectroscopy (SERS). Further the capsules are incorporated into the self-healing coating and applied on a galvanized steel substrate. The multiple action self-healing coating is then evaluated by electron microscopy, SERS, X-ray photoelectron spectroscopy, and electrochemical techniques (electrochemical impedance spectroscopy and scanning vibrating electrode technique).

The use of SERS for this purpose seems unique, and also very promising as it has the advantage to detect very small amounts, even monolayers.

References

- [1] Chen, H.; He, J.; Tang, H.; Yan, C. *Chemistry of Materials* **2008**, 20, 5894.
- [2] Poznyak, S.K.; Tedim, J.; Rodrigues, L.M.; Salak, A.N.; Zheludkevich, M.L.; Dick, L.F.P.; Ferreira, M.G.S. *ACS Applied Materials & Interfaces* **2009**, 1, 2353.

Metal Dusting Protection by a Novel Coating, Providing a Classical Oxide Barrier as well as Catalytic Inhibition

*S. Madloch, M.C. Galetz, M. Schütze,
DECHEMA-Forschungsinstitut, Frankfurt/Main, Germany*

Metal dusting is a severe form of corrosion, which occurs in high carbon activity atmospheres at temperatures of 400-900°C (e.g. in reformer or coal gasification plants). Affected materials are steels and nickel base alloys because of the catalytic effect of nickel and iron on the dissociation of carbon containing gas species, uptake and subsequent graphite nucleation inside the material. Conventional protection is given by dense oxide scale forming coatings and the use of alloys with high amounts of oxide scale forming elements.

Since metal dusting involves catalytic surface interactions, a new functional coating approach was developed at the DECHEMA-Forschungsinstitut DFI. Combination of an electrochemical nickel plating step with subsequent tin powder pack cementation led to the formation of an intermetallic Ni-Sn layer. Alloying nickel with tin, blocks the catalytically active centers for surface reactions with carbon. It has been reported that graphite nucleation on nickel or cementite could be correlated with epitaxial similarities between those species. The change of the crystal structure of nickel by tin seems to inhibit the nucleation of graphite as well. Exposure tests of Ni-Sn coated samples (coating thickness 7-10 µm) at 650°C under metal dusting conditions (74% H₂; 24% CO; 2% H₂O) showed great improvement. Since the Ni-Sn coating is prone to oxidizing environments, the functional coating was further supplemented by an enrichment of oxide scale forming elements to provide a sufficient oxygen protection. The resulting coating gives a dual protection, classical oxide barrier (conventional approach) combined with catalytic inhibition.

Combination of CVD coatings and halogen effect to prevent high-temperature embrittlement in titanium aluminides

J. Grüters, M.C. Galetz, M. Schütze

DECHEMA-Forschungsinstitut, Theodor-Heuss-Allee 25, 60486 Frankfurt/Main, Germany

With increasing ecological and economical requirements intermetallic TiAl-based alloys represent an important class of high temperature structural materials providing a unique set of physical and mechanical properties that can lead to substantial payoffs in industrial applications, e.g. for turbine blades or turbolader wheels. With less than half the weight of nickel-base alloys, which are currently in use in combination with excellent high temperature properties, TiAl-based alloys have the ability to reduce the engine weight and to improve efficiency. Because of their insufficient oxidation resistance and embrittlement at higher temperatures ($> 700^{\circ}\text{C}$) the surface of titanium aluminide alloys has to be modified in order to effectively replace the heavier nickel-base alloys.

A combination of Al enrichment plus additional fluorine treatment is used to protect the alloy against rapid inward diffusion of oxygen at high temperatures which leads to structural damage of the material. Indeed, Al-rich coatings plus fluorine are expected to promote the formation of a protective alumina layer at high temperatures which not only protects the alloy from oxidation, but also impedes embrittlement at high temperatures.

To achieve this aim advanced coatings are produced either by pack cementation or by metal-organic chemical vapor deposition (MOCVD) and additionally fluorine is deposited by spraying with a fluorine polymer. It turns out that Al pack powder mixtures produce a multi-layered coating with the brittle TiAl_3 and TiAl_2 and an inner zone of TiAl. Whereas Cr-Al pack powder mixtures of reduced chemical Al activity form thinner Al-rich coatings. Here, thin bi-layered coatings of TiAl_2 and TiAl are formed. Surface modification via MOCVD produces a very thin coating consisting of Al, O and C. The coating effect on the oxidation behavior of the titanium aluminide alloys is examined under isothermal and thermocyclic conditions ($800\text{--}1000^{\circ}\text{C}$) in air and the mechanical properties of coated and uncoated samples after atmospheric exposure are compared using 4-point bend tests to investigate the room temperature strength and ductility.

Surface modification of thermal barrier coatings by defocused laser phosphate and treatments

M. Shoeib, CMRDI, Cairo/ET; K. Ahmed, Arab Institute for Advanced Technology, Cairo/ET

Aerospace gas turbine engines are now designed such that the heat resistant super alloys operate at temperature very close to their melting, so current strategies for performance improvement are centered on thermal barrier coatings. Lower thermal conductivities lead to temperature reductions at the substrate/bond coat interface which slows the rate of the thermally induced failure mechanisms. Alternatively, lower thermal conductivity TBC layers might allow designers to reduce the TBC thickness there by decreasing the significant centrifugal load that the mass of the TBC imposes on the rotating turbine engine components. One approach to improve TBC system is to optimize the pore morphologies in order to reduce the thermal conductivity while still retaining high in-plane compliance. The second approach to improve TBC system performance is to optimize the surface microstructure, surface densification, phase structures mechanical characteristic, chemical structure, and thermo-physical properties. The main focus of this work is to study the influence of Al PO₄ (and laser)-sealed ZrO₂-MgO coatings on thermal barrier coating system comprised of zirconia stabilized with magnesia top coat to predict the best improvement of TBC system and to optimize the surface microstructure, surface densification, phase structures, mechanical characteristic, chemical structure, and thermo-physical properties as well as their properties with those obtained using reference techniques. Thermal expansion studies were used to study the high temperature stability of the different coatings (reference and modified coatings) structures. As low thermal conductivity is one of the most important features of TBC, thermal diffusivity and specific heat measurements were carried out. Also the mechanical measurements (e.g. micro-hardness, tensile bond strength, young's modulus), phase analyses using XRD and chemical analysis using electron dispersive X-ray (EDX) for elemental analysis in scanning microscopy studies.

Improvement of turbine blade by using protective ceramic coating

Saeid sohrabi, azad university of najaf abad, Isfahan-iran

Ahmad Saatchi, Isfahan university of technology, Isfahan-iran

Reza ebrahimi, azad university of najaf abad, Isfahan-iran

Abstract

Turbines are considered as an initial element of power station factories, which have a key role in functionality of the power station. Due to high cost production of turbine components, increasing service time and efficiency has been one of the most important issues for manufacturer. Super alloys are most favorite materials for this special application. However, corrosion is inevitable cause for the super alloys, thereby reducing service cycle. One of reliable solution for enhancing of the turbine blade is to be protective ceramic coating, by which super alloys are protected in corrosive ambient. In this research, a protective layer of aluminum oxide was coated by electrolyte plasma method on super alloy inconel 738LC. The passive layer is being characterized from both mechanical and physical point of view. Moreover, corrosion resistance properties were evaluated by *potential static* test. Morphological investigation, which is done by electron microscopy, shows a protective layer with 13.3 μm in thickness. X-ray diffraction and EDX analysis confirmed aluminum oxide as major phase of the layer. Mechanical performance of sample with protective coating is considerably enhanced rather than that sample without coating. In addition corrosion characterization showed that the layer increased sensibly resistance to corrosion.

Keyword: Turbine, Superalloy, protective coating, electrolyte plasma

Wavelet transform electrochemical noise analysis for intermetallic coatings at 750 °C in molten salt environment

A. García, Departamento de Investigación en Física-Universidad de Sonora, Sonora, México;

E.F. Díaz, S. Serna, J. Colin, A. Torres-Islas, M. A. Lucio-García, CIICAp-FCQel-UAEM, Cuernavaca, México;

Localised corrosion at high temperature is the most dangerous form of corrosion, which often causes unexpected and rapid damage to a very small portion of a metal structure. Electrochemical noise (EN) measurement can provide information about both the rate and the mechanism of a corrosion process. The intensity of the corrosion process is associated to the amplitude of the fluctuations observed in electrochemical noise records (ENRs) and their shape related with the type of corrosion process. Most ENRs are characterised by a high number of overlapped transients. Hence, the signal analysis requires adequate mathematical tools. The wavelet analysis is a mathematical tool for data processing and has been proposed since 90 decade as an alternative to Fourier transform when a precise time-scale analysis is required or to study transients into a signal. The aim of this work is to show that wavelet analysis can be a valuable option to process ENRs data obtained from high temperature intermetallic coating corrosion.

Development of Fe doped Ni-Co spinel for use in SOFC interconnects

*Alexander Bervian, Gustavo A. Ludwig, Matias A. de Korb, Célia de F. Malfatti,
University Federal of Rio Grande do Sul, Porto Alegre/Brazil*

Fuel cells are an attractive alternative for the production of energy with few environmental impacts and high yield conversion of chemical energy into electrical energy. Interconnects in Intermediate Temperature Solid Oxide Fuel Cell (ITSOFC) provide electric contact between the electrodes as well as separation of air and fuel. The metallic interconnect has many advantages of low material cost, good mechanical properties, high thermal conductivity and easy manufacturing process to large area. However, one major concern with metallic interconnects is their oxidation during ITSOFC operation (600 – 800 °C), which affects their long-term stability and contact resistance. One approach to improving the oxide growth resistance of metallic interconnects is to apply a coating that may reduce the rate of oxide formation as well as modify the properties of the oxide that is generated by the substrate. Therefore, compact, electronically conductive and low-cost surface coatings for metallic interconnects need to be developed. The oxides of type spinel are more applicable due to its thermal expansion coefficient compatible with the other components, barrier volatilization of chromium and oxygen diffusion. The aim of this work is to obtain coatings based Fe doped Ni-Co, using the technique of dip-coating on ferritic stainless steel. After heat treatment, we obtain the phase of the spinel in order to protect stainless steel against oxidation, other than those previously reported. The films are characterized by SEM, EDS, XRD and also for adherence. We intend to develop a uniform film, adherent and without cracks.

Influence of CaO and CeO₂ coatings on the oxidation of nickel polycrystals

N. Halem, Z.Halem*, M. Abrudeanu**, G. Petot-Ervas***

Materials Physico-Chemical laboratory, University Mouloud Mammeri, 15000 Tizi-Ouzou, Algérie

*Campus Chaab Ersas, Constantine, Algeria.

** University of Pitesti, LSIM I134, Pitesti, Romania

***SPMS/CNRS Ecole Centrale Paris, Châtenay Malabry and CEA/DEN,DMN, Saclay, Gif sur Yvette, France

Abstract The present study is concerned with the influence of CaO or CeO₂ sputter-coatings on the oxidation behaviour of specpure Ni polycrystals. The experiments were performed in air, in the temperature range 800°-1200°C. These coatings, which are incorporated in the growing oxide scale, reduce the oxidation rates at $T < 1200^{\circ}\text{C}$. The oxidized specimens were examined by SEM, X-Ray diffraction, and EPMA analysis. The calcium and cerium profiles through the layer are smooth. However, they show a local higher concentration than the limit of solubility near the position of the original metal surface, at $T < 1100^{\circ}\text{C}$. The presence of precipitates leads then to a diffusion blocking effect, which contributes to the beneficial influence of these coatings. Furthermore, a higher amount of calcium was observed in the outer layer, while the amount of cerium increases in the inner layer. This observation shows that $D_{\text{Ca}} > D_{\text{Ni}} > D_{\text{Ce}}$, due to a kinetic demixing of the cations in the growing oxide layer.

The effect of the a double coating layer–oxide phase (NiFe_2O_4) combined with perovskite phase ($\text{La}_{0.6}\text{Sr}_{0.4}\text{CoO}_3$) on a ferritic stainless steel

*Diego Afonso da Silva Lima , Gustavo Alberto Ludwig, Matias de Angelis Korb,
Alexander Bevia, Célia de Fraga Malfatti, Iduvirges Lourdes Müller
LAPEC – Laboratory of Corrosion Research
PPGE3M
Federal University of Rio Grande do Sul, Brazil*

Considering the reduction on the solid oxide fuel cells working temperatures to a range from 600 °C and 800 °C, metallic alloys have been used as interconnects for these cells (ITSOFC). In this way, the ferritic stainless steels have been considered due to their adequate properties such as electrical and thermal conductivity, thermal expansion coefficient compatible with other cell components and low cost comparing to other metallic alloys. However, at high temperatures the ferritic stainless steel starts to suffer oxidation, forming a chromium oxide layer, which acts as electrical insulator. Furthermore, chromium migration may happens from the interconnector to the cathode, originating new phases, which in general act impairing the device performance. In order to solve this problem, ceramic protective coatings have been considered. Among the proposed coatings, ceramic perovskite type and the spinel type oxide have been used. The oxides of the spinel type are proposed to have the diffusion barrier property of chromium through the coating. In this context, the aim of the present work is coated AISI 430 stainless steel with a double layer constituted firstly of a Fe-Ni based coating produced by the electrodeposition technique, coated with a second La, Sr and Co layer produced then by the spray pyrolysis technique. The coatings were heat treated, in order to obtain the desired spinel (NiFe_2O_4) and perovskite ($\text{La}_{0.6}\text{Sr}_{0.4}\text{CoO}_3$) type phases. The coatings were characterized regarding their morphology, chemical composition and crystalline structure using Scanning Electron Microscopy (SEM), Energy Dispersive Spectroscopy (EDS) and X-Ray Diffraction respectively. Besides that, the oxidation resistance of the coatings will be analysed. It is expected to produce a homogeneous and oxidation resistant coating while avoiding the formation of chromium oxide.

Oxidation resistance ferritic stainless steel AISI 430 coated with spinel based Fe doped Ni-Co

Alexander Bervian, Gustavo A. Ludwig, Matias A. de Korb, Célia de F. Malfatti, Laboratory of Corrosion Research (LAPEC), PPGE3M, Federal University of Rio Grande do Sul, Porto Alegre/Brazil

Fuel cells are an attractive alternative for the production of energy with few environmental impacts and high yield conversion of chemical energy into electrical energy. In order to multiply the SOFC electrical power, a series of single cells is connected by interconnects. The Interconnects provide electric contact between the electrodes as well as separation of air and fuel. The metallic interconnect has many advantages of low material cost, good mechanical properties, high thermal conductivity and easy manufacturing process to large area. However, one major concern with metallic interconnects is their oxidation during the ITSOFC (intermediate temperature solid oxide fuel cell) operation, which in a temperature range between 600 and 800 °C. The oxidation can affect their long-term stability and contact resistance. One approach to improving the oxide growth resistance of metallic interconnects is to apply a coating that may reduce the rate of oxide formation as well as modify the properties of the oxide that is generated by the substrate. Therefore, compact, electronically conductive and low-cost surface coatings for metallic interconnects need to be developed. The aim of this work is to develop a conductive ceramic coatings for application as interconnector in Intermediate Temperature Solid Oxide Fuel Cell. The oxides of type spinel are more applicable due to its thermal expansion coefficient compatible with the other components of the cell. Besides, this coating can promote a barrier to the chromium volatilization and oxygen diffusion. In this work coatings based Fe doped Ni-Co will be to attain by of dip-coating process on ferritic stainless steel AISI 430. After heat treatment, it is intended to obtain the phase of the spinel in order to protect stainless steel against oxidation, other than those previously reported. The films will be characterized by SEM, EDS, XRD, oxidation resistance and also for adherence. It is porpuse to develop a uniform film, adherent and without cracks and fissures.

Risk Based Inspection

Angelo Pette, Bureau Veritas Italia S.p.A., Rome/Italy,

The most rapid way in order to reduce maintenance and inspection costs

The OIL&GAS industry performance indicator (Solomon) shows that some companies are falling behind their competitors in terms of maintenance costs. The main areas of concern are the on-stream maintenance costs and shutdown costs.

It is believed that inspections can have a significant part to play in improving the situation, however this will require a change in the strategy for scheduling inspection activities.

In considering these aspects more and more often the OIL&GAS companies (but not only the OIL&GAS companies), have embarked on the development of "Risk Based Inspection Projects". The objectives of those projects is to develop a new and improved strategy of inspection management of pressure equipment.

Today almost all sites have developed RBI (Risk Based Inspection) studies on pressure vessels, but the RBI methodology could cover also the Inspection of piping and the Inspection of Atmospheric Storage Tanks.

For piping systems most of the refineries adopt an approach that schedules all inspection activities at major turnaround periods. Little or no effort is made to take the advantage of other unit outages to complete routine examinations. During this short period, significant effort is made to complete the examinations and analysis of the trends of piping systems, the cost of this exercise is considerable. It is considered that the piping system inspection task could be completed as part of the routine on-stream inspection activities. This option should be used as part of a new inspection strategy.

Some recent incidents in the world have raised concern for the reliability of storage tanks and also the danger of environmental pollution. Some new guides for the maintenance and inspection of storage tanks have been drafted and issued. Those new approaches to inspection of tanks should be used as part of a new inspection strategy. The application of reliability and risk based techniques to optimize the inspection and maintenance of the storage tanks follows global trends to move away from 'time based' to 'condition/risk based inspection and maintenance'. During the last decade it has been recognized that the techniques can be usefully applied to the total maintenance approach for conventional storage tanks.

Also the RBM (Risk Based Maintenance) is a methodology to determine and document in a cost effective way the optimum maintenance requirements of the asset in order to assure its functionality.

Risk Based Inspection (RBI), applied on piping and tanks is recognized as one of the most common methodology to ensure and improve the integrity and safety of an asset but it's also one of the most rapid way to reduce maintenance and inspection costs. Case studies will be presented accordingly.

Integrity assurance of process facilities at Adriatic LNG Terminal through Risk Based Inspection

Filippo Belloni
Adriatic LNG
Milan
Italy

Vittorio Colombo, Giacomo Benassi
Cescor srl
Milan
Italy

Adriatic LNG operates a LNG terminal off the coast of Italy. The terminal consists of a reinforced concrete Gravity Based Structure (GBS) with dimensions of 180 m long, 88 m wide and 47 m high. The GBS contains all the process piping and equipment necessary to perform the regasification process and to send the gas onshore into the Italian gas network. The paper presents the steps and the activities carried out to apply the Risk Based Inspection procedure to the LNG plant. The RBI approach allows to make a screening of the most critical items in order to optimize the inspections. The paper describes in particular the criteria adopted for grouping all the piping and equipment, belonging to both process and utility systems, into homogeneous circuits. A fundamental step of the RBI process is the identification of the expected degradation mechanisms due either to corrosion or to other sources (e.g. thermal cycles, vibrations, mechanical stresses, etc.) and which depend on the combination of material, conveyed fluid, service conditions (such as cryogenic / non-cryogenic service), stress level and external environment. The methodology followed to accomplish the risk assessment task is also discussed, focusing on the adopted approach for the definition of the probability and consequences of a possible failure and the overall criticality of an item / homogeneous circuit. In addition, the guiding normative and principles for the selection of the most suitable inspection techniques are addressed in the paper. Finally, a brief overview on the regulatory requirements that are mandatory is provided in order to comply with the national law and how they were captured in the planning of inspections.

Towards a first global assessment of corrosion issues in advanced biorefineries as preliminary learnings from ECORBIO

G. Marlair, W. Benaissa, Accidental Risks Division, INERIS, Verneuil-en-H. (F)
M. Nonus, C. Len, E. Hondjuila-Miokono, UTC, E. TIMR, EA4297 Compiègne, (F)
Nicolas Thiébault, ESCOM, Compiègne (F)
C. Sarazin GEC, UMR 6022, UPJV, Amiens, (F)
J. Garcia, CETIM, Senlis, France
B. Nancy, LEREM, Montataire (F)
G. Doreau, A. Darraspen, MAGUIN SAS, (F)

Advanced biorefining is a versatile concept that promotes the sustainable production of a portfolio of biobased products including biomolecules, biomaterials, bioenergy and energy vectors from various biomass resources. Early development of so-called 1G (first generation) biorefineries that were essentially concentrating on mass production of biodiesel or bioethanol has shown a number of limitations in the related value chains in terms of sustainability issues. Among those issues, a number of corrosion problems have been reported and identified, at least partially understood and sometimes solved. We can quote for example the corrosion of some metallic components of engines due to heat driven conversion of ethanol into acidic species before combustion, the high temperature corrosion in biomass burning furnaces due to the presence of alkali salts as well as stress corrosion cracking in ethanol carbon steel tanks and in pipelines. However no global assessment of corrosion issues in the biorefineries of the future has been made so far, hence leaving significant interrogations where research efforts have to be deployed to accompany their sustainable implementation. This paper first offers a presentation of a project named ECORBIO (for Evaluation of CORrosion in BIOrefineries of the future), the main aim of which is to cover this gap by delivering useful information to process managers, engineering companies and investors for evaluation of corrosion in bioprocesses.

The project (Oct 2012 to Sept 2015) lies on a diversity of scientific approaches comprising: a) literature review of known corrosion issues relating to biorefining and consolidation of related data into dedicated databases, b) consolidation of return from experience from existing accident statistics, exchanges with stakeholders and first visits of biorefineries c) testing with existing procedures and developing screening procedures with focuses on “biocorrosion”, organic acids and ionic liquids, the former being a key corrosion mode of corrosion due to emergence of biotechnologies the latter being key products or reagents in integrated biorefineries.

Preliminary results exposed in this paper comprise: a) the analysis of the corrosive environment potentially developed by key microbial products such as organic acids (lactic acid, acetic acid, succinic acid, citric acid....) with sulphuric and distilled water as reference substances for three different grades of steels ; b) corrosive potencies of some imidazolium and phosphonium based ionic liquids that may play a role e.g. in lignocellulosic biomass defragmentation and/or in cellulose dissolution c) first lessons from experience in biorefining and from more general statistics d) first learnings on the pertinence of the “C1 test protocol” that is used to state whether or not a given substance (e.g. a process juice) is “corrosive to metals” as an identified “dangerous phys-chem intrinsic property, according to the recently implemented CLP Regulation in the EU (also included in the Globally Harmonised System at UN level).

Corrosion behaviour of AISI 1006 steel in aqueous extracts of biodiesel and petrodiesel

Luís F. P. Dick & Maria Denise de Oliveira, Universidade Federal do Rio Grande do Sul, Porto Alegre/Brazil

All diesel currently commercialized in Brazil contains 5 vol.% of biodiesel added to petrodiesel (B5). Most of the added biodiesel is obtained from soja beans and contains salts, emulsified water and aggressive organic substances that corrode carbon steels used for the transportation of the washed fuel, as well as stainless steels used in the production of pure biodiesel. This attack to metallic materials, added to polymers deterioration in contact with biodiesel constitutes the most important limitations to the use of higher biodiesel concentrations.¹ The corrosivity of biodiesel has been studied usually by exposure to the pure product¹ that does not adequately simulate the most aggressive conditions, when emulsified water decants. Thus, the major concern of this work was to evaluate the corrosion attack of low carbon steel (AISI1006) exposed to water extracts of pure washed biodiesel (B100) before and after its thermal degradation. For this, cyclic voltammetry curves were measured in aqueous extracts using oil:water volumetric ratios ranging from 1:1 to 100:1. For comparison, the corrosion behaviour in aqueous extracts of petrodiesel was also studied.

Accelerated thermal degradation of pure biodiesel was carried out for 5 days at 90°C. The aqueous extracts were prepared with a 0,01 mol L⁻¹ KClO₄ support electrolyte, stable under the considered experimental conditions.²

As seen in Fig. 1, the aqueous extract of B100 is much more aggressive to low carbon steel than pure 0,01 mol L⁻¹ KClO₄. The currents observed on the steel cannot be attributed to reactions of the electrolyte, as the comparison with the curves on Pt show.

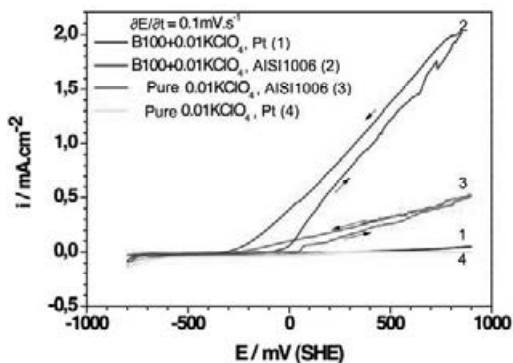


Fig.1 Curves 3 and 2: CV of AISI1006 (3, 2), respectively in pure 0.01KClO₄ and in 1:1 aqueous extract of pure biodiesel in 0.01KClO₄ (B100+0.01KClO₄). Curves 4 and 1: CV of Pt in the same solutions.

References

1. Akita, A. H., Fugivara, C. S., Aoki, I. V., Benedetti, A. V., *ECS Transactions* (Online), v. 43 (2012) p. 71-77.
2. Bakos, I. and Horanyi, G., *J. Electroanal. Chem.*, 347 (1993), p. 383-391.

CORROSION IN SYSTEMS FOR STORAGE AND TRANSPORTATION OF PETROLEUM PRODUCTS AND BIOFUELS

Alec Groysman

Israeli Society of Chemical Engineers & Chemists, Tel Aviv, Israel

Technion, Haifa, Israel

E-mail: alecgroysman@gmail.com

The *aim* of this work is to describe the conditions in which petroleum products (fuels) are corrosive to metals; corrosion mechanisms in petroleum products; which parts of storage tanks containing crude oils and petroleum products undergo corrosion; dependence of corrosion in tanks on type of petroleum products; how fuel additives and oxygenates improve properties of fuels; how microorganisms take part in corrosion of tanks and pipes containing petroleum products; which corrosion monitoring methods are used in systems for storage and transportation of petroleum products; what corrosion preventive and control measures should be chosen; how to choose coatings for inner and outer surfaces of tanks containing petroleum products; cases of typical and unusual corrosion of tanks; biofuels (bioalcohols and biodiesel); and how different components of fuels (including oxygenates and aromatic solvents) and biofuels influence metallic and polymeric materials. The results are summarized in the books “*Corrosion for Everybody*” and “*Corrosion in Systems for Transportation and Storage of Petroleum Products and Biofuels*” published by Springer.

Keywords: *petroleum products, fuels, biofuels, corrosion, polymeric materials*

Laboratory test method for corrosion under thermal insulation

*Ole Øystein Knudsen, SINTEF, Trondheim, Norway
Jorunn Aaneby, Jotun, Sandefjord, Norway*

Background

Corrosion under thermal insulation is one of the most costly and significant corrosion problems, both in the petrochemical industry and other industries. Even though this problem is highly related to the quality of the coating application and insulation work at the installation, it is nevertheless important to have test methods to study the phenomenon in lab. Evaluation of coatings, insulation materials and new designs will benefit from relevant laboratory test methods. ASTM G-189 "Standard guide for laboratory simulation of corrosion under insulation" is such a test, but this test is not suitable for e.g. testing of coatings.

Objectives

The objective with the work is to develop a test method for studying protective coatings under insulation.

Results

An apparatus is designed, as shown in the sketch below. A test pipe with one or more protective coatings is electrically heated from the inside. The pipe is exposed in a cabinet with humid atmosphere or salt water. The test cycle includes varying temperature, salt water and humid atmosphere. 30 test cycles are run during over a period of six weeks. The apparatus and test cycle is based on the ASTM G-189 test method, but modified in order to make the test more suitable for testing of protective coatings.

A number of coatings with different expected temperature tolerance and protective properties are tested in the apparatus and compared with the Houston Pipe Test¹. Pros and cons with the two methods are discussed.

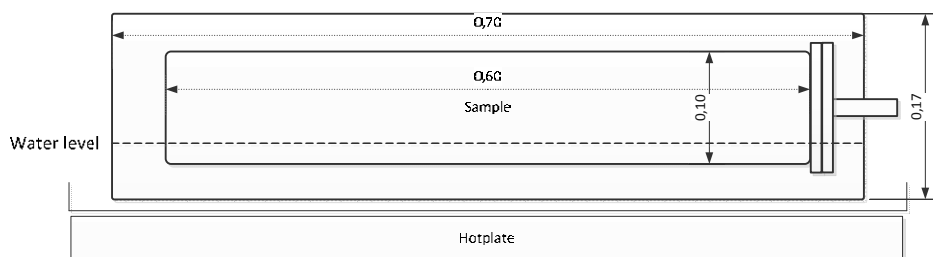


Figure 1. Apparatus for testing protective coatings and insulation materials with respect to corrosion under insulation.

¹ M. Halliday, CORROSION/2005, Paper No. 05020 (NACE, Houston TX) 2005

Case Study of Axulary Burner Fuel Ring Failure Experienced at Sulfur Recovery Unit at Saudi Aramco

Khaled Al-Hajri
Saudi Aramco, ShGP Gas Plant
Abqiaq, Saudi Arabia

Summary:

This paper presents a case study for the experienced repetitive failure at Sulfur Recovery Unit, Axulary Burner Fuel Ring. Failure took place at one of Saudi Aramco's gas plant facilities in Saudi Arabia.

This failure was experienced at 304 SS material which is not the right material for these services. High temperature services will require 310 SS.

Failure Finding:

- Material of Construction of the fuel ring is 304 SS which is lower grade material not susceptible for HT services
- Corrosion & Crack at 6 O'clock Position
- Parsons of conditions at the material



Failure Analysis:

This Failure was investigated and assessed where this ring was send to lab for analysis and examinations. Close-up micrographs revealed and showed that Fuel Ring has exposed to two type of corrosion damage:

- **The first Damage was Sensitization Damage** that happened for 304 SS when it is held at High Temperature which led to Chromium react with Carbon

to form chromium carbide. This chromium carbide precipitated at the grain boundaries which means that there is a chromium depleted zone around the grain boundaries. This depletion weak the metal and less corrosion resistant, specifically to intergranular corrosion.



- The 2nd Damage was **Polythionic Acid Crack** which is a form of Acid Cracking normally occurring during shutdowns and startups due to formation of Sulfur Acids (Polythionic Acid) acting on sensitized stainless steels. **Polythionic Acid formed** when SS exposed to sulfur compounds (H_2S) to form a surface sulfide scale. Moreover, during Shutdowns these scales react or combine with air (oxygen) and moisture to form weak acid known as sulfur acids (polythionic acid).



Recommendations:

The Recommendations & Proposed Solution to prevent future reoccurrence are as follows:

- Improve resistance to corrosion & PAC cracking that can be achieved with upgrading the fuel ring to 309 SS Material which containing more amounts of Cr and Ni.

SS Type	Cr %	Ni %
304	18 - 20	8 - 10.5
316	16 - 18	10 - 14.5
309	22 - 24	12 - 15.5

- Prevent condensation formation
- Control & Minimize temperature to which the ring is exposed that will prevent Sensitization Damage

Chemical Treatment of Un-treated Close Cooling Water System

Faraj Hammad OMER
Ras Lanuf Oil & Gas processing Co.

Ras Lanuf- Libya

Abstract

Ras Lanuf Complex consists of a variety process units including refinery, ethylene plant, polyethylene plant, utility plants and loading facilities for export purposes. The entire complex is provided with Treated Cooling Water (TCW-I) System. TCW-I is a closed loop cooling system with total volume of 12,000 m³ which removes heat from process units and equipment to the sea water cooling system, by Indirect contact through titanium plate heat exchangers, during all modes of plant operation. The cooling system is fully equipped with appropriate storage tanks, make-up tanks, pumping system, heat exchangers and a lengthy intricate piping network throughout the entire complex. In addition, a de-oiling unit is incorporated to remove possible hydrocarbon contaminant in the water system. Chemical injection system is provided to inject corrosion inhibitor, biocide, and oil dispersant into the system. Zinc Chromate was used with different dosages as a corrosion inhibitor since commissioning of utility plants in 1982. For health and safety concerns, the treatment by this inhibitor was stopped completely after 24 years of operation. For the last 7 years the cooling system was operated without any corrosion protection, however measurement of corrosion rate indicate the system is still within safe limits. The chemical analysis of residual Zn⁺⁺ and CrO₄⁻ ions showed residual traces of these ions remaining in the system and negligible figures of dissolved iron content. The biological analysis did not revealed any presence of sulphate reducing bacteria. New treatment was recommended to start by injection of synergized of silicate corrosion inhibitor, liquid biocides and oil dispersant to the system. Close follow up to the new treatment trial for three months was performed and results were presented.

Keywords: Cooling water, corrosion inhibitor, corrosion rate, chemical treatment.

Successful Trial of Using Non-Metallic Cladding in Saudi Aramco Facility

Abstract

In Oil & Gas, Chemical, Petrochemical, and Refining industries, Corrosion Under Insulation (CUI) is a major problem effecting production, safety, and the economics of the facility. The integrity of piping and process equipment is often compromised by CUI. It is now commonly accepted within industry and Health & Safety Executives as an integrity issue that requires urgent attention. Annually CUI results in the loss of millions of dollars. The main root cause of CUI is external water ingress through traditional metallic cladding systems.

New Non-Metallic Cladding system has been successfully tried in one of Saudi Aramco Facilities. During more than two years, the non-metallic cladding exposed to different tests and lab analysis and was having positive results which approve the successful of the trial. In This presentation I will share our successful trial and experience in using non-metallic cladding instead of metallic cladding

3D TRASAR Cooling Water Technology combined to Refined Knowledge System will help to optimize total cost of operation, to improve reliability at any time even during process leaks and to minimize the impact of process leaks on asset management.

*Dr Valerie Bour Beucler, Nalco, Wasquehal/France;
Sr Industry Technical Consultant*

The good management of a recirculating cooling water system is the preservation of the balance between the corrosion, the scaling and the microbiology. Any event that destabilizes this balance is going to increase the corrosion rate, microbiology growth and scaling risk. In refineries we are frequently fighting process leaks into cooling water systems. This process leaks, mainly hydrocarbons, will very strongly impact this balance. The recovery will require time and corrective actions, and will increase the total cost of operation. The recovery and the life time equipment impact will mainly depend on two critical parameters, the time to detect the leak and the time to stop it after leak identification. The action plan efficiency is also critical, but it will impact the results in a second phase.

In a refinery, a leak detection protocol, a leak identification action plan and a leak management program are recommended by Best Practices.

The combination of 3D Trasar cooling system monitoring (data analysis) and Refined Knowledge System implemented in site is the right tool to confirm a leak, to help in leak detection and to implement in on time the right action plan.

3D Trasar Technology combined with Refined Knowledge System will help to optimize total cost of operation, to improve reliability at any time, even when process leaks occur, and to minimize the impact of process leaks on asset management.

Precipitation and dissolution of critical phases in Alloy 625

R. Lackner¹, G. Mori¹, R. Egger², F. Winter², W. Grogger³, M. Albu³

¹ *Christian Doppler Laboratory of Localized Corrosion, University of Leoben, Franz-Josef-Str. 18, 8700 Leoben, Austria, roland.lackner@unileoben.ac.at*

² *voestalpine Grobblech GmbH, Voest-Alpine-Straße 3, 4031 Linz, Austria*

³ *FELMI - ZFE, Steyrergasse 17, 8010, Graz*

ABSTRACT

Alloy 625 is used in oil and gas industry as a cladding material for high diameter pipes. Different conditions of Alloy 6225 are solution annealed, stable annealed and as rolled. All three conditions have been isothermally sensitized in a laboratory furnace. Different time-temperature combinations up to an annealing time of 10 h and annealing temperatures up to 1050 °C were applied. Corrosion tests according to ASTM G28A were used for determination of time – temperature – sensitization – diagrams. Sensitized specimens have been further treated at high temperatures to re-establish high corrosion properties. High temperature repair was done between 950 and 1050 °C for 0.3 to 10 hours. Microstructure of the investigated samples was evaluated by High Resolution Scanning Electron Microscopy (HR-SEM). Chemical composition of precipitated phases and depletion zones were characterized by Transmission Electron Microscopy (TEM). Concentration profiles of Molybdenum can be used to determine the degree of sensitization

Key words: Alloy 625, intergranular corrosion, depletion zone, sensitization.

Laboratory Examination of Two Olefin Cracking Radiant Tube Materials

*Jian-Zhong Zhang, Lee Allcock, Abdulaziz Al-Meshari, Esteban Morales Murillo,
Mohammad W. Diab and Shahreer Ahmad
Materials and Corrosion Section, SABIC Technology Centre, SABIC,
Jubail, Saudi Arabia*

Two centrifugally cast olefin cracking furnace radiant tube materials were examined in laboratory after 3.5 years' service in an olefin plant. The two materials examined are of an Aluminium containing 25/35 and an Aluminium free 35/45 metallurgies.

The tube materials were examined using chemical analysis, optical microscopy and SEM/EDX. The effects of metallurgy on carburization and nitridation resistances of the materials are discussed.

Effective Parameters on Bottom Plates Corrosion Phenomenon of Storage Tanks during Construction Time Interval: A Case Study, Investigations, and Solutions.

*Hamed Aldaghi, Soehil Easapour, Yavar Haghighat,
Pars oil and gas company, Asalouyeh, Iran*

The external surface of storage tank bottom plates, in contact with moist soil, faces a level of corrosion that makes cathodic protection unavoidable. The risk of this type of corrosion increases dangerously during the time interval, (usually more than 2 years) between the final installation of storage tank bottom plates and commissioning of storage tank cathodic protection systems.

As a practical case study, the corrosion phenomenon of storage tank bottom plates, during the above mentioned time interval has been investigated in this paper. Magnetic Flux Leakage (MFL) technique was carried out to investigate the extent of general corrosion occurred in the bottom plates. Soil composition has been scrutinized, regarding its pH value, chloride and sulfate ion contents and presence of sulfide reducing bacteria (SRB). XRD technique was used to investigate the chemical nature of corroded plate surfaces and corrosion products. Results derived from fore different plants and the effect of two more parameters on the corrosion behavior of the plates has been compared: foundation layer adjacent to the bottom plates including asphalt or sand cushion, and application of coating on the plates.

Finally according to site survey data, laboratory results and standard recommendations, the applicable solutions were concluded and represented. Results showed that soil contamination with chloride and sulphate ions is the main reason of catastrophic corrosion at the absence of cathodic protection. Furthermore it has been concluded that, the presence of asphalt layer has a significant role in the corrosion protection during interval time.

Key words: bottom plate corrosion; tank's foundation; aboveground storage tank;

Corrosion resistance of austenitic steels used in biodiesel fuel plant

Amanda Petronilha Pereira¹, Vanessa de Freitas Cunha Lins², Cintia Gonçalves Fonseca Costa², Maria das Mercês Reis de Castro², Carlos Eduardo de Almeida Souza Torres³

1 Fiat Automobile S.A., Materials Science Technology Center, Betim, Brazil

2 Federal University of Minas Gerais, Chemistry Engineering Department, Belo Horizonte, Brazil

3 PETROBRAS Biofuell, Montes Claros, Brazil

This study evaluated the corrosion behaviour of the stainless steel 304L, 316L, 317L and 904L in glycerine A (load 11,000 kg / h) and glycerine B (load 6,500 kg / h). The objective is the material selection for equipment operating in a biodiesel plant. The open circuit potential (OCP) measurement, the electrochemical impedance spectroscopy (EIS) and the anodic potentiodynamic polarization were used in this work. The corrosion potential of the AISI 904L steel was the highest, indicating that the AISI 904L has a lower propensity to corrode in acidic glycerine media. According to the values of the polarization resistance (R_p) obtained using the EIS analysis, the 317L ($R_p = 1.51 \times 10^4 \Omega \cdot \text{cm}^2$) and 904L ($R_p = 5.28 \times 10^4 \Omega \cdot \text{cm}^2$) had a polarization resistance an order of magnitude greater than the other. The steels showed a breakdown potential only in glycerine B. The 317L and 904L steels showed the highest value of breakdown potential of 0.3V (Ag/AgCl). Considering the technical and economical feasibility, the AISI 317L steel was selected to be used in the biodiesel plant, in media of acid glycerine.

Corrosion of steels used in a biodiesel fuel plant

Amanda Petronilha Pereira¹, Vanessa de Freitas Cunha Lins², Cintia Gonçalves Fonseca Costa², Maria das Mercês Reis de Castro², Carlos Eduardo de Almeida Souza Torres³

1 Fiat Automobile S.A., Materials Science Technology Center, Betim, Brazil

2 Federal University of Minas Gerais, Chemistry Engineering Department, Belo Horizonte, Brazil

3 PETROBRAS Biocombustíveis, Brazil

The search for alternative forms of energy that generate a lower carbon dioxide and pollutants content conducts to an increase in biodiesel fuel production in Brazil. The corrosion of steel equipment is a problem in biofuel plants. This work evaluates the corrosion resistance of the AISI 304 L steel, that is actually used in biofuels production plants, and two alternative materials, the AISI 904L stainless steel and a 2205 duplex stainless steel. Open circuit potential (OCP) measurements, electrochemical impedance spectroscopy and anodic potentiodynamic polarization were performed in acid glycerine solution provided by a biodiesel plant. The OCP measurements showed that AISI 904 L steel had the highest corrosion potential in acid glycerine and the AISI 304L showed the lowest corrosion potential. The electrochemical impedance spectroscopy results indicated that the AISI 904L stainless steel and the 2205 duplex stainless steel showed higher values of polarization resistance (10^5 - 10^6 ohm.cm²) than the AISI 304L stainless steel (10^3 - 10^4 ohm.cm²). The breakdown potential of the 2205 duplex stainless steel was 520mV (Ag/AgCl), the highest among all studied steels. The AISI 904L and the AISI 316L steel showed breakdown potential values of 180mV(Ag/AgCl) and 265mV (Ag/AgCl), respectively.

in situ AFM and FTIR spectroscopy coupled with electrochemical techniques studies on naphthenic corrosion of API 5L X70 steel

Emerson C. Rios, Aloadir L. Oliveira, Alexsandro M. Zimer, Renato G. Freitas, Roberto Matos, Lucia H. Mascaro, Ernesto C. Pereira*

Federal University of São Carlos (UFSCar), São Carlos – SP/Brazil.

**emersoncostarios@yahoo.com.br*

Abstract

The corrosion caused by organic acids is a major concern in the petroleum industry. The presence of naphthenic acid in petroleum considerably increases the corrosion rate in distillation units. Therefore, equipment failures have become a critical safety and reliability issue. In this work, we used the Fourier transform infrared spectroscopy *in situ* (FTIR) and atomic force microscopy (AFM) to qualitatively characterizing the formation of iron naphthenate film on the API 5L X70 steel surface at room temperature. Mineral oil containing organic acids was used to simulate the naphthenic corrosion of petroleum on steel. The FTIR measurements were made *in situ* and coupled with electrochemical noise (ECN) measurements. The ECN data were analyzed with the wavelet transform, and, from the energy distribution plots general corrosion was observed, frequently observed in systems containing organic acid. Figure 1 shows the temporal evolution of the FTIR spectra. The main regions that evidence the formation of iron naphthenate film are: (i) 2923 cm^{-1} and 2853 cm^{-1} : asymmetric and symmetric C-H stretching, respectively, of CH_3 and CH_2 groups; (ii) 1452 cm^{-1} and 1376 cm^{-1} : CH_2 and CH_3 deformations (bending); (iii) 1700 cm^{-1} and 3380 cm^{-1} : due to the carbonyl ($\text{C}=\text{O}$), hydroxyl (OH) and amine groups (N-H). To observe the morphology of the initial iron naphthenate film and its evolution a long the time, *in situ* AFM images were obtained. The images in Figure 1 shown the early formation of the film: 11 minutes and 95 minutes after immersion of steel plate in oil. Before the onset of corrosion, steel plate presented a roughness medium square (RMS) $\approx 5\text{ nm}$, and after 5 hours immersion RMS $\approx 134\text{ nm}$. The set of results obtained in this work confirmed the presence of naphthenic corrosion of steel API 5L X70 oil even at room temperature.

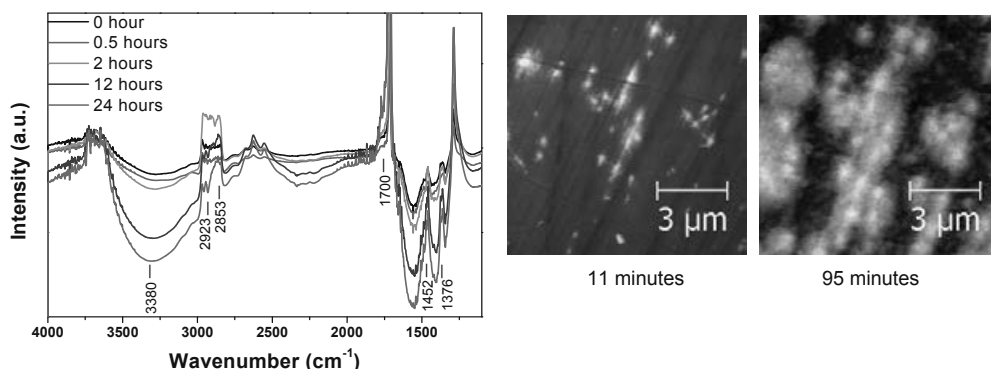


Figure 1: *in situ* FTIR spectra of the API 5L X70 steel surface during the onset of naphthenic corrosion. The AFM image shows the growth of iron naphthenate film.

Detection and Sizing of Corrosion under Fireproofing (CUF) with Welded Wire Mesh Using MR-MWM-Array

Salman A. Dossary and Ali Minachi
Saudi Aramco, Dhahran, KSA 31311

Neil Goldfine and Scott Denenberg
JENTEK Sensors, Inc., 110-1 Clematis Avenue, Waltham, MA 02453-7013

This presentation describes a new capability for imaging of external and internal corrosion under fireproofing (CUF) in refinery vessels (and other structures such as the legs of LPG spheres and I-beam structures) without removal of fireproofing. These methods allow for inspection during normal plant operation from outside of vessels, skirts, and other structures. This presentation focusses specifically on a demonstration performed at a Saudi Aramco facility in July 2013 for the skirt region of a drum with fireproofing and wire mesh with welded vertical and horizontal segments. This welded wire mesh presents a different challenge to magnetic field based inspection technologies than non-welded wire mesh. The welded mesh is typically comprised of horizontal and vertical wire segments with spacing ranging from 4-8 inches (10-20 cm) and with welds at each of the wire segment crossing nodes. These welds create a pathway for induced eddy currents to circulate, producing a substantial contribution to the sensor response that must be removed to enable reliable corrosion (skirt wall thickness) imaging.

The MR-MWM®-Array uses a novel linear drive winding construct with a linear array of solid state Magneto-Resistive (MR) sensing elements. Data is acquired simultaneously on multiple channels with the fully parallel GridStation® impedance instrument and rapidly converted into corrosion images using a HyperLattice™ based multivariate inverse method (MIM) that also removes the contribution from the wire mesh. The Hyperlattice MIM uses pre-computed databases of sensor responses to rapidly convert two dimensional maps of sensor impedance over large surface areas into skirt wall thickness and magnetic permeability images (where the remaining wall thickness provides the quantitative corrosion image and the permeability is correlated with relative stress variations in the steel). A vertical scanner was used to allow relatively rapid coverage of large surfaces. The demonstration unit provided a 9 inch (23 cm) scan path width using an 18 channel system. Systems with up to 119 channels can be configured with the new GridStation® 8200 family of fully parallel impedance instruments. This paper describes the underlying technology and the results of the field demonstrations at a Saudi Aramco facility in the Kingdom of Saudi Arabia.

Electrochemical investigation of carbon-based conductive coatings for application as anodes in ICCP system of reinforced concrete structures

Gino Ebell, Marina Poltavtseva, Jürgen Mietz

BAM Federal Institute for Materials Research and Testing, Berlin (Germany)

Carbon based conductive coatings are complex composites, consisting of an organic or inorganic binder and conductive carbon components, for application as anodes in impressed current cathodic protection systems (ICCP) of reinforced concrete structures. These mixtures can be painted as paste or aqueous dispersion at the prepared concrete surface. For current supply of the rectifier to the coating are used different materials like wires made of platinised titanium, copper or mixed metal oxide coated titanium (primary anode). The minus pole of the rectifier is connected to the reinforcing steel (cathode) and the positive pole to the primary anode. By supplying a protective current between anode and cathode, the potential of the reinforcing steel should be lowered below -720 mV (versus Ag/AgCl/0,5 M KCl) into an electrochemical inactive range [1]. An industrial research project in cooperation between the Federal Institute for Materials Research and Testing (BAM, Berlin) and the Institute of Building Materials and Research (RWTH-Aachen University) should assess the applicability of three commercial carbon-based conductive coatings as secondary anode in ICCP systems. As part of this research project, extensive electrochemical and morphological investigations of carbon based conductive coatings were carried out to determine important parameters such as applied current density, pH value of the electrolyte solution, humidity and, type of binder and their influence to the degradation behaviour of these coatings. The electrochemical properties in saturated calcium hydroxide solution were studied by electrochemical methods, such as electrical impedance measurement, measuring of open circuit potential over time and galvanostatic polarisation. For the galvanostatic polarisation with in situ pH-value measurements we designed a special corrosion-measurement-cell (Fig. 1).

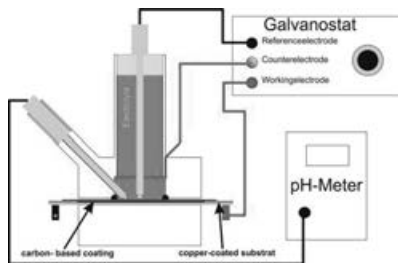


Fig. 1: Measurement cell for polarisation experiments at conductive coatings

The dissolved organic and inorganic carbons in electrolyte solution were quantified by using a photometric method. The structures of the coatings were investigated before and after the electrochemical investigations by microscopy and SEM/EDX analysis.

References

- [1] DIN EN ISO 12696:2012-05, Cathodic protection of steel in concrete, Beuth, Berlin 2012.

EXAMPLES OF C.P. REMOTE MONITORING INSTALLATIONS CARRIED OUT BY A EUROPEAN GAS TRANSMISSION COMPANY

Christine AKNOUCHE^a, Clara Calvi^b

^aGRT GAZ - 5, Rue Ferdinand Lesseps 5 60203 Compiègne Cedex,
christine.aknouche@grtgaz.com

^bTECNOSYSTEM GROUP – Via Vigentina 2, 27010 San Genesio ed Uniti (PV),
c.calvi@tecnosystemgroup.com

ABSTRACT

Having daily information about the state of Cathodic Protection systems of the entire transmission network allows to increase the reactivity level and to obtain a better overview of the CP.

Grt Gaz, with the most extended high pressure transmission network in Europe, has been the first gas transmission company to decide to remotely monitor the whole network: this paper describes the key passages which led Grt Gaz in its choice of materials and services associated with the installation of the CP remote monitoring system.

Corrosion of Cathodically Polarized TSA in Subsea Mud at High Temperature

Ole Øystein Knudsen, SINTEF, Trondheim, Norway

George Clapp and Graeme Duncan, Woodside Energy Ltd., Perth, Australia

Jan van Bokhorst, Shell Global Solutions International B.V., Amsterdam, The Netherlands

Background

Thermally sprayed aluminium (TSA) is not immune to corrosion when polarized by sacrificial aluminium anodes. However, the corrosion rate is usually rather low due to a protecting surface oxide on the TSA, keeping the TSA passive. A certain cathodic reaction rate is found on the TSA, producing hydroxide. This hydroxide is a potential threat to the TSA, since aluminium is not passive in alkaline environments. When the TSA is exposed to seawater the hydroxide may be transported away from the TSA surface by diffusion and convection, and the pH is maintained within the passive range. However, in mud there is no convection and the diffusion is limited. This may result in accumulation of hydroxide at the TSA-mud interface and activation of the TSA. The cathodic polarization may therefore result in decreased lifetime of the TSA in mud.

Objectives

The objective with this paper is to discuss corrosion rate of TSA as function of cathodic polarization and temperature, when exposed in subsea mud.

Results

Excessive cathodic polarization of TSA in mud, e.g. by impressed current or magnesium anodes is detrimental to the TSA. The TSA activates and corrodes rapidly.

The pH at the TSA/mud interface seems to adjust itself to the upper pH limit for passivity of aluminium. The hydroxide produced by the cathodic reaction is consumed by corrosion of the aluminium, preventing pH to increase significantly.

The corrosion rate of the TSA at -1100 mV vs Ag/AgCl increased with temperature, from about 10 $\mu\text{m}/\text{year}$ at ambient temperature to about 20 $\mu\text{m}/\text{year}$ at 95 °C (after 170 days exposure). The corrosion rate decreased with time. The corrosion rate correlated with cathodic current density, which indicates that the hydroxide formed by the cathodic reaction results in corrosion of the TSA. However, as long as the TSA is not polarized excessively the cathodic reaction rate remains quite low and the corrosion rate of the TSA is moderate.

Cross-sectional post-test investigation of the samples in SEM showed that little or no calcareous deposits were formed on the TSA surface. This is probably explained by limited diffusion of Ca^{2+} and Mg^{2+} ions to the TSA surface when exposed in mud. Aluminium oxide was found on the TSA surface of all the samples, which probably contributed to decrease the cathodic reaction rate. A layer of firmly attached mud was also found on the TSA, which probably also has contributed to limit the cathodic reaction rate.

Cased-pipeline: presentation and experience of annular space wax filling

Cased pipeline construction creates operational challenges for cathodically protecting and assessing the condition of the carrier pipe inside a casing. Filling the annular space between the casing and carrier pipe with wax is a method commonly used to control corrosion on the exterior surface of the carrier pipe in a casing.

Presentation of the process and evolution during the last 30 years to improve it.

Review of the norms mentioning this process.

Case studies of the assessment of filled casings using Inline Inspection (ILI) and Direct Assessment (DA) will be presented to evaluate the effectiveness of filling casings to control corrosion. The study covers 328 casings from Consumer Energy pipeline network.

The a.c. corrosion rate: A discussion of the influencing factors and the consequences on the durability of cathodically protected pipelines

M. Büchler, SGK, Zürich/CH

Most of the knowledge gained on a.c. corrosion was obtained by means of coupon measurements. They allowed building a profound understanding of the relevant parameters, explaining their significance as well as the corresponding threshold values based on thermodynamic and kinetic concepts. The corrosion rates derived from the theoretical models are often confirmed by coupon measurements, demonstrating the validity of the concepts as well as the corresponding measuring techniques. However, the significant corrosion rates obtained on coupons are typically not observed on pipeline systems. The reasons for this discrepancy are addressed by means of theoretical considerations and numerical simulations. The obtained results are compared with field data. Based on the good agreement between calculation and experimental data a new approach to assessing the a.c. corrosion risk is proposed that is based on the current threshold values of EN 15280.

Electrochemical Phenomenon of a.c. Corrosion Likelihood of Cathodically Protected Steel Pipelines

Fumio Kajiyama, Tokyo Gas Co., Ltd., Tokyo, Japan

Electrochemical phenomenon of a.c. corrosion likelihood of a cathodically protected steel pipeline paralleling a 25 kV a.c. powered rail transit system which operated at frequency of 50 Hz, was studied using coupon technology developed by the author. The pipeline had polyethylene coating. Measurements on coupon current and potential were made at intervals of 0.1 ms over a period of 24 hours. Positive values in coupon current indicate the current flowing through electrolyte to the coupon (i.e., cathodic current flowing). The coupon instant-off potential was obtained by averaging 200 coupon potentials measured 80 to 100 ms after the interruption of the coupon from the pipe. Coupon d.c. current and coupon a.c. current density were obtained from the calculation of coupon current. Based on the data analyses using Pourbaix diagram considerations, the results were drawn as follows:

- (1) If the measured coupon current for a single period meets the following results, frequency of the coupon current is considered to be commercial frequency (16-2/3, 50 or 60 Hz).
 - Coupon current exhibits polarity reversal.and
 - The difference in appearance time between the maximum and the minimum value is half of a period.
- (2) The coupon current with commercial frequency was not symmetrical for the positive (cathodic) and the (negative) parts. The magnitude of cathodic current was greater than that of anodic current.
- (3) By calculating 8640 data, correlation coefficient of 0,866 between average coupon d.c. current density and average coupon a.c. current density was obtained, indicating coupon a.c. current density was well directly proportional to coupon d.c. current density. This suggests that high a.c. current density, together with high d.c. current density at holidays on cathodically protected natural gas high pressure pipelines increases the risks of hydrogen embrittlement and a.c. corrosion due to the formations of hydrogen and dissolved HFeO_2^- by enhanced cathodic reaction ($2\text{H}_2\text{O} + 2\text{e}^- \rightarrow 2\text{H}(\text{H}_2) + 2\text{OH}^-$). In the case where dissolved HFeO_2^- is formed, the dissolution of steel proceeds as irreversible reaction.
- (4) By taking coupon instant-off potential into account, possible anodic and cathodic reactions were thought according to the pH value and potential shifts.

Detecting and quantifying damage evolution of coated, cathodic protected buried pipelines by combining AC monitoring and stochastic analysis

X. Li¹, A. Yajima², R. Liang² and H. Castaneda^{1*}

Chemical and Biomolecular Engineering¹

National Center for Research and Education in Corrosion¹,

Civil Engineering Department²

The University of Akron

Akron, Ohio, 44325-9006

Abstract

The susceptibility of pipeline to soil corrosion is always minimized by imposing an insulating barrier or coating at the pipe surface. When the coating fails or loss the functionality as a physical barrier, the soil surrounding the metallic structure influences the initiation and propagation of localize corrosion damage. The stochastic nature of the soil properties and metallic corrosion influences the reliability of the pipelines in operation conditions. Electrochemical impedance spectroscopy (EIS) technique has been used previously to detect and characterize the electrolyte/coating/metal interface degradation in real time under laboratory conditions.

In this work EIS tests are performed to identify and characterize the damage evolution of different coal tar enamel coating status conditions (intact and defect) for buried cathodically protected pipelines in laboratory scale. Generalized Exponential (GE) distribution is used to model and quantify the damage evolution of localized corrosion induced by a coating defect. The distribution of metal degradation rate has been modeled with the family of extreme value distributions (e.g., Weibull, Gumbel, and Generalized Extreme value distributions); however, these families of distribution often do not consider the property of metal degradation rate when one or more parameters take certain values. The extreme family also is hard to estimate with analytical solutions because of their non-linear characteristics. The generalized exponential distribution contains the parameters that permit the damage evolution process modeling be more effective than the extreme value families. The parameters of GE can be time dependent with their own distributions. These parameters are estimated via Markov Chain and Monte Carlo methods. The proposed models are validated based on the EIS laboratory data obtained for different pipelines simulating soil conditions for a period of 320 days.

CORTracer™, an innovative monitoring instrumentation for the ac corrosion risk assessment of cathodically protected buried pipelines

Elisabeth FLEURY^a, Didier CARON^a, Michel MEYER^a, Sylvain FONTAINE^b

^a GDF SUEZ – DRI – Centre de Recherche et d'Innovation sur le Gaz et les Energies Nouvelles, 361 avenue du Président Wilson 93211 SAINT-DENIS La Plaine, elisabeth.fleury@gdfsuez.com / didier-jean-christophe.caron@gdfsuez.com / michel.meyer@gdfsuez.com

^b GRTgaz – Pôle Expertise de Compiègne, 5 rue Ferdinand de Lesseps BP 50309, 60203 COMPIEGNE CEDEX, sylvain.fontaine@grtgaz.com

Abstract

A.c.-induced corrosion threat on buried transmission pipelines is currently controlled through a two-step approach, which demands:

- 1) Implementation of specific grounding devices aimed at mitigating the interference effect by lowering the pipeline's a.c. voltage below a specific threshold, and
- 2) Acquiring measurements of some electrical parameters along the right of way of pipeline sections affected by the a.c. interference, and confronting the measurements to "CP-mitigation" criteria, effectively reducing the a.c. corrosion likelihood. The goal of this step is to check that mitigation of the interference (step 1) is adequately implemented and compliant with the CP dosage on the line, so that pipeline integrity is not impaired by the interference.

A.c. voltage's threshold and "CP mitigation" criteria have been established from semi-empirical data, including laboratory works and field feedback data, as well as from considerations on the a.c. corrosion mechanisms.

However, in the field, levels of a.c. interferences depending on numerous conditions may change including significant fluctuations in a.c. voltage levels due to daily and seasonal changes in electrical load, soil conditions, etc. Performing a continual monitoring of suitable parameters such as a.c. voltage potential and/or a.c. corrosion current density may improve the corrosion risk assessment diagnosis.

Moreover GDF SUEZ R&D center developed new criteria based on the understanding of a.c. corrosion mechanisms and specifically the faradic rectification impact on corrosion severity. The new criterion is based on faradic rectification monitoring and comparison to several thresholds. It is believed to improve the current practices by introducing a new parameter which can track the actual impact of a.c. corrosion on corrosion risk. It has been patented under reference FR1161133. This new criteria has been introduced in an innovative monitoring device so-called CORTracer™ dedicated to evaluate a.c. corrosion risk through standardized criteria and faradic rectification monitoring.

This article deals with an introduction to CORTracer™ monitoring tools as well as with first results of laboratory and field trials of the device.

Key words : ac corrosion ; cathodic protection ; monitoring ; instrumentation.

Effects of anodic interference on carbon steel under cathodic protection condition

M. Ormellese¹, A. Brenna¹, L. Lazzari¹, F. Brugnetti²

*¹Politecnico di Milano, Dipartimento di Chimica, Materiali e Ingegneria Chimica
"Giulio Natta", Milan, Italy*

²APCE – Associazione per la Protezione dalle Corrosioni Elettrolitiche, Milan, Italy

Abstract

Stray currents originating from direct current systems may cause severe corrosion damage on buried metal structures, as steel pipelines for the transport of hydrocarbons. Depending on stray current source, stationary or fluctuating interference may occur, even under cathodic protection condition. In order to assess the risk of corrosion to which the structure is exposed, the positive (anodic) potential shift of the affected metal shall be compared with the acceptance criteria provided by international standards.

The duration and the magnitude of the anodic potential shift during the operating period of the interfering systems should be taken into account to evaluate the corrosion effects of stray current on the interfered structure.

This paper deals with the effect of anodic interference on buried carbon steel structures both in free corrosion and in cathodic protection condition, in particular as regards the interference acceptable criteria provided by cathodic protection guidelines. Weight loss tests were carried out on steel specimens in soil-simulating environment varying the protection condition, i.e. the protection potential, and the anodic current density (from 0.1 to 10 A/m² for 3600 s daily) in order to evaluate corrosion rate and the acceptability of stray current interference. IR-free potential and interfering currents were measured during the period of interference.

Keywords: carbon steel, cathodic protection, anodic interference, stray current, potential shift.

Presentation made by Sylvain FONTAINE (GRTgaz)

Mail : sylvain.fontaine@grtgaz.com

Address :

GRTgaz
Pôle Expertise Compiègne
Département Opérationnel Expertise Protection contre la Corrosion
5 rue Ferdinand de Lesseps
BP 50309
60203 Compiègne Cedex
France

Mobile : +33 6 61 12 20 45

Office : +33 3 44 23 41 12

Title : Proposed method to define the maximal accepted error made in the metrology line of measurements

Abstract

GRTgaz has more than 15 years of experience in the monitoring of the metrology of all its measurements devices used in cathodic protection according to its insurance quality management. Nowadays, GRTgaz uses the EN ISO 10012 standard which defines rules to respect for the metrology management of measurement devices.

The process presents the advantage to guarantee the accuracy of measurements made for the operation and the maintenance of cathodic protection equipment.

The EN 12954 standard defines cathodic protection criteria using IR free potential measurements. GRTgaz has consequently defined its calculation method to quantify an acceptable error made during IR free potential measurements. This error has been calculated taking into account the metrology chain composed by the multimeter and the reference electrode. As a consequence, the accuracy of IR free potential measurements has been calculated to ± 50 mV. This value is the so called Maximum Acceptable Error (MAE).

CP design of internal components

H. Osvoll, Force Technology Norway AS, Trondheim/N

In order to perform a CP design one has to collect information on the components to protect, the conditions and the CP standards to use. For internal components as e.g. smaller tanks, piping, filters, etc, the CP design is not straight forward and is not fully cover by existing standards. Since this is protection of an internal area there will be limited space for current transport which will introduce extra potential drop and reduce the protection capability. This design limitation is also seen for e.g. pump caisson where this have caused major failures on caissons. This paper will look into these factors through CP modelling, practical calculations and actual measurements.

**Abstract: Cathodic protection of extended sheet piling in soil.
A practical case.**

U. Marinelli, E. Barbaresi, F.M.Engineering S.r.l., Ancona, Italy.

The paper describes the study, execution and start-up of the cathodic protection system for a 5 km sheet piling. The sheet piling lays in the south of Italy (Sicily) and it is used to contain an area characterized by surface's pollution of the ground water. Because the sheet piling was intended to seal the ground water and not to hold the soil mechanically, cathodic protection was needed to prevent every kind of decay due to corrosion that could have nullify the functionality of this significant structure. The elements leading the planning of this cathodic system and its realization till the start-up, have been the size of the structure, the impossibility to execute big digging works, the need to avoid interferences with existent structures, even with a high protection current, and the little literature concerning cathodic protection of sheet piling in non-marine environment. The realization of the system entailed the installation of 36 current feeders for cathodic protection, in conjunction with the same number of anodic deep wells (Figure 1). During the calibration of the plants, the introduction of E-log I test allowed reducing the current supply of the feeder, still granting the sheet piling protection.

Keywords: Cathodic protection, sheet piling, soil, corrosion, corrosion potential, Tafel curves, E-log I test.

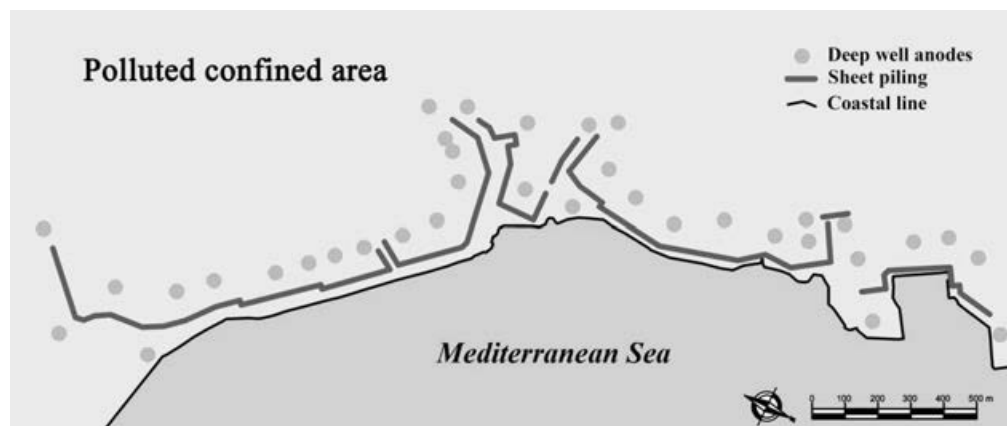


Figure 1. Polluted area, sheet piling position and deep wells location.

Cathodic protection assessment of oil storage tank farm

*Massimo Diminich, Fabio Mari, TAL Società Italiana per l'Oleodotto Transalpino SpA,
San Dorligo della Valle, Trieste, Italy*

Giorgio Lecardi, Tiziana Caglioni, Fabio Duranti, Cescor Srl, Milan, Italy

Abstract

SIOT has 32 crude oil above ground storage tanks in its Tankfarm for the storage of the product prior to export. These tanks have a storage capacity from 20'000 to 100'000 cubic meters.

Hydrocarbons leaks/spillages resulting from tank failures, if any, could be very expensive and could pose serious fire hazards apart from major environmental issues. With the aging tank farm facilities, it become even more important to implement a corrosion management strategy that is able to provide a reliable picture of the integrity status. Therefore, in order to carry out a comprehensive assessment of structures integrity, an RBI approach in conjunction with a dedicated cathodic protection survey has been performed.

The paper is an overview of the adopted methodologies to identify the corrosion threats and used for the calculation of corrosion rates. Finally, the paper provides a brief overview on the applicable cathodic protection inspection techniques, describing how the cathodic protection survey helps in identifying hidden corrosion.

New tool for CP inspection

H. Osvoll, J.C. Werenskiold, Force Technology Norway AS, Trondheim/N

Inspection and monitoring of offshore structures and pipelines protected by CP are important factors in maintaining the integrity. As the offshore structures and pipelines get older, sacrificial anodes become depleted and coating gets damaged or deteriorates, methods for quantifying the various parameters affecting the protection become increasingly important. This paper describes the capability of a new tool for CP inspection both through modelling and inspection cases.

The new tool, The Field Gradient Sensor (FiGS), has been developed in order to measure electric fields in the seawater very accurately. It will quantify the current density of the surface and detect coating damages at a level which has never been seen before. It can be used to detect small coating damages even on buried pipes. It will accurately measure anode current, thereby enabling accurate estimates of remaining anode lives. It will determine the current density on the steel surface, which in turn can be used to optimise a CP retrofit design. It will enable detection of leakage currents from ICCP systems, cables and subsea power supply units and it is a tool for quantifying current flow from anodes of a pipeline equipped with Direct Electrical Heating (DEH).

Evaluation of ICCP system over API X52 steel tested in two types soils in the state of Campeche, Mexico.

C. Lizárraga¹, L. Quej-Aké², A. Contreras², V. Moo-Yam¹, T. Pérez¹

¹Universidad Autónoma de Campeche, Campeche, México, ave. Agustín Melgar s/n, Col Buenavista, P.O. Box 24039, Campeche, México.

²Instituto Mexicano del Petróleo, Eje Central Lázaro Cárdenas Norte 152, Col. San Bartolo Atepehuacan, P. O. Box 07730, México D.F.

The investigation and studies of the corrosion soils in the current days have become of interest for the researchers in the area of the preservation of materials, by economics, mechanical and safety needs. Many industries are being based on the use of soil as a support for countless buried structures for efficiency from the engineering activities in a more simple and economical form. However, ecological, human and economic losses suggest a considerably research on topics related to steel corrosion in soils. As for the corrosion control of these buried structures, two types of the protection are mainly used: a good coating, and/or a cathodic protection system.

In this work, two types of soils common of the State of Campeche, Mexico, one natural calcareous origin and the other cropland, were analyzed by physicochemical methods determining: chloride, sulfate, carbonates and bicarbonates ions, organic matter, resistivity, moisture, pH and redox potential. Was evaluated in laboratory essays, the corrosion process of witness samples of API X52 steel in the two soils. Similar samples were tested under cathodic protection by using Impressed Current Cathodic Protection (ICCP) by the criteria of potential -850 and -950 mV vs Electrode Cu/CuSO₄. Corrosion behavior was evaluated by gravimetry (weight loss) and electrochemical techniques: potentiodynamic polarization curves and polarization resistance. Tests were carried out at open circuit potential and with ICCP system.

Weight loss results show that the calcareous soil presents corrosion rates higher than those obtained in the cropland. Similarly, the polarization curves and polarization resistance analysis confirms this trend of higher corrosivity of the calcareous soil. Are discussed the corrosion behavior of API X52 steel due to characteristics of soils and of the ICCP polarization applied.

Soil side corrosion of storage tank bottom plate, failure causes and mitigation provisions

Sahar Afroukhteh, Pars Oil and Gas Company, Tehran/Iran

Mehdi Askari, Pars Oil and Gas Company, Tehran/Iran

Daryoush Masouri, Pars Oil and Gas Company, Tehran/Iran

Abstract

Above ground storage tanks are affected by corrosion from soil side with different mechanisms. This is common failure especially for tanks living without cathodic protection or insufficient protection at early life after construction in which temporary sacrificial cathodic protection is not usually considered. Soil side corrosion risk remains latent at this short stage considering controlled properties of infill material beneath tanks. Achieving the polarized potential criteria will be reliable and safe protection for tank operator.

Aim of this work is to discuss the parameters contributing in soil side corrosion on some corroded tanks in coastal regions, review the protection techniques intended in design process and remedial solutions to achieve minimal risk and get integrity of tank bottom plates.

Cathodic protection of bare bottom tank in field is also studied in this survey. The effects of soil resistivity, presence of corrosive agents in soil, anode spacing and other design factors are analysed. Even though it was believed that corrosion rate can be predicted based on the soil survey, but the field experience shows surprising results in moderate corrosive soil. Risk assessment as per API Standards is also part of this work.

Sacrificial Anode Key Design Parameters for the Internal Surfaces of Vessel, Tank and Structures

Saleh Al-Sulaiman

Hasan Sabri

Kuwait Oil Company, Ahmadi, Kuwait

The internal protection of the carbon steel storage and vessels against corrosive media raise high level of threat from corrosion. For extended protection against corrosion, a combination of internal coating and cathodic protection normally is utilized. The use of cathodic protection for the protection of carbon steel storage and vessels have varied success rate. This is mostly due to improper design, installation, operation, planning or a combination of all. This has raised a great challenge on the corrosion engineers to provide effective cathodic protection for the internal immersed carbon steel inside storage and vessels. This paper discuss case studies that took into consideration the cathodic protection key parameters during the design stage and had improved the life of galvanic anodes, which in return would help in achieve increased cathodic protection life.

EPIC new 16" Jet A1 Fuel Pipeline (External Coating Case Study)

**Nabil Hamdy Head of Coatings
PETROJET**

**NabilHmdy@yahoo.com
+974 501 406 84 +20 111 30 73 200**

ABSTRACT

Oil and gas still our main sources of energy production, otherwise eco-compatible alternatives are costly and their industrial application is limited or they are economically valid but undesirable owing to potential environmental risk factors like nuclear power which their use is consequently limited in some countries. In future, hydrogen may become a valid option, but for the time being, fuel demand is satisfied by fossil resources that are being continually identified by technological developments for prospecting in deep waters, thus putting off the time when they run out.

Pipelines, whether buried in the ground, exposed to the atmosphere, or submerged in water, are susceptible to corrosion. Without proper maintenance, every pipeline system will eventually deteriorate. Corrosion can weaken the structural integrity of a pipeline and make it an unsafe vehicle for transporting potentially hazardous materials. However, technology exists to extend pipeline structural life indefinitely if applied correctly and maintained consistently.

Although data management, system quantification through the use of global positioning surveys, remote monitoring, and electronic equipment developments have provided significant improvement in several areas of pipeline corrosion maintenance, there have few basic changes in the approach to the management of corrosion on pipelines until recently. The use of integrated External Corrosion Control System for Pipelines is the most affective toll for corrosion protection in the pipeline sector.

Therefore we forced to face the challenge in design the most suitable strategy in corrosion protection to pipelines used for hydrocarbons transport which will achieved by the combination of a materials development and selection, protective coating (factory coating and field coating) and cathodic protection (CP) to preserve the metal exposed to corrosive environments and also in operation phase (corrosion monitoring / inspection plans – maintenance plans).

Hence the effectiveness of protection strategy will depend upon the equilibrium between all variables including: basic materials, coating condition and the CP level, in integrated engineering process.

This case study demonstrates the strategies used in external corrosion protection for our project (EPIC new 16" Jet A1 Fuel Pipeline) during engineering / construction / operating phases and discuss coating in more details including coating performance / coating properties / design / factors effect selection...etc. including required tables and diagrams.

The proposal of this work is simply to study and recognize the integrated external coating system applied for this pipeline and give required recommendations needed for future projects.

1. INTRODUCTION

The coating is the primary corrosion mitigation system and the CP is the supportive system that protects the pipeline metal where the coating has failed, however in spite of all these precautions a coating disbondment may locally occur It leads to the penetration and the stagnation of the electrolyte contained in the soil in confined space between the coating and the pipeline. In the past few years, new techniques have emerged to assist the corrosion engineer in the evaluation of the best corrosion control of their pipelines.

Impressed Current Cathodic Protection (ICCP) Ti-MMO Grid System for 61m diameter Methanol Tank

F. Al-Fawaz, Saudi Basic Industries Cooperation-SABIC, Jubail Industrial City/SAR

Abstract

The corrosion of metallic structures buried in soils or in contact with soils has long been a serious engineering and economic problem. All over the world many of buried structures such as (storage tanks, pipelines and critical structures foundations) are suffering from soil corrosion problems which affect mainly the external surfaces of these structures.

This paper emphasizes a model defining adequate CP technique including detailed design requirements in accordance with SABIC standards & specification, international codes and standards for the external bottom of newly constructed tank.

ICCP Ti-MMO grid system is one of important CP technique where can be used to protect aboveground storage tank bottom. A Ti-MMO anode grid system placed between an aboveground storage tank's bottom surfaces and the secondary High Density Poly Ethylene (HDPE) liner with properly distributed power-feed connections can protect the tank's bottom plates against external corrosion. Such systems can achieve uniform potentials along the tank bottom surfaces.

Light weight Technologies for Innovative Mobility Society

A. Dogan, *Toyota Motor Europe, Technical Centre Hoge Wei 33, B-1930 Zaventem, Belgium*

Abstract

We are in challenging times...

Economic uncertainties, energy demand beginning to exceed supply, increasing consumption of natural resources, reduced ambient air quality, climate change are the main ones.

Automotive manufacturers, while MAXIMIZING the value of their products for their customers, on the other hand pursuing to ZERONIZE energy consumption, greenhouse gases, and usage of natural resources and waste.

Light Weight Design is not only as a trend to increase vehicle driving performance, but to reduce the environmental footprint, through manufacturing, and increasing vehicle efficiency.

As a company, pursuing the philosophy of "Right Material at Right Place", we first would like to discuss how we see each sector, namely Steel, Aluminium, and Plastic industries, making their most efforts to secure their future.

At my speech, I will present the Toyota light weight philosophy with an emphasis on value to the customers considering their needs, diversity and durability aspects.

- Continue Steel Sheet, by expanding the usage of advanced high strength grades, partial thickness optimization, partial strength optimization, and improvement of material joining technologies,

- Using low density materials, Aluminium, Magnesium, and Plastics,

During the presentation more focus will be given in CFRP materials by concrete examples from Lexus Super Sport vehicle LFA, and discuss how to expand its usage by tackling the problems of cost and productability.

Final portion will summarise challenges of multi-material design, such as joining technologies, surface treatment of various different material, galvanic corrosion, necessity of innovative low temperature coating material and complexity and availability of global supply.

Effect of Welding Heat on Microstructure and Corrosion of Ferritic Stainless Steel 409M

Sachin P. Ambade, , Phd Scholar, Department of Metallurgical and Materials Engineering VNIT, Nagpur India,

Yogesh M. Puri, Associate Professor, Department of Mechanical Engineering VNIT, Nagpur, India,

Awanikumar P. Patil, Professor, Department of Metallurgical and Materials Engineering VNIT, Nagpur, India 440001

Presenting author's email: sachinamb2@rediffmail.com

ABSTRACT

Ferritic stainless steel 409M is becoming a preferred choice as construction material for railway wagon and containers owing to its better corrosion resistance and strength. While the steel has useful properties in the wrought condition, welding is known to reduce toughness, ductility, and corrosion resistance because of grain coarsening and formation of martensite. The grain coarsening takes place when the base metal is heated above a critical temperature (i.e. 955°C) and causes rapid grain growth of the ferrite. This coarse grain zone lacks ductility and presence of small amount of martensite worsens the situation. Excessive grain growth can be avoided, of course, by using lower welding heat inputs. Welding procedure for SS409M is already established but there is paucity of published literature on the topic. Present investigation, therefore, is aimed at studying effect of welding heat on microstructure and corrosion of ferritic stainless steel 409M. The sheet of 409M (3mm thick) was welded by shielded metal arc welding (SMAW) as bead-on-plate. The surface of the sheet was carefully cleaned and the sheet was anchored during welding to minimise distortion. Welding electrode of 308L (3.15mm Φ) was used and welding currents of 80A (at 23V), 90A (at 23.5V) and 100A (at 24V) were used to vary heat input. Microstructure was observed at transverse section; width of heat affected zone (HAZ) was noted. It was found that width of HAZ increased with increasing heat input. It was also noticed that grain growth increased with increasing heat input. Potentiodynamic polarisation (PDP) tests were performed on samples cut from HAZ and base metal in H_2SO_4 (0.1M and 0.5M) and mixture of H_2SO_4 (0.1M and 0.5M) + NH_4SCN (0.01M). It was observed that test steel shows passivity in 0.5M H_2SO_4 (with or without NH_4SCN). The current at the middle of the passive region increased on increasing welding heat and also on addition NH_4SCN . Test steel shows active corrosion in 0.1M H_2SO_4 (with or without NH_4SCN). The anodic current density increased on increasing welding heat and also on addition NH_4SCN . It is attributed to precipitation of chromium carbide at grain boundaries and grain growth.

Pickling process for high-strength steels before coating

Christiane Schreiber, Susanne Friedrich

Institut für Korrosionsschutz Dresden GmbH, Dresden/Germany

Pickling of high-strength steels is used predominantly to remove present oxide layers. Subsequently organic coatings combined with conversion processes are applied. The continuous increase of using laser cutting as well as welding of high-strength steels in automotive engineering and lightweight construction demonstrates the necessity of this measure. In order to ensure an optimal adhesion, the thereby resulting strongly adhering scale must be removed by suitable methods, e. g. by pickling baths.

The pickling process is less critical for steels with normal tensile strength, in contrast to high-strength steels, which are more or less susceptible to absorption and permeation of hydrogen as well as hydrogen embrittlement.

Therefore a new pickling method for the treatment of high-strength steels was developed. The research was focussed on the evaluation of suitable pickling substances with low hydrogen permeation. Hence the danger of damaging high-strength steels caused by hydrogen embrittlement or hydrogen induced brittle fracture should mostly be prevented.

For the specific variation of critical parameters an appropriate test method was applied. Furthermore the iron concentration and the reaction of corrosion inhibitors in the pickling baths with regard to hydrogen embrittlement and hydrogen generation were investigated. Within this research project dual-phase steels, retained austenite steels and martensitic-phase steels with several tensile strength R_m were applied. Picklings containing sulphuric and phosphoric acid and also weakly acidic picklings based on organics were used for the investigations. The correlation between hydrogen concentration and possible hydrogen embrittlement was complemented by simultaneous tensile tests of pickled steel samples.

In summary it could be shown, that the dual-phase steel HCT500X with a tensile strength R_m of 500 MPa has a hazard potential regarding hydrogen absorption. In addition a negative impact on the mechanical values after pickling by not inhibited sulphuric-phosphoric acid exists. Especially for the use of this mineral acidic pickling several corrosion inhibitors were applied. All further studied high-strength steels indicated no significant differences in their mechanical values after pickling. Particularly the hydrogen absorption of these steels has mostly been decreased by the application of weakly acidic organic picklings.

Limits of Rapid Heating for the Press-Hardening of Ultra-High-Strength Steel from Aluminum-Silicon-Coated Blanks

Todzy, T., Daimler AG, Benzstrasse, 71059 Sindelfingen

Wortberg, D., Daimler AG, Benzstrasse, 71059 Sindelfingen

Engel, B., University of Siegen, Chair of Metal Forming Technology, Paul-Bonatz-Strasse 9 - 11, 57076 Siegen

Weyrich, M., University of Stuttgart, Institute for Automation and Software Technology, Pfaffenwaldring 47, 70550 Stuttgart

Lightweight construction with ultra-high-strength steel is an excellent way to reduce emissions from motor vehicles while at the same time enhancing occupant protection. Accordingly, many automobile manufacturers have in recent years considerably increased the number of body shell components made from press-hardened steel. These components are usually manufactured in the direct press-hardening process, in which the blanks are initially heated to around 925°C over a period of several minutes in a roller hearth furnace (normally between 30 m and 40 m in length) to achieve austenitization. The long heating times include the time it takes for the furnace to heat up, which takes place via the comparatively slow method of convection and radiation. To minimize corrosion and high-temperature oxidation, however, an aluminum-silicon coating is often applied to the components. But this first has to be stabilized while the furnace is heating up by alloying iron from the base material so that it does not "melt away" at the austenitization temperature of more than 900°C. Once the semi-finished part has been heated in the furnace, it is formed in a water-cooled tool and then hardened by keeping the tool closed for several seconds. As a result, the cycle times are much higher than in the cold-forming process. Furthermore, the current press-hardening process requires considerable investment, is not very flexible and takes up large production areas. This problem would be exacerbated further if the cycle times were reduced because the length of the furnace would have to be increased. To avoid these drawbacks of press-hardening, various concepts for reducing the time it takes to heat the blanks are currently being investigated, with the focus in most cases on looking at different heating methods (e.g. induction-based) for achieving the quickest-possible rate of heating. However, the following question has yet to be clarified: For how long can the blanks be heated before both the base material and coating lose their function? This is why this paper specifically investigates the influence of rapid heating on the surface. For this purpose, the influence of different heating parameters (e.g. heat-up rate and temperature profile) on the aluminum-silicon coating is first determined. To do this, the samples are heated both in a conventional furnace heating process as well as via rapid, induction-based heating. Besides the coating's properties (e.g. roughness), its functions (e.g. corrosion and paint adhesion) are also characterized as a function of the different heating profiles on the basis of the coating currently being applied and used to define a process window for rapid heating. Finally, the same tests are performed on samples whose coating has been heat-treated in advance. The aim is to investigate the extent to which this kind of preconditioning improves the coating performance (i.e. specifically, a process window for shorter heating times) for rapid heating.

Controlling and monitoring the risks of hydrogen induced stress corrosion cracking in automotive body parts

Roland Scharf¹, Andreas Muhr², Gerald Luckeneder², Karl-Heinz Stellnberger², Josef Faderl², Gregor Mori³

¹*CEST Kompetenzzentrum GmbH, Viktor-Kaplan-Strasse 2, 2700 Wiener Neustadt, Austria*

²*voestalpine Stahl GmbH, Research and Development, voestalpine-Strasse 3, 4021 Linz, Austria*

³*Montanuniversität Leoben, Franz-Josef-Straße 18, 8700 Leoben, Austria*

Automotive industry is forced to reduce the weight of cars for environmental protection. This is in conflict with increasing safety (crash performance) demands and comfort requirements.

The application of advanced high strength steels in car body design is a very powerful approach to meet those conflicting goals. But for very high strength levels, 1 GPa or more, hydrogen embrittlement becomes an issue and has to be taken into account. Prerequisites for hydrogen induced stress corrosion cracking (HISCC) are a critical diffusible hydrogen content in the component, a certain stress level and a certain susceptibility of the chosen material to hydrogen embrittlement. For appropriate steel development minimizing the risks of hydrogen embrittlement is of crucial importance. Therefore, an effective and reliable tool to measure the hydrogen embrittlement susceptibility for different steel grades is necessary.

A qualified testing method to determine the risks of HISCC (Hydrogen Induced Stress Corrosion Cracking) during production or during operation (service) has been established and is presented. The constant load test contains a small corrosion chamber surrounding the sheet tensile specimen and is adequately notched.

Tests have been performed with and without zinc coating of the specimen under different loads. Fracture surfaces have been investigated by SEM and optical microscopy. The specimens have been characterised by measurements of the hardness. Different specimen geometries and preparation methods are critically discussed.

Crevice corrosion of hot stamping steels for the automotive industry

Martin Jönsson¹ Lisa Levander²

[1] Gestamp HardTech, Ektjärnsvägen 5, SE-97125 Luleå, Sweden, mjonnsson@se.gestamp.com

[2] Gestamp HardTech, Ektjärnsvägen 5, SE-97125 Luleå, Sweden, llevander@se.gestamp.com

Abstract

Hot stamping steels have seen a major increase in the automotive industry during the last decade.

These steels ensure the required safety directives in a light weight car body construction. The use of tailored blanks is a further step in the strive towards weight decrease of the car body. One solution is the pre-patched blanks where the patches are attached to the blanks before the hot stamping step. Using the patched blanks the mechanical strength can be enhanced solely in areas where it is further needed, e.g. areas on a B-pillar that protects vital parts of the human body. The use of patched blanks saves expensive production steps. Further, the welding of the patches onto the blanks is made before the hot stamping process; hence the problems with a heat affected zone will be eliminated.

However with the increasing use of hot stamped steels and the desire to use them in areas more exposed to the elements an increased focus needs to be directed towards the corrosion questions. Since a crevice is unavoidable between the blank and the patch, crevice corrosion will be an issue that's needs to be taken into consideration. In this work the crevice corrosion of these patched blanks has been investigated and is discussed.

A century with salt spray testing; Time for a final phasing-out by a replacement based on newly developed more capable test regimes

Mats Ström, Volvo Car Corporation, Gothenburg, Sweden

1914, i.e. hundred years ago, salt spray corrosion testing was suggested by Capp(). 25 years later the first ASTM B117 standard was issued and since the fifties the neutral salt spray method remains essentially the same and has been dominating the scene of corrosion testing. (We will in the following only address the neutral variant). 35 years ago, in the university department on corrosion where I was a graduate student, there was a saying that neutral salt spray testing, at best, might correlate to the environment of a submarine periscope. At the time the consequence of a severe misjudgement, based on salt spray testing, was too obviously manifested on the rusty cars running through our streets. A work life later and with a solid experience in atmospheric corrosion, I have not found much to add to the merit list of this test method. In industrial sectors dealing with corrosion protection as a core concern, like surface treatment of car bodies, the problem was soon realized and development of alternative, more realistic test regimes, based on alternating wet/dry climate cycles and moderated salt loads, was started. This process has continued since and substantial progress has been achieved. These findings do not appear to have penetrated into areas of the manufacturing industry, where surface treatment is more of an externality, however. In spite of numerous publications dealing with the problem, neutral salt spray testing is still 2014 regarded state-of-the-art for quality assurance against corrosion problems, even if more often just a tic-in-the-box-test. The procedure is well established, testing equipment is readily available and comparably low-cost and the test looks hard and relevant.

This presentation systematically summarizes why continuous salt spray testing lacks essential elements to be capable of reproducing almost any field environment. Examples from the most important materials and modes of atmospheric corrosion are given and explained to detail. From a car industry perspective another aspect associated with its high penetration among the suppliers is that the use of the test blocks and prevents meaningful communication around real corrosion risks and issues ("but it passed XX hours in our salt spray cabinet"). In the academies, on the other hand, the knowledge can also be missing. Many corrosion studies utilizing advanced electrochemical equipment or computer modelling, have addressed salt spray testing as a control reference, in order to validate the achieved results.

It is time to utilize the significant progress in test development made in the automotive industry to define a simple enough replacement to the ubiquitous salt spray method. Such a test is based on climate cycling combined with periods of wet loads, containing one or more corrosive constituents (most frequently NaCl). In spite of the high number of seemingly different set of test cycles found in this area (many brand unique tests) there are certain key variables and proportions that are common denominators for those tests that show the best and broadest correlation to field. Here is shown how such a base test shall be designed in detail to become relevant, reliable and easily performed without high investments in equipment. It is also suggested how to improve the notorious problems with repeatability and reproducibility found in corrosion testing, by controlling/eliminating the sensitive parameters.

Analysis of Perforation Corrosion Morphology of Steel Sheets for Automobiles using Laser Displacement Meters

*Hiroshi Kajiyama **, *Masataka Omoda **, *Mitsuo Kimura **

** JFE Steel Corporation, Japan*

In evaluations of the perforation corrosion resistance of steel sheets for automobiles, corrosion loss and maximum corrosion depth are commonly measured. It is empirically known that corrosion morphology is affected by the corrosion test conditions and the kinds of steel sheets, but the corrosion morphology cannot be evaluated by current conventional methods. In order to analyze the distribution of corrosion depth, a new measurement system using two laser displacement meters and an X-Y stage was developed. In this report, the newly-developed system was applied to analysis of the perforation corrosion morphology of steel sheets for automobiles. From the results of cold-rolled steel sheets, it is found that the corrosion morphology of steel sheets was affected by the structure of specimens. In the flat specimens, the distribution of corrosion depth had a minute uniform roughness. However, in the lapped specimens, non-uniform roughness was observed on the surface of the specimens. Furthermore, from the results of the lapped specimens of Zn-coated steel sheets, it is found that Zn-coating could inhibit the initial progress of perforation corrosion.

Methodology for the definition of Failure Assessment Diagram of AHSS exposed to aggressive environments

M. Beghini, L. Bertini, C. Colombo, B. Monelli, R. Valentini

Department of Civil and Industrial Engineering, Largo L. Lazzarino 1, 56122

University of Pisa (Italy), email: beghini@ing.unipi.it, l.bertini@ing.unipi.it,

costanza.colombo@for.unipi.it, bernardo.monelli@ing.unipi.it,

r.valentini@diccism.unipi.it

Abstract

The increasing demand of weight and cost reduction, and higher safety levels of the automotive industry is favouring the spread of Advanced High Strength Steels (AHSS) as structural materials. This class of steels is promising owing to their very good strength properties combined to ductility and formability. Although these very attractive properties, AHSS can suffer from phenomena induced by service environment which can jeopardize the material strength such as Hydrogen Embrittlement (HE) and Stress Corrosion Cracking (SCC). Experimental works have confirmed that AHSS mechanical resistance also depends on the applied stress and plastic strain states. Design and manufacturing practices have to take into account these issues for which traditional know-how may be no longer applicable. The knowledge of the dependence of the material strength on the stress-strain states, and environmental conditions, represents a crucial problem to be challenged. The present work is aimed at defining a methodology for identifying these kind of relationships. The research has been structured into three phases. Material selection and aggressive environment definition were firstly faced. The preliminary analysis led to three representative AHSS (M1200, HS1500 and TRIP800), for which standard characterization has been carried out. Salt aqueous solution (3.5% NaCl), with the application of different values of potential (0, -1 and -1.5 V SCE), was selected to reproduce service life conditions. Consistent stress and strain states were introduced adopting U-bend configuration. Specimens were bent by three points bending process, according to the prescriptions of VDEh SEP 1970 - 2011. Stress and strain distributions were estimated by an *ad-hoc* Finite Element Model (FEM) simulating the used process for specimen drawing. The proposed methodology allows to establish a direct correlation between the stress-strain states and the occurrence of failure and time for each combination of considered material and environment. This methodology appears to be successfully used for the definition of useful failure assessment diagrams.

Influence of key climatic parameters in accelerated test on the corrosion and mechanical properties of joined materials used in the automotive industry

*Nathalie LEBOZEC, Olivier CLAUZEAU, Dominique THIERRY,
French Corrosion Institute, Brest, France*

Steel and aluminum based materials are the most important construction materials for the mass production of automotive structure, which implies joining of dissymmetric assemblies with appropriated joining techniques. From a previous work, it was shown that the strength loss measured on a large numbers of joined materials was largely dependent upon the type of corrosion test used [1]. No correlations were observed when comparing the mechanical properties obtained after three different corrosion tests e.g. VDA621-415, VDA233-102 and a BMW SCAB test. In particular, the VDA 233-102 test which has a low temperature phase (-15°C) did not contribute to higher strength loss for adhesives more than the VDA 621-415.

Hence from those results, additional studies were conducted in order to better understand the effect of climatic parameters in a cyclic corrosion test on the mechanical properties of different assemblies. Thus, the effect of selected climatic parameters including the freezing temperature (room, -15 and -25°C) and the composition of the salt solution (NaCl or a mixture of NaCl and CaCl₂) in a VDA233-102 cycle was investigated using 20 different assemblies with a lap-shear design. These joined materials included steel based substrates such as carbon steel, high strength steel and zinc coated steel (conventional zinc coating as well as ZnAlMg coating) and two different aluminium alloys (AA6016 and AA5182). Joining techniques integrated spot welding, clinching and adhesive bonding. The results were also compared with field data from long term exposure under a trailer in snow belt area.

1. N. LeBozec, A. LeGac and D. Thierry, Materials and Corrosion, 63(5), 408, 2012

Concentration effect of salt solution on the corrosion of carbon steels investigated by salt spray test

Ha Sun Park, Yun Ha Yoo, POSCO, Incheon/Korea

Salt spray test (SST, ASTM B-117) and cyclic corrosion test (CCT) are widely used to evaluate the corrosion properties of carbon steels in automotive industry. It is very well known that SST is a faster method (typically 3-6weeks) than CCT (typically 6-10weeks) but corrosion results by CCT are recognized to more reliable to the field exposure than that by SST. The corrosion results by some CCT modes such as VDA621-415, Honda and Nissan mode show good correlation with SST, however, others such as GM and ECC1 show the weak correlation with SST. Moreover, there are many kinds of CCT modes which are very specific to auto company and different from each other. Any CCT mode does not show the exactly matched corrosion performance to that of field test. Results from corrosion test by those CCT to carbon steels show the broad range in corrosion performance. Cosmetic/perforation corrosion of cold rolled (CR) steels are better than that of hot-dip galvanized (HDG) steel in some CCT mode but reverse results would be shown in other CCT mode. These CCT modes could be categorized into two region based on which corrosion performance is better among CR and HDG. We have doubt why two categorized CCT modes show different corrosion performance to the same material. We guessed that the key factor in CCT modes is not the differences in the mode (that is, combination of salt spray, dry and humid condition), but the concentration of salt solution used in the test. Typically, salt concentration of 1% and 5% are used for CCT salt solution. Any CCT mode using 5% concentration of salt solution, shows better cosmetic corrosion performance of CR than that of HDG, but CCT mode using 1% concentration of salt solution shows opposite results. These results strongly suggest that concentration of salt solution could affect the corrosion behavior of carbon steels. We tried to investigate the concentration effect of salt solution on the corrosion behavior of carbon steels by SST and to correlate SST results with CCT results.

Adequacy between lighter multimaterial vehicle and car body corrosion resistance

P. Buttin, P.-Y. Cam, G.-A. Balmont, J. Bovin

Renault SAS, Guyancourt, France

To reduce fuel consumption and CO₂ emission, car body weight has to be reduced. A good way to get this is to change materials body, and choose lighter materials as aluminium and magnesium. This material modifications lead to different forms of corrosion issues. Galvanic corrosion appears to be one of the main risks that may occur in a weight reduced car body. Our point is to improve its corrosion resistance by keeping a not expensive car.

Therefore, manage the interface between two metals becomes an important point to reach a good corrosion resistance of the body. Assembly needs to have isolated flange to avoid galvanic corrosion. A way to get this is to choose an adhesive with a high electrical resistivity.

Finally, efficiency of paints protections are tested in a synthesis corrosion test. Dynamics test is important to consider the use of the vehicle. A good understanding of the corrosion mechanism of metals involved in this car is important to determine the validation criteria which asset a good quality requirement.

The influence of Ca^{2+} in de-icing salt on the corrosion behavior of AM50 magnesium alloy

M. W. Grabowski, Prof. Dr. S. Virtanen, University of Erlangen / Nuremberg, Germany; Dr. D. B. Blücher, Dr. M. Korte, AUDI AG, Ingolstadt, Germany;

To lower the freezing point of de-icing salt, CaCl_2 is commonly used. This also affects the deliquescence of the solution. The influence of Ca^{2+} on the corrosion behavior and morphology of die cast AM50 magnesium alloy was investigated by using an electrolyte close to the de-icing salt composition with and without Ca^{2+} addition. The aim of the work is to point out the difference of corrosion mechanism with and without Ca^{2+} addition by electrochemical investigations, H_2 -evolution and weight loss characterization. It was shown that under polarizing conditions (potentiostatic and -dynamic) the resulting current densities were significantly lower in presence of Ca^{2+} , which could be attributed to the inhibiting effect of Ca^{2+} . During corrosion testing at the OCP (immersion), an ambivalent behavior was shown. During short time corrosion experiments (up to 4 h), an inhibiting effect with increasing charge transfer resistance R_{CT} with time could be observed in presence of Ca^{2+} . After about 4 h, a breakdown of R_{CT} could be observed with and without Ca^{2+} , leading to slightly higher R_{CT} values in absence of Ca^{2+} . Nevertheless, the mass loss in presence of Ca^{2+} is lower than without Ca^{2+} up to 3 days. After 3 days the mass loss in presence of Ca^{2+} is increasing significantly up to 7 days (by factor of 3). The inhibiting effect of the Ca^{2+} in the first 4.5 h cannot be attributed to the incorporation of Ca^{2+} into the surface layer, shown by XPS measurements. XPS depth profiling indicates that an increase of the thickness of the corrosion product layer in presence of Ca^{2+} seems to be responsible for the inhibiting effect. After 12 days of immersion in the presence of Ca^{2+} , the element Ca could be detected on the surface by EDX. XRD proved the presence of calcite with layer thicknesses up to 155 μm , shown by REM investigations. The alkalization of the electrolyte during Mg alloy corrosion triggers the deposition of CaCO_3 , whilst the carbonate anion stems from the CO_2 in the atmosphere. The investigations have also shown that during immersion of AM50 magnesium alloy, the pH does not exceed a value of 9.5 because of reaching the maximum solubility of $\text{Mg}(\text{OH})_2$ which leads to its precipitation. Therefore, under these conditions it is not possible for the system to reach the passivating pH of 12.

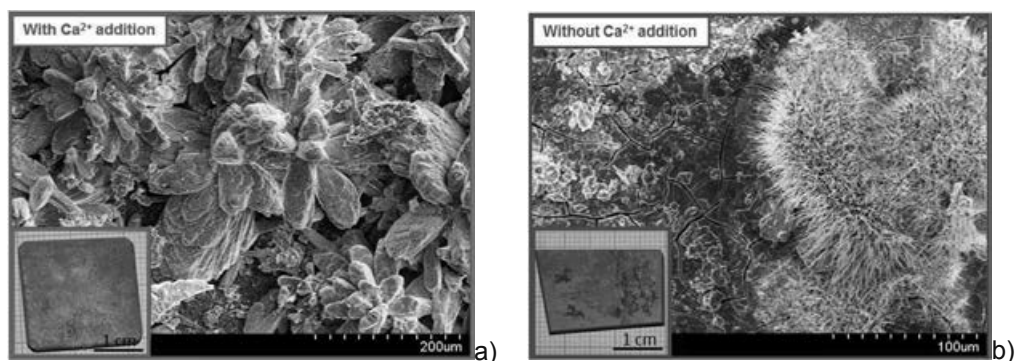


Figure 1: SEM images of corrosion morphologies after 12 day immersion in presence a) and absence b) of Ca^{2+} . a) Calcite precipitation. b) $\text{Mg}_x(\text{OH})_y\text{Cl}_z$ corrosion products

Study of polymer coating delamination kinetics on zinc modified with zinc oxide of different morphologies

*D.Iqbal, R.Singh_Moirangthem, A.Bashir and A.Erbe,
Max-Planck-Institut für Eisenforschung GmbH, Düsseldorf/Germany,*

Keywords: zinc oxide, rough model interfaces, cathodic delamination, microparticles, morphology

Abstract

Zinc is extensively used as a protective metallic coating for steels. Moreover to enhance its corrosion resistance it is often coated with polymers. Zinc is always covered with a thin oxide layer, which determines its adhesion to the polymer that is related to its resistance against corrosion. Industrially prepared materials surfaces often possess complex morphologies and topographies, which also affects their adhesion to polymers and eventually resistance to corrosion. Using rough model interfaces, the effect of the surface morphology on the delamination of a polymer coating from zinc surfaces is investigated in this work. [1] Zinc oxide particles of different shapes with characteristic dimensions $\sim 1\ \mu\text{m}$ were deposited on zinc surfaces to serve as model corrosion products with well-defined morphologies. Surfaces with spherical, rod-shaped and twin-plate-shaped zinc oxide particles were prepared and characterised by scanning electron microscopy (SEM) as well as X-ray diffraction (XRD). The surfaces were subsequently coated with poly(vinyl butyral) (PVB) as a model for a weakly bound polymer coating. Scanning Kelvin probe (SKP) measurements were carried out in humid air to study the delamination kinetics. Results were compared to PVB on zinc. While delamination is fastest on zinc without zinc oxide particles, the delamination rate on the particle-covered surfaces strongly depends on the particle morphology. Delamination rate increases in the order sphere < rod < twin-plate, with differences by one order of magnitude between fastest and slowest. The differences in delamination rate can be understood based on the surface energies of the terminating surfaces of the particles, and the resulting differences in stability under conditions of zinc oxide dissolution.

[1] D.Iqbal, R.Singh_Moirangthem, A.Bashir, A.Erbe, Mater. Corros., 2014, DOI: 10.1002/maco.201307533

Investigation on the effect of impurities on the corrosion behaviour of various A356 secondary alloys

A. Niklas¹, R. González-Martínez¹, A. I. Fernández-Calvo, J.J.de Damborenea²,
S. Méndez¹

1. IK4-AZTERLAN, Engineering, R&D and Metallurgical Processes, Spain

2. Centro Nacional de Investigaciones Metalúrgicas, CENIM (CSIC), Spain

Keywords: Al-Si secondary alloys, impurities, intermetallic iron compounds, electrochemical tests, salt spray and immersion tests

Abstract

In this study, the microstructure and corrosion behaviour of secondary A356 aluminium alloys with various amounts of Mn, Cr, V, Fe, Cu and Zn were examined and compared to the corresponding primary alloy. The aim was to develop new secondary alloys suitable for high mechanical property applications in the automotive industry having a corrosion resistance comparable to the one of the primary alloys. Fe and Zn are common impurities in Al-Si secondary alloys which adversely affect mechanical properties and/or corrosion resistance. Small quantities of Mn, Cr and V were added to counteract the negative effect of Fe on mechanical properties, due the formation of needle/platelet shaped β -Al₅FeSi by replacing them by α -iron compounds with a less harmful morphology. The effect of these compounds on the corrosion behaviour was studied. On the other hand, small copper additions can further enhance the mechanical properties of the A356 alloy. However Cu is also known to reduce the corrosion resistance of these alloys. Therefore, various additions of Cu were made in order to determine the optimum concentration where the corrosion resistance is still not affected. Electrochemical tests, salt spray test and immersion tests in 3.5 % NaCl were used to characterise the corrosion behaviour of the alloys. Based on the results of mechanical and corrosion tests an optimised secondary alloy composition has been proposed.

Effect of experimental parameters on AA6xxx intergranular corrosion during immersion in acidified NaCl solutions (ISO11846)

Lionel Peguet, Eric Chassagnolle, Romain Bergeron, Andreas Afseth

*Constellium Research Centre, 725 rue Aristide Bergès, CS 10027, 38341 Voreppe
cedex, France*

Intergranular corrosion (IGC) resistance of Al-Mg-Si (6xxx-series) wrought aluminium alloys is frequently assessed by assessing the mode and measuring the depth of corrosion attack after 24h immersion in a solution of NaCl (30 g l^{-1}) acidified with HCl according to the ISO 11846 test standard. However, poor repeatability and reproducibility (R&R) is considered a major issue when using this test for alloy development and optimization or process quality control.

Several experimental parameters, not always accurately defined in the standardized experimental protocol, were investigated in the present work: (1) Ratio between test solution volume and sample surface area, (2) immersion time, (3) solution temperature and (4) removal of the corrosion products by brushing. Rolled sheet material of AA6016-T4 containing 0.18 wt% Cu was used as a reference alloy. The copper content was chosen to ensure an intermediate level of IGC susceptibility. After corrosion testing, a statistical analysis of the maximum attack depths measured on several sub-sections defined on sample cross section was carried out. The use of a cumulative distribution function showing probability vs. attack depth proved very efficient to detect changes in the test response as a function of each unique parameter. The simple method consisting in measuring only the maximum depth of attack is much less discriminating.

The single most significant experimental factor was found to be the ratio between volume of the test solution and surface area of the sample: Increasing this volume/surface ratio from 5 to 40 ml cm^{-2} led to more than a doubling of the IGC penetration depth. The strong effect of the surface/volume ratio means that this parameter should be fixed in a narrow range for improved R&R of the test. The current ISO 11846 defines only a minimum value (5 ml cm^{-2}). Temperature variation, in the ambient range of 25 to 35°C , was not found to significantly influence the test results. Mechanical brushing of the sample surface following test completion may lead to underestimation of the depth of attack for corrosion susceptible materials, as whole rows of grains can be removed. Consequently, this practice is advised against. Variation in immersion time, within the tolerances accepted in ISO 11846, have no significant effect on the test results. However the study demonstrated how the IGC penetration develops as a function of immersion time in the solution. The corrosion morphologies observed after different immersion times were compared with those of samples in accelerated cyclic test simulating atmospheric exposure, and provide an improved understanding of the relevance of the test to predict atmospheric corrosion resistance.

The effect of surface conditioning on the deposition of Zr-based conversion coatings on aluminium alloys

J. Cerezo^{1,2}, P. Taheri^{1,2}, I. Vandendael³, R. Posner⁴, J.H.W. de Wit², J.M.C. Mol², H. Terry^{1,2,3}

¹*Materials innovation institute (M2i), Delft, The Netherlands*

²*Delft University of Technology, Department of Materials Science and Engineering, Delft, The Netherlands*

³*Vrije Universiteit Brussels, Group of Electrochemistry and Surface Engineering, Brussels, Belgium*

⁴*Henkel AG & Co. KGaA, Düsseldorf, Germany*

Abstract

Conversion coatings are used in the industry to improve the corrosion resistance and adhesion properties of organic coatings. Among the new generation of environmentally friendly conversion coatings, the application of Zr-based films by immersion in a hexafluorozirconic based acid solution has gained considerable acceptance [1-3]. The first stage in the formation of the Zr-based conversion layers is the chemical dissolution of metal oxides by the free fluorides present in the conversion bath. Then, local precipitation of Zr-oxide starts due to local alkalization at readily present cathodic particles at the metal surface. Finally, lateral Zr-oxide precipitation, complete surface coverage and Zr-oxide thickness growth occurs [4-5].

Chemical and thermal surface conditioning prior to the conversion coating application alter oxide chemistry and thickness of metal surfaces: these variables have an important effect on the formation of the conversion layers [3]. For that purpose, different model pre-treatments were applied on AA6014 before the conversion coating formation process in order to investigate the effect of the hydroxyl fraction and oxide layer thickness on the resulting Zr-based film. The elemental distribution and surface chemistry of the treated samples before and after the formation of the Zr-based conversion layer was evaluated by Auger Electron Spectroscopy (AES) depth profiling and X-ray Photoelectron Spectroscopy (XPS). Moreover, the Open Circuit Potential (OCP) evolution as a function of time was recorded during the formation of the Zr-based conversion layers in order to study the electrochemical surface activity and formation mechanism in-situ. The results have shown that especially high initial hydroxyl fractions are beneficial for the formation of the Zr-based layer. This study demonstrates and stresses the pivotal role of surface conditioning of metal surfaces prior to conversion coating formation.

[1] O. Lunder, F. Lapique, B. Johnsen, K. Nisancioglu, *Int. J. Adhes. Adhes.* 24 (2004) 107-117.

[2] R. Posner, N. Fink, M. Wolpers, G. Grundmeier, *Surf. Coat. Technol.* 236 (2013) 286-295.

[3] P. Taheri, K. Lill, J.H.W. de Wit, J.M.C. Mol, H. Terry, *J. Phys. Chem.* 116 (2012) 8426-8436.

[4] F. Andreatta, A. Turco, I. De Graeve, H. Terry, J.H.W. de Wit, L. Fedrizzi, *Surf. Coat. Technol.* 201 (2007) 7668-7685.

[5] J. Cerezo, I. Vandendael, R. Posner, K. Lill, J.H.W. de Wit, J.M.C. Mol, H. Terry, *Surf. Coat. Technol.* 236 (2013) 284-289.

Effect of Sr and Ti addition on the corrosion behavior of Al-7Si-0.3Mg alloy

M. Uludağ^a, M. Kocabaş^b, D. Dişpınar^c, R. Çetin^a, N. Cansever^b

^aSelçuk University, Faculty of Engineering, Metallurgical and Materials Eng. Dept., Konya-Turkey

^bYıldız Technical University, Faculty of Chemistry-Metallurgy, Metallurgical and Materials Eng. Dept., Istanbul-Turkey

^cIstanbul University, Faculty of Engineering, Metallurgical and Materials Eng. Dept., Istanbul-Turkey

Abstract

Among the various classes of aluminum alloys, Al-Si-Mg base alloys hold superior properties such as excellent castability, weldability, pressure tightness and corrosion resistance and are hence widely used in the aerospace and automotive industries. The applications include engine block, cylinder head, piston, wheel etc. In this work, one of the most commonly used A356 (Al-7Si-0.3Mg) alloy was studied. The alloy was provided in the unmodified form and it was then modified with AlTi5B1 for grain refinement and with Sr for Si modifications. These modifications yield to better strength and improved properties. However, it is well known that improper casting conditions may lead to the deterioration of the properties. These processes can be summarized as degassing for hydrogen removal and the holding time after the modifiers are added.

Therefore, in this study, cylindrical bars were cast in the before/after conditions such as: degassing, Si modifications (Sr), grain refinement and Si modifications (Sr+Ti). In all the tests, the hydrogen content of the melt was measured by AlSpek. Degassing was carried out with Ar for 20 minutes. It was found that hydrogen level was 0.25-0.30 ml/100g Al before degassing and 0.10-0.15 ml/100g Al after degassing. Reduced pressure test (RPT) samples were collected in order to determine the quality of the melt by means of measuring bifilm index. The cast samples were sectioned and subjected to metallographical examination. The microstructures of samples were investigated by optical microscope and SEM. XRD and SEM analysis were used for phase characterization. The electrochemical experimental set-up was composed of a classic three electrodes cell using a carbon rod as counter electrode and a saturated calomel electrode (SCE) as the reference one, the samples being connected to the working electrode. The solution used was 3.5% NaCl.

After the corrosion tests, it was found that casting operations had significant effect over the corrosion behavior of the alloy. In the degassed samples, corrosion resistance was increased and, highest resistance was achieved in the Sr+Ti modified alloy. As the bifilm index was increased, corrosion resistance was decreased. SEM images of the corroded sample surfaces also supported these findings.

Keywords: A356 alloy, bifilm index, grain refinement, modification, corrosion.

Electrochemical profiling of multi-clad aluminium sheets used in automotive heat exchangers

*K. Bordo, R. Ambat, Technical University of Denmark, Kgs. Lyngby, Denmark;
L. Peguet, A. Afseth, Constellium Research Centre, Voreppe, France*

Aluminium alloys are widely used in automotive heat exchangers due to the favourable combination of properties, such as low density, high thermal conductivity and good corrosion resistance. During the last two decades, mechanical assembly in the production of heat exchangers has been continuously replaced by brazing of aluminium alloys. This change was caused by cost and safety requirements as well as recycling issues [1]. Brazed heat exchangers are generally manufactured from clad aluminium sheet materials where a high melting point core alloy, typically Al-Mn (AA3xxx), is clad on one or both sides with a low melting point alloy Al-Si (AA4xxx) family.

The effects of the coolant composition on the corrosion of aluminium-based heat exchanger materials have been extensively studied [2]. On the other hand, corrosion occurring on the outer side of heat exchanger tubes caused by chloride from the environment (e.g. salty water from the road and de-icing reagents) is also a very important issue and is currently a blocking point for continued down-gauging and weight reduction of several types of heat exchangers. Recently significant increase in this air-side corrosion resistance has been achieved by using clad sandwich materials with multiple layers of different alloys.

The objective of the present study is to understand the mechanisms of corrosion propagation across the multi-clad structure of Al alloys sheets as a function of local alloy composition and microstructure. Electrochemical behaviour at different depths was profiled using a combination of GDOES sputtering, microelectrochemistry, and zero resistance ammetry (ZRA) method in 0.1M NaCl solution. Multi-clad structure used was a four layer sandwich consisting of a copper-containing AA3xxx long-life core alloy, AA4343 brazing clad on both sides and a copper-free AA3xxx interlayer on the air-side of the sandwich sheet. Local microstructure and corrosion behaviour through the thickness were systematically investigated. The polarization behaviour of both as-rolled and brazed materials (i.e. corrosion potential, pitting potential, cathodic and anodic reactivities) was determined as a function of depth using a localized electrochemical cell and glow discharge optical emission spectroscopy (GDOES) sputtering [3, 4]. Galvanic corrosion behaviour of individual cladding layers was studied by zero resistance ammetry (ZRA). The changes in the microstructure of the material caused by the brazing process were investigated by scanning electron microscopy (SEM) and energy-dispersive X-ray spectroscopy (EDX). The observed evolution of the electrochemical parameters throughout the material depth was analysed and correlated to the respective microstructural features. The obtained results were compared to those obtained for a conventional, three-layer long-life alloy product.

References

1. S. Tierce, N. Pebere, C. Blanc, C. Casenave, G. Mankowski, H. Robidou. *Corr. Sci.* 49 (2007) 4581-4593
2. Y. Liu, Y.F. Cheng. *J. Appl. Electrochem.* 41 (2011) 151-159
3. F. Norouzi Afshar, R. Ambat, C. Kwakernaak, J.H.W. de Wit, J.M.C. Mol, H. Terryn. *Electrochim. Acta* 77 (2012) 285-293
4. R. Ambat, P. Møller. *Corr. Sci.* 49 (2007) 2866-2879

Investigation by electrochemical impedance spectroscopy of filiform corrosion of electrocoated steel substrates

A.-P. Romano, M.-G. Olivier

*University of Mons - UMONS, Faculty of Engineering Materials Science
Department, Place du Parc, 20 - 7000 Mons, Belgium*

In automotive industry, the body car is composed of different metallic substrates such as steel, galvanized steel and aluminium alloys of 6xxx series. The corrosion protection of all the substrates is often obtained by a cathaphoretic coating. For economic reasons, steel is more and more used but this substrate is very reactive and sensitive to corrosion and particularly to filiform corrosion. This specific type of corrosion is produced between the coating and the substrate by formation of filaments. The aim of this work is to study by electrochemical impedance spectroscopy the susceptibility to filiform corrosion of steel.

Electrochemical impedance spectroscopy can be used to evaluate in short time the sensitivity to filiform corrosion of the different substrates through the estimation of the exposed metallic area. This is possible if the corrosion products are correctly dissolved before characterization. Their presence may indeed hinder the metal activity leading to an underestimation of the delaminated area.

Different steel grades with and without pretreatment were analysed by EIS on scratched samples.

In order to remove the corrosion products and to avoid subsequent corrosion during the measurement, many parameters were optimized such as the choice of electrolyte solution, acid and dissolution time, EIS electrolyte and immersion time before EIS measurements, exposure time to climatic chamber. The steel is a very complex substrate and thus an additional cathodic polarization step must be added (time and potential to define) to evacuate corrosion products and homogenize pH underneath the delaminated coating.

Influence of water, chloride, sulphate and acetic acid on corrosion behavior of aluminum materials in ethanol-containing fuels

Rüdiger Reitz, Georg Andersohn, Matthias Oechsner, Technische Universität Darmstadt, Institute for Materials Technology (IfW), Darmstadt / Germany

Abstract

Fuels containing ethanol with biogenic origin plays an increasing role in the transport fuel market, because of their CO₂-saving potential and the limited oil resources. Especially in the European countries, legal restrictions with regard to sustainable energy supply will accelerate this trend.

Ethanol with its hygroscopic properties has the ability to solvate water in fuel. As expected, with increasing content of ethanol, fuels tend to have a larger concentration of water. Along with the higher water content, there is also a risk to contaminate the fuel with corrosive ions such as chloride or sulfate, for example by atmospheric exchange processes. Hence, electrochemical corrosion can occur at the used metals in tanks or in fuel systems and the risk of corrosion damage is given.

In this study, the influence of corrosive components in gasoline fuels on the corrosion behavior of various aluminum wrought alloys (EN AW-1050A, EN AW-3003, EN AW-5182, EN AW-6060) has been analyzed. As a function of the ethanol content, the components water, chloride, sulfate, and acetic acid were varied. The interactions between these components were determined by applying the methods of statistical experimental design. On the material side, corrosion features such as mass change, hole depth and corrosion morphology were investigated in relation to the fuel composition. In accordance to the guideline VDA 230-207, the experiments have been carried out in pressure-tight reactors at environmental and increased temperatures (up to 60 °C).

Time-dependent corrosion and layer formation reactions of EN AC- AlSi10Mg in coolants for combustion engines under various boiling conditions

*Thomas Duchardt, Georg Andersohn, Matthias Oechsner, Technische Universität
Darmstadt, Institute for Materials Technology (IfW), Darmstadt/Germany*

Even with an increasing share of electrical vehicles, the combustion engine can be assumed to be the main drive technology in automobiles for the next 20 years. Increasing demands to the engine, such as the reduction of CO₂ emissions and minimization of fuel consumption while maintaining performance, require new concepts regarding the engine design.

Concepts like "downsizing" and "thermal management" are state of the art. Start-stop systems which reduce fuel consumption while waiting at traffic lights or in traffic jams are increasingly used.

These measures often result in increased engine temperature, which have to be balanced by the coolant to avoid overheating of the materials. The increased thermal loading, associated with local boiling processes result in unknown implications in terms of corrosion, the formation of corrosion protective layers, and coolant long-term stability. At this point, the interaction between materials and the respective coolant is of particular importance.

In this report, the development of corrosion and the formation of reaction or inhibition layers along with stable and unstable boiling and changing flow conditions are discussed. The presented results are based on experiments with AlSi10Mg specimens and Si- and OAT based coolants. An evaluation of the results is given on basis of mass loss and SEM analysis. Furthermore cross sections and 3D-Microscope analysis are used to show the dependency of the test duration with its implemented heat, rest, and vapour phases to the corrosion- and layer-formation process. The evaluation is also based on electrochemical OCP and EIS in situ analysis, which were recorded directly in the coolant flow.

The obtained results provide information on damage relevant parameters and their interaction with coolant induced corrosion on hot aluminum surfaces. In particular, the influence of boiling processes with complete coolant evaporation is investigated. It can be shown that under use of coolant OAT the evaporation phase triggers pitting corrosion at the specimen surface.

The impact of condensates containing sulphate and chloride on automotive exhaust systems – in solution and in vapour-

*R. Hashimoto, G. Mori, Christian Doppler Laboratory of Localized Corrosion,
Montanuniversität Leoben, Franz-Josef-Straße 18, A-8700 Leoben, Austria,
H. Wieser, Faurecia Emission Control Technologies,
Biberbach-Straße 9, 86154 Augsburg, Germany*

Internal corrosion of exhaust systems is of significant interest in the automotive industry. So far, it has been informally recognized that the corrosion rate differs with the regions, where vehicles are driven. In some regions, the particularly high return rate within a warranty period due to severe corrosion inside the muffler has been seen, even though the material and design of mufflers are similar to other regions. In the present study, the chemical composition of the condensates recovered from a test car in the different regions was compared. It was shown that the condensates in the region of the severe internal corrosion issue contain higher concentrations of both chloride and sulphate than that in the region of less corrosion issue. Chloride causes a pitting corrosion, while acidification of the condensate due to sulphate could induce a uniform corrosion. Consistently, the microscopic analyses revealed that the internal parts of the used mufflers in the region of a severe corrosion issue suffer from more number of pits and greater extent of uniform corrosion. During a car operation, the internal environment in the muffler changes dramatically and also the elements to cause corrosion differs depending on the geometric position in the muffler. The bottom surface of a muffler is often in a wet environment due to a pool of condensate and the top surface of a muffler is more affected by humid air. In order to consider the influence of condensate under these different circumstances, immersion tests in the solution along with the exposure tests to the vapour deriving from the identical solution were performed by using a variety of solutions containing 0.01-1000mM sulphate and chloride. The difference of types and degree of corrosion was analysed between in-solution and in-vapour conditions, and compared to the types and extents of corrosion on the internal top and bottom surfaces in the used mufflers. In addition, the broader concentrations of sulphate and chloride in the condensate, in which uniform and pitting in the 1.4512 and 1.4513 ferritic stainless steels start occurring, were investigated. The impact of vapour from acidic condensates on uniform and pitting corrosion is intensively discussed in this study.

High-temperature corrosion of materials for cast exhaust-components

Madeleine Ekström, Royal Institute of Technology, Stockholm, Sweden

Baohua Zhu, Scania CV AB, Södertälje, Sweden

Peter Szakalo, Royal Institute of Technology, Stockholm, Sweden

Stefan Jonsson, Royal Institute of Technology, Stockholm, Sweden

The exhaust regulations for heavy-duty trucks are becoming more restrict in order to limit the environmental effects from the exhaust gases and particles. By increasing the specific power-output of diesel engines, the fuel efficiency is improved and emissions greatly reduced. However, a drawback is that it leads to an increased exhaust-gas temperature putting higher demands on the materials for the exhaust manifolds. Furthermore, the fuel flora for heavy duty vehicles will change, going towards new bio fuels. This will result in a more corrosive exhaust-gas composition.

Today, a ferritic ductile cast iron, SiMo51, is generally used for these components but as it shows poor corrosion resistance above 700°C, other materials need to be used or new ones developed. In the present study, some alternative materials to SiMo51, of both the austenitic and ferritic types, listed in table 1, were tested for high-temperature corrosion and oxide spallation during thermal cycling.

Table 1. Chemical composition of studied materials (given in wt%, Fe bal.).

Alloy	Type ¹	C	Si	Mn	Cr	Ni	Nb	W	Co	Mo	Mg
SiMo51	FDI	3.71	4.15	0.40	0.10	0.04				0.86	0.05
Ni-resist D5S	ADI	2.41	5.38	0.28	1.77	33.12				0.18	<0.06
HF	ACS	0.33	1.50	1.43	18.76	8.87	0.01	0.01	0.02		
A3N	ACS	0.57	0.58	1.05	19.59	10.15	1.75	2.28	0.29		
HK30	ACS	0.51	1.50	1.45	25.41	18.67	<0.01	0.01	0.03		
HK-Nb	ACS	0.37	1.29	0.96	25.38	22.40	1.39	0.02	0.03		
4509	FCS	0.02	0.81	0.75	17.90	0.12	0.36	<0.01	0.02		

¹ Ferritic ductile iron (FDI), austenitic ductile iron (ADI), austenitic cast steel (ACS) and ferritic cast steel (FCS).

The oxidation resistance was tested at 900°C in three different atmospheres: air, 5%O₂-10%H₂O-85%N₂ and 5%CO₂-10%H₂O-85%N₂ for exposure times of 6h, 24h and 96h. The oxide spallation was tested in an engine test cell for 1000h where the exhaust-gas temperature was cycled between 120°C and 730°C as the load on the test engine was varied. Among the tested materials, the austenitic cast steels, HF and A3N, show the worst oxidation behavior with severe oxide spallation and rapid growth of porous Fe-oxides whereas the best oxidation behavior was observed for the austenitic cast steels, HK30 and HK-Nb, forming compact and adherent Cr-oxides.

Role of corrosion products in corrosion mechanisms of Zn(Mg)(Al) coatings on steel

P. Volovitch*, M. Salguero Azevedo^{1,2}, J.D. Yoo¹, C. Allely², K. Ogle¹

¹Chimie-ParisTech, 11 rue Pierre et Marie Curie, Paris 7005, France (polina.volovitch@chimie-paristech.fr)

²Arcelor Mittal Research, Maizières les Metz, France

The best strategy to improve the life time of metallic coated steel is to maximize the barrier resistance while maintaining a sufficient galvanic effect. The barrier resistance in presence of mobile metal cations can be achieved through the formation of insoluble corrosion products, which is particularly known for zinc containing coatings and is often referred as a self-healing effect. Even for relatively simple coatings like galvanized steel numerous mechanisms of the zinc action were proposed and are still under discussion, for more complex alloys containing Al and / or Mg the effect is even more complex.

The formation conditions of different Zn, Al and Mg compounds during corrosion and their role for protection mechanisms are still poorly understood. The present work aim to review the recently obtained knowledge about the electrolyte composition and exposure conditions necessary to form different Zn, ZnAl and ZnAlMg containing corrosion products and to identify the possible inhibiting mechanisms related to their presence. *We will try to differentiate between the barriers effects of the corrosion products already formed on the material, the dynamic pH buffering effect and the simple coincidence of the reduced reactivity and the presence of a selected product because the conditions correspond to its stability domain.*

The study consists of two parts. First of all, the recent bibliographical data about corrosion products formed in different exposure conditions on Zn, ZnAl and ZnMgAl alloys are reviewed and an analysis of the conditions necessary for the formation of different corrosion products is done. In the second part, the electrochemical behavior of coating or steel substrate covered by selected synthetic corrosion products is tested. Three classes of corrosion products are studied: Mono-action oxides and hydroxides, zinc layered basic salts (LBS) and ZnAl and MgAl based layered double hydroxides (LDH).

Selected patinas were obtained by electrochemical dissolution-precipitation process on coated steel and the stability of the formed systems in varying pH and solution composition was studied. The behavior of the systems during spontaneous reactivity, under potentiodynamic polarization and under applied potential was tested. Barrier effect of some LBS on the oxygen reduction was directly demonstrated by the measurement of the cathodic reactivity of cold rolled steel in presence of electrochemically synthesized LBS and during the galvanic coupling between the steel under selected patina and coating [1-3]. The role of the exposure conditions and the role of different soluble cationic and anionic species on the stability of LBS and on their transformations are also discussed.

The formation of LDH compounds on ZnAlMg and MgAl alloys is sometimes considered as a benefit for corrosion resistance due to the low air permeability of several LDH powders. In other works the formation of LDH is regarded as not specifically protecting for the underneath substrate and is considered as a mandatory consequence of the high pH during corrosion of Al-containing coatings. In this work we communicate for the first time the conditions of the accelerated tests in which LDH is not formed and explain the dynamic role of Mg ions in corrosion mechanisms with and without LDH formation.

[1] J.D. Yoo, P. Volovitch, A.A. Aal, C. Allely, K. Ogle, "The effect of an artificially synthesized simonkolleite layer on the corrosion of electrogalvanized steel" Corros. Sci. 70 (2013) 1-10

[2] J. D. Yoo, K. Ogle, P. Volovitch "The effect of synthetic zinc corrosion products on corrosion of electrogalvanized steel: I. Cathodic reactivity under zinc corrosion products" Corros. Sci. 81 (2014) 11-20

[3] J. D. Yoo, K. Ogle, P. Volovitch "The effect of synthetic zinc corrosion products on corrosion of electrogalvanized steel. II. Zinc reactivity and galvanic coupling zinc/steel in presence of zinc corrosion products." Corros. Sci. 83 (2014) 32-37

[4] M. Salguero Azevedo, C. Allely, K. Ogle, P. Volovitch "Corrosion mechanisms of Zn(Mg, Al) coated steel in accelerated tests and natural exposure: 1. The role of electrolyte composition in the nature of corrosion products and relative corrosion rate" Corros. Sci. (2014) doi 10.1016/j.corsci.2014.05.014

[5] M. Salguero Azevedo, C. Allely, K. Ogle, P. Volovitch "Corrosion mechanisms of Zn(Mg,Al) coated steel: 2. The effect of Mg and Al alloying on the formation and properties of corrosion products in different electrolytes" Corros. Sci. (submitted)

Influence of Corrosion on Fatigue Behaviour for Automotive Exhaust Systems

Uwe Troeger¹, Daniel Knoll¹, Helmut Wieser¹, Kursat Duru², Ferdinand Haider²

1 Faurecia Emissions Control Technologies, Augsburg, Germany

2 Institute of Physics, University of Augsburg, Germany

Abstract

Corrosion in automotive exhaust components is familiar worldwide. The life time of a silencer is shorter as compared to any other part of an exhaust system. The reason is salt corrosion from outside and condensate corrosion from inside. It's obvious that this kind of corrosion will affect the fatigue behaviour of the exhaust systems and due to that the life time.

The effect of different corrosion phenomena on fatigue behaviour will be shown.

The stainless steel samples tested exhibited different level of corrosion attack (realized by different cycles of salt spray test) and also various temperature treatments. The fatigue tests were performed by means of high frequency pulsation and/or with tensile tests. Important for the analysis of the samples was the comparison of the Wöhler curve (S/N-curve) with the analysis of the cracking area by means of Scanning Electron Microscopy.

On the basis of the obtained results, it can be concluded that due to the corrosion the fatigue can be decreased rapidly.

Keywords: Automotive exhaust system, silencer, stainless steel, corrosion, fatigue, pitting corrosion, intergranular corrosion.

Investigation on galvanic effect in automotive body corrosion

E. Szala*, A. Dogan**, F. Hannour***

**On leave from Tata Steel Research and Development, at Toyota Motor Europe - Technical Centre Hoge Wei 33, B-1930 Zaventem, Belgium*

***Toyota Motor Europe, Technical Centre Hoge Wei 33, B-1930 Zaventem, Belgium*

****Tata Steel Research and Development, PO Box 10.000, 1970CA IJmuiden, the Netherlands*

Abstract

Cosmetic corrosion in automotive has become of higher interest for automotive makers. This is a result of different market criteria:

- Car's evolving in-service requirements such as automobile increasing lifetime, developing markets with new corrosion conditions...
- Customer's higher aesthetic expectation (for instance rising in second-hand market).

Recently, increasing amount of multi- material combinations has been observed in body structure either to comply with lightweight restrictions or to improve aesthetics customer demands in vehicles.

This evolution in car design has led to inevitable galvanic coupling between the added materials and the Body-in-White.

Method for predicting the corrosion resistance of painted steel sheets have been developed and standardized by OEMs. However, they often require the material to be subjected to strong defects (i.e. scratch on painted material to observe paint creep and discriminate either metal substrate or paint system). These pre-requisite are not necessarily reproducing field conditions where blistering can be observed without the presence of paint scratches.

Based on a test developed at Volvo Cars to investigate blister corrosion occurrence, a study was carried out to investigate different parameters susceptible to play a role in galvanic coupling effect in vehicles:

- Coupling the automotive body with a strong cathode
- Effect of mechanical micro-defects in the body corrosion
- Influence of body surface conditions (sanding the metal substrate, presence defects such as pinholes in the Electrodeposited coating)

Application Relevant Polymer Testing - Impact of Media on the Viscoelastic Behaviour of Engineering Polymers

*Peter Guttmann, Montanuniversitaet Leoben, Leoben/Austria;
Gerald Pilz, Montanuniversitaet Leoben, Leoben/Austria*

In general the performance of engineering polymers in structural applications is strongly dependent on the specific service conditions such as service temperature, loading time and ambient media. The present study discusses efficient mechanical testing methods for the evaluation of viscoelastic behaviour of engineering polymers under media influence, exemplarily shown for fibre reinforced PA 66, PPA and PPS grades. For the characterization of time and temperature dependency of the elastic modulus E , which is a characteristic value for structural applications, primarily dynamic-mechanical tests (DMA) and creep tests were performed for the conditioned materials state.

Based on the use of standard specimens which were immersed in various media (ph from 2 to 12) until saturation the temperature dependent modulus curves were determined in order to find application relevant modulus levels and critical thermal transition ranges. For the determination of the time dependency of creep modulus E_C the preconditioned specimens were tested under constant loading and water immersion, which provides the conservation of the saturated materials state along the total testing time of 24 hours. The stepwise increased test temperatures (stepped isothermal method (SIM)) enabled the generation of creep modulus mastercurves for an extended time range up to 50 years. Moreover, the correlation of the DMA results with the corresponding creep behaviour shows characteristic dependencies of the mechanical long term properties on the thermo-mechanical behaviour. Additional materials analysis such as DSC and infrared spectroscopy (IR) provided informations about relevant physical and chemical aging effects.

Compatibility of sealing materials with biofuels, biodiesel-heating oil blends and premium grade fuel at different temperatures

*Margit Weltschev, Jan Werner, Frank Heming and Frank Jochems
Federal Institute for Materials Research and Testing, Unter den Eichen 87, 12205
Berlin, Germany*

Biofuels including ethanol and biodiesel (fatty acid methyl ester) represent an important renewable fuel alternative to petroleum-derived transport fuels. Increasing biofuel use would bring some benefits, such as a reduction in oil demands and greenhouse gas emissions, and an improvement in air quality.

Materials compatibility is a major concern whenever the fuel composition is changed in a fuel system. The question arises of whether sealing materials are resistant to fuels with bioethanol and biodiesel (rapeseed oil fatty acid methyl ester).

The aim of this work is to study the interaction between sealing materials such as FKM (fluorocarbon rubber), EPDM (ethylene-propylene-diene rubber), CR (chloroprene rubber), CSM (chlorosulfonated polyethylene), NBR (acrylonitrile-butadiene rubber), IIR (butyl rubber), VMQ (methyl-vinyl-silicone rubber), FVMQ (methyl-fluoro-silicone rubber) and PA (polyamide) and biofuels such as biodiesel, E10, E85 (fuel with 85% ethanol) and B10 (heating oil with 10% biodiesel) at 20°C, 40°C and 70°C for 84 days. Experiments were conducted with specimens of these elastomers to document the changes in the mass and tensile properties of these sealing materials according to ISO 1817.

The mass, tensile strength and breaking elongation of the test specimens were determined before and after exposure for 84 days to E85, non-aged and two years aged biodiesel, and one year aged B10 and compared with premium-grade fuel at 20°C, 40°C and 70°C. Visual examination of some elastomer test specimens clearly showed a great volume increase until breakage or partial dissolution.

The sealing materials FVMQ, VMQ and PA were evaluated as resistant in E85 at 20°C and 40°C with a reduction of tensile properties limited to 15%. None of the examined materials was evaluated as resistant at 70°C with even fluorocarbon rubber losing 20% of its tensile strength in E85.

When exposed to biodiesel, elastomers were affected in two ways: firstly, by absorption of liquid by the elastomers and, secondly, by dissolution of soluble components from the elastomers into the liquid medium. Swelling was the result of the high absorption by the elastomers CR, CSM, EPDM, IIR and NBR in comparison to their dissolution in non-aged and two years aged biodiesel. FKM, VMQ and PA were evaluated as resistant sealing materials in non-aged biodiesel at 40°C. FKM was still resistant in aged biodiesel at 40°C but only to a limited degree at 70°C.

The sealing materials CR, CSM, EPDM and IIR were damaged to a high extent in one year aged B10 as a result of swelling up to 70°C. However, FKM was evaluated as resistant in aged B10.

The exposure tests showed that FKM was the most resistant sealing material in premium-grade gasoline at 70°C, while the elastomers EPDM, NBR, CR und IIR even lost 100% of their breaking elongation.

Monitoring the Process of Polymer Degradation by Imaging Techniques

*Tobias Schuster, Subin Damodaran, Karsten Rode, Robert Brüll,
Fraunhofer Institute for Structural Durability and System Reliability (LBF), Division
Plastics, Group Material Analytics, Schlossgartenstr. 6, 64289 Darmstadt, Germany*

*Britta Gerets, Mirko Wenzel, Martin Bastian, SKZ - German Plastics Center,
Friedrich-Bergius-Ring 22, 97076 Würzburg, Germany*

The degradation of polymers can be triggered by light, heat or aggressive media. The elemental steps are the loss of stabilizing additives, and finally oxidation and chain scission of the polymer. The current approach of analysis is to mechanically abrade layers and then analyze the individual samples by various techniques. Imaging techniques (e.g. polarized light-, infrared- or Raman-microscopy) excel by superior spatial resolution and reproducibility. These advantages enable to profile the degree of crystallinity, molecular orientation and additive content.^{1, 2} Furthermore, the degradation and extraction of antioxidants from polypropylene pipes during use³ and the loss of stabilizers from polyethylene surfaces upon UV-exposure can be monitored.⁴

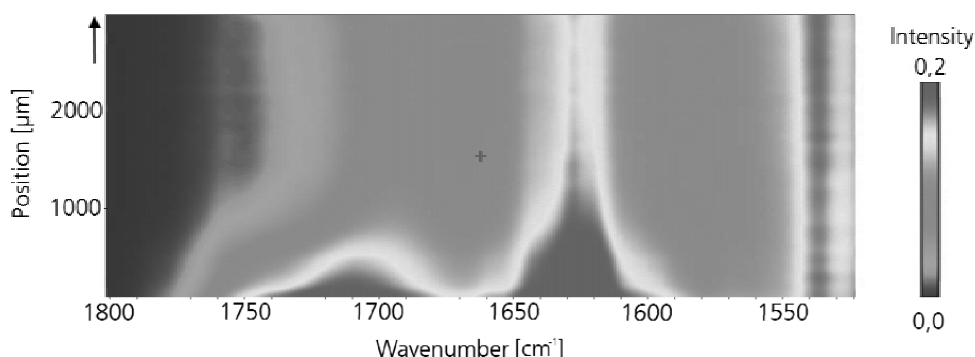


Figure 1: Locally resolved IR-spectra over the cross section of a PP-R pipe. The pipe was hydrostatic pressure tested for 3000 h at 110 °C.

New strategies to comprehensively monitor the process of degradation and examples for economically relevant applications will be presented.

Reference:

1. Brüll, R.; Geertz, G.; Kothe, H.; Macko, T.; Rudschuck, M.; Wenzel, M.; Engelsing, K.; Wüst, J.; Bastian, M. *Macromolecular Materials and Engineering* **2008**, 293, (5), 400-408.
2. Schuster, T.; Rode, K.; Brüll, R.; Heinemann, J.; Haupt, H. *J Appl Polym Sci* **2013**, 130, (6), 4182-4190.
3. Geertz, G.; Brüll, R.; Wieser, J.; Maria, R.; Wenzel, M.; Engelsing, K.; Wüst, J.; Bastian, M.; Rudschuck, M. *Polymer Degradation and Stability* **2009**, 94, 1092-1102.
4. Maria, R.; Rode, K.; Brüll, R.; Dorbath, F.; Baudrit, B.; Bastian, M.; Brendlé, E. *Polymer Degradation and Stability* **2011**, 96, 1901-1910.

Lifetime Analysis for Plastic Pipes by Statistical Evaluation of Creep Rupture Data

*Dipl.-Wirtsch.-Ing. Jürgen Heinemann, Dipl.-Ing. Hansgeorg Haupt,
Dipl.-Ing. Alexander Bockenheimer, Prof. Dr.-Ing. Matthias Oechsner,
Technische Universität Darmstadt, Zentrum für Konstruktionswerkstoffe (MPA/IfW),
Darmstadt, Germany*

Almost six decades ago, plastic pipes have been introduced on a large industrial scale. Since then they have gained strong significance amongst others in the areas of drinking water and gas supply as well as sanitary and heating installations. An important criterion for the success of plastic pipes is their long lifetime verified on the basis of international standards. The lifetime analysis necessarily takes place based on an accelerated test with a subsequent extrapolation of the material behaviour, as described in ISO 9080 in conjunction with ISO 1167.

The so-called internal pressure creep rupture test according to ISO 1167 represents the fundamental test method for the evaluation of the long-term hydro-static strength behaviour of plastic pipes. The applied stress collective consists of mechanical stress due to internal pressure and thermal stress due to temperature and accordingly focuses on factors of prominent importance determining the lifetime of plastic pipes.

The obtained test results provide the basis for a lifetime analysis by statistical extrapolation according to ISO 9080. A multiple linear regression analysis with two, three or four parameters using the method of ordinary least squares is applied to predict the mean long-term hydrostatic strength as well as the corresponding lower prediction limit for the intended operating time and temperature.

To prove the suitability of this statistical approach, different datasets obtained from internal pressure creep rupture tests on samples made of different materials and sizes are evaluated. At first the goodness of fit of the regression functions is studied focusing the coefficient of determination, standard error of estimation and significance of regression function and regression coefficients. Furthermore the distribution of the residuals resulting from the difference of observed and estimated values is examined to verify the statistical assumptions for an unbiased and efficient regression estimation as well as to identify possible outliers.

Fluoropolymers in Corrosion Resistance – Long Term Experience Opens a Broad Spectrum of Applications

Dr. Brigitte Neubauer, Solvay Specialty Polymers, Brussels, Belgium; Mr. Giorgio Maggi, Solvay Specialty Polymers, Bollate, Italy

Since the 1940's fluoropolymers have been successfully applied in situations where a high level of corrosion resistance is required. The chemical structure of these polymers leads to a shielding of the polymer backbone to attack by chemicals. Data obtained from immersion tests is the basis to determine the resistance of these polymers to chemicals. The picture is completed by exposure tests under mechanical load. For practical purposes, case stories are the most precious piece of information demonstrating the fit for the application which includes also other important factors like the permeation resistance, surface properties, temperature resistance as well as economic aspects.

Fluoropolymers have been classically employed in acid environments but their field of applications extends to fields including drinking water transport or pharmaceutical synthesis. It is their distinctive set of properties, which allows for their use in a broad spectrum of demanding applications.

Fluorothermoplastic-lined steel and FRP equipment for highly corrosive environments – An overview

Dr Mirko Lotz, Quadrant EPP AG, Switzerland

Equipment made of steel and FRP (fibre reinforced plastic) is used in manifold applications in industry, subject to corrosive conditions of most aggressive nature. Examples are tanks, vessels, scrubbers and pipelines in chemical industry, or condensing heat exchangers and the surrounding equipment in fossil- or waste-fired power production plants. The combination of strong acids, strong bases and aggressive organic media with high temperatures thereby often exceed the chemical resistance of conventional steel and polymeric materials by far, and in many cases even special metal alloys or exotic materials cannot be used.

Fluorothermoplastic liners made from polymers like PVDF, ECTFE, FEP and PFA provide an excellent corrosion and temperature protection without the fabrication drawbacks of sintered fluoropolymers or for example wall thickness restrictions as known for coatings.

The ability to choose between partially and fully fluorinated polymers renders possible fluorothermoplastic lining solutions for almost every chemical media and concentration. Well established manufacturing methods for bonded linings on steel and FRP as well as mechanically fixed linings for steel or other surfaces provide lining solutions suitable up to high temperatures, and with a wide range of possible pressure including vacuum, the latter also depending on the method chosen. Likewise, pipelines for the transport of corrosive, hot and potentially permeating chemical media can be constructed beneficially with fluorothermoplastic lined FRP.

Objective of the presentation is to provide an overview about the fluorothermoplastic polymers, the lining materials and their key properties. Principle lining technologies and best practices will be introduced, and application benefits as well as limitations discussed. Application examples will be shown in order to illustrate the versatility of these valuable materials of construction.

Fluoropolymers in Corrosion Resistance – Protective organic coatings based on ECTFE

Dr. Brigitte Neubauer, Solvay Specialty Polymers, Brussels, Belgium; Mr. Giorgio Maggi, Solvay Specialty Polymers, Bollate, Italy

Fluoropolymers have been used in corrosion resistance for almost 7 decades. Partially fluorinated polymers have often lower permeation rates and better mechanical properties than fully fluorinated polymer or commodity polymers. Among the partially fluorinated polymers, ECTFE combines best barrier properties with a broad chemical resistance and thus has been successfully used for anticorrosion coatings for almost two decades. ECTFE coating, classically applied as electrostatic powder coating, is used for corrosive fume protection in desulphurization plants or in semiconductor fabs, in desalination plants in the sensitive sea water inlet area, where corrosion is combined with high abrasion, or in pharmaceutical plants where corrosion resistance has to be paired with high cleanliness. In specific areas, new grades with antistatic properties or particularly high layer build up have recently been introduced.

Corrosion of Copper alloy fittings in a combined Plastic/Metal installation for hot drinking water

J.W. Erning, Federal Institute of material research and testing, Berlin, Germany

A household installation for drinking water was analysed for the water quality after an incident concerning the water distribution system in the city. Chemical analysis showed very high levels of lead in the hot water circulation system. The installation was made from multi-layer-pipes, the hot water tank from stainless steel, no obvious source of lead could be determined. After a thorough cleaning of the piping system and the tank the lead levels rose again after short time.

Investigations

Water samples and samples of the pipe connectors made from different copper alloys were taken during an inspection of the building. Results for water analysis and metallographic investigations of the samples are given. Close examination of the connectors showed selective corrosion along the grain boundaries for the connectors made from brass but not for the connectors made from gun metal.

Results

The lead found in the hot drinking water was released from the brass connectors. Obviously the contact time of the water with the metal surfaces in the system investigated was much longer as the contact times used for the evaluation of metallic materials according to EN 15664-1. The standards for the dimensioning of hot water circulation systems available are outdated and do not consider retention time in the system but are driven by maximum availability of hot water at any time.

Innovative high corrosion resistant systems for chrome plating on plastics

L. Thiery COVENTYA HOLDING, H. Sahrhage COVENTYA GmbH, D. Dal Zilio COVENTYA SpA, GL Schiavon COVENTYA SPA.

Chrome electroplating has been used since decades to give a shiny aspect to many objects of our daily life. Chrome finish is present on furniture items, mobile phones, and plastic parts for the automotive industry...

The electrolytes considered to plate chrome are based on the use of chromium trioxide.

The REACH regulation has set the sunset date for the use of chromium trioxide without authorization on the 21st of September 2017. The latest date to apply for an authorization is the 21st of March 2016. Any authorization delivered by the ECHA is subjected to a time limited review period.

Amongst the alternatives to hexavalent chrome, trivalent chrome plating has been the most promising candidate, but the behavior of the deposits obtained from these electrolytes is often quite different than the one obtained from a hexavalent chrome bath.

With a focus on the application on plastic parts, the article will review the benefits and drawbacks of the deposits obtained from trivalent electrolytes versus hexavalent ones.

The different behavior in accelerated corrosion tests will be discussed, especially the CASS test, the Russian Mud test that is more favorable to the trivalent chrome based deposits, and also neutral salt spray test and specific automotive tests.

The critical role of the different nickel based deposits under the chrome will be reviewed. The latest developments will show the ability of the deposits made from trivalent chrome baths to resist to the various accelerated corrosion and outdoor exposure tests thanks to the use of a dedicated combination of Nickel based under layers.

Particularly, the benefit of introducing a noble Nickel alloy layer prior to the chrome deposit has shown an outstanding advantage over the present technologies and will be discussed.

Imaging Techniques: Tool for the quantification of oriented additives

*Tobias Schuster, Karsten Rode, Subin Damodaran, Robert Brüll,
Fraunhofer Institute for Structural Durability and System Reliability (LBF), Division
Plastics, Group Material Analytics, Schlossgartenstr. 6, 64289 Darmstadt, Germany*

The rate of crystallization and the size of the resulting crystals have a strong impact on the mechanical and optical properties after conversion of the plastics, especially in polypropylene (PP). Therefore nucleating agents, such as the β nucleating agent N,N'-dicyclohexyl-naphthalene-2,6-dicarboxamide (NU-100) are widely used to control the crystallization process. The direction of crystallite growth is highly dependent on the orientation of nucleating agent.¹ Figure 1 shows optical images of an extruded PP sample in the planes TD-ND and MD-ND and the respective IR absorptions.

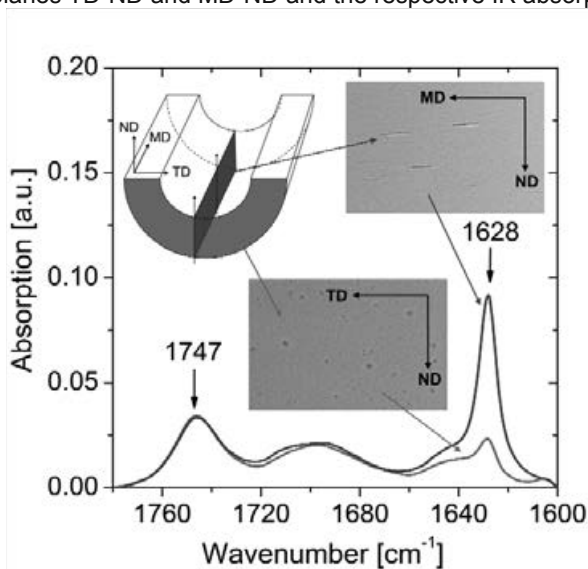


Figure 1: Optical images of orthogonal microtome cuts of an extruded pipe and enlargement of corresponding IR spectra in the range between 1780 and 1600 cm^{-1} .

NU-100 exhibits an intense Infrared- (IR) absorption at 1628 cm^{-1} , which can be assigned to its two amide groups. Analyzing the perpendicular cuts of the extruded PP sample by IR, a strong influence of the cutting direction on the intensity of the band at 1628 cm^{-1} can be recognized. In contrast to the band at 1747 cm^{-1} , caused by the carbonyl group of an antioxidant, the band at 1628 cm^{-1} shows strong dichroism. The dichroic effect can be used to calculate the orientation of nucleating agents and polymer chains with regard to the three directions of the processed material from IR-spectroscopic measurements.^{2,3}

Reference:

1. Yamaguchi, M.; Fukui, T.; Okamoto, K.; Sasaki, S.; Uchiyama, Y.; Ueoka, C. *Polymer* **2009**, 50, (6), 1497-1504.
2. Brüll, R.; Maria, R.; Rode, K. *Macromolecular Chemistry and Physics* **2010**, 211, (20), 2233-2239.
3. Schuster, T.; Rode, K.; Brüll, R.; Heinemann, J.; Haupt, H. *J Appl Polym Sci* **2013**, 130, (6), 4182-4190.

Three Dimensional Orientations by FTIR- and Polarized Light Microscopy

Subin Damodaran, Tobias Schuster, Karsten Rode, Robert Brüll,
Fraunhofer Institute for Structural Durability and System Reliability (LBF), Division
Plastics, Group Material Analytics, Schlossgartenstr. 6, 64289 Darmstadt, Germany

The welding of polymers is an important way to realise complex product geometries. The type of welding as well as the applied parameters have a significant influence on the morphology of the resulting welding seam. Welding seams were already studied with regard to their morphology,¹ however, no quantitative information with regard to the degree of crystallinity and no information at all about the orientation of the macromolecules in the welding zone has been available so far. Since both are crucial morphological parameters in explaining macroscopic properties of polymers, it is of pivotal importance to precisely analyse them.

The absorption of linear polarized infrared light by functional groups depends strongly on their orientation in the polymer matrix. A three dimensional model developed by transforming the Frasers equation into spherical coordinates enables to calculate the spatially resolved orientation.²

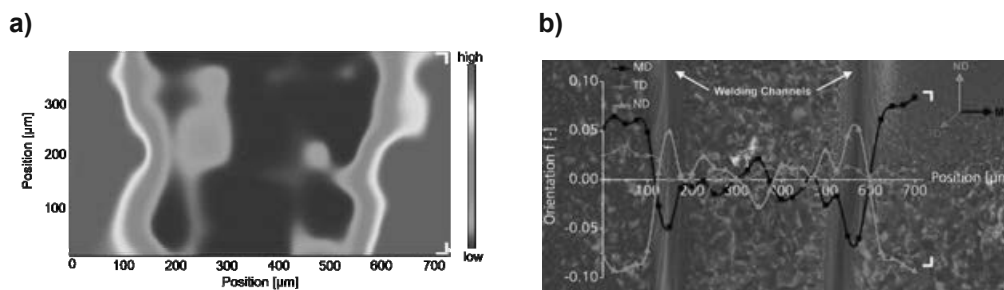


Figure 1: a) Crystallinity map in the weld seam of the polypropylene (marked by white corner in b) b) Orientation of polymer chains using the 3D model overlaid with the polarized light microscopic image

The spatially resolved orientation of the welded channel is calculated by the 3D model. The values of the orientation function are in good agreement with the images from polarised light microscopy, reflecting the flow profile of polymer and the kinetics of crystallisation in the channel. As illustrated in Figure 1a) the crystallinity of the welded region over an $800 \times 400 \mu\text{m}$ area is also calculated using IR microscopy. The area within the welding channels shows a significant drop in crystallinity compared to the outer zone (bulk).

Reference:

- Schmachtenberg, E.; Tüchert, C. *Macromolecular Materials and Engineering* **2003**, 288, (4), 291-300.
- Brüll, R.; Maria, R.; Rode, K. *Macromolecular Chemistry and Physics* **2010**, 211, (20), 2233-2239.

Modeling water quality by water treatment for corrosion control in water distribution networks

Angelika Becker

IWW Water Centre, Muelheim an der Ruhr, Germany

The main goal of a water supplier is to distribute drinking water to the customer in a quality to comply with the European Drinking Water Directive, in a sufficient pressure and in a sufficient quantity.

The costs for producing a drinking water of high level may be unsuccessful if the water quality is negatively affected by corrosion processes. So one requirement is the knowledge about the significant influences of interactions between drinking water and material consideration to maintain the drinking water quality and avoid limitations for the lifetime of materials and integrity of water nets.

Due to the fact that the corrosion behaviour of materials in contact with drinking water is strongly influenced by different water parameter, an effective water treatment which adapts the conditions in the water net is able to minimize corrosion problems. Special challenges are necessary by changing the corrosion system material/drinking water due to the modification of water treatment or by distributing water with alteration of the composition in plant and distribution system.

However, moderating the corrosivity of water by water treatment is one step of a corrosion control system due to the fact that this approach is complicated by the fact that different pipe and component materials are affected by water quality parameters in a different way. But nevertheless, a well-structured corrosion risk analysis provides control systems with relations of adequate treatment procedures and corrosion protection.

The presentation shows on basis of a corrosion risk assessment, case studies and practical investigations in test rigs the possibility to minimize corrosion problems by a fine-tuned water treatment. Also the limitations, e.g. corrosion indices as characteristic variable for corrosion control by water treatment, are discussed.

Observations on the Graphitic Corrosion of Cast Iron Trunk Main: Mechanisms and Implications

*Ron Logan¹, Mike Mulheron¹, David Jesson¹, Paul Smith¹, Tim Evans²,
Nic Clay-Michael², Jeff Whiter³*

¹University of Surrey, Guildford, Surrey, GU2 7XH, United Kingdom

²Thames Water Utilities Ltd, Clearwater Court, Vastern Rd, Reading, RG1 8DB, United Kingdom

³Environment Agency, Ergon House, Horseferry Rd, London, SW1P 2AL, United Kingdom

The Greater London area is serviced by a subterranean water network that includes over 6,000 km of large diameter cast iron pipe (commonly known as trunk main), much of which has been in service for over 100 years. Cast iron trunk main failures can be catastrophic in the damage they can cause and it is therefore imperative to understand how cast iron deteriorates in order to help predict those areas of the network which are at greatest risk of failure.

Unlike other ferrous metals, such as steels, which usually corrode in a uniform, mostly predictable manner, grey cast irons undergo a different form of corrosion. Within the water industry it is commonly referred to as “graphitisation”, whilst the corrosion literature, defines this as graphitic corrosion. Although this is a well reported phenomena, there is still a great deal to be understood about this insidious form of deterioration. The traditional view of graphitic corrosion is that it is a process of dissolution and transport of the iron matrix with the graphite flake structure being left intact. Scanning electron microscopy, in conjunction with both energy and wavelength dispersive x-ray spectroscopy, Scanning electron microscopy, in conjunction with energy dispersive and wavelength x-ray spectroscopy, has been used to characterise the microstructure and chemistry of the graphitic corrosion that occurs on the external surface of the pipe during time in service. The results suggest that the graphite flakes themselves are in fact deteriorating as part of the corrosion process. Archaeological studies concerned with the preservation of iron objects buried for many decades have found that contamination of iron by chlorides in the soil is a major factor in the corrosion process. The results of this study have also found chlorides present at the interface between the bulk metal and the corrosion product. It is proposed that the continuous graphite flake matrix acts as transport network for chloride ions that are found at the corrosion interface. It is proposed that the continuous graphite flake matrix acts as a transport network for chloride ions that are found at the corrosion interface. The implications of these observations for both the prevention and mitigation of trunk main deterioration are discussed.

Corrosion failure analysis of galvanized steel pipes in a closed water cooling system

Alessandra Colombo, Luca Oldani, Stefano P. Trasatti

Dipartimento di Chimica, Università degli Studi di Milano, Milan, Italy

The present study is focused on the failure analysis of water cooling systems serving a PET (polyethylene terephthalate) preform moulding plant. PET preforms have application in the field of drinking water, fresh milk and soft drink bottles.

Cooling systems under examination operate at 6 °C and 20 °C.

When the plant was set up, the cooling circuits were made from carbon steel. Mixture of water and ethylene glycol was used as coolant. Ethylene glycol was added with corrosion inhibitor to prevent corrosion.

The lack of proper control of plant management led to dramatic corrosion in the form of high dissolution rate of the base metal. This involved the risk of severe loss of functionality of the plant itself.

The following critical factors were identified:

- In 2009, carbon steel pipes were completely replaced with galvanized steel ones. Nevertheless, the corrosion inhibitor was added again to the coolant.
- The plant was equipped with a water softener that didn't operate properly, thus promoting the release of chlorides.
- Ethylene glycol was not replaced and its decomposition to organic acids brought to an increase of acidity.

All these factors contributed to corrosion initiation and propagation.

Chemical analysis were carried on water from both well and closed cooling circuits.

Analysis of water from the circuits revealed a very high amount of metals in solution (mainly Zn and Fe) and in the sediment. High chloride content was also determined.

The water pH was slightly acidic as a consequence of ethylene glycol decomposition e iron hydrolysis reactions.

It is possible to say that the failure of the pipes before their expected lifetime was induced by acidic corrosion. Zinc dissolution rapidly exposed the steel surface. Moreover, the deterioration of the pipes was enhanced by the mechanical wear resulting from a substantial amount of suspended solids in the flowing water.

Material durability and biofilm development in drinking water network – Comparison of stainless steel grades with commonly used materials

Audrey Allion^a, Sophie. Jacques^b, Jérôme Peultier^b, Pauline Boillot^b, Jean-Michel Damasse^a, Marie-Claude Bonnet^{c†}

^aAperam Isbergues Research Center, Corrosion & Surface Dept., BP 15, F-62330 Isbergues, France

^bArcelorMittal, Global R&D Le Creusot, Industeel, 56 rue Clémenceau, BP19, 71201 Le Creusot Cedex, France

^cEPI, ZI du Parc, 42490 Fraisses, FRANCE

Corrosion & Corrosion Protection of Drinking Water Systems

For micro-organisms, the preferred living state is adhering to surfaces that can lead to the development of a biofilm. In drinking water networks, a biofilm can affect the organoleptic quality of the water as well as whether it's safe to drink. This is due to the probable presence of pathogens inside the biofilm which may be spread in the water. Furthermore, by locally modifying the environment in terms of pH, RedOx potential or by secreting corrosive species, biofilms can induce changes on the surface of material, sometimes causing degradation.

It is well known that some materials are really prone to fouling and biofilm development while others, which are less sensitive to fouling, suffer from general corrosion leading to a non negligible ion release.

The aim of this work was to compare the behaviour of stainless steel grades with materials commonly used in drinking water networks in terms of biofouling and corrosion resistance.

The tested stainless steels included ferritic (444/EN 1.4521), three austenitic (304L/EN 1.4307, 316L/EN 1.4404 and 316LN/EN 1.4429) and two duplex (2304 /EN 1.4362 and 2205/EN 1.4462) grades. The materials used for comparison were copper, galvanised steel, polyethylene and cement. The experiments were performed in a pilot specially designed to assess the material biocontamination on a natural drinking water loop for more than 2 years.

The results evidence that even after a 2-year exposure biofilms are still dynamic systems leading to the modifications of the biofilm structure and composition with time. These modifications could be the source of the evolution of Open Circuit Potential (OCP). Evidence of neither free chlorine content variation nor localized corrosion on stainless steels was found. Corrosion attacks were only observed on galvanised carbon steel. While for stainless steels, negligible release rates, much below international health requirements were measured. So stainless steels are good candidates to make drinking water pipes.

Long term corrosion test of stainless steel for water heater applications

*Elisabeth Johansson, Sukanya Hägg Mameng, Avesta Research Centre,
Outokumpu Stainless AB, Avesta/Sweden*

Abstract

Stainless steels are used in domestic water heaters where their inherent corrosion resistance in potable water can be utilized without the use of lining or anode. In the case of duplex stainless steel their high strength can be utilized for a lighter design. It has been shown that proper design, welding procedures and post weld cleaning are important factors for achieving optimum corrosion resistance for stainless steel in water heater applications.

In this study long term test corrosion tests have been carried out for up to 1 year in water with 250 and 500 ppm chlorides at a temperature of 75 °C. The tested materials include ferritic, austenitic and duplex stainless steel grades. Results were evaluated with regard to pitting and crevice corrosion. Special emphasis was placed on the effect of weld oxide and different degrees of post weld cleaning, as well as different types of weld joints.

The long term test results are compared with short term electrochemical measurements such as pitting potential and critical pitting temperature (CPT). Also experiences from stainless steel in domestic water heaters are discussed and compared with the laboratory corrosion results.

Fatigue behavior of high quality steels in water

M. Borchert¹, M. Panzenboeck¹

*Department Metallkunde und Werkstoffprüfung, Montanuniversität Leoben,
Roseggerstr. 12, 8700 Leoben, Austria
marlies.borchert@unileoben.ac.at*

ABSTRACT

Gear boxes for hydraulic equipment are normally filled with oil in order to prevent corrosion. Today for many applications oil is replaced by water. In this paper the influence of an added corrosion inhibitor on corrosion fatigue is examined. The investigated materials are a high alloyed stainless steel (X3CrNiMo13-4) and a structural steel (20Mn5). Electrochemical studies have shown that both materials exhibit pitting attack although the medium contained an inhibitor. Additionally, the fatigue behavior is strongly influenced. The level of the fatigue strength of X3CrNiMo13-4 obtained in the medium without inhibitor is about 50 MPa lower than that within air. However, in the medium with inhibitor it is about 100 MPa lower. The 20Mn5 steel shows a fatigue limit in air, whereas in the medium (with and without inhibitor) all samples fail due to corrosion attack. Thus, the investigated inhibitor is not suitable for application at ambient temperature and in untreated water.

Key words: corrosion fatigue, fatigue strength, inhibitor, pitting, high quality steel.

Influence of disinfection chemicals on corrosion of various metals for drinking water supply systems

Mirjam Bajt Leban, Tadeja Kosec, Slovenian National Building and Civil Engineering Institute, Dimičeva 12, SI-1000 Ljubljana Slovenia

Drinking water supply systems mostly consist of pipes and accessories (valves, T species, etc.) made from different type of metals: galvanized carbon steel, stainless steel and copper and its alloys. Lifetime of installations for drinking water should be designed for at least 50 years, but in many cases they fail much earlier - usually due to corrosion. The main reason for corrosion of drinking water supply systems is the corrosivity of water as well as an increase in corrosion due to chemical and physical methods of disinfection of water systems due to infections caused by micro-organisms hazardous to health. In Europe and the world, there are known standardised tests for determination of impact of the disinfectants on sustainability of materials used for drinking water systems. However, the duration of such tests is very long and the price high.

The main aim of our research was to characterize corrosion behavior of commonly used metal materials in Slovenia (galvanized steel, stainless steel and copper and its alloys) in local water with additions of disinfectants (concentration for continuous disinfection and increased concentration used for chemical shocks). In addition, tests were performed at room and at elevated temperature. The methods used for corrosion characterization of chosen metal materials in the contact with drinking water were electrochemical methods (potentiodynamic polarization and polarisation resistance) and exposures in selected environment and condition for particular time (the condition of exposed surface was examined by scanning electron microscope and Raman spectroscopic methods after 7 and 40 days of exposure).

The results of tests have shown increased corrosion activity at elevated temperatures. Also, different disinfectants have different influence (aggressiveness) to different types of metals. It was observed that the results of electrochemical tests are in accordance to observations obtained by visual examination of surfaces after exposures.

Limiting conditions of pitting corrosion for lean duplex stainless steel as a substitute for standard austenitic grades

*Sukanya Hägg Mameng¹, Rachel Pettersson²,
Avesta Research Centre, Outokumpu Stainless steel AB, Avesta/Sweden¹,
Jernkontoret, The Swedish Steel Producers' Association Stockholm,
Stockholm /Sweden²*

Summary

Lean duplex stainless steels such as LDX 2101[®] are today used in many applications where they can substitute for the standard austenitic stainless steel 304L and 316L. The advantages include higher strength, better resistance to stress corrosion cracking, good uniform corrosion resistance and better price stability due to the lower nickel content.

This paper focuses on the performance of the lean duplex stainless steel LDX 2101[®] as a substitute for type 304L and 316L in chloride containing environments ranging from potable water to seawater. A combination of short term electrochemical testing and long term exposures is used to investigate the tendency to pitting corrosion as a function of chloride concentration and temperature. This is used to define the limiting conditions for pitting corrosion and construct engineering diagrams showing the risk areas for localised corrosion as a function of environmental parameters. Results are discussed in terms of the role of alloying elements and microstructure.

Keywords: Lean duplex stainless steel, LDX 2101[®], temperature, potential, chloride concentration, pitting potential, engineering diagram

Effectiveness of induction annealing process for the ferritic stainless steel AISI 444

A. Acquesta^a, C. Bitondo^a, A. Bossio^a, A. Carangelo^a, M. Curioni^b and F. Bellucci^{a,*}

^a University of Naples "Federico II", Dept. of Chemical Engineering, Materials and Industrial Production, 80125 Naples, Italy

^b Corrosion and Protection Centre, The University of Manchester, Manchester, M139PL, UK

* Corresponding author. Tel. (+39) 081 7682402, Email address: bellucci@unina.it

Abstract

The objective of this work was to investigate the effect of an induction annealing process of the ferritic stainless steel AISI 444 on its corrosion resistance. Due to the absence of Ni, this alloy can be used in drinking water facilities without problems related to the release of such metal. On the other hand different distribution agency could choose to add different amount of chlorine to the water, so it is fundamental to study the influence of concentration of chloride ions on its corrosion resistance. The pitting and crevice corrosion susceptibility of both, annealed and not annealed AISI 444, were examined by Cyclic potentiodynamic macro (large area) and micro (small area) polarization measurements (CPP) and by salt spray test. The influence of annealing process on the microstructures of specimens was analyzed by using SEM and EDS analysis. The pitting and crevice corrosion resistance were not improved by heat treatment, as shown by micro CPP tests, anyway this result was not confirmed by macro CPP.

Failure analyses of localised corrosion damages on stainless steels – practical examples

Ivan Juraga, Vesna Alar, Vinko Šimunović, Ivan Stojanović

*University of Zagreb, Faculty of Mechanical Engineering and Naval
Architecture, I. Lučića 5, 10000 Zagreb, Croatia*

Summary

High alloyed corrosion resistant Cr-Ni stainless steels are, as it is well known and confirmed by countless examples of their successful application over the last hundred years, a unique kind of materials with extraordinary corrosion resistance properties in many different media. Without these steels, many modern industrial fields would be unthinkable. However, these steels are not, contrary to their name in almost all world languages, absolutely immune to various corrosion processes, especially not to localized corrosion. In this paper, from a practical point of view, an overview of the various stainless steel corrosion failures caused by pitting corrosion, crevice corrosion, stress corrosion cracking and microbiologically influenced corrosion is presented, as well as possibilities of their avoidance based on the conducted failure analysis investigations.

Keywords: Stainless steels, Localized corrosion, Failure analyses

Investigations of the Corrosion behaviour of stainless steel in contact with ECA-generated disinfectant fluids

*M. Dimper, J.W. Erning, Federal Institute of material research and testing, Berlin,
A. Ahrens, S. Reimann, Research and Teaching Institute for Brewing, Berlin
Germany*

The generation of active disinfectants by electrochemical processes gains market share due to the lack of need for transportation and storage of dangerous goods as well as the ease of operation. Usually the process involves the use of specific electrodes for electrolysis of water to produce active chlorine species, sometimes supported by addition of chlorides to the process water.

Investigations

The research project involves the investigation of the passive and repassivation behaviour of stainless steels typical for the beverage industry in contact with industrially available disinfectant fluids. Measurements will be conducted according to EN 16056 in Cells according to ASTM G 150. Samples will be taken from new sheets as well as from sheets exposed to laboratory cleaning cycles with the disinfectant fluids. The combination of the influence of oxidant and chloride concentration will be examined in detail.

Results

The investigations will show the influence of oxidant and chloride concentration and combinations of both on the corrosion resistance of stainless steels like 1.4404 (316 L) used in the beverage industry. The final aim is to develop a matrix for the combined influence and give specifications for the use of ECA-based disinfectants regarding the material of the plants.

FAILURE ANALYSIS OF FIREWATER PIPELINE

Saud Al Subai, Keshab Barai and Esteban Morales Murillo

Saudi Basic Industries Corporation, P.O Box 11669, Jubail 31961, Saudi Arabia, T +966 (3) 359 9134, F +966 (3) 359 9112

This paper presents the failure analysis of a fire water pipe line from a petrochemical industry. Leakages were noticed at the top portion of the pipeline. Severe deep pits were observed at the top inner surface and deposits found at the bottom inner surface of the pipe line. Visual inspection, microscopic examination, and chemical and water analyses were employed in the present failure analysis. Final analysis results showed that the failure occurred due to the severe oxygen corrosion attack at the top portion of the pipe while the bottom surface of the pipe suffered from under deposit corrosion. The fire water pipe line was made of low carbon steel. A number of recommendations were proposed to prevent recurrence of such type of failure in future.

Keywords: Fire water, oxygen, under deposit, corrosion, failure

In-plant Corrosion Investigation on Steels in Distillery Effluents

Ajay K. Singh

Department of Applied Science & Engineering, IIT-Roorkee, Saharanpur, India

Chhaya Sharma

Department of Paper Technology, IIT-Roorkee, Saharanpur, India

Chhotu Ram

Department of Applied Science & Engineering, IIT-Roorkee, Saharanpur, India

Abstract

Steels have been widely used as a construction material for effluent treatment plant (ETP) of distillery. Present study deals with corrosion investigations on mild steel and stainless steels i.e. 304L, 316L, 2205 in distillery effluents. Accordingly, in-plant corrosion test were conducted on these coupons which were exposed to primary tank having untreated effluent and secondary tank having effluent from anaerobic biogas digester. Corrosion rate and localized corrosion has been evaluated by weight loss and pit depth respectively on coupons. The corrosivity of both untreated and treated effluents were compared and correlated with different chemical constituents. The various corrosion influencing parameters in both untreated and treated effluents has been discussed from our previous reports. In these studies, electrochemical polarization test were performed in both effluents and untreated effluent was observed to be more corrosive than treated effluents. Mild steel has shown maximum corrosion rate followed by stainless steels 304L, 316L and lowest in case of 2205. Intensity of pitting on mild steel was observed maximum followed by stainless steels 304L, 316L and minimum on 2205. The corrosion resistance against uniform and localized corrosion was correlated with presence of alloying elements such as Cr, Ni and Mo content in stainless steels.

Biocorrosion Evolution in a Laboratory Copper Pipe Ageing System

Diego Fischer¹, Leslie Daille², Carlos Galarce¹, Rodrigo De La Iglesia², Gonzalo Pizarro^{1,3} and Ignacio Vargas^{1,3}

¹ Department of Hydraulic and Environmental Engineering. Pontificia Universidad Católica. Santiago, Chile

² Biological Science. Pontificia Universidad Católica. Santiago, Chile.

³ Centro de Desarrollo Urbano Sustentable. Santiago, Chile.

Copper is widely used as a plumbing material due to its resistance to corrosion and antibacterial properties. Nevertheless under certain conditions an accelerated process of corrosion influenced by microorganisms may occur. The biocorrosion can cause material failure and health concerns due to high copper concentration in potable water.

This study aims to help understanding how microbial communities and their relative abundance influence the corrosion process and the copper release to the water. To answer these questions, we have implemented a laboratory copper pipe ageing system and inoculated it with 4 known bacterial isolates extracted from real drinking water system affected by biocorrosion. Synthetic water was replaced three times a week during 16 weeks. It consisted of tap water adjusted to pH 6.4 using HNO₃ and supplemented with 60 mg/L of acetate as electron donor and carbon source to accelerate bacterial growth. During the ageing process we studied the copper release under controlled flux conditions. Specific tests for copper release under flowing conditions were performed on weeks 1, 2, 3, 5, 8 and 16. Surface analysis was conducted by combining SEM-EDS observation with electrochemistry. Finally, DNA samples were extracted to observe changes on the relative abundance of the four community members during the ageing period.

The copper concentration in the water reached 3 mg/l since the first week, exceeding the OMS recommendation (2 mg/l). Until the 5th week copper release under flux conditions seems to fit a plug flow, which would mean no significant biosorption is occurring. Nevertheless the SEM analysis shows a biofilm grew on the pipe inner surface.

This research will help us understand first stage of the biofilm formed on the pipe inner surface and how the first colonizer that attach to the surface of the copper pipe will promote the attachment of other bacteria, which in turn can accelerate the copper corrosion. These effects may also be correlated with the bacterial communities that might change in time, before reaching a steady state.

Corrosion of gold imitations in illuminated manuscripts

*Milan Kouril, Eliska Jindrova, Tereza Jamborova, Jana Dernovskova**

Institute of Chemical Technology, Prague, Czech Republic

** National Library of the Czech Republic*

The manuscript illumination developed in the Czech countries with the emergence of the first monasteries and education extension. The painting technique was gradually changing, but materials used for illumination craft, remained the same - the binder, the materials, pigments. One of the techniques was painting and gilding and replacement of gold with other metals such as brass, which occur mainly in Byzantine code books and oriental manuscripts. The survey of 10 centuries old illuminations from the collections of the National Library showed that the gold-like areas were made with a use of a brass powder. Currently, this layer shows significant damage and the degradation mechanisms of such a rare manuscript is to be found.

Illuminations show degradation of the pseudo-gilded areas, such as darkening of the metal phase and disintegration of the binder. The aim was to compare the corrosivity to brass by binders using artificial aging tests modelling the conditions for the deposition of illuminated documents in the archives. Samples were made by means of pseudo-gilding on parchment, glass, brass sheets and the brass electrical resistance probes. Egg white, Arabic gum, fish glue and parchment glue were applied as most often used binders in the manuscript illuminations. The samples on pseudo-gilded parchment, glass, brass sheets and probes were subjected to artificial aging comprising of alternating wet and dry 24-hour periods. The second part of the sample glasses, sheets and probes were exposed to the atmosphere containing acetic acid vapour and the effect of increased relative humidity on the corrosion behaviour of brass was evaluated. Colour change of the samples, IR spectra change and corrosion depth of the electrical resistance probes in time were evaluated as well.

The results show that the presence of the binder layer on brass increases the corrosion rate of brass at higher relative humidity of ambient air. Protein-based binders provided the higher corrosion rate of the brass probes compared to that of polysaccharide-based binder – Arabic gum. IR spectroscopy has not demonstrated any changes in the polymer chain of binders which would indicate degradation of the binder by the corrosion products of brass. The colour change of samples was negligible. When evaluating the effect of cupric ions on the polymer chain integrity (by using the vibration viscometer), a decrease of the viscosity of samples with added brass powder and cupric ions was observed, but the polymer chain splitting was not proven. In presence of the acetic acid vapours, the corrosion attack is most intensive, as expected. Corrosion loss after exposure in acetic acid polluted air is directly proportional to the concentration of source acid solution and copper and zinc acetate based corrosion products were identified by means of IR spectroscopy.

The bronze panel (*paliotto*) of *San Moise* in Venice: materials and causes of deterioration

C. Chiavari¹, C. Martini², S. Montalbani³,
E. Franzoni⁴, M.C. Bignozzi⁴, M.C. Passeri⁵

¹ C.I.R.I. (Centro Interdipartimentale di Ricerca Industriale) Meccanica Avanzata e Materiali
Università di Bologna, Via Risorgimento 2, 40136 Bologna (Italy); cristina.chiavari@unibo.it

² Dipartimento di Ingegneria Industriale,
Università di Bologna, Via Risorgimento 4, 40136 Bologna (Italy); carla.martini@unibo.it

³ Dipartimento di Chimica "Giacomo Ciamician", Via Selmi 2, 40126 Bologna;
simona.montalbani2@unibo.it

⁴ Dipartimento di Ingegneria Civile, Chimica, Ambientale e dei Materiali
Università di Bologna, Via Terracini 28, 40131 Bologna (Italy); elisa.franzoni@unibo.it,
maria.bignozzi@unibo.it

⁵ RE.CO. Restauratoriconsortiati - Via F. Sivori, 6 - 00136 Roma - reco@recorestauratori.com

The Church of *San Moisé* in Venice (Italy) has a beautiful bronze panel (a so-called "*paliotto*") with high-relief figures, which is located in front of the altar in the sacristy. The bronze panel was made by Nicolò Roccatagliata and his son Sebastiano in 1633 and represents the Passion of Christ.

At the beginning of the last restoration intervention, diagnostic investigations were carried out so as to identify the materials and the causes of deterioration. In particular, both the bulk metal alloy and surface layers (consisting of corrosion products and organic compounds, related with previous restoration actions or from original protective treatments) were investigated.

A range of microscopic/spectroscopic techniques was applied: the alloy composition and microstructure was determined by VP-SEM/EDS, whilst the corrosion products were analysed by Raman micro-spectroscopy (wavelength 514.5 nm, power: 5 W). The organic compounds in surface layers were analysed by Pyrolysis Gas Chromatography Mass Spectrometry (Py-GC-MS). The adjacent mortars were analysed as well, in order to highlight their role in the degradation processes which took place in the contact areas between the wall and the bronze panel.

The results showed that the alloy is a quaternary bronze (Cu-Sn-Zn-Pb): the high-relief figures were cast separately then mechanically joined to the body of the panel. Traces of the clay core were detected in the back of the panel. The bronze surface was artificially patinated by liver of sulfur (K_2S). The organic protective layer consisted of stearin and paraffinic wax. However, siccative oil was detected in the layer at the interface with the metal, likely corresponding to the original protective treatment. Also pine resin was detected among the organic compounds.

The corrosion products mainly consisted of basic copper chlorides (paratacamite, atacamite) and mixed Cu and Na carbonates (calconatronite), deriving from the interaction with the surrounding mortar.

Single- and multiple-layer coatings for bronze statuary: preliminary study and in situ evaluation after five-year outdoor exposure

Barbara Salvadori, Emma Cantisani, Cecilia Gaia Rachele Tognon, CNR-Institute for the Conservation and Valorization of Cultural Heritage, Sesto Fiorentino (Florence)/I; Merj Nesi, private restorer, Florence/I; Andrea Cagnini, Monica Galeotti, Simone Porcinai, Opificio delle Pietre Dure, Florence/I

In recent years, several studies have been carried out to individuate or develop new successful coatings for metals conservation. However, only a small range of polymers is still used in the common practice. Acrylic resins with a topcoat of wax (the so-called double layer) are extensively used by restorers on outdoor bronze statuary, and both laboratory researches and field tests show the better performance of this combined application compared to the single products. Indeed, it has been reported that the acrylic resin hinders the onset of fresh corrosion, while the sacrifice wax topcoat preserves the underlying coating. On the other hand, a few information is available on the lifespan of these systems upon natural weathering. Moreover, some commercial formulations (in particular Incralac™ and Soter) contain the corrosion inhibitor benzotriazole (BTA), in this case as a UV stabilizer, but its suspicious toxicity makes it necessary to individuate safer products. Nevertheless, these commercial blends continue to be used in the absence of any quantitative proof of significantly better performing alternatives.

A comparative study was carried out on artificially aged bronze coupons treated with reference traditional products and different BTA-free coatings. In addition, a triple-layer system (wax/acrylic/wax) was tested, where the application of a wax priming layer on the metal was presumed to impart reversibility.

Aesthetical features and resistance against acid attack were documented with colour measurements, SEM-EDS and FTIR spectroscopy; moreover, the reversibility of the most promising coatings was checked after aging in the corrosive environment.

Triple-layer and reference double-layer systems were also applied on a bronze fountain, the *Fontana dei putti* by Mario Moschi in Florence (1952), following its restoration. After five-year outdoor exposure, a diagnostic campaign provided service-life information for the applied coatings.

In-situ EIS characterization of outdoor corrosion behaviour of bronze and gilded bronze

A. Balbo^{1,2}, M. Abbottoni¹, C. Chiavari³, C. Martini⁴, E. Bernardi⁵, C. Monticelli^{1,2}

¹ Centro Studi Corrosione e Metallurgia "A. Daccò", Università di Ferrara, Italia;

² Teknehub, Università di Ferrara, Italia

³ C.I.R.I. (Centro Interdipartimentale di Ricerca Industriale) Meccanica Avanzata e Materiali, Università di Bologna, Italia

⁴ Dipartimento di Ingegneria Industriale, Università di Bologna, Italia

⁵ Dipartimento di Chimica Industriale "Toso Montanari", Università di Bologna, Italia

Abstract

The corrosion monitoring of bronze and gilded bronze artefacts exposed outdoor is an important issue helping to develop proper conservation strategies of our cultural heritage. The corrosion process is particularly critical in the case of gilded bronzes because the contact with the large cathodic gold surface galvanically stimulates the corrosion of bronze substrate at the flaws (pores and defects) of the gold layer. As a result, an interlayer of corrosion products grows at the bronze/gold interface causing further damage and detachment of the gilded layer.

In this research an in situ non-destructive EIS technique was adopted to monitor the corrosion rate process developed in the presence of synthetic rainwater on bronze and gilded bronze coupons produced with the ancient techniques adopted during the Renaissance period. In particular, a "contact probe" similar to that already used in the field of cultural heritage by other researchers [1] was used to collect EIS data and to discriminate the severity of the corrosion process under different experimental conditions. The sensitivity of the technique was checked by varying both the aggressiveness of the environment (rainwater composition) and by testing as received and pre-corroded coupons. Electrochemical impedance spectra on gold sheet were also collected as reference data. The accelerated corrosion conditions applied to bronze and gilded bronze to get pre-corroded specimens involved wet & dry exposures to artificial acidic rain, producing surface degradations representative of those actually developed during outdoor exposition. The obtained pre-corroded surfaces were properly characterized by surface analysis techniques to help EIS data interpretation.

[1] Letardi P., Laboratory and field test on patinas and protective coating systems for outdoor bronze Monuments, in: J. Ashton, D. Hallam (Eds.), Metal2004 – Proceedings of the International Conference on Metals Conservation, Canberra, 4–8 October 2004, National Museum of Australia, 2004, pp. 379–387.

Staining of Bronze Sculptures, Determining the Causes

Anna Ramus Moreira, IPT Institute for Technological Research, São Paulo/Brazil

Karen Barbosa, MASP Museu de Arte de São Paulo

Neusvaldo Lira de Almeida, IPT Institute for Technological Research, São Paulo/Brazil

Zehbour Panossian, IPT Institute for Technological Research, São Paulo/Brazil

Since prehistory, copper and its alloys are the most known metals by man. Its importance is primarily related to its good corrosion resistance in various environments. Additionally, they have an excellent workability, high electrical and thermal conductivity and good mechanical properties. When copper and its alloys are exposed to “clean” atmospheres (non-contaminated) at room temperature, it starts to grow on the surface a thin layer of copper oxides which provide excellent corrosion resistance. When exposed to rural atmospheres with low contamination of hydrogen sulfide, it can be observed on copper and its alloys surface a darkening to black that persists over time and also provides a very low corrosion rate. It is worth to mention that hydrogen sulfide is a gas formed from the decomposition of organic matter. In urban and industrial environments, atmospheres typically contaminated with sulfur dioxide, the color of the corrosion products changes over time from black to green. This green layer is called patina. Patina is highly protective and provides excellent corrosion resistance. The presence of sulfur dioxide is necessary to the patina formation, but other pollutants can also contribute which are carbon dioxide and chlorides. Despite the excellent corrosion resistance of copper and its alloys, when the layer of corrosion products is not formed in the proper way, interference colors can be assumed. And when the aesthetic aspect is important, as it is for works of art, the loss of the original appearance can result in a huge prejudice. In this sense, this work presents all the study conducted for the identification of the causes that led to the appearance of brilliant gray stains on bronze sculptures surface.

The role of microstructure on initial corrosion and metal release of Cu-Zn alloys in a chloride-containing laboratory atmosphere

*Xian Zhang, Inger Odnevall Wallinder and Christofer Leygraf
KTH Royal Institute of Technology, Div. Surface and Corrosion Science,
Dr. Kristinas v. 51, SE-100 44 Stockholm, Sweden*

Bare copper sheet and three commercial Cu-Zn alloys, Cu15Zn, Cu30Zn and Cu40Zn, have been exposed to chloride containing environments in the laboratory. The aim was to explore the role of chloride deposition and of alloy microstructure on the initial corrosion mechanisms and on initial differences in copper and zinc release. The subject is of principal interest for the outdoor exposure of copper-based artifacts, since chlorides are expected to increase in relative importance in coastal areas of, e.g., Europe (1).

In earlier studies (2,3) it was found that the single phase Cu15Zn alloy exhibits lower tendency of corrosion product flaking than bare Cu sheet and Cu4Sn in chloride containing atmospheres. This was attributed to the early formation of zinc hydroxycarbonate, $\text{Zn}_5(\text{OH})_6(\text{CO}_3)_2$, which delayed the formation of nantokite, CuCl, a precursor of atacamite, $\text{Cu}_2(\text{OH})_3\text{Cl}$. The flaking process was attributed to an observed volume expansion during transformation of CuCl to $\text{Cu}_2(\text{OH})_3\text{Cl}$. Significantly lower runoff rates than corresponding corrosion rates were observed for bare Cu sheet and Cu15Zn at marine field conditions (3).

In this study the investigation was extended to include not only single phase alloys (Cu15Zn and Cu30Zn) but also Cu40Zn, a two-phase alloy containing the Cu-Zn matrix (α -phase) and an additional secondary Cu-Zn phase (β -phase). The laboratory exposure was based on predeposition of NaCl followed by cyclic wet/dry conditions to study corrosion initiation, and subsequent successive simulated rainfall events to assess differences in released copper and zinc quantities. The evolution of corrosion products was followed with a series of complementary analytical techniques, which included Fourier transform infrared reflection absorption spectroscopy (IRAS), confocal Raman spectroscopy (CRM) and grazing incidence X-ray diffraction (GIXRD). Unique sets of data were extracted though in situ IRAS measurements and an environmental scanning electron microscope (ESEM). Phases were post-analyzed with CRM at submicron lateral resolution. Released amounts of copper and zinc were determined by means of atomic absorption spectroscopy (AAS).

The same dominating corrosion products were observed in the laboratory exposures as at field conditions, findings in accordance with the general scenario for corrosion product evolution of bare copper and zinc sheet (2). The multi-analytical approach allowed the influence of microstructure to be explored, in particular the corrosion initiation in the slightly zinc-richer β -phase adjacent to the α -phase. The results confirmed the barrier effect of zinc hydroxycarbonate, $\text{Zn}_5(\text{OH})_6(\text{CO}_3)_2$, leading to reduced interaction of chlorides with the alloy surface, and thereby to reduced formation rates of corrosion products and release rates of copper.

References:

1. J. Tidblad, Atmospheric Environment, 55 (2012) 1-6
2. X. Zhang, I. Odnevall Wallinder and C. Leygraf, Manuscript submitted
3. I Odnevall Wallinder, X. Zhang, S. Goidanich, N. Le Bozec, G. Herting and C. Leygraf, Science of the Total Environment, 472 (2014) 681-694

Atmospheric corrosion of fire gilded bronze: accelerated ageing in runoff conditions

¹C. Chiavari, ²C. Martini, ³E. Bernardi, ³S. Raffo, ⁴A. Balbo, ⁴M. Abbottoni, ⁵M.C. Bignozzi, ⁴C. Monticelli

¹C.I.R.I. (Centro Interdipartimentale di Ricerca Industriale) Meccanica Avanzata e Materiali, Università di Bologna, Via Risorgimento 2, 40136 Bologna (Italy); cristina.chiavari@unibo.it

²Dipartimento di Ingegneria Industriale, Università di Bologna, Via Risorgimento 4, 40136 Bologna (Italy); carla.martini@unibo.it

³Dipartimento di Chimica Industriale "Toso Montanari", Università di Bologna, Via Risorgimento 4, 40136 Bologna (Italy).

⁴Centro di Studi sulla Corrosione e Metallurgia "A. Daccò", University of Ferrara, Via Saragat 1, 44122 Ferrara (Italy)

⁵Dipartimento di Ingegneria Civile, Chimica, Ambientale e dei Materiali, Università di Bologna, Via Terracini 28, 40131 Bologna (Italy); elisa.franzoni@unibo.it, maria.bignozzi@unibo.it

Gilded bronzes, widely used in historical monuments as well as in architectural elements, are often severely affected by corrosion damages due to the galvanic coupling between the gold layer and the bronze substrate. The growth of corrosion products at the gold/bronze interface may lead to blistering or break-up and loss of the gold layer, and specific cleaning procedures as well as conservation actions are required for safeguarding gilded bronze artefacts.

The present work was carried out within a research project dealing with conservation methods for gilded bronzes, based both on preventive actions (microclimate control) and on active methods (protective coatings). The results presented here are dealing with fire gilded bronze samples (replicating the composition and microstructure of the materials used in Lorenzo Ghiberti's Paradise Door (Baptistry of Florence, 1452)), which were aged in runoff conditions by accelerated exposure tests in synthetic acid rain. Both unprotected and organosilane-coated gilded bronzes were investigated, so as to assess the protective efficiency of nanoparticle-containing 3-mercaptopropyltrimethoxy-silane on these substrates.

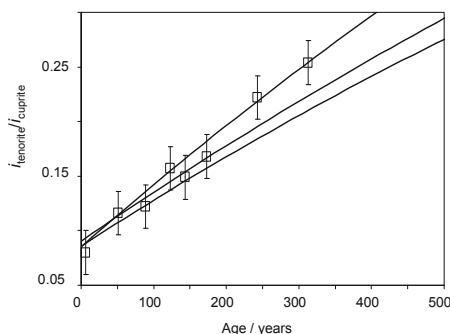
A detailed characterization of fire gilded bronze samples was carried out by FIB/FEG-SEM both before and after accelerated ageing. Surface analysis and cross-sections analysis of the samples were performed also by VP-SEM/EDS and micro-Raman spectroscopy. The protective efficiency of the organosilane coating was assessed by the measurement of the metal release in the ageing solution.

Dating copper-based archaeological materials using the voltammetry of microparticles

Antonio Doménech-Carbó^a, Sofia Capelo^b, María Teresa Doménech-Carbó^c

^a Departament de Química Analítica. Universitat de València. Dr. Moliner, 50, 46100 Burjassot (València) Spain; Departamento de Paisagem, Ambiente e Ordenamento, Escola de Ciências e Tecnologia, Universidade de Évora, Rua Romão Ramalho 59, 7000-671 Évora Portugal, ^cInstitut de Restauració del Patrimoni, Universitat Politècnica de València, Camí de Vera 14, 46022, València.

The voltammetry of microparticles, an electrochemical technique providing information on the composition of archaeological materials using an essentially non invasive analysis [1,2] was previously applied for dating lead-based materials [3,4]. It is described the application of this methodology for dating copper-based archaeological materials based on a theoretical model for long term metal corrosion [5]. Dating is based on the measurement of the voltammetric signals of cuprite and tenorite formed as a corrosion products in artifacts submitted to aging in atmospheric environments with no exigent corroding conditions. Assuming that the composition and conditions of aging can be considered as similar for all samples, and that the corrosion proceeded uniformly during the entire corrosion time, the time variation of the tenorite/cuprite ratio fits to a potential law from calibration using a set of copper-based coins (see Figure). As a result, absolute dating can be obtained.



References

- [1] Doménech, A.; Doménech, M.T.; Costa, V. *Electrochemical methods applied to archaeometry, conservation and restoration*, (Scholz, F. Edit.) Springer, Berlin-Heidelberg, 2009.
- [2] Doménech, A.; Doménech, M.T.; Pasíes, T.; Bouzas, M.C. *Electroanalysis*, 2011, 23, 2803-2811.
- [3] Doménech, A.; Doménech, M.T.; Peiró, M.A. *Analytical Chemistry* 2011, 83, 5639-5644.
- [4] Doménech, A.; Doménech, M.T.; Peiró, M.A.; Martínez, I.; Barrio, J. *Journal of Solid State Electrochemistry* 2012, 16, 2349-2356.
- [5] Doménech, A.; Doménech, M.T.; Pasíes, T.; Bouzas, M.C. *Electroanalysis*, 2012, 24, 1945-1955.

Prediction of long-term corrosion rate of copper alloy objects

Katerina Kreislova¹, Hana Geiplova²

¹SVUOM Ltd., Prague/Czech Republic; ²UTAM/CET, Telc/Czech Republic

Abstract

Comparative atmospheric corrosion data for different metal alloys can be used to predict the service life of a component, maintenance requirements, and metal loss to the environment. In some international projects there were derived some prediction models for atmospheric corrosion rate of metals – dose/response functions – including copper alloys.

In paper there are presented the real corrosion studies of two long-term exposed objects – bronze statue of Johan from nepomuc from Charles bridge, Prague, and copper roof of Summer Palace of Queen, Prague. Both these objects had been exposed in urban atmospheres for more than 300 years.

The thickness of materials had been measured and the analysis of patina was done. In case of bronze the effect of bronze alloy composition is important. The limiting property for the serviceability of the roof was not corrosion (material) loss but the decreasing of mechanical properties.

A multi-technique approach for characterizing patina formed on the surface of brass used for musical instrument of the XIX century

F. Cocco¹, M. Fantauzzi¹, G. Peschke², B. Elsener^{1,2}, A. Rossi¹,

¹ Dipartimento di Scienze Chimiche e Geologiche S.S. 554 bivio per Sestu,
Università degli Studi di Cagliari, Monserrato (Cagliari) / Italy

² ETH Zurich, Institute for Building Materials, ETH Hönggerberg, CH-8093 Zurich,
Switzerland

corresponding author: rossi@unica.it

Scientific reports on the characterization of patinas formed on brass alloys used for the fabrication of musical instruments are scarce despite the interest of musicians in the execution of music using instruments built at the same age of the compositions. It is widely acknowledged that the sound depends on the manufacturing characteristics of the instrument. Very often the surface of the instruments in contact with saliva are covered by a biofilm and corroded: there is on one hand the need of characterizing the patina, of choosing how to remove it and clean the brass surface without compromising the performances of the instrument, and last how to effectively maintain the instrument upon time.

In this investigation, electrochemical methods which include potentiodynamic polarization curves, open circuit potential (OCP) and linear polarization (LP) were applied together with light optical microscopy (OM), scanning electron microscopy (SEM) equipped with energy dispersive X-ray analyser (SEM-EDX), X-ray photoelectron spectroscopy (XPS) and X-ray excited Auger electron spectroscopy (XAES). These complementary analytical techniques allowed characterizing the brass surfaces of five different brass alloys, whose zinc content ranges from 18 wt% to 37 wt%, before and after exposure to saliva solutions at pH 7.4 and at ambient temperature. Two alloys with 1 and 2wt% of Pb were also studied for comparison.

Electrochemical results

The results of the electrochemical measurements showed that the corrosion rate of all the alloys after one hour of immersion is relatively high (35 – 85 $\mu\text{m}/\text{year}$), with the formation of the patina it is expected to decrease after prolonged immersion. The alloys can be separated in two groups: alloys with low zinc content (Cu18Zn, Cu28Zn) show lower corrosion rates and more positive corrosion potentials, the alloys with higher zinc content exhibit higher corrosion rates. The anodic and cathodic Tafel slopes were determined from potentiodynamic polarization curves, indicating $\beta_a = 70 \text{ mV}/\text{dec}$ and $\beta_c = 130 \text{ mV}/\text{dec}$.

XPS surface characterization

Analysis of brasses by XPS is particularly challenging, as it is known that the XPS signals of $\text{Cu}2p_{3/2}$ and $\text{Zn}2p_{3/2}$ do not exhibit chemical shifts. Thus in this work emphasis was put on the analysis of the x-ray induced Auger signals and the Auger parameter with the Wagner chemical state plot. After immersion in artificial saliva for *one hour* the XPS survey spectra revealed the presence of nitrogen, phosphorus and sulfur in addition to the components of the alloy. The detailed spectra showed a clear shift of both binding energies and kinetic energies of the x-ray induced signals. On all the brass alloys studied after immersion in artificial saliva an inorganic surface film composed of CuSCN and zinc orthophosphate has been revealed by the application of the Auger parameter concept and the Wagner chemical state plot. Composition of the surface films formed in the different conditions will be reported at the conference.

In situ study of long term atmospheric corrosion of iron by μ Raman spectroscopy

Marie Bouchard, Delphine Neff, Jean-Paul Gallien, Philippe Dillmann

LAPA SIS2M UMR3299 CEA/CNRS and IRAMAT UMR5060 CNRS, CEA Saclay, 91191 Gif sur Yvette Cedex, France

A lot of cultural heritage iron alloys are submitted to atmospheric corrosion for several centuries. One of the most famous examples are the reinforcements used to build gothic cathedrals during medieval times. One important issue, concerning these metallic artefacts is to diagnose their corrosion state. To that purpose, a very important step is the fine understanding of the corrosion mechanisms. The corrosion layers are constituted of Fe(III) phases (oxyhydroxydes and oxides as goethite, lepidocrocite, ferrihydrite, maghemite and magnetite). Some of these phases can be very reactive electrochemically. This is the reason why some scholars proposes that they could be reduced and provoke the anodic corrosion of metallic iron during a so-called wet/dry cycle. Nevertheless because this process is transient, this assertion was, up to now, never assessed experimentally despite its formalism is accepted in several models already used for corrosion diagnoses.

Using a home designed cell, the wetting stage of the W/D cycle, during which the reduction of FeIII phases potentially occur, was simulated on a 500 hundred year old sample coming from an iron clamp from the Metz cathedral and submitted to atmospheric corrosion since it was put in the building. The layer of this sample is of several 10 micron thick and constituted mainly of ferrihydrite ($\text{Fe}_2\text{O}_3 \cdot 0.5\text{H}_2\text{O}$), a very electrochemically reactive phase, connected to the metallic substrate. The in situ cell allowed us to monitor by μ Raman spectroscopy on a transverse section the structural modification of the corrosion layer. Experiments took place with the external part of the layer in contact with deaerated water. Different structural mapping of the layer at different times allowed us to demonstrate that a part of the ferrihydrite is reduced after a certain duration. The results will be presented in details in the paper and discussed in function of the nature of the wet/dry cycles

An integrated EIS-Raman approach to study the corrosion mechanism of iron artefacts

S. Grassini¹, M. Bouchar², E. Angelini¹, M. Parvis³, D. Neff², P. Dillmann²

¹*Dipartimento di Scienza Applicata e Tecnologia, Politecnico di Torino, Italy*

²*IRAMAT LMC CNRS UMR5060 et SIS2M LAPA CEA/CNRS UMR3299, France*

³*Dipartimento di Elettronica e Telecomunicazioni, Politecnico di Torino, Italy*

Iron artefacts exposed for centuries to indoor atmospheric corrosion are subjected to very complex degradation mechanisms, which can be understood only through a complete investigation of the nature of the corrosion products layer and of its corrosion behaviour.

In this study an integrated approach based on electrochemical impedance spectroscopy (EIS) and μ -Raman spectroscopy is proposed to study the corrosion mechanisms affecting the iron artefacts of the Metz Cathedral in France. Saint-Étienne de Metz is a historic Roman Catholic cathedral, whose structure was reinforced after it was built in the 13th century, by iron tie rods or clamps, which have been either exposed to indoor atmosphere or subjected to corrosion in a sealing mortar for long times.

EIS and μ -Raman measurements have been carried out in order to correlate the microstructure and distribution of the different corrosion products with the electrochemical reactivity of the corrosion system under investigation. As a matter of facts, the corrosion mechanism of the iron artefacts exposed to long-time atmospheric corrosion is linked not only to the chemical composition of the corrosion products and to the reactivity of the single phases, but it is also mainly affected by the distribution of the different constitutive phases and by their porosity degree.

Assessing the electrochemical reactivity of the single corrosion product phase, outside the contest of the corrosion system, is of course a fundamental starting point, but several questions on the corrosion mechanisms affecting these artefacts are still open, requiring further investigations.

The experimental set-up has been, therefore, specifically design to allow collecting the EIS measurements and the μ -Raman maps at the same time on the same sample in order to study the distribution of the different corrosion products in the corrosion layer and at the same time to evaluate their corrosion reactivity.

The typical microstructure of the corrosion system investigated is constituted by a matrix of oxyhydroxides, more precisely of goethite, α -FeOOH, with local spots of lepidocrocite, γ -FeOOH, and akaganeite, β -FeO(OH_xCl_{1-x}). Other reactive phases have been also detected; in particular the presence of ferrihydrite/maghemite, $5\text{Fe}_2\text{O}_3 \cdot 9\text{H}_2\text{O}$ and γ -Fe₂O₃, respectively, has been observed on the surfaces exposed to atmospheric corrosion, while maghemite/magnetite, γ -Fe₂O₃ and Fe₃O₄, respectively, have been detected on the iron artefacts embedded in mortar.

Electrochemical reduction experiments have been also carried out in order to correlate the evolution of the different corrosion products and to propose corrosion mechanism hypotheses.

Study of iron sulphides origin in archaeological artefacts by determination of sulphur isotopic ratio

S.Grousset¹, F. Mercier¹, A.Dauzeres², D.Crusset³, L.Raimbault⁴, A. Galtayries⁵, J-P. Gallien¹, P. Dillmann¹, D.Neff¹

1. SIS2M/LAPA, CEA/CNRS UMR3299, 91191 Gif-sur-Yvette Cedex, France

2. IRSN, PRP-DGE/SRTG/LETIS, B.P. 17, 92262 Fontenay aux Roses Cedex, France

3. ANDRA, Direction Recherche et Développement

4. MINES ParisTech, Centre de Géosciences, Fontainebleau, France

5. Laboratoire de Physico-Chimie des Surfaces, Chimie ParisTech, Paris, France

*Corresponding author – Tel: +33 (0) 6 50 13 02 40 – e-mail: sophie.grousset@cea.fr

In a biologically active environment, the corrosion of ferrous object in anoxic conditions can be influenced by the action of micro-organisms. [1] For instance, sulfate-reducing bacteria may lead to localized corrosion. Therefore, it is important to determine these corrosion mechanisms in a double context. The first one is the preservation *in situ* of ferrous archaeological objects. Indeed soil analyses combined with sufficient knowledge of the corrosion mechanisms will ensure good storage conditions. The second one is the French concept for geological disposal of nuclear waste. It is based on a multi-barrier system including the metallic containers confined in natural clay in which microorganisms could be present. Yet, this barrier has to resist to long term corrosion over thousand years to secure such a disposal facility.

The presence of iron sulfides and other iron/sulfur-containing compounds in the corrosion layers has been reported in the corrosion product layers of iron in anoxic conditions and can be the fingerprint of the role of sulfate-reducing bacteria. [2-3] However the nature of iron sulfides is the same when these phases are formed by inorganic or metabolic pathway. Five different sulfur-containing compounds are observed: nanocrystalline mackinawite FeS_{1-x} , crystalline mackinawite, $\text{Fe(III)-mackinawite}$, greigite Fe_3S_4 and pyrite FeS_2 . [3-4] Nevertheless, isotope fractionation occurs during the microbial sulfate reduction (MSR) [5]. Indeed sulfate-reducing bacteria use preferentially sulfates containing the lightest isotopes of sulfur. Thus the sulfides ions produced are depleted in heavy isotopes (^{33}S , ^{34}S , and ^{36}S) relative to the starting sulfate. Then these sulfides ions can react with the Fe^{2+} ions issued from the anodic dissolution of iron to form iron sulphides depleted in heavy isotopes of sulfur. The iron sulfides produced are isotopically depleted in ^{34}S relative to remaining sulfates by up to ~75‰ only by MSR.

In our study, the archeological objects studied are nails from different anoxic sites, terrestrial (Site of Glinet, 16th century, Seine-Maritime, France & Site of Radhùspladsen, 16th century, Copenhagen, Denmark) or subaquatic (Site of Rhône 3, 1st century, Arles, Bouche-du-Rhône, France). Complementary techniques are used to characterize the sulfur-bearing compounds in the corrosion products of the nails: Field-Emission Scanning Electron Spectroscopy (FESEM) for the distribution of sulphur, μ -Raman spectroscopy for the nature of sulfur phases. For the determination of $^{34}\text{S}/^{32}\text{S}$ ratio, μSIMS (point measurements) and ToF-SIMS (imaging) have been carried out on iron sulfides borders in the corrosion product layers of different archeological nails.

1. Esnault, L., Jullien, M., Mustin, C., Bildstein, O., & Libert, M. (2011). *Physics and Chemistry of the Earth*(36), 1624-1629.
2. AlAbbas, F., Williamson, C., Bhola, S., Spear, J., Olson, D., Mishra, B., et al. (2013). *International Biodeterioration & Biodegradation*(78), 34-42.
3. Rémaizeilles, C., Saheb, M., Neff, D., Guilminot, E., Tran, K., Bourdoiseau, J., et al. (2010). *Journal of Raman Spectroscopy*(41), 1425.
4. Sherar, B., Power, I., Keech, P., Mitlin, S., Southam, G., & Shoesmith, D. (2011). *Corrosion Science*(53), 955-960.
5. Thode, H. (1991). Sulphur Isotopes in Nature and the Environment : an Overview. In *Stable Isotope in the Assessment of Natural and Anthropogenic Sulphur in the Environment*. John Wiley & Sons Ltd.

Study of archaeological ferrous objects in sulfide-containing media

*Jacques-André Bourdoiseau, Marc Jeannin, René Sabot, Céline Rémazeilles,
Philippe Refait,*

*Laboratoire des Sciences de l'Ingénieur pour l'Environnement (LaSIE),
UMR 7356 CNRS-Univ. La Rochelle, Bât. Marie Curie, Av. Michel Crépeau,
F-17042 La Rochelle cedex 01, France.*

Corrosion of iron and steel in natural and oxygen poor environments is likely to be microbiologically influenced. Anaerobic sulfate reducing bacteria (SRB) are often mentioned to be involved in this type of corrosion processes. SRB are able to reduce the sulfate species present in the environment into sulfide and one of the consequences of the metabolic activity of SRB is then the occurrence of iron sulfides in the corrosion products layer. In a context of long term materials durability, as required for nuclear waste storage, the corrosion mechanisms of steel in biologically active media has to be thoroughly studied. In order to understand the influence of BSR on corroded steel after long term burial in soils, experiments were conducted on archaeological artefacts (16th century). As archaeological analogues, such samples are often studied to predict long term corrosion in the field of nuclear research. In this context, archaeological nails were immersed for 2 months in different sulfide-containing solutions (Na_2S). The corroded artefacts were then exposed directly to sulfide species in order to simulate the action of SRB on rust. The corrosion system of such samples was previously thoroughly characterized through the analysis of a large corpus of similar nails extracted from the same excavation site (Glinet, France) [1,2]. Besides, the identification of iron sulfides by micro-Raman spectroscopy is now possible since the study of phases synthesized in laboratory that provided reference spectra [3,4]. Consequently, the evolution of the corrosion products of each sample could be clearly understood through the analysis of the corrosion products layers by micro-Raman spectroscopy and scanning electron microscopy. From a phenomenological point of view, the results revealed that the corrosion products, consisting initially mainly in carbonated phases (FeCO_3 siderite and $\text{Fe}_2(\text{OH})_2\text{CO}_3$ chukanovite) could transform into FeS mackinawite. This transformation occurred in the external part of the corrosion products layer. An interaction mechanism between the corrosion system and sulfides could then be proposed. This mechanism provides a global understanding of a possible action of SRB on corrosion products of ferrous materials buried in soils. Some questions remain however about the kinetics of the various reactions involved in the overall process.

[1] M. Saheb, D. Neff, P. Dillmann, H. Matthiesen, E. Foy, J. Nuclear Mat. 379 (2008) 118-123.

[2] M. Saheb, D. Neff, L. Bellot-Gurlet, P. Dillmann, J. Raman Spectroscopy 42 (2011) 1100-1108.

[3] J.-A. Bourdoiseau, M. Jeannin, R. Sabot, C. Rémazeilles, Corros. Sci. 50 (2008) 3247-3255.

[4] J.-A. Bourdoiseau, M. Jeannin, C. Rémazeilles, R. Sabot, Ph. Refait, J. Raman Spectroscopy 42 (2011) 496-504.

Study of the Role of Ammonium Ions on the Corrosion of Copper in Sulphate Containing Media

de Melo, H.G., Abrahão, D.F., Polytechnic School of the University of São Paulo/BR

Copper was one of the first metals shaped by humans. Its importance is evidenced by its wide use in different technological domains. Among them, we highlight its use to build historical monuments. When exposed to natural weathering copper develops a corrosion product layer that goes through a series of change [1]. The composition and appearance of this layer, generally denominated patina, depends both on the exposure time and on the composition of the atmosphere. Many historical monuments are exposed outdoors in urban environments. Therefore, they are constantly exposed to pollution and to weather. Ammonium sulfate is a major constituent of urban atmospheric dust, and, consequently, must play a major role in the formation of copper patinas.

Lobnig *et al.* [2,3] and Odnevall *et al.* [4], studied the corrosion of copper in the presence of submicron ammonium sulfate particles and have clearly demonstrated that they play a major role in the formation of copper patinas. They suggested [2,3] that ammonia originated from the dissociation of NH_4^+ ions stabilizes Cu^+ ions as a complex ($\text{Cu}(\text{NH}_3)_2^+$) in solution, which can, afterwards, react with water forming a dense cuprite layer. Continuous exposure of these samples to atmospheres with controlled humidity gave rise to the formation of copper sulfates, which precipitated from solution when the relative humidity was below the critical value. However, these authors did not investigate the effect of ammonium concentration in the corrosion rate of copper. In the present work, the corrosion of copper samples immersed in 0.5 M sulfate solutions with different concentrations of ammonium ions was investigated. For this purpose, copper samples were immersed in such solutions for different time spans, and the corrosion products were evaluated both by visual examination and by SEM/EDS, furthermore, the composition of the solution was analyzed by ICP-AES. In addition, the electrochemical behavior of the copper samples was studied by polarization curves and EIS experiments after short immersion times.

Examination of the surfaces of the samples after different immersion times in the 0.5 M sulfate solution with different concentrations of ammonium revealed that the corrosion product layer developed unevenly on the samples surface, and that the smaller the concentration of ammonium ions the sooner a thick dark layer of corrosion product was developed. SEM observations of these samples showed the development of cubic-octahedral crystals, which sizes increased as the samples surface darkened for increasing immersion time. EDS analysis also showed that the darker the region the higher the amount of oxygen in the corrosion product layer, confirming its thickening.

Anodic polarization experiments showed that increased depolarization with ammonium concentration. Results of the cathodic curves and of the EIS experiments will also be presented and discussed.

[1] K.P. FitzGerald, J. Nairn, G. Skennerton, A. Atrous *Corrosion Science* 48 (2006) 2480–2509

[2] R. E. Lobnig, R. P. Frankenthal, D. J. Siconolfi, J. D. Sinclair *J. Electrochem. Soc.*, 140(7), (1993) 1902

[3] R. E. Lobnig, R. P. Frankenthal, D. J. Siconolfi, J. D. Sinclair, M. Stratmann *J. Electrochem. Soc.* 141(11), (1994) 2935

[4] I. Odnevall and C. Leygraf *J. Electrochem. Soc.*, 142(11), (1995) 3682

Mill scale on historic wrought iron: impact on corrosion and coating performance

Nicola Emmerson, Eric Nordgren & David Watkinson, Cardiff University, Cardiff, United Kingdom

Mill scale, the oxide layer formed on the surface of iron and steel during hot rolling and forging, is well understood for modern steels but less so for ancient and historic ferrous material. Recent studies on atmospheric corrosion of historic wrought iron reinforcements in French gothic cathedrals identified surviving mill scale in corrosion layers and studied its effect on corrosion processes. Anecdotal evidence from conservators working on heritage iron also attests to the presence of mill scale and they report that it has a protective effect on the wrought iron substrate. Better understanding of the properties of mill scale will lead to improved conservation rationales and the design of evidence based procedures. Determining whether mill scale represents the original surface of corroded ironwork, if it survives only as fragmented layers and whether its presence influences corrosion rate will develop this understanding, as will determining its impact on the adhesion of protective coatings applied over it.

Surface preparation advice from coating and steel manufacturers and the use of industrial standards conflict with the experience of heritage ironworkers and conservation ethics. Removing all oxide layers to 'optimise' performance of protective coating systems inevitably leads to complete loss of the information contained therein, yet the evidence that removal of oxide layers reduces post coating corrosion rates is limited.

Work at Cardiff University aims to characterise mill scale on wrought iron and mild steel samples and assess how its removal impacts on corrosion rates and the adhesion of coatings. The morphology and composition of mill scale on 2nd century AD archaeological forged nails, mid/late 19th century rolled wrought iron bar and plate and modern mild steel samples have been investigated. Location and thickness of 'mill scale' layers and their degree of continuity have been determined using optical microscopy and SEM-EDS. X-ray diffraction has been used to characterise mill scale in the context of the corrosion profiles on un-cleaned, cleaned to mill scale, and cleaned to bright metal samples. The results give insight into the nature of mill scale on archaeological and historic wrought iron produced using differing technologies.

The corrosion behaviour of these samples is being investigated using Electrochemical impedance spectroscopy and corrosion rates derived by measuring oxygen consumption of samples sealed in controlled high relative humidity environments. Effect of mill scale retention on adhesion of coating systems to samples cleaned to mill scale and bright metal is tested using a standard hydraulic pull-off rig. The decision whether to remove or retain mill scale during a conservation process can now be made with an enhanced understanding of its impact on corrosion rate and coating performance.

Protective coatings for historic wrought iron: epoxy resins versus oil-based systems

Nicola Emmerson & David Watkinson, Cardiff University, Cardiff, United Kingdom

The heritage ironwork community is debating the practical and moral disadvantages of coating wrought iron with two-pack epoxy coating systems versus their potential for corrosion prevention. Their promotion by manufacturers as highly engineered, long-lasting 'wonder-coatings' is being called into question and weighed against the issues of cost, requirement for blasting substrates to Sa2.5 (near white metal), a relatively short pot life, reversibility challenges, and the lack of compatibility between the inflexible cured polymer and the dimensionally thermo-responsive ironwork which is reported to cause cracking of the epoxy resin at joints with resultant ingress of water. Currently absent from this discussion is empirical evidence of the impact of epoxy resin coatings on the corrosion rate of wrought iron as compared with other coating types.

A project investigating the surface treatment and protective coating of historic wrought iron is under way at Cardiff University with sponsorship from Historic Scotland. The effect of surface preparation methodology prior to coating on the corrosion rate of the uncoated substrate was reported at EUROCORR 2012. Current work aims to provide a cost benefit comparison between the use of two-pack epoxy resin coating systems and oil-based systems. This paper presents the results of corrosion rate investigations and electrochemical impedance spectroscopy (EIS) analyses of samples coated with a commonly used epoxy resin system and two household name oil-based systems.

Mid-19th century rolled plate wrought iron samples were prepared by blasting to Sa2.5 with aluminium oxide powder or by wire brushing, in accordance with the coating manufacturers' recommendations. Similarly prepared samples were contaminated with synthetic seawater (BS3900-F10:1985) to simulate wrought iron exposed to a coastal environment. All three coatings were applied as per the manufacturers' instructions.

The samples were sealed within individual glass reaction vessels containing silica gel conditioned to 90% RH. Depletion of oxygen within the vessels over 12 months was remotely recorded using a World Precision Instruments OxyMini oxygen meter to measure the quenching of fluorescence of an oxygen sensor spot attached to the wall of each vessel. Oxygen consumption of the coatings was determined using controls and subtracted from that of the coated wrought iron samples to give the corrosion rates of the metal substrates. Comparative performance of the coatings was investigated using EIS to support the real time long-term tests employing oxygen consumption.

Interpretation of the outcomes will build towards evidence based advice for contractors choosing coatings for corrosion prevention of heritage wrought iron monuments in coastal and inland contexts.

Pre-corroded electrical resistance corrosion monitors to mimic, monitor and guide the conservation of heritage iron

*James Dracott & Stuart Lyon, University of Manchester, Manchester, UK
David Watkinson & Melanie Rimmer, Cardiff University, Cardiff, UK*

Heritage iron objects are usually covered in thick corrosion layers which will alter corrosion rates and habits. Accurate monitoring of their corrosion rates is crucial for continued preventative conservation and active intervention of at risk artefacts. Measurement of storage environment corrosivity is commonplace for a variety of metals, but use un-corroded metal as a proxy. Corrosion rates measured will be different with respect to chloride infused and corroded artefacts and data recovered difficult to reconcile with actual artefact degradation.

Pre-corrosion of electrical resistance monitors has been shown to be an effective way to alter proxy measurements to a closer approximation of heritage iron corrosion rate. The methodology of creation and pre-corrosion; salt deposition by inkjet printer and subsequent controlled atmospheric corrosion of photo-chemically milled patterns; was reported at Eurocorr 2013. The methodology has since been refined further to give set levels of corrosion thickness and product. Corrosion products formed have been compared to those on recovered archaeological iron artefacts from soil contexts, using Scanning electron microscopy and Raman spectroscopy.

Rates of corrosion of the sensors have been monitored in a climate chamber over the short and medium term. Constant and fluctuating relative humidities were used to replicate storeroom and display environments and scenarios. Sensor corrosion rates, accuracy, reaction time and data reproducibility have been examined. Cumulative corrosion and changes in corrosion products after exposure to the low relative humidity environments were investigated. The results are compared to oxygen consumption rates, as a proxy for corrosion rate, of actual archaeological objects in identical conditions.

The final outcomes of the project are discussed with respect to the closeness of fit between proxy and archaeological iron corrosion rate data, benefits and shortcomings of the system and how the corrosion data affects current conservation understanding. The result of field testing at the SS. Great Britain is discussed and applications and suggested methodologies considered against the current heritage iron conservation framework. It is concluded that the technique can detect corrosion rates down to storage relative humidity levels, provides more accurate representation of corrosion rate for chloride infested iron objects than bare metal ECRM, can be calibrated to suite specific objects and could represent excellent cost-effectiveness for environmental monitoring in heritage institutions.

Corrosion products transformations during subcritical stabilization of archaeological iron artefacts

*M. Bayle, Laboratoire Archéomatériaux et Prévion de l'Altération, NIMBE/LAPA
CEA/CNRS UMR3299 CEA Saclay, 91191 Gif-sur-Yvette,
France, marine.bayle@cea.fr*

*D. Neff, Laboratoire Archéomatériaux et Prévion de l'Altération, NIMBE/LAPA
CEA/CNRS UMR3299 CEA Saclay, 91191 Gif-sur-Yvette,
France, delphine.neff@cea.fr,*

*Ph. de Viviés, A-CORROS Expertise, 23 chemin des Moines 13200 Arles, France
devivies@a-corros.fr*

*J-B. Memet, A-CORROS Expertise, 23 chemin des Moines 13200 Arles, France,
jbmemet@a-corros.fr*

*Ph. Dillmann, Laboratoire Archéomatériaux et Prévion de l'Altération, NIMBE/LAPA
CEA/CNRS UMR3299 CEA Saclay, 91191 Gif-sur-Yvette, France,
philippe.dillmann@cea.fr*

Stabilization of archaeological iron artefacts is essential to avoid the loss of the information contained on the original surface due to the transformation of the corrosion product microstructure. The nature of the corrosion phases is determined by the environmental conditions such as the oxygen rate, alkalinity and presence of chlorides during periods of burial or immersion. After excavation, these conditions are disturbed and the corrosion layers transform rapidly. Severe reactivation of the corrosion processes may also occur. Therefore, restorers carry out stabilization treatments in order to remove elements responsible of this phenomenon such as chlorides. These processes, mainly based on immersing artefacts in chemical baths also induce microstructural transformations [1]. One of these processes recently developed in the conservation field consists of pressurizing and heating an alkaline fluid (NaOH, 35 bar, 180°C) to the subcritical liquid phase. In our study we try to understand the impact of the process on the archaeological corrosion products [2].

A-CORROS Expertise has established a prototype chamber to perform several experiments on synthetic and archaeological samples. Phases commonly found on corroded archaeological artefacts have been synthetized, treated at several temperatures and pressures and then analyzed with Raman spectroscopy, X-ray diffraction and SEM-EDX. The crystalline structure of some ferric oxyhydroxides such as akaganeite (chlorinated, $\beta\text{-FeO}_{1-x}(\text{OH})_{1+x}\text{Cl}_x$), lepidocrocite ($\gamma\text{-FeOOH}$) or oxides such as ferrihydrite have transformed into hematite ($\alpha\text{-Fe}_2\text{O}_3$). For others, the nature of the phases remains the same (magnetite Fe_3O_4 , hematite, goethite $\alpha\text{-FeOOH}$) but the process modifies the crystals' morphology. The archaeological phases' reactivity during the process is compared to synthetic phases' behavior. Furthermore, cross-sections of representative sets of artefacts from several archaeological environments are analyzed before and after treatment. They are treated in the experimental chamber at various durations to follow the corrosion profile transformation steps with a specific attention to the crystals' morphology evolution during the subcritical treatment. The understanding of chemical and physical transformations of iron corrosion layers inside the sub-critical chamber could optimize the stabilization of archaeological artefacts.

1. Kergourlay, F., et al., Corros. Eng., Sci. Technol. 2010. **45**(5): p. 407-413.
2. deViviés, P., et al., METAL 2007 Proceedings: p. 26-30.

Predicting corrosion: chloride form and the response of archaeological iron to humidity

David Watkinson and Melanie Rimmer,

Department of Archaeology and Conservation, Cardiff University, CF10 3EU, United Kingdom. Watkinson@cf.ac.uk

Chloride is known to drive the corrosion of archaeological wrought iron objects and lowering its concentration in objects has been shown to decrease their corrosion rate^{1,2}. The quantity of chloride in objects is considered by most conservators to be significant for determining the rate of corrosion in any humidity. We have examined corrosion rate and chloride content of archaeological iron objects to address questions about corrosion-influencing variables and their relationships, using oxygen consumption measurements over long periods of time as a measure of corrosion.

Using a WPI OxyMini remote oxygen sensor, the individual oxygen consumption rate ($\text{mbar g}^{-1} \text{yr}^{-1}$) of 143 wrought iron nails from two archaeological sites was measured at 10% relative humidity (RH) intervals across the 20-80% range. Following this, each object was digested and its chloride concentration (ppm) determined using a specific ion meter. The data revealed that, at any given RH, chloride was a predictor of corrosion over the concentration range 200-4000 ppm but that many anomalies existed where objects of similar chloride content returned very different oxygen consumption rates. Across the RH range, each archaeological site showed a different humidity response pattern; objects from the Billingsgate medieval site did not significantly increase their oxygen consumption rate until RH exceeded 60%, whereas the Roman objects from the Caerleon site began noticeable rate increases from 30% and a rapid increase from 50% RH onwards. Although the overall slower oxygen consumption rates of Billingsgate objects could be explained by the typically lower chloride content returned from this site, this did not directly explain the different shape of the response curve across the RH range.

The hypothesis that the different responses of the two sites to humidity could be explained by two different forms in which chloride is known to occur in archaeological iron objects, $\beta\text{-FeOOH}$ and FeCl_2 , was examined experimentally. Each of these compounds is hygroscopic and is capable of corroding iron in contact with it³. Depending on the amount of chloride in archaeological iron objects and their storage environment, the occurrence and proportion of these compounds in objects will differ. $\beta\text{-FeOOH}$ was synthesised and assayed. The hydration response of $\beta\text{-FeOOH}$ powder and FeCl_2 powder was measured in a climate chamber using a balance to determine the mass of water gained as the RH was raised in 10% intervals from 20% to 80%. The outcomes of these tests are reported and there is a discussion of their potential impact on understanding corrosion patterns in archaeological iron and their impact on preservation strategies.

1. **Watkinson, D. and Rimmer, M. (2013)** *Quantifying effectiveness of chloride desalination treatments for archaeological iron using oxygen measurement.*

Metal 2013 Edinburgh, Scotland. Interim meeting of the international Council of Museums Committee for Conservation Metal Working Group, 16th -20th September 2013. (Eds.) Hislop, E., Gonzalez, V., Troalen, L. and Wilson, L., 95-102.

2. **Rimmer, M., Watkinson D. and Wang Q. (2013)** *The impact of chloride desalination on the corrosion rate of archaeological iron* . Studies in Conservation., **58** (4): 326-337
3. **Watkinson D. and Lewis M. (2005)** *Desiccated storage of chloride contaminated archaeological iron objects*. Studies in Conservation, **50**, 241-252.

Testing the Durability of Modified Corrosion Protection Systems for Iron Monuments Conservation

Martina Raedel, Michael Bucker,
BAM Federal Institute for Materials Research and Testing
Division 4.2
Richard-Willstätter-Str. 11, 12489 Berlin
Contact: martina.raedel@bam.de, scientist

The performance of anti-corrosion systems is improved and optimized constantly. Nevertheless after an indefinite time maintenance and replacement of the corrosion protection will be necessary. In a research project the performance of modern anti corrosion systems and red lead based systems, which are often used in the conservation of historic iron- and cast iron monuments, were evaluated. Additionally modified systems and a combination of systems were tested. The motivation for the project was to show alternatives for the use of red lead priming coat, a material which endangers health as well as environment.

To meet the requirements in the conservation of historic iron and cast iron monuments better, anti corrosion systems are often modified, e.g. matting agents were used to improve the adaption of new coatings by matting the surface. Another frequently applied practice is the repair of damaged coatings or the combination of modern anti corrosions systems with traditional oil based systems to improve the authentic appearance. But no examination was conducted till now concerning the influence of these adaptations to the corrosion resistance of the systems.

Besides coatings containing red lead several rust compatible systems with different anti corrosion pigments were examined. Systems for industrial were used just as systems developed especially for conservation purpose. They were investigated together with the modified systems. The coatings were applied to both historical samples and to newly prepared model samples.

The samples were underwent two different ageing procedures: artificial ageing in a climate chamber and the exhibition on at an outdoor exposure test site. Evaluation of the aged samples was carried out under the aspect of coating degradation. The degree of rusting, cracking and flaking was examined and mechanical testing procedures were performed. Furthermore analytical examinations with the Environmental Scanning Electron Microscope (ESEM) or with the Fourier-Transform infrared microscope (FT-IR) were conducted.

The results of the research with optical evaluation and the various test procedures will be presented. The two ageing methods (naturally and artificially ageing) showed different results. They will be presented together with the tests of the modified systems. The results show an at least similar eligibility of modern anti corrosion systems in comparison with red lead systems for the use in conservation.

EVALUATION OF THE CONSERVATION STATE OF METALLIC ARTEFACTS FROM THE VILLA DEI QUINTILI IN ROME

E. Angelini, S. Grassini, Dip. Scienza Applicata e Tecnologia, Politecnico di Torino, Torino, Italy

G. Galli, Soprintendenza Speciale per i Beni Archeologici di Roma, Roma, Italy

M. F. La Russa, S.A. Ruffolo, Dipartimento di Biologia, Ecologia e Scienze della Terra, Università della Calabria, Arcavacata di Rende, Italy

Several metallic artefacts, coming from the Villa dei Quintili in Rome, have been selected for investigation of their chemical composition, metallurgical features and corrosion products. The Villa dei Quintili is an archaeological site located along the Via Appia and its nucleus, belonging to the Quintili brothers Condianus and Maximus, dates back to the late Adrian age, ie the first half of the second century A.D..

Over the centuries repeated excavation campaigns have been carried in different areas of the villa, bringing to light the various building steps and allowing to find large amounts of artifacts, from ceramics to statues to metallic artefacts. In particular in the excavations of 2002-2004 and 2007-2009 a large portion of the gardens arcades, of the reception area and of some tepidarium rooms between the caldarium and the frigidarium have been discovered. The metallic artefacts under study come from these campaigns: fragments of lead plates, fragments of iron and bronze braces that were used to secure to the wall the tiles that covered the caldarium, iron nails.

The metallic artefacts have been studied by means of the combined use of scanning electron microscopy combined with energy dispersive spectrometry (SEM-EDS), X-ray diffraction (XRD), in order to identify the corrosion mechanisms that affected the various typologies of alloys in the same environment, with the ultimate goal of finding tailored conservation strategies.

The fragments of the lead-based artefacts appear in good conservation conditions, covered by a soft and adherent layer of corrosion products mainly constituted by white lead carbonate, with soil traces relatively evenly distributed over the metal surface. Contact with the soil discoloured the outer corrosion layer.

The fragment of the copper-based artefact is covered by a crust that varies in shades of blue and green, mainly constituted by copper carbonates, azurite, and malachite, overlying a powdery red compact layer. Spots of softer, pale green corrosion products are also visible in the layers.

The current appearance of the examined iron-based artefacts (pitting, cracking, discolouration, flaking) is largely the result of the formation of iron oxides, process that occurs when untreated iron is exposed to an oxygen-rich environment.

Iron oxides with different oxidation states of iron have been found in the corrosion products layer. The interior of the artefact is mainly constituted by a dark grey magnetite layer, Fe_3O_4 , surrounded by a dark brown maghemite layer ($\gamma\text{-Fe}_2\text{O}_3$), that contains minerals from the soil, and that could not match the original surface not always clearly identifiable. The outer layer of orange-brown color is less compact and more porous than the interior one and is mostly constituted by goethite ($\alpha\text{-FeOOH}$) mixed with soil components.

Atmospheric corrosion effects of air pollution on materials and cultural property in Kathmandu, Nepal

*Johan Tidblad, Swerea KIMAB, Stockholm, Sweden (johan.tidblad@swerea.se),
Kevin Hicks and Johan Kuypenstierna Stockholm Environment Institute, York, UK
Bidya Banmali Pradhan and Pradeep Dangol, ICIMOD, Kathmandu, Nepal
Iyngarasan Mylvakanam, UNEP*

Ten racks with materials (carbon steel, zinc and limestone) and passive samplers for pollutants (gaseous SO_2 , NO_2 , O_3 and HNO_3 as well as particulate matter, total mass and ions), were exposed in the Kathmandu area for one year. The results show that the rates of corrosion for iron, zinc and limestone vary considerably across the Kathmandu valley and are correlated mainly with the SO_2 concentration. The data range from 2 - 20 $\mu\text{g m}^{-3}$ (SO_2), with 5 - 13 $\mu\text{m year}^{-1}$ (limestone recession), 5 - 60 $\mu\text{m year}^{-1}$ (carbon steel corrosion) and 0,4 - 1,1 $\mu\text{m year}^{-1}$ (zinc corrosion). It was possible to obtain a tolerable SO_2 concentration for protection of cultural heritage of 5-6 $\mu\text{g m}^{-3}$ (for carbon steel, Figure 1, below) and 6-7 $\mu\text{g m}^{-3}$ (for limestone) for the Kathmandu valley based on this these data.

The paper also presents an overview of corrosion results from exposures of carbon steel, zinc, copper, limestone and paint coated steel where corrosion attack after one, two and four years of exposure was obtained from more than twenty test sites in Asia and Africa. These results obtained within the Swedish Sida funded Programme on Regional Air Pollution in Developing Countries (RAPIDC) also identify SO_2 as the main pollutant but HNO_3 is also important for zinc and limestone as is also the case for samples exposed in Europe. Absolute corrosion rates are also similar in magnitude compared to Europe with the exception of some individual sites in Asia/Africa with very high pollution levels. For some materials, especially for limestone, there is also generally higher degradation levels in Asia/Africa compared to Europe.

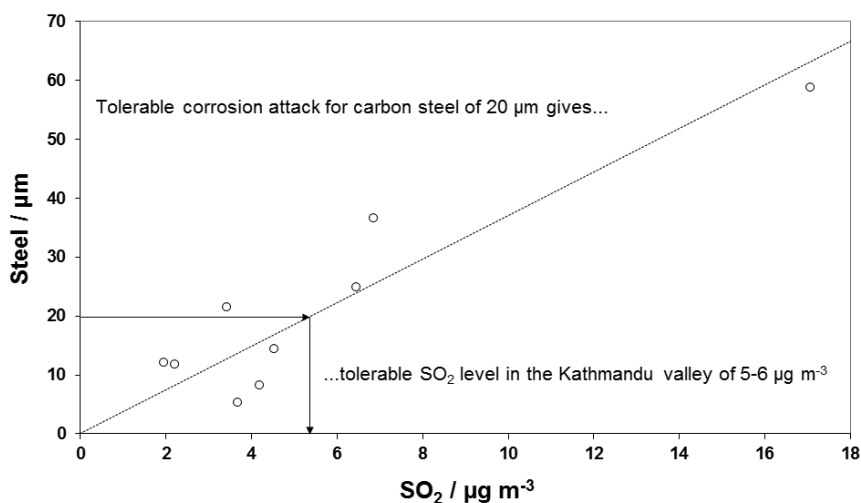


Figure 1 Carbon steel corrosion vs SO_2 concentration in Kathmandu, Nepal.

Innovative biological approaches for metal conservation

Edith Joseph^{1,2}, Paola Letardi³, Monica Albini¹, Lucrezia Comensoli¹, Wafa Kooli¹, Lidia Mathys¹, Emmanuelle Domon Beuret^{2,4}, Laura Brambilla², Christian Cevey⁴, Régis Bertholon², Pilar Junier¹, Daniel Job¹

¹Laboratory of Microbiology, Institute of Biology, University of Neuchâtel, Switzerland.

²Haute Ecole Arc Conservation-Restauration, Neuchâtel, Switzerland.

³CNR, Institute of Marine Sciences, Genova, Italy.

⁴Archaeological park and museum Laténium, Hauterive-Neuchâtel, Switzerland.

While often considered as harmful for cultural heritage, microorganisms can also be used for its safeguarding. Indeed, biotechnology has been applied with success in different domains, such as bioremediation or corrosion control. Its interest lies in the exploitation of environmental friendly processes that are close to ambient temperature and pressure and do not require toxic materials. Two research projects (BIOPATINAS and MAIA) using the capacities of microorganisms for the conservation-restoration of metal artistic and archaeological objects are presented in this study. Both research projects combine innovative aspects in biogeochemistry of microorganisms and conservation science.

The objective of the BIOPATINAS project is to propose an alternative biological treatment for copper alloys artefacts. Taking advantage of unique properties of carefully selected fungal strains, the project relies on the conversion of existing corrosion patinas into more stable copper oxalates. In fact, thanks to their insolubility and stability (even under acidic conditions), copper oxalates could provide long-term stabilization to the treated objects and low aesthetical alteration. After initial successful attempts (FP6-EU-ARTECH, 2004-2009 and FP7-BAHAMAS, 2010-2012), the efficacy of the fungal treatment is now improved on naturally corroded samples and validated on real case studies such as outdoor sculptures and archaeological objects. The results of the ageing procedures suggested a different weathering behaviour of the biopatina compared to standard treatments such as waxes or inhibitors. A specifically designed delivery system is also developed. Based on the outcome of this study, a prototype could be proposed and further developed as a user-friendly commercially available kit dedicated to conservator-restorers. In parallel, a complementary research work aims at proof-testing aesthetical fungal patinas for art and architecture.

In the MAIA project, the unique capacities of some fungi and bacteria are studied for the stabilization of archaeological iron. To this purpose, three different strategies are adopted either leading to the formation of stable iron compounds of low molar volume or using chloride-translocation properties. Based on the results achieved, a synergetic microbial consortium will be designed for the formation of stable iron compounds and the simultaneously removal of chloride ions that are the instigators of further corrosion after excavation. A careful assessment of the methodology is currently carried out over iron- and chloride-rich phases and preliminary results will be discussed here.

Acknowledgements

The MAIA project was supported by the Swiss National Science Foundation Ambizione grant PZ00P2_142514, 2013-2015. The Biopatina project was supported by the Commission for Technology and Innovation CTI (grant agreement n° 14573.2 PFLS-LS, 2013-2014) and the Gebert Rûf Stiftung (grant agreement n° GRS 054/12, 2013-2016). Transnational access time to the experimental marine station of the CNR-ISMAR was supported by the European Union Seventh Framework Programme (FP7/2007-2013) under grant agreement n° 262584, JERICO (2013-2015).

Insoluble decanoate salts as anticorrosion additives in acrylate varnish

Stoulil J., Nikendey V., Institute of Chemical Technology, Prague/Czech Republic

This work deals with an use of insoluble decanoate salts (Ca, Mg, Zn) as anticorrosion additives in acrylate varnish (Paraloid B72). Solubilities were estimated by atomic absorption spectroscopy. Their influence on corrosion of carbon steel was studied in salt extracts in artificial rain water and solution of sodium sulfate by means of impedance spectroscopy. A migration of cations and anions on the surface was observed by means of infrared spectroscopy and SEM/EDS on samples exposed in condensation chamber. Real influence on corrosion performance of painted coupons was tested on scribed samples in condensation chamber.

Protection of patinas on various bronzes by different types of inhibitors

Tadeja Kosec^a, Katarina Marušić^b, Polonca Ropret^{c,d}, Helena Otmačić Ćurković^b

^aSlovenian National Building and Civil Engineering Institute, Dimičeva 12, Si-1000 Ljubljana, e-mail: tadeja.kosec@zaq.si

^bFaculty of Chemical Engineering and Technology, University of Zagreb, Savska cesta 16, 10000 Zagreb, Croatia

^cConservation Centre, Institute for the Protection of the Cultural Heritage of Slovenia, Poljanska 40, 1000 Ljubljana, Slovenia

^dMuseum Conservation Institute, Smithsonian Institution, 4210 Silver Hill Rd., Suitland, MD 20746

Numerous cultural and historical artefacts are made of bronze. In humid air, bronze is spontaneously covered by oxide films, called patina. However, in urban atmospheres the aggressive air species concentrate in acid rain which dissolves patina and the bronze itself. This leads to enhanced deterioration of bronze artefacts and formation of secondary corrosion product.

In protection of historical and cultural artefacts, only methods that do not change the visual appearance of the artefact itself can be applied. Such methods include protection of bare metal as well as the patina covering it. One of the possible methods is the use of corrosion inhibitors. Recent research has shown that imidazole based inhibitors can be successfully used to protect patinated bronze.

Aim of this study is to investigate the use of imidazole and benzotriazole type inhibitors (TMI, BTAH) in protection of different types of bronzes, namely CuSnZn bronze, CuSnZnPb bronze and CuSnSi bronze. Bronzes that will be studied, will be bare or covered by two types of patinas: sulphide brown type of patina and electrochemically formed patina that simulates naturally formed patina on bronze exposed to atmosphere.

Morphology and structure of the patinas will be determined using SEM/EDX and Raman spectroscopy. Then both chemical and electrochemical patina will be studied in environments that simulate urban environments.

The protection properties of corrosion inhibitors will be studied on different bronzes and on differently patinated bronze samples by the use of electrochemical techniques, such as potentiodynamic measurements and electrochemical impedance spectroscopy in simulated urban rain. SEM /EDX analysis as well as Raman spectroscopy will be used to evaluate the differently formed patinas before and after the electrochemical experiments. The combination of electrochemical and spectroscopic techniques will enable the study of inhibition mechanisms and inhibition efficiency of the chosen protection method.

Plasma deposited DLC coatings for the conservation of bronze artefacts

E. Angelini¹, D. Caschera², F. Faraldi¹, S. Grassini¹, G.M. Ingo²

¹*Dipartimento di Scienza Applicata e Tecnologia, Politecnico di Torino, Italy*

²*Istituto per lo Studio dei Materiali Nanostrutturati - CNR, Area della Ricerca di Montelibretti, Roma, Italy*

Bronze artefacts are affected by dangerous post-burial corrosion phenomena, such as “bronze disease”, that, gradually, cause the complete mineralization of the metallic bulk. It has been investigated that the chloride ions (Cl⁻) are the main corrosion agents responsible of bronze artefact corrosion since they form cuprous chloride (CuCl) at the interface between the *patina* and the surviving metal. The exposure of the reactive cuprous chloride to the atmosphere gives rise to cyclical dissolution reactions of the copper substrate.

The study of innovative materials and strategies to preserve bronze artefacts is, therefore, very important to ensure the chemical-physical long-lasting stability of ancient objects. The development of innovative protective coatings able to avoid the interaction between the metallic surface and the surrounding environment, without altering the chemical composition and the aesthetical appearance of the artefact, is a valid solution to preserve ancient objects from further corrosion.

In this contest, plasma enhanced chemical vapour deposition (PECVD) is a very promising environmentally friendly process for the deposition of a variety of amorphous and nano-structured thin films, such as SiO₂-like films, that have been already successfully investigated for the conservation of ancient silver and bronze artefacts.

The purpose of this study is, therefore, to investigate the barrier properties of Diamond-like carbon (DLC) coating deposited by PECVD on Cu-based reference alloys, whose metallurgical features and chemical composition is very similar to those of ancient alloys.

DLC coatings have been deposited in a RF capacitively coupled reactor, in plasma fed with different CH₄/H₂ flow ratios at a total working pressure of 10⁻¹ mbar and by applying 50W of input power. The deposition experiments have been carried out at a temperature of 300 K by placing the substrates either on the electrically powered electrode (cathodic mode) or on the grounded electrode (anodic mode) in order to assess the effect of the substrate ion bombardment on the coating microstructure.

The chemical and morphological characterization of DLC coatings was performed by Raman Spectroscopy, X-ray photoelectron Spectroscopy (XPS), optical electron microscopy and colorimetric measurements. The protective effectiveness of the DLC layers has been investigated by means of Electrochemical Impedance Spectroscopy (EIS) performed in 0.1M NaCl aerated solution.

Furthermore, a set of Cu-based reference samples coated with DLC films has been submitted to an accelerated ageing procedure in order to simulate the coatings behaviour in real exposure conditions.

Self-Assembling Monolayers of Organic Acids for Protection of Bronze from Polluted Urban Atmospheres

*Katarina Marušić, Natalija Devetak, Sanja Špoljarić, Helena Otmačić Ćurković
University of Zagreb, Faculty of Chemical Engineering and Technology,
Marulićev trg 19, 10000 Zagreb, Croatia*

Cultural heritage made of bronze can be found exhibited in cities all around the world. Such artefacts, after long-term exposure to air and humidity, form a thin film of corrosion products with a characteristic greenish colour, called patina. Patina protects the substrate bronze, but also enhances its beauty. Such works of art are exposed to the aggressive effect of polluted urban environments. Different ways of treating and protecting both bronze and its patina are common: coatings, mainly waxes and varnishes, and corrosion inhibitors. Since protection is applied to artefacts that are cultural heritage and exposed in urban outdoors it is expected for the protection to have additional characteristics beside corrosion inhibition: it should not change the aesthetics of the work of art, as colour or surface structure, it should be easy to apply and it should not be harmful for the restaurateur.

This is the reason why application of self-assembling monolayers of organic acids is interesting in this field of application. Organic acids are not harmful, a monolayer on the metal's surface cannot be seen with bare eyes and the fact that these molecules are self-assembled by pure exposure of the bronze artefact to the solution containing molecules with self-assembling properties makes it easier to apply than any other protection.

Two types of organic acids are investigated for protection of CuSn6 bronze and its patina: stearic and palmitic acid. They are both dissolved in ethanol and bronze is exposed to the solution.

The corrosion inhibition efficiency is investigated by electrochemical methods (potentiodynamic polarization and electrochemical impedance spectroscopy) in a solution simulating urban atmospheres. Different concentrations are investigated on bare bronze and the optimal concentrations are applied for patinated bronze. The corrosion products of both bare and patinated bronze exposed to the corrosion test solution are investigated by SEM and EDX.

Soil- induced Corrosion of Ancient Roman Brass: a case study

O. Papadopoulos*, P. Vassiliou*, V. Gouda[^], F. Faraldi[°], S. Grassini[°], E. Angelini[°]

*Lab. Physical Chemistry, School of Chem. Engineering, NTUA, Athens, Greece
[^] National Research Centre, Cairo, Egypt

[°]Dipartimento di Scienza Applicata e Tecnologia, Politecnico di Torino, Italy

*e-mail: olpap@central.ntua.gr

This work focuses on the results of solid state processes occurred on a naturally corroded copper-based metal fragment, which dates back to the Roman period, after a detailed, systematic examination and chemical analysis of its surface and cross-section. The original artefact was recovered from burial during technical works at the riverbed of Tiber and was of unknown chemical composition and origin.

The characterization of metallurgical characteristics and corrosion processes was performed by a combination of XRF and SEM-EDS analyses, derivative calculations and OM observation of the corrosion stratification under polarized light. The findings were critically discussed after literature review [1-4].

The fragment was identified as leaded brass (Cu 84.4, Zn 12.7, Pb 2.2, Fe 0.7 wt %). The study of the heterogeneous multi-layer corrosion depositions testified that the artefact has undergone a sequence of corrosion cycles. During the first period of burial the formation of corrosion layers was under the control of slow dealloying processes (Zn and Cu migration). At a second stage the artefact has undergone more severe attack from corrosion agents and the corrosion reactions were controlled by anions moving inwards. The gradual mineralization of the insoluble surface corrosion products created a protective crust which stabilized the metal, preventing total metal dissolution. Metallographic observations of the remaining metal substrate provided interesting information about the manufacturing history of the ancient brass as well.

The chloride content in the patina was detected locally and at limited concentrations. Thus there were no indications of active 'bronze disease' and that explains the good preservation condition of the ancient fragment.

References

- [1] Oudbashi O., Emami S.M., Ahmadi H. Davami P, *Heritage Science*, 1-21, 2013
- [2] Ingo G.M., Bustamante A., Alva W., Angelini E., Cesareo R., Gigante E., et. al., *Applied Physics A: Materials Science and Processing*, 113 (4) , 877-887, 2013
- [3] Riccucci, C., Ingo, G.M., Faustoferri, A., Pierigè, M.I., Parisi, E.I., Di Carlo, G., De Caro, T., Faraldi, F., *Applied Physics A: Materials Science and Processing*. 113 (4) , 959-970, 2013
- [4] Faraldi, F., Çilingiröglu, A., Angelini, E., Riccucci, C. DeCaro T., Batmaz A., Mezzo A., Caschera D. Cortese B., *Applied Physics A: Materials Science and Processing*, 113 (4) , 911-921, 2013

Corrosion of sheet piling in the soil: results of a literature review and practical research

ing. P. Kraaijenbrink, dr.ir. G.A.M. van Meurs, dr.ir. S. Jansen and dr.ir. H. Senhorst

Sheet piling, made of steel, is frequently used in the Netherlands as measure to strengthen dikes whenever space is not available for strengthening dikes by putting a layer of soil at the inner side of the dike. During exposure to soil, corrosion occurs and the thickness, as well as the mechanical strength, of the sheet reduces. Corrosion surcharge is applied to compensate this reduction. Corrosion surcharge not only increases the thickness, it also increases the costs of the material. Responsible reduction of corrosion surcharge can lower the costs (significantly) while water safety is maintained.

To come to a responsible corrosion surcharge, data for sheet pile corrosion in soil was collected both by a literature survey as well as by practical research. We studied the effect of exposure time and soil conditions. Both literature and practical data demonstrate that the position of the groundwater level and the degree of disturbance of the soil, are the most determining factors for the rate of corrosion: in undisturbed soil and below groundwater level, corrosion rates are lowest. With increasing exposure time, corrosion rates decrease. The results show that corrosion surcharge could be reduced to a few millimetres. The costs for strengthening can now responsibly be reduced substantially; in the area of only one of the Water Authorities with about 5 to 10 million euros.

Effects of *Juniperus communis* leaves extracts on tin bronze corrosion

Refka BEN CHANNOUF^{1,2}, Nébil SOUISSI^{1,2}, Sandrine ZANNA³, Helene ARDELEAN³, Nizar BELLAKHAL², Philippe MARCUS³

1- *Tunis El Manar University, Institut Préparatoire aux Etudes d'Ingénieur d'El Manar, BP 244, 2092 El Manar II – Tunisia*

2- *Carthage University, Institut National des Sciences Appliquées et de Technologie, Unité de Recherche « catalyse, électrochimie, nanomatériaux et leurs application et didactique (CENAD) », BP 676, 1080 Tunis Cedex, Tunisia.*

3- *Ecole Nationale Supérieure de Chimie de Paris, Laboratoire de Physico-Chimie des Surfaces (LPCS), 11 rue Pierre et Marie Curie, F-75005 Paris, France.*

This work aims the investigation of the effects of a *Juniperus communis* leaves (JC) methanolic extract on the interfacial behaviour of a Cu₁₀Sn modern bronze analogous to a punic material. Polarization curves and X-Ray Photoelectron Spectroscopy (XPS) were used in order to understand the alloy corrosion behaviour in aqueous 0.5M chloride medium without and with the extract addition.

The I-E curves obtained when the bronze was immersed in the corrosive medium showed that the anodic current decreased in the entire potential domain explored whereas the cathodic curve shape was almost unchanged when the JC extract added. When analysing the electrochemical parameters obtained in the Tafel field it was concluded that the extract affected both anodic and cathodic reactions.

XPS semi quantitative characterization revealed that the cationic composition at the material surface when submitted to the aggressive medium was 97.9%, 1.8% and 0.3% respectively for Cu(I), Sn(II) and Sn(IV). Furthermore, the bronze surface composition was 7.2%, 24.9% and 67.9% respectively for Sn(II), Cu(I) and Cu(II) when the JC extract was added.

The decuprification factor f_{Cu} was -1 and 0.23 respectively without and with the plant addition. The JC methanolic extract was concluded inhibiting tin oxidation and promoting Cu(I) transformation.

Pollutant permeability in acrylate varnishes

Švadlena J., Stoulil J., Institute of Chemical Technology, Prague/Czech Republic;
presenting author underlined

This work compares permeability of pollutants (H_2O , H_2S , SO_2 , NO_x , NH_3 and acetic acid) in two acrylate varnishes (Paraloid B72 and B48N). Water permeability was estimated in liquid water by means of impedance spectroscopy at constant frequency. In vapour water was estimated only diffusion coefficient by means of resistometry (time to change of corrosion rate after water vapour permeation). Difference in effect of permeation of other gaseous pollutants was estimated directly by resistometry (corrosion rate under varnish after pollutant permeation). Permeability is the same in both varnishes for H_2S , SO_2 , NH_3 and acetic acid. B72 is less permeable for water, while B48N is significantly less permeable for NO_x .

Corrosion of cans in collections: the case study of Burghalde museum

Laura Brambilla¹, Stefano Mischler², Laurence Nicolay³, Rudolf Schmitt³, Christine Von Arx⁴, Isabelle Böhmler⁴ and Régis Bertholon¹

¹Haute Ecole Arc Conservation-Restauration, Neuchâtel, Switzerland.

²Tribology and Interface Chemistry Group, EPFL, Lausanne, Switzerland.

³Institute of Life Technology, HES-SO, Sion, Switzerland.

⁴Burghalde Museum, Lenzburg, Switzerland.

Cultural heritage consists in artworks (painting, sculpture...) but also in usual and everyday objects (tools, machines...) sometimes unexpected, such as food preserves. Nowadays, cans are represented in several museum collections as witnesses of different time periods and significances: from industrial evolution to food habits. They are also present in modern and contemporary artworks, such the ones of Daniel Spoerri and Ben Vautier.

The conservation of those objects, however, is particularly problematic. In fact, severe corrosion phenomena occur due to interaction with environment as well as between the organic content and the metallic sealer. The interventions of conservation restoration should be carried out taking into account both the material conservation and the immaterial values of the objects.

The Hero group, founded in 1886 in Lenzburg, Switzerland, is an international company producing consumer food. The production of canned food is one of its selling points since the beginning. In 2010 the Hero company offered to the Lenzburg's municipal museum (museum Burghalde) its whole cans collection. This includes a can sealed the first day of large scale production (1896) and still filled its original content. The Hero cans collection has been exposed for more than two years in the framework of the exhibition entitled "Hero – seit 1886 in aller Munde". However, the exhibition conditions and other factors damaged, sometime in an irreparable way, some cans.

In this work are presented preliminary results of a three-years project about preservation of cans in museum collections supported by the Swiss National Foundation for Scientific Research. In particular first analysis on cans from the Hero collections will be pointed out.

The goals of these preliminary studies were to define and suggest the best preservation condition for cans with their original content and to understand corrosion phenomena on selected cans from Hero collection. This first approach to face such complex objects allowed to point out the difficulties and to establish the bases for defining criteria for the choice of intervention methodologies or preventive conservation strategies.

CANS – Conservation of cAns in collectionNS project is supported by the Swiss National Science Foundation under grant CR12I1_152946/1.

Investigation into the impact of lithium additions on the corrosion response of Al-Cu alloys for Aerospace Applications

David .M. Carrick,

Department of Materials, Loughborough University, United Kingdom

Simon .C. Hogg,

Department of Materials, Loughborough University, United Kingdom

Geoffrey .D. Wilcox,

Department of Materials, Loughborough University, United Kingdom

Lithium is one of only a small number of elements that, when alloyed with aluminium, will simultaneously increase its elastic modulus but also a reduction in density. Additions of 1 % can offer as much as a 6 % increase in elastic modulus and a 3 % reduction in density. Lithium has, however, been linked to reduced corrosion resistance. Li-containing Al alloys are becoming more widespread within aerospace applications, with the Airbus A380 being the first commercial airliner to utilise Al-Cu-Li alloys within its airframe. In addition, Al-Li alloys will also be used within the fuselage of the next generation of civil airliners. As such an understanding of their corrosion behaviour is critical to ensure safe operation over many years of service.

This paper compares the microstructure and corrosion behaviour of the lithium containing AA2099-T8E77 (Al-Cu-Li) alloy with a commercial AA2024-T3 alloy (Al-Cu). Immersion testing and anodic polarisation have been conducted in a 3.5 wt.% NaCl electrolyte. Samples atmospherically exposed for up to 12 months have also been examined using XPS and FEGSEM to observe any differences in corrosion response between the two alloys. Detailed alloy characterisation was conducted prior to corrosion analysis using FEGSEM and FEGTEM together with EBSD and EDS analysis. Localised corrosion was also investigated using FEGSEM and FEGTEM techniques.

Microstructural characterisation revealed a significant difference in grain size between the Al-Cu-Li and Al-Cu alloys with the latter having a relatively fine homogeneous grain structure whilst large recrystallised grains were present within the AA2099-T8E77 alloy. FEGTEM Characterisation of both alloys showed discontinuous Cu rich films on grain boundaries; however, the population of these films was much greater in the Li containing AA2099-T8E77 alloy. Immersion testing revealed that AA2099-T8E77 had more active phases present, with sub-micron pits initiating. FEGTEM revealed these sites to be active T_1 (Al_2CuLi) phase particles. Cross-sectioning of anodically polarised samples showed on average pit depths of 80 to 100 μm on AA2099-T8E77, compared with 60 to 70 μm on AA2024-T3. Both alloys showed evidence of intergranular corrosion, however, it was more pronounced on AA2024-T3, suggesting that microstructure plays an important role in the development of pitting and intergranular corrosion. For atmospherically exposed samples the corrosion product that built up on the surface of both alloys is substantially different in composition to that present on electrochemically tested specimens, with elements such as Cl, S, Si and P being present. With regards to the atmospheric corrosion response, both alloys show evidence of intergranular corrosion, however, limited pitting corrosion has been observed to date.

Effect of microstructure on the corrosion resistance of AA2524-T3 and AA2198 T-851 aluminum alloys used in the aeronautic industry

Aline Fatima Silva Santos¹, Silvana Zacarelli¹, Sidnei Ramis de Araujo², Maysa Terada¹, Isolda Costa¹

¹ IPEN/CNEN-SP, Av. Prof. Lineu Prestes, 2242, São Paulo, SP, CEP 05508-000, Brazil., ² Centro Nacional de Pesquisa em Energia e Materiais, LNLS, Rua Giuseppe Maximo Scolfaro, 10000, Campinas, SP, CEP 13083-970, Brazil.

New types of 2XXX alloys have been developed in the last years to attain better corrosion resistance performance besides weight and cost saving benefits. Among these alloys, there are the AA 2524 that contains lower amounts of alloying elements comparatively to the AA2024 alloy, and the AA 2198, an Al-Li alloy of third generation. The microstructure of the alloy, mainly the presence of intermetallic precipitates, is dependent on its chemical composition and strongly affects the localized corrosion resistance of the material in the presence of chloride ions. In this investigation the effect of intermetallic precipitates on the corrosion resistance of the AA 2524-T3 and the AA2198-T851 alloys has been investigated. The microstructure of the aluminum alloys surface was analyzed by Field Emission Gun (FEG) scanning electron microscopy (SEM) and X-ray energy dispersive analysis (EDX). The samples were immersed in the electrolyte for various periods and then removed and analyzed by FEG-SEM-EDX. The electrochemical behavior of the aluminum was monitored by electrochemical impedance spectroscopy as a function of time in a 0.01 mol L⁻¹ sodium chloride solution. The electrochemical results were compared with those of the AA2024-T3 alloy. Similarly to this last alloy, the localized attack on the AA2524-T3 alloy starts at the Al-Cu-Mg small precipitates since the first hours of immersion leading to the removal of a large number of this type of intermetallics and to impedance increase due to surface "cleanliness". Subsequently, the selective attack of the Al-Fe-Mn occurred leading to crevice conditions mainly at the interface intermetallic precipitate – aluminum alloy matrix. Localized attack occurred at the surface of the AA2198-T851 alloy since the first hours of immersion and the pits showed a dynamic behavior, consisting of repassivation and reactivation along the period of immersion. Relatively to the AA2524-T3 alloy, the electrochemical behavior of the AA2198-T851 alloy was more stable along the immersion test period. Comparatively to the AA2024-T3, both tested alloys, AA 2524-T3 and AA2198-T851, showed superior localized corrosion resistance.

Corrosion resistance of Direct Metal Laser Sintering (DMLS) AlSiMg alloys

M.Cabrini, S.Lorenzi, T.Pastore, University of Bergamo (Dalmine, BG) Italy
D.Manfredi, Center for Space Human Robotics @Polito, Istituto Italiano di
Tecnologia, Corso Trento, 21, 10129 Torino
S.Biamino, P.Fino, C.Badini, Politecnico di Torino, Italy

Abstract

Direct Metal Laser Sintering (DMLS) is an additive manufacturing technology for the fabrication of near net-shape parts by melting together different layers of metal powders. Significant business benefits could be obtained by using DMLS production techniques: time and cost savings in terms of tooling time, virtually unlimited geometric complexities, advanced design, and reduced scrap production with respect to traditional manufacturing processes. Unfortunately, the surface finishing obtained with DMLS technique is generally worst as compared to conventional manufacturing. The macrostructure is characterized by the presence of porosities which may affect the mechanical, chemical and functional properties (1). In the last years Manfredi et al. (2) studied and optimized the process parameters for AlSi10Mg alloy. The main objective was the manufacturing of prototypes characterized by higher hardness and strength than conventional and high pressure casted AlSi10Mg alloy. The DMLS components showed, in fact, a very fine microstructure and distribution of the Si phase in aluminium due to the rapid cooling and solidification, and probably the presence of Mg_2Si .

The paper is oriented to evaluate the influence of DMLS on the corrosion resistance of the AlSi10Mg alloy. Three different surface conditions were considered: as received, after blasting and after alumina polishing. Free corrosion potential monitoring, potentiodynamic, electrochemical impedance spectroscopy (EIS) tests were performed in aerated diluted Harrison solution. Weight loss tests were also carried out for comparison. The results evidenced the role of porosities on localised attacks initiation (figure 1a). The highest susceptibility to pitting initiation was evidenced for the specimens in as received condition. The specimens obtained after alumina-polishing showed the lowest susceptibility. The morphology of localised corrosion showed selective attack of the aluminium matrix in the interdendritic second phase precipitates (figure 1b).

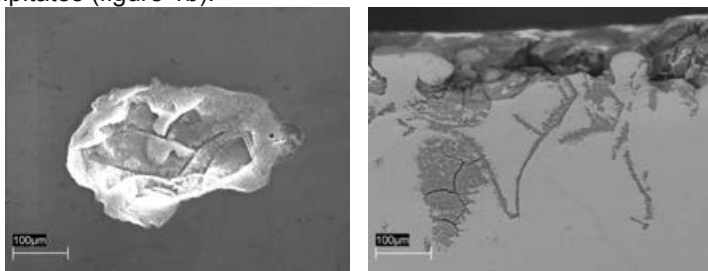


Fig.1: a) localised attack on potentiodynamic test on polished specimen, b) selective corrosion after 15 days of exposures in dilute Harrison solution

References

- (1) Y.Sun et al. (2013) *Journal of Mat. Eng. and Perfor.*, published on line
- (2) D.Manfredi et al. (2013) *La metallurgia italiana*, 105 (10), 15-24.

Effect of Deicing Compounds on Aircraft Materials

Astrid Bjørgum, Ann-Karin Kvernbråten, Anne Støre, SINTEF Materials Chemistry, Norway and Tor Arne Gustavsen, Per Ivar Lohne, and Geir Willy Karlsen, Royal Norwegian Air Force, Norway

Safe operation of airfields in Norway demands deicing of runways during the winter time. In addition to removing snow and ice mechanically, chemical deicing is needed. Traditionally, solid urea has been used as an effective deicer. Due to environmental problems replacement of urea is required. However, the experience with new, more environmental friendly runway deicers clearly shows that acetate- and formiate based chemicals result in corrosion of cadmium plated steel and catalytic oxidation of carbon-carbon brakes. Thus, this investigation was undertaken to evaluate the effect of deicing chemicals on materials used in existing and new aircrafts.

The effect of urea, potassium formiate based Aviform L50, potassium acetate based Clearway 1, and mixtures of urea and Aviform L50 on corrosion of Cd plated AISI 4130 and DC04 steel samples have been investigated according to AIR6130. The results showed generally minor weight changes. Several tests gave weight increases, particularly exposure in as received Clearway 1 and in a urea/Aviform L50 mixture. Weight increases are due to insoluble corrosion products settled on the Cd plated surface during exposure. Generally, an etched surface appearance and micropitting were seen by visual examination of exposed samples had. Figure 2 shows that weight loss of samples exposed in diluted Aviform L50 were above 0.3 g/cm² which according ti AIR6130 is the limit for undesirable corrosion for aircrafts and airport equipment. By assuming uniform corrosion of the Cd coating this corresponds to corrosion rates of 10 – 12 µm/yr, indicating that the entire Cd coating may corrode within one year exposure in the applied test conditions. SEM investigations showed that the coating still covered the steel surfaces after two weeks testing.

The effect of the same deicers on oxidation of carbon-carbon brakes was investigated in accordance to AIR5567. As shown in Figure 1, exposure in Aviform L50 and Clearway 1 deicing solutions gave a significant increase in oxidation weight loss. The result confirms the catalytic effect of potassium formiate and potassium acetate based deicers on oxidation experienced for carbon-carbon brakes. Exposure in the urea/Aviform L50 mixture also showed a catalytic effect while exposure in urea alone resulted in oxidation weight loss comparable to unexposed reference samples.

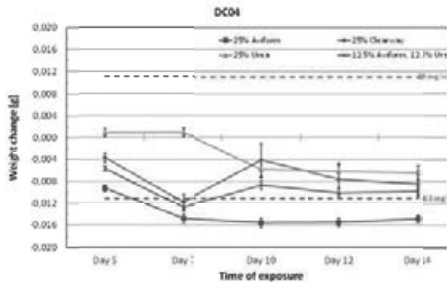


Figure 2. Weight change for Cd plated DC04 samples in 25 weight% deicing solutions tested in accordance to AIR6130. Stippled lines are test limits ($\pm 0.3 \text{ mg/dm}^2$) for undesirable corrosion.

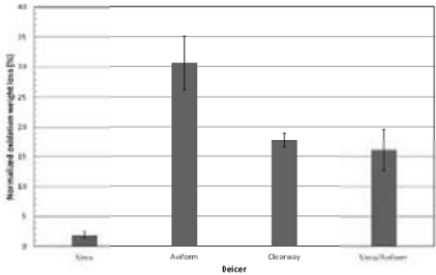


Figure 1. Oxidation weight loss of carbon-carbonbrake samples in 25 weight% deicing solutions tested in accordance to AIR5567.

Surface treatments in space environment

Asensio Zapata, AIRBUS DEFENCE&SPACE, Toulouse-France

Abstract

Space environment far from being soft, quiet and friendly (regarding materials) is aggressive and could provoke failures on spacecraft's and/or degradation of the performances of the instruments and equipment's.

The surface treatments in space environment have to be characterised and evaluated to ensure the compliance with mission requirements.

Accelerated test to simulate the effect of 15 years mission under aggressive factors presents in space environment like radiation (solar particles, high-energy electrons, protons, ultraviolet radiation, like atomic oxygen, the effect of vacuum and the high and violent temperature variations as well as vibrations, electrostatic discharge and space debris, have to be done to characterise the surface treatments in space environment.

The evaluation of main properties of a surface treatment used as general purpose layer or as functional layer (corrosion resistance, thermo optical properties, electrical properties, adhesion, layer structure...) at T0 (fresh layer) and the comparison with values obtained at T11 (after accelerated ageing when submitted to test campaign) is the key to verify the adequacy of the surface treatment with the mission profile.

This presentation is showing the main aggressive factors in space environment, the potential effects on spacecraft's (materials and processes) and how the industrials lead with accelerated test to simulate this unfriendly environment and evaluate the potential degradation of the performances of the surface treatments used in spacecraft's.

Asensio Zapata

Materials and Processes –Surface Treatment Expert

E-mail: asensio.zapata@astrium.eads.net

Phone: +33(0)5 62 19 75 51

Mobile: +33(0)6 77 92 10 84

AIRBUS DEFENCE&SPACE

31,rue des Cosmonautes – Z.I. du Palays- 31402 Toulouse (France):

Complex oxide morphologies by potentiodynamic anodizing of aluminium

M. van Put ¹, O. Elisseeva ², J. de Kok ², S.T. Abrahami ^{1,3}
J.M.C Mol, ¹ H. Terry ^{3,4}

¹ Delft University of Technology, Delft, The Netherlands

² Fokker Aerostructures BV, Papendrecht, The Netherlands

³ Materials innovation institute (M2i), Delft, The Netherlands

⁴ Vrije Universiteit Brussel, Brussels, Belgium

The aerospace industry progressively develops alternatives for chromic acid anodizing (CAA), since Cr^{6+} is known to be toxic and carcinogenic. In this work, anodizing of AA1050 and AA2024-T3 clad was performed in phosphoric sulfuric acid (PSA) and sulfuric acid (SAA) solutions. The electrochemical response and porous film growth was studied under potentiodynamic anodizing conditions. It was found that pore, cell and barrier layer dimensions are dependent on the anodizing voltage. Coarse morphologies were developed at higher voltages, and fine morphologies at low voltages. By changing the voltage during the process, differences in morphology were developed across the film thickness. However, the relation between voltage and pore morphology was not always linear for fast voltage changes, and less pronounced for decreasing voltages than increasing voltages due to recovery effects. Moreover, for prolonged anodizing in PSA, coarsening of the upper film part was observed, due to the high solubility of Al_2O_3 in phosphoric acid. The anodic oxide formation efficiency was therefore higher for SAA than for PSA.

Application of surface wetness sensors for the evaluation of corrosivity of the atmosphere to aerospace aluminium alloys

Startsev O.V., Medvedev I.M.

Gelendzhik climatic testing center (GCTC VIAM), Gelendzhik, Russia

One of the most important factors responsible for corrosion of aerospace aluminium alloys in the maritime atmosphere is the surface moisture. To monitor the surface moisture, the time of wetness according to ISO 9223, GOST 9.039 and Davis leaf wetness sensor were continuously measured for 5 years. Additionally, the chloride deposition rate and the corrosion rates of 1163 aerospace aluminium alloy and technically pure A5M aluminium were measured. Exposure was conducted at Akimov Gelendzhik climatic testing center; a branch of All-Russian scientific research institute of aviation materials. A disagreement in time of wetness estimated using ISO 9923 and GOST 9.039 methodology and the Davis leaf wetness sensor was shown. To improve estimation of the Davis leaf wetness, the dew point methodology was applied. It was shown that the dew point is a better way to predict the Davis leaf wetness. Additionally, long-time degradation of the leaf wetness sensors exposed to the marine atmosphere was investigated and it was shown that the exposed sensors are less sensitive to the changes in surface moisture. The promising technology is self-powered wireless data acquisition systems that collect environmental data (temperature, relative humidity and time of wetness) and can be placed in locations, which are difficult to access for inspection.

Choosing a Corrosion Prevention Compound Surface Science Helping to Preserve Aeronautical Equipment

Dr. Christine Bilke-Krause^{1*}, Dr. Christopher Rulison²

¹ Krüss GmbH, Borsteler Chaussee 85, 22453 Hamburg, Germany

² Augustine Scientific, 12300 Kinsman Road, Newbury, Ohio, USA

* corresponding author: C.Bilke-Krause@kruss.de, phone: 0049 40 51440136

Corrosion prevention compounds (commonly referred to as CPC's) are low viscosity, oily liquids commonly sprayed onto metal structures to slow corrosion. They are designed to prevent water, and therefore the reactions which it facilitates, from getting to metal surfaces in large quantities. CPC's have a variety of chemistries, and on boldly exposed and freshly produced surfaces they are largely effective. However, the ability of CPC's to penetrate into secluded regions of complex structures varies fairly substantially from supplier to supplier and compound to compound. One of the largest areas of concern is "lap" joints. As the name implies, these are joints are formed by overlapping metal, such that there is effectively a capillary between two pieces of metal. Several such joints exist on a standard airplane body, and we have investigated the abilities of CPC's to penetrate these joints in particular. The most demanding situation for a CPC is when the joint is already formed and somewhat corroded, and the application of the CPC is intended to prevent further corrosion.

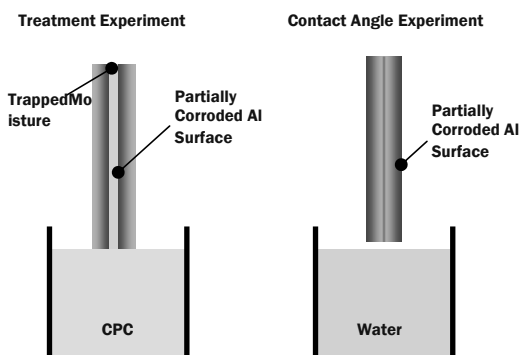
In the first part of this talk we illustrate the optical sessile drop technique. Samples of a separated lap joint with minor corrosion inside the joint were tested for surface energy and surface polarity (fraction of the overall surface energy which is made up of polar component). This was done according to the Fowkes method based on the measured contact angle with test liquids on partially corroded aluminum lap joint and on freshly formed and pre-treated aluminum stock. In the second part of talk we illustrate the influence of surface tension and the measuring technique of Wilhelmy plate and pendant drop technique. We measured the surface tensions of these samples, and also measured their contact angles on poly(tetrafluoroethylene) PTFE used to characterize the aluminum samples. All of the CPC's show much lower surface tensions than the surface energy of the corroded aluminum from the joint – so one would think the wetting would be very favorable if the joint was dry and exposed. Also, some of the higher surface polarity CPC's have surface polarities approaching that of the corroded aluminum. So, initially at least, it would appear we could easily pick the most compatible CPC for the corroded aluminum surface from this list.

However, when we consider that the goal is to find the best CPC for potentially moist lap joints, the choice proves not to be so easy. When the surface is wet you are trying to replace a water/aluminum interface with two interfaces within the joint: a CPC/aluminum interface and a CPC/water interface. Interfacial tensions between the corroded aluminum and the CPC's, as well as for corroded aluminum and water, must be calculated based on the known properties of water and the properties of the aluminums and CPC's as given above. There is no direct way to measure the interfacial tension at a liquid/solid interface. The calculation can be made using Good's equation. CPC/Water interfacial tensions can be measured directly, since both are liquids. And, they were measured for this work using the pendant drop method used to characterize the CPC's themselves and the aluminum surfaces. The interfacial tensions for the CPC's are what is high, and what drives some of the free

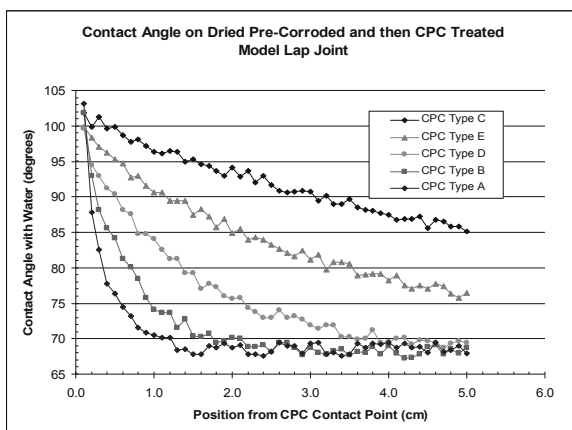
energies to be higher than is desirable. There is, however, some trade-off to be had with CPC's regarding interfacial tension.

The interfacial tension with water cannot be made too low or else it will be easy for water to displace the CPC once it is in place. In other words, the CPC will wash off, and/or, the CPC film will emulsify water – thus bringing water closer to the surface. On the other hand, as we see here, if the interfacial tension is too high then the free energy for water displacement is high. We continue to focus on the ability of CPC's to displace water and penetrate lap joints. To that end, we designed one more experiment which attempts to directly confirm the impressions which the free energy of water displacement data above give us.

The experiment was conducted as follows. We took corroded aluminum pieces from the customer's separated lap joints, wet them with water by dipping, and combined them in pairs corroded-face to corroded-face, thus creating moistened lap joints.



These dual sided surfaces were then tested for water contact angle as a function of dipping distance experiments, using the Wilhelmy technique. We also had measured the following average contact angles for the corroded surface when treated directly with each of the CPC's.



The obtained data clearly suggest which CPC is the best choice for a corrosion prevention compound for this described application.

The Prevention of Corrosion and Stress-Corrosion Cracking on European Space Programme

Tommaso Ghidini, European Space Agency, Noordwijk, The Netherlands

Andreas Tesch, European Space Agency, Noordwijk, The Netherlands

Adrian Graham, European Space Agency, Noordwijk, The Netherlands

Corrosion and in particular Stress-Corrosion Cracking (SCC) are generally presented as failure phenomena associated with industrial applications (most commonly the oil and chemical industry), where materials are exposed to salt water or highly corrosive environments. However, corrosion and SCC can be insidious failure mechanisms in aircraft and even spacecraft applications. Materials for space use are often fabricated by revolutionary manufacturing processes for near net shape, special heat treatments for grain optimisation and with unusual surface protection processes and are often exposed to severe environmental conditions.

The paper presents a detailed overview of documented occurrences of corrosion in space hardware and describes the European Space Agency (ESA) approach for controlling and preventing corrosion and stress-corrosion cracking failures in spacecraft and launchers.

An overview of recent SCC testing programme ranging from new and promising Al-Li alloys, to Particle Metal Matrix Composites (PMMC) alloys and Metal Laminates (GLARE®), as well as innovative Stainless Steels for bearings applications and Magnesium Alloys for Mars rovers potential use are presented. The effects of microstructure, surface finishing as well as the influence of innovative manufacturing processes such as Friction Stir Welding (FSW) and Additive Layer Manufacturing (ALM) on the SCC behaviour of materials are presented and discussed.

Moreover components, fracture mechanics based and near application SCC testing campaigns as well as future planned activities are also described.

The role of anodic oxide chemistry in the interfacial bonding of aluminium in the aerospace industry

S.T. Abrahami^{1,2}, J. de Kok³, J.M.C Mol¹, H. Terryn^{2,4}

¹ *Materials innovation institute (M2i), Delft, The Netherlands*

² *Delft University of Technology, Delft, The Netherlands*

³ *Fokker Aerostructures BV, Papendrecht, The Netherlands*

⁴ *Vrije Universiteit Brussel, Brussels, Belgium*

Anodizing is the central part of a multi-step pre-treatment process, which aims at preparing the aluminium surface for adhesive bonding in the aerospace industry. These anodizing processes are performed in acid solutions that lead to the formation of a duplex oxide structure with a compact barrier layer at the bottom and a relatively regular porous structure on top [1]. In the transition towards an environmentally friendly production replacements are desired for chromic acid anodizing, which is still largely used for this purpose. While research efforts with new types of acid anodizing are often directed towards controlling the film morphology, studies show that the oxide surface chemistry plays an essential role in the subsequent interfacial bonding with an organic coating [2, 3]. To focus on this aspect, thin anodic oxide layers without porous structure were prepared on AA1050 samples by stopping the anodic oxide growth during barrier layer formation. To vary the film chemistry, anodizing has been conducted in phosphoric, sulphuric and mixed phosphoric-sulphuric acid solutions. To further modify the hydroxyl activity, some samples were given a post-anodizing treatment in either acid or alkaline solutions. This set of samples were analysed by X-ray Photoelectron Spectroscopy (XPS) to determine the oxide chemistry as a function of the pre-treatment. A link was then made between the oxide chemical properties and its capability to interact with model organic molecules by means of XPS and FTIR. The organic molecules in this study are representative of the functionalities found in common aerospace adhesion primers.

- [1] Sheasby P.G., & Pinner R., *The surface treatment & finishing of Al and its Alloys*, 6th ed., (2001).
- [2] Van den Brand, J., Blajiev O., Beentjes, P.C.J., Terryn, H., de Wit, J.H.W., *Langmuir*, 20, 6318-6326, (2004).
- [3] Salgin, B., Özkanat, Ö., Mol, J.M.C., Terryn, H., Rohwerder, M., *J. Phys. Chem.* 117, 4480-4487, (2012).

Plasma electrolytic oxidation processes for aeronautic applications and their technical application

Norica Godja¹, M. Pölzler¹, A. Schindel¹, J. Wosik¹, A. Gavrilović¹, Ch. Kleber¹

¹. CEST Center of Electrochemical Surface Technology,

A- 2700 Wiener Neustadt, Austria

Email: norica.godja@cest.at

Abstract

Plasma electrolytic oxidation (PEO) processes of light metals have been introduced for several applications and are considered as a “green surface technology”. PEO improves surface properties of light metals like hardness, corrosion stability, chemical resistance and wear behaviour; therefore it is an attractive topic in the field of surface modification/protection. Aeronautic industry is a major user of lightweight materials and thus on large field for targeted research on high performance materials and coatings based on light metals. PEO processes are in use or at least in evaluation for many components and applications in this field. Within this work a detailed study of the correlation between experimental parameters and the resulting layer properties of PEO processes has been performed focusing on aeronautically relevant aluminum alloy substrates. The nature and chemical composition of the coatings formed by PEO can be controlled by matching specific process parameters such as electrolyte composition, voltage, current density, type of applied current (DC, AC or pulsed), electrolyte temperature, speed of stirring, total anodization time etc.

The incorporation of particles into the growing PEO layer is improving the pore size distribution and increasing the obtained layer hardness but will add a new challenge to the industrial PEO system. This work is a contribution to relate the effects of various process parameters on the resulting layer properties. This knowledge is important for the development of industrially applicable, robust processes where the control of the parameters ensure the reproducibility of the resulting properties. Only when the processes reach this point they can be considered for application in quality-sensitive areas like aeronautics.

Acknowledgement

This research at CEST was sponsored by the FFG and the Government of Lower Austria within the Comet program.

Tartaric/Sulphuric Acid Anodizing of Aluminium-Copper-Lithium Alloy AA2198

A. Schindel, N. Godja, T. Vanka, J. Wosik, Ch. Kleber, CEST - Kompetenzzentrum f. elektroch. Oberfltech. GmbH, Wiener Neustadt/Austria

Aerospace application and energy saving strategies in general boosted the interest and the research in the field of lightweight materials, typically on alloys based on aluminium. However, with a standard electrode potential of -1.66 V , it is an ignoble metal – therefore it is essential to protect aluminium and its alloys from corrosion. A commonly known method of protecting aluminium is anodization and subsequent sealing of the pores to achieve a dense protective oxide layer.

In the scope of this work, anodization of sheets of the new generation aluminium-copper-lithium alloy AA2198 (2.9-3.5 % Cu, 0.8-1.1 % Li) with a tartaric/sulphuric acid electrolyte (TSA) with a layer thickness of approx. $3\text{ }\mu\text{m}$ has been investigated. The specimens have been followed through the course of the entire process, comprising pre-treatment (alkaline cleaning, acidic pickling and etching), anodization and hot water sealing. After each step, specimens have been taken out of the process and characterized with various methods, including intergranular corrosion (ASTM F2111) after pre-treatment, mass-loss-investigation after each pre-treatment step, layer thickness and characterization of the anodic layer (with and without sealing) with ESEM (environmentally scanning electron microscope) at the surface and in cross-cuts prepared by means of FIB (focussed ion beam), metallurgical cross-section and breaking after immersion in liquid nitrogen, respectively.

8 different potentiodynamic anodization cycles have been investigated and compared with respect to layer thickness, size of the pores prior to sealing, contact angle on the anodized specimens with water and corrosion protection of anodized and hot-water-sealed specimens, determined by means of salt spray test (SST, EN ISO 9227).

Acknowledgement

This research at CEST was performed in cooperation with Hellenic Aerospace Industry S.A. in the framework of the JTI-CS-2012-3-ECO-01-058 “Validate TSAA” project, funded by the Clean Sky Joint Technology Initiative within the 7th Framework Programme.

Characterization and performance of passive layers generated from lithium based inhibitors for corrosion protection of AA 2024-T3

P. Visser^{1,3}, J.M.C. Mol¹, H Terryn^{1,2}

¹ *Delft University of Technology, Department of Materials Science and Engineering, Delft, The Netherlands.*

² *Vrije Universiteit Brussel, Group of Electrochemistry and Surface Engineering, Brussels, Belgium.*

³ *AkzoNobel Aerospace Coatings, Sassenheim, The Netherlands*

Over the years, a wide range of corrosion inhibitors has been studied to find suitable alternatives for hexavalent chromium based inhibitors to protect aerospace aluminum alloys. As from the 1980s, aluminum is reported to exhibit passivity in alkaline lithium salt solutions¹. Therefore, lithium salts were proposed and studied in the field of chemical conversion coatings^{2,3}. Our work presents the characterization and performance analysis of lithium based corrosion inhibitor chemistry for organic coatings. Suitable inhibitors need to be soluble and should generate an irreversible protective layer fast and effectively. Passive and inhibitive layers were generated from lithium based inhibitor doped coatings and aqueous solutions in the presence of sodium chloride on AA 2024-T3 high strength aluminum alloys. The main goal of this work was to characterize the morphology and chemistry of the generated layers as a function of parameters such as concentration and pH in order to develop a fundamental understanding of the formation mechanism. The layers generated were characterized using (ex-situ) surface analytical and electrochemical techniques. The morphology has been studied with Scanning Electron Microscopy (SEM) and Auger Electron Spectroscopy (AES) was used for chemical depth profiling. The surface chemistry of the layers was analyzed with X-Ray Photoelectron Spectroscopy (XPS). The generation of the passive layer was followed by open circuit potential measurements. The electrochemical response of the formed layers was studied using Electrochemical Impedance Spectroscopy (EIS) and potentiodynamic polarization experiments. The formation of these passive layers in the presence of sodium chloride and their protective properties indicate that lithium based inhibitors may represent potential alternatives to hexavalent chromium based inhibitors in organic coatings.

- (1) Gui, J.; Devine, T. M. *Scripta Metallurgica* **1987**, 21, 853.
- (2) Buchheit, R. D. *Corrosion* **1994**, 50, 205.
- (3) Rangel, C. M. *Surface & coatings technology* **2006**, 200, 5823.

Experimental study of the effect of mass transfer on the efficiency of inhibitors released from an inhibited-primer

F.Peltier, R.Oltra, G.Zalamansky*

Laboratoire ICB, Equipe EIC UMR 6303 CNRS – Université de Bourgogne, France

* DASSAULT Aviation, Saint Cloud, France

In a series of papers [1], the effect of different inhibitor release profiles on the pitting behaviour inside paint defects (scratch) was modelled. In atmospheric corrosion conditions or standard neutral salt spray test (surface covered by droplets) it was demonstrated that the main factor controlling the localized corrosion was the availability of the corrosion inhibitor which was clearly dependent of its diffusional path from the cut edge of the primer to drops in the centre of the scratch.

Consequently, the size of the scratch becomes a major controlling parameter because for larger scratch, as the probability for coalescence of droplets was very low, the inhibitor could not diffuse into most drops covering the slot and then the time to initiate pits was found to be reduced compared to narrow scratches for which a “continuous film” of electrolyte can be reasonably expected allowing to reach the critical inhibitor concentration to avoid localized corrosion initiation.

In our work this feature was revisited for immersion tests by studying the behaviour of cut-edge electrodes of various size machined from a coated AA2024-T3 plate designed for an aircraft structure. The cut-edge geometry has been used to mimic the electrochemical response occurring after a mechanical scratch on a coated structure [2]. The corrosion initiation occurring by trenching around coarse intermetallic phases was characterized [3] as function of the thickness of the primer-coated cut-edge electrodes. It was found that the existence of a competition between the released rate of inhibitors and the local corrosion activity around coarse intermetallic phases and consequently the inhibitor efficiency is depending of the size of the cut-edge electrodes. On the other hand, by ageing artificially the primer coating, it was possible to separate the role of the transport of inhibitors inside the primer (release) from the transport outside the primer by diffusion in the electrolyte. To simplify the demonstration, all the experiments were carried on an AA 2024-T3 alloy coated with a chromate-inhibited primer layer containing mainly zinc dichromate (corrosion inhibitor) but the methodology can be applied to support modelling of any inhibitor efficiency on the corrosion resistance of self-repairing aircraft structures.

[1] S.A. Furman, F.H. Scholes, A.E. Hughes, D. Lau, P. A. Corrigan, P. A. White, T. H. Muster, T. G. Harvey, S. G. Hardin, *Modelling inhibitor release kinetics in self repairing systems, Proceedings of the First International Conference on Self Healing Materials, 18-20 April 2007, Noordwijk aan Zee, The Netherlands*

[2] R.L. Howard, I.M. Zin, J.D. Scantlebury, S.B. Lyon, *Inhibition of cut edge corrosion of coil-coated architectural cladding, Prog. Org. Coat., 37 (1999) 83-90.*

[3] F. Peltier, R. Oltra, B. Vuillemin, *Inhibition Probing on a Cut-Edge Electrode Machined from a Primer-Coated 2024-T3 Alloy, ECS Electrochemistry Letters, 2 (8) (2013) C31-C33*

Advanced protective coatings for AA2024 alloys with combination of pH- sensitive active containers filed with corrosion inhibitors

D. Snihirova¹, S.V. Lamaka¹, P. Taheri², J.M.C. Mol², M.F. Montemor¹

¹ICEMS, Instituto Superior Tecnico/ULisboa, Lisbon/Portugal,

²Department of Materials Science and Engineering, Delft University of Technology, Delft/The Netherlands

Nowadays, there is a strong demand on the search of thinner, but more effective organic coatings for corrosion protection of aluminium alloys 2024 used for aeronautic applications. This strategy allows at saving raw materials and energy and at decreasing the CO₂ footprint. In order to guarantee effective corrosion protection of these coatings one of the most attractive strategies consists of the modification of the organic coating with particles or containers loaded with corrosion inhibitors, which can be triggered by external stimulus, releasing the inhibitor to the active sites.

In this work, two different pH sensitive additives were explored as potential self-healing materials for the development of smart coatings. These pH sensitive particles were added to commercial water based epoxy primer, individually, or by combining the two types of containers loaded with different corrosion inhibitors in order to study the active corrosion protection properties in coatings of industrial relevance.

The anticorrosion activity of these additives with respect to aluminium alloy AA2024 was investigated by electrochemical impedance spectroscopy, scanning vibrating electrode technique and localized electrochemical impedance spectroscopy. The results reveal that that an enhancement of the active protection effect can be reached when additives loaded with different inhibitors are combined in the same protective system.

Acknowledgment: Portuguese Foundation of Science and technology (FCT) for PhD grant SFRH/BD/72497/2010

Self-healing anticorrosive hybrid sol-gel coatings based on loaded nanocontainers for 2XXX serie aluminium alloys

*Romain Noiville¹, Marie Gressier¹, Marie-Joëlle Menu¹, Jean-Pierre Bonino¹,
Sandrine Duluard¹, Benoit Fori², Celine Gazeau², Pierre Bares²*

¹*CIRIMAT-UMR CNRS 5085, Université Paul Sabatier, 118 route de Narbonne,
31062 Toulouse, France*

²*Mecaprotec Industries, 34 Boulevard Joffrery, 31605 Muret Cedex, France*

Keywords: AA2024-T3 aluminium alloy; sol-gel hybrid coatings; active protection; nanocontainers; boehmite nanoparticles ; silica nanoparticles

The 2XXX series aluminum alloys occupy a very important place in aerospace components, especially in the structure of an aircraft (70%) due to their lower density and their high mechanical properties. However, the presence of copper in the AA 2024-T3 alloy in order to improve the mechanical strength leads to an heterogeneous microstructure, which makes the alloy highly vulnerable to corrosion. Therefore, it is necessary to develop an efficient anti-corrosion system to protect it against atmospheric conditions. Since few years, great efforts have been made to research environmental friendly substitutes of hexavalent chromium which are the most efficient to protect aluminium alloys. In this way, hybrid sol-gel coatings of silica-epoxy have been developed as a barrier layer to protect against diffusion of corrosive agents such as water, oxygen and chloride ions at the coating/metal interface [1, 2]. In addition, when the coating is damaged, an active corrosion protection can be achieved with the incorporation of nanocontainers loaded with corrosion inhibitors. The nanostructured coating reveals enhanced long-term corrosion protection in comparison with the unloaded hybrid [1, 3].

In this work, we have investigated the development of sol-gel coatings with distinctive nanocontainers which include cerium(III) as an inorganic corrosion inhibitor. Coatings are deposited by dip-coating method on AA2024-T3 alloy. Our objective is to raise the amount of cerium physisorbed on nanocontainers to improve anticorrosion performances. The first step is the synthesis of nanoparticles presenting a high specific area: two kinds of nanoparticules have been evaluated, the first one based on silica and the second one on Boehmite in order to keep a chemical consistency with coating and substrate. Then the loading of the inhibitor was realized by physisorption in aqueous solution. The last step consists to evaluate by Electrochemical Impedance Spectroscopy (EIS) the inhibitor release of the loaded nanoparticles to highlight the nanocontainer effect involving in the active protection. Further characterizations to evaluate the morphology and the microstructure of the nanocontainers such as Scanning Electronic Microscopy, FEG-SEM, Transmission Electronic Microscopy (TEM), were undertaken. Anticorrosion performances of such nanocomposite coatings were evaluated by Electrochemical Impedance Spectroscopy (EIS) during immersion in a representative corrosive medium together with the resistance to accelerated corrosion test in neutral salt spray (NSS).

[1] *Jaubert et al. patents UN 643-BF 14311 – cas 33 EP/CA 10/2011 et UN 643-BF 14630 – cas 37 EP/CA 10/2011*

[2] *M. L. Zheludkevich, I. M. Salvado. Sol-gel coatings for corrosion protection of metal. J. Mater. Chem., 2005, 15, 5099-*

[3] *D. G. Shchukin, M. L. Zheludkevich, H. Möhwald. Feedback active coatings based on incorporated nanocontainers. J. Mater. Chem., 2006, 16, 4561-456*

Silica mesoporous thin films hosting benzotriazole for protection of 2024 aluminum alloy – Study of healing mechanism

I. Recloux, M. Mouanga, F. Khelifa, M-G. Olivier, University of Mons, Mons/Belgium

Sol-gel coatings are increasingly studied for the replacement of hexavalent chromium based conversion due to their strong adhesion to metallic substrates and due to their high corrosion protection. However, due to their nature, they only act as passive physical barriers and cannot hamper corrosion propagation when the film presents failures. The introduction of organic or inorganic corrosion inhibitors in the layer has already been reported as a solution to provide defect-healing ability to the coating. The incorporation way of these agents is particularly important to obtain high performance. For example, introducing directly inhibitive compounds in the sol in high concentration may induce a deterioration of integrity and physical barrier properties of the sol-gel matrix. The use of inert nanostructures (such as halloysite, ion-exchange clays, nanoparticles...) as mediators to encapsulate corrosion inhibitors has consequently been considered to prevent detrimental interactions between the chemical compound and the sol-gel medium. In case of scratch or when stimulated by external action, nanocontainers release active species which form a local protective layer healing the defect.

In the present work, a silica mesoporous thin film synthesized through "Evaporation Induced Self-Assembly" process was used as inhibitor nanocontainer for 2024 aluminum protection. The mesoporosity developed through the layer was employed to host benzotriazole which is known as an efficient corrosion inhibitor of AA 2024.

From transmission electron microscopy (TEM) and adsorption porosimetry measurements, it was possible to determine high specific surface area and well-organized pores providing high-load ability for active species [1]. The inhibitor loading as well as the releasing rate from the film were determined by desorption in aqueous medium using UV/visible spectroscopy. A second copolymer based layer was applied on the loaded mesoporous film as a topcoat to confine corrosion inhibitors close to the metallic surface. An enhanced anticorrosion protection was observed using Electrochemical Impedance Spectroscopy (EIS) when the corrosion inhibitor is incorporated in the porosity. EIS measurements were complemented with Scanning Vibrating Electrode Technique (SVET) measurements in order to get a better understanding of the positive effect related to benzotriazole and to highlight healing mechanism.

[1] I. Recloux, M. Debligny, A. Baroni, Y. Paint, A. Lanzutti, L. Fedrizzi, M-G. Olivier, Optimization of synthesis parameters of mesoporous silica sol-gel thin films for application on 2024 aluminum alloy substrates, *Applied Surface Science*, 277 (2013) 201-210.

Eco-friendly primer treatments for corrosion protection of Al 2024

*I. Bertoli, M. Trueba, S.P. Trasatti
Università degli Studi di Milano, Italy*

This paper presents an investigation of pyrrole-, aniline- or thiophene-functionalized silanes for corrosion protection of Al 2024-T3. Primers were deposited on the alloy by immersion in the corresponding hydrolyzed silanes solutions using methylacetate (MeOAc) as main solvent. This non-HAP, VOC-exempt and biodegradable solvent was chosen to replace methanol (MeOH), as the solubility of the above mentioned silanes in water is limited. Protection capacity was investigated mainly by impedance experiments (Mott-Schottky analysis), considering also the effect of copper enrichment on the surface that was promoted by an alkaline pre-treatment. Comparison with MeOH-based treatments [1-4] indicates that the use of MeOAc does not cause important structural changes in both solution and film phases. The barrier protection is notably improved, though active protection is still manifested by specific interactions at the metal/film interface. Copper enrichment influences the protection capacity though differently for given silane and solvent used in the surface treatment step.

- [1] (a) M. Trueba, S.P. Trasatti, Prog. Org. Coat. 66 (2009) 254-264; (b) Ibid, 265-275.
- [2] D.O. Flamini, M. Trueba, S.P. Trasatti, Prog. Org. Coat. 74 (2012) 302-310.
- [3] M. Trueba, S.P. Trasatti, D.O. Flamini, Corros. Sci 63 (2012) 59-70.
- [4] S. Bianchi, M. Trueba, S.P. Trasatti, Prog. Org. Coat. (2014) (accepted)

Characterization of corrosion resistance of chromium-free coatings for aeronautical application

Lucrezia Belsanti^{*}, Emiliano Forchin[§], Roberto Stifanese^{*}, Milena Toselli^{*}, and Pierluigi Traverso^{*}

^{*}National Research Council (C.N.R.) – Institute of Marine Sciences (I.S.MAR.) U.O.S of Genoa, via A. de Marini 6, 16149 Genoa Italy

[§]Agusta Westland, Via G. Agusta 520, 21017 Cascina Costa di Samarate (VA) Italy,

Coatings protect metallic substrates from environmental corrosion attack. However, although giving good insulation, the presence of specific metal ions in their composition represents a potential source of environmental contamination. The necessity to conciliate corrosion protection with environmental impact is, thereby, primary.

This work was designed to study the performance of low environmental impact protective systems (surface treatment and primer), such as those free from chromium (Cr), layered on different substrates of aluminum (Al) alloy [Al 7075 (T6) unclad and Al 2024 (T3) unclad] for aeronautical applications. Substrates were first surface-treated in different ways: Cr-based anodizing/passivation or more environmentally friendly Cr-free treatments. Successively, on substrates treated as above, Cr-containing or Cr-free epoxy primers were used.

The capability to protect substrates from corrosion phenomena was evaluated following exposure of 10 groups of samples to *in situ* marine atmosphere. To this aim, specimens were exposed at the Experimental Marine Station of C.N.R.-I.S.MAR.-Ge, located in the port of Genoa, for 8, 16, and 24 months and in accordance with UNI EN ISO 8565:1997 standard.

Before and at the end of the different periods of exposure, a detailed photographic documentation was collected and some sample features, such as the thickness of superficial treatment and primer, the contact angle and the color (L,a,b parameters) of the surface were evaluated. Accelerated degradation of coating systems was also studied by electrochemical impedance tests carried out in 5% NaCl solution. Sections from some selected samples were submitted to optical and scanning electron microscopy analyses to evaluate the thickness of superficial treatment and primer, and characterize the interface metal/superficial treatment and superficial treatment/primer.

Altogether, the experimental results obtained identify some groups of samples that show a higher corrosion resistance and suggest the combination of Cr-free or Cr-containing treatment and primer that has a significant protective power among those tested. Moreover, they give useful information to design Cr-free systems that protect metallic structures from corrosion but have, at the same time, a lower impact on workers and the environment.

Anticorrosion Sol-Gel Coatings for Anodised Aluminium

Mohamed Oubaha, Cecilia Agustin Saenz, Uxoa Izagirre Etxeberria, Brendan Duffy

Centre for Research in Engineering Surface Technology (CREST), FOCAS Institute,

Dublin Institute of Technology, Dublin 8, Ireland, mohamed.oubaha@dit.ie

*Tecnalia, Donostiako Teknologi Parkea, Mikeletegi Pasealekua, 2, E-20009
Donostia-San Sebastián - Gipuzkoa (Spain)*

This study results from the collaborative AVCOP-FP7 project, which aims at investigating the potential of nanostructured hybrid organic-inorganic sol-gel materials in the sealing process of anodised aerospace grade aluminium AA2024-T3. A range of hybrid materials prepared from hydrolysis and condensation reactions of organosilane and metal transition precursors have been synthesised, characterised and employed as coating systems for the anodic layer. In addition to the effect of the function group contained in the organosilane, emphasis has been placed on understanding the fundamental mechanism related to the nanostructuration of the metal transition complex and the subsequent effect this would provide to anti-corrosion performances. The corrosion and chemical resistance of the sealed anodic films has been evaluated and compared to conventional sealing technologies such as hydrothermal treatments. Field Emission Scanning Electron Microscopy was utilised to characterise the pore morphology of the anodic films and to determine the sealing mechanism. Accelerated exposure tests have been conducted including neutral salt spray, acidified salt spray and strong alkaline resistance. The synergistic anti-corrosion mechanism of the hybrid sol-gel and oxide film of the corrosion prone alloy was determined with and without the use of the sol-gel sealants. The technique described offers numerous opportunities for industrial applications.

A study of the films formed on an AA2024 alloy clad layer by hydrothermal treatments involving cerium (III) and propylene glycol

W. I. A. Santos¹, V.R. Capelossi¹, S. Hinder², M. A. Baker², R. Grilli², I. Costa¹,

¹Instituto de Pesquisas Energéticas e Nucleares, Av. Prof. Lineu Prestes, 2242, CEP 05508-000, São Paulo, SP, Brazil

²Faculty of Engineering and Physical Sciences, University of Surrey, Guildford, Surrey, UK

Surface treatments using cerium (III) ions have been largely studied for the corrosion protection of aluminum alloys. These treatments are being proposed as alternatives to chromating treatments due to their environmentally friendly properties, as no toxic waste is generated. Most of the cerium treatments reported are based on cerium conversion coatings involving the immersion of the surface in corrosive acid solutions. This study investigates the effect of hydrothermal treatments on the corrosion resistance on the AA2024 alloy clad layer. The hydrothermal treatment was carried out by immersion in solutions either containing cerium ions or propylene glycol, both at 75 °C. The chemical composition, morphology and corrosion resistance of the films formed by the hydrothermal treatment has also been studied by XPS, FTIR, SEM and electrochemical impedance spectroscopy (EIS). The results showed that $\text{Ce}^{3+}/\text{Ce}^{4+}$ ions were incorporated into the boehmite layer formed on the clad layer during the hydrothermal treatment in the solution with Ce (III) ions. This incorporation caused a large increase in the surface impedance of the clad material. The results also suggested that propylene glycol acts as a catalytic agent promoting the formation of a protective boehmite film on the clad surface. The clad surface film after a two-step treatment that combined hydrothermal treatment in solution with Ce (III) ions with hydrothermal treatment in solution with propylene glycol showed impedances much superior to that of the treatment associated to only a one step treatment in Ce (III) containing solution or to the clad material with a chromate conversion coating.

Mitigating corrosion in sweet gas units: a comparison between laboratory data and field survey

J. Kittel⁽¹⁾, M. Bonis⁽²⁾, G. Perdu⁽³⁾

⁽¹⁾ IFP Energies nouvelles, Rond-point de l'échangeur de Solaize, BP3 69360 Solaize, France

⁽²⁾ Total, avenue Larribau, 64018 Pau Cedex, France

⁽³⁾ Prosernat, 100/101 Terrasse Boieldieu, 92042 Paris La Défense Cedex, France

An extensive review of acid gas removal units covering 5 decades and more than 120 amine units showed that sweet gases (i.e. with CO₂ only) presented the worst risks of corrosion. In some extreme cases, a quite uniform corrosion in an active mode was observed on stainless steel grades such as AISI 410 and 304L, despite apparently mild corrosive conditions. Strong scaling of the heat exchangers by corrosion products was also observed. A detailed analytical survey of those corrosive DEA units was then performed over more than two years. Immediately after fresh solvent swap, dissolved iron concentration increased until stabilization at several hundreds of mg/L after a few months. Good correlation was found between dissolved iron, amine degradation, and the amount of corrosion products that was recovered in the heat exchangers. Comparisons with similar units using activated MDEA revealed dissolved iron levels several orders of magnitude below those in DEA.

In order to understand more precisely the driving forces for steel corrosion and for the precipitation of corrosion products, a laboratory program was launched. Comparisons between different amines in rich and lean conditions were performed in autoclave. A specific protocol was developed which aimed at degrading the amine solutions and providing dissolved iron before corrosion tests. Some tests were also performed with an industrial DEA solution sampled in a sweetening unit having experienced corrosion problems. Active corrosion of AISI 304L was reproduced in laboratory conditions in hot rich DEA and in industrial DEA solution as well. Precipitation of iron carbonate could also be explained. Iron solubility was found to depend on amine loading, with a lower solubility in rich conditions, thus a strong tendency to precipitate.

The experience and know-how gathered from the feed-back, inspection and laboratory experiments is applied to improve the performance of existing units, for which carbon steel has been used extensively. The key corrosion mitigating issues are exposed in term of appropriate amine selection for sweet or sour gases, flow velocities and procedures for solvent preservation. The article also discusses about material selection and replacement of carbon steel by appropriate corrosion resistant alloy (CRA) when needed and only on selected areas, as normal maintenance operations following periodic inspections. This considerably extends the service life, while also enabling operation above the initial specifications.

For newly built compact units, the design criteria focus on application of AISI 316L, now preferred instead of lower grades like 304L or AISI410, to areas potentially prone to corrosion. With appropriate use of CRA's, acid gas loadings of 0.85 or even higher are easily achieved, without velocity limitations on the rich amine lines. Furthermore, the amine unit remains fully versatile and flexible to encompass the widest range of amines, including some in development.

Keywords : alkanolamines, corrosion, gas sweetening, scaling

Corrosive and protective behaviour of MEA in dense phase CO₂

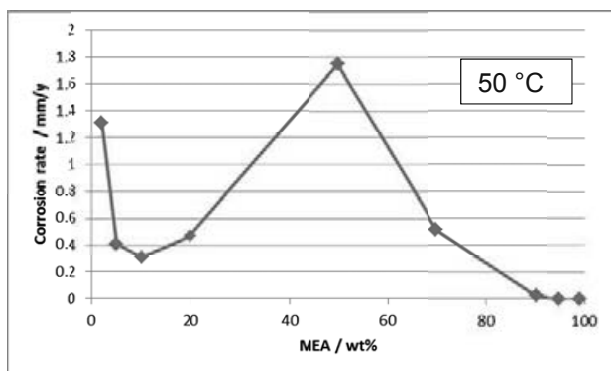
Arne Dugstad, Malgorzata Halseid, Bjørn Morland

Institute for Energy Technology, Kjeller, Norway

Amines are commonly used in the CO₂ catching process and carryover of small amounts from the process plant might contaminate the CO₂ in the pipeline. The amine solubility in dense phase CO₂ is not known, but if a separate amine-water phase is formed corrosion will take place. The presence of amines increases the pH in the water phase. Due to this effect, amines are used as pH stabilisers and both lab experiments and field experiences show that the corrosion rate can be significantly reduced (< 0.1 mm/year) when MEA is added in moderate amounts (< 5 wt%) at CO₂ partial pressures less 10 bar. In contrast, amines are reported to be corrosive when used at high concentration (> 30 wt%) in amine plants for CO₂ removal.

A series of corrosion experiments were performed in 50 cm long slim 200 ml autoclaves that were half filled with an aqueous phase containing MEA (Mono Ethanol Amine) and pressurised to 50-150 bar with CO₂. Cylindrical test specimens were mounted on small cylindrical racks that slid from one end to the other when the autoclaves were rotated vertically on a shaft inside a temperature controlled cabinet. That gave good mixing and disturbed flow around the test specimen.

The effects of test duration, temperature (25, 50 °C), MEA concentration (2, 5, 10, 20, 70, 90, 95 and 99 wt%) and oxygen content (0, 500 ppmv) were studied. A



reduction in corrosion rate was observed when the MEA concentration was low and this is attributed to the formation of protective corrosion product films. Lowest corrosion rate was observed at 10 wt% MEA. The protection was apparently lost when the MEA concentration was increased to 20 and 50 wt% MEA. The loss of protection might be

related to the formation of dissolved iron complexes. The corrosion rate decreased when the MEA concentration was increased from 50 to 70, 90, 95 and 99 wt% respectively. The mechanism for this decrease has not been studied, but is assumed to be closely related to the decreased water activity and increased viscosity.

The paper discusses the experimental approach, the results obtained and the corrosive vs. the protective properties of MEA when present as a contaminant in dense phase CO₂ and when added deliberately as pH stabiliser in gas condensate pipelines.

Thermally sprayed corrosion resistant alloy coatings on carbon steel for use in CCS

S. Paul, TWI, Cambridge, UK

Carbon dioxide capture and storage (CCS), a carbon sequestration method, is recognised as one means of utilising carbon-based fuels whilst minimising the release of CO₂ into the atmosphere. Primarily, this involves capturing the CO₂ arising from industrial and energy-related sources, separating it from some other gases if needed, compressing it, and then transporting and injecting it into a storage site such as depleted oil and gas wells or saline aquifers to ensure long-term isolation from the atmosphere.

Although the CCS concept is based on a combination of known technologies, large scale adoption and integration of individual existing technologies poses challenges. These technological challenges range from corrosion and structural integrity of materials to safety inspection during operation. Understanding these issues, mitigating if necessary, and filling the technology gaps in full scale implementation of CCS is important for its wider adoption as a CO₂ emission reduction tool.

This paper reports the use of a thermal spray corrosion resistant alloy (CRA) coating to mitigate corrosion of carbon steel conduits used in carbon dioxide capture plants. CRA coatings were sprayed onto carbon steel substrate and these were tested in 3.5wt.% NaCl solution saturated with 100bar supercritical CO₂ at 40°C for 30days. Microstructural characterisation revealed that the thermally sprayed layer protected the steel substrate from carbonic acid corrosion. The bare steel formed a siderite (FeCO₃) scale while no such scale was seen in the case of CRA-coated steel. It can be concluded that thermally sprayed CRA coatings provide a cost-effective corrosion mitigation method for infrastructure likely to be in contact with wet supercritical CO₂. The same coatings can be used as inner lining of pipes for transport of impure CO₂. However, care must be taken to ensure that the thermally sprayed layer does not have any through porosity; else, such coatings may accelerate corrosion of the underlying steel due to galvanic interactions.

Effect of microstructure on scale protectiveness and corrosion rate of carbon steel in CCTS environments

M.Cabrini, S.Lorenzi, T.Pastore

University of Bergamo, Dalmine/Italy

The role of microstructure on the corrosion behaviour of carbon steel in environments containing CO₂ is well known in oil and gas industry, where failures are often explained by varying the tenacity of protective corrosion scales due to different carbon steel microstructures. The same effects have not been yet demonstrated in Carbon Capture Transport and Storage Environments (CCTS). CCTS is the technology for capturing waste CO₂ from combustion gases of fossil fuels used for the production of energy, its compression and liquefaction, transport in pipelines and storage in the deep underground sites (below 800 meters), generally depleted oil and gas fields or in deep saline aquifers.

Microstructure is considered to play a crucial role on scale adhesion on the steel surface. The adhesion of the corrosion product film and hence its protectiveness has often been related to the presence of iron carbide and its morphology (laminar, globular, etc.). The carbide phase is able to strengthen the film and improve the bond with the steel substrate. Consequently the size and distribution of these carbides becomes more and more important.

The high pressure of CO₂ in CCTS systems causes very high corrosion rates in the first times of exposure but the high concentration of carbonate species favours the the supersaturation conditions and the precipitation of a protective scale.

The paper is devoted to study the effect of carbon steel microstructure on the scale morphology and protectiveness in water saturated with supercritical CO₂, at 80 bar pressure and 40-60°C temperature.

Four different carbon steel microstructures were considered. The microstructures were modified by different heat treatments, in the specific: normalizing, annealing, quenching, quenching and tempering.

Weight loss tests were performed in order to estimate the average corrosion rates. The morphology of corrosion products scales was observed by means of scanning electron microscope. The chemical composition was evaluated by X-ray spectroscopy.

Potentiodynamic and electrochemical impedance spectroscopy tests were performed in dilute sulphuric acid (pH 3.5) saturated with 1 bar CO₂ to evaluate the effect of the scale microstructure and composition on the electrochemical behaviour of steel.

The results evidenced the effect of iron carbide network in the scale formation and growth. The effect of the presence of such networks on the corrosion rate was also highlighted.

Safe transport of dense phase CO₂ – how much flue gas impurities can be accepted?

*Arne Dugstad, Malgorzata Halseid, Bjørn Morland
Institute for Energy Technology, Kjeller, Norway*

Transport of anthropogenic CO₂ is a new technology and there is limited knowledge about possible corrosion and bulk phase reactions when the CO₂ contains flue gas impurities like SO_x, NO_x, O₂ and CO in addition to H₂O, H₂S. A number of CO₂ specifications and recommendations for maximum impurity concentrations have been published, but there is presently no consensus on the operation window for safe transport of dense phase CO₂.

National Energy Technology Laboratory (NETL) issued recently a table of recommended limits for CO₂ stream compositions based on a review of 43 CO₂ specifications found in the literature.¹ A large variation in the reported impurity concentrations can be seen as the impurities in the CCS/CCUS stream will depend on the fuel type, the energy conversion process (post-combustion, pre-combustion or oxyfuel) and the capture process.

Various CO₂ compositions with impurity concentrations within the recommended ranges given by NETL have been tested with respect to corrosion and bulk phase reactions. The experiments were performed in long (1-2 m) slim autoclaves that were mounted vertically on a shaft inside a temperature controlled cabinet and tilted alternately $\pm 180^\circ$. Cylindrical test specimens were mounted on small cylindrical racks that slide from one end to the other when the autoclave is tilted. This gives good mixing and disturbed flow around the test specimen. The autoclaves were continuously fed with CO₂ and impurities (H₂O, H₂S, O₂, NO₂ and SO₂) and the consumption of the impurities due to corrosion and bulk phase reactions (reactions between impurities) were measured in the CO₂ vented from the autoclave. The experiments were run at 100 bar CO₂ pressure at 25 and 45 °C.

The experiments showed that precipitation of acids and elemental sulfur can occur when the dense phase CO₂ contains small amount of H₂O, O₂ and SO₂ or NO₂.

The paper discusses the experimental techniques and results obtained in a few selected experiments. The paper also discusses how the lack of fundamental data and understanding makes it difficult to predict corrosion rates and define a safe operation window for transport of dense phase CO₂ originating from different sources with different contaminants.

1 NETL Quality Guidelines for Energy System Studies, "CO₂ impurity design Parameters", DOE/NETL-341/011212, 2012

Corrosion susceptibility of steels under transport and injection exploitation conditions possible in CCS process chain.

Oleksandra Yevtushenko, Ralph Bäßler, Dirk Bettge, BAM Federal Institute for Materials Research and Testing, Berlin/Germany

Once sequestered, CO₂ will be transported and injected in its gaseous, liquid or supercritical state. The presence of impurities significantly influences the corrosion behavior of pipeline steels even with small concentrations of water below its saturation limit.

Within the project COORAL (German acronym for “CO₂ purity for capture and storage”) studies on piping steels exposed to circulating supercritical impure CO₂ have been carried out. The impurities such as H₂O, CO, SO₂, NO₂ and O₂ were added to the CO₂ stream before compression. Without acid condensation even carbon steels like L485MB or L360NB can be used [1]. They exhibit general corrosion with low corrosion rates less than 0.1 mm/year also by water content up to 2000 ppm(V) at 10 MPa and 333 K.

In the absence of brine the limiting factor for metallic materials will be acid condensation from the CO₂ stream when containing water and SO_x. Even small amounts of SO₂ may cause corrosion problems inside the pipeline due to the formation of acidic droplets. General corrosion followed by strong shallow pit formation was observed on L360NB in condensates saturated with CO₂ at ambient pressure and 278 K. The corrosion products were fluffy and did not exhibit much protection against further surface attacks. General uniform corrosion with growth of a dense corrosion layer was observed on X46Cr13 after 14 days exposure to condensates saturated with CO₂. Localized corrosion was observed on material X1NiCrMoCu32-28-7. It has been shown that even high alloy materials might be susceptible to general as well as to localized corrosion in the acidic condensates with pH below 2 [2].

Dealing with CO₂ stream and saline brine at the same time, a much higher corrosion resistance is needed because of chlorides. In the experiments in CO₂ saturated saline brine 42CrMo4 exhibits general corrosion with high corrosion rates up to 1.4 mm/a, and, therefore, cannot be recommended for application under the investigated conditions. Cr13 steels and X5CrNiCuNb16-4 are not resistant to pitting corrosion in CO₂ saturated saline brine at 60 °C. Their corrosion rates cannot be predicted, therefore, these materials cannot be recommended for applications under conditions investigated in this study. Only the highest alloyed and most expensive X2CrMnNiN22-5-2 and X1NiCrMoCu32-28-7 are resistant to CO₂ saturated saline brine at 60 °C and can be used under above mentioned conditions, however, in case of X2CrMnNiN22-5-2 no crevices may be present.

[1] O. Yevtushenko, D. Bettge, S. Bohraus, R. Bäßler, A. Pfennig, A. Kranzmann, Corrosion behavior of steels for CO₂ injection. Process Safety and Environmental Protection (2013), in press

[2] O. Yevtushenko, D. Bettge, R. Bäßler and S. Bohraus, Corrosion of CO₂ transport and injection pipeline steels due to the condensation effects caused by SO₂ and NO₂ impurities, Materials and Corrosion 2013, DOI: 10.1002/maco.201307368

Perspectives on the climatic reliability issues of electronic devices

Rajan Ambat

*Materials and Surface Engineering, Department of Mechanical Engineering,
Technical University of Denmark, DK 2800 Kgs Lyngby, Denmark*

Email: ram@mek.dtu.dk

Corrosion reliability is a serious issue today for electronic devices, components, and bare printed circuit boards (PCBs) due to factors such as miniaturization, globalized manufacturing practices, and global usage. The result is reduced life span for electronic products and heavy economic loss due to failures. Miniaturization at all levels is one of the key factors reducing the corrosion reliability. Over the last 10 years, size of the electronics has been reduced by over 70%. For the flip chip ICs, miniaturization amounts to ~ 90%. The closer spacing increases the electric field ($E = V/d$), which makes the corrosion cell formation easier during local condensation under humid environments. Process related residues (contamination) on the PCB surfaces results from all stages of the manufacturing process starting from the base PCB production to the components mounting, soldering, inspection and testing, device assembly, and packing are all process that will have great influence on corrosion. A particularly important factor is the residue resulting from no clean flux especially from the wave soldering process. Such residues can easily absorb water under humid conditions, and can accelerate the corrosion problems by providing conducting ions, participating in corrosion reaction, or as a site for entrapment of dust.

This paper provides an overview of the climatic reliability issues of electronic devices and components with a focus on materials used, components, process related cleanliness, humidity interaction on PCBA surface, and PCBA design and device design aspects.

Key words: Electronics, reliability, corrosion, cleanliness, humidity

Brief Introduction to the Mechanism of Electrochemical Migration

Helmut Schweigart
Zestron Europe, D-Ingolstadt, Germany

To cause electrochemical migration humidity is necessary, which form few monolayers of water film. Only few layers of molecular water is enough to start corrosion processes above the critical humidity levels of 60-70 % RH at room temperature depending on the substrate polarity and its surface energy. Hygroscopic pollutions lower the critical humidity in extreme cases down to 40 % RH. So even in normal interior climatic conditions computers are indangered. Under a constant climate, the epoxy resin substrates with tin-lead metallization, the humidity adsorption is concentrated at the polymer surface. In nearly pure condensed water, the migration tendency can be connected to pH-value and potential-pH diagrams, so-called Pourbaix diagrams. In the presence of chlorides and other complexes forming pollutions normal stable elements like gold, indium, palladium and platinum also migrate.

Electrochemical migration with dendritic bridges that are tree-like, band-like and fibrous type growing from the cathode to the anode can be observed in dependence of the concentration gradient at the cathode. The composition of the short circuiting bridges between cathode and anode can be metallic in nature or made of metal salt complexes depending on the stability of the dissolved metal ions in water layer. This provides an overview of the mechanism of electrochemical migration based on the influence of various influencing factors.

Influence of the Printed Circuit Board Design on Electrochemical Migration and Surface Insulation

*Mathias Nowottnick, University of Rostock, Rostock/Germany;
Saskia Mattern, Robert Bosch GmbH, Stuttgart/Germany*

A better understanding of chemical, electrical and geometrical effects on the surface resistance (SIR) on printed circuit boards is essential for manufacturing of high quality electrical appliances. This is particularly important because the distances on PCB's are getting smaller, the electrical voltages and currents are becoming higher, and the requirements on reliability are becoming increasingly demanding. The usual standard tests with comb structures only consider the distances and widths of the copper traces. However, a number of other factors need to be considered for real assemblies. Contaminations by fluxes are usually not uniformly distributed, but will be also influenced by the solder resist, gaps among components and the different surface tensions. The same applies of course to the afterwards used cleaning agents. This paper describes theoretical approaches and experimental results of different design influences.

Electrochemical migration in electronics: effect of contamination and bias conditions

*Vadimas Verdingovas, Morten Stendahl Jellesen, Rajan Ambat
Materials and Surface Engineering, Department of Mechanical Engineering,
Technical University of Denmark, DK-2800 Lyngby, Denmark vaver@mek.dtu.dk*

A number of reliability issues are caused by mechanisms different from the conventional corrosion due to specific aspects of the printed circuit board assembly (PCBA). The size of the components and the distance between them, combinations of dissimilar metals, voltage and temperature gradients – all together influence susceptibility of electronic PCBA to corrosion. When electronics is operating under humid conditions, the cleanliness of the PCBA becomes essential, since corrosion related failures in electronics can occur at extremely low levels of moisture and contamination. A synergetic effect of the aspects mentioned above makes it challenging to predict the lifetime of electronic device.

The aim of this work is to investigate corrosion influencing factors, which at a later stage improve capabilities of predicting the functioning and herewith reliability of electronics under certain climate, contamination, and bias conditions. In this work, the effect of ionic contamination such as sodium chloride and weak organic acids, as they are used in no-clean fluxes, was studied under water droplet and humidity elevation at room temperature conditions. The effect of pH and tin ion dissolution on the probability for electrochemical migration was studied on surface mount chip components under water droplet conditions, as a function of applied voltage (DC and square wave unipolar/ bipolar). The leakage current and impedance was studied on the surface insulation resistance patterns precontaminated with sodium chloride and weak organic acids exposed to accelerated humidity conditions.

The results from pH and tin ion dissolution study under water droplet condition showed electrochemical migration dependence on duty cycle and period, which was dependent on the amount of sodium chloride in the water droplet. Overall the tendency of increase in time to electrochemical migration with decrease of duty cycle was observed. The testing of the printed circuit boards under humid conditions showed a correlation between the hygroscopic property of contaminants and leakage current measured on the boards. A significant increase of leakage current was observed at humidity levels close to the critical or deliquescence of the contaminants.

Contamination profile of Printed Circuit Board Assemblies in relation to soldering types and conformal coating

Hélène Conseil, Morten S. Jellesen, Rajan Ambat

Materials and Surface Engineering, Department of Mechanical Engineering,

Technical University of Denmark, Hélène Conseil

Building 425, Kongens Lyngby, Denmark, helco@mek.dtu.dk

Abstract

Electronics industry has been adopting no-clean flux technology, with the assumption that there is no requirement to clean the printed circuit board assemblies (PCBAs) after soldering. However, substantial amounts of flux residues, including the activator components, mainly weak organic acid (WOA), are found left on the PCBAs surface after processing. These ionic residues of hygroscopic nature can cause increased water absorption to the surface and when in solution they increase leakage current and corrosion such as electrochemical migration resulting in intermittent or permanent failures. Reflow, wave, and selective wave soldering are three major types of soldering process used in industry, and the amount and distribution of the flux residue vary considerably with the specific type of soldering and related parameters, especially the soldering temperature profile and other process aspects.

Relevant surface conditions on actual production PCBAs, including distribution, composition, and concentration of ionic contaminations have been analysed. Localization and identification of flux residues have been done with a pH gel test method, and Fourier Transform InfraRed (FT-IR) analysis. Localized contaminations have been extracted using a steam purge, with a C3 (Critical Contamination Control) equipment, and quantified by ion chromatography analysis and leakage current measurement, in order to get information about the localized WOA and NaCl equivalent concentrations. In order to determine the effect of cleaning after soldering processes, some PCBAs were carefully washed with a solution of Millipore water and isopropyl alcohol with ratio of 1:3 and analysed for contamination profile. The effect of ionic contaminants on the adhesion of silicone conformal coating has been observed as a function of soldering processes and contamination level following blisters formation after exposure of PCBAs to aggressive environment. The results reveal that the distribution and concentration of flux residues left after soldering on PCBA surfaces are directly correlated to the type of processing, with an average localized NaCl equivalent concentration of $1.8 \mu\text{g}.\text{cm}^{-2}$ on reflow soldered PCBs and 2.1 and $4.0 \mu\text{g}.\text{cm}^{-2}$ respectively on wave and selective wave soldered PCBs. The presence of flux residues result in the degradation of the coating adhesion on PCBAs by assisting water intake and blister formation.

Key words: printed circuit boards, solder flux, ionic residues, contamination profile, conformal coating

Corrosion reliability of electronics: the influence of solder temperature on the decomposition of flux activators

Kamila Piotrowska, Hélène Conseil, Morten S. Jellesen, Rajan Ambat

Materials and Surface Engineering, Department of Mechanical Engineering,

Technical University of Denmark,

Building 425, DK-2800 Kongens Lyngby, Denmark, kampio@mek.dtu.dk

The climatic reliability issues of electronic devices and their components have increased during the past few decades due to different environmental, manufacturing, and application factors. One among them, while the most important one, causing acceleration of corrosion in electronics, is the process related contamination found on the Printed Circuit Board Assembly (PCBA). The contamination originates mainly from the soldering process (hand, wave, selective or re-flow) carried out when mounting the components on PCBAs. Although the current use of fluxes for soldering relies on using so-called 'no-clean' fluxes, it is expected that their use should only result in low levels and benign contamination left on the surface of PCBA. However, flux systems with different types of activators combined with factors related to application of flux and temperature distribution over the surface of PCBAs can result in substantial amounts of activator residues (acid residues in the case of WOA fluxes) left on the surface. The fact of no existing strict requirements for cleaning the PCBA's surface after soldering process leads only to the increase of residues left on the boards after the manufacturing process.

As commonly used flux types differ in their composition, the kind and level of residues can differ also. Typically, the residues consist of the solvent, resin, and activators. The activators are usually Weak Organic Acids (WOA) or halogenides. They are highly hygroscopic and therefore increase the level of water absorption on the PCBA surface in addition to the increased leakage currents and corrosion effects.

The investigation in this paper focus on the decomposition nature of activators used in different 'no-clean' flux systems of WOA type and some of the selected 'no-clean' flux systems. The studies include Fourier transform infrared spectroscopy (FT-IR) analysis of the activators as a function of temperatures and their possible influence on PCBA reliability including the effect on performance on conformal coating. Decomposition of the activator can be correlated with the water absorption on the PCBA surface and through the coating.

Cleaning in Electronics: Understanding Today's Needs

P.J.Duchi, Anne-Marie Laügt

INVENTEC PERFORMANCE CHEMICALS, Bry Sur Marne, France

pduchi@inventec.dehon.com

Abstract

Because of the phase out of CFC's and HCFC's, standard solder pastes and fluxes evolved from RA and RMA fluxes, to No-Clean, low residue No-Clean, and very low residue No-Clean. Many companies came out with their cleaning solutions, aqueous and semi-aqueous, with each product release being more innovative than the previous one. Unfortunately for most of the suppliers of cleaners, two other trends appeared; lead-free soldering and the progressive miniaturization of electronic devices. Miniaturization in electronics means reduction of solder pads, smaller components with lower stand off and tight spaces where flux can be entrapped. In addition new components are being introduced with higher capacities and functions: MEMS, microBGAs, LEDs, etc.

Traditional chemicals like CFC's, HCFC's, brominated solvents, detergents and glycols cannot do a good cleaning job anymore because most flux formulations have changed. Also, assembly processes have been modified due to smaller components and more compact board assemblies. The world is composed of two main things: organics and inorganics. Organics are made of resins and activators, whereas inorganics are made of salts, metallic salts and fillers.

Cleaning performance is affected by three main criteria. The first involves the Hansen Parameters which is a characterization of a contaminant to be dissolved and can be simplified by the solvency power of a product also known as the Kauri Butanol Index (KB Index). The second is surface tension, expressed in mN/m. This parameter must be considered because when the cleaning product cannot make contact with the contaminants under or around components, the contaminants cannot be dissolved.

The third criteria are the physical parameters like temperature, mechanical activities, and the process cycle.

The mastery to manage all of these parameters while facing high-tech miniaturization and environmental regulations, like ROHS, REACH, etc. brings innovation to cleaning in this electronic world.

Solder Paste Residue Corrosivity Assessment: Bono Test

Céline Puechagut, Anne-Marie Laügt, Emmanuelle Guéné, Richard Anisko
Inventec Performance Chemicals
Bry sur Marne, France

Abstract

Lead free soldering with no clean solder pastes represent nowadays the most common process in electronic assembly. A solder paste is usually considered as no-clean if it passes all IPC J-STD-004 corrosion tests: copper mirror, copper panel corrosion test, Surface Insulation Resistance (SIR) and Electrochemical Migration (ECM). Other SIR and ECM tests are described in Bellcore GR-78-CORE and JIS Z3197 standards.

Miniaturization is a common trend in electronics: boards have higher densities and narrower spacings between tracks and pads. Thus dendritic growth by electrochemical migration can become a big problem. Although SIR and ECM tests are recognized by all standards authorities to evaluate the solder paste residue corrosivity after reflow, a more selective method, the Bono test, has been developed and implemented in some French companies as a qualification criterion. It has been proven that compared to common corrosion tests, the Bono test better differentiates the nature of solder paste residues.

Corrosion in electronics: Overview of failures and countermeasures

Morten Stendahl Jellesen, Vadimas Verdingovas, H  l  ne Conseil, Rajan Ambat
Materials and Surface Engineering, Department of Mechanical Engineering, Technical
University of Denmark, DK-2800 Lyngby, Denmark, msj@mek.dtu.dk

The overall corrosion reliability of electronics depends on many aspects including the materials involved for the printed circuit boards assembly (PCBA), its fabrication and assembly processes, its electrical bias, and external service life environmental conditions such as humidity, temperature, and contamination. These aspects can individually or in combination lead to premature failure of the PCBA.

Many field failure returns of electronics are marked as “no failure found”, yet numerous of these failures are likely due to corrosion, since corrosion related failures are not easily detected during subsequent failure analysis. In some cases failures are intermittent and occur because of service life conditions (humidity and contamination) where water film formation on the PCBA leads to leakage currents resulting in wrong output signal of the electronic device. If the leakage current itself will not result in malfunctioning of the electronics, the formed water film and potential bias of the PCBA will eventually lead to failure caused by more easily recognisable corrosion. Typical corrosion failure types seen in electronics are galvanic corrosion, electrochemical migration, and other types of bias induced corrosion.

This paper describes the most commonly used metals and alloys in electronic devices including aluminium, gold, copper, silver, tin, lead and their alloys. Galvanic series performed in a flux solution is presented together with examples of galvanic corrosion causing failure of electronics.

Failures that find root cause in the manufacturing process are described in details, e.g. flux activator related failures and degassing from laminates during soldering. Failures caused by service life conditions with high humidity, sodium chloride aerosols and sulphur containing gaseous environments are also described.

Finally it is described how the architecture of the PCBA (the placement of components) will affect the corrosion reliability. Infrared camera imaging is used to show the thermal distribution of the PCBA during power on periods and can reveal the local cold spots on the PCBA being prone to condensation and corrosion.

Salt Spray Corrosion Test Methods – an overview

Anders B. Kentved and Kim A. Schmidt, DELTA, Hoersholm/Denmark

Salt spray corrosion testing can be performed according to many different test methods and for different purposes. This poster will give a schematic overview illustrated by several practical examples for electronic products.

Background

Failures in electronics and mechanics due to corrosion in harsh salt-laden environments, such as off-shore and automotive, is a well-known problem. A large number of different salt mist tests have been developed in order to test the corrosion resistance of products used in environments with salt mist. As the number of salt mist corrosion tests have increased, it has become more and more important to know the strategy behind and the purpose of each test. This is relevant both when selecting the right test for a given situation, as well as in order to interpret the results in the right context.

Corrosion Test Overview

The poster will give a graphical overview of different salt mist corrosion tests relevant for electronic products. The overview will include short descriptions of different test strategies and different test purposes. Illustrations and photos from a number of practical cases with different electronic products will be included. The poster will link between the examples to relevant international recognized testing standards. It may be the new IEC 62506 “Methods for product accelerated testing”, the generic EN/IEC 60068-2 series, and specific ISO. Examples from actually performed Highly Accelerated Corrosion Testing (HACT) will also be included.

The poster will also link to the Danish Innovation Consortium “IN SPE” project to be initiated in 2014. The consortium will deal with corrosion aspects relevant for development and production of reliable products to be used in harsh corrosive environments.

An On-site Atmospheric-corrosion Sensor

*Rintaro Minamitani, Hitachi Research Laboratory, Hitachi, Ltd.,
832-2 Horiguchi, Hitachinaka, Ibaraki, 312-0031, Japan*

Introduction

An on-site measurement sensor for evaluating the corrosivity of environments installing electronic equipment was developed. The sensor measures the thickness of corrosion products on the basis of the difference in the colors of non-corroded metal and a corrosion product. It requires no professional knowledge of instrumental analysis.

Measurement principle

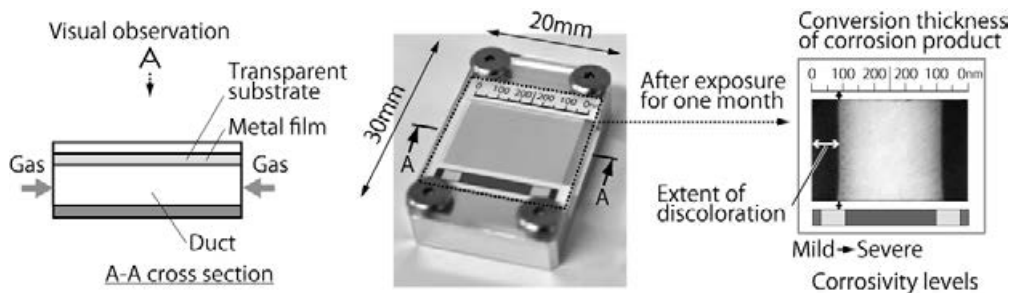
The on-site sensor consists of a metal film (on a transparent substrate) and a duct. The metal film corrodes when exposed to corrosive gas. Under such a condition, the corrosion product forms on the exposed surface of the metal film and proceeds down through the film towards the transparent substrate; that is, it does not form from the transparent side. The metal film near the inlet of the duct corrodes through its full thickness, while the metal film away from the inlet of the duct corrodes partially. In the former case, the color of the corrosion product can be seen through the transparent substrate. In the latter case, the color of the non-corroded metal can be seen because the film has not yet corroded all the way through. The extent of discoloration can be converted by a corrosion simulation to measured thickness of corrosion product of an exposed metal coupon by the conventional method. The levels of corrosivity are classified in terms of the measured thickness of corrosion product.

Applicability

Silver corrosion sensors and conventional silver coupons were used to investigate the corrosion behaviour when exposed in a mixed-flowing-gas test. Since the silver film is corroded by the same mechanism as the coupon, it was possible to use the sensor instead of the coupon to measure the thickness of the corrosion product.

Conclusion

This sensor is compact, inexpensive, and does not require a power supply; therefore, it can be easily and safely used in any location installing electronic equipment. Additionally, corrosivity can be determined on-site, without the need for data collection or analysis.



Environmental Stress Corrosion of Polybutylenterephthalate: A Common Material for Electronic Housings

G. Klett, M. Fürtsch, A. Hachtel and L. Müller
Robert Bosch GmbH, Reutlingen, Germany
Email: Lutz.Mueller@de.bosch.com

The glass fibre reinforced PBT Polybutyleneterephthalate is used in high volumes for housings for second level packaging of electronics. Water tight PBT housings are used to protect against corrosive environments. These housings are mounted with metallic fixtures (screws, bushings, brackets and sheet metal). Corrosion of these fixtures will occur under exposure to external environments. Bimetallic and crevice corrosion can produce alkaline conditions. Increase in pH upto 13.5 was measured. The PBT is sensitive against alkaline induced stress cracking (ESC environmental stress cracking). A combination of internal stress in PBT and impact of alkaline conditions produced by corrosion can cause crack-formation in the housing. If these cracks reach internal electric conductors of the housing, the second level package fails.

Remedies: Avoidance of bimetallic or crevice corrosion of the housing fixtures and on the other hand reduction of residual internal stress in the PBT and change to hydrolysis resistant PBT. Hydrolysis resistant PBT's, i.e. PBT's with additives against hydrolytic decay due to hot water, are significantly less sensitive against alkaline induced ESC.

The effect of a post-electroplating electrochemical oxidation treatment on whisker formation from tin coatings

M.A. Ashworth¹, D. Haspel¹, L. Wu¹, G.D. Wilcox¹ and R.J. Mortimer²

¹ *Department of Materials, Loughborough University, Leicestershire, LE11 3TU, UK*

² *Department of Chemistry, Loughborough University, Leicestershire, LE11 3TU, UK*

Electroplated tin finishes are widely utilised in the electronics industry due to their excellent solderability, electrical conductivity and corrosion resistance. However, the spontaneous growth of tin whiskers during service can result in localised electrical shorting or other harmful effects. Tin whiskers have been responsible for a wide range of electrical equipment failures in consumer products, safety critical industrial and space based applications. Until recently, the growth of tin whiskers was effectively mitigated by alloying the tin with lead. However, EU legislation prohibiting the use of lead in electronics (RoHS) has led to renewed interest in finding a successful alternative mitigation strategy.

Different strategies have been developed to mitigate the formation of tin whiskers, including the use of a post-electroplating anneal, the application of a polymeric conformal coating that acts as a physical barrier to impede whisker growth and the use of a nickel underlay to prevent the formation of Cu_6Sn_5 intermetallic at the interface. The aim of the current study was to investigate the influence of the surface oxide on whisker growth using electrochemical oxidation in potassium bicarbonate-carbonate and borate buffer electrolytes to produce oxide films of controlled thickness.

The effect of oxide thickness on whisker growth has been investigated for tin electrodeposition onto both copper and brass substrates. The influence of applied oxidation potential on the thickness of the Sn oxide film has also been investigated using x-ray photoelectron spectroscopy (XPS). Whisker growth for electrochemically oxidised Sn-Cu deposits on Cu and Sn deposits on brass has been investigated and compared with samples left to develop a native air-formed oxide.

Whisker growth studies demonstrate that electrochemically oxidised Sn-Cu electrodeposits on Cu and Sn deposits on brass are significantly less susceptible to whisker growth than those left to develop a native oxide film. For Sn deposits on brass, the electrochemically formed Sn oxide greatly reduces Zn oxide formation at the surface of the tin deposit, which results in whisker mitigation. For Sn-Cu deposits on Cu, the reduction in whisker growth is derived from the increased thickness of the Sn oxide, i.e. the Sn oxide film has an important role in stemming the development of whiskers.

Tin Electrodeposits Produced using Non-Aqueous Ionic Liquid Electrolytes: Whisker Formation

*C. J. Stuttle, Department of Materials, Loughborough University, LE11 3TU, UK.
M. A. Ashworth, Department of Materials, Loughborough University, LE11 3TU, UK.
G. D. Wilcox, Department of Materials, Loughborough University, LE11 3TU, UK.
R. J. Mortimer, Department of Chemistry, Loughborough University, LE11 3TU, UK.*

Tin electrodeposited coatings on copper are commonly utilised in the electronics industry for their inherent beneficial properties, such as a high solderability and high corrosion resistance. However, these coatings have been reported, at times, to initiate whisker formation leading to electronic shorts, with an example whisker seen in Figure 1. Tin alloying and different aqueous electroplating solutions have been shown to lead to varying whiskering propensities; increasing or decreasing levels of whisker mitigation.

Deep eutectic solvents, a subgroup of ionic liquids, are an emerging novel electrolyte class from which Sn and Sn alloys may be electrodeposited. Due to the markedly differing chemistries of deep eutectic solvents compared to traditional aqueous solutions the resulting electrodeposits require investigation into their suitability as a pure tin replacement and the extent of their whiskering propensity. In this study three deep eutectic solvents were examined; ethaline, propeline and reline.

All three solvents permitted the reduction of Sn(II) from SnCl_2 at varying concentrations and rates onto static 4 cm^2 Cu substrates. Although reduction has been possible for all trials only a few specific conditions resulted in electrodeposits deemed to be acceptable in terms of coating quality, as seen in Figure 2. The resulting acceptable Sn electrodeposits formed uniform coatings with low dendritic growth but within two weeks after electrodeposition filament whiskers were observed on the surface. The whiskers formed from these deposits feature diameters ranging between $0.2 \mu\text{m}$ to $1 \mu\text{m}$ and maximum lengths of $\sim 20 \mu\text{m}$. Although to date these tin coatings have formed whiskers the electrolytes used in this study will, in future investigations, allow the deposition of novel tin alloys. This is due to their large potential window compared to aqueous systems, thus allowing the formation of novel alloy electrodeposits which may result in successful tin whisker mitigation.

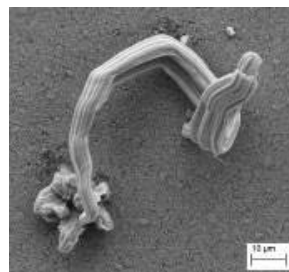


Figure 1: SEM micrograph of tin whisker from a tin electrodeposit on brass substrate.

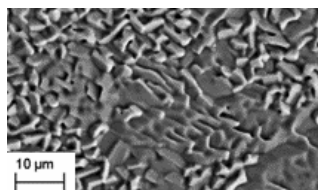


Figure 2: SEM micrograph of tin electrodeposit created from a propeline based electrolyte.

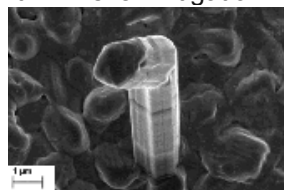


Figure 3: SEM micrograph of tin whisker from an electrodeposit surface created from a propeline based electrolyte.

Basic physics of moisture challenges in electronic packaging - a tutorial overview

J.B. Jacobsen, A. Holm, J.P. Krog, L. Rimestad and A. Riis
Grundfos A/S, Poul Due Jensens Vej 7, 8850 Bjerringbro, Denmark
Email: jbjacobsens@grundfos.com

More and more electronics are being used in climatically harsh environments. Therefore, the challenge of climate-protective packaging increases. Compared to thermo-mechanical loads, relatively little is known among design engineers on how to design for robustness and how to predict lifetime for electronics in moist environments and in condensing applications.

In response, this presentation offers a tutorial overview on how moisture problems can be understood by appreciation of basic physical mechanisms, which are intuitively clear to most people as they are observed in our daily environment. Furthermore, the paper points to design pitfalls – such as over-emphasizing formal ingress protection rating – and it offers the basics of a systematic design approach.

Climatic durability of modern assembly technologies in electronics

Pavel Žák¹, Kateřina Kreislová², Dušan Majtas³

¹ Czech Technical University, department of electrotechnology, Prague/ Czech republic,

² SVÚOM Ltd., Prague/Czech Republic,

³ UTAM/CET, Telč/Czech Republic

The paper presents the current results of the experiments conducted in the field of climate durability of materials permitted by the EU RoHS Directive for the assembly of electrical and electronic equipment. The biggest technological change in current electrical production was legislatively the transition to lead-free soldering technology and finishes in all the parts of electrical equipment due to the necessary performance of requirements of the RoHS Directive and its subsequent amendments.

The authors focused primarily on the issue of climate durability of circuit made of lead-free solders based on alloys with a predominance of pure tin and electrically conductive adhesives based on epoxy resin filled with silver particles. Corrosion represents one of the major degradation mechanisms for these mounting technologies which reduce their reliability. Experiments were performed in the laboratory conditions, in which the mounting technologies, both solders and adhesives achieved very satisfactory results in terms of both the electrical and the mechanical properties.

Laboratory research has resulted into the verification of the results by performing long-term experiments under the real climatic conditions. Degradation was studied in standard environment as well as in the the harsh environment of motorway tunnel.

Basic electrical and mechanical properties were studied during the ageing processes. In this segment of the research, quite unexpected result was achieved, particularly in the solder alloy.

At the same time in the paper authors discusses a new and currently very topical issue of the relationship between durability and reliability of the products in relation to their ecological characteristics and possibilities of their practical and subsequent recycling.

Obtained results justify the author's to express doubts about the possibility of replacing the previously used SnPb mounting technology and some existing surface treatment methods by the one proposed in the RoHS Directive across the spectrum of manufacturing of electrical and electronic equipment.

Based on the experimental results, the paper also evaluate the climatic, technological and reliability implications of this legislation forced transition to lead-free assembly technology.

Understanding moisture protection of coated electronic circuits in terms of water permeation and electrochemical corrosion

J.P. Krog*, M.Ahmed, M.S. Jellesen, J.B. Jacobsen*, and R. Ambat
Department of Mechanical Engineering, Technical University of Denmark, DK 2800
Lyngby, Denmark

*Grundfos A/S, Poul Due Jensens Vej 7, 8850 Bjerringbro, Denmark

Does conformal coating and silicone gel potting improve the robustness and lifetime of printed circuit board assemblies against moist environments? This question is frequently debated but a consensus has not been reached. The lack of consensus seems to be related to different perceptions of what kind of protection to expect from a coating and on which time scales and against which moisture load such measures should protect the printed circuit board assembly (PCBA).

In this paper we formulate a framework of understanding moisture-related deterioration of PCBAs and of protection mechanisms provided by conformal coating and potting materials. Further, we report on material data obtained on coating materials and on findings on failure mechanisms on coated PCBAs. The framework and the results enable a more detailed discussion of when and how to benefit from using conformal coatings or potting on PCBAs. The water transport characteristics for coating and potting materials described based on the electrical measurements on coated test-boards including impedance spectroscopy. The observed relations between well-defined contamination levels and time to failure in well-defined climates will also be discussed.

Development and evaluation of atmospheric corrosion sensors using printed circuits.

*E. Roblero, F. Corvo, V. Moo-Yam, E. García-Ochoa, T. Pérez
Universidad Autónoma de Campeche, Campeche, México, ave. Agustín Melgar s/n,
Col Buenavista, P.O. Box 24039, Campeche, México.*

Atmospheric corrosion evaluations take a long time due to the relatively low corrosion rate of the process. Many factors are involved in atmospheric corrosion process. It is the summa of different meteorological and pollution events occurring as time goes on.

The use of corrosion sensors allow to determine corrosion rate in short periods of time. The corrosive effect of different meteorological and pollution events can be determined individually using sensors.

Interdigital corrosion sensors have been developed using screen printing technique. Printed circuits based on a copper layer deposited on Bakelite were used.

Corrosion rate was determined using three electrochemical techniques: Electrochemical Noise, EIS and Polarization Resistance. In parallel, corrosion rate was evaluated by weight loss using copper wires.

In order to a complete characterization of sensors, corrosion behaviour was evaluated in five solutions having wide differences: Acid solutions: HCl 0.1 N and HNO₃ 0.1N, Neutral solutions: NaCl 3% and (NH₄)₂SO₄ 0.01 M and NaOH 0.1 N as basic solution.

Corrosion rate was evaluated under complete immersion and under a thin layer of electrolyte.

A comparison of the results obtained by different electrochemical techniques under complete immersion and under thin layer of electrolyte and weight loss is made. Respecting the electrolyte layer, measurements were made under evaporation conditions. Significant differences have been observed between the different solutions and between immersion and thin layer conditions.

Influence of single surface ash layer on dual corrosion

Maria Mosquera Feijoo¹, Axel Kranzmann¹, Alba Baselga Zapater²

¹Federal Institute for Materials Research and Testing (Berlin)

²Institut Químic de Sarrià (Barcelona)

In a number of technical heat transfer devices both media can corrode the heat exchanger material. (1) In our experiments we are focused on steam oxidation and flue gas ash corrosion attacking the opposite surfaces of the metal specimen. Dual effect corrosion was also observed on SOFC interconnectors, where ash plays no role.

Different dual atmosphere exposures have been tested with different metals, including VM12, P92, Fe-14%Cr, Fe-9%Cr and Fe-armco. The exposures were performed at 600°C for 24, 240 and 960 hours. For the first condition, both sides (with and without artificial ash) were exposed to a flue gas (27H₂O-60CO₂-1SO₂-10N₂-2O₂). For the second condition, the flue gas was used on the ash side and steam was applied on the other side.

The specimen was laid flat in the constant temperature region of the chamber, with the help of a gold ring. The heat treatment takes place in a ceramic tube, because of its inert character. The gas is applied at a constant volumetric rate in the middle of the sample.

In this study the effects of ash in flue gas atmospheres covers an analysis of the impact of temperature, steam flow rate, specimen shape and specimen surface finish of oxidation of resistant materials. The resulting dual effect was analyzed and compared with standard coupon tests.

References

1. **D. Huenert, W. Schulz, A. Kranzmann.** Corrosion behavior of ferritic and martensitic power plant steels under conditions of dual atmospheres. *Nace Corrosion*, 66. 2010.

Acoustic emission analysis coupled with thermogravimetric experiments dedicated to high temperature corrosion studies on metallic alloys

PERES Véronique^a, AL HAJ Omar^a, SERRIS Eric^a, GROSJEAN François^b, KITTEL Jean^b, ROPITAL François^b, COURNIL Michel^a

^a Ecole Nationale Supérieure des Mines, SPIN-EMSE, CNRS:UMR 5307, LGF, 42023 Saint-Etienne France,

^b IFP Energies nouvelles, Rond-point de l'échangeur de Solaize BP3, 69360 Solaize France.

High temperature corrosion of metallic alloys (like Iron, nickel, cobalt alloys) can damage equipment of many industrial domains (refinery, petrochemical ...). It represents a major challenge. Acoustic emission (AE) is an interesting method owing to its sensitivity and its non-destructive aspect to quantify the level of damage in service of these alloys under various environmental conditions. High temperature corrosive phenomena create stresses in the materials; the relaxation by cracks of these stresses produces transient elastic waves which can be recorded and analyzed using the AE system. The study of these transient waves enables the anticipation of the degree of damage of the alloys. Several methods are used to record and analyze these transient elastic waves. Piezoelectric sensors fixed directly on the structure can be used. But in case of high temperature environments, a waveguide may be used to transmit waves from the sample to the sensors. The goal of our study is to establish an acoustic signals database which assigns the acoustic signals to the specific corrosion phenomena. This database will then be useful for the monitoring of industrial equipment using acoustic emission methods. For this purpose, thermogravimetric analysis (TGA) has been coupled with acoustic emission (AE) devices. Simultaneous measurements of the mass variation and of the acoustic signals emitted during the corrosion of samples at high temperature provide complementary information. For this purpose a specific alumina waveguide (WG) has been developed.

The oxidation of a zirconium alloy, zircaloy-4, was firstly studied using thermogravimetric experiment coupled to acoustic emission analysis to validate the waveguide operation at 900 °C. An inward zirconium oxide scale, preliminary dense, then porous, grows during the isothermal isobaric dwell. The kinetic rate increases significantly after a kinetic transition (breakaway). This acceleration is accompanied by an acoustic emission activity. Most of the acoustic emission bursts were recorded after the kinetic transition. Acoustic emission signals were also observed during the cooling of the sample. AE numerical treatments completed by SEM and in-situ Raman microscopy characterizations allow us to distinguish the different populations of cracks.

Metal dusting represents also a severe form of corrosive degradation of metal alloy. Iron metal dusting corrosion, with or without pre-oxidized layer, was studied by EA coupled with TGA at 650°C under $C_4H_{10} + H_2 + He$ atmosphere. Acoustic emission signals were detected after a significant increase of the sample mass (carbon deposit).

From these innovative studies we can conclude that reversible mechanisms as diffusion of atoms (Fe cations in case of iron outward oxidation) are not emissive. Irreversible mechanisms, as cracks initiation and propagation, are audible.

INTEGRATED RISK MANAGEMENT PROGRAM TO ALLOW SAFE, PROFITABLE PROCESSING OF OPPORTUNITY NAPHTHENIC ACID CRUDES

Philip Thornthwaite, Nalco Champion, Northwich, United Kingdom

Kevin Clarke, Permasense, Horsham, United Kingdom

Dr Jacob Davies, Permasense, Horsham, United Kingdom

Abstract

Continuing economic pressures on the European refining industry are forcing more refiners to evaluate the possibilities of processing lower priced, opportunity naphthenic acid crudes in order to improve margins. The processing of naphthenic acid crudes introduces significant challenges to the refiner, with the risk of high temperature naphthenic acid corrosion being one of the primary concerns.

If refiners are to take full advantage of these discounted opportunity crudes, these challenges need to be addressed in order to avoid margin attrition caused by decreased equipment reliability and run length. In order to safely process naphthenic acid crudes, a comprehensive risk management program is developed with the refinery in order to assess, monitor and mitigate naphthenic acid corrosion and other processing impacts associated with these crudes.

One of the most critical aspects of this risk management methodology is the implementation of a corrosion monitoring program robust enough to ensure corrosion rates are not excessive when TAN levels are increased. Recent developments in permanent ultrasonic thickness measurements provide the refiner with a cost effective, reliable means to install a rigorous corrosion monitoring program that provides comprehensive coverage of the areas identified to be at elevated risk of naphthenic acid corrosion.

With a rigorous monitoring program in place, the applied corrosion control strategies can be optimised to ensure corrosion rates are not excessive and asset reliability and integrity is not compromised.

This paper provides an overview of the risk assessment methodology and how it is applied to assess and monitor the risks in conjunction with a rigorous corrosion monitoring program comprising of multiple ultrasonic sensor placements.

Passivation behaviour of stainless steel (UNSN-08028) in industrial phosphoric acid contaminated with chlorides and sulfates at 80°C

Authors: M. BenSalah ^{a,b}, R. Sabot ^b, E. Triki ^a, L. Dhouibi ^a, Ph. Refait ^b and M. Jeannin ^{a,*}

(a) Unité de Recherche de Mécanique et Energie, ENIT, Université de Tunis-El-Manar, BP 37, Tunis Belvédère, 1002, Tunisia.

(b) Laboratoire des Sciences de l'Ingénieur pour l'Environnement (La SIE), UMR 7356-Univ. La Rochelle, Bât. Marie Curie, Av. Michel Crépeau, F-17042 La Rochelle cedex 01, France.

Phosphoric acid in pure state is not very corrosive compared to nitric or sulphuric acids. Nevertheless, ninety-five percent of phosphoric acid is obtained by the wet process [1], which generates severe corrosion problems due to high temperature and impurities such as chlorides, fluorides and sulphides [2–5]. So, the choice of materials used in this industrial process plays an important role since they must have both good chemical and mechanical resistance. In this sense, austenitic stainless steels are a good choice for phosphoric acid solution contaminated with 0, 34 wt% of SO_4^{2-} , 0.026 wt. % Cl^- and 0.32 wt. % F^- . In this study the corrosion behaviour of a highly alloyed austenitic stainless steel (UNSN-08028) Sanicro 28 was evaluated in 50 wt. % industrial phosphoric acid medium at 80°C. The corrosion resistance was also investigated by increasing the chloride concentration up to 0.46% in order to improve the resistance of the passive film.

The electrochemical experiments were carried out in open to atmosphere and non-stirred conditions in a classical three electrodes glass cell. Potentiodynamic experiments and potentiostatic tests at different potentials were performed in order to characterize the kinetic of formation and the behaviour of the passive film. OCP measurement at 80°C during 48h were performed to evaluate at long time exposition to different chloride concentration on the resistance of the passive film used to the power low model was used to analyzed the EIS experiments and to evaluate the passive film thickness

The main conclusions drawn from the research are summarized as follows:

Even with the highest chloride concentration, no pits were observed after 48h of immersion. OCP values remained high for the lowest concentration of Cl^- indicating that the stainless steel was spontaneously passivated. Although OCP decreased in the active domain for higher concentrations, no pits were observed after 48h of immersion. Potentiodynamic experiments have shown the presence of a passive state, whatever the chloride concentration although a slight increase in the passive current densities and a decrease in the transpassive potential were observed. The very high impedance values observed for the lowest concentration were due not only to the resistive passive film composed of chromium oxides and nickel oxides but to the formation of iron phosphate and chromium phosphate underneath a polyphosphate film identified by micro-Raman spectroscopy. At higher concentrations, the passive film resistance decreased due to the aggressiveness of chloride ions but the presence of phosphate and the subsequent formation of iron phosphates inhibit the formation of pits.

References

- [1] Pierre becker , *Technology, and Economics of the wet process*, second ed, M. Dekker, NewYork, 1989.
- [2] A. Bellaouch , A. Guenbour, A. Benbachir, *Corrosion* 49 (1993) 656-662
- [3] S. El Hajjaji, L. Aries, J. Audouard, F. Dabousi, *Corros, Sci*, 37 (1995) 927-939.
- [4] H. Iken, R. Basseguy, A.B. Bachir, *Electrochemical. Acta* 52 (2007) 2580-2587.
- [5] A. Guenbour, M.A .Hajji, E.M. Jallouli, A.B Bachir, *appl. Surf. Sci.* 253 (2006) 2362-2366.

FAILURE ANALYSIS OF BOILER FURNACE WALL TUBE

Mohammed Al Muaisub, SABIC Technology Center, Saudi Arabia
Avtandil Bayramov, SABIC Technology Center, Saudi Arabia

This paper discusses a failure analysis of a furnace side wall tube of the package boiler in utility. Before the failure, the chemical cleaning was carried out. Then, the hydrostatic testing was performed. During the testing, one tube was ruptured. This tube has been in service for 8 years and its material of construction is SA 178 Gr. C. The failed tube has been analyzed using stereoscope, optical microscope, scanning electron microscopy and energy dispersive spectrometer. It is concluded from the investigation that the failure was associated with multimode failure mechanisms, primarily caustic gouging followed by creep rupture. Damages were attributed with localized overheating. It is important to note that no spheroidization of carbides was found.

Heavy metal inputs from anodic dissolution of Al-Zn-In galvanic anodes to the marine environment: TALINE Project

Samuel PINEAU, ACCOAST, Arradon/France
Jonathan DEBORDE, ACCOAST, Arradon/France
Anne-Marie GROLLEAU, DCNS, Cherbourg/France
Philippe REFAIT, Université de La Rochelle/LaSIE, La Rochelle/France
Christelle CAPLAT, Université de Caen/BiOMEA, Cherbourg/France
Olivier BASUYAUX, SMEL, Blainville-sur-mer/France
Marie-Laure MAHAUT, Cnam/Intechmer, Cherbourg/France
Stéphane LE GLATIN, LDA, Saint Lô/France
Paco BUSTAMANTE, Université de La Rochelle/LIENSs, La Rochelle/France
Jean-Louis GONZALEZ, Ifremer, Seyne-sur-mer /France
Christophe Brach-Papa, Ifremer, Nantes/France
Patrick HONORE, CCI-CO Port de Calais, Calais/France

Due to the lack of informations about the environmental impact of cathodic protection of marine steel structures using sacrificial anodes, a research program, called *TALINE (Transfers of metallic elements from ALuminium-INdium galvanic anodes to marine Environment)* has been implemented in 2012 in the Calais Harbor (France).

This study focuses on three objectives: (i) implement and test a five-year in situ monitoring of the metallic elements from sacrificial anodes; (ii) assess with laboratory experiments the nature and the transformation of the corrosion products; and (iii) examine the transfers of anode corrosion products toward the aquatic system and the sediments.

The first step of this work supported a qualitative and quantitative statement of metal concentrations in marine waters, sediments and biota in the harbor before the sacrificial anode installation. These results will enable to compare long-term evolution of the metal concentrations and the potential environmental impact of galvanic anodes. Laboratory experiments provided the preliminary analytic results of corrosion product nature and transfers from sacrificial anodes to water; and qualify the appropriate methods, which initiate new and innovative research perspectives.

Design of Cathodic Protection retrofitting of subsea pipelines assisted by FEM modeling

Paolo Marcassoli, Monica Ginocchio, Bruno Bazzoni, Cescor srl, Milan, Italy

Abstract

The wide installation of subsea pipelines during '70s and '80s, related to the increased number of exploited oil and gas field, currently poses a problem with respect to their integrity. In fact, several pipelines reached or are now approaching the end of design life, but the still high productivity of relevant connected wells and platforms require an operating life extension. From the internal corrosion point of view, ILI, hydraulic tests or direct assessment procedures allow to evaluate the conditions of pipeline in terms of wall thickness and to estimate residual life. However, as far as the external conditions, particularly Cathodic Protection (CP), are concerned, due to subsea pipelines are almost protected with galvanic anode systems installed before laying, it is necessary a retrofitting in order to preserve protection conditions. Whenever possible, CP retrofitting shall be performed before complete anode depletion, in order to maintain steel polarization and the beneficial calcareous deposit, limiting the initial current demand. CP retrofitting can be performed with both galvanic or impressed current systems, depending on the specific application and its main characteristics.

This paper analyse the Cathodic Protection retrofitting of subsea pipelines with the use of galvanic anode sleds or impressed current anode sleds. Although the design of cathodic protection systems was performed with traditional approach, the potential and current distribution along the pipeline were also evaluated by means of FEM modelling. This allows to minimize the number of anode sleds and to optimize their locations, thus ensuring a reliable but easier installation in field. The geometry and main environmental parameters typical for the cases under study were modelled. Boundary conditions take into account for the corrosion electrochemical processes through the Butler-Volmer equation, i.e. the secondary current distribution was analysed. The anode interference was investigated by varying the distance between the sleds and the pipelines and by varying the anode to anode distance. Coating breakdown was also considered. Furthermore, the effect of presence of a localized coating holiday was introduced and evaluated.

Volume synthesis of a calcareous deposit on steel under cathodic protection by impressed current

Alaric ZANIBELLATO, René SABOT, Philippe REFAIT, Marc JEANNIN

Laboratoire des Sciences de l'Ingénieur pour l'Environnement (LaSIE) UMR CNRS 7356, Université de La Rochelle, France

Cathodic protection, applied on steel in marine environment, leads to the formation of calcium carbonate and magnesium hydroxide deposit to the metal surface (calcareous deposit). In the case of protection by imposed potential (-0.9 V/SCE to -1.1 V/SCE), numerous laboratory studies on gold, stainless steel or construction steel have shown that a thin calcareous layer cover the metal surface leading to a decrease in current demand. Our objective in the context of the Ecocorail project (supported by the French National Research Agency) is different as we seek to promote the formation of the deposit in volume (several centimeters thick) in semi-natural conditions. Thus, this calcareous conglomerate could serve as natural cement allowing a global cohesion between marine sediments, sand, shells...

In order to avoid the surface blocking by the deposit, impressed current was used. Different conditions of current density were imposed. An experimental device was developed consisting of aquarium (10L) where filtered and sterilized natural seawater circulates. Concrete steel rods were cathodically polarized at different current densities for 10 days. The calcareous deposit obtained, and the steel surface, were then analyzed by μ -Raman spectrometry and X-Ray Diffraction.

The results show that at low current density (-0.1 mA/cm²), the steel surface was covered by a thin layer of pyroaurite instead of calcareous deposit. Pyroaurite is a Mg(II)-Fe(III) hydroxycarbonate resulting from the residual corrosion of the steel and the presence of Mg ions. The oxygen reduction leads to an increase of pH and then to the precipitation of Mg(II)-Fe(II) hydroxide sheets that is afterwards oxidized into pyroaurite. This hydroxide covers the entire surface whereas the potential given by the steel remains around -0.9 V/Ag/AgCl. For a current density of -0.15 mA/cm², leading to a potential of -1.1 V/Ag/AgCl, some calcareous deposit in the form of monohydrocalcite are observed whereas the remainder of the rod was covered by corrosion products as akaganeite, pyroaurite and magnetite. The presence of these corrosion products results also from the residual steel corrosion even at those cathodic potentials. The absence of calcareous deposition could be explained by the effect of pyroaurite blocking, which covers a large part of the steel rod. Stronger currents (-0.20 mA/cm² and -0.25 mA/cm²) should be applied to allow calcareous deposit to develop. The steel potential is then -1.2 V/Ag/AgCl. The quantification of the different phases making up the deposit, obtained by using the XRD MAUD software, shows that the deposit consists generally of about 80% by weight of brucite (Mg(OH)₂). The other phases are aragonite (10%), calcite (5%) and monohydrocalcite (5%). Analysis by ionic chromatography after dissolving of such deposits results in a Ca / Mg ratio of 5/10 in agreement with the XRD results.

Experimental study is also focused on growing calcareous deposit on steel rod with different sediments, such as sand or shell. Those experiments run for two months at -1 mA/cm² in natural seawater from English Channel, revealed some promising results on the ability of the calcareous deposit to act as cement.

Coating deterioration and corrosion on offshore wind power structures: A review of inspection results

Andreas Momber, Muehlhan AG, Hamburg, Germany

The paper reports about causes for coating deterioration and substrate corrosion on offshore wind power structures in the North Sea and the Baltic Sea. This includes tower structures and transformation platforms. The report is based on regular coating inspections performed by certified coating inspectors. Damage types include the following: blistering, underrusting, flaking, mechanical damage, wear. Steel construction details, such as corners, weld seams, difficult-to-paint areas, were found to be critical to the protection performance of the coating systems. Damages caused during transportation, erection and handling contributed notably to coating deterioration. A frequently observed substrate corrosion type was bi-metal corrosion.

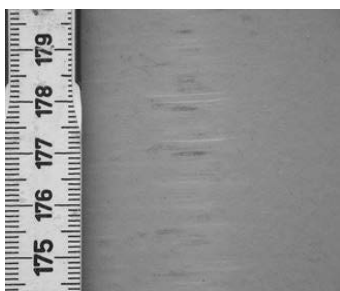
Typical examples are shown below.



Impact damage



Coating deterioration



Transport damage



Bi-metal corrosion

Cathodic protection for marine structures: 3 case studies

Sameer Ayyar & Jacob Jansson, COWI A/S, Copenhagen, Denmark

Abstract

The article presents three case studies on cathodic protection design for marine structures and compares the experiences learned from the three different cases.

The first case involves the steel shaft in the foundation of a suspension bridge in slightly brackish water (Marmara Sea).

The second case involves steel monopile foundation of an offshore wind turbine foundation in normal sea water (North Sea).

The third case involves a jacket foundation of an offshore wind turbine foundation in brackish water (Baltic Sea).

In the first case, a sacrificial anode system was initially considered in view of simplicity of installation and operation. However as the structure was bare steel, it was found during design simulation that the sacrificial anode system would not polarize the structure adequately. In lieu, an impressed current system was designed. The design presented challenges with cable routing. The challenges were solved, and the project is now in the installation stage.

In the second case, a sacrificial anode system was considered in view of simplicity of operation. However, the installation of sacrificial anodes on to the monopile required a different approach with anodes installed on an external cage as a ring at the top section of the monopile for the deep foundations. For the deep foundations the solution with mounting the anodes at the bottom of the transition piece was expected to deliver inadequate protection at the lowest part of the structure. Boundary element method simulation was carried out which confirmed this, and validated the protection level offered by the anodes.

In the third case, a sacrificial anode system was considered in view of simplicity of operation. However, the design of sacrificial anodes presented challenges considering the high resistivity of Baltic Sea. It was decided to coat the submerged section of the jacket foundation to reduce the current demand of the anodes. Boundary element method simulation was carried out and it was seen that the protection level offered by the anodes is adequate.

Based on the three cases the advantage and disadvantages of sacrificial anode systems and impressed current systems are discussed for marine foundations, also taking coating system and installation factors into account.

Corrosive environment inside offshore monopile structures and challenges in monitoring

*Birit Buhr Jensen, DONG Energy, Denmark
Frits Grønvold, FORCE Institute, Denmark*

Offshore wind farms are typically designed with an anticipated service life of 25 years. Earlier it was assumed that the internal side of foundations below the lower working platform was airtight. If airtight, corrosion was assumed to cease when the oxygen present inside the foundation was consumed. This assumption has been shown not to be fully valid as both seawater and oxygen have access to the inside of the monopile under certain conditions. This may result in active corrosion, which can compromise the durability of the wind farm and reduce the service life if not prevented.

A marine offshore environment is highly aggressive with variable corrosion rates which can be high. In order to assess the actual corrosion rates and thus decide on appropriate corrosion prevention a series of measurements have been made. These comprise both manual measurements together with measurements on a permanent monitoring system installed on one DONG Energies wind turbine farms. Dissolved oxygen, temperature, salinity, pH-values and potentials are being measured manually and in the automated system.

The automatic monitoring system has been installed in 10 individual monopiles, and manually measurements conducted on these and another 11 monopiles.

The monopiles have been equipped with sacrificial anode cathodic protection systems. The effectiveness of the cathodic protection and corresponding water quality measurements have been tested. Also water quality measurements on foundations prior to embedment of anodes were made and serves as reference.

This paper will present details of the automatic monitoring system used, the effectiveness and the effect of cathodic protection on corrosion and water quality.

Durability of coating repair systems for offshore service

A. R. Black, P. K. Nielsen, FORCE Technology, Brøndby/Denmark

It is well-known that coating damage may occur on offshore wind structures during their structural lifetime due to climatic breakdown since the offshore location exposes the structures to heavy stresses and a marine corrosive environment. Construction and installation actions may also induce mechanical damage of the protective coating. Furthermore, structures may even be installed offshore without any proper coating protection in local areas due to e.g. production delay.

For damage to the immersed surfaces, good repair is not possible, and it must be trusted that the cathodic protection is effective. For the atmospheric zone and the upper part of the splash zone, coating repairs are possible.

Change in the weather offshore is a challenge to a reliable surface preparation and paint application. Consequently, versatile preparation methods and paints are mandatory to offshore coating repair.

The aim of this study has been to evaluate the effect of pre-treatment quality, number of coating layers and paint type on the durability of coating repairs under realistic application conditions. In total three different pre-treatment methods, three paint types and two painting systems have been evaluated through laboratory performance test methods, including neutral salt spray and water immersion tests.

Greater knowledge of the durability of coating repair systems under realistic application conditions may provide valuable information to wind farm owners when specifying coating repair procedures. Optimised paintwork specifications may reduce the number of offshore working days and thus provide significant savings in operating costs.

Kinetic of passivation of two stainless steel microstructures under tribocorrosion solicitations

Effect of pH and anodic applied potential.

V. Dalbert¹, N. Mary¹, B. Normand¹, C. Verdu¹, S. Saedlou²

¹ INSA-Lyon, MATEIS CNRS UMR5510, F-69621 Villeurbanne, France

² APERAM Research Center, rue Roger Salengro BP15, F-62330 Isbergues, France

Passivity of stainless steel is usually attributed to the formation on the metal of an oxide film which is a mixture of iron and chromium with oxygen inducing semiconducting properties. The film composition varies with both material and solution chemistry. Indeed, a major issue is to understand the role of these parameters on the rate of growth of passive films. To activate in-situ the depassivation - repassivation on stainless steels surfaces, electrochemical measurements have been implemented in tribocorrosion experiments. These provide a method of examining the electrochemical properties of metal surface initially free of oxide.

Electrochemical measurements consist in measuring the current-potential signal under the wear. From converted charge densities required for the film growth, models of repassivation have been proposed. More recently, electrochemical noise measurements and impedance spectroscopy measurement under wear have been used to access to the mechanism of repassivation. Results highlight that current transient for repassivation are obeying to a two-time constant law. Based on this two steps mechanism, wear current transients have been studied either under applied potential or various pH solutions under OCP to identify the impact of these parameters on the passivation kinetics.

Results obtained on two stainless steels microstructures with a nominal chemical composition indicate that repassivation is affected by the applied potential when it is located closed to the activity peak without an impact of the microstructure. To the opposite, time-constants become pH and microstructure dependant under wear at the OCP.

Tribocorrosion behaviour of stainless steel under cathodic potential.

N. Mary¹, V. Dalbert¹, B. Normand¹, B. Ter-Ovanesian¹, T. Borgna^{1,2}, L. Lefebvre^{1,2}, S. Saedlou²

¹ INSA-Lyon, MATEIS CNRS UMR5510, F-69621 Villeurbanne, France

² APERAM Research Center, rue Roger Salengro BP15, F-62330 Isbergues, France

Tribocorrosion studies are usually performed at open circuit potential or under anodic potentials in order to describe the total wear degradation of material. Such approach needs to define a reference concerning the mechanical degradation in absence of corrosion. Indeed, experiments in the cathodic domain can be performed. Several authors have pointed out that mechanical wear can evolve as a function of the applied cathodic potential. Most of them suggest a role of hydrogen embrittlement on the wear mechanism [1]–[3].

To understand the effect of hydrogen in the mechanical wear, results from tribocorrosion and nano-indentation have been compared. Wear volumes and surface morphologies are compared to the surface hardness evolution measured by nano-indentation. Two stainless steels have been selected: (i) a ferritique with carbides distributed homogenously in volume and (ii) a dual phase ferrite-martensite. Both have the same chemical composition in order to avoid an effect of nickel, carbon and chromium.

Results show an interaction between the hydrogen absorption mechanisms resulting on the surface hardness evolution and wear increase for lower cathodic potential applied, whereas the hydrogen evoluion to the surface for higher cathodic potential turn the wear from a wet to a dry mechanism.

- [1] S. Akonko, D. Y. Li, and M. Ziomek-Moroz, "Effects of cathodic protection on corrosive wear of 304 stainless steel," *Tribol. Lett.*, vol. 18, no. 3, pp. 405–410, Mar. 2005.
- [2] Q. Zhou, J. Li, and W. Chu, "Effect of hydrogen on the friction and wear of Ni-P coatings," *Int. J. Miner. Met. Mater.*, vol. 17, no. 2, pp. 241–245, Apr. 2010.
- [3] Y. Yao, L. J. Qiao, and A. A. Volinsky, "Hydrogen effects on stainless steel passive film fracture studied by nanoindentation," *Corros. Sci.*, vol. 53, no. 9, pp. 2679–2683, Sep. 2011.

The effect of surface condition on the friction coefficient of different dental archwires

Tadeja Kosec^a, Petra Močnik^a, Uroš Mezeg^d, Andraž Legat^a, Jasmina Primožič^b

*^aSlovenian National Building and Civil Engineering Institute,
Dimičeva 12, SI-1000 Ljubljana, e-mail: tadeja.kosec@zag.si*

*^bMedical Faculty, University of Ljubljana,
Zaloška 2, SI-1000 Ljubljana, Slovenia*

NiTi alloys as important technological material finds its wide application in different fields. Due to shape memory and superelastic properties it is widely used in biomedical applications. Generally, nickel titanium alloys are known for their good corrosion resistance, but in some circumstances they suffer from different forms of corrosion, like pitting and crevice. Beside corrosion, the wear resistance of this alloy is of critical concern in many applications. Since NiTi dental archwires experience severe failures in applications or reduced performance, it is of great importance to study the causes for such performance or failures.

The aim of this paper is to analyse the influence of the nature of the orthodontic archwires on the friction coefficient and wear rate against Al_2O_3 and materials commonly used as brackets (316L Stainless Steel). The materials selected as orthodontic archwires will be stainless steel and NiTi archwire. Unused and already used dental archwires with oral deposits will be examined in order to define the effect of plaque presence on friction coefficient and the performance of the wire. The roughness and hardness will be defined before and after wear tests. Wear tests will be carried out in an artificial saliva. A relationship between the hardness of the materials and the friction coefficients as well as the effect of material and different surface conditions of the dental archwire will be studied in order to correlate and understand different properties of dental archwires.

New advances and perspectives in the electrochemical study of tribocorrosion.

Michel KEDDAM¹, Pierre PONTIAUX², Vincent VIVIER¹

¹ *LISE-Laboratoire Interfaces et Systèmes Electrochimiques, Université P. et M. Curie, CNRS. 4, place Jussieu, 75252 Paris Cedex 05, France.*

² *Laboratoire LGPM, Ecole Centrale, Rue des Vignes, 92290, Châtenay – Malabry, France.*

Damages due to abrasion, wear, slurries, particle impact...in wet environment result from an intricate reciprocal interactions between mechanical and electrochemical phenomena, defined as tribocorrosion. Electrochemical techniques have been applied in an increasingly successful way in the last decade for understanding the underlying mechanisms. This was possible owing to the improved control of the mechanical parameters particularly by sophisticated tribometers. New trends in the field will be illustrated in the case of austenitic stainless steel in acidic and neutral media.

Electrochemical Impedance Spectroscopy (EIS) can be implemented only under steady-state conditions. This contribution will focus first on the incorporation of mechanical parameters in a general input-output description of the interface response to any external perturbations. Conditions for reaching steady-state under mechanical disturbance of the interface are defined within the accepted concepts in tribocorrosion. They can be fulfilled by so-called pin-on-disc tribometers.

Impedance techniques can be considered in various ways depending on the input-output pair. Classical EIS based on ac current-voltage correlations are applied over a range of mechanical parameters such as rotation speed and applied pressure. EIS behaviours of stainless steels will be presented. Frequency and potential dependences are consistent with dissolution-passivation reactions on these materials. The extension of classical impedance models to the exotic case of triboelectrochemistry is a real challenge. Specific and totally original structure of impedance models accounting for the competition between mechanical removal of surface films and their electrochemical healing will be presented and applied to samples covering a range of the ratio abraded to non-abraded areas.

Mechano-electrochemical transfer functions can also be defined. They are likely to provide more relevant information about the intimate interactions between the various processes at work in tribocorrosion. A new mechano-electrochemical impedance has been defined on the basis of a sine wave modulation of the rotation speed of the pin-on-disc setup and the electrochemical ac current hence generated. It has been demonstrated that the frequency dependence of this transfer function (Tribo-Electrochemical Impedance, TEI) is the Fourier transform of the repassivation transient of the material under investigation, a key function in most of the electrochemical models in tribocorrosion. A thorough analysis of the TEI yielded by a 316 SS established that the repassivation takes place by a mechanism generating a two time-constant transient. The likely meaning of these data will be discussed.

Sensitivity to liquid metal embrittlement of the T91 steel by the liquid sodium : influence of the pre-immersion in liquid sodium

Ingrid Proriot Serre, Unité Matériaux et Transformations UMR CNRS 8207 – Université Lille 1, 59650 Villeneuve d'Ascq/France; Ouadie Hamdane, Unité Matériaux et Transformations UMR CNRS 8207 – Université Lille 1, 59650 Villeneuve d'Ascq/France; Jean-Bernard Vogt, Unité Matériaux et Transformations UMR CNRS 8207 – Université Lille 1, 59650 Villeneuve d'Ascq/France

The use of the T91 martensitic steel was considered to constitute structural material of future sodium fast reactors of fourth generation where it will be deformed between 150 and 550 °C in presence of liquid sodium. The effect microstructure on the mechanical behavior of T91 steel in presence of liquid sodium has been studied by means of Small Punch Test (SPT), carried out inside a Plexiglas cell where the atmosphere is severely purified and controlled. The change in the state of precipitation and the dislocation structure of the T91 steel by a tempering heat treatment at 550 °C or without tempering heat treatment provokes Liquid Metal Embrittlement (LME) of the steel by liquid sodium between 200 and 550 °C. Sodium penetrates prior austenitic grains boundaries and induces brittle crack initiation under a plastic deformation as showed by Secondary Ions Mass Spectroscopy (SIMS) analyses and observations.

In order to take into account the influence of the corrosion effect on the mechanical properties, pre-immersion tests of various heat treatments of T91 steel were carried out in a static liquid sodium at 503 °C, for 169 hours. Then, the mechanical behavior of pre-immersed materials has been evaluated in air at room temperature and in presence of sodium at 200°C and 300 °C, by Small Punch Test (SPT). Surfaces have been characterized by Scanning Electron Microscopy (SEM) and Secondary Ion Mass Spectroscopy (SIMS) not only after the pre-immersion in sodium but also after mechanical tests. After sodium pre-immersion, defects due to corrosion by liquid sodium at the outer surface are created, preferentially in prior austenitic grains boundaries and martensitic laths boundaries. The pre-immersion by creating this surface defects induces or accentuates sodium penetration under loading and so a further LME of T91 steel by sodium.

Tribocorrosion effects on offshore mooring chain steel

*Ainara Lopez, Francesco Pagano, Raquel Bayon, Amaya Igartua
IK4-Tekniker, Eibar, Spain*

Abstract

Corrosion is a critical problem affecting many parts of the off-shore oil extraction platforms. The mooring chain is one of the parts that are continuously exposed to the aggressive marine environment and as a consequence suffers different kind of environmental attacks: corrosion, corrosion fatigue, hydrogen embrittlement, tribocorrosion and erosion.

This paper analyzes the tribocorrosion phenomena that occur in marine water on typical mooring chain steels (steel R4 and steel R5). Electro impedance spectroscopy (EIS) and open circuit potential measurements were employed during tribological experiments in order to distinguish the isolated contribution of corrosion and wear and the contribution due to the joint effect of corrosion and wear. The wear scars produced during the tests were analyzed by optical microscope, confocal microscope and Scanning Electron Microscopy / Energy-Dispersive X-ray Spectroscopy (SEM-EDS).

Tribocorrosion behavior of commercially pure titanium in biomedical application of dental and orthopedic implants

Yaqin Yang and Pierre Ponthiaux, Ecole Centrale Paris, Grande Voie des Vignes,
92295 Chatenay-Malabry, France*

**Corresponding author. Tel.: +33 1 41 13 12 44; Fax: +33 1 41 13 12 62.*

E-mail address: pierre.ponthiaux@ecp.fr

Tribocorrosion is the interplay between chemical, electrochemical and mechanical processes that leads to a degradation of passivating materials in a corrosive environment. Recently, more and more attentions have been paid to tribocorrosion and its effects on the lifetime of materials in marine and offshore equipments, cutting tools, chemical pumps, nuclear reactor components, and biomedical industry. Due to the good mechanical properties, excellent corrosion resistance, and adequate biocompatibility, titanium and its alloys are well used as dental and orthopedic implants. The passive film, formed spontaneously, is highly stable and protects the surface against chemical attacks in corrosive medium. However, the low wear resistance of titanium and its alloys, resulting from the easy damage of the passive film under mechanical solicitations, limits their further development as more efficient and economic biocompatible implants. Although surface modifications have been conducted to improve wear resistant capability, fundamental researches are necessary to well understand the degradation mechanism of titanium and its alloys in tribocorrosion system.

In this work, the aim is to apply a tribocorrosion protocol for passivating materials to evaluate the contributions of normal force, depassivation/repassivation phenomena in material loss of commercially pure titanium (cp Ti) during continuous and intermittent unidirectional sliding tests. Tribometers were used to impose different loading forces in a pin-on-disc mode. Electrochemical measurements such as open circuit potential (OCP) and electrochemical impedance spectroscopy (EIS) were applied to in situ characterize the corrosion behaviour of cp Ti before, during and after sliding in phosphate buffered saline (PBS) solution. Scanning electron spectroscopy (SEM) coupled with energy dispersive spectroscopy (EDS) and profilometer were employed to analyze the surface morphology/chemical composition and the total wear volume at the end of sliding tests. The experimental results showed that the applied normal force affects the corrosion-wear degradation of cp Ti in PBS. The material loss due to corrosion of active material and the materials loss due to mechanical wear of active material on the sliding track enlarge simultaneously with the increase of normal force under continuous unidirectional sliding tests. The effect of latency time on the depassivation/repassivation behavior of passive film is also discussed under intermittent unidirectional sliding tests. It was observed that the material loss due to mechanical removal predominates and the formation of passive film on the surface in off-time periods accelerates the mechanical removal of cp Ti.

Corrosion investigations of ultrasound supported friction stir welded Al/Mg-hybrid joints

S. Benfer¹, B. Straß², G. Wagner², W. Fürbeth¹, ¹DECHEMA-Forschungsinstitut, Frankfurt/Germany; ²TU Kaiserslautern, Kaiserslautern/Germany

Light-weight metals like Al- and Mg-alloys are of great interest in transport technology (aerospace, automotive). Only with hybrid construction it is possible to combine the advantages of both materials. However fusion welding of these dissimilar materials is often impossible as a result of the different melting ranges. Moreover in many cases unrequested mixed phases occur in the weld area, whereby the attainable strength of the joints will be reduced. Within the project Al-cast- and Mg-cast alloys are joined by friction stir welding (FSW), because there is no possibility to realize joints between them by fusion welding. FSW enables a joining by plastic deformation. Additionally power ultrasound is submitted into the welded area to eliminate strength reducing effects by occurring brittle phases and to improve the stirring in the joining area.

To understand the development of the microstructure in the bonding zone a detailed analysis has been carried out. The resulting microstructure may influence the corrosion properties of the hybrid materials, which are investigated by different methods and are the main purpose of the work presented here.

Besides integral methods (immersion test and electrochemical measurements) local investigations (scanning kelvin probe, scanning kelvin probe force microscopy (SKPFM)) have been carried out. Open circuit potential measurements give information about the passivation behavior of the different alloys and potential differences between them. Corrosion activity of the alloys is measured by potentiodynamic polarization. As expected the Mg-alloy exhibits a much stronger corrosion in sodium chloride solution than the Al-alloy. In the area of the Al/Mg-butt weld the overall corrosion rate increases while the corrosion of the Al-alloy is reduced at the expense of the Mg-alloy.

Local methods have been used to investigate the influence of noble intermetallics which are formed in the Al-alloy (AC-48000) that contains some noble alloying elements (e.g. Cu, Ni). The aim is to correlate the observed corrosion properties with the microstructure in the bonding zone which is a result of the applied welding parameters.

Study of the corrosion behaviour of friction stir welded AA 2024-T3 using global and local electrochemical techniques

Hercílio Gomes de Melo, University of São Paulo, USP, São Paulo, Brazil, Vincent Vivier, University Pierre et Marie Curie, Paris/França, Idalina Vieira Aoki, University of São Paulo, USP, São Paulo, Brazil, Camila Molena de Assis University of São Paulo, USP, São Paulo, Brazil

Friction-stir welding (FSW) is an innovative process to join metals developed by The Welding Institute (TWI) where the parts to be welded do not reach the melting temperature. It avoids several drawbacks involved in welding procedures that are more common, being a major achievement for welding of high strength Al alloys used in the aerospace industry. In the process, a non-consumable rotating tool composed of a shoulder and a threaded pin moves along the butting surfaces of two rigidly clamped plates placed on a backing plate. The heat generated by the tool rotation and displacement along the seam causes severe plastic deformation and flow of the plasticized metal creating the weld, which is typically composed by three different zones. The heat affected zone (HAZ), which is only submitted to a temperature gradient with no mechanical deformation, the thermomechanically affected zone (TMAZ), affected both by heating and plastic deformation, and the nugget, where the parts to be joined reach the highest temperature and deformation. This latter region is characterized by fine equiaxed grains due to recrystallization [1]. These differences in deformation and temperature cycles of the welding zones introduce changes in the microstructures of the parts to be joined and, consequently, affect their corrosion resistance.

In the literature, a number of works devoted to the investigation of the corrosion behaviour in FSW of high strength Al alloys has been published. However, only few of them have used EIS or local techniques to perform the investigation and, to the best of the authors' knowledge, none of them has used both techniques together.

In the present work, the corrosion behaviour of FSW in 2024-T3 Al alloy in 0.001 M NaCl solution was investigated by means of polarization curves, EIS, local electrochemical impedance spectroscopy (LEIS) and SVET. SEM observations of corroded specimens were used to consolidate the interpretation of the electrochemical results.

The study of each weld region individually revealed that the ensemble nugget + TMAZ had the lowest corrosion potential. This sample also presented a defined passive region and did not exhibited localized type of corrosion, at variance with the behaviours observed for the HAZ and the base metal, both showing the classical pitting corrosion morphology associated with 2024 alloys. This sample also displayed the best EIS response, with higher impedance values, even though the diagrams for the three individual samples presented similar shape.

SVET measurements for the nugget + TMAZ zone revealed that the electrochemical activity was mainly concentrated in the TMAZ, with higher activity being observed in the advancing side of the tool. On the other hand, the analyses of the HAZ showed that the temperature gradient plays a major role in the electrochemical activity of the sample.

Results obtained with LEIS and with galvanically coupled samples will also be presented and discussed.

[1] M. Jariyaboon, A.J. Davenport, R. Ambat, B.J. Connolly, S.W. Willians, D.A. Price *Corr. Sci.* 49 (2007) 877.

Active self-healing coating for galvanically coupled multi-material assemblies

Maria Serdechnova, Silvar Kallip, Daniel Vieira, Luís Filipe Santos Barbosa, Mario G.S. Ferreira, Mikhail L. Zheludkevich, DEMaC, CICECO, University of Aveiro, Aveiro/Portugal

A new “self-healing” coating concept to be used for active corrosion protection on galvanically coupled multi-material structures is reported in the present work. The main novel approach is based on the combination of two types of nanocontainers with two different inhibitors in the same coating system. The nanocontainers confer a triggered release of both inhibitors which act in a synergistic way when an aluminum alloy is galvanically coupled with carbon fiber reinforced plastic (CFRP). The combination of an aluminium alloy with CFRP is selected because of its high relevance for aeronautical applications. Moreover this galvanic couples is challenging because of high difference of galvanic potentials of Al and carbon.

The layered double hydroxide and bentonite were used as functional nanocarriers for 1,2,3-benzotriazole and Ce^{3+} inhibitors respectively. The synergistic inhibiting properties of this combination were previously reported in our recent work [1]. Scanning vibrating electrode technique (SVET) has been applied for monitoring the galvanic corrosion activities and the kinetics of self-healing processes in confined defects. The effective inhibition of electrochemical activity in the defects on coated galvanically coupled aluminium alloy with carbon fiber reinforced plastic was demonstrated for the first time.

References

1. S. Kallip, A.C. Bastos, K.A. Yasakau, M.L. Zheludkevich, M.G.S. Ferreira, Synergistic corrosion inhibition on galvanically coupled metallic materials, *Electrochemistry Communications*, 20 (2012) 101-104.

A controlled experimental approach of the effect of confinement on the damage inside an aluminium alloy lap joint

T.M.L. Le, R. Oltra, A. Zimmer,

Laboratoire ICB, Equipe EIC UMR 6303 CNRS – Université de Bourgogne, France

For aircraft structures, corrosion sensitive areas are mainly those where the protection of the structure may suffer local breakdowns, as encountered inside lap joints. The assemblies of metal plates by overlapping (riveting, bonding, hybrid joining) may present some defects in contact and consequently a gap can exist between the two parts of the assembly. Typically this gap is isolated from the outside environment by a sealant. But there is always a risk of trapping of moisture more or less concentrated in aggressive ions which can induce corrosion of the bare metal inside the cavity.

The objective of this work was to develop a methodology to reproduce in a controlled manner and in the most representative way regarding actual cases, the corrosion of a lap joint made of aluminium alloy 2024-T3 plates, to perform chemical and electrochemical measurements.

An instrumented cavity (gap thickness of 200 μm) was designed allowing simultaneous pH, potential or current measurements. Various conditions were tested to simulate the nature of the chemical transport and the existence or not of an electrical coupling between the bare metal exposed inside the cavity and the metallic surface exposed at the outside the cavity.

The same experimental set up was used to simulate humid-dry cycling of the outer part of the lap joint.

It was demonstrated that the time variation of the pH inside the cavity and the pH outside the cavity is highly dependent on the existence or not of the chemical and electrical coupling between the inner and the outer part of the cavity.

Assuming the outer part of the lap joint is an electrical insulator (painted sheet of aluminium alloy) it was confirmed that in free corroding conditions the pH inside the lap joint tends more towards alkalisation than to acidification, as described by other authors [1]. In the opposite, if the outer part of the lap joint is electrochemically active (unpainted sheet) the pH inside the cavity tends towards an acidic value. This latter trend was confirmed using the same cell but in potentiostatic conditions. These trends can be discussed as function of the spatial distribution of the cathodic reactions on the inner and outer parts of the lap joint.

[1] K.S. Ferrer, R.G. Kelly, *Development of an aircraft lap joint simulant environment*, *Corrosion* 58 (2002) 452.

1st Author: Roland Oltra

E-mail: roland.oltra@u-bourgogne.fr

Phone: 33 380 39 6162

CNRS - University of Burgundy -

Address: Laboratoire ICB, Equipe EIC UMR 6303

CNRS – University of Burgundy, France

Galvanic corrosion behaviour of titanium in lightweight construction

Stefan Wibiha, CEST, Wr. Neustadt/Austria; Günter Faflek, Vienna University of Technology, Vienna/Austria; Theo Hack, Airbus Group Innovations, Munich/Germany; Martin Beneke, Airbus Operations, Bremen/Germany

The "Flightpath 2050" of the European Commission plans a 75% reduction of CO₂ emission. To achieve this ambitious goal the optimization of the aircraft design or the development of new propulsion technologies will not be enough, it will be also necessary to reduce the aircraft weight. Therefore lightweight structural materials such as titanium or aluminium are becoming more and more important but may also lead to new problems regarding corrosion.

Both metals are ignoble, with a standard potential of -1.21 V for the Ti/Ti³⁺-couple and -1.66 V for the Al/Al³⁺-couple, but they are usually protected by a stable and compact oxygen layer. In the presence of chloride ions aluminium and especially its copper rich alloys are susceptible to pitting corrosion. The corrosion of aluminium is might be further increased in combination with titanium, as active titanium might work as a cathode. Different ways to activate titanium are possible. One way is related to titanium oxide being a n-type semiconductor. The band gap of titanium oxide is approximately 3.0 eV (respectively a wavelength of 415 nm) and therefore visible light can create holes in the valence band. [1]

Another way to activate Ti is cathodic polarization as can be seen in Figure 1. In this case the hysteresis between forward and reverse scan depends on the reverse potential. A more negative reverse potential leads to a more active electrode surface and an increase of the oxygen reduction current density. This can be related to the reduction of surface species which mediate the oxygen reduction. [2]

Using a rotating electrode the cathodic reaction kinetics on a titanium disc was investigated with the focus on the previously mentioned cathodic activation of titanium alloys.

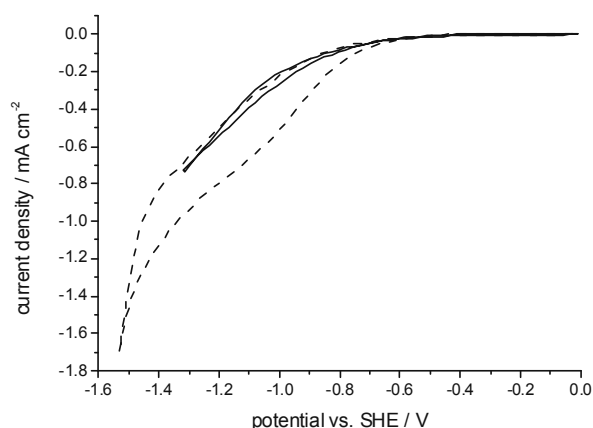


**Figure 1: Ti6Al4V rotating disc electrode
(500 rpm, 0.1 M NaCl)**

[1] A. Fujishima and K. Honda, *Nature*, 238, (1972) 37.

[2] B. Parkinson, F. Decker, J.F. Julião, M. Abramovich and H.C. Chagas, *Electrochimica Acta*, 25, (1980) 521.

Inhibitor-enriched composite protective coating for WE43 magnesium alloy

S.V. Lamaka, M. M. Lourenço,

Instituto Superior Técnico, ICEMS, University of Lisbon, Portugal

D. K. Ivanov, M.L. Zheludkevich, M.G.S. Ferreira,

University of Aveiro, CICECO, Dep. Materials and Ceramic Eng., Aveiro, Portugal

T. Hack,

EADS Innovation Works, Munich, Germany

Addition of an efficient corrosion inhibitor into protective coating greatly extends its service life. Mechanically impacted inhibitor-enriched protective coatings are able to restore their main functionality – corrosion protection – by releasing inhibitor that stops corrosion propagation. Three main functional components contribute to success of a self-healing coating: durable polymer matrix, inhibitor carrier and efficient corrosion inhibitor. The presentation will describe our approach to composite protective coatings for WE43 magnesium alloy disclosing the details of said three main protective components. Special emphasis will be placed on newly identified corrosion inhibitors for magnesium alloys.

The composite protective coatings are based on porous anodic layer formed on magnesium alloy by DC plasma electrolytic oxidation in spark regime [1]. Individual corrosion inhibitors and their mixtures are incorporated in the pores of anodic layer. Leaching of inhibitor is moderated by its sealing in anodic pores with epoxy-silane hybrid coating [2], which also provides strong barrier for corrosive species. Inhibitors of magnesium corrosion incorporated in the composite coating considerably improved its cumulative protective performance and impaired its fault-tolerance. The results of laboratory and industrial tests will be presented.

Acknowledgement

Portuguese Foundation for Science and Technology (FCT), projects PTDC/CTM-MET/112831/2009, PTDC/CTM-NAN/113570/2009 and PTDC/CTM-MET/113645/2009.

1. D.K. Ivanou, M. Starykevich, A.D. Lisenkov, M.L. Zheludkevich, H.B. Xue, S.V. Lamaka, M.G.S. Ferreira. Plasma anodized ZE41 magnesium alloy sealed with hybrid epoxy-silane coating. *Corrosion Science* 73 (2013) 300–308.
2. F. Brusciotti, D.V. Snihirova, H.B.Xue, M.F.Montemor, S.V.Lamaka, M.G.S. Ferreira. Hybrid epoxy-silane coatings for improved corrosion protection of Mg alloy. *Corrosion Science*. 67 (2013) 82–90.

The influence of hot forming on the microstructure and corrosion behavior of magnesium alloy

A. Juliawati¹, X. Zhou¹, G.E Thompson¹

1- Corrosion and Protection Centre, School of Materials,

The University of Manchester, M13 9PL, UK

juliawati.alias@postgrad.manchester.ac.uk

xiaorong.zhou@manchester.ac.uk

george.thompson@manchester.ac.uk

Abstract

Magnesium is the lightest of all structural metals and known to potentially promoting energy efficient transportation. However, magnesium and its alloys are known to exhibit poor formability via conventional forming operations at ambient temperatures, but relatively high at elevated temperature due to activation of non-basal slip system. The forming operation at elevated temperature also adversely affects its corrosion properties. The reason for poor corrosion resistance lies on the aspect of quasi-passive hydroxide films, galvanic corrosion caused by impurities, secondary phases and the post processing effect of heat treatment such as grain size and twinning. This study is concerned on the influence of hot forming process of AZ31B magnesium alloy sheets on its grain and intermetallic particle distribution, twinning and its corrosion behaviour in 3.5 wt% NaCl solution. The alloy sheets were heated to 450°C, transferred to the die immediately, stamped and quenched rapidly by cold-die quenching. The microstructures of the alloy have been characterised using optical microscope (OM) and scanning electron microscope (SEM). The role of twinning on the corrosion behaviour also further examined using electron backscattered diffraction (EBSD) analysis.

It was observed that the hot forming process decrease the amount of intermetallic particle distribution, but increase in grain size. The corrosion measurements were performed by the hydrogen evolution test and electrochemical measurement, in the 3.5 wt.% NaCl solution. The corrosion was found to initiate on the impurity contamination and highly degraded on the stressed region of the deformed alloys. The reduction in particle distribution is expected to result in good corrosion resistance, however, the role of twinning was found to deteriorate the alloy severely due to its active dissolution rate.

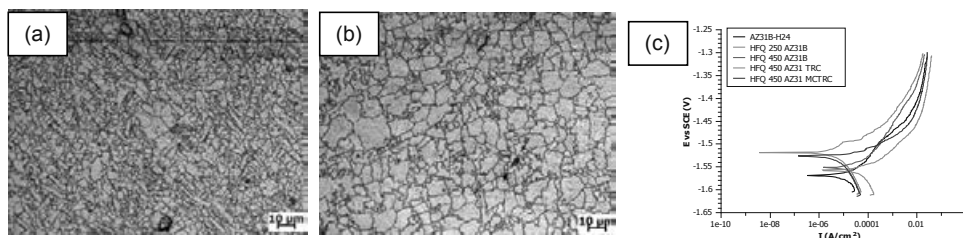


Fig 1. The micrograph of: (a) AZ31B-H24; (b) hot formed AZ31B-H24 at 450°C and (c) is the polarisation curve of the alloys showing its corrosion behaviour in 3.5 wt.% NaCl solution.

Keywords: hot forming, magnesium alloys, twinning

In-Situ Al/TiC Nanocomposites: The Effect of Sintering Temperature on The Corrosion Behavior

B. Dikici¹, M. Gavgali², F. Bedir³ and T. Kiyak⁴

¹ Yuzuncu Yil University, Department of Mechanical Engineering, 65080 Van, Turkey

² Ataturk University, Department of Mechanical Engineering, Erzurum 25240, Turkey

³ Suleyman Demirel University, Department of Mechanical Engineering, 32260 Isparta, Turkey

⁴ Gazi University, Art & Sciences Faculty, Department of Chemistry, 06500 Ankara, Turkey

Abstract

In this study, in-situ TiC nanoparticles with a diameter of 70–400 nm have been successfully synthesized in liquid aluminum by conventional hot pressing method. The effect of production temperature on the corrosion behavior of the composites was investigated by potentiodynamic polarization technique. in aqueous NaCl solutions. The corrosion rates of the samples were determined by using E_{pit} , E_{corr} and I_{corr} values obtained from polarization curves. The corroded surface morphologies of the composites were determined by a scanning electron microscopy (SEM). Also, X-ray diffraction (XRD) technique has been used in order to determine the in-situ phases occurred in the matrix. The obtained results indicate that the corrosion resistance of the nanocomposites was higher than the matrix material.

Keywords: Al/TiC, nanocomposites, corrosion, polarization

* **Corresponding author:** Tel: +90 432 225 1040 (1109); Fax: +90 432 225 1730

E-mail: burakdikici@yyu.edu.tr (B. Dikici)

Research Activity for the Restoration and Maintenance of the Pisan Objects at The University of Pisa

Alessia Andreotti¹, Ilaria Bonoduce¹, Valter Castelvetro¹, Francesco Ciardelli^{1,2}, Maria Perla Colombini^{1,3}

¹ Dipartimento di Chimica e Chimica Industriale, Università di Pisa, Italy

² SPIN-PET s.r.l., Pontedera, Italy

³ Institute for the Conservation and Enhancement of Cultural Heritage, ICVBC-CNR, Firenze, Italy

The researchers at the Department of Chemistry of the University of Pisa have been involved for more the 25 years in activities aimed at the protection, restoration and conservation of art objects and historical buildings. The work performed regarded the development of both innovative fluorinated polymer coating coatings for for the protection of monumental stones and the development of new micro-invasive analytical procedures for the characterization of the degradation products in works of art and archaeological objects, and related approaches for the restoration and conservation.

In cooperation with the ICVBC Institute of CNR in Firenze and other researchers from CNR and Italian Universities and Superintendencies of North Italy, a series of new fluorinated polymeric materials were produced by free radical polymerization and their potential in the conservation and protection of various lithotypes typically found in relevant historic buildings was evaluated. Both solvent-based and water-based formulations of such fluorinated acrylic-based copolymers have been tested as protective coatings on different stones, including Carrara and Candoglia Marble (the latter used in the Duomo of Milan), other carbonatic stones as well as sandstones of various chemical compositions and porosities. The polymers were designed to systematically investigate the effect of comonomer composition and of the presence of various functional groups (fluorinated, polar, reactive) in their side chain on their hydrophobic protection efficiency and photooxidative self-stabilization. In a case study, both surface and bulk properties (water repellency, capillary water absorption) of two carbonatic stones, Carrara Marble and the porous Vicenza Stone, were greatly improved by application of a semifluorinated terpolymer bearing a sol-gel reactive silane group in the side chain; the terpolymer showed exceptionally good performance when compared with the commercial acrylic Paraloid B72 and the silicone Rhodorsil H224.

Seventy years have passed since 27 July 1944, the "dies horribilis" for art history - the day an incendiary device landed in the middle of the Monumental Cemetery of Pisa. The result was the devastation, partial collapse and especially the charring of a vast area of frescoes that together made up the most important pictorial anthology of the history of Italian art between the Middle Ages and the Renaissance. The right artistic media needed to be selected for the missing frescoes, along with suitable experiment protocols for cleaning and pictorial integration, and how to fix them on the wall. Finally, the best ways were needed to make the environment compatible from a climate point of view. Now, in front of the north walls, the Monumental Cemetery of Pisa is coming back to life. It is again made understandable in the living memory of its lost but not forgotten beauty and its symbolic functions.. Great care and special methods are required for the cycle of the "Triumph of Death" and "Stories of Holy Fathers", given that they are relatively well conserved, and still rich in layers / depth and chromatic materials. The results of the relocation on the walls of the frescoes of the Cemetery are beginning to be visible. Probably two more years will be needed before the restoration of all the frescoes on the wall is completed ,but the effect is already comforting and you all are invited to enjoy a visit while in Pisa.

World War One fortresses and artifacts in Trento area: from historical corrosion to a durable maintenance work

arch. Fiorenzo Meneghelli

consultant of Soprintendenza per i Beni architettonici e archeologici della
Provincia Autonoma di Trento.

via Bevilacqua, 25

37063 Isola della Scala (VR)

Tel. 045/7301783

mf@architettomeneghelli.191.it

The start of World War 1 was one century ago. Trenton, a contact area between the Austro-Hungarian Empire and the Italian kingdom, has been deeply wounded by the conflict, both in human terms, due to the unavoidable social, economical, cultural repercussions and by a materials point of view, because of the dissemination on the territory of a huge number of concrete objects and locations, still visible and available for excursions. The Trento area actually, where the frontline winded along 230 kilometers, hosts one of the most important concentration of defense systems built up by the Empire. On the whole territory of the Austro.Hungarian Empire 510 fortresses were built, about hundred of which stay on the Trentino mountains.

Such structures, conceived for a totally obsolete function, stay over the time subjected to corrosion and degradation, as strongholds, foxholes, and cannons emplacements. Part of them were spared from war damages, and suffer the natural degradation as abandoned objects, other ones show the hits of heavy bombardments and assaults. And also some of them, surviving intact the war, were dismantled by the hysterical action of ran sackers, eager to reuse materials. Even if fortresses are the most evident mark of the storm of the "Great War" on the territory, they are not the only one voice to tell about the war years: the remains of the foxholes and other buildings, widespread allover trentino, (leaving alone single objects recovered from the glaciers), bring back glances of the war operations but also of everyday life of the soldiers.

The great cultural enterprise known as "Progetto Grande Guerra", established by the Trenino local Government in collaboration with most of local both private and public Institutions aims to study, know, recover, maintain and appraise all cultural values relevant to the war period. The will to maintain structures copes with the will to keep in mind history, in order to read it also in terms of mute but always reliable witness of Architecture, as a warning for such events never to happen again, changing those war artifacts into peace messengers

**Cutting-edge technologies for the renewal and care of historical buildings:
the thirty-year experience gained in restoring the painted facades of the
ligurian historical buildings.**

abstract

The intervention has the aim to deepen the technical features of some families of finishing products particularly suitable for the restoration and protection of historical building's heritage and more. The choice, once limited to only limed based products, is today much wider. The qualities demanded to a finishing products, were those of resistance in an aggressive exterior setting, aggressions nowadays much harder than in the past due to the pollution and the aesthetic aspect that, instead, needed to be very close to that of the traditional products, the experience and the interventions made in a lot of ancient and very important historical buildings of Genoa (like Palazzo San Giorgio, via del Campo, via San Lorenzo, sea station and more) allowed us to carry out these typologies of interventions, interacting for the diagnosis and the substrates study and afterwards for the choice of the applications systems with both the superintendence and the works directions

Genoa's elevated highway (Soprelevata) : 1964 -1984 -2014 - a successful maintenance project

P.L. Bonora, University of Udine, Italy

The town of Genoa, 35 Km long along the sea and only a few Km wide towards the inner hills, is crossed in its most crowded eight kilometer long downtown by a steel structured elevated highway, called "Soprelevata" and named "Strada Aldo Moro" which was built in an extremely short time (six months) in 1965. The design, among many excellent features, bore some genetic mistakes, mainly due to the erroneous presumption that the whole supporting metal structure was waterproofing. The second problem concerned the malfunction of the expansion joints.

Some maintenance work was carried out on the paint of the external structure during the first years of use, but a major inspection carried out in the eighties showed, a part of an expected degradation of the external organic coating, an apparently dangerous generalized corrosion, with more than one cm thick rust layers, together with stagnant water inside the trapezoidal metal support of the highway.

A plan aimed to completely clean and protect the interior of the 16 km long supporting tunnel was carried out, including designing and testing a surface tolerant one hand organic protecting coating. A new external coating was also designed, bearing both esthetical and durability features.

The paper shows the experimental methods, including electrochemical Impedance spectroscopy, employed both to determine the possible reduction of reliability of the structure due to heavy corrosion damage and to forecast the performances of the protecting coating, both inside and outside the supporting tunnel.

A survey of the present situation, both by an esthetic and a structural point of view is shown in the paper after about thirty years from the major maintenance work carried out in 1985

More than 20 years of proven durability of fluorinated architectural coatings onto concrete; 1992 – 2014 Genoa's Aquarium case.

dr. eng. Angelo Locaspi, Innoventions srl, Via Alberto da Giussano 3C/1 - 20092 Cinisello Balsamo (MI) Italy; e-mail: angelo.locaspi@innoventions.eu

Genoa's Aquarium, designed by architect Renzo Piano, was inaugurated in 1992 to celebrate the 500th anniversary of the discovery of America. The exterior walls of the building are made of precast concrete painted with fluorinated coatings. The project required the building to be perceived like a ship moored in the harbor. Technically it was necessary to achieve a smooth coated surface, defects free, having a high level of finish to look like painted steel.

After 23 years of exposure in hostile marine environment, the original fluorinated coating has never been maintained or touched-up; the fluorinated coating is integer, well adhered to the substrate with a negligible change in brightness and color. There is no dirt pick up or degradation due to acidic attack of bird droppings by seagulls. Carbonation depth of concrete was < 2 mm .

On last 2013, for the construction of the second building of the Aquarium, it was decided to use the same fluorinated coating applied in 1992 without any touch-up of the original part. The result was the excellence of fluorinated coatings both in aesthetics and economics.

The effect of soiling and oxidation on architectural titanium

M.V. Diamanti¹; MP. Peddeferri¹
¹ *Politecnico di Milano, Milan, Italy*

The advanced structural properties of titanium, together with its fascinating interference colours, have opened the way to architectural applications as façade claddings¹. In fact, anodised titanium can exhibit fascinating interference colours due to the presence of a thin oxide layer on its surface. The hue produced depends on oxide thickness, therefore it can provide information on the oxidation degree of the surface itself². In outdoor applications the amphiphilic surface of titanium undergoes both soiling and a slow oxidation; few experimental studies have been carried out to understand its durability when exposed to the atmosphere³, and none of them considers this dual surface modification. This work investigates through spectrophotometry the two contributions to titanium surface alterations upon outdoor exposure, and evaluates different anodising treatments to improve its behaviour.

Non-anodised titanium and differently anodized titanium plates were subjected to a preliminary characterisation, including oxide thickness and crystal structure. Specimens were then exposed outdoor by hanging them on a wood table that was placed on the roof of a building in Milan, which caused a fast soiling of the surfaces. Colour monitoring along time allowed to observe not only a gradual soiling, but also a variation of oxide thickness, which may be due either to further oxidation – in case of thin oxides unable to protect the metal surface completely – or to a chemical modification of the oxide – e.g., formation of hydrates by reaction with the outdoor environment and in particular with rain. The latter effect may cause not only a thickness alteration, but also a change in the optical properties of the outer layer, namely its refractive index: this property is commonly used to estimate oxide thickness, therefore such effect would hinder a straightforward evaluation of the damage undergone by the surface.

Finally, from the experimental tests performed and from the observed mixing of soiling and oxidation effects it is possible to assert the need for a clear distinction between the two, in order to design the most suitable cleansing or maintenance procedure. In fact, while the removal of atmospheric particulate deposits can be performed with conventional methods, colour alterations due to further titanium oxidation necessitate heavy duty maintenance with fluorine-based chemicals to remove the undesired oxide layers.

References

1. C. Santilli, *Architecture* 88, 1999, 140-142.
2. M.V. Diamanti, B. Del Curto, MP. Peddeferri, *Color Res. Appl.* 33, 2008, 221-228.
3. M. Kaneko, K. Takahashi, T. Hayashi, K. Tokuno, J. Tamenari, *Mater. Selection Design* 2006, 38-42.

Study of protective coatings for outdoor bronzes by means of in situ electrochemical techniques

S. Goidanich¹, E. Guerrini², A. Colombo², S. Porcinai³, A. Cagnini³, M. Galeotti³, B. Salvadori⁴, A. Vincenzo¹, L. Brambilla⁵, L. Rosetti¹, S. Trasatti²

¹ Politecnico di Milano, Department CMIC, Milan, Italy

² Università degli Studi di Milano, Department of Chemistry, Milan, Italy

³ Laboratorio Scientifico Opificio delle Pietre Dure, Florence, Italy

⁴ ICVBC-CNR, Florence, Italy

⁵ Haute Ecole Arc Conservation-Restauration, Neuchâtel, Switzerland

Protective coatings for cultural heritage applications should not alter the visual appearance of the surfaces and should be removable, as may be required by conservation issues. In addition, research has been recently focused particularly on the development of eco-friendly treatments.

In this study, six different protective coating (Soter; Incral 44; Reswax; Fluoline HY; polysiloxane; polylactic acid) and four corrosion inhibitors (benzotriazole (BTA); sodium oleate; 2-mercaptobenzoxazole; tolyltriazole) have been tested on a quaternary bronze (Cu 88.3%, Sn 5.7%, Zn 3.9%, Pb 1.6%). The coatings have been applied as single, double and triple layer both on bare and patinated samples. The patina was artificially formed by applying on the surface liver of sulphur (a commercial mixture of potassium polysulphide and thiosulfate) and ammonium chloride (NH₄Cl). The protective treatments have been characterised by stereo and electronic microscopy, spectrophotometry, linear polarisation resistance (LPR) and electrochemical impedance spectroscopy (EIS). Electrochemical measurements were performed using a contact probe which is also suitable for in situ measurements.

As expected, double and triple layers provided a higher protection against corrosion. Among the single layers, polysiloxane showed the best performance, while Fluoline the worse. In general, the addition of corrosion inhibitors improved the performance of the protective coatings.

All the samples have been then exposed to outdoor weathering in Milan, unsheltered and 45° South, for two years. The characterisation of the protective treatments after exposure is on-going.

Corrosion resistance of anticorrosive film formed on Mg alloy by steam coating

Takahiro Ishizaki, Naosumi Kamiyama, Department of Material Science and Engineering, Shibaura Institute of Technology, Tokyo/Japan;

Development of effective corrosion protection is an issue of major economic importance, because the market of metal and metal alloys are constantly growing and environmental issues are becoming more important.¹ Magnesium and its alloys have been used as advanced structural and functional materials in aerospace, automobile, and railway industries because of excellent physical and mechanical properties such as low density, good electromagnetic shielding, and high strength/weight ratio.² Their low corrosion resistance, however, hinders their use on a larger scale. To improve the corrosion resistance of the magnesium alloys, the development of a novel coating technology has been highly desirable. In this presentation, we report a novel preparation method of an anticorrosive Mg-Al layered double hydroxide/oriented magnesium hydroxide composite film on magnesium alloys by steam coating. The corrosion resistance of the composite film was also investigated.

Magnesium alloy AZ31 was used as the substrate. The substrates were ultrasonically cleaned in absolute ethanol for 10 min. The cleaned magnesium alloys were set in the autoclave. The cleaned AZ31 substrates were introduced in a Teflon-lined autoclave with a 100 ml capacity. 20 mL of ultrapure water containing 10mM NaNO_3 was located at the bottom of the autoclave to produce steam. The autoclave was heated to a temperature of 433 K, and then held at this temperature for 3 to 9 h, and was subsequently cooled naturally to room temperature, resulting in the formation of anticorrosive films on magnesium alloys. The resulting films were characterized by XRD, XPS, SEM, FT-IR, and electrochemical measurements.

Some peaks at approximately $2\theta = 18, 33, 38, 51, 58, 62$, and 72° , which could be assigned to the 001, 100, 101, 102, 110, 111, and 201 reflections of brucite type $\text{Mg}(\text{OH})_2$ were clearly observed in the XRD patterns. In addition, two peaks at around $2\theta = 11$ and 22° assigned to the 003 and 006 diffraction peaks were clearly observed, which could be assigned to Mg-Al LDH. These results indicates that the film formed on AZ31 by steam coating was composed of crystal $\text{Mg}(\text{OH})_2$ and Mg-Al-LDH. The corrosion resistance of the film were investigated by electrochemical measurements. The potentiodynamic polarization curves of the film coated and uncoated AZ31 after immersion in the 5 wt% NaCl aqueous solution for 30 min revealed that the corrosion current density, j_{corr} , of the AZ31 coated with films decreased by more than four orders of magnitude as compared to that of the uncoated one. This indicates that the film coated AZ31 has a better corrosive resistance than uncoated one.

References

1. R.C. Newman, K. Sieradzki, Science. 1994, 263, 1708.
2. Z. Yong, J. Zhu, C. Qiu, and Y. Liu, Appl. Surf. Sci. 2008, 255, 1672.

Acknowledgement

This research was partially supported by Grant for Advanced Industrial Technology Development, New Energy and Industrial Technology Development Organization (NEDO) of Japan (No.11B06024d).

Development of Inhibitor-Containing Zeolites for Protection Coatings

Mario G.S. Ferreira, University of Aveiro, Aveiro/Portugal

Zeolites loaded with different inhibitors and incorporated in sol-gel coatings were prepared for protection of AA2024-T3. The zeolites were loaded with Cerium, Lanthanum and Molybdate species. The sol-gel coatings modified with mixture of zeolites showed the best protective properties. A synergistic effect between Cerium or Lanthanum and Molybdate species occurred. The inhibiting effect took place by release, by ion exchange, of the inhibiting species contained in the microparticles, with adsorption of Mg^{2+} or/and Cu^{2+} from intermetallic particles dissolution that are mainly the cause of corrosion. The enriched zeolites showed also the ability to adsorb chloride ions from the solution, making it, locally, less aggressive.

AUTHORS INDEX



A

Aaneby J.	O-7408	467
Abbasov V.M.	P-7859	346
Abbottoni M.	O-7259, O-7192, O-7261, O-7551	555, 558, 266, 268
Abd-El-Naby B.	P-7677	218
Abdel Hamid Z.	P-7112, P-7111, O-7113	211, 367, 386
Abdelghany N.A.	P-7596	43
Abdelrahman A.	P-7516	436
Abdullatef O.	P-7677	218
Abdurrahim A.	O-7106	313
Abe H.	O-7149	79
Abolghasemi S.	O-7576	307
Abrahami S.T.	O-7180, O-7179	591, 596
Abrahao D.F.	O-7651	566
Abrudeanu M.	P-7574	459
Achour M.	O-7173	14
Acquesta A.	O-7223, O-7852	409, 546
Adam K.	O-7360	68
Addison O.	O-7846	249
Afroukhteh S.	O-7619, O-7634	334, 496
Afseth A.	O-7385, O-7482	515, 518
Agafonkina M.O.	P-7212	34
Aghajani A.	O-7434	174
Aguirre I.	O-7265	279
Agullo J.	O-7381	94
Ahmad I.	P-7172, P-7174	49, 335
Ahmad S.	O-7554	475
Ahmed K.	O-7115	455
Ahmed M.	P-7689, P-7826	47, 630
Ahrens A.	P-7405	548
Aiad I.	O-7280	28
Akçay C.	O-7169	8
Akid R.	O-7490	110
Aknouche C.	O-7853	482
Al Ameri M.	P-7435	185
Al Haj O.	O-7240	633
Al Muaisub M.	P-7423	636
Al Ridy M.	O-7102	472
Al Saadi S.	P-7435	185
Al Subai S.	O-7737, P-7738	17, 549
Al-Fawaz F.	P-7739	499
Al-Hajri K.	O-7841	468
Al-Hammad M.	O-7724	316
Al-Mahamedh H.	O-7357	258
Al-Meshari A.	O-7554	475
Al-Sulaiman S.	O-7146	497
Alanazi N.	O-7093	330
Alaoui Mouayd A.	O-7245	152
Alar V.	P-7396	547
Albayrak S.	O-7751	414
Albini M.	O-7562	576
Albores O.	O-7395	326
Albu M.	O-7500	474
Aldaghi H.	O-7120	476
Alhambra T.	P-7714	236

Ali Y.	P-7580	365
Alias J.	O-7415	657
Alieva L.I.	P-7859	346
Alkhimenko A.	O-7776	309
Allcock L.	O-7554	475
Allely C.	O-7678	524
Alleva L.	O-7491	320
Allion A.	O-7703, O-7548	243, 541
Almaaesab S.	O-7357	258
Almeida A.	O-7627	230
Almeida N.L.	O-7563, O-7197	317, 556
Alneemi M.	O-7093	330
Alshamsi A.	P-7304	392
Altin A.	P-7443	451
Alvarez Pampliega A.	O-7369	349
Amar S.	O-7093	330
Amaral C.	P-7476, P-7326	193, 202
Amaya H.	O-7205	333
Ambade S.P.	O-7315	501
Ambat R.	P-7337, P-7601, O-7302, O-7482, O-7822, O-7447, O-7082, O-7495, O-7426 P-7826	393, 399, 430, 518, 614, 617, 618, 619, 622, 630
Andersohn G.	O-7434, O-7428, O-7460, O-7481	174, 381, 520, 521
Andreatta F.	O-7132, O-7584, O-7185	167, 382, 443
Andreev N.	O-7307	23
Andreeva N.P.	P-7212	34
Andreotti A.	O-7835	659
Andrieu E.	O-7542, O-7210	83, 112
Angeli G.	O-7243, P-7143	169, 368
Angelini E.	O-7474, O-7671, O-7519, O-7727	563, 574, 579, 581
Angst U.	O-7060	270
Anisko R.	O-7225	621
Ankita P.	P-7201	387
Ansell R.	P-7181	427
Anselmi M.	P-7534, O-7266	213, 300
Antony H.	O-7129	228
Aoki I.V.	O-7287, O-7585, O-7643	438, 444, 652
Arancón J.	O-7394	7
Aranda L.	O-7568, P-7573	66, 69
Araujo S.R.	O-7622	587
Ardelean H.	O-7376	583
Arenas M.A.	P-7844	369
Argandoña G.	P-7696	219
Arkan S.	P-7270	262
Arkipushkin I.A.	O-7352	13
Arndt M.	O-7243, O-7244, P-7143	169, 354, 368
Arnell S.	O-7815	20
Ashrafizadeh F.	P-7844	369
Ashworth M.A.	O-7236, O-7403	626, 627
Askari M.	O-7619, O-7634	334, 496
Assis K.	P-7079	342
Assowe O.	P-7175	178
Atrens A.	O-7806	115
Attallah M.M.	O-7676	140
Augros M.	O-7593, O-7597	378, 383

Auzoux Q.	O-7542	83
Awad M.K.	P-7164	46
Aylor A.	O-7271	114
Ayyar S.	O-7375	641
Azoulay I.	O-7137	157
Azumi K.	O-7478, O-7399	138, 355

B

Babutzka M.	O-7455	146
Bacic I.	P-7591	398
Badini C.	O-7536	588
Badrak R.	O-7776	309
Bagcivan N.	O-7428	381
Baghni I.	O-7299	10
Bairamov A.	O-7737	17
Bajt Leban M.	O-7636, O-7358	81, 544
Baker B.A.	O-7539	57
Baker M.A.	P-7680	607
Balbo A.	O-7138, O-7261, O-7551, O-7265, O-7253, O-7259, O-7192	151, 266, 268, 279, 304, 555, 558
Baldermann A.	O-7791	252
Balduyck J.	O-7369	349
Balmont G.-A.	O-7221	511
Balzer M.	O-7473	384
Bangsgaard D.	O-7446	117
Barai K.	P-7738	549
Barariu Gh.	O-7429	89
Barbaresi E.	O-7694	492
Barbosa K.	O-7197	556
Barbosa L.F.S.	O-7257	653
Bardi U.	P-7470	363
Bares P.	O-7749	602
Barker E.	P-7664	109
Barnel N.	O-7542	83
Barnes P.	O-7226	310
Barnett A.	O-7439, P-7215	321, 403
Baroux B.	O-7158	142
Barros C.D.R.	P-7475, P-7332	192, 203
Baselga Zapater A.	O-7400	632
Bashir A.	O-7493, O-7526	405, 513
Basseguy R.	O-7384	241
Bäßler R.	O-7235, O-7157	121, 613
Bastian M.	O-7248	529
Bastidas D.	O-7265	279
Basuyaux O.	O-7222	637
Bataillon C.	O-7381	94
Bavarian B.	KN-7108, O-7107, P-7855	5, 282, 299
Bayle M.	O-7390	570
Bayon R.	O-7772	649
Bayramov A.	P-7423	636
Bazzoni B.	O-7754, O-7729	493, 638
Becker A.	O-7388	538
Becker-Willinger C.	O-7751, P-7761	414, 424
Bedir F.	O-7198	658

Bedolla A.	P-7768	205
Beese-Vasbender P.	O-7077	242
Beghi M.	O-7505	95
Beghini M.	O-7670	508
Begic Hadzipasic A.	P-7710	48
Bellakhal N.	O-7376	583
Bellezze T.	O-7546, P-7457	276, 295
Belloni F.	O-7740	463
Bellucci F.	O-7842, P-7825, O-7223, O-7852	285, 372, 409, 546
Beloglazov G.	P-7050	214
Beloglazov S.	P-7050	214
Belsanti L.	P-7715	605
Ben Channouf R.	O-7376	583
Ben Salah M.	P-7386	635
Benaissa W.	O-7579	464
Benassi G.	O-7740	463
Beneke M.	O-7786	655
Benfer S.	O-7232, O-7170	375, 651
Bengu B.	P-7178	418
Bentfeld R.	P-7363	428
Bentiss F.	O-7234	27
Bentz D.	P-7761	424
Berge H.E.	O-7229	247
Berger M.-H.	O-7703	243
Bergeron R.	O-7385	515
Berlanga C.	P-7696	219
Bernardi E.	O-7259, O-7192	555, 558
Berne C.	O-7210	112
Berthod P.	O-7561, O-7568, P-7573, P-7575, P-7615, P-7611	63, 66, 69, 70, 71, 74
Bertholon R.	O-7562, P-7847	576, 585
Bertini L.	O-7670	508
Bertoli I.	O-7292	604
Bertolini L.	O-7624	273
Bervian A.	P-7588, P-7667, P-7668	458, 460, 461
Bestetti M.	P-7099	190
Bettge D.	O-7157	613
Bettini E.	O-7572	145
Biamino S.	O-7536	588
Bianco A.	O-7187	439
Biezma M.V.	P-7696, O-7709	219, 223
Bignozzi M.C.	O-7261, O-7551, O-7190, O-7192	266, 268, 553, 558
Bilke-Krause C.	O-7577	593
Birbilis N.	O-7545, O-7265	131, 279
Bitondo C.	P-7825, O-7852	372, 546
Björgum A.	O-7196	589
Björkbacka Å.	P-7218	100
Black A.R.	O-7230	643
Blackwood D.J.	O-7354	280
Blagojevic A.	O-7241	288
Blanc C.	O-7542, O-7486, O-7210	83, 97, 112
Bleck W.	O-7232	375
Bluecher D.B.	O-7161	512
Blumer D.	O-7173	14
Board J.E.	O-7070	128

Bobzin K.	O-7428	381
Bockenheimer A.	O-7820	530
Boduch A.	O-7235	121
Bogdanov R.	O-7074	113
Böhmeler I.	P-7847	585
Boillot P.	O-7548	541
Bolzoni F.	P-7406, P-7520, O-7508	180, 209, 322
Bonaccorsi L.	P-7515, P-7534, O-7522	208, 213, 440
Bonino J-P.	O-7749	602
Bonis M.	O-7811	608
Bonnaud L.	O-7452	412
Bonnet C.	O-7548	541
Bonoduce I.	O-7835	659
Bonora P.	O-7816	662
Borchert M.	O-7380	543
Bordenet B.	O-7756	51
Borderon A.	O-7051	278
Bordo K.	P-7337, P-7601, O-7482	393, 399, 518
Borgna T.	O-7532	645
Borioli C.	P-7099	190
Borodin S.	O-7529	60
Bosch C.	O-7233	311
Bosch R.-W.	O-7661, P-7837	82, 99
Bossio A.	O-7842, P-7825, O-7852	285, 372, 546
Böttcher M.	O-7791	252
Bouchar M.	O-7186, O-7474	562, 563
Bour Beucier V.	O-7817	473
Bourdoiseau J.A.	O-7136	565
Boutoba M.	O-7593, O-7597	378, 383
Bouvet G.	O-7560	407
Bovin J.	O-7221	511
Bozzo G.	O-7807	661
Bracarense A.Q.	P-7719, P-7653	103, 235
Braccini M.	O-7531	61
Brach-Papa C.	O-7222	637
Braga Soares R.	P-7569	340
Brambilla L.	O-7562, P-7847, O-7849	576, 585, 665
Branca T.A.	P-7566	210
Braunstein Faldini S.	O-7709	223
Brenna A.	O-7513, O-7518	164, 489
Brenne F.	O-7635	406
Brögelmann T.	O-7428	381
Broughton A.	O-7638	385
Brugnetti F.	O-7518	489
Brüll R.	O-7248, P-7247, P-7249	529, 536, 537
Brunella M.F.	P-7099	190
Brunelli K.	O-7239	379
Brusciotti F.	P-7730	388
Büchler M.	O-7080	485
Bücker M.	O-7734	573
Buelens C.	O-7369	349
Bueno A.H.S.	O-7674	29
Buggio D.	O-7290	130
Buhrow J.W.	O-7195	446
Burkert A.	O-7207	274

Burns W.	KN-7830	220
Bustamante P.	O-7222	637
Buttin P.	O-7221	511
Byrne G.	O-7805	305
Bystrianský V.	O-7665	98

C

Caballero Hinostroza J.	O-7133	78
Cabañas M.	O-7394, P-7566	7, 210
Cabrini M.	P-7451, O-7536, O-7524	191, 588, 611
Caglioni T.	O-7754	493
Cagnini A.	O-7464, O-7849	554, 665
Calabrese L.	O-7523, P-7515, P-7534, P-7522	119, 208, 213, 440
Caldeira N.	O-7593, O-7597	378, 383
Calle L.M.	O-7195	446
Calvi C.	O-7853	482
Cam P.-Y.	O-7221	511
Camacho-Chab R.	P-7632	297
Campos F.R.	P-7719	103
Campos W.R.C	P-7600	107
Cansever N.	P-7270, O-7614	262, 517
Cantisani E.	O-7464	554
Canulescu S.	P-7337	393
Cao F.	O-7271	114
Cao J.	P-7098	234
Capelo S.	O-7311	559
Capelossi V.R.	P-7680	607
Caplat C.	O-7222	637
Caporali S.	P-7470	363
Cappuccini F.	O-7523, P-7534, O-7266	119, 213, 300
Capri A.	P-7534, O-7522	213, 440
Carangelo A.	O-7852	546
Cardoso Junior R.	P-7719, P-7653	103, 235
Caron D.	O-7543	488
Carrascal D.	O-7394	7
Carreno Velasco J.A.	P-7813	341
Carrick D.	O-7421	586
Carvalho M.L.	O-7794, O-7797	239, 256
Caschera D.	O-7519	579
Cassagne T.	O-7821	306
Castaneda H.	P-7341, O-7361	394, 487
Castelvetro V.	O-7835	659
Castro M.M.R.	P-7721	477
Caylar P.	KN-7691	76
Ceppek C.	O-7584	382
Céré S.	P-7090	188
Cerezo J.	O-7511	516
Cetier J.	O-7227, O-7225	620, 621
Çetin R.	O-7614	517
Cevey C.	O-7562	576
Chahboun N.	O-7593, O-7597	378, 383
Chakri S.	O-7553	272
Chapon P.	P-7404, O-7666	179, 377
Chartier A.	P-7175	178

Chassagnolle E.	O-7385	515
Chauveau E.	O-7701	284
Chaves I.	O-7200	265
Chaves Pereira E.	O-7618	163
Chekroude S.	P-7574	459
Cheldi T.	O-7255	15
Chen J.	O-7603	93
Chen S.	P-7089	261
Chess P.	O-7662	292
Chiavari C.	O-7261, O-7551, O-7190, O-7259, O-7192	266, 268, 553, 555, 558
Chikova A.	P-7308	199
Chisholm C.	P-7181	427
Chizhikov V.	O-7776	309
Cho P.	P-7435	185
Christensen C.	O-7446	117
Chyrkin A.	O-7059	54
Ciardelli F.	O-7835	659
Cicolin D.	P-7291	196
Cigna R.	O-7206	224
Clapp G.	O-7413	483
Clarke K.	O-7135	634
Clauzeau O.	O-7193	509
Clay-Michael N.	O-7466	539
Cocco F.	O-7787	561
Cohendoz S.	O-7560	407
Cole I.	O-7353	240
Colin J.	P-7768, P-7732	205, 457
Colla V.	P-7566	210
Collazo A.	O-7790	231
Colombini M.P.	O-7835	659
Colombo A.	O-7753, O-7849	540, 665
Colombo C.	O-7684, O-7670	325, 508
Colombo V.	O-7740	463
Comensoli L.	O-7562	576
Conde A.	O-7224	514
Conejero O.	O-7394	7
Conrath E.	O-7561, P-7575, P-7615, P-7611	63, 70, 71, 74
Conseil H.	O-7082, O-7495, O-7426	618, 619, 622
Conti C.	P-7457	295
Contreras A.	O-7333	495
Corrales-Luna M.	P-7336	338
Correra S.	O-7255, O-7541	15, 328
Corsinovi S.	O-7684	325
Corvo F.	P-7335	631
Cosenza E.	O-7842	285
Costa C.G.F.	P-7719, P-7720	103, 478
Costa I.	P-7552, P-7124, O-7622, P-7680	376, 426, 587, 607
Cotting F.	O-7585	444
Cournil M.	O-7240	633
Courouau J.-L.	O-7687	648
Courouau J.L.	O-7659	96
Couvant T.	O-7133	78
Cox K.	O-7233	311
Crépin J.	O-7133	78
Crespy D.	O-7228, P-7219	448, 449

Creton N.	P-7759, P-7762	104, 204
Cristiani P.	O-7794, O-7533, O-7797	239, 245, 256
Crusset D.	O-7631, O-7486, O-7264, O-7594	90, 97, 161, 564
Cuevas Arteaga C.	O-7778, P-7771	26, 187
Cunha A.	O-7627	230
Curioni M.	O-7310, O-7852	132, 546
Curkovic L.	P-7591	398

D

D'Ávila C.R.	P-7813	341
da Rocha J.C.	P-7325	39
Dabalà M.	O-7239	379
Dahl K.V.	P-7535	73
Daille L.	P-7609	551
Dal Bianco C.	O-7542	83
Dal Zilio D.	O-7831	535
Dalbert V.	O-7528, O-7532	644, 645
Dalvit M.	O-7506	147
Damasse J.-M.	O-7548	541
Damodaran S.	O-7248, P-7247, P-7249	529, 536, 537
Dangol P.	O-7459	575
Darraspen A.	O-7579	464
Daumas S.	O-7631, O-7486	90, 97
Dauzeres A.	O-7594	564
Davenport A.J.	O-7676, O-7846	140, 249
Davies J.	O-7430, O-7135	351, 634
de Almeida L.H.	P-7047	344
de Araujo Figueiredo C.	O-7661	82
de Arenas J.J.	O-7224	514
de Bonnafos P.	O-7833	484
de Damborenea J.J.	O-7224	514
De Filippo B.	P-7617	400
de Freitas Cunha Lins V.	P-7719, P-7653, P-7569, P-7721, P-7720	103, 235, 340, 477, 478
De Graeve I.	O-7373, O-7608, O-7282, O-7145, P-7374	155, 408, 445, 447, 452
de Kok J.	O-7180, O-7179	591, 596
de la Fuente D.	P-7566	210
De la Iglesia R.	P-7609	551
de Melo H.	O-7651	566
de Mendonca R.	P-7837	99
De Nicolo A.	O-7584	382
De Sanctis M.	P-7566	210
de Sousa Garcia D.C.	P-7569	340
de Souza S.M.	P-7813	341
de Viviés Ph.	O-7390	570
de Vooy A.C.A.	O-7549	170
de Wit J.H.W.	O-7313, O-7511	153, 516
Deborde J.	O-7222	637
Deconinck J.	KN-7708, O-7237	127, 136
Deflorian F.	O-7506, O-7625	147, 359
Dejardin S.	P-7759	104
del Ángel Meraz E.	P-7771	187
Delacoux D.	KN-7691	76
Delafoy C.	O-7542	83
Delaunoy F.	O-7081	358
Dellabiancia C.	O-7586	118

Deloye E.	P-7762	204
Delpoux O.	P-7777	345
Demeter A.	KN-7708	127
Demizieux M.	P-7836	108
Denenberg S.	P-7858	480
Depner-Miller U.	O-7428, O-7481	381, 521
Dercz G.	P-7274	371
Derfouf Talbi H.	P-7461	36
Dernovskova J.	O-7139	552
Desamais N.	P-7777	345
Desgranges C.	P-7836	108
Devetak N.	O-7319	580
Dewonck S.	O-7631	90
Dhouibi L.	P-7386	635
Di Biase L.	O-7100	314
Di Fonzo F.	O-7505	95
Di Iorio C.	O-7255	15
Di Pietro D.	O-7523, P-7515, O-7266	119, 208, 300
Di Sarli A.R.	P-7124	426
Di Tanna G.	O-7807	661
Diab M.	O-7554	475
Diamanti M.V.	O-7448, O-7450	324, 664
Díaz E.F.	P-7732	457
Dick L.F.P.	O-7699	465
Dietzel M.	O-7791	252
Díez J.A.	O-7418	357
Dikici B.	O-7198	658
Dillmann P.	PL-7838, O-7501, O-7623, O-7186, O-7474, O-7594, O-7390	1, 91, 238, 562, 563, 564, 570
Diminich M.	O-7754	493
Dimper M.	P-7405	548
Din R.	O-7302	430
Diniz A.F.	O-7674	29
Diomidis N.	O-7503	88
Dispinar D.	O-7614	517
Dogan A.	KN-7850, O-7854	500, 526
Doi T.	O-7205	333
Dolgikh O.	KN-7708, O-7237	127, 136
Dolley E.	O-7283	85
Doménech A.	O-7311	559
Doménech T.	O-7311	559
Domon Beuret E.	O-7562	576
Donato A.	P-7534	213
Dos Anjos Moraes J.	P-7525, P-7530	396, 402
dos Santos D.C.	P-7078	212
dos Santos F.C.	P-7194	421
Dossary S.A.	P-7858	480
Dove P.	P-7431	419
Dracott J.	O-7589	569
Dragolici F.	O-7429	89
Du C.	P-7654	343
Dubois P.	O-7452	412
Duchardt T.	O-7481	521
Duchi P.J.	O-7227	620
Duchoslav J.	O-7243, O-7244, P-7143	169, 354, 368

Duffó G.	P-7086, O-7088, P-7087	101, 281, 294
Dugstad A.	O-7743, O-7744	609, 612
Duhamel C.	O-7133	78
Duluard S.	O-7749	602
Dumas L.	O-7452	412
Duncan G.	O-7413	483
Duquesnes V.	P-7762	204
Duranti F.	O-7754	493
Duret C.	O-7821	306
Duru K.	O-7497	525
Dusquesnes V.	P-7759	104

E

Easapour S.	O-7120	476
Ebell G.	O-7207, O-7489	274, 481
Ebrahimi R.	O-7316	456
Eckert R.	O-7229	247
Egger R.	O-7500	474
Egorkin V.S.	O-7338	139
Eguchi E.	O-7368	302
Eissa M.M.	P-7044	293
Eken A.E.	P-7134	401
Ekpe U.J.	O-7728	18
Ekström M.	O-7383	523
El-Mahallawy N.	P-7580	365
El-Mahdy G.M.	P-7044	293
El-Sharif M.	P-7181	427
El-Shishtawy R.M.	P-7596	43
El-Sukkary M.	O-7280	28
Eliezer A.	KN-7830	220
Elisseeva O.	O-7180	591
Elsener B.	O-7060, O-7787	270, 561
Elsner C.I.	P-7124	426
Emmerson N.	O-7496, O-7555	567, 568
Engel B.	O-7269	503
Engelberg D.L.	O-7436, O-7213, O-7226	80, 143, 310
Eom M.J.	P-7297	197
Erbe A.	O-7077, O-7233, O-7493, P-7443, O-7526	242, 311, 405, 451, 513
Erbil M.	O-7498, P-7567, P-7814	12, 42, 45
Eremias B.	P-7068	176
Erni A.	O-7411	350
Erning W.	O-7183	534
Escobar J.	O-7452	412
Escobar-Morales B.	P-7632	297
Escrivà-Cerdán C.	P-7514	207
Estupiñan H.	P-7707	389
Evans C.	O-7490	110
Evans T.	O-7466	539

F

Faderl J.	O-7244, O-7433	354, 504
Faflek G.	O-7641, P-7372, P-7663, O-7786	166, 417, 437, 655
Fajardo S.	O-7265	279
Fako R.	O-7429	89
Falcón J.M.	O-7287	438

Fallahmohammadi E.	P-7520, O-7508	209, 322
Fan Z.	O-7246	129
Fang Z.	P-7094	420
Fantauzzi M.	O-7787	561
Faraldi F.	O-7519, O-7727	579, 581
Farina S.	P-7086, P-7091, P-7090, P-7092, P-7087	101, 102, 188, 189, 294
Fathy A.M.	P-7044	293
Favergeon J.	P-7836	108
Favilla M.	P-7451	191
Feaugas X.	O-7560	407
Fedel M.	O-7506	147
Fedorova E.	O-7531	61
Fedrizzi L.	O-7132, O-7584, O-7185	167, 382, 443
Fenker M.	O-7473	384
Ferguson D.	P-7431	419
Fernandes J.C.	O-7775	373
Fernandes J.C.S.	O-7810	411
Fernández-Calvo A.I.	O-7224	514
Fernández-Domene R.	P-7504, P-7514	206, 207
Ferrari G.M.	O-7313	153
Ferrari V.	O-7563	317
Ferreira J.Z.	P-7268	422
Ferreira M.C.	P-7813, O-7810	341, 411
Ferreira M.G.S.	O-7627, O-7257, O-7640, O-7860	230, 653, 656, 667
Ferreiro J.	P-7714	236
Ferro D.	P-7617	400
Feser R.	O-7322, O-7323	257, 352
Fickert J.	O-7228	448
Filatov Y.V.	P-7317	201
Fino P.	O-7536	588
Finsgar M.	O-7465	329
Firouzi A.	O-7187	439
Fischer D.	O-7613, P-7609	248, 551
Fitzpatrick L.	O-7195	446
Flachet M.	O-7623	238
Flanagan K.	P-7857	429
Fleischanderl M.	O-7641, O-7477, P-7372	166, 168, 417
Fletcher S.	O-7576	307
Fleury E.	O-7543	488
Fluch R.	O-7605	122
Foct F.	O-7631	90
Fontaine S.	O-7543, O-7834	488, 490
Forchin E.	P-7715	605
Foret C.	O-7114	6
Fori B.	O-7749	602
Foy E.	O-7486	97
Franchi M.	O-7206	224
Francis D.	O-7783	165
Francis R.	O-7805	305
Frandsen F.J.	O-7604	56
Frankel G.S.	O-7545	131
Franz S.	P-7099	190
Franzoni E.	O-7190	553
Fratesi R.	P-7457	295
Frateur I.	O-7553	272

Freitas E.	P-7799	194
Freitas R.	O-7627, P-7645	230, 479
Friedrich S.	O-7209	502
Frignani A.	O-7138	151
Fumagalli G.	P-7406, P-7520, O-7508	180, 209, 322
Fumei G.	O-7100	314
Fumei O.	O-7206, O-7100	224, 314
Fürbeth W.	O-7232, O-7170	375, 651
Fürtsch M.	O-7824	625
Fushimi K.	O-7278, O-7167, O-7364	134, 160, 162

G

Gabetta G.	O-7713, O-7541	222, 328
Gaillard N.	O-7088	281
Galarce C.	O-7613, P-7609	248, 551
Galeano M.	O-7523, P-7515	119, 208
Galeotti M.	O-7464, O-7849	554, 665
Galetz M.C.	O-7168, O-7414	453, 454
Galli G.	O-7671	574
Gallien J.P.	O-7623, O-7186, O-7594	238, 562, 564
Galtayries A.	O-7594	564
Ganta R.	O-7756	51
Gao J.	P-7652	425
Gao L.X.	O-7147	62
Garcia A.	P-7799, P-7732	194, 457
Garcia E.	O-7395	326
García Ferré F.	O-7505	95
Garcia J.	O-7579	464
García-Antón J.	P-7517, P-7504, P-7514, P-7525, P-7530	40, 206, 207, 396, 402
García-Blanco B.	O-7418	357
García-Lecina E.	O-7418	357
García-Ochoa E.	P-7335	631
García-Urrutia I.	O-7418	357
Garrecht H.	O-7204	158
Garrelfs J.	O-7077	242
Gartner N.	O-7656	283
Gastaldi M.	O-7624	273
Gauquelin C.	O-7384	241
Gavgali M.	O-7198	658
Gavrilovic A.	O-7208	597
Gazeau C.	O-7749	602
Ge H.	O-7683	251
Geary S.	O-7549	170
Gehrke J.	P-7427	183
Geiplova H.	O-7425	560
Geis-Gerstorfer J.	P-7216	435
Gelling V.J.	O-7265, O-7262	279, 434
Genchev G.	O-7233	311
Gennaro M.E.	O-7510	318
Gentaz L.	O-7501	91
Gerengi H.	O-7169	8
Gerets B.	O-7248	529
Gheno T.	O-7109	58
Ghiara G.	O-7377	253
Ghidini T.	O-7803	595

Gholinia A.	O-7783	165
Gibalenko A.N.	P-7317	201
Gibbon S.	O-7783	165
Gierth U.	O-7144	229
Gin S.	O-7501	91
Ginocchio M.	O-7729	638
Giorgi M.L.	O-7659	96
Gipon E.	KN-7691	76
Giray E.S.	O-7498	12
Girginov C.	P-7300	391
Glover C.	O-7547	413
Gnedenkov A.	O-7202	172
Gnedenkov S.V.	O-7338, O-7202, O-7166	139, 172, 361
Gobessi A.	O-7584	382
Godja N.	O-7208, O-7367	597, 598
Goidanich S.	O-7849	665
Goldfine N.	P-7858	480
Golenishcheva O.	O-7434, O-7460	174, 520
Golozar M.A.	P-7845	370
Gomez C.	O-7458	227
Gomez Sanchez A.	P-7090	188
Goncharova O.A.	O-7658	19
Gonzalez J.L.	O-7222	637
González Rodríguez J.G.	P-7126, P-7770	44, 186
González V.	O-7265	279
González-Martínez R.	O-7224	514
Gorewoda T.	P-7274	371
Gorgulho H.F.	O-7674	29
Gosselin I.	O-7579	464
Gouda V.	O-7727	581
Grabowski M.W.	O-7161	512
Gracco A.	O-7625	359
Gracenea J.	O-7725	431
Graham A.	O-7803	595
Grassi V.	O-7138, O-7253	151, 304
Grassini S.	O-7474, O-7671, O-7519, O-7727	563, 574, 579, 581
Grattieri M.	O-7533	245
Graver B.	O-7488	332
Grengg C.	O-7791	252
Gressier M.	O-7749	602
Grilli R.	P-7680	607
Grimes W.D.	O-7576, O-7571	307, 319
Grogger W.	O-7500	474
Grolleau A.M.	O-7222	637
Grønvold F.	O-7662, O-7365	292, 642
Grosjean F.	P-7777, O-7240	345, 633
Grousset S.	O-7594	564
Groysman A.	O-7062, O-7061	221, 466
Grundmeier G.	O-7635	406
Grüters J.	O-7414	454
Guastaferro D.	P-7291	196
Gudla V.	P-7337, P-7601	393, 399
Guene E.	O-7225	621
Guerrini E.	O-7794, O-7533, O-7797, O-7849	239, 245, 256, 665
Gulli G.	O-7522	440

Gümpel P.	P-7155	177
Guo L.	O-7829	123
Gustavsen T.A.	O-7196	589
Gutierrez A.	O-7362	374
Guttmann P.	O-7660	527

H

Hachtel A.	O-7824	625
Hack T.	O-7786, O-7640	655, 656
Hägg Mameng S.	O-7424, O-7410	542, 545
Haghighat Y.	O-7120	476
Hagler J.	O-7243	169
Haider F.	O-7497	525
Hajdari Z.	O-7289	11
Hakeem M.	O-7069	32
Halamová M.	P-7406	180
Halem N.	P-7574	459
Halem Z.	P-7574	459
Halle T.	O-7455	146
Hallen J.M	P-7336	338
Halseid M.	O-7743, O-7744	609, 612
Hamdane O.	O-7687	648
Hamdani F.	O-7149	79
Hamdy N.	P-7041	498
Hammer P.	P-7194	421
Hammouti B.	O-7234	27
Han E.H.	KN-7830	220
Hannour F.	O-7854	526
Harb S.V.	P-7194	421
Harek Y.	P-7461	36
Härkönen E.	O-7242	380
Harvey M.D.F.	O-7458	227
Hasegawa R.	O-7075	260
Hasegawa Y.	O-7278, O-7167, O-7364	134, 160, 162
Hashimoto R.	O-7327	522
Hashimoto T.	O-7246, O-7783	129, 165
Hashizume S.	O-7095	312
Haslehner G.	O-7477	168
Haspel D.	O-7236	626
Hassan N.	P-7596	43
Hassel A.W.	O-7484, O-7477, O-7485	156, 168, 404
Hater W.	O-7114	6
Haupt H.	O-7820	530
Havlik W.	O-7610	16
Hawkins T.	P-7341	394
Hays G.	KN-7830	220
Hegazy M.A.	P-7163, P-7164	37, 46
Hegazy M.H.	P-7044	293
Heinemann J.	O-7820	530
Helm C.	O-7583	291
Heming F.	O-7072	528
Herrera-Gutiérrez H.	P-7771	187
Herrmann M.	O-7602	171
Heyn A.	O-7455, O-7473	146, 384
Hicks K.	O-7459	575

Hill A.	O-7773	353
Hinder S.	P-7680	607
Hintze-Bruening H.	O-7417, O-7379	137, 442
Hirano S.	O-7171	301
Höche D.	O-7142	173
Hochmannova L.	P-7068	176
Hogg S.	O-7421	586
Holm A.	O-7823	628
Holper B.	O-7605	122
Homborg A.M.	O-7313	153
Hondjuila-Miokono E.	O-7579	464
Hong S.J.	P-7297	197
Hönig S.	O-7610	16
Honoré P.	O-7222	637
Hoshi Y.	P-7442	362
Hosseinpour S.	P-7218	100
Hoxha G.	O-7491	320
Huang W.	O-7271	114
Huang Y.L.	O-7808	232
Huttunen-Saarivirta E.	O-7752	433

I

Iannuzzi M.	P-7284	195
Ibrahim A.	O-7729	638
Igarashi T.	O-7096	86
Igartua A.	O-7772	649
Igetoft L.	O-7815	20
Iglesias M.	P-7558	41
Ignatenko V.	O-7074	113
Ilhan-Sungur E.	P-7270	262
Ingo G.M.	O-7519	579
Iqbal D.	O-7526, O-7493	513, 405
Ishak R.	O-7586	118
Ishiguro Y.	O-7368	302
Ishizaki T.	O-7782	666
Ismailov T.A.	P-7859	346
Isotahdon E.	O-7752	433
Itagaki M.	P-7442	362
Ito D.	O-7171	301
Ivanov D.	O-7640	656
Ivashechkin P.	P-7566	210
Izagirre Etxeberria U.	P-7730	388

J

Jacklin R.	O-7603	93
Jackson J.	O-7465	329
Jacobsen J.	O-7823, P-7826	628, 630
Jacques S.	O-7548	541
Jalowicka A.	O-7252	65
Jama C.	O-7234, P-7231	27, 390
Jamali S.S.	O-7697	154
Jamborova T.	O-7139	552
Jang C.	P-7435	185
Jansen S.	O-7843	582
Jansson J.	O-7375	641

Jeannin M.	O-7156, O-7137, O-7129, KN-7848, O-7136, P-7386, O-7306 92, 157, 228, 237, 565, 635, 639	
Jeffrey R.	O-7199	246
Jellesen M.S.	O-7302, O-7447, O-7082, O-7495, O-7426, P-7826 430, 617, 618, 619, 622, 630	
Jensen B.	O-7365	642
Jensen F.	P-7337, P-7601	393, 399
Jensen M.	O-7262	434
Jesson D.	O-7466	539
Jezequel T.	O-7542	83
Jiang H.	P-7652	425
Jiang X.	O-7728	18
Jindrova E.	O-7139	552
Jivkov A.P.	O-7436	80
Job D.	O-7562	576
Jochems F.	O-7072	528
Jochum M.	O-7751	414
Johansson E.	O-7424	542
Johnsson M.	P-7218	100
Joiret S.	P-7777	345
Jolley S.T.	O-7195	446
Jonkers H.M.	O-7301	259
Jonsson M.	P-7218, O-7540	100, 505
Jonsson S.	O-7383	523
Jonsson T.	P-7535	73
Jorcin J.B.	P-7714	236
Joseph E.	O-7562	576
Jovancicevic V.	O-7238	327
Jung W.S.	P-7297	197
Jung Y.H.	P-7297	197
Junier P.	O-7562	576
Juraga I.	P-7396	547

K

Kaesche S.	O-7204	158
Kajiyama F.	O-7148	486
Kajiyama H.	O-7655	507
Kakaroglou A.	O-7608	408
Kallip S.	O-7257	653
Kalume R.	P-7813	341
Kaluzhina S.	P-7298, P-7308	198, 199
Kamiyama N.	O-7782	666
Kapor F.	P-7710	48
Kapp M.	O-7605	122
Kappes M.	P-7284	195
Karlsen G.W.	O-7196	589
Kashi K.	O-7262	434
Katayama H.	P-7442	362
Kazansky L.P.	O-7352	13
Keddam M.	O-7798	647
Keech P.G.	O-7603	93
Keil P.	O-7417, O-7379	137, 442
Kek Merl D.	O-7177	416
Kentved A.B.	O-7521	623
Keppert T.	O-7243	169

Kestens L.	O-7373	155
Khalil S.	P-7596	43
Kharkiov A.	O-7776	309
Khelifa F.	O-7131	603
Khobragade N.	O-7570	159
Khorsand S.	P-7844, P-7845	369, 370
Khosravi J.	O-7407	323
Khrisanfova O.A.	O-7338	139
Kiamehr S.	P-7535	73
Kicir N.	P-7814	45
Kilic A.	O-7781	55
Kim J.S.	O-7125	348
Kim K.Y.	P-7294	38
Kim M.	O-7366	415
Kim S.H.	O-7125	348
Kim S.Y.	O-7125	348
Kim T.C.	O-7125	348
Kim T.Y.	P-7297	197
Kimura M.	O-7655	507
Kittel J.	P-7777, O-7811, O-7240	345, 608, 633
Kivisäkk U.	O-7572	145
Kiyak T.	O-7198	658
Kleber Ch.	P-7663, O-7208, O-7367	437, 597, 598
Klein L.H.	O-7211, O-7217, O-7373, O-7242	141, 150, 155, 380
Klein M.	O-7576	307
Klesen C.	O-7232	375
Klett G.	O-7824	625
Klimaytys G.	O-7436	80
Klinghoffer O.	O-7662	292
Kloewer J.	O-7434	174
Kluger F.	O-7598	52
Knoll D.	O-7327, O-7497	522, 525
Knudsen O.	O-7408, O-7413	467, 483
Kocabas M.	O-7614	517
Koch G.	O-7229	247
Koenders E.A.B.	O-7260	271
Kok J.	O-7393	286
Kokalj A.	O-7581	9
Kolesov S.	O-7776	309
Koleva D.A.	O-7301, O-7260, O-7116, O-7241, O-7557	259, 271, 287, 288, 290
Köliö A.	O-7741	289
Koltsov A.	O-7245	152
Komatsu A.	O-7096	86
Kooli W.	O-7562	576
Korb M.A.	P-7588, P-7667, P-7668	458, 460, 461
Korolov V.	P-7317	201
Korte M.	O-7161	512
Kosalla M.	O-7550	269
Kosec T.	O-7656, O-7358, O-7628, O-7630	283, 544, 578, 646
Kostitsyna I.V.	P-7214	336
Kouril M.	O-7139	552
Kozelj M.	P-7178	418
Kozhukharov S.	P-7300	391
Kraaijenbrink P.	O-7843	582
Kranzmann A.	O-7598, O-7400	52, 632

Krausová A.	O-7130, O-7665	84, 98
Krawiec H.	O-7626, O-7480	133, 148
Krebs A.	O-7322	257
Krecanová E.	O-7665	98
Kreislova K.	O-7425	560
Kreislová K.	P-7453	629
Kremmer K.	O-7602	171
Kritsky V.G.	P-7856	347
Krog J.P.	O-7823, P-7826	628, 630
Kroke E.	O-7362	374
Krumm M.	O-7773	353
Kudo T.	O-7205	333
Kumai T.	O-7055	356
Kunst S.R.	P-7558, P-7509	41, 395
Kuokkala V.-T.	O-7752	433
Kurauchi K.	O-7278	134
Kuriki Y.	O-7735	226
Kurtay M.	O-7169	8
Kuylenstierna J.	O-7459	575
Kuznetsov Yu.I.	O-7658, P-7212	19, 34
Kuznetsova A.	O-7627	230
Kvarekvål J.	O-7472	315
Kvernbråten A.-K.	O-7196	589
Kwak Y.J.	P-7297	197

L

L'Hostis V.	O-7381	94
La Iglesia V.	O-7265	279
La Russa M.F.	O-7671	574
Labrenz E.	O-7411	350
Lackner R.	O-7500	474
Lahdensivu J.	O-7741	289
Lamaka S.V.	O-7700, O-7640	601, 656
Landfester K.	O-7228, P-7219	448, 449
Landim R.V.	P-7813	341
Lange M.M.	O-7529	60
Langklotz U.	O-7144	229
Lanneluc I.	KN-7848	237
Lanzutti A.	O-7132	167
Lapeire L.	O-7373	155
Larché N.	O-7370, O-7154	225, 303
Laügt A.M.	O-7227, O-7225	620, 621
Law D.	O-7353	240
Lazzari L.	O-7513, P-7520, O-7518	164, 209, 489
Le Boulch D.	O-7542	83
Le Glatin S.	O-7222	637
Le Manchet S.	O-7151, O-7480	124, 148
Le T.M.L.	O-7789	654
Lebozec N.	O-7193	509
Lecardi G.	O-7754	493
Lee D.Y.	P-7297	197
Lee J.-S.	O-7364	162
Lefebvre L.	O-7532	645
Legat A.	O-7636, O-7656, O-7630	81, 283, 646
Legendre S.	P-7404	179

Lehrer S.	O-7238	327
Leining E.	KN-7830	220
Leinum B.	O-7488	332
Leis A.	O-7791	252
Leitner H.	O-7605	122
Leiva-García R.	P-7517, P-7514, P-7530	40, 207, 402
Lemos Menezes T.	P-7509	395
Len C.	O-7579	464
Lengwin F.	O-7244	354
León E.J.	O-7301	259
Léon Y.	O-7623	238
Leroux F.	O-7417, O-7379	137, 442
Leroy A.	O-7568, P-7573	66, 69
Letardi P.	O-7562	576
Levander L.	O-7540	505
Levasseur A.	O-7756	51
Leygraf C.	P-7218, O-7572, O-7382	100, 145, 557
Li W.	O-7195	446
Li W.J.	P-7184	450
Li X.	P-7654, P-7652	343, 425
Li X.	O-7361	487
Liang R.	O-7361	487
Liang S.	O-7246	129
Lignola G.P.	O-7842	285
Lijanová I.V.	P-7336	338
Likhanova N.V.	P-7336	338
Lima D.A.S.	P-7667	460
Lima Junior D.R.	P-7763	263
Lima L.I.L.	P-7813	341
Lima M.A.G.A.	P-7763	263
Lin M.	O-7829	123
Lindgren M.	P-7182	33
Lindsay R.	O-7587	21
Linhardt P.	P-7696	219
Liptáková T.	P-7406	180
Liu C.-N.	O-7635	406
Liu H.	O-7246	129
Liu Q.	O-7806	115
Liu Y.	O-7783	165
Liu Z.	P-7654	343
Lizárraga C.	O-7333	495
Llorente I.	O-7265	279
Lo Piccolo E.	O-7255	15
Loable C.	O-7701	284
Locaspi A.	O-7812	663
Loch J.	O-7626	133
Loepp D.	P-7617	400
Logan R.	O-7466	539
Lohne P.I.	O-7196	589
Lojewski C.	O-7151	124
Lollini F.	O-7624	273
Lønvik K.	O-7488	332
Lopez A.	O-7772	649
Lorenzi S.	P-7451, O-7536, O-7524	191, 588, 611
Lotfollahi Yaghin A.	O-7084	244

Loto C.A.	O-7774	30
Loto R.T.	O-7774	30
Lotz M.	O-7188	532
Loureiro S.	O-7627	230
Lourenço M.M.	O-7775, O-7640	373, 656
Lovicu G.	O-7586, O-7684	118, 325
Lu C.J.	P-7184	450
Lu K.	KN-7108	5
Lu L.	P-7652	425
Lucca C.	P-7566	210
Lucca G.	P-7066	215
Lucio-Garcia M.A.	P-7770, P-7768, P-7732	186, 205, 457
Luckeneder G.	O-7243, O-7433	169, 504
Ludwig G.A.	P-7588, P-7667, P-7668	458, 460, 461
Lukaszczyk A.	O-7626	133
Lunkenheimer R.	O-7114	6
Lutz A.	O-7282, O-7145, P-7374	445, 447, 452
Lv L.-P.	P-7219	449
Lyon S.B.	O-7783, P-7642, O-7226, O-7638, O-7589	165, 182, 310, 385, 569

M

Macák J.	O-7130, O-7665	84, 98
Maciej A.	P-7274	371
Maciel P.	KN-7708, O-7237	127, 136
Madloch S.	O-7168	453
Maeng W.	O-7366	415
Maggi G.	O-7250, O-7251	531, 533
Maggi V.	P-7268	422
Magnabosco R.	P-7078	212
Magot M.	O-7623	238
Magrini M.	O-7239	379
Mahaut M.L.	O-7222	637
Mahmoud H.	O-7439	321
Maia F.	O-7627	230
Majtás D.	P-7453	629
Malfatti C.F.	P-7558, P-7509, P-7588, P-7667	41, 395, 458, 460
Malina J.	P-7710	48
Malki B.	O-7158	142
Mallarino S.	O-7560	407
Manfredi D.	O-7536	588
Manfredi G.	O-7842	285
Mansur F.	P-7600	107
Mantel M.	O-7531, O-7701	61, 284
Manzi S.	O-7261, O-7551	266, 268
Marcantelli P.	P-7470, O-7729	363, 638
Marcassoli P.	O-7729	638
Marcus P.	KN-7695, O-7211, O-7217, O-7373, O-7703, O-7242, O-7376	126, 141, 150, 155, 243, 380, 583
Mari F.	O-7754	493
Marinelli U.	O-7694	492
Marion A.	O-7264	161
Mariscotti M.	O-7088	281
Marlair G.	O-7579	464
Marney D.	O-7353	240
Marotta F.	P-7086	101

Marsal F.	O-7623	238
Marshakov A.I.	O-7074	113
Martelli P.B.	O-7674	29
Martikainen M.	P-7182	33
Martinelli L.	P-7836	108
Martinez Lombardia E.	O-7373	155
Martini C.	O-7190, O-7259, O-7192	553, 555, 558
Martins B.	O-7669	410
Martins M.	P-7764, P-7637	296, 298
Martins R.	O-7627	230
Marusic K.	O-7289, O-7628, O-7319	11, 578, 580
Mary N.	O-7528, O-7532	644, 645
Mascaro L.H.	P-7618, P-7645	163, 479
Mashtalyar D.V.	O-7202	172
Masiu P.C.	O-7757	360
Masouri D.	O-7606, O-7619, O-7634	233, 334, 496
Masquelier C.	O-7369	349
Massoud T.	O-7211	141
Matheis J.	O-7114	6
Mathiesen T.	O-7446	117
Mathys L.	O-7562	576
Matos R.	P-7645	479
Matsuda T.	O-7262	434
Mattedi S.	P-7558	41
Mattern S.	O-7818	616
Mattos O.R.	P-7079, P-7047	342, 344
Maurice V.	O-7211, O-7217, O-7373, O-7242	141, 150, 155, 380
Maya E.	P-7341	394
Mayrhofer K.J.J.	O-7545, O-7077	131, 242
McCoy S.A.	O-7539	57
McMurray H.N.	O-7070, O-7549	128, 170
Medina Da Silva M.	O-7618	163
Medina E.	O-7265	279
Medvedev I.M.	P-7312, O-7784	200, 592
Melchers R.E.	O-7084, O-7199, O-7200	244, 246, 265
Mele A.	O-7448	324
Melilli E.	P-7291	196
Melis G.	O-7395	326
Memet J-B.	O-7390	570
Mendes Zimer A.	O-7618	163
Mendez S.	O-7224	514
Mendonça Lima M.	P-7569	340
Mendonça R.	O-7661	82
Meneghelli F.	O-7828	660
Meneguzzi A.	P-7268	422
Meng X.	O-7683	251
Meng Y.	O-7147	62
Menu M-J.	O-7749	602
Mercier-Bion F.	O-7623, O-7594	238, 564
Merlin M.	O-7253	304
Mertke A.	O-7323	352
Mesquita T.J.	O-7701	284
Meyer J.J.	P-7855	299
Meyer M.	O-7543	488
Meynial-Salles I.	O-7384	241

Mezeg U.	O-7630	646
Michalska J.	P-7274	371
Michau N.	O-7631, O-7486	90, 97
Mietz J.	O-7207, O-7489	274, 481
Mihelcic M.	P-7178	418
Mikhail S.	P-7565	397
Mille C.	O-7815	20
Mills D.J.	O-7697	154
Milosev I.	P-7748, P-7745	35, 50
Min J.K.	P-7297	197
Minachi A.	P-7858	480
Minakova T.A.	P-7308	199
Minamitani R.	O-7203	624
Mindos L.	P-7068	176
Mirhashemihaghighi S.	O-7242	380
Mischler S.	P-7847	585
Mittermayr F.	O-7791	252
Miyahara R.	P-7442	362
Miyanaga K.	O-7075	260
Miyasaka M.	O-7735	226
Mizukami Y.	O-7095	312
Mobili A.	O-7546	276
Močnik P.	O-7630	646
Mohammed-Ali H.B.	O-7676	140
Mol J.M.C.	O-7313, O-7301, O-7260, O-7511, O-7180, O-7179, O-7616, O-7700	153, 259, 271, 516, 591, 596, 599, 601
Molena de Assis C.	O-7643	652
Molina J.	O-7725	431
Momber A.	O-7792	640
Monceau D.	O-7109, O-7531	58, 61
Monelli B.	O-7670	508
Monetta T.	O-7842, P-7825, O-7223	285, 372, 409
Montalbani S.	O-7190	553
Monteiro M.V.C.	P-7325	39
Montemor M.F.	O-7669, O-7810, O-7700	410, 411, 601
Montesin T.	P-7759	104
Montesperelli G.	O-7187	439
Montgomery M.	O-7604, P-7535	56, 73
Monticelli C.	O-7261, O-7551, O-7265, O-7259, O-7192	266, 268, 279, 555, 558
Moo-Yam V.	O-7333, P-7335	495, 631
Moradi M.	O-7334, P-7809	250, 264
Moraes R.	O-7563	317
Morando C.	P-7092	189
Morcillo M.	P-7566	210
Moreira A.R.	O-7197	556
Moreira F.M.A.	O-7674	29
Mori G.	O-7610, O-7605, O-7500, O-7433, O-7327	16, 122, 474, 504, 522
Morimoto T.	O-7055	356
Morland B.	O-7743, O-7744	609, 612
Morozov Y.	O-7669	410
Mortali G.	O-7255, O-7395	15, 326
Mortimer R.J.	O-7236, O-7403	626, 627
Moshira Y.	O-7280	28
Mosquera Feijoo M.	O-7598, O-7400	52, 632
Mouanga M.	O-7132, O-7185, O-7131	167, 443, 603

Mousa M.E.	P-7565	397
Moutrille M-P.	KN-7691	76
Msallem A.	O-7729	638
Mueller T.	O-7473	384
Muhr A.	O-7433	504
Mulheron M.	O-7466	539
Müller I.L.	P-7667	460
Müller L.	O-7824	625
Muñoz-Portero M.J.	P-7517	40
Murillo E.M.	O-7554, P-7738	475, 549
Muzeau B.	O-7381	94
Mylvakanam I.	O-7459	575

N

Nad'kina E.A.	O-7658	19
Nafikova N.	P-7298	198
Naitoh M.	O-7104	77
Najmi M.	O-7606	233
Nakahashi T.	O-7368	302
Nakamura H.	O-7275	144
Nakanishi T.	O-7278, O-7167, O-7364	134, 160, 162
Nakayama G.	O-7176	87
Nam K.H.	P-7297	197
Nam T.	O-7275	144
Narcy B.	O-7579	464
Nassif M.	P-7516	436
Natali M.E.	O-7261, O-7551	266, 268
Naumenko D.	O-7252	65
Navet A.	O-7568, P-7573	66, 69
Nayak S.	O-7077	242
Neacsu E.	O-7429	89
Necib S.	O-7631, O-7486	90, 97
Neff D.	O-7501, O-7623, O-7186, O-7474, O-7594, O-7390	91, 238, 562, 563, 564, 570
Nelemans A.	O-7141	308
Nesi M.	O-7464	554
Neubauer B.	O-7250, O-7251	531, 533
Neville A.	O-7439	321
Ngo H.-L.	O-7579	464
Nice P.I.	O-7141	308
Nicolay L.	P-7847	585
Nielsen P.K.	O-7230	643
Niendorf T.	O-7635	406
Niewolak L.	O-7140	59
Nikendey V.	O-7272	577
Niklas A.	O-7224	514
Nikolaev F.V.	P-7856	347
Nimrova A.	O-7666	377
Nishikata A.	O-7275	144
Nishiura Y.	O-7055	356
Nisol B.	O-7608	408
Nogueira P.	P-7600	107
Nogueira R.P.	O-7701	284
Noh J.	O-7366	415
Noiville R.	O-7749	602

Nonus M.	O-7579	464
Nordgren E.	O-7496	567
Normand B.	O-7149, O-7499, O-7528, O-7532	79, 149, 644, 645
Nóvoa X.R.	O-7790	231
Nowak W.	O-7252	65
Nowotnick M.	O-7818	616
Nygaard P.V.	O-7662	292

O

Oakey J.E.	O-7544	53
Obike A.	O-7728	18
Obot I.	O-7438	25
Ochoa M.	P-7091	102
Oder G.	O-7598	52
Odnevall Wallinder I.	O-7382	557
Oechsner M.	O-7434, O-7428, O-7460, O-7481, O-7820	174, 381, 520, 521, 530
Oelzant D.	O-7660	527
Ogle C.	O-7678	524
Ogle K.	O-7417	137
Oh M.S.	O-7125	348
Ohtsuka T.	O-7278	134
Okada H.	O-7104	77
Okafor P.C.	O-7728	18
Okazaki S.	O-7171	301
Okoro S.C.	O-7604	56
Oldani L.	O-7753	540
Olivares-Xometl O.	P-7336	338
Oliveira A.L.	P-7645	479
Oliveira M.D.	O-7699	465
Oliveira S.H.	P-7763	263
Oliveira T.	P-7079	342
Olivero C.	P-7404, O-7666	179, 377
Olivier M.-G.	O-7132, O-7452, O-7185, O-7152, O-7131	167, 412, 443, 519, 603
Oltra R.	P-7759, O-7264, O-7263, O-7789	104, 161, 600, 654
Omer F.	O-7127	471
Omoda M.	O-7655	507
Omori Y.	O-7055	356
Opsoelder M.	O-7751	414
Oquab D.	O-7531	61
Orel B.	P-7178	418
Ormellese M.	O-7505, O-7513, O-7448, O-7518	95, 164, 324, 489
Ormiga F.	P-7476, P-7326	193, 202
Örnek C.	O-7213	143
Ortega Vega M.R.	P-7558, P-7509	41, 395
Osmond M.	P-7664	109
Osório W.	P-7799	194
Osvoll H.	O-7747, O-7746	491, 494
Otmacic Curkovic H.	O-7289, P-7591, O-7628, O-7319	11, 398, 578, 580
Otsuka N.	O-7205	333
Oubaha M.	P-7760	606
Ozcan O.	O-7635	406

P

Pagano F.	O-7772	649
Palmieri B.I.	P-7813	341

Palomino L.E.M.	P-7552	376
Pan J.	O-7572	145
Panossian Z.	O-7197	556
Pantleon K.	O-7604	56
Panzenböck M.	O-7605, O-7380	122, 543
Papadopoulou O.	O-7727	581
Pargar F.	O-7260	271
Park H.S.	O-7349	510
Park J.H.	P-7294	38
Parry V.	O-7531	61
Parshukov V.P.	P-7214	336
Partovi-Nia R.	O-7603	93
Parvis M.	O-7474	563
Pascal C.	O-7531	61
Passeri C.	O-7190	553
Pastore T.	P-7451, O-7536, O-7524	191, 588, 611
Pasturel A.	O-7158	142
Patil A.	O-7570	159
Patil A.P.	O-7315	501
Paul S.	O-7458, O-7456	227, 610
Paussa L.	O-7584, O-7185	382, 443
Pearman B.P.	O-7195	446
Peca D.	O-7581	9
Pedefferri M.P.	O-7448, O-7450	324, 664
Peguet L.	O-7385, O-7482	515, 518
Peltier F.	O-7263	600
Peltola H.	P-7182	33
Peña D.	P-7707	389
Peng H.	O-7217	150
Pepenar I.	O-7314	277
Perdu G.	O-7811	608
Pereira A.P.	P-7721, P-7720	477, 478
Pereira E.C.	O-7618, P-7645	163, 479
Peres V.	O-7240	633
Perez A.	O-7623	238
Pérez C.	O-7790	231
Pérez T.	P-7632, O-7333, P-7335	297, 495, 631
Perfect E.	O-7173	14
Perini R.	P-7451	191
Perre E.	O-7751	414
Peschke G.	O-7787	561
Petot-Ervas G.	P-7574	459
Pette A.	O-7726	462
Pettersson R.	O-7512, O-7410	111, 545
Peultier J.	O-7548	541
Pezzato L.	O-7239	379
Pfeifer S.	O-7362	374
Phan T.	P-7231	390
Piçarra S.	O-7669	410
Piccardo P.	O-7377	253
Pichler M.	O-7641, P-7372	166, 417
Pillai R.	O-7059	54
Pilz G.	O-7660	527
Pineau S.	O-7129, O-7222	228, 637
Pinger T.	O-7369, P-7191	349, 364

Piotrowska K.	O-7495	619
Pizarro G.	O-7613, P-7609	248, 551
Plennevaux C.	O-7821	306
Pogliana M.	P-7291	196
Poltavtseva M.	O-7489	481
Pölzer M.	O-7208	597
Ponciano Gomes J.A.C.	P-7325, P-7475, P-7476, P-7326, P-7328, P-7494	39, 192, 193, 202, 337, 339
Ponthiaux P.	O-7798, P-7330	647, 650
Poorteman M.	O-7452	412
Popova T.A.	P-7308	199
Porcinai S.	O-7464, O-7849	554, 665
Pori P.	P-7178	418
Porta R.	O-7491	320
Posner R.	O-7511	516
Potgieter H.	P-7409	181
Potter A.	O-7544	53
Pradhan B.B.	O-7459	575
Pranovi P.	O-7206	224
Prethaler A.	O-7610	16
Prieto A.	P-7714	236
Primožic J.	O-7630	646
Proriol Serre I.	O-7688, O-7687	120, 648
Prota A.	O-7842	285
Provazi de Souza K.	P-7552	376
Proverbio E.	O-7523, P-7515, P-7534, O-7522	119, 208, 213, 440
Pruzzo C.	O-7377	253
Puechagut C.	O-7225	621
Pulcinelli S.H.	P-7194	421
Puri Y.M.	O-7315	501
Puricelli G.	P-7099	190
Puz' A.V.	O-7338	139
Pyshmintsev I.Yu.	P-7214	336

Q

Qian H.	P-7652	425
Qiao L.	O-7829	123
Qu D.R.	O-7728	18
Qu W.J.	O-7808	232
Quadackers W.J.	O-7059, O-7140, O-7252	54, 59, 65
Queiroz F.M.	P-7124	426
Quej-Aké L.	O-7333	495
Quinan M.A.D.	P-7600	107

R

Raedel M.	O-7734	573
Raeissi K.	P-7844, P-7845	369, 370
Raffo S.	O-7192	558
Raheem K.A.	P-7215	403
Raimbault L.	O-7594	564
Rajendran S.	O-7056, O-7069	31, 32
Ram C.	P-7281	550
Ramachandran S.	O-7238	327
Ramamurthy S.	O-7603	93
Ramos L.	P-7707	389

Rance A.P.	O-7503	88
Rankin S.	O-7173	14
Rasheed A.	O-7093	330
Rassow A.	P-7566	210
Raupach M.	O-7550, O-7583	269, 291
Rauter A.	O-7177	416
Rayon Lopez N.	O-7778	26
Re G.	P-7520, O-7508	209, 322
Rebak R.B.	O-7283, P-7284, P-7590	85, 195, 366
Rebiscoul D.	O-7501	91
Reby J.	O-7210	112
Recloux I.	O-7185, O-7131	443, 603
Reddy B.	O-7503	88
Refait P.	O-7156, O-7137, O-7129, KN-7848, O-7136, P-7386, O-7222, O-7306	92, 157, 228, 237, 565, 635, 637, 639
Regis P.P.	O-7069	32
Rehfeldt S.	O-7598	52
Reimann S.	P-7405	548
Reiner L.	KN-7108, O-7107, P-7855	5, 282, 299
Reis C.M.	P-7552	376
Reis de Castro M.M.	P-7569	340
Reitz R.	O-7460	520
Remazeilles C.	O-7137, O-7136	157, 565
Renciuková V.	O-7130	84
Reniers F.	O-7608	408
Renner F.U.	O-7529	60
Rese H.	O-7141	308
Resende C.	O-7674	29
Reyes-Hernandez R.	P-7768	205
Ribeiro Piaggio Cardoso H.	P-7509	395
Riener C.K.	O-7243, P-7143	169, 368
Righetti M.	O-7625	359
Riis A.	O-7823	628
Riis K.	O-7393	286
Rimestad L.	O-7823	628
Rimmer M.	O-7589, O-7258	569, 571
Rincon Ortiz M.	P-7284	195
Rios E.C.	P-7645	479
Ritala M.	O-7242	380
Rivollier M.	O-7659	96
Roblero E.	P-7335	631
Robson J.	O-7246	129
Rocca E.	O-7593, O-7597	378, 383
Roche V.	O-7701	284
Rode K.	O-7248, P-7247, P-7249	529, 536, 537
Rodosek M.	O-7177, P-7178	416, 418
Rodriguez J.	O-7132	167
Rodríguez J.M.	O-7265	279
Rodriguez M.A.	P-7091, P-7284	102, 195
Rodríguez-Ripoll M.	O-7360	68
Rohuma F.	P-7172	49
Rohwerder M.	O-7391, O-7493, O-7228, P-7219, P-7443	116, 405, 448, 449, 451
Rojacz H.	O-7360	68
Rolla L.	O-7586	118
Romaine A.	O-7156	92

Romano A.-P.	O-7152	519
Ronceray M.	P-7215	403
Roos C.	O-7802	255
Ropital F.	O-7240	633
Ropret P.	O-7628	578
Rosemann P.	O-7455	146
Rosenberg E.	O-7610	16
Rosetti L.	O-7849	665
Rossi A.	O-7787	561
Rossi S.	O-7506	147
Rossrucker L.	O-7545	131
Rouvre I.	O-7384	241
Roventi G.	O-7546, P-7457	276, 295
Rubio-Cervera J.	P-7517	40
Rückemann M.	O-7610	16
Rückle D.	O-7204	158
Ruel F.	O-7151	124
Ruffolo M.	O-7088	281
Ruffolo S.A.	O-7671	574
Ruiz-Camargo C.	O-7587	21
Rulison Chr.	O-7577	593

S

Saatchi A.	O-7316	456
Sable S.	KN-7848	237
Sabot R.	O-7156, O-7137, O-7129, KN-7848, O-7136, P-7386, O-7306 92, 157, 228, 237, 565, 635, 639	
Sabri H.	O-7146	497
Saedlou S.	O-7151, O-7528, O-7532	124, 644, 645
Sagara M.	O-7205	333
Sahrhage H.	O-7773, O-7831	353, 535
Saint-Victor F.	O-7488	332
Sajdl P.	O-7130, O-7665	84, 98
Sakai J.	O-7735	226
Sakairi M.	O-7095	312
Sakakibara Y.	O-7176	87
Salguero Azevedo M.	O-7678	524
Salvadori B.	O-7464, O-7849	554, 665
Salvin P.	O-7802	255
Samy M.	O-7280	28
Sánchez-Tovar R.	P-7504, P-7514, P-7525, P-7530	206, 207, 396, 402
Sangeetha M.	O-7056	31
Santana A.I.C.	P-7047	344
Santilli C.V.	P-7194	421
Santos A.F.S.	O-7622	587
Santos W.I.A.	P-7680	607
Sarazin C.	O-7579	464
Sarfraz A.	O-7233	311
Sathiyabama J.	O-7056	31
Sato H.	O-7368	302
Sato Y.	O-7399	355
Sawczen T.	O-7287	438
Sayed F.M.	P-7044	293
Scamans G.	O-7246	129
Scatena A.	O-7266	300

Scharf R.	O-7433	504
Scheltjens G.	O-7608	408
Schiavon G.L.	O-7831	535
Schiek M.	O-7140	59
Schille C.	P-7216	435
Schimo G.	O-7484	156
Schindel A.	P-7663, O-7208, O-7367	437, 597, 598
Schlegel M.	O-7631	90
Schlegel M.L.	O-7486	97
Schmid-Fetzer R.	O-7246	129
Schmidt K.A.	O-7521	623
Schmitt G.	O-7736	22
Schmitt R.	P-7847	585
Schmitz-Stöwe S.	O-7751, P-7761	414, 424
Schneider M.	O-7602, O-7144	171, 229
Schodl J.	P-7663	437
Schreiber C.	O-7209	502
Schulz F.M.	P-7086, P-7087	101, 294
Schulz Z.	O-7805	305
Schuster T.	O-7248, P-7247, P-7249	529, 536, 537
Schütze M.	O-7168, O-7414	453, 454
Schvartzman M.	P-7600	107
Schweigart H.	O-7819	615
Schweitzer Th.	O-7568, P-7573	66, 69
Schweizer E.	P-7216	435
Seemann P.	P-7155	177
Sempf K.	O-7602	171
Senatore E.	P-7494	339
Senhorst H.	O-7843	582
Serdechnova M.	O-7257	653
Seré P.R.	P-7124	426
Serna S.	P-7770, P-7768, P-7732	186, 205, 457
Serris E.	O-7240	633
Servidio D.	P-7617	400
Seyeux A.	KN-7695, O-7211, O-7217, O-7703, O-7242	126, 141, 150, 243, 380
Sgorlon S.	O-7510, O-7541	318, 328
Shabadi R.	P-7337	393
Shalaby H.	P-7516	436
Sharma C.	P-7281	550
Shel N.V.	P-7296	423
Shemet V.	O-7059	54
Sherik A.	O-7093	330
Shi W.	P-7642	182
Shinoda N.	O-7735	226
Shitanda I.	P-7442	362
Shkirskiy V.	O-7417	137
Shoeib M.	P-7580, P-7565, P-7516, O-7115	365, 397, 436, 455
Shoemaker L.E.	O-7539	57
Shoesmith D.W.	O-7603	93
Shutko K.	P-7801	106
Sigircik G.	O-7498, P-7567	12, 42
Silva A.	P-7799	194
Silva A.P.	O-7627	230
Silva G.V.	P-7813	341
Silva R.S.	P-7268	422

Silva S.	P-7328	337
Silveira D.M.	P-7719, P-7653	103, 235
Simar A.	P-7337	393
Simillion H.	KN-7708, O-7237	127, 136
Simka W.	P-7274	371
Simms N.J.	O-7544	53
Simoës A.M.	O-7775	373
Simunovic V.	P-7396	547
Sinebryukhov S.L.	O-7338, O-7202, O-7166	139, 172, 361
Singh A.	P-7201, P-7281	387, 550
Singh Moirangthem R.	O-7526	513
Singheiser L.	O-7059, O-7252	54, 65
Sivokon I.S.	O-7307	23
Skeldon P.	O-7666	377
Skovhus T.L.	O-7229	247
Slemenik Perse L.	O-7177, P-7178	416, 418
Sloof W.G.	O-7059	54
Smart N.R.	O-7503	88
Smit J.P.	O-7576	307
Smith A.	O-7395	326
Smith G.	O-7783	165
Smith G.D.	O-7539	57
Smith P.	O-7466	539
Snihirova D.	O-7669, O-7700	410, 601
Soares A.M.V.M.	O-7627	230
Sobetzki J.	O-7235	121
Sobrinho J.-M.	O-7210	112
Sociu F.	O-7429	89
Sof'in M.V.	P-7856	347
Sohn H.K.	P-7297	197
Sohrabi S.	O-7316	456
Soliman H.	P-7565	397
Soliman S.	O-7280	28
Somers M.A.J.	P-7535	73
Song G.	O-7366	415
Song Y.K.	O-7349	510
Song Z.	O-7334, P-7809	250, 264
Sørensen R.E.	O-7393	286
Souissi N.	O-7376	583
Souza C.S.	P-7719, P-7653	103, 235
Spark A.	O-7353	240
Speakman A.	P-7181	427
Spiegel M.	O-7781, O-7529, O-7233	55, 60, 311
Spinelli J.E.	P-7799	194
Spoljaric S.	O-7319	580
Stammose D.	P-7664	109
Startsev O.V.	P-7312, O-7784	200, 592
Stauder M.	O-7377	253
Steck T.	O-7244	354
Stefanoni M.	O-7437	267
Steinberger R.	O-7244	354
Stellnberger K.H.	O-7477, O-7243, O-7433	168, 169, 504
Stifanese R.	P-7715	605
Stifter D.	O-7243, O-7244, P-7143	169, 354, 368
Stimpfling T.	O-7417, O-7379	137, 442

Stojanovic I.	P-7396	547
Støre A.	O-7196	589
Storni G.	O-7797	256
Stoulil J.	O-7272, P-7273	577, 584
Straß B.	O-7170	651
Stratmann A.	O-7114	6
Stratmann M.	O-7077	242
Ström M.	O-7639	506
Stuttle C.J.	O-7403	627
Styazhkin P.S.	P-7856	347
Suay J.	O-7725	431
Sumner J.	O-7544	53
Sun J.	P-7098	234
Sun W.	O-7271	114
Sunaba T.	O-7171	301
Sundararajan G.	P-7590	366
Sunetci O.	P-7178	418
Surca Vuk A.	O-7177, P-7178	416, 418
Surma J.M.	O-7195	446
Susanto A.	O-7116	287
Sutter E.	O-7245, O-7553	152, 272
Suzuki T.	O-7368	302
Svadlena J.	P-7273	584
Swiatowska J.	O-7242	380
Szkalos P.	O-7383	523
Szala E.	O-7854	526

T

Tada E.	O-7275	144
Taheri P.	O-7260, O-7511, O-7700	271, 516, 601
Takabatake Y.	O-7167	160
Tan E.	P-7134	401
Tan Y.T.	O-7354	280
Tang Y.	P-7098	234
Tanji Y.	O-7075	260
Tansug G.	O-7498	12
Taravel-Condât C.	P-7777	345
Tarquini B.	P-7451	191
Tasçioğlu C.	O-7169	8
Tatehara J.	O-7095	312
Taxen C.	O-7578	135
Tedim J.	O-7627	230
Tejero M.	P-7714	236
Tempez A.	P-7404	179
Tenié A.	O-7232	375
Teo S.	O-7370	225
Ter-Ovanessian B.	O-7149, O-7499, O-7532	79, 149, 645
Terada M.	O-7622	587
Terryn H.	O-7237, O-7373, O-7608, O-7282, O-7145, P-7374, O-7511, O-7180, O-7179, O-7616	136, 155, 408, 445, 447, 452, 516, 591, 596, 599
Tesch A.	O-7803	595
Tharandt D.	O-7757	360
Theil H.	O-7379	442
Thiébauld N.	O-7579	464
Thierry D.	O-7578, O-7370, O-7154, O-7193	135, 225, 303, 509

Thiery L.	O-7831	535
Thomas E.	O-7369	349
Thompson G.E.	O-7246, O-7783, O-7666, O-7415	129, 165, 377, 657
Thornthwaite P.	O-7135	634
Tidblad J.	O-7459	575
Tigges B.	O-7232	375
Tinga T.	O-7313	153
Tiroel L.	O-7563	317
Tittarelli F.	O-7546	276
Tjelta M.	O-7472	315
Todesco F.	O-7510	318
Todzy T.	O-7269	503
Tognon C.G.R.	O-7464	554
Tohyama K.	O-7075	260
Tomachuk C.R.	P-7552, P-7124	376, 426
Tomandl A.	O-7369, O-7411	349, 350
Tomaszewski J.	P-7191	364
Tomio A.	O-7205	333
Tomoe Y.	O-7171	301
Tonholo J.	P-7764, P-7637	296, 298
Torres C.E.A.S.	P-7721, P-7720	477, 478
Torres-Islas A.	P-7770, P-7768, P-7732	186, 205, 457
Torri L.	O-7510	318
Tosar F.	O-7081	358
Toselli M.	P-7715	605
Touzain S.	O-7560	407
Traisnel M.	O-7234	27
Tran T.H.	O-7228, P-7219	448, 449
Trasatti S.P.M.	O-7290, P-7291, O-7794, O-7533, O-7797, O-7437, O-7541, O-7753, O-7292, O-7849	130, 196, 239, 245, 256, 267, 328, 540, 604, 665
Traverso P.	P-7715	605
Trévin S.	KN-7691	76
Tribollet B.	O-7245, O-7553	152, 272
Triki E.	P-7386	635
Triquenaux C.	O-7579	464
Tröger U.	O-7327, O-7497	522, 525
Trueba M.	O-7290, P-7291, O-7292	130, 196, 604
Tsai C.Y.	P-7184	450
Tsygankova L.E.	P-7296	423
Tüken T.	O-7498, P-7567, P-7814	12, 42, 45
Tuma L.	O-7665	98
Turcu E.F.	O-7391	116
Turek L.	P-7068	176
Tyurin A.G.	P-7214	336

U

Uchida S.	O-7104	77
Uchoa S.B.B.	P-7764, P-7637	296, 298
Ueda M.	O-7278	134
Ueno F.	O-7096	86
Uludag M.	O-7614	517
Umoren S.	O-7303	24
Unsal T.	P-7270	262
Unzurrunzaga Iturbe A.	P-7730	388

Urios L.	O-7623	238
Urquidi-Macdonald M.	O-7794	239
Urtiga Filho S.L.	P-7763	263
Uryadnikov A.A.	P-7296	423

V

Valencia V.	P-7341	394
Valentini R.	O-7684, O-7670	325, 508
Valladares-Cisneros M.G.	P-7126	44
Valle L.C.M.	P-7047	344
Van Assche G.	O-7608	408
van Bokhorst J.	O-7413	483
van Breugel K.	O-7301, O-7260, O-7116	259, 271, 287
Van Brutzel L.	P-7175	178
Van den Steen N.	KN-7708	127
Van der Merwe J.W.	O-7757	360
Van Mele B.	O-7608	408
van Meurs G.A.M.	O-7843	582
van Put M.	O-7180	591
van Renterghem W.	P-7837	99
van Rodijnen F.	O-7058	331
van Westing E.P.M.	O-7313	153
Vandendael I.	O-7511	516
Vanka T.	O-7367	598
Vankeerberghen M.	O-7661	82
Varga M.	O-7360	68
Vargas I.	O-7613, P-7609	248, 551
Vaßen R.	O-7140	59
Vassiliou P.	O-7727	581
Vastra M.	O-7802	255
Velardi U.	O-7448	324
Velázquez-González M.A.	P-7126	44
Vera Jimenez M.	O-7778	26
Verbeken K.	O-7373	155
Verbruggen H.	P-7374	452
Verdingovas V.	O-7447, O-7426	617, 622
Verdu C.	O-7528	644
Vesely S.S.	O-7307	23
Veys-Renaux D.	O-7593, O-7597	378, 383
Viana A.	P-7079	342
Vicenzo A.	P-7099, O-7849	190, 665
Viçosa I.N.	O-7701	284
Vieira D.	O-7257	653
Vieira M.R.S.	P-7763	263
Vigdorovich V.I.	P-7296	423
Vignal V.	O-7626, O-7480	133, 148
Villumsen F.	O-7393	286
Vimalanandan A.	O-7228, P-7219	448, 449
Virtanen S.	KN-7153, O-7204, O-7161	125, 158, 512
Visser A.	O-7605	122
Visser P.	O-7616	599
Vitry V.	O-7081	358
Vivas B.P.	P-7566	210
Vivier V.	O-7553, O-7798, O-7643	272, 647, 652
Vogt J-B.	O-7688, O-7687	120, 648

Volaric B.	P-7748	35
Volovitch P.	O-7417, O-7678	137, 524
Volpi E.	O-7437	267
von Arx C.	P-7847	585
Vrtílková V.	O-7130	84
Vucko F.	O-7154	303
Vuillemin B.	O-7264	161
Vysotskyy Y.B.	P-7317	201

W

Wagner G.	O-7170	651
Walczak M.	O-7613, O-7412	248, 441
Walczak M.S.	O-7587	21
Walkner S.	O-7485	404
Walraven J.C.	O-7241	288
Wang P.	P-7089	261
Wang X.-J.	O-7683	251
Warburton G.	O-7805	305
Ward L.	O-7353	240
Watanabe Y.	O-7149	79
Watkinson D.	O-7496, O-7555, O-7589, O-7258	567, 568, 569, 571
Weiss R.	O-7428	381
Weltschev M.	O-7072	528
Wenzel M.	O-7248	529
Werenskiold J.C.	O-7747, O-7746	491, 494
Werner J.	O-7072	528
Wessman S.	O-7512	111
Weyrich M.	O-7269	503
Whiter J.	O-7466	539
Wibihal S.	P-7371, P-7372, O-7786	217, 417, 655
Widdel F.	O-7077	242
Wieser H.	O-7327, O-7497	522, 525
Wijesinghe S.L.	O-7370, O-7354	225, 280
Wilcox G.D.	O-7421, O-7236, O-7403	586, 626, 627
Wild M.	P-7761	424
Williams G.	O-7070, O-7430, O-7547	128, 351, 413
Wilms M.E.	O-7576, O-7571	307, 319
Wint N.	O-7549	170
Winter F.	O-7500	474
Wittebroodt C.	P-7664, O-7623	109, 238
Wojczykowski K.	O-7773	353
Wolf F.	O-7114	6
Wolpers M.	O-7641	166
Wolski K.	O-7151	124
Worterg D.	O-7269	503
Wosik J.	O-7208, O-7367	597, 598
Wouters Y.	O-7531	61
Wu L.	O-7236	626

Y

Yajima A.	O-7361	487
Yakuwa H.	O-7735	226
Yamamoto M.	O-7096	86
Yang L.	O-7246	129
Yang Y.	P-7330	650

Ye C.	O-7688	120
Yekehtaz M.	O-7232	375
Yevtushenko O.	O-7157	613
Yi Y.	P-7435	185
Yilmaz C.	P-7134	401
Yoo J.D.	O-7678	524
Yoo Y.H.	O-7349	510
You M.	O-7366	415
Young D.	O-7109	58
Yu F.	O-7846	249
Yu X.M.	O-7808	232
Yurmanov E.	P-7800	105
Yurmanov V.	P-7800	105

Z

Zacarelli S.	O-7622	587
Zagidulin D.	O-7603	93
Zajec B.	O-7636	81
Zák P.	P-7453	629
Zalamansky G.	O-7263	600
Zanella C.	O-7506, O-7625	147, 359
Zanibellato A.	O-7306	639
Zanna S.	O-7217, O-7703, O-7376	150, 243, 583
Zanotto F.	O-7261, O-7551, O-7253	266, 268, 304
Zapata A.	O-7785	590
Zavidnaya A.G.	O-7338	139
Zehethofer G.	O-7610	16
Zerjav G.	P-7745	50
Zhang D.	P-7089	261
Zhang D.Q.	O-7147	62
Zhang J.	KN-7108, O-7554	5, 475
Zhang L.	O-7147, P-7094	62, 420
Zhang M.	O-7683	251
Zhang X.	O-7313, O-7195, O-7382	153, 446, 557
Zhao X.	P-7094	420
Zheludkevich M.L.	O-7627, O-7257, O-7640	230, 653, 656
Zhilenko D.Yu.	O-7352	13
Zhong X.	O-7246, O-7783	129, 165
Zhou X.	O-7246, O-7783, O-7415	129, 165, 657
Zhu B.	O-7383	523
Zhu M.	P-7654	343
Ziebermayr S.	O-7477	168
Zimer A.M.	P-7645	479
Zimmer A.	O-7789	654
Zimmer P.	O-7598	52
Zomorodian A.	O-7669, O-7810	410, 411
Zoppas-Ferreira J.	P-7525, P-7530	396, 402
Zucchi F.	O-7138, O-7253	151, 304
Zuo Y.	P-7098, P-7094	234, 420
Zychová M.	O-7665	98

Sponsored by:



ASSOCIAZIONE PER LA PROTEZIONE
DALLE CORROSIONI ELETTROLITICHE
www.apce.it • info@apce.it

